CHALMERS

Vehicle Dynamics

Compendium

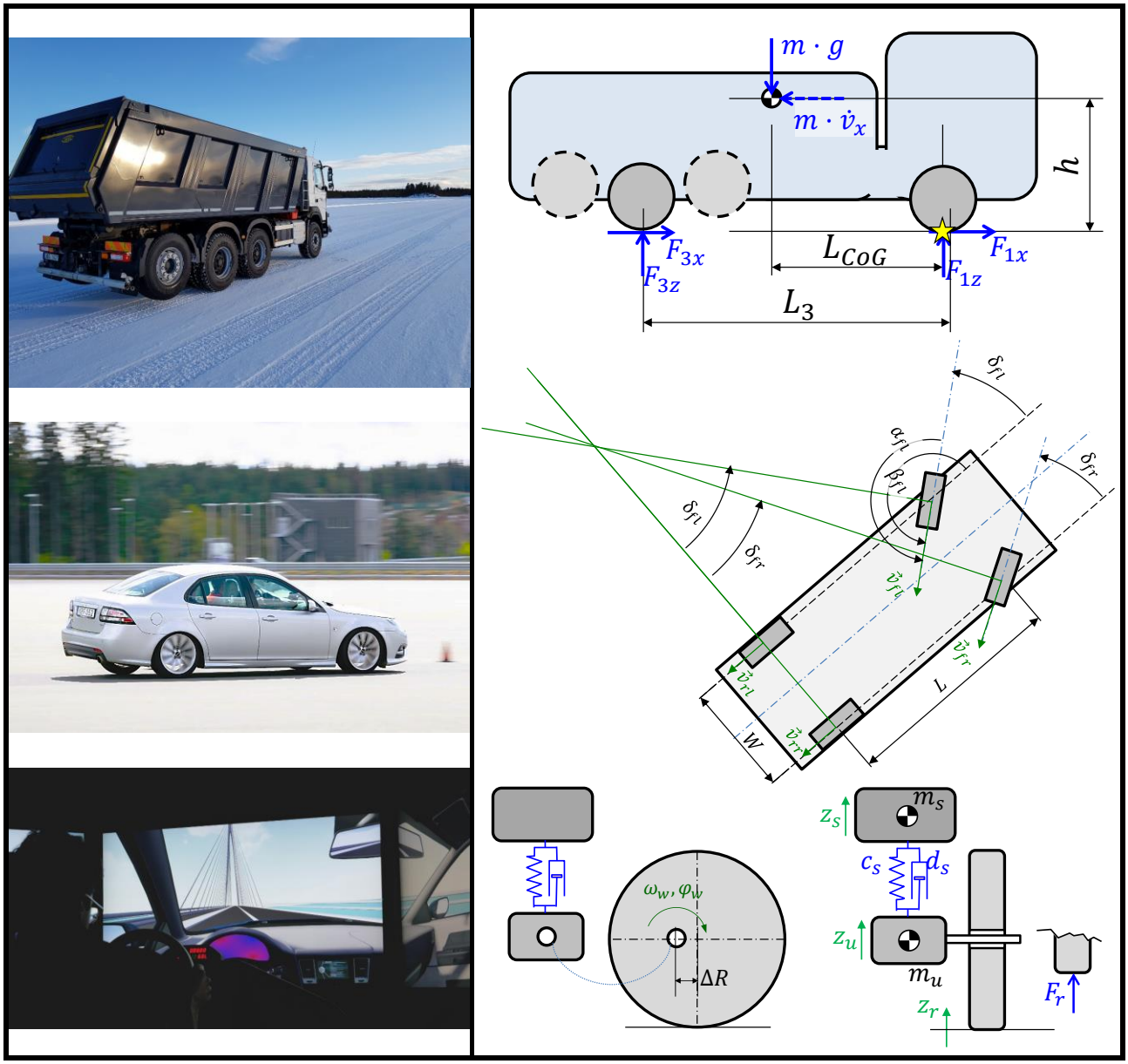

2019, variant: Printed on paper

Bengt Jacobson et al
Vehicle Dynamics Group, Division Vehicle and Autonomous Systems,
Department Mechanics and Maritime Sciences, Chalmers University of Technology, www.chalmers.se

Preface 2019

The compendium 2019 is published in 2 variants: “Printed on paper” and “Digital only”. Both are available as pdf-file. The “Digital only” variant contains some additional material; search for “#DigitalOnly”. The numbered items (figures, equations, etc) in the “Digital only” variant does not have numbering, in order to keep same numbers of each item between the variants. However, note that page numbering varies between the variants.

Thanks to Tobias Brandin, Fredrik Bruzelius, Edo Drenth, Niklas Fröjd, Toheed Ghandriz, Patrick Gruber, Mats Jonasson, Mathias Lidberg, Anders Lindström, Oscar Ljungcrantz, Peter Nilsson, Luigi Romano, Juliette Utbult and errata reporting from students. Sorry, if I forgot some contributor!

/Bengt Jacobson, Göteborg, October 2019

Preface 2018

One large rearrangement is done: Subsystem descriptions has been collected from Chapter 3, 4 and 5 to 2.3-2.7. Also, minor changes and additions has been done throughout all chapters. Many thanks to, among other, Niklas Fröjd Volvo GTT, Toheed and Fatemeh Ghandriz, Ingemar Johansson CEVT, Mats Jonasson VCC, Mathias Lidberg, Simone Sebben, Alexey Vdovin. Thanks also to many students that have found and reported errors in the previous edition.

/Bengt Jacobson, Göteborg, October 2018

Preface 2017

This edition has various smaller changes and additions. Thanks to Fredrik Bruzelius (VTI), Tobias Brandin (VCC), Niklas Fröjd (Volvo GTT), Assar Jarlsson (Kinnarps), Pär Pettersson (Chalmers), among others. Thanks also to many students that have found and reported errors in the previous edition. */Bengt Jacobson, Göteborg, October 2017*

Preface 2016

This edition has various changes and additions. Some of these are: Chapter 1: Control engineering, Chapter 2: Tyre models, Driver models, Chapter 3: Propulsion systems, Varying road pitch, Non-reactive truck suspensions, Chapter 4: Track-ability, Articulated vehicles, and Cambering vehicles.

Thanks to Cornelia Lex (TU Graz), Fredrik Bruzelius (VTI), Niklas Fröjd, Anders Hedman, Kristoffer Tagesson, Peter Nilsson, Sixten Berglund (Volvo GTT), Tobias Brandin, Edo Drenth, Mats Jonasson (VCC), Mathias Lidberg, Artem Kusachov, Anton Albinsson, Manjurul Islam, Pär Pettersson, Ola Benderius (Chalmers), Mats Sabelström, and Roland Svensson among others.

/Bengt Jacobson, Göteborg, October 2016

Preface 2015

This edition has various changes and additions. Some of these are: brush model with parabolic pressure distribution, typical numerical data for heavy vehicle, added “2.2.3 Tyre”, “4.5.3.2 Example of explicit form model”, more about tyre relaxation, introduction of neutral steering point, introduction of steady state roll-over wheel lift diagram. Thanks to Anton Albinsson, Edo Drenth (VCC), Gunnar Olsson (LeanNova), Manjurul Islam, Mathias Lidberg, Mats Jonasson (VCC), Niklas Fröjd (Volvo GTT), Ola Benderius, Pär Pettersson, and Zuzana Nedelkova among other. */Bengt Jacobson, Göteborg, 2015*

Preface 2014

This edition has various small changes and additions. The largest changes are: Function definitions added and major update of sections 2.3, 4.1.1, 0, 6.1.1.

Thanks to Lars Almefelt from Chalmers, Jan Andersson from VCC, Kristoffer Tagesson from Volvo GTT and Gunnar Olsson from Leannova and Karthik Venkataraman. */Bengt Jacobson, Göteborg, 2014*

Preface 2013

This edition has various small changes and additions. The largest additions were in: Functional architecture, Smaller vehicles, Roll-over, Pendulum effect in lateral load transfer and Step steer.

Thanks to Gunnar Olsson from LeanNova, Mathias Lidberg, Marco Dozza, Andrew Dawkes from Chalmers, Erik Coelingh from Volvo Cars, Fredrik Bruzelius from VTI, Edo Drenth from Modelon, Mats Sabelström, Martin Petersson and Leo Laine from Volvo GTT. */Bengt Jacobson, Göteborg, 2013*

Preface 2012

A major revision is done. The material is renamed from “Lecture notes” to “Compendium”. Among the changes it is worth mentioning: 1) the chapters about longitudinal, lateral and vertical are more organised around design for vehicle functions,

2) a common notation list is added, 3) brush tyre model added, 4) more organised and detailed about different load transfer models, and 5) road spectral density roughness model is added.

Thanks to Adithya Arikere, John Aurell, Andrew Dawkes, Edo Drenth, Mathias Lidberg, Peter Nilsson, Gunnar Olsson, Mats Sabelström, Ulrich Sander, Simone Sebben, Kristoffer Tagesson, Alexey Vdovin and Derong Yang for review reading.

/Bengt Jacobson, Göteborg, 2012

Preface 2011

Material on heavy vehicles is added with help from John Aurell. Coordinate system is changed from SAE to ISO. Minor additions and changes are also done. */Bengt Jacobson, Göteborg, 2011*

Preface 2007

This document was developed as a result of the reorganization of the Automotive Engineering Master's Programme at Chalmers in 2007. The course content has been modified in response to the redistribution of vehicle dynamics and power train education.

These lecture notes are based on the original documents developed by Dr Bengt Jacobson. The text and examples have been reformatted and edited but the author is indebted to the contribution of Dr Jacobson. */Rob Thomson, Gothenburg, 2007*

Keywords: Vehicle Engineering, Automotive Engineering, Vehicle Dynamics, Vehicle Motion, Modelling, Modelica, Simulation

Cover: Left column, from top: Brake testing in Colmis in Arjeplog with Haldex and Volvo GTT, Test of avoidance manoeuvre with Direction Sensitive Locking Differential by DsenseD technology AB (photo by CFFC), and Simulator test at CASTER for a planned floating bridge across Björnafjorden in Norway. Right column: Figures from written examinations in MMF062 Vehicle Dynamics, academic year 2018/2019.

This compendium is also available as pdf file at https://research.chalmers.se/en/person/bengtja#publications

Paper version printed at Repro-centralen, Chalmers, Göteborg, Sweden, 2019

Contents

1 INTRODUCTION

1.1 Definition of Vehicle Dynamics

Vehicle Dynamics is an engineering subject about motion of vehicles in relevant user operations. The subject is applied, and applied on a certain group of products, i.e. vehicles. Vehicle Dynamics always uses terms, theories and methods from Mechanical/Machine engineering, but often also from Control/Signal engineering and Human behavioural science.

1.2 About this compendium

This compendium is initially written for the course "MMF062 Vehicle Dynamics" at Chalmers University of Technology. The compendium covers more than included in that course; both in terms of subsystem designs and in terms of some teasers for more advanced studies of vehicle dynamics. Therefore, the compendium can also be useful in general vehicle engineering courses, e.g. in the Chalmers course "TME121 Engineering of Automotive Systems"; and as an introduction to more advance courses, which at Chalmers is the course "TME102 Vehicle Dynamics Advanced".

The overall objective of the compendium is to educate automotive engineers for development of vehicles. The compendium focuses on road vehicles, primarily passenger cars and commercial vehicles. Smaller road vehicles, such as bicycles and single-person cars, are only very briefly addressed. It should be mentioned that there exist a lot of ground-vehicle types not covered at all, such as: off-road/construction vehicles, tracked vehicles, horse wagons, hovercrafts or railway vehicles.

Functions are needed for requirement setting, design and verification. The overall order within the compendium is that models/methods/tools needed to understand each function are placed before the functions. Chapters 3-5 describes (complete vehicle) "functions", organised after vehicle motion directions:

- Chapter 3: Longitudinal dynamics
- Chapter 4: Lateral dynamics
- Chapter 5: Vertical dynamics

Chapter 1 introduces automotive industry and defines/repeats required pre-knowledge from different traditional academic disciplines. It is important to qualitatively understand the characteristics of the vehicle's subsystems and, from this, learn how to quantitatively predict and analyse the complete vehicle's behaviour. The reader of this compendium is assumed to have knowledge of mathematics and mechanics, to the level of a Bachelor of Engineering degree. Previous knowledge in dynamic systems, e.g. from Control Engineering courses, is often useful.

The vehicle is a component or subsystem in a superior transport system consisting of other road users, roads, and transport missions. A vehicle is also, itself, a system within which many components or subsystems interact. Chapter 2 describes what interacts with the vehicles from outside, like aerodynamics and driver. Chapter 2 also describes the other subsystems relevant for vehicle dynamics:

- Wheels and Tyre in 2.2
- Suspension System in 2.3 (and 3.4.5.2 and 4.3.9)
- Propulsion System in 2.4
- (Wheel) Braking System in 2.5
- (Wheel) Steering System in 2.6
- Environment Sensing System in 2.7

1.3 Automotive engineering

This section is about the context where Vehicle Dynamics is mainly applied, i.e. the automotive industry. *OEM* means Original Equipment Manufacturer and is, within the automotive industry, used for a vehicle manufacturer. OEM is a legal status in some countries. In the automotive industry, the word

Supplier means supplier to an OEM. A *Tier1* supplies directly to an OEM. A *Tier2* supplies to a Tier1 and so on. Primarily, suppliers supply parts and systems to the OEMs, but suppliers can also supply competence, i.e. consultant services.

From an engineering view, an OEM does Product Development and Manufacturing. But it is good to remember that there is also Purchasing, Marketing & Sales, After Sales, etc. However, Product Development is the main area where the vehicles are designed. It is typically divided into Powertrain, Chassis, Body, Electrical and (Complete) Vehicle Engineering. Vehicle Dynamics competence is mainly needed in Chassis, Powertrain and Vehicle Engineering.

On supplier side, Vehicle Dynamics competence is mainly needed for system suppliers that supplies propulsion, brake, steering and suspension systems. Additional to OEMs and suppliers, Vehicle Dynamics competence is also needed in authorities for legislation and testing as well as research institutes.

There are engineering associations for automotive engineering. FISITA (Fédération Internationale des Sociétés d'Ingénieurs des Techniques de l' Automobile, www.fisita.com) is the umbrella organisation for the national automotive societies around the world. Examples of national societies are IMechE (United Kingdom), JSAE (Japan), SAE (USA), SAE-C (Kina), SATL (Finland), SIA (France), SVEA (Sweden, www.sveafordon.com) and VDI FVT (Germany). There is a European level association also, EAEC.

1.3.1 Vehicle Dynamics Engineers' Industry Roles

The activity type that sets the pace in automotive industry are vehicle programme or projects. It defines the **technology** to be developed, the **time** and **cost** aspects. The work is organised around such programmes, both at vehicle manufacturers and their sourced subsystem supplier. One way to exemplify such is Figure 1-1. Engineers with vehicle dynamics profile are typically active at departments called Chassis, Complete Powertrain, Electrical or Vehicle Engineering. They are responsible for deliverables to vehicle programme in the form of:

- **Hardware**: Geometry, Strength and function per subsystem, ECUs
- **Software**: SW per subsystem, Functions such as ABS, ESC, ACC
- **Requirement setting and verification**: Handling, Driveability, Brake performance, Ground clearance, Ride comfort, Energy consumption. Verification in **real and virtual tests**.

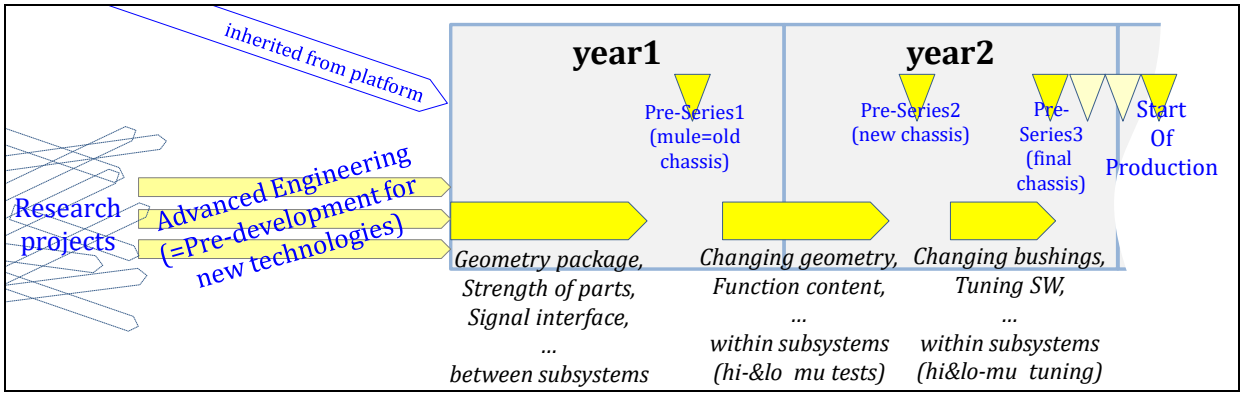

Figure 1-1: An example of vehicle programme and Vehicle Dynamics related activities.

1.4 Requirement Setting

Development of a vehicle is driven by **Requirements**, coming from:

- Manoeuvres/Vehicle operations/Use cases, representative for the need of the customers/users
- Legislation from the authorities and Rating from consumer organisation, and
- Engineering constraints from the manufacturer's platform/architecture on which the vehicle should be built.

One way of organising requirements is to define **Attributes** and **Functions**. The terms are not strictly defined and may vary between vehicle manufacturers and over time. With this said, it is assumed that the reader understand that the following is an approximate/exemplifying and simplified description.

In this compendium, both attributes and functions concern the **complete vehicle**; not the subsystems within the vehicles and not the superior level of the transportation system with several vehicles in a road infrastructure.

Attributes and Functions are used to establish processes and structures for requirement setting and verification within a vehicle engineering organisation. Such processes and structures are important to enable a good overall design of such a complex product as a vehicle intended for mass production at affordable cost. Figure 1-2 gives an overview, with reference to the well-known V-process, of how a vehicle is developed. Note that these kinds of figures are very idealized, and one should neither trust the process too much nor neglect them. A vehicle is a very complex product. First, one has several levels of functions and subsystems. Secondly, it is difficult to keep a clean hierarchical order between functions and subsystems. Thirdly and most conceptually difficult, is the fact that each subsystem gets requirements from many functions as showed by the dashed lines; this makes the complexity explode.

1.4.1 Attributes

An attribute is a high-level aspect of how the users perceive the vehicle. Attributes which are especially relevant for Vehicle Dynamics are listed in Table 1.1. The table is much generalised and the attributes in it would typically need to be decomposed into more attributes when used in the engineering organisation of an OEM. Also, not mentioned in the table, are attributes which are less specific for vehicle dynamics, such as Affordability (low cost for user), Quality (functions sustained over vehicle lifetime), Styling (appearance, mainly visual), etc.

A set of Attributes is a way to categorise or group functions, especially useful for an OEM organisation and vehicle development programs. A set of Functions is a way to group requirements. **Legal** requirements are often, but not always, possible to trace back to primarily one specific attribute. Requirements arising from OEM-internal **platform and architecture constraints** are often more difficult to trace in that way. Hence, "platform/architecture" is a "requirement container", beside the attributes.

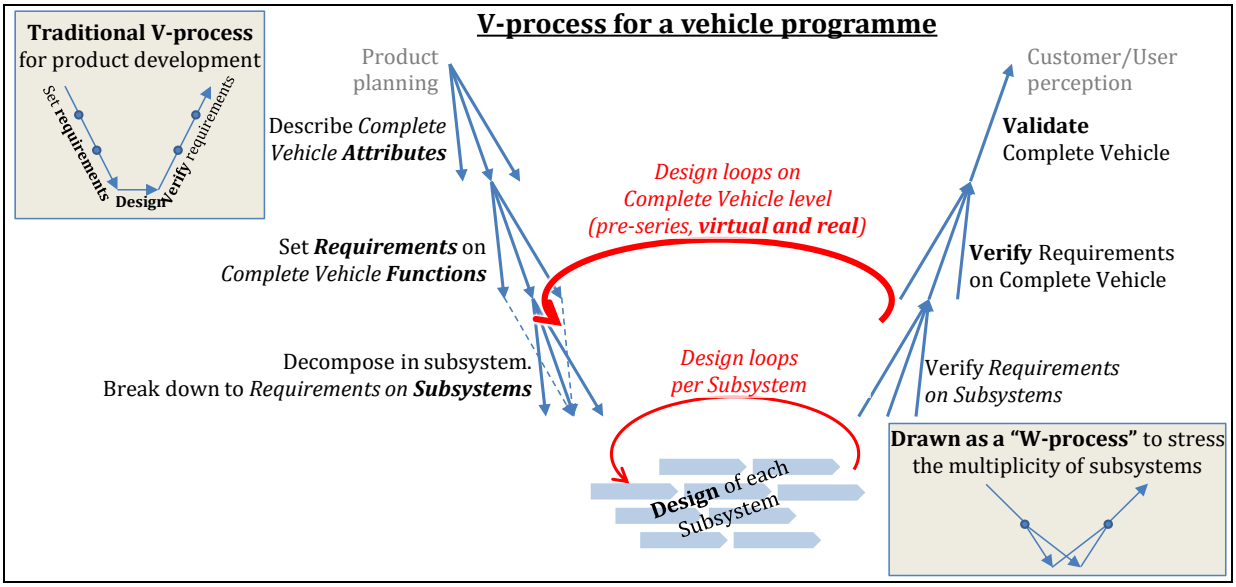

Figure 1-2: V-process for a vehicle program. The more design loops are utilized, the more "agile".

1.4.2 Functions

In this compendium, a *function* is more specific than an attribute. A function should define measures of something the (complete) vehicle does, so that one can set (quantitative) requirements on each measure, see 1.4.3. The function does not primarily stipulate any specific subsystem. However, the realisation of a function in a certain vehicle programme, normally only engages a limited subset of all subsystems. So, the function will there pose requirements on those subsystems. Hence, it is easy to mix up

whether a function origin from an attribute or a subsystem. One way to categorise functions is to let each function belong to the subsystem which it mainly implies requirements on rather than the source attribute. Categorizing functions by subsystems tends to lead to "carry-over" function realisations from previous vehicle program, which can be good enough in many cases. Categorizing functions by source attribute facilitates more novel function realisations, which can be motivated in other cases.

The word "function" has appeared very frequently lately along with development of electrically controlled systems. The function "Accelerator pedal driving" in 3.5.2.1 has always been there, but when the design of it changed from mechanical cable and cam to electronic communication and algorithms (during 1990's) it became much more visible as a function, sometimes referred to as "electronic throttle". The point is that the main function was there all the time, but the design was changed. The change of design enabled, or was motivated by, improvement of some sub-functions, e.g. idle speed control which works better in a wider range of engine and ambient temperature.

At some places, the compendium emphasizes the functions by adding an **asterisk "*"** in section heading and a "**Function definition**" in the following typographic form:

> *Function definition:* ***{The Function}*** *is the {Measure} … for {Fixed Conditions} and certain {Parameterized Conditions}.*

The word "conditions" should be understood as a manoeuvre, operation or use case. It is often possible and efficient to define multiple measures from one "condition".

The {*Measure*} should be one unambiguously defined measure (such as time, velocity or force) of something the vehicle does. The {*Measure*} is ideally a continuous, objective and scalar physical quantity, subjected for setting a requirement on the vehicle. The {*Fixed Conditions*} should be unambiguously defined and quantified conditions for the vehicle and its surroundings. The keyword "*certain*" identifies the {*Parameterized Conditions*}, which need to be fixed to certain numerical values or probabilistic distributions, before using the Function definition for requirement setting, see 1.4.3.

Since the term "Function" is defined very broadly in the compendium, these definitions become very different. One type of Function definition can be seen in "3.2.3.1 Top Speed *", which includes a well-defined measure. Another type of Function definition is found in "3.5.2.3 Anti-Lock Braking System, ABS *" and "4.3.3 Under-, Neutral- and Over-steering *". Here, the definitions are more on free-text format, and an exact measure is not so well defined.

Table 1.1: Attributes relevant for Vehicle Dynamics / Vehicle Motion

↓Attribute	Description↓
Transport Efficiency	This attribute means to maximize output from and minimize costs for transportation. Transport output can be measured in $person \cdot km$, $ton \cdot km$ or $m^3 \cdot km$. The costs are mainly energy costs and time, but also wear of vehicle parts influence. The attribute is most important for commercial vehicles but becomes increasingly important also for passenger vehicles. The attribute is mainly addressing long-term vehicle usage pattern, typically 10 min to 10 hours. There are diverse ways to define such usages, e.g. (Urban / Highway / Mixed) driving cycles. So far, the attribute is mainly required and assessed by the vehicle customers/users. The attribute can also be seen to include "Environmental Efficiency", which means low usage of natural resources (mainly energy) and low pollution, per performed transport task. This is to a substantial extent required and assessed by society/legislation.
Safety	Minimizing risk of property damages, personal injuries and fatalities both in vehicle and outside, while performing the transportation. This attribute is to a considerable extent required and assessed by society/legislation. In some markets, mainly developed countries, it is also important for vehicle customers/users.

↓Attribute	Description↓
User Experience (Driver Experience)	How the occupants (often the driver) experiences the vehicle during transport; from relaxed transport (comfort) to active driving (sensation). This attribute contains sub-attributes as: • **Ride comfort**. Ride comfort often refers to vibrations and harshness of the occupants' motion, primarily vertical but secondly longitudinal and lateral. So, V and H in NVH (=Noise, Vibration and Harshness) is included. If expanding to "comfort" it would include also N (noise) and compartment air conditioning, but these sub-attributes are less related to vehicle dynamics. • **Performance** describes how the vehicle can perform at the limits of its capabilities; acceleration, deceleration or cornering. Most often, it refers to longitudinal limitations due to propulsion and brake systems limitations. • **Driveability, Handling and Road-holding** describes how the vehicle responds to inputs from driver and disturbances, and how driver gets feedback from vehicle motion e.g. through steering feel. It is also the corresponding response aspects for a "virtual driver", i.e. a control algorithm for automated driving. Driveability often refers to longitudinal (acceleration, braking gear shifting). Handling and Road-holding often refer to lateral manoeuvres. • **Trust** in automated driving becomes increasingly important and needs to be balanced; high trust but not over-trust. This attribute is to a considerable extent required and assessed by the vehicle customers/users, both through own experience but also indirectly via assessments by experts, e.g. in motor journals.

1.4.3 Requirements

A requirement shall be such that it is possible to verify how well a product fulfils it. A requirement on the complete vehicle is typically formulated as:

"The vehicle shall … do something or have measure … $<$ or $>$ or $\approx$ … number·[unit] …
… under certain conditions."

Examples: The vehicle shall…

- … accelerate from 50 to 100 km/h in <5 s when full acceleration pedal. On level road.
- … decelerate from 100 to 0 km/h in <35 m when brake pedal is fully applied, without locking any rear wheel. On level road.
- … turn with outermost edge on a diameter <11m when turning with full steering at low speed.
- … have a characteristic speed of 70 km/h (±10 km/h). On level ground and high-friction road conditions and any recommended tyres.
- … give a weighted RMS-value of vertical seat accelerations $< 1.5\ m/s^2$ when driving on road with class B according to ISO 8608 in 100 km/h.
- … keep its body above a 0.1 m high peaky two-sided bump when passing the bump in 50 km/h.

To limit the amount of text and diagrams in the requirements it is useful to refer to ISO and OEM specific standards. Also, it is good to document the purpose and/or use cases with the requirement.

The above listed requirements stipulate the function of the vehicle, which is the main approach in this compendium. Alternatively, a requirement can stipulate the design of the vehicle, such as "The vehicle shall weigh <1600 kg" or "The vehicle shall have a wheel base of 2.5 m". The first type (above listed) can be called *Performance based requirement*. The latter type can be called *Design based requirement* or *Prescriptive requirement* and such are rather "means" than "functions", when seen in a function vs mean hierarchy. It is typically desired that requirements are Performance based, else they would limit the technology development in society.

1.4.4 Models, Methods and Tools

The attributes, functions and requirements are top level entities in vehicle development process. But to design and verify, the engineers need knowledge in form of models, methods and tools.

As mentioned above, some sections in the compendium have an asterisk "*" in the section heading, to mark that they explain a function, which can be subject for complete vehicle requirement setting. The remaining section, without an asterisk "*", are there to give the necessary knowledge (models, methods and tools) to verify (including understand) the function and the requirements on it. It is the intention that the necessary knowledge for a certain function appears before the description of that function. One example is that the "2.4 Propulsion System", "3.2.1 Traction Diagram" and "3.2.2 Power and Energy Losses" are placed before "3.2.3.1 Top Speed *". Functions only appear in Chapters 3, 4 and 5.

1.5 Engineering

Engineering (or Design Engineering, in Swedish often "Ingenjörsvetenskap", in German "Ingenieurwissenschaft"), as a science has an important portion of *Synthesis.* As support for synthesis, it also relies on *Analysis*, *Inverse analysis* or *(Nature) Science*, see Figure 1-3. Figure 1-4 distinguishes between Analysis and Synthesis, which shows that Analysis is a step in the whole design loop. The actual Design step requires Synthesis. The overall purpose is to propose a design, e.g. numerical values of *Design parameters* of a product. The distinction between Analysis and Inverse Analysis can be made when there is a natural causality ("cause-effect-direction").

In 1.5 some useful general methods and tools are described. Parts of these are probably repetition for some of the reader's previous education, in mechanical and control engineering. In the end of 1.5, there is a stronger connection to the vehicle engineering.

1.5.1 Model Based Engineering

An analysis step as in Figure 1-4, can use either real or virtual verification. For real verification one need to build prototypes. For Virtual Verification, models are needed. A (dynamic) model is a representation of something from real-world varying over a time interval, such as a car during longitudinal acceleration from 0..100 km/h. Models are always based on assumptions, approximations and/or simplifications. However, when using models as a tool for solving a particular problem, the models at least have to be able to reproduce the engineering problem one is trying to solve. Also, models for engineering have to reflect design changes in a representative way, so that new designs can be evaluated. Too detailed models tend to be a less useful, since they require and produce a lot of data.

The models typically used in vehicle dynamics can be called *physical dynamic* models (many alternative names: functional models, lumped models, discretized models, system models, DAE-model, ODE-models, etc.). The models are typically multi-domain type, involving mechanics, hydraulics, pneumatics, electric, control algorithms, driver's actions, etc. Examples of modelling methods which more seldom are used directly in vehicle dynamics are: Finite Elements, Computational Fluid Dynamics, CAD geometry models, etc.

One can identify **modelling** in 3 stages in the overall process: 1.5.1.1.2 *Physical Modelling,* 1.5.1.1.3 *Mathematical Modelling,* and 1.5.1.1.4 *Explicit Form Modelling.* See Figure 1-5. The compendium spends most effort on the first 2 of those 3.

Physical models are assumed. As opposite to this, one can think of formulating a mathematical model without motivation from established physics. (Without a physical model, the parameters are generally not interpretable to real design parameters; an indication of this is when the modeller does not know the units of parameters and variables in the model, and the parameters needs real tests to be found. Methods for such modelling can be regression, machine learning, etc and such models can only be used for interpolation, not extrapolation.) However, for vehicle engineering, the vehicle model should be physical, so that its real-world design parameters can be identified. However, a driver model can be useful also without strict physical model, since the driver is not to be designed during vehicle

engineering. But it is important to consider that the driver do change its behaviour when vehicle design parameters are changed.

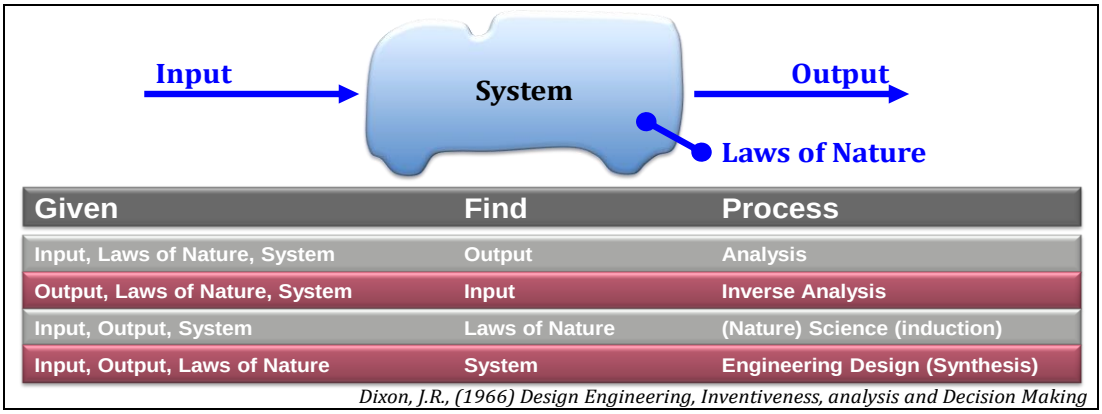

Figure 1-3: Engineering Design and related activities. Picture from Stefan Edlund, Volvo Trucks.

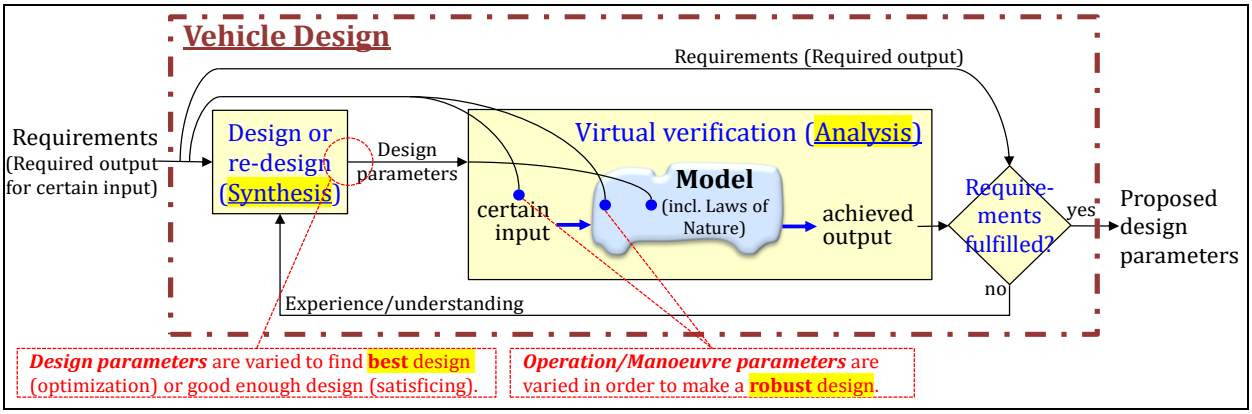

Figure 1-4: How Analysis/Synthesis and Design/Operation parameters appears in Vehicle Design.

1.5.1.1 Stages in (Dynamic) Model Based Engineering

1.5.1.1.1 Formulate the Engineering Design Task

Based on a problem description, one formulates the **engineering design task**, which describes the required design decisions (if possible, appoint design parameters) for an existing vehicle or a concept. Also, requirements on how the output of the system should react in certain vehicle operations (or manoeuvres or situations) have to be identified. Requirements can be either constraints (something<number) and/or optimization (some scalar to be minimized).

The conceptual idea with requirements in vehicle industry is that they are set independently of the design solution. However, the general requirements are seldom neither enough for a certain engineering design task; one often have to reformulate or add requirements. The operation parameters often have a range/spread/stochasticity to design for, see Figure 1-4. Examples of such parameters describe traffic situation, driver, tyre/road characteristics, weather, see 1.5.1.3.1. The range can be searched for in feedback or logged data from customers and accident statistics. But it is also very important with experienced engineering judgment, to forecast how the problem will appear in a future context, with a future fleet of vehicles and a future road infrastructure. Design methodology can be used to reason about and categorize parameters (e.g. Taguchi's: "signal, response, noise and control factors").

One design task is typically influenced by several requirements and can therefore need multiple models of the same system. This stresses the importance of parameterization, which help to secure that the same design is assessed in the different models.

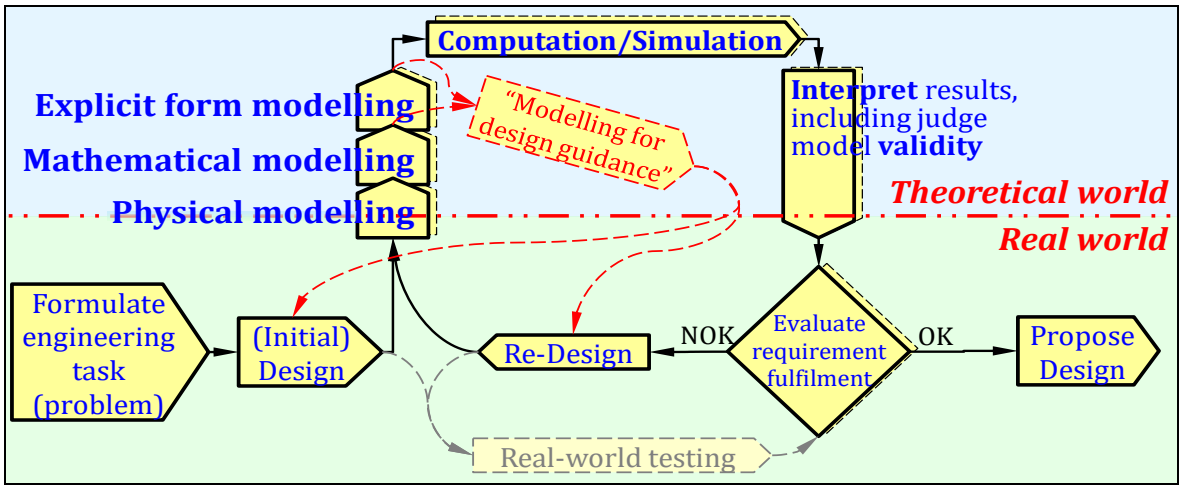

Figure 1-5: (Dynamic) Modelling stages. Real versus Theoretical world. The dashed boxes in the background indicate that same design has to fulfil multiple requirements, which might require multiple models.

1.5.1.1.2 Physical Modelling

In this stage, one should generate a **physical model**, which in this compendium means sketches and text. Free-body diagrams (see 1.5.2.1) and operating conditions (see 1.5.6) are always important ingredients in the physical model of a vehicle, but also other domains than mechanical are often represented, such as hydraulics, electrics, driver and control algorithms. The physical model shall clarify assumptions/approximations/simplifications, e.g. rigid/elastic, inertial/massless, small angles, etc. Discrete dynamics, see 1.5.1.4, such as ideal dry friction, backlash or end stop does not exist in real world, so such assumptions are typical examples of clear differences between real system and physical model. How to model here should be based on what phenomena is needed to be captured and what variations (e.g. which design parameters) are intended for simulations with the model. A list of parameters and variables are suitably introduced and defined, for reuse in the mathematical model. A physical model is often not executable, but it can be. One example of executable format is a model build in an MBS tool, see 1.5.4.9 and Figure 1-18.

1.5.1.1.3 Mathematical Modelling

In this stage, one should generate a **mathematical model**, which means equations. Basically, it is about finding the right equations; equally many as unknowns. For dynamic systems, the unknowns are unknown variables of time. In the mathematical model, the assumptions are transformed into equations. For dynamic systems, the equations form a "DAE" (Differential-Algebraic system of Equations). It is seldom necessary to introduce derivatives with respect to other independent variables, such as positions, i.e. one does seldom need PDE (Partial Differential Equations). The general form of a DAE:

- $\boldsymbol{f_{DAE}}(\dot{\boldsymbol{z}}, \boldsymbol{z}, t) = \boldsymbol{0}$;

The $\boldsymbol{z}$ are the (dependent) variables and t is time (independent variable). The mathematical model is complete only if there are equally many (independent) equations in $\boldsymbol{f_{DAE}}$ as there are variables in $\boldsymbol{z}$. (Since DAE, we don't counte $\dot{\boldsymbol{z}}$ and $\boldsymbol{z}$ as different variables.)
Note that it is not only a question of finding suitable equations, but also to decide *parameterisation*, which is how parameters are defined and related to each other. Parameterisation should reflect a "fair" comparison between different design parameters, which often requires a lot of experience of the product and the full set of requirements on the vehicle. To underline the parameters, $\boldsymbol{p}$, they can be included in the DAE form as $\boldsymbol{f_{DAE}}(\dot{\boldsymbol{z}}(t), \boldsymbol{z}(\boldsymbol{t}), t, \boldsymbol{p}) = \boldsymbol{0}$;.

Selection of output variables is important so that output variables are enough to evaluate the requirements on the system. Selecting more might drive unnecessary complex models.

The Mathematical model is *acausal*, i.e. describes relations between the variables, not how and in which order they are computed.

There is a strong tradition to in mechanical engineering to model with 2nd order differential equations, where accelerations of inertial bodies appear as 2nd derivative of position. However, numerical

methods for solving first order differential equations are much more mature and Vehicle Dynamics mainly aims at such. Hence, the compendium aims at first order differential equations. It is easy to go from few higher order to many first order differential equations; variables appearing in 2nd order derivative $\ddot{z}_i$ are replaced with $\dot{z}_{new,j}$ and one equation $\dot{z}_i = z_{new,j}$; is added. The opposite is not generally as easy, but often possible. An example is a linear model $\dot{\boldsymbol{z}} = \boldsymbol{A} \cdot \boldsymbol{z}$;, which can be converted from many 1st order to fewer 2nd order becomes as follows:

$$\underbrace{\begin{bmatrix}\dot{\boldsymbol{z}}_1\\ \dot{\boldsymbol{z}}_2\end{bmatrix}}_{\dot{\boldsymbol{z}}} = \underbrace{\begin{bmatrix}\boldsymbol{A}_{11} & \boldsymbol{A}_{12}\\ \boldsymbol{A}_{12} & \boldsymbol{A}_{22}\end{bmatrix}}_{\boldsymbol{A}} \cdot \underbrace{\begin{bmatrix}\boldsymbol{z}_1\\ \boldsymbol{z}_2\end{bmatrix}}_{\boldsymbol{z}}; \Rightarrow \left\{\begin{matrix}\text{differentiate}\\ \text{equation for } \dot{\boldsymbol{z}}_1\end{matrix}\right\} \Rightarrow \left\{\begin{matrix}\text{eliminate}\\ \boldsymbol{z}_2 \text{ (and } \dot{\boldsymbol{z}}_2)\end{matrix}\right\} \Rightarrow$$

$$\Rightarrow \ \ddot{\boldsymbol{z}}_1 - \left(\boldsymbol{A}_{11} + \boldsymbol{A}_{12} \cdot \boldsymbol{A}_{22} \cdot \boldsymbol{A}_{12}^{-1}\right) \cdot \dot{\boldsymbol{z}}_1 - \boldsymbol{A}_{12} \cdot \left(\boldsymbol{A}_{21} - \boldsymbol{A}_{22} \cdot \boldsymbol{A}_{12}^{-1} \cdot \boldsymbol{A}_{11}\right) \cdot \boldsymbol{z}_1 = \boldsymbol{0};$$

A mathematical model can have a format which is executable, e.g., a Modelica model, see 1.5.4.10.

1.5.1.1.4 Explicit Form Modelling

In this stage, one should generate an **explicit form model**, which means equations rearranged to assignment statements, i.e. to an explicit form (algorithm) which outputs the state derivatives. The explicit form model is generally causal. You probably recognize this formulation as "ODE" (Ordinary Differential Equation) or "IVP" (Initial Value Problem). The general form is:

- $\dot{\boldsymbol{x}} \leftarrow \boldsymbol{f}_{\boldsymbol{ODE}}(\boldsymbol{x}, \boldsymbol{u}(t), t); \quad \boldsymbol{y} \leftarrow \boldsymbol{g}(\boldsymbol{x}, \boldsymbol{u}(t), t);$

The $\boldsymbol{x}$ is the state variables, $\boldsymbol{u}$ is the input variables, and $\boldsymbol{y}$ the output variables. In the mathematical model, there was no distinction between different dependent variables in $\boldsymbol{z}$. However, to reach the explicit model, each variable in $\mathbf{z}$ has to be identified as belonging to either of $\boldsymbol{x}$, $\boldsymbol{y}$ or $\boldsymbol{u}$. Simply speaking, states $\boldsymbol{x}$ are the variables which appears both as z_i and $\dot{z}_i$, inputs $\boldsymbol{u}$ are variables that cannot be solved for within the system of equations and outputs $\boldsymbol{y}$ are the remaining variables. In some cases, a Linear State Space Form can be identified (or found to be a good approximation):

- $\dot{\boldsymbol{x}} \leftarrow \boldsymbol{A}(t) \cdot \boldsymbol{x} + \boldsymbol{B}(t) \cdot \boldsymbol{u}(t); \quad \boldsymbol{y} \leftarrow \boldsymbol{C}(t) \cdot \boldsymbol{x} + \boldsymbol{D}(t) \cdot \boldsymbol{u}(t);$ where $\boldsymbol{A}, \boldsymbol{B}, \boldsymbol{C}, \boldsymbol{D}$ are matrices.

Sometimes one need to get rid of constant terms by linear variable transformations, starting from the "affine" form:

- $\dot{\boldsymbol{x}} \leftarrow \boldsymbol{A}(t) \cdot (\boldsymbol{x} - \boldsymbol{x_0}) + \boldsymbol{B}(t) \cdot \left(\boldsymbol{u}_0 - \boldsymbol{u}(t)\right); \quad \boldsymbol{y} \leftarrow \boldsymbol{C}(t) \cdot (\boldsymbol{x} - \boldsymbol{x_0}) + \boldsymbol{D}(t) \cdot \left(\boldsymbol{u}_0 - \boldsymbol{u}(t)\right);$

If the system is neither linear and nor affine it can at least be approximated with a **linearization** around $[\boldsymbol{x_0}, \boldsymbol{u_0}]$:

- $\dot{\boldsymbol{x}} \leftarrow \boldsymbol{A}(\boldsymbol{x_0}, \boldsymbol{u_0}, t) \cdot (\boldsymbol{x} - \boldsymbol{x_0}) + \boldsymbol{B}(\boldsymbol{x_0}, \boldsymbol{u_0}, t) \cdot \left(\boldsymbol{u}_0 - \boldsymbol{u}(t)\right);$
  $\boldsymbol{y} \leftarrow \boldsymbol{C}(\boldsymbol{x_0}, \boldsymbol{u_0}, t) \cdot (\boldsymbol{x} - \boldsymbol{x_0}) + \boldsymbol{D}(\boldsymbol{x_0}, \boldsymbol{u_0}, t) \cdot \left(\boldsymbol{u}_0 - \boldsymbol{u}(t)\right);$

In many cases, the matrices are not dependent of time t which makes the analysis easier. However, many methods for linear systems can handle the time dependencies.

A dataflow diagram (see Figure 1-9 and Figure 1-15) is a graphical representation of the explicit form. It is drawn using blocks with input and output ports and arrows representing signals between; integration is represented by integration blocks with $\dot{\boldsymbol{x}}$ as input and $\boldsymbol{x}$ as output.

If the explicit form cannot be found, there are computation methods also for solving the semi-explicit form: $\dot{\boldsymbol{x}} \leftarrow \boldsymbol{f}_{\boldsymbol{semi}}(\boldsymbol{x}, \boldsymbol{y}, \boldsymbol{u}(t), t); \ \boldsymbol{0} = \boldsymbol{g}_{\boldsymbol{semi}}(\boldsymbol{x}, \boldsymbol{y}, \boldsymbol{u}(t), t);$.

A generalisation of the semi-explicit form is when we cannot even find explicit expression for all state derivatives $\dot{\boldsymbol{x}}$. We can still formulate an Explicit form model, but then using "implicit form expressions". As extreme example, when no variabels can be solved for:

- $[\dot{\boldsymbol{x}}, \boldsymbol{y}] \leftarrow solve\left(\boldsymbol{f}_{\boldsymbol{ODE,impl}}(\dot{\boldsymbol{x}}, \boldsymbol{x}, \boldsymbol{y}, t) = \boldsymbol{0}\right);$

The operator "$solve$" is here meant to be implemented as a (numerical) iteration during the Computation (compare 1.5.1.5). The only difference to the original $\boldsymbol{f}_{\boldsymbol{DAE}}$ is that the states $\boldsymbol{x}$ are identified among the variables $\boldsymbol{z}$. But, it should also be noted that this is no general cure to avoid doing Mathematical manipulations, because far from all iterations succeed; so, explicit form expressions should be strived for as far as possible! Often, some parts of the Explicit form can be explicit form and only a few variables appear in a $solve$ epression. When implicit form expressions appear in the Explicit form model,

we have a situation where causality is not defined for the involved variables, although the model is on an overall Explicit form.

1.5.1.1.4.1 Time Sampling and Time Events

In vehicle dynamics, the dynamics occurring in the digital control is essential. A control algorithm can of course be modelled with continuous equations, but the effect of time sampling and signal communication delays are often essential to include. A mathematical method to model this phenomenon is "time events".

Time events are similar to, but not same as, discrete dynamics in 1.5.1.4. The similarity is that both time events and state events (used for discrete dynamics) uses transition conditions, $\boldsymbol{h} > \boldsymbol{0}$. But for time events, the transition conditions are only a function of time $\boldsymbol{h}(t)$. Time events appear since algorithms are executed on digital processors or are delayed sin signal communication. Time events are generally more established and easier to get physically consistent than the more general *state events*, $\boldsymbol{h} = \boldsymbol{h}(\boldsymbol{x_c}, \boldsymbol{x_d}, \boldsymbol{u}, t)$.

In Modelica, a continuous model with its time sampled controller can be modelled as in Figure 1-6. The example is speed control of a vehicle in uphill. The longer sample time gives an unstable solution.

```
model SampledAlgorithm
  parameter Real m=1500, RollGradeResist=(0.01+0.05)*m*9.80665;
  Real vx, axReq, Fx;
  parameter Real SampleTime, PGain=1/0.5; //0.5 is seconds
initial equation
  vx = 10;
equation
  //vehicle (continuous DAE)
  m*der(vx) = min(Fx, 0.8*m*9.80665) - RollGradeResist;

  //control and actuation (time sampled discrete DAE)
  when sample(0,  SampleTime) then
    axReq =  Pgain*(20 - pre(vx));
    Fx = m*axReq; //Model, without resitances
  end when;
end SampledAlgorithm;
```

discrete part

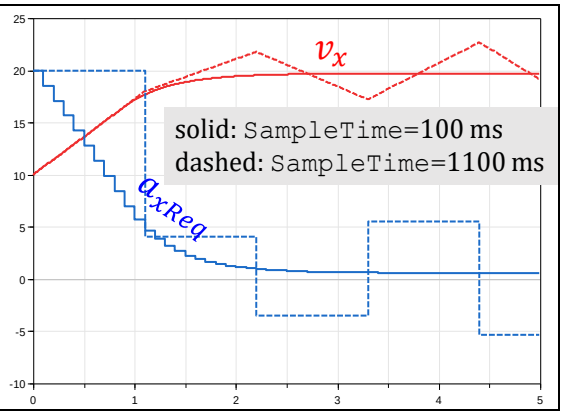

Figure 1-6: Dynamic model with time sampled part.

1.5.1.1.4.2 Discretization of Continuous Models

When a simulation tool solves a dynamic model it typically does time discretization, but as engineers we still see the model as continuous. However, continuous dynamic models often have to be intentionally (time) discretized; as they shall become parts of the product, the vehicle. The integral part of a PID controller is one example. Another example is when an algorithm is derived as continuous, which is often the case with filters and estimators, 1.5.4.6. Yet another example is when the algorithms shall perform simulations of dynamic models which are derived as continuous. An example of converting a continuous dynamic model to a time discrete is shown in Figure 1-7.

1.5.1.1.5 Computation

Computation, is to find a numerical solution. Several ways can be of interest, e.g.:

- *(Time domain) Simulation* (e.g. Initial value problem, IVP or End value problem, EVP). There are many advanced pre-programmed integration methods which one can rely on without knowing the details. It is often enough to the concept of the simplest "Euler forward with constant time step", in which the state variables are updated in each time step, Δt, as follows:
  $\dot{\boldsymbol{x}}_{\boldsymbol{now}} \leftarrow \boldsymbol{f}_{\boldsymbol{ODE}}(\boldsymbol{x}(t_{now}), \boldsymbol{u}(t_{now}), t_{now})$; (Explicit form model)
  $\boldsymbol{x}(t_{now} + \Delta t) \leftarrow \boldsymbol{x}(t_{now}) + \Delta t \cdot \dot{\boldsymbol{x}}_{\boldsymbol{now}}$; (Derivative approximation)
  Typically, the time step Δt is varied by the integration methods itself to minimize computation time, but maintaining a certain accuracy. The Δt should not be mixed up with the *sample time* in time discrete systems, see 1.5.1.4.
- For linear models and simple excitation one can find the solution without time integration, by using the *"exponential matrix"*, $e^{\boldsymbol{Matrix}}$. E.g., the solution to a linear system without input, $\dot{z} = A \cdot z$;, starting from a given initial state $\boldsymbol{x}(0) = \boldsymbol{x_{iv}}$ is found as $\boldsymbol{x}(t) = e^{\boldsymbol{A} \cdot t} \cdot \boldsymbol{x_{iv}}$;.

- *Frequency domain analyses.* The model can sometimes be linearized around an operating condition by differentiating and $A_{ij} = df_i/dx_j$ and $B_{ik} = df_i/du_k$. (Compare with 1.5.1.1.4, where the A_{ij} and B_{ik} was identified in the algebraic expressions and linearity was not limited to around a certain operating condition.) The matrices are very useful for eigen-modes, eigen-frequencies, step response, stability, or use as model base in model-based control design methods.
- *Stability analysis* is to study when small disturbances lead to large response and how. (In linear models, when limited disturbances lead to unlimited solutions, typically oscillating or exponentially increasing.) Stability analysis is normally done for one operating point $[\boldsymbol{x_0}, \boldsymbol{u_0}]$, around which one linearizes. Instability is detected as when any eigenvalue to $\boldsymbol{A}$ has positive real parts. If there are inputs ($\dim(\boldsymbol{u}) > 0$), the stability is "for the open loop system", e.g. for the vehicle without driver. If the equations for $\boldsymbol{u}$ is included in the model, there will be no $\boldsymbol{B}$ matrix, and the stability is then "for the closed loop system", e.g. for the vehicle with driver. Adding a driver can make the vehicle with driver more or less stable.
- *Optimization*. Either optimizing a finite number of defined design parameters or time trajectories, e.g. $u(t)$. There are many optimization methods, ranging from trial-and-error to mathematically/numerically advanced gradient based or evolutionary inspired methods. If optimizing time trajectories, one often discretize the model in time, which converts the differential equations into difference equations, using a certain derivative approximation, such as $\boldsymbol{x_{k+1}} \leftarrow \boldsymbol{x_k} + \Delta t \cdot \dot{\boldsymbol{x}}_{\boldsymbol{k}} = \boldsymbol{x_k} + \Delta t \cdot \boldsymbol{f}(\boldsymbol{x_k}, \boldsymbol{u}(t_k), t_k) = \boldsymbol{x_k} + \Delta t \cdot \boldsymbol{f}(\boldsymbol{x_k}, \boldsymbol{u_k}, k \cdot \Delta t)$;. Typically, very simple derivative approximations, compared to today's integration methods for simulation, should be used.

```
model DiscreteIntegrator
  parameter Real SampleTime=0.5;
  Real u, yc,   udF, ydF, prederydF,  udB, ydB, derydB;
initial equation
  yc=0.2; pre(ydF)=yc; pre(ydB)=yc;
equation
  //input:
  u=0.1*sin(2*time);
  //model (continuous):
  der(yc)=-yc+u;

  //discrete, EulerFwd: pre(deryd)=(yd-pre(yd))/SampleTime
  when sample(0, SampleTime) then
    udF=u;
    prederydF = -pre(ydF)+pre(udF); //model
    ydF=pre(ydF)+prederydF*SampleTime;
  end when;

  //discrete, EulerBwd: deryd = (yd-pre(yd))/SampleTime
  when sample(0, SampleTime) then
    udB=u;
    derydB = -ydB+udB; //model
    ydB=pre(ydB)+derydB*SampleTime;
  end when;
end DiscreteIntegrator;
```

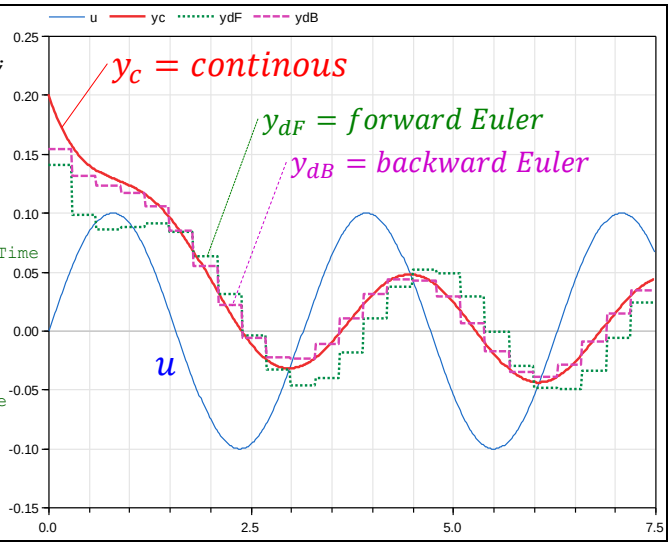

Figure 1-7: A continuous dynamic model, $\dot{y}_c = -y_c + 0.1 \cdot sin(2 \cdot t)$; and two discretizations: y_{dF} and y_{dB}.

1.5.1.1.6 Evaluate Requirement Fulfilment

This is often called *Requirement Verification* and means to find out *how well the vehicle fulfils the requirements*. Also, *Model Validity* should be evaluated. (One can also do "*Requirement Validation*" which is to judge whether a suitable selection of requirements was selected in 1.5.1.1. This requires much experience.)

Often, there is an old design which was the cause for the whole engineering task and then there might be test data to validate model with. Such validity check will be for one certain design. If directly comparing one simulation with one test it is an **absolute model validity**. If comparing the change between two tests where something has been changed, it is a **relative model validity**, e.g. telling if the model reflects design parameter changes well. The relative model validity is often more important than the absolute. Since one often don't know exactly how the model is going to be used, it can be a good habit to include a boolean auxiliary variable for validity. One clear reason to set the validity "false" is when the physical model assumptions are not met, such as if a wheel lifts from ground (assuming equations

to handle wheel lift is not included). In other cases, it can be more of an engineering judgement on what threshold to set the validity false. Then, if validity is false during only a tiny fraction of the whole studied time, it is again a judgement whether to disqualify the simulation result or not.

Evaluation of **requirement fulfilment** (or Analysis, as opposed to Synthesis) involves understanding and interpretation of the computation results to real world. New requirements can appear, typically when new constraints become active with the new design.

1.5.1.1.7 Redesign

Redesign (or Synthesis, as opposed to Analysis) is a creative part where experience and intuition is important. In some rare cases, one can inversely calculate the new design or use numerical methods optimize to a new better design.

1.5.1.1.8 Final Design

Final design, meaning a concrete proposal of design, such as a numerical design parameter value or a drawing or control algorithm.

1.5.1.1.9 Modelling for Design Guidance

The activity "Modelling for Design Guidance" in Figure 1-5 marks another "branch" than the straight-forward computation/simulation for virtual verification described in 1.5.1.1 to 1.5.1.1.8. It refers to activities that adjust the mathematical model with purpose to generate knowledge that can support the design. Examples of such adjustments are:

- Linearization of the models, helps control or estimator designs,
- Simplified models which can be simulated in the vehicle for on-line predictions,
- Simplified models which can be optimized in the vehicle for optimal predictive control, and
- General understanding of how parameters (both physical such as suspension hardpoints, spring stiffnesses, actuator capabilities and SW parameters such as control gains) influence the vehicle in the studied manoeuvres.

To do these model adjustments, one often aims at a *Closed form expression* or *Analytical expression*, $\dot{\boldsymbol{x}} = \boldsymbol{f}_{\boldsymbol{ClosedForm}}(\boldsymbol{x}, \boldsymbol{u})$. In some cases, one can even find *Closed form solution* or *Analytical solution*, $\boldsymbol{z} = \boldsymbol{f}_{\boldsymbol{ClosedForm}}(t)$;. Examples where closed form solutions are possible are linear models with inputs $\boldsymbol{u}(t)$ expressed as a simple time functions, such as step, harmonic and/or exponential functions, see 4.4.3 and 5.4.

To reach closed form expressions/solutions, one often has to, after the mathematical model, reduce the number of equations by eliminating variables. This can help to understand the behaviour of the whole system. The Mathematical model is still important since it documents better which physical phenomena has been modelled. The differentiation order can often increase when eliminating variables, so that $\ddot{\boldsymbol{z}}, \dddot{\boldsymbol{z}}, \cdots$ appears in the equations.

1.5.1.2 Approximations

As mentioned above, assumptions (or simplifications or approximations) are made during *Physical modelling*. These can be directly motivated by **vehicle design**, such as assuming that some part is rigid or massless. They can also be directly motivated by the **manoeuvre** to be studied with the model. Examples of approximations during Physical modelling are massless bodies, steady state conditions and small angles. These have implications on the *Mathematical modelling* stage: some fictive forces do not appear in the equations, and $angle$ replaces $\sin(angle)$ in the equations.

We can also assume that some variables or parameters are *small*. If a term in the final Explicit form model gets a high order, one can approximate mathematically by removing it. For example, a term $small^N$ where $N \geq 2$ can be removed if the other terms have $N < 2$. Note that such approximations can not be done in an *equation* (during Physical or Mathematical modelling), but in the final *expression* (in Explicit form model). For example, a term with order $small^N$ in Mathematical model, it can end up in denominator in final Explicit form model, which correspond to order $small^{-N}$. Removing terms can also be done by keeping only the first terms in a Taylor expansion of $\boldsymbol{f}_{\boldsymbol{ODE}}$ in the Explicit form: $\boldsymbol{f} \approx \boldsymbol{f_0} + (\boldsymbol{df}/\boldsymbol{dx})|_{\boldsymbol{x_0},\boldsymbol{u_0}} \cdot (\boldsymbol{x} - \boldsymbol{x_0}) + (\boldsymbol{df}/\boldsymbol{du})|_{\boldsymbol{x_0},\boldsymbol{u_0}} \cdot (\boldsymbol{u} - \boldsymbol{u_0})$;.

1.5.1.3 Constants, Parameters, Variables and Signals

Variables and **Signals** vary with time during an experiment with the model. **Constants** and **parameters** do not. In the following, it is understood that all have physical interpretation, e.g. a corresponding (physical) quantity with a known unit. Units are central for engineering. A $\{quantity\} = measure \cdot [unit]$; such as $\{Length\} = L \cdot [m] = 2 \cdot [m]$;. If using a consistent set of units, such as SI-units, each equation can be seen as either a relation between quantities or relation between measures. The compendium assumes SI-units, (ISO 80000-3, 2013),where else is not stated. Angle units are not stipulated by SI, but the recommendation is to use radians. It is recommended to not use numerical constants directly in the equations unless they are dimensionless=unitless, such as π *or* 2.

1.5.1.3.1 Constants and Parameters

A parameter can be changed between experiments. A constant does not even change between experiments. Typical constant is π or gravity constant g. Typical parameters are vehicle wheelbase and road friction coefficient.

From vehicle engineering point of view there is a significant difference also between *Design parameters* and *Operation/Manoeuvre parameters*. The first ones are varied to fulfil the requirements as good as possible. The latter ones should also be varied, but as disturbances for which the vehicle need to be robust.

It is often natural to have different parameter sets to describe the design and operation/manoeuvre and another for use in the equations. For example, the kerb weight (design) and load (operation) are good for description while the total weight (sum of kerb and load) is the parameter that appears in the equations. Therefore, the parameters that appears in the equations cannot always be categorized as either design or operation/manoeuvre parameters. It is easy to forget that the selection of parameters and the relations between parameters are often an equally important part of the engineering problem, as the relations between variables (the equations) is for the dynamic system. A good question to ask oneself is often: Is the comparison “fair” if I vary parameters as I do?

1.5.1.3.2 Variables

Variables vary during the studied time interval. Consequently, their time derivatives are not identical zero, which is important when going from DAE to ODE formulation since some DAE equations might need to be differentiated. In Mathematical model (DAE), a variable and its time derivatives are counted as one variable. In Explicit model (ODE), one can count each time derivative of a variable as an additional variable, but then one also should count each integration ($z_i = \int \dot{z}_i \cdot dt$;) as one equation.

It can be noted that, during parameter optimization, some model parameters are *varied* and could therefore potentially be called variables, causing terminology confusion. To avoid such confusion, a prefix could be used: *model parameters* or *optimization variables*, depending of context.

A very important type of variable is a **state variable**. The variables used as (continuous) state variables are given initial values and then updated through integration along the time interval studied. Which variables to use as state variables is **not** uniquely defined by the physical (or mathematical) model. See 1.5.2.2.

1.5.1.3.3 Signals

Since vehicle dynamics so often requires models of the control algorithms, one often use the words variable and signal interchangeable. It is suggested to, at least, reflect over the difference:

- A signal can represent an ODE variable with prescribed **causality**. So, a variable cannot be represented by a signal before the modelling stage “Explicit Form Model”.
- Signals **can** appear already in mathematical model (DAE), typically as interface on models of mechatronic subsystems or subsystems consisting purely of algorithms (software). For such signals, the causality is normally prescribed already in the mathematical model and one have to differ between **differentiation orders**, so that z_i and $\dot{z}_i$ are counted as two variables. A strict way to implement this is given in the Modelica modelling format, see 1.5.4.10.

1.5.1.4 Discrete Dynamics

Only continuous dynamics, as opposed to **discrete dynamics**, were considered in 1.5.1.1.3 to 0. Discrete dynamics modelling can be used for computational efficient models of, e.g., ideal dry friction or ideal backlash but also to model time sampled (digital) systems. See Figure 1-8. The way the states evolve over time differs between continuous and discrete dynamics: During the modelling, the continuous states, $\boldsymbol{x_c}$, should be thought of as changing continuously. In the computation there has to be a discretization in time steps since computers are digital (not analogue). Hence the $\boldsymbol{x_c}$ are updated only between each time step but thought of as continuously changing in between. The update is based on a derivative approximation, e.g. $\dot{\boldsymbol{x}}_{\boldsymbol{c}} = (\boldsymbol{x_c}(t + \Delta t) - \boldsymbol{x_c})/\Delta t$;. Discrete states, $\boldsymbol{x_d}$, should be thought of as constant except that they step-wise change value at the time instants *when* one of the *transition conditions* becomes true (not between these time instants!). These time instants are called *(state) events*, and can be implemented as *when* event indicators, $\boldsymbol{h}(\boldsymbol{x_c}, \boldsymbol{x_d}, \boldsymbol{u}(t), t) > 0$, becomes true.

At a first glance, the x_c should not change in the events, but are two reasons why one sometimes model them to change (stepwise) at an event: one is to reinitialize to physically obvious values (e.g. a bouncing ball need to start from the surface it bounces at when the bounce happens) and the other is if one change physical model at an event, e.g. introduce an inertia or elasticity. The latter can be powerful to solve an engineering task, but the engineer has to be especially observant on how credible the numerical solution is, because the simulation tools can typically not estimate errors in such model. The latter way is here described as one model, but in another context it can be seen as "splicing" of several models.

A system which includes both types (*hybrid dynamics*) evolves as follows:

$\boldsymbol{x_c}(t + \Delta t) \leftarrow \boldsymbol{x_c} + \Delta t \cdot \dot{\boldsymbol{x}}_{\boldsymbol{c}} = \boldsymbol{x_c} + \Delta t \cdot \boldsymbol{f_c}(\boldsymbol{x_c}, \boldsymbol{x_d}, \boldsymbol{u}(t), t)$; and

when $\boldsymbol{h}(\boldsymbol{x_c}, \boldsymbol{x_d}, \boldsymbol{u}(t), t) > \boldsymbol{0}$ *then* $\boldsymbol{x_d}(t^+) \leftarrow \boldsymbol{f_d}(\boldsymbol{x_c}, \boldsymbol{x_d}, \boldsymbol{u}(t), t)$;.

Note that a "knee" (discontinuous derivative but continuous value) in an equation does generate an event, but no discrete state, since no "memory" is needed. But a step (mathematical discontinuity in value) or a hysteresis (mathematical function with multiple values depending on which branch is active) generate state event with discrete state.

One can see discrete dynamics as if the physics get stuck on the steep part of a step or in a branch in a hysteresis, until when an exit condition becomes true. Examples where this occur is dry friction, one-way clutches, and back-lash. Another example appears if one changes physical models, e.g. remove a mass or compliance, during some parts of the simulation, governed by certain events. See more in 2.4.3. Examples which typically appears in control algorithms or driver models are *state machines*.

It can be needed to reinitialize continuous state variables ($\boldsymbol{x_c}(t^+) = \cdots$) in events, e.g. motivated by impact dynamics. There is a risk that the numerical solution gets stuck in undesired high frequency switching of discrete states which is called *chattering*. Chattering can be caused by coding errors of the event handling or inconsistent physical modelling. Discrete dynamics is not as well established in most basic engineering education as continuous dynamics.

1.5.1.5 Algebraic Loops or Simultaneous Equations

One problem that can appear when generating the Explicit form model is *Algebraic loops*. The name is most intuitively understood when Data flow diagram is used for the Explicit form model, see 1.5.4.7. Then, an Algebraic loop is a signal loop which does not include and integrator blocks; meaning that each branch of the loop needs input from the other to calculate its output. Algebraic loops can also be called *Simultaneous equations*. The smallest possible can actually be one single equation, e.g. a transcendent equation, such as "$x = \sin(x)$;", which has no closed form solution.

A simple mechanical example where two equations need to be solved before each other is given in Figure 1-9. The example is a vehicle decelerating with locked wheels; Vertical forces are needed to calculate friction forces, which are needed to calculate acceleration, which is needed to calculate vertical forces.

Loops appear often between bigger chunks of equations than in Figure 1-9, namely between modules in the model. The decomposition in certain modules is often desired for model modularity. A typical

other example where a loop occurs is when doing quasi-steady state assumptions about roll moment distribution between axles (4.3.9.3).

Loops can always be solved by setting up an iteration in each evaluation of time derivatives. This can sometimes be accepted, but it gives poor computational speed. Other ways are to handle the loops by sacrificing simplicity in model is to model an additional elasticity or inertia between the modules, or simply a (non-physical) filter. "Memory blocks" can work but are not recommended, since the simulations will be dependent on solver. Best is if the loop can be symbolically solved, as in Figure 1-9.

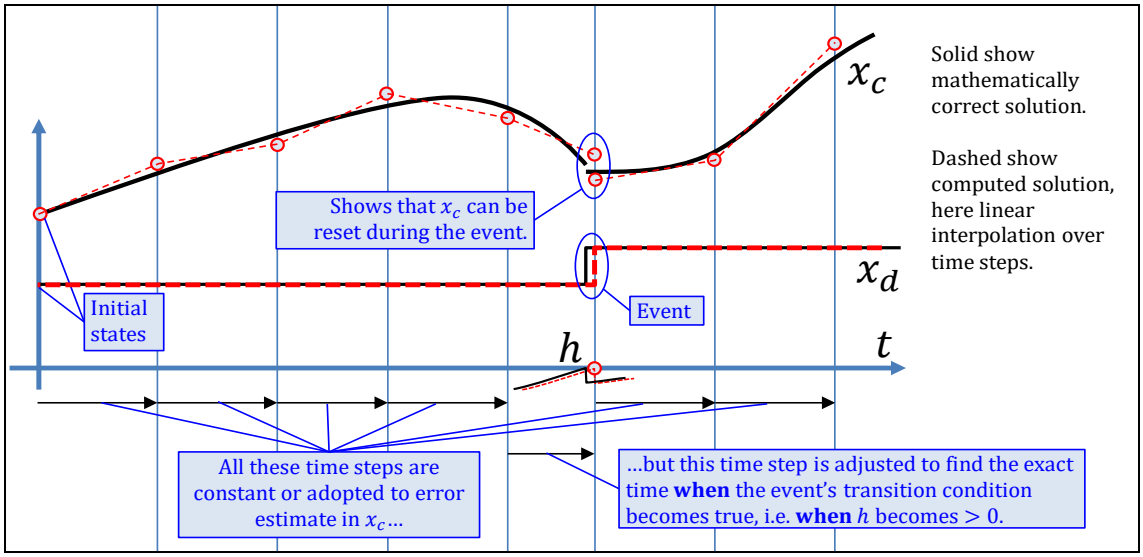

Figure 1-8: A visualization of a model and computed solution with both continuous and discrete states.

1.5.1.6 High Index

A possible problem for a mathematical model is High index. A simple mechanical example of High index system of equations is when two inertias are rigidly connected, see Figure 1-10, where a working causality cannot be found with retained modularity. Similarly to algebraic loops, it can be solved with equation manipulations, but for high index problems, the manipulations include differentiation of some equations. It is tempting to try a "differentiating" block ($\dot{v}_2 = (d/dt)v_2$; instead of $v_2 = \int \dot{v}_2 \cdot dt$; in Figure 1-10) but that will not work. Other examples where high index occurs is when modelling purely rolling wheels (3.3.2).

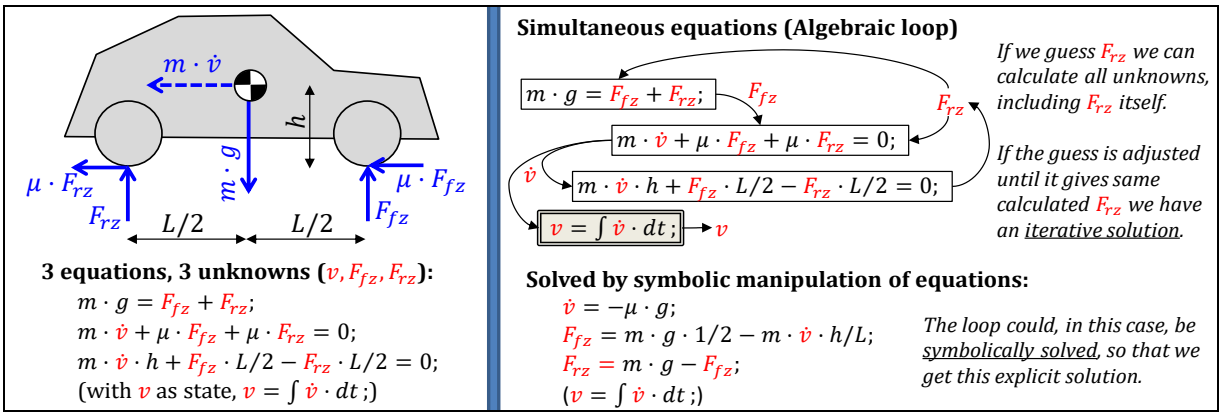

Figure 1-9: An example of Algebraic loop, also called Simultaneous equations.

1.5.1.7 Modularity in Models

Another aspect of modelling is the modularity. For complex products as vehicles, it is often important to keep a modularity in the models, which reflects the subsystems in the product. This is for reuse of subsystem models and co-operation between engineering teams at vehicle manufacturer and suppliers. Reuse cuts modelling time, but also improves the models over time since bugs are found when models are used. Modularity is also important for replacing one subsystem model with a real ECU with

software or splitting model between several processors for increasing the computational capability. Methods for above motivated "co-simulation" are typically based on that each module are on explicit form but also include its own time integrator. This can create big challenges in numerical stability and accuracy of the whole system.

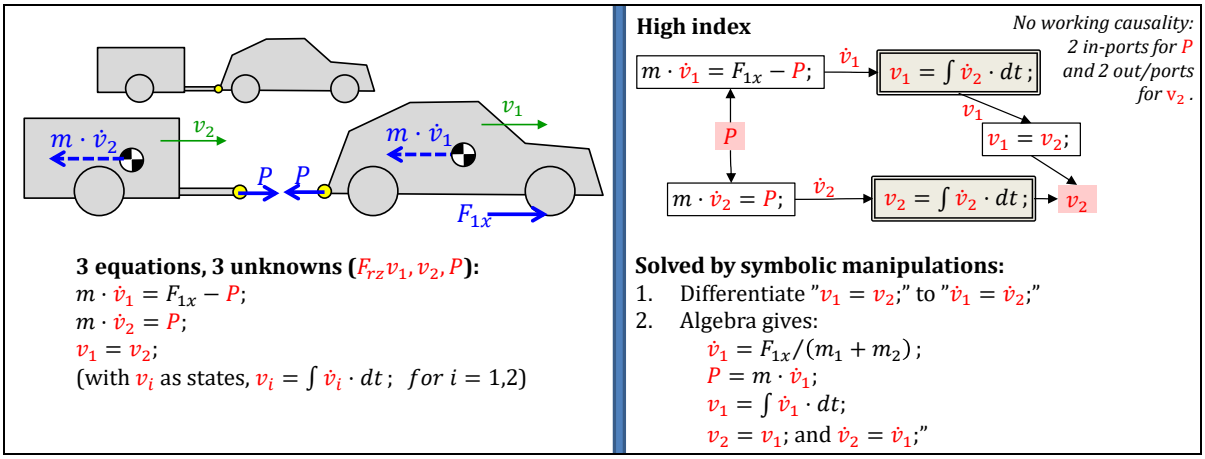

Figure 1-10: An example of a High index model; an accelerating rigidly connected car and trailer.

An alternative way where models of sub-systems are connected on Mathematical form, as opposed to Explicit form. It could be called "co-modelling" and make it easier to organize libraries of models since one would not need to keep different versions of part models for different causality on interface variables. However, co-modelling would require a globally accepted and used standard of Mathematical modelling format, which does not exist yet; Modelica is the closest to reach such status.

1.5.1.8 Causality

Systems can be modelled with **Natural causality**. For mechanical systems, this is when forces on the masses (or motion of the compliance's ends) are prescribed as functions of time. Then the velocities of the masses (or forces of the compliances) become state variables and have to be solved through time integration. The opposite is called **Inverse dynamics** and means that velocities of masses (or forces of compliances) are prescribed. For instance, the velocity of a mass can be prescribed and then the required forces on the mass can be calculated through time differentiation of the prescribed velocity. Cf. Analysis and Inverse Analysis in Figure 1-3.

1.5.1.9 Drawing

Drawing is a very important tool for engineers to understand and explain. Very often, the drawing contains free body diagrams, FBD, see 1.5.2.1, but also other diagrams are useful. Beyond normal drawing rules for engineering drawings, it is also important to draw motion and forces. The notation for this is proposed in Figure 1-11.

It is often necessary to include more than just speeds and forces in the drawings. In vehicle dynamics, these could be: power flow and signal or data flows. These can preferably be drawn as arrows, but of another kind than the motion and force arrows.

When connecting components with signal flow, the resulting diagram is a *data flow diagram*. Physical components and physical connections can be included in such diagram, and if arrows between them it would represent data flow or causality. Physical components can also be connected by "Physical connections", which does not have a direction, see 1.5.1.9.1. It should be noted that a *(computation) flow charts* and *(discrete) state diagram* represent something quite different from data flow diagrams, even if they may look similar; in state diagrams, an arrow between two blocks represents a transition from one (discrete) state or operation mode, to another.

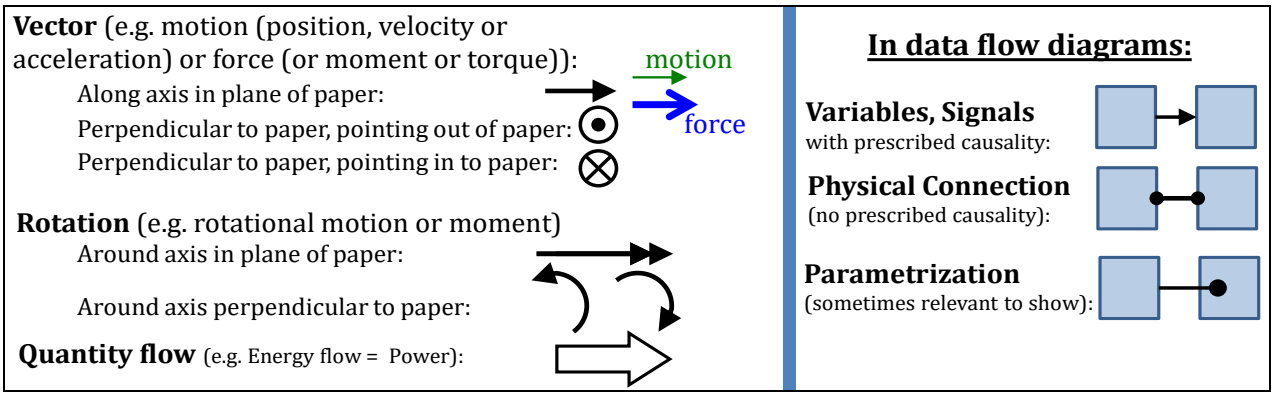

Figure 1-11: Arrow-like drawing.

1.5.1.9.1 Physical Connections and Power-Factorized Interface

It is recommended to use interface variables which factorize power P, e.g. use force F and velocity v, because $P = F \cdot v$. Similar factorization is found in all other domains, on a general form $P = effort \cdot flow$. Connection via such "power-factorized interfaces" is sometimes referred to as "power bonds". Effort and flow often get opposite variable flow causality or signal flow causality in the explicit form model.

If modelling with only P as interface variable, it is easier to miss validity limits of the models, such as supplying a certain non-zero power to a stand-still vehicle requires infinite forces ($F = P/v \rightarrow P/0$).

When connecting physical components in a data flow diagram with "Physical connections", there can be two main concepts:

- Connecting in "nodes", see Figure 2-61. Here, each node has typically potential and flow variables (velocities and forces in Mechanical systems). And there are only two components connected to each node. The node variables appear in both components' equations. The connection itself generates these equations: "Potential variable in node and both connected components are equal" and "Flow variable in node and both connected components are equal".
- Connecting with "connections between connectors", see Figure 2-74. Here, the same variables are defined in connectors at the components. A connection can be made with lines between the connectors at the components, possibly connecting more than two components. The equations in each component is formulated in the connector's variables. The connection itself generates these equations: "Effort variables are equal" and "Sum of flow variables are zero".

The first is often the easiest (least number of equations and variables) for small models with a fixed topology. The latter is a more systematic which easier handles larger models and models with varying topology. The latter is supported in the standard modelling language Modelica, see 1.5.4.10 and the open book on internet in Reference (Tiller, 2019).

1.5.1.10 Mathematical Notation Conventions

Generally, a variable is denoted x or $x(t)$, where t is the independent variable time. In contexts where one means that variable's value at a certain time instant, t_0, it can be denoted $x(t_0)$. In contexts where one wants to mark that the variable's time history over a time interval (infinitely many values over an infinite or finite time interval) is referred to, it can be denoted $x(\cdot)$.

Differentiation (of x) with respect to time (t): $\frac{dx}{dt} = \dot{x} = der(x)$.

Matrices (two-dimensional arrays) are denoted with bold letters, often uppercase $\boldsymbol{A}$. Column and row vectors (one-dimensional arrays) are denoted with bold, often lowercase $\boldsymbol{b}$. When elements in arrays are written, brackets are used: $\begin{bmatrix} x & y \\ y & z \end{bmatrix}$.

Geometric vector (or physical vector, or spatial vector), denoted by $\vec{v}$. In order to use geometric vectors in calculations, they are often expressed as one-dimensional arrays with components. It has to be clear for each component, which direction it is expressed in, e.g. by a subscript, e.g. $\boldsymbol{v_{xyz}}$.

Multiplication symbol (* or · or × or •) shall be used to avoid ambiguity, e.g. $a \cdot bx$, not abx (assuming bx is one variable, not two). Stringent use of multiplication symbol enables use of variables with more than one token, cf. programming. Stringent use of multiplication symbol reduces the risk of ambiguity when using operators, e.g. it shows the difference between $f(x)$ and $f \cdot (x)$. Compendium denotes multiplication between scalars and matrices equally, using "·". Multiplication between geometric vectors are denoted: Cross multiplication, denoted $\vec{a} \times \vec{b}$ and scalar multiplication, denoted $\vec{a} \bullet \vec{b}$.

Parentheses shall be used to avoid ambiguity, e.g. $(a/b) \cdot c$ or $a/(b \cdot c)$, and not $a/b \cdot c$.

An **interval** has a notation with double dots. Example: Interval between a and b is denoted $a..b$.

An **explanation**, between two consecutively following steps in a derivation of equations is written within {} brackets. Example: $x + y = \{a + b = b + a\} = y + x$;.

An **inverse function** is denoted with superscript inv, $y = f(x); \Leftrightarrow x = f^{inv}(y)$. The use of superscript -1 can cause an ambiguity whether f^{-1} means inverse function or inverted function value $(1/f)$. When a name of the inverse function is available, it can be used, e.g. arctan(⋯) instead of $\tan^{\text{inv}}(\cdots)$.

Fourier and Laplace **transform** of function $f(t)$ are denoted $\mathcal{F}\big(f(t)\big)$ and $\mathcal{L}\big(f(t)\big)$, respectively:

$$\mathcal{F}\big(f(t)\big) = \int_{-\infty}^{+\infty} f(t) \cdot e^{-j \cdot \omega \cdot t} \cdot dt\,; \quad where\ \omega \in Re$$

$$\mathcal{L}\big(f(t)\big) = \int_{0}^{\infty} f(t) \cdot e^{-s \cdot t} \cdot dt\,; \quad where\ s = \sigma + j \cdot \omega \quad where\ \sigma\ and\ \omega\ \in Re$$

There are many practical rules for manipulation transformed differential equations, such as $\mathcal{F}\left(\dot{f}(t)\right) = j \cdot \omega \cdot \mathcal{F}\big(f(t)\big)$;.

1.5.2 Mechanical/Machine Engineering

Vehicle dynamics originates from Mechanical engineering (in Swedish "Maskinteknik", in German "Maschinenbau"). Therefore, it is important to be fluent with the following mechanical basic relations:

- [Torque or Moment] = Force · Lever: T or $M = F \cdot length$;
- Power = Force · Translational velocity: $P = F \cdot v$;
  or Power = Torque · Rotational velocity: $P = T \cdot \omega$;
- Energy = time integral of Power: $E = \int P \cdot dt$; or: $E = \int F \cdot dx$; or: $E = \int T \cdot d\varphi$;.
- (Torque) Ratio = Output torque/Input torque: $ratio_T = T_{out}/T_{in}$;
- (Rotational velocity) Ratio = Input velocity /Output velocity: $ratio_\omega = \omega_{in}/\omega_{out}$;
- (Power) Efficiency = Output power/Input power: $\eta = P_{out}/P_{in}$;
  or, in a wider meaning, Efficiency = Useful/Used;

Interfaces in mechanical systems are recommended to use $[F, v]$ or $[T, \omega]$, which is a "power-factorized interface", see 1.5.1.9.1.

1.5.2.1 Free-Body Diagrams

In the physical model, see 1.5.1.1.2, a *free-body diagram, FBD* is often central. See example in Figure 1-12 and Figure 1-13. Also, division into subsystems is often practical, e.g. to implement moment-free connection points or other vehicle internal behaviour. The subsystem split typically goes through:

- Connection point between towing unit and towed unit (typical interface quantities: 2 positions (with their derivative, velocities) and 2 forces).
- Driveshaft close to each wheel (typical interface quantities: 1 shaft torque, 3 forces, and 2 angles (steering and shaft rotation), sometimes 1 wheel camber angle).
- Surface between driver's hand and steering wheel (typical interface quantities: 1 angle and 1 torque).
- Sensed signals and request signals, which cuts out control algorithms as subsystem.

One can draw free-body diagrams with two purposes: Understand the real-world problem/manoeuvre or as a help to set up (equilibrium) equations. A FBD with the 1st purpose, typically has force arrows

with the actual force directions and named $|F|$ or an explicit numerical value. A FBD with the 2nd purpose has force arrows as the corresponding force variables are defined positive and named F (or $-F$, if drawn as drawn negative). The reasoning about naming with $|F|, F, -F$ also applies to other signed or vector quantities: velocities, displacements and distances; in translation and rotation.

It is recommended to **not** draw two forces acting at the same point of part and having same direction, F_1 and F_2. With such unsuitable drawing, it is very easy to set up wrong equations, e.g. friction limitation as $F_1 < \mu \cdot F_N$, while it often is more physically correct with $F_1 + F_2 < \mu \cdot F_N$.

A short-cut, which avoids one equation, is to use same notation on two forces in the FBD, e.g. denote F_{fz0} as F_{fz} in Figure 1-12. If using this, one should keep in mind that the naming itself includes a physical assumption between 2 forces. Compare this to action/reaction force in a cut, which actually is the same force and should have the same name.

When using FBD as a help to set up equilibrium equations, a short-cut that can be to express a force in other, in a way that equilibrium is already fulfilled in the FBD. This eliminates one equilibrium equation. An example of this could be to use F_{fz} instead of F_{fz0} in Figure 1-12, which would make the vertical force equilibrium for the front axle ($F_{fz} - F_{fz} = 0$) unnecessary and not useful.

1.5.2.2 Choice of State Variables

From 1.5.1.3.2, we know state variables has to be selected and that selection is not unique. For mechanical systems, one often selects positions and velocities of (inertial) bodies as state variables, but it is quite possible and sometimes preferable, to use forces in compliances (springs) and velocities of bodies as state variables. With mass-spring system as example, the two alternatives become:

- v, x states: [$\dot{v} = F/m\,; \quad F = c \cdot x; \quad \dot{x} = v;$] (or [$\ddot{x} = F/m\,; \quad F = c \cdot x;$]) and
- v, F states: [$\dot{v} = F/m; \quad \dot{F} = c \cdot v; \quad x = F/c\,;$], respectively.

The latter alternative is especially relevant when position is not of interest, typically in propulsion systems. If v, F states, one equation ($x = F/c$) can then be omitted which can simplify. It is also often easier to express steady state initial conditions for a pre-tensioned system, e.g. wheel suspension where spring forces can be states. A drawback might be that, if overdetermined pre-tensioned systems (e.g. mass suspended in two springs: [$\dot{v} = (F_1 + F_2)/m; \; \dot{F}_1 = c_1 \cdot v; \dot{F}_2 = c_2 \cdot v; \; x = F_1/c_1\,; \; x = F_2/c_2\,;$]), more states than necessary will be used, which means that positions (x) can be calculated in two ways ($x = F_1/c_1\,; \; x = F_2/c_2\,;$). These two ways can drift apart. The drift can be eliminated by completely disregard the original spring constitutions ($x = F_1/c_1\,; \; x = F_2/c_2\,;$) and instead use position as a state ($\dot{x} = v;$).

The mathematical system is then effectively:

- v, F, x states: [$\dot{v} = F/m\,; \quad \dot{F} = c \cdot v; \quad \dot{x} = v;$].

One can see the latter alternative as if the states are the variables which represents the two energy forms kinetic and potential energy, respectively, see Lagrange mechanics in 1.5.2.3.5.

1.5.2.3 Equation Types

The step from physical model (see 1.5.1.1.2) to mathematical model (1.5.1.1.3) means basically to identify variables and parameter and find the relationship between them, i.e. the equations. Models for Vehicle Dynamics always includes mechanics, and for these parts we can identify 3 main types of equations: Equilibrium, Compatibility and Constitution.

1.5.2.3.1 Equilibrium

Equilibrium gives relations between forces (including moments). For a static system, we can use the (static) equilibria: Sum of forces in any direction is zero: $\sum \boldsymbol{F} = \boldsymbol{0}$; and Sum of moments around any axis is zero: $\sum \boldsymbol{M} = \boldsymbol{0}$;

In a dynamic system, there is typically inertia effects. Inertia effects can be seen as "fictive forces" and "fictive moments" (or "d'Alembert forces or moments"). Typically, the fictive forces are $F_{fict} = m \cdot a$ (where a =translational acceleration) and the fictive moments are $M_{fict} = J_{CoG} \cdot \dot{\omega}$. These are counter-directed to a and $\dot{\omega}$, respectively. We can find the equations either as "Dynamic equilibria":

- Sum of forces, including F_{fict}, in any direction is zero: $\sum_{\boldsymbol{incl.fict}} \boldsymbol{F} = \boldsymbol{0}$;
- Sum of moments **around any axis**, including both M_{fict} and "$F_{fict} \cdot lever$", is zero: $\sum_{\boldsymbol{incl.fict}} \boldsymbol{M} = \boldsymbol{0}$;

or as "Equations of motion" or "Newton's 2nd law":

- Sum without fictive in a direction have to be equal to $m \cdot a$: $\sum_{\boldsymbol{excl.fict}} \boldsymbol{F} = \boldsymbol{m} \cdot \boldsymbol{a}$;
- Sum without fictive **around axis through CoG** in direction of $\dot{\omega}$ have to be equal to $J_{CoG} \cdot \dot{\omega}$: $\sum_{\boldsymbol{CoG,excl.fict}} \boldsymbol{M} = \boldsymbol{J_{CoG}} \cdot \dot{\boldsymbol{\omega}} + \boldsymbol{\omega} \times (\boldsymbol{J_{CoG}} \cdot \boldsymbol{\omega})$;

The J_{CoG} is the mass moment of inertia matrix in CoG along the same coordinate axes as ω is expressed in. In this compendium, the alternative with Dynamic equilibria is mainly used. The fictive forces are introduced in the free-body diagrams with dashed arrows, see Figure 1-12 and Figure 1-13. The general form for the fictive forces is:

$$\vec{F}_{fict} = \frac{d}{dt}(translational\ momentum) = \frac{d}{dt}(m \cdot \vec{v}) = m \cdot \frac{d}{dt}\vec{v} = m \cdot \frac{d}{dt}\left(\frac{d}{dt}\vec{r}\right) =$$
$$= m \cdot \dot{\boldsymbol{v}} - \underbrace{m \cdot 2 \cdot \boldsymbol{\omega} \times \boldsymbol{v}}_{Coriolis\ force} - \underbrace{m \cdot \boldsymbol{\omega} \times (\boldsymbol{\omega} \times \boldsymbol{r})}_{Centrifugal\ force} - \underbrace{m \cdot \dot{\boldsymbol{\omega}} \times \boldsymbol{r}}_{Euler\ force};$$

The $\vec{r}$ is the *position vector*. The Coriolis and Euler forces can often be assumed as zero in examples in this compendium due to no motion within the vehicle and rigidity of rotating bodies. The general form for the fictive moments is:

$$\vec{M}_{fict} = \frac{d}{dt}(rotational\ momentum) = \frac{d}{dt}(\boldsymbol{J_{CoG}} \cdot \vec{\omega}) = \boldsymbol{J_{CoG}} \cdot \dot{\boldsymbol{\omega}} + \boldsymbol{\omega} \times (\boldsymbol{J_{CoG}} \cdot \boldsymbol{\omega});$$

The term $\boldsymbol{J_{CoG}} \times (\boldsymbol{J_{CoG}} \cdot \boldsymbol{\omega})$ can often be assumed as zero in examples in this compendium due to symmetries and rotation in one plane at the time.

Figure 1-12 and Figure 1-13 show examples of free-body diagrams (FBDs) with all forces, including fictive forces. With such FBDs, the equilibrium equations are implicitly defined. In Figure 1-12 we can note that the axles' rotational inertia and mass are assumed to be zero, else there would have been fictive moments ($J_{axle} \cdot \dot{\omega}$) on the axles and fictive force ($m_{axle} \cdot a_x$) on the free axle.

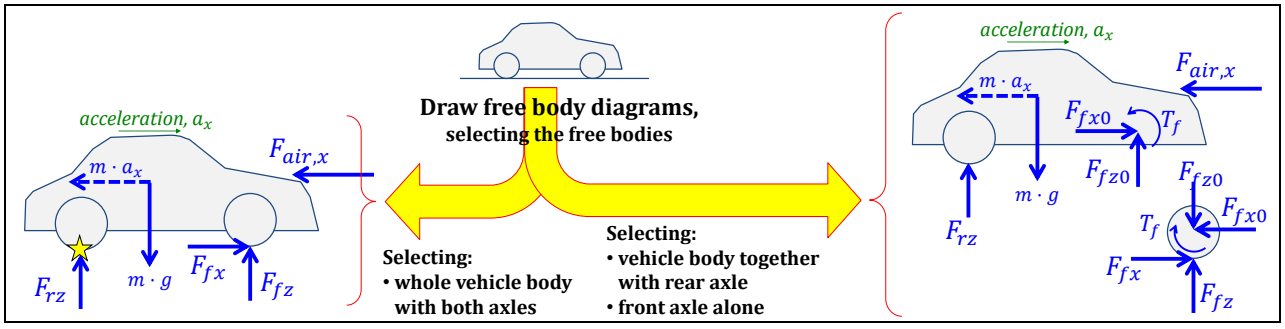

Figure 1-12: Free body diagram. The dashed arrow is a "fictive force". The star is a way to mark around which point(s) moment equilibrium is taken in the later stage "Mathematical model".

1.5.2.3.1.1 Centrifugal Forces in General 3D Motion

Centrifugal force terms appear as $m \cdot v_i \cdot \omega_j$ where $i \neq j$, i.e. for rotation perpendicular to translational velocity:

$$\begin{bmatrix} a_x \\ a_y \\ a_z \end{bmatrix} = \begin{bmatrix} \dot{v}_x \\ \dot{v}_y \\ \dot{v}_z \end{bmatrix} + \begin{bmatrix} 0 & +v_z & -v_y \\ -v_z & 0 & +v_x \\ +v_y & -v_x & 0 \end{bmatrix} \cdot \begin{bmatrix} \omega_x \\ \omega_y \\ \omega_z \end{bmatrix} = \begin{bmatrix} \dot{v}_x \\ \dot{v}_y \\ \dot{v}_z \end{bmatrix} + \begin{bmatrix} 0 & -\omega_z & +\omega_y \\ +\omega_z & 0 & -\omega_x \\ -\omega_y & +\omega_x & 0 \end{bmatrix} \cdot \begin{bmatrix} v_x \\ v_y \\ v_z \end{bmatrix} =$$
$$= \begin{bmatrix} \dot{v}_x + v_z \cdot \omega_y - v_y \cdot \omega_z \\ \dot{v}_y - v_z \cdot \omega_x + v_x \cdot \omega_z \\ \dot{v}_z + v_y \cdot \omega_x - v_x \cdot \omega_y \end{bmatrix} \approx \left\{ \begin{matrix} in\ most\ relevant \\ vehicle\ operations: \\ v_x \gg v_y\ and\ v_x \gg v_z \end{matrix} \right\} \approx \begin{bmatrix} \dot{v}_x \\ \dot{v}_y \\ \dot{v}_z \end{bmatrix} + \begin{bmatrix} 0 \\ +\omega_z \\ -\omega_y \end{bmatrix} \cdot v_x;$$

In most vehicle operations, the most important centripetal acceleration terms are: $\omega_z \cdot v_x$ (see Eq [4.45]) and $\omega_y \cdot v_x$ (see Eq [3.25]).

1.5.2.3.2 Constitution

Constitution are relations between forces (including moments) and motions, e.g.

- For a (linear) spring: $Force = F_0 + c \cdot Deformation$; or $\frac{d}{dt} Force = c \cdot DeformationSpeed$;. Metallic materials typically follow such linear behaviour, cf. Hooks law, if not deformed too much or too fast.
- For a (linear) damper: $Force = d \cdot DeformationSpeed$;. Shearing of thin liquid films typically follows such linear behaviour, e.g. in lubricated bearing where shear force is proportional to sliding speed.
- For a dry friction contact: $Force = Constant \cdot sign(SlidingSpeed)$;. This is the most common friction model in mechanical engineering, explained by adhesion between molecules and hysteresis when material is deforming over micro level asperities. So, the proportionality constant depends on both cooperating bodies material and surface roughness. Note: When a friction contact sticks, the equation switches to a compatibility equation ($SlidingSpeed = 0$;).
- For a more general model component: $Force = function(Position, Speed)$;. Even more general would include models of actuators: $Force = function(Position, Speed, Signal)$;, where $Signal$ often is a request signal, e.g. $ForceRequest$.

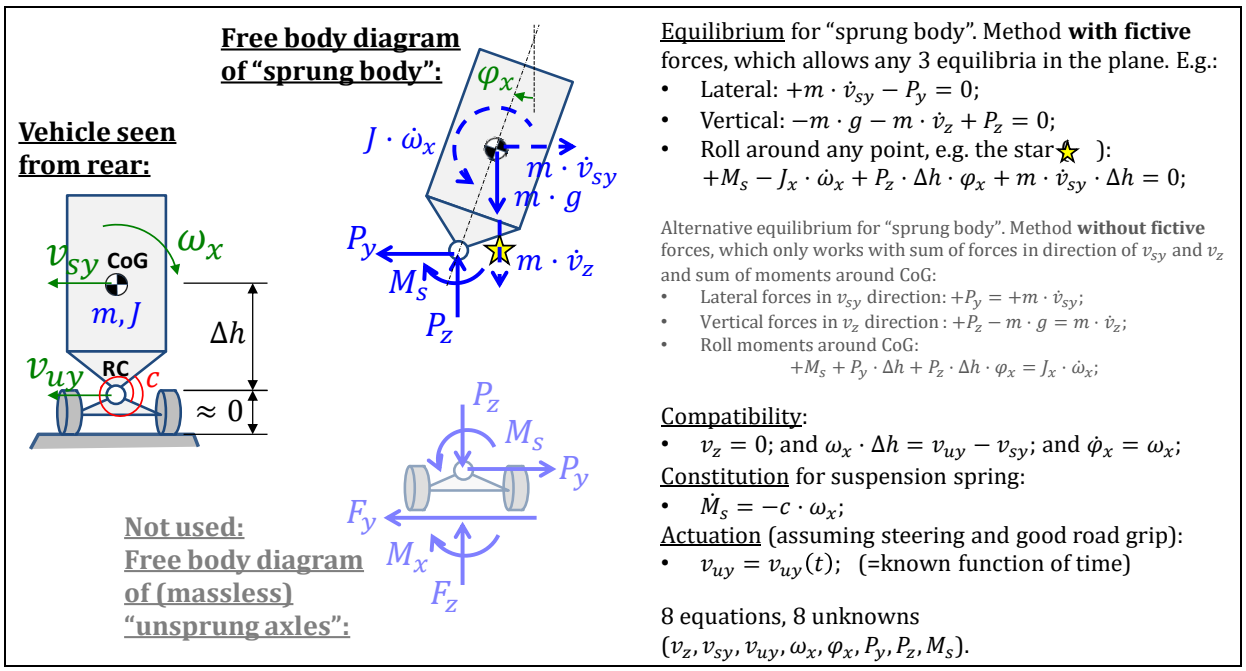

Figure 1-13: Free body diagrams for combined translation and rotation. The figure also shows the two ways of setting up equilibria, with and without fictive forces. Angle φ_x is assumed small.

1.5.2.3.3 Compatibility

Compatibility gives relations between motions (positions, velocities, accelerations, …). One example is $Speed = Radius \cdot Rotational\ speed$; for a purely rolling wheel or $\beta_f \approx (v_y + l_f \cdot \omega_z)/v_x$; for body side slip angle over front axle for a vehicle body moving in road plane.

(A special case of compatibility is a coordinate transformation for motion quantities.)

1.5.2.3.4 Algorithms and Other Equation Types

The listing of equation types in 1.5.2.3.1..1.5.2.3.3 is a help to model but it is not claimed to be complete. There are many other equation types that can appear, e.g. from electrical and chemical science. Among these others there are two sub-types (algorithms and driver) that are especially important for vehicle dynamics, so they will be discussed here in 1.5.2.3.4.

Via sensors and actuators, control algorithms can operate with the mechanics, mechatronics. The control algorithms with their interface to sensors and actuators is here included in the equation type

"algorithms". We also include models of how the human driver controls and experience the mechanical quantities. This equation type cannot be sorted into the traditional 1.5.2.3.1..1.5.2.3.1.2. Conceptually, any quantities that can be sensed or actuated in, and outside of, the subject vehicle can occur in these equations. (Finite) State machines are often useful when modelling (and designing) algorithm-based functions but also the driver, see discrete state machine in 1.5.1.4.

A model of control algorithm can often be the same artefact as the design of it, especially if using a modelling tool that allows automatic generation of real-time code, like Simulink. However, note that the algorithms in real system is implemented in a time discrete digital computation platform and digital communication, so using a time continuous version as model is an approximation in itself. For best fidelity, the models need to be formulated as time discrete dynamics. Then one can properly represent the influence from the design parameter sample time on the vehicle functions.

1.5.3 Control Engineering

Vehicle dynamics is more and more influenced by electronics, where algorithms are the main artefact to engineer. For this reason, this section introduces some relevant theory and methods and their *connection to vehicle models as they are described in vehicle dynamics*. From Figure 1-14, we realize that there are many other types of Vehicle Level Algorithms needed than just the Vehicle Motion Controller. It should be underlined that the control structure in today's vehicles are not as clean and structured as in Figure 1-14, very much depending on that vehicle level control is distributed in several ECUs, each belonging to its own subsystem.

Control algorithms can be designed without utilizing knowledge about the controlled system, such as neural networks, tuned only on observations on how the system responds. However, in this section we only consider Model based controllers. For those, the input and output signals, as well as parameters inside, has a clear interpretation in vehicle motion quantities and units. For instance, the requests on vehicle, $\boldsymbol{y_{req}}$, is typically forces on vehicle $[F_x; F_y; M_z]$ or accelerations of the vehicle $[\dot{v}_x; \dot{v}_y; \dot{\omega}_z]$. The model base is helpful when tuning the controller parameters. Moreover, the model base helps to find a consistency between derivatives order in the controller and the controlled system, such as if P, I or D gains should be used in a PID-controller.

Four conceptual categorizations of vehicle control will be presented in 1.5.4.2 to 1.5.4.5.

The control, or algortihms, can be cathegorized in different types, such as:

- Decision Making or Execution
- Momentaneous or Predictive Control
- Open or Closed Loop Control
- Degree of Over-Actuation
- Filtering, Estimation and Differentiation

1.5.4 Tools & Methods

This section presents some tools and methods for modelling and computation.

1.5.4.1 General Mathematics Tools

Examples of tool: Matlab, Matrixx, Python

We will take Matlab as example. Matlab is a commercial computer program for general mathematics. It is developed by Mathworks Inc. Compendium will use some simple Matlab code to describe models in this compendium. The following are useful for dynamic models:

Solve linear systems of equations, $\boldsymbol{A} \cdot \boldsymbol{x} = \boldsymbol{b}$: `>> x=inv(A)*b;`

Solve non-linear systems of equations, $\boldsymbol{f}(\boldsymbol{x}) = \boldsymbol{0}$: `>> x=fsolve('f',...);`

Solve ODE as initial value problems, $\dot{\boldsymbol{x}} = \boldsymbol{f}(t, \boldsymbol{x})$: `>> x=ode23('f',x0,...);`

Find Eigen vectors (V) and Eigen values (D) to linear systems: $\boldsymbol{D} \cdot \boldsymbol{V} = \boldsymbol{A} \cdot \boldsymbol{V}$: `>> [V,D]=eig(A);`

Find the $\boldsymbol{x}$ which minimizes $f(\boldsymbol{x})$ under constraints that $\boldsymbol{A} \cdot \boldsymbol{x} \leq \boldsymbol{b}$: `>> x=fmincon(f,x0,A,b);`

Find the $\boldsymbol{x}$ which minimizes $0.5 \cdot \boldsymbol{x}^T \cdot \boldsymbol{H} \cdot \boldsymbol{x} + \boldsymbol{f}^T \cdot \boldsymbol{x}$: `>> x=quadprog(H,f);`

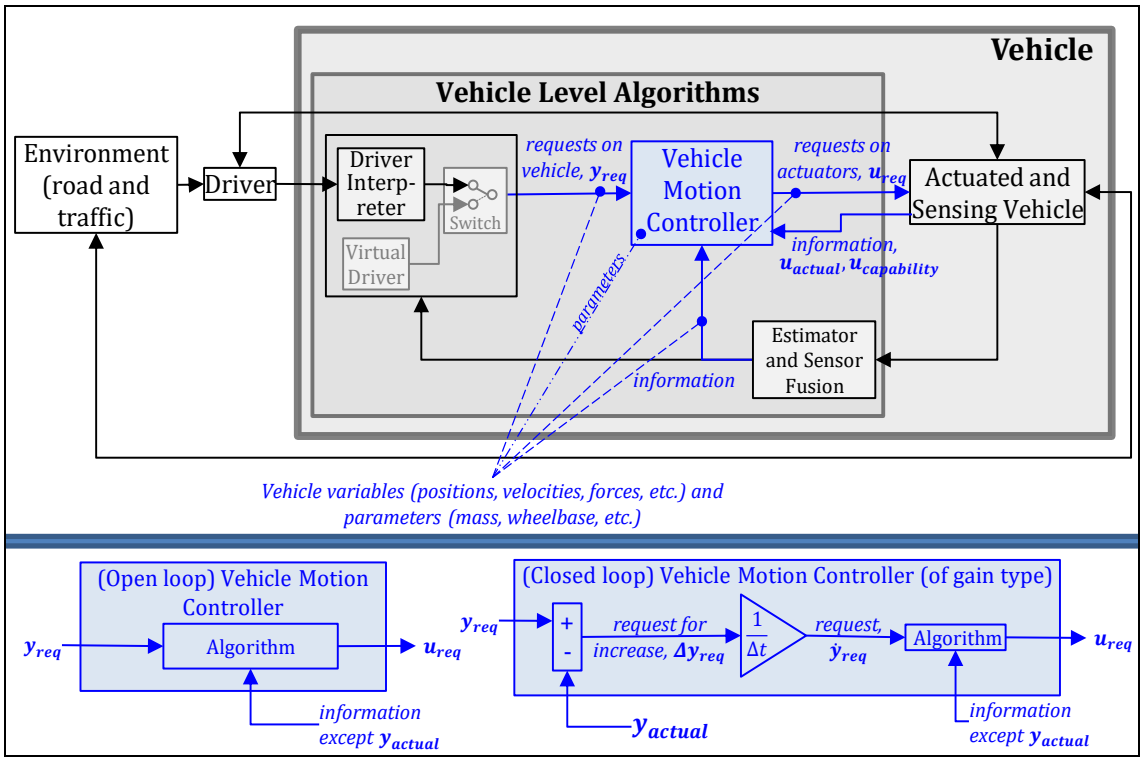

Figure 1-14: Context for Vehicle Level Algorithms and Vehicle (Motion) Controller. "Virtual Driver" takes vehicle driver into account and closes the loop in vehicle speed and lateral position.

Matlab is mainly numerical, but also has a symbolic toolbox:

```
>> syms x a; Eq=a/x+x==0; solve(Eq,x)   %symbolically solve equation
ans =   (-a)^(1/2)
       -(-a)^(1/2)
>> diff(a/x+x,x)   %symbolically differentiate expression
ans = 1 - a/x^2
>> int(x^3+log(x),x)   %symbolically integrate expression
ans = (x*(4*log(x) + x^3 - 4))/4
```

Of special interest for dynamic systems is that Matlab has a built-in function for "exponential matrix", mentioned in 1.5.1.1.5. E.g., if $\dot{\boldsymbol{x}} = \boldsymbol{A} \cdot \boldsymbol{x}$; with $\boldsymbol{x}(0) = \boldsymbol{x}_{\boldsymbol{iv}}$ the solution is $\boldsymbol{x}(t) = e^{\boldsymbol{A} \cdot t} \cdot \boldsymbol{x}_{\boldsymbol{iv}}$ which can simply be computed as:

```
>> x=expm(A*t)*x_iv;   %with A as (square) matrix
```

1.5.4.7 Dataflow Diagram Based Tools

Examples of tools: Simulink, Systembuild, Altair Activate, Xcos, Modelica with Blocks library

In these tools, the Explicit form model (or an ODE) is built with a graphical representation, around "integrator blocks", often marked "1/s" or "$\int$ ". An example using Simulink is shown in Figure 1-15. Simulink is designed for designing/modelling signal processing and control design. It can also be used for modelling the physics of the controlled systems. There are no dedicated vehicle dynamics tools/libraries from Mathworks (but there are in-house developed specific libraries in automotive companies).

From this type of tools, it is often possible to automatically generate real time code, which is more and more used instead of typing algorithms. It can be used for rapid prototyping of control functions, or even for generation of executable code for production ECUs.

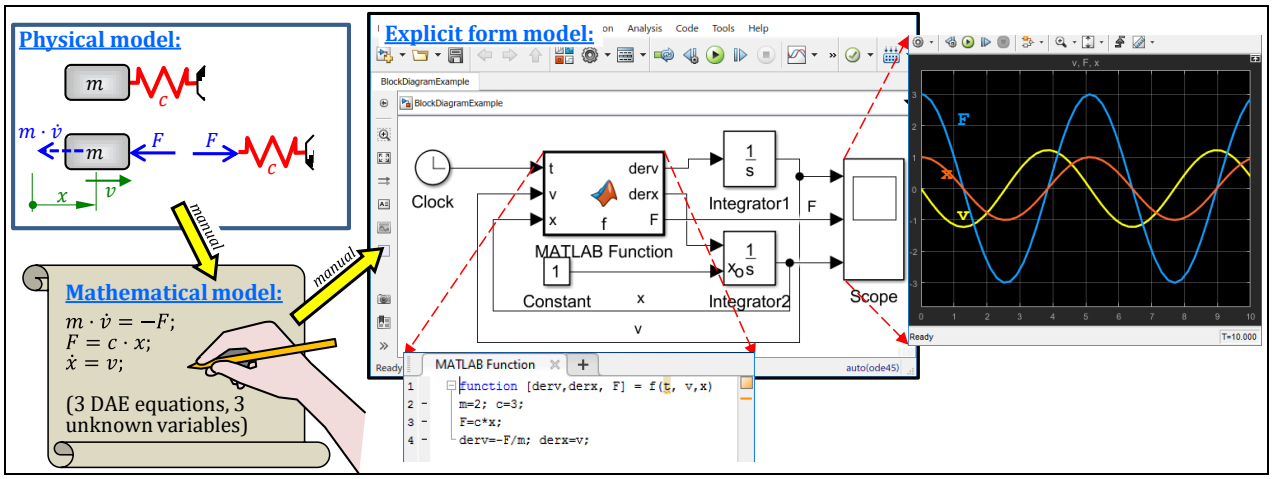

Figure 1-15: Graphical modelling using Simulink for Explicit form model.

1.5.4.8 Vehicle Dynamics Specialized Simulation Tools

Examples of tools: CarMaker, TruckMaker, veDYNA, CarSim, TruckSim.

These tools are specialized for vehicle dynamics. They contain purpose-built and relatively advanced models of vehicles, drivers and scripts for test manoeuvres. They are well prepared for parameter changes. However, they are generally less prepared for modelling conceptually new vehicle designs, which can make these tools less useful for vehicle manufacturers. For this reason, many of these tools offer also an interface to Simulink or FMU, so that the user can add in their own vehicle models.

1.5.4.9 MBS Tools

Examples of tools: Adams, Simpack, LMS Virtual Lab, Simscape Multibody, Modelica with Mechanics library.

These are general 3D mechanics modelling and simulation tools, so called MBS (Multi-Body Simulation) tools. As one example, Adams contains libraries of general bodies, joints and force elements. But there are toolboxes in Adams for vehicle dynamics, where template models and special components (such as tyre models and driver models) are available for vehicles dynamics. The models are very advanced and accurate for 3D mechanics, and there are import/export interfaces to Simulink.

1.5.4.10 Modelica Based Modelling Tools

Examples of tools: Dymola, Maplesim, System-Modeler, AMESim, Optimica Studio, Jmodelica, OpenModelica

Modelica is not a tool but a globally standardized format for lumped dynamic models on DAE form (or Mathematical form, see 1.5.1.1.3). There are several tools which supports the format. Specification of Modelica is found at https://www.modelica.org/. When learning Modelica, http://www.xogeny.com/ is helpful. The model format is acausal and all variables and parameters are declared. An example of model is given in Figure 1-16. Declaration of which are parameters and variables is a necessary part for a DAE model, see "`parameter Real`" and "`Real`", respectively.

The model format is also object oriented, which means that libraries of model components are facilitated. These are often handled with graphical representation, on top of the model code. There are some open-source libraries for various physical domains, such as hydraulic, mechanics, thermodynamics and control. There are also commercial libraries, where we find vehicle dynamics relevant components: Vehicle Dynamics Library and Powertrain Library. Some simple Modelica code will be used to describe models in this compendium.

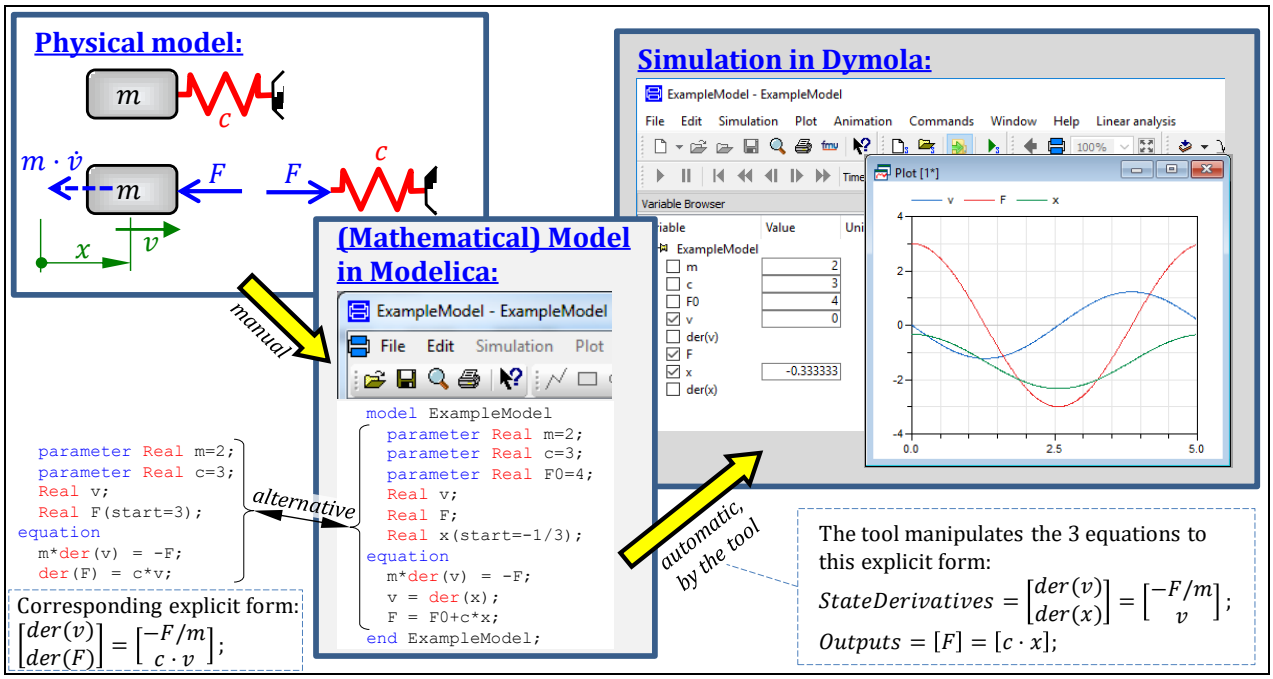

Figure 1-16: Example of model in Modelica format (using the tool Dymola). Two alternative models are given, leading to either [x, v] or [v, F] as states.

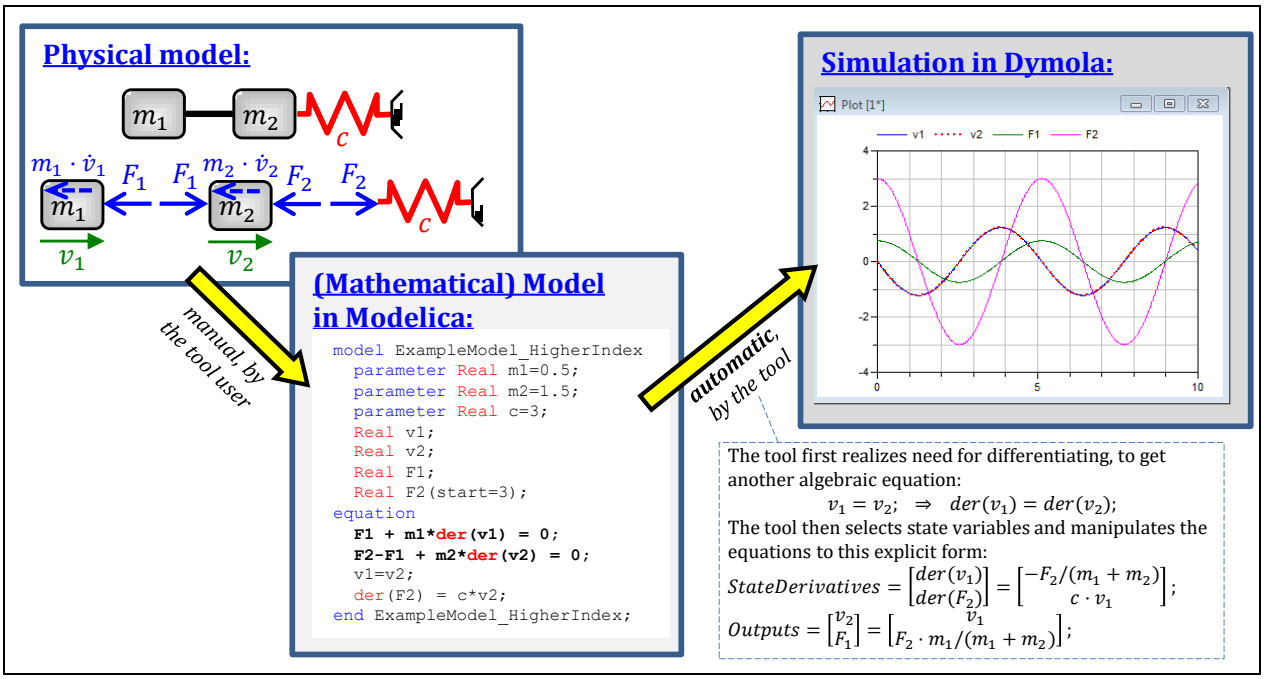

Figure 1-17: Example of "higher index problem" model in Modelica format.

Mathematical modelling is more efficient than Explicit form modelling, since the engineer does not need to spend time on symbolic/algebraic manipulation of the equations. This is especially true when a model is reused in another context which changes the causality or for so called "higher index problems", see Figure 1-17. In this compendium, many models are only driven to Mathematical model, since it is enough if assuming there are modern tools as Modelica tools available. One the other hand, an explicit form model has the value of capturing the causality, i.e. the cause-to-effect chain. The causality can sometimes facilitate the understanding and in that way help the engineer, which is why at least one and rather complete model is shown as explicit form model, see 4.5.3.1.

One can also declare variables with prescribed causality, i.e. signals, in Modelica. Declaration of input signal: "`input Real z;`". Modelica can also handle sampled signals and discrete states.

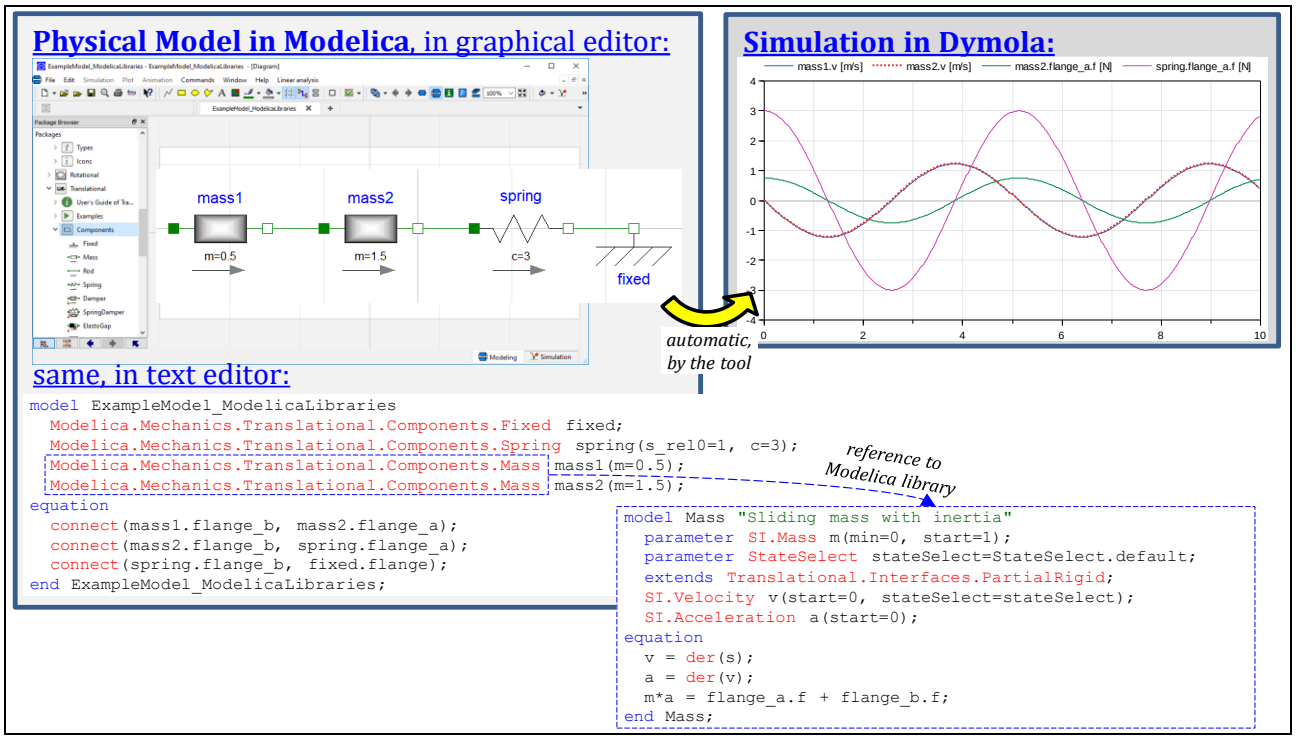

Figure 1-18: Example of model in Modelica format, using Modelica libraries of component.

1.5.4.11 FMI Supporting Simulation Tools

Examples of tools: Most of the tool examples in 1.5.4.10, but also Simulink, CarMaker

FMI (Functional Mock-up Interface) is not a tool but a globally standardized format for dynamic models on explicit form (see https://fmi-standard.org/). There are several tools which supports this format. FMI enables model export/import between tools. It also allows to hide Intellectual Property (IP) by using "black-box format", i.e. models compiled (non-human readable) for certain processors, which is important in relation between OEMs and suppliers.

1.5.5 Vehicle Motions and Coordinate Systems

A vehicle's (motion) degrees of freedom are named as in marine and aerospace engineering, such as heave, roll, pitch and yaw, see Figure 1-19. Figure 1-19 also defines the 3 main geometrical planes, such as transversal plane and symmetry plane. For ground vehicles, the motion *in-road-plane (irp)* is the primary motion, and has the dofs longitudinal, lateral and yaw. The remaining degrees of freedom (dof) describes the *out-of-road-plane (oorp)* motion. Also, the forces and moments on the vehicle body can be categorized in irp forces (longitudinal forces, lateral forces and yaw moments) and oorp (vertical forces, roll moments and pitch moments). Along each dof one defines velocity, such as longitudinal velocity v_x in $[m/s]$ and yaw velocity (or yaw velocity) ω_x in $[rad/s]$.

The consistent use of parameters that describe the relevant positions, velocities, accelerations, forces, and moments (torques) for the vehicle are critical. Unfortunately, there are sometimes disparities between the nomenclature used in different text books, scientific articles, and technical reports. It is important to apply ISO coordinate system, Reference (ISO 8855). It is the predominant coordinate system used nowadays. Historically, a coordinate system with other positive directions, Reference (SAEJ670), has been applied.

The distinction of vehicle fixed and inertial (= earth fixed = world fixed) coordinate systems is important. Figure 1-20 depicts the four most relevant reference frames in vehicle dynamics: the inertial, vehicle, wheel corner and wheel reference frames. All these different coordinate systems allow for the development of equations of motion in a convenient manner.

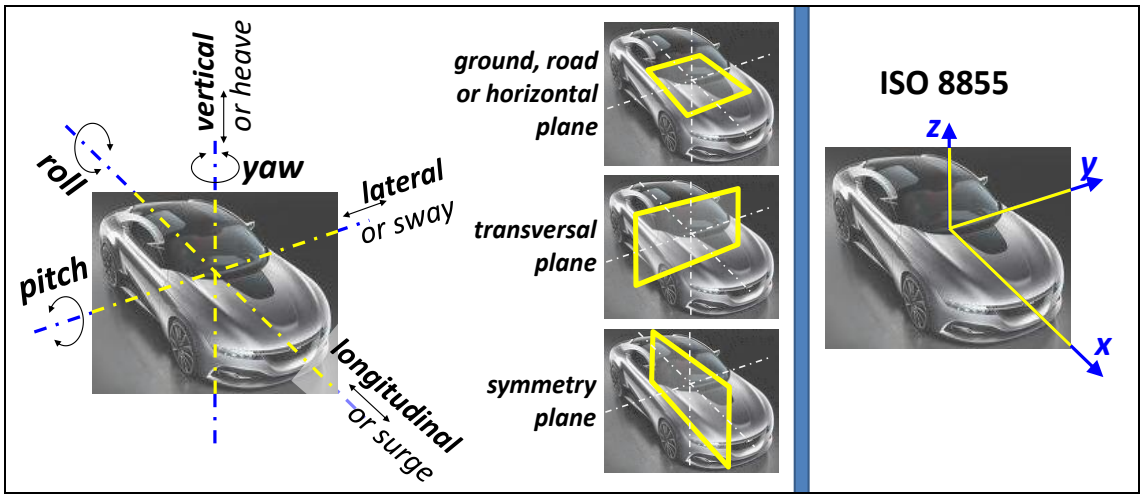

Figure 1-19: Left: Vehicle (motion) degrees of freedom and important planes. Right: ISO coordinate system

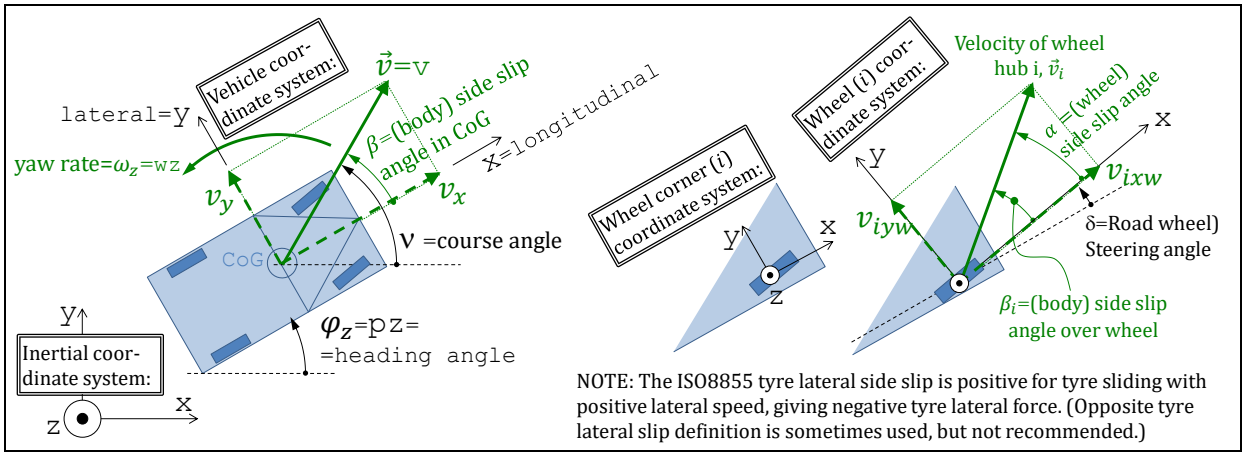

Figure 1-20: Coordinate systems and motion quantities in ground plane.

The orientation of the axes of an inertial coordinate system is typically either along the vehicle direction at the beginning of a manoeuvre or directed along the road or lane. Road or lane can also be curved, which calls for curved longitudinal coordinate.

Origin for a vehicle coordinate system is often centre of gravity of the vehicle, but other points can be used, such as mid front axle (ground contact or wheel centre height), mid of front bumper, outer edge of body with respect to certain obstacle, etc. Figure 1-20 defines velocities $\vec{v}$. Note that they are relative to inertial system, "velocities over ground", not relative to the other coordinate systems. However, the velocity components v_x, v_y are depent of which coordinate system $\vec{v}$ is decomposed in. Positions are often not included in the models. When positions are needed, e.g. for lane markings, road edges, other moving vehicles and varying friction, they are typically defined in inertial coordinate systems but algorithms on-board the vehicle use positions expressed in vehicle coordinate system.

In ISO and Figure 1-20, wheel side slip is defined so that it is positive for positive lateral speed. This means that lateral tyre forces on the wheel will be negative for positive side slip. Some would rather want to have positive force for positive side slip. Therefore, one can sometimes see the opposite definition of wheel side slip, as e.g. in (Pacejka, 2005). It is called the "modified ISO" sign convention.

Often there is a need to number each unit/axle/wheel. The numbering in Figure 1-21 is proposed. It should be noted that non-numeric notations are sometimes used, especially for two axle vehicles without secondary units. Then front=f, rear=r. Also, to differentiate between sides, l=left and r=right.

Using these motion dofs and coordinates for modelling is further described in 1.5.6.

1.5.5.1 Wheel Orientation

For steered wheels, there are often reason to translate forces and velocities between vehicle coordinate system and wheel coordinate system, see Figure 1-22 and Eq [1.1].

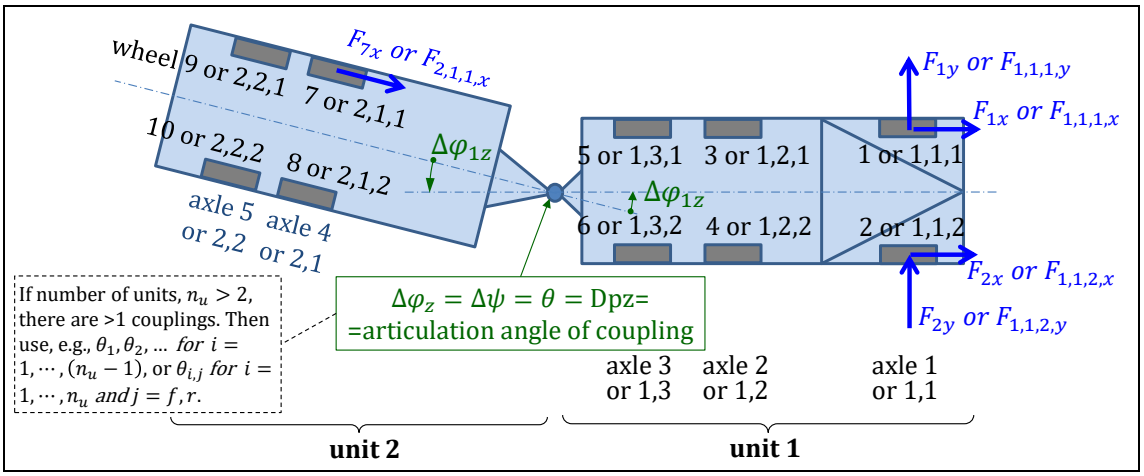

Figure 1-21: Proposed numbering of units, axles, wheels and articulation angle. Example shows a rigid truck with trailer. If multiple units: $\Delta\varphi_{n,z} = \varphi_{n-1,z} - \varphi_{n,z}$;

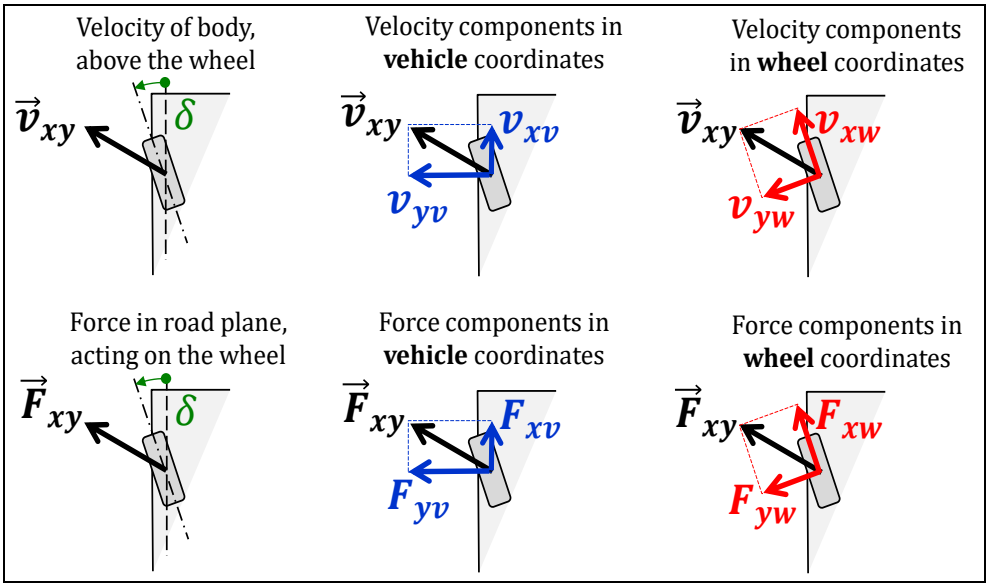

Figure 1-22: Transformation between forces and velocities in vehicle coordinate system and wheel coordinate system.

Transformation from wheel coordinates to vehicle coordinates:

$$\begin{bmatrix} v_{xv} \\ v_{yv} \end{bmatrix} = \begin{bmatrix} \cos(\delta) & -\sin(\delta) \\ \sin(\delta) & \cos(\delta) \end{bmatrix} \cdot \begin{bmatrix} v_{xw} \\ v_{yw} \end{bmatrix}; \quad and \quad \begin{bmatrix} F_{xv} \\ F_{yv} \end{bmatrix} = \begin{bmatrix} \cos(\delta) & -\sin(\delta) \\ \sin(\delta) & \cos(\delta) \end{bmatrix} \cdot \begin{bmatrix} F_{xw} \\ F_{yw} \end{bmatrix};$$

Transformation from vehicle coordinates to wheel coordinates:

$$\begin{bmatrix} v_{xw} \\ v_{yw} \end{bmatrix} = \begin{bmatrix} \cos(\delta) & \sin(\delta) \\ -\sin(\delta) & \cos(\delta) \end{bmatrix} \cdot \begin{bmatrix} v_{xv} \\ v_{yv} \end{bmatrix}; \quad and \quad \begin{bmatrix} F_{xw} \\ F_{yw} \end{bmatrix} = \begin{bmatrix} \cos(\delta) & \sin(\delta) \\ -\sin(\delta) & \cos(\delta) \end{bmatrix} \cdot \begin{bmatrix} F_{xv} \\ F_{yv} \end{bmatrix};$$

[1.1]

1.5.5.2 Slip of Tyres and Wheels

Slip (longitudinal s_x and lateral s_y) for a tyre or wheel will be defined in Chapter 2, see Eq [2.1], Eq [2.32] and 2.2.4.1.1.1. Slip is central for relating tyre forces in ground plane F_x, F_y to vehicle and wheel motion and wheel vertical force F_z. Note that rotational speed of each wheel ω_i comes in as additional variables to Figure 1-20. Slip is a dimensionless speed, "sliding speed divided by a reference speed". It appears as an intermediate variable to compute forces: $[F_x, F_y] = \boldsymbol{f_s}(F_z, s_x, s_y) = \boldsymbol{f\_s}\left(F_z, s_x(v_x, \omega), s_y(v_y, \omega)\right) = \boldsymbol{f_v}(F_z, v_x, \omega, v_y)$;. One can sometimes define slip also for an axle or even for an axle group, but it becomes less strict, since v_x, ω, v_y can generally differ between the wheels within the axle or axle group.

1.5.5.3 Compatibility between Tyre and Vehicle

When implementing lateral tyre models in a vehicle model for lateral dynamics, there are two major ways of formulating the compatibility that relates vehicle motion (body slip angle β) to wheel side slip ($s_{iy} \approx \tan(\alpha)$) via wheel steering angle (δ). One way is to express longitudinal and lateral velocity components with sine and cosine, as done in Eqs [4.3], [4.6] and [4.46]. The other way is to use the angle sum $\beta_i = \delta_i + \alpha_i$;.

$$\begin{bmatrix} v_{xv} \\ v_{yv} \end{bmatrix} = \begin{bmatrix} \cos(\delta) & -\sin(\delta) \\ \sin(\delta) & \cos(\delta) \end{bmatrix} \cdot \begin{bmatrix} v_{xw} \\ v_{yw} \end{bmatrix}; \quad or \quad \begin{cases} \sqrt{v_{xv}^2 + v_{yv}^2} = \sqrt{v_{xw}^2 + v_{yw}^2}; \\ \arctan(v_{yv}/v_{xv}) = \delta + \arctan(v_{yw}/v_{xw}); \\ or, for\ small\ angles: \beta \approx \delta + \alpha; \end{cases} \quad [1.2]$$

If approximating with small angles, it is easier to approximate to a linear vehicle model, see 4.3.2.4 and 4.4.2.2. For reversing, the angles β, α are close to $\pm\pi$ instead of close to 0.

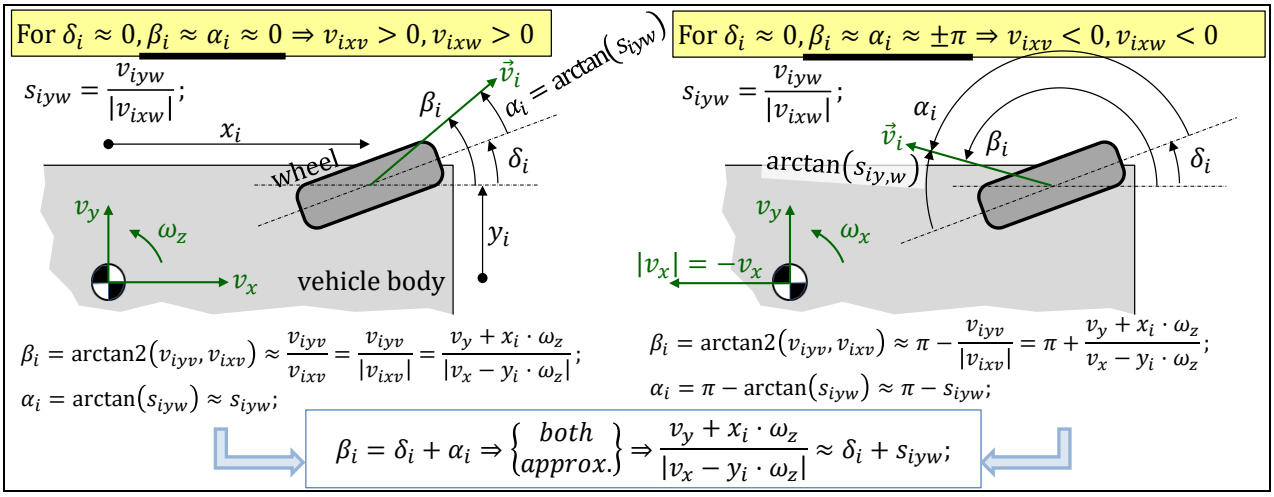

Figure 1-23: Approximate compatibility relation for small side slip v_{yw}. Left: For forward driving. Right: For reversing. Both lead to same final equation.

1.5.6 Complete Vehicle Modelling Concepts

The (Dynamic) Equilibria (or Equation of Motion) can be seen as the main equations in a mathematical model of a complete vehicle. A summarizing view of this is given in Eq [1.3].

In the left approximations, only the most important centrifugal effects, $m \cdot v_x \cdot \omega_i$, are included see also Eqs [3.29] and [4.45]. The sums refer to forces and moments acting on the vehicle body; from tyre/ground caused by actuation and rolling resistance, from gravity and from aerodynamics. Equations for forces and moments in the summations are not given here, but are needed for the model to be complete, i.e. "simulate-able".

In-road-plane (irp) equilibria:

$$\begin{cases} m \cdot \dot{v}_x \approx m \cdot (\dot{v}_x - v_y \cdot \omega_z) = \sum forces_x; \\ m \cdot (\dot{v}_y + v_x \cdot \omega_z) \approx m \cdot (\dot{v}_y + v_x \cdot \omega_z) = \sum forces_y; \\ J_z \cdot \dot{\omega}_z = \sum moments_z; \end{cases}$$

Out-of-road-plane (oorp) equilibria:

$$\begin{cases} m \cdot (\dot{v}_z - v_x \cdot \omega_y) \approx m \cdot (\dot{v}_z - v_x \cdot \omega_y + v_y \cdot \omega_x) = \sum forces_z; \\ J_x \cdot \dot{\omega}_x = \sum moments_x; \\ J_y \cdot \dot{\omega}_y = \sum moments_y; \end{cases} \quad [1.3]$$

Chapter **3** and **4** requires complete vehicle models that can measure complete vehicle functions expressed in *irp* motion. A major categorization, see 1.5.6.2 and 1.5.6.3, of those are whether the models considers *only* **irp** motion or *also* **oorp** motion. Another important categorization is to differ between **1-track** and **2-track** models, see 1.5.6.2.2. A third important categorization is which "dynamic operating conditions" that is assumed, among those listed in the following:

- ***Low speed*** condition means that vehicle moves with low speed, forward or reverse. Also, accelerations are low. No fictive forces ($mass \cdot acceleration$) is modelled. All terms on left side in Eq [1.3] are neglected.
- ***Steady State*** condition means that time history is irrelevant for the quantities studied. Seen as a manoeuvre over time, the studied quantities are constant. Explained for a certain model, it means that the influence of the derivatives of the corresponding variables, that else would generate state variables, is neglected. In physical model of a mechanical system this often means that "$mass \cdot acceleration\ [N]$" or "$velocity/stiffness\ \ [m/s]$" is neglected (in mathematical model: equation "$\dot{z}_i = 0$;" is added, in explicit form model: "$\dot{z}_i$" is replaced with "0"). If only some quantities are treated in this way, one might call the conditions steady state with respect to these quantities. Only the $m \cdot v_i \cdot \omega_j$ terms (centrifugal forces) on left side in in Eq [1.3] are kept.
- ***Transient*** (or Transient State, as opposed to Steady State) condition means that time history is relevant; i.e. there are delays, represented by "state variables" when simulated. All terms on the left side in in Eq [1.3]are kept.
- ***Stationary Oscillating*** condition is a special case of transient, where cyclic variations continue over long time with a repeated pattern. Long time means to that all none-cyclic components of the variation is damped out. The pattern is often modelled as harmonic (sinus and cosine variations in time) with constant amplitudes and phases. Example is sinusoidal steering with small enough steering amplitude, see 4.4, but also driving with over an undulated road surface, see Chapter 5. All terms on left side in in Eq [1.3] are kept, as for transient operation.
- ***Quasi-Steady State*** condition have a more diffuse meaning. It can refer to steady state with respect to some quantities, i.e. some terms on left side in in Eq [1.3] are neglected but not all. Alternatively, it can refer to that the quantities are prescribed to an explicit function of time, e.g. $v_x = f(t)$;, which means that also $\dot{v}_x$ is known.

Let us also briefly list some other possible categorizations for Chapter 3 and 4:

- Categorization referring to **small angles** ($\sin(angle) = 1; \cos(angle) = 0;$) or not, applied to steering/articulation angles and/or tyre/body side-slip angles.
- Categorization referring to **tyre models** are further explained in 2.2.6.
- One can also categorize referring to **subsystem models**.
  - The suspension can add states per wheel or axle i, at least the vertical spring force F_{si}.
  - The propulsion and brake system can be actively controlled. They give wheel torques $\boldsymbol{T}(t) = [\omega_1, \omega_2, \cdots]$. Such models often add one state per wheel or axle i, the rotational speed ω_i.
  - Chapter 3 uses different models of propulsion, brake and suspension. E.g., the propulsion system can add more states: engine delay, gear shifting, torsional shaft, control algorithms.
  - Chapter 4 adds the steering subsystem, with its control algorithms. Also, more about model categorisation is found in 4.1.1.

Chapter **5** is very different since it treats vehicle functions expressed in *out-of-road-plane* motion. So, most models in Chapter **5** uses only the oorp equations, i.e. not the irp equations, above.

To make the overall model simulate-able one needs some form of driver model and environment model. A rather complete example model is described in 4.5.3.1.

1.5.6.1 1D Models

In some cases, it can be enough to model motion in 1 dimension. Some examples are:

- **Longitudinal 1D** in 3.2 and 3.3, it can be enough to model v_x: $m \cdot \dot{v}_x = \sum forces_x$;. A 1D longitudinal model can lump all wheel, axles and units to one wheel, or treat them separately.
- **Roll 1D** in 4.3.11, it can be enough to model ω_x: $J_x \cdot \dot{\omega}_x = \sum moments_x$;
- **Heave 1D** in 5.4, it can be enough to model v_z: $m \cdot \dot{v}_z = \sum forces_z$;

1.5.6.2 In-road-plane Models, 2D

When modelling longitudinal dynamics, one has to involve at least v_x. When modelling lateral dynamics, one has to involve at least v_y and ω_z. So, models in xy-plane (irp) are often useful. (Other 2D models, in xz- or zy-planes, can also be relevant, e.g. for load transfer.)

1.5.6.2.1 Particle and Body Models

In some cases, e.g. threat estimation in 3.5.2.7 and 4.6.2.4, a particle model can be of use. The alternative is a body model, see Figure 1-24. A particle model cannot resolve F_z per wheel or axle, which means that tyre slip, neither s_x nor s_y, can be properly captured which is a problem for both longitudinal and lateral dynamics. The force $\vec{F}$ can be decomposed in global directions $[F_X, F_Y]$ or $[F_{xg}, F_{yg}]$. Other decompositions are road $[F_{xr}, F_{yr}]$, path $[F_{xp}, F_{yp}]$ or vehicle $[F_{xv}, F_{yv}]$. Road can be tracked using a map. Path can be tracked by remembering position from previous time history. Vehicle heading is most difficult, since a particle model do not capture yaw dynamics well.

1.5.6.2.2 1-Track and 2-Track Models

The models can assume that each wheel on the axles have their own ground contact (2-track models) or if there is only one "virtual tyre" modelled per axle (1-track model or single-track model or bicycle model). See Figure 1-24 and Figure 1-25. For multi-axle vehicles, one can even simplify one step further and model only one "virtual tyre" per axle group, see Figure 1-24. It should be noted that the simplifications have limitations, they are not suitable when the forces of the different tyres are significantly different, e.g. differences in actuated wheel torques or different wheel side slips.

Lateral dynamics phenomena which 1-track models do not capture well are, e.g.:

- Deviations from Ackerman geometry within an axle, see 0.
- Roll motion
- Lateral load shift (4.3.6.2) and combined tyre slip (4.3.6.6).
- Added yaw moment due to left/right-asymmetric wheel torque, such as ESC interventions.

The in-road-plane (irp) models does not capture the out-of-road-plane motion, v_z, ω_x, ω_y. However, they can still capture the transfer of loads (vertical forces on wheels).

For longitudinal dynamics, 1-track models are often enough. For longitudinal functions in "3.2 Steady State Functions" and "3.3 Functions Over (Long) Cycles", even particle models are often enough. But, it is important to understand the validity limit of the model!

1.5.6.3 Adding Out-of-road-plane Motion, >2D

The expression ">2D" as opposed to "3D" reflects that sometimes it can be enough and preferable to combine equations from several 2D views (xy-, xz- and yz-plane) without adding all cross-coupling effects. This is as opposed to a full 3D model, following rigid body dynamics theory in all details.

An example of a 2-track model including both irp and oorp motion is given in 4.5.3.

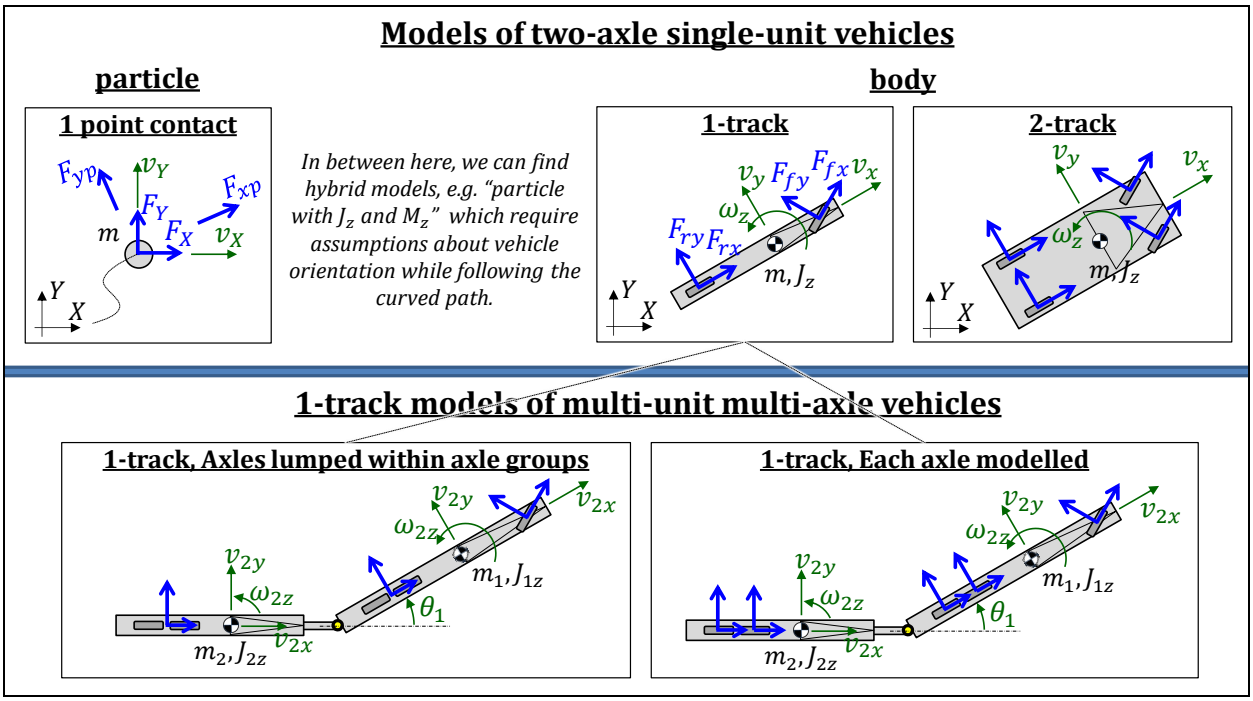

Figure 1-24: Different in-road-plane vehicle model concepts. The forces are from tyre contacts acting on vehicle body. Fictive forces (m · acceleration) and body forces (gravity and aerodynamic) are not drawn.

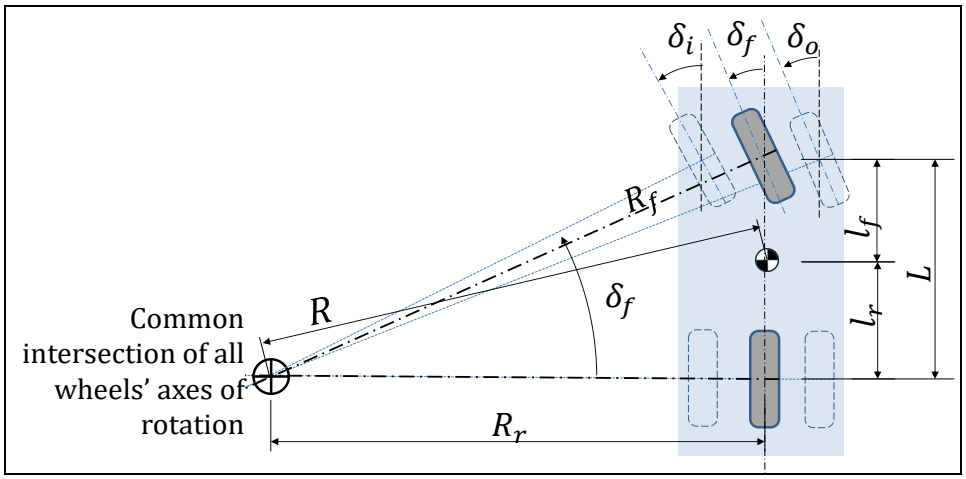

Figure 1-25: Collapsing a 2-track vehicle to a 1-track model.

1.5.7 Vehicle Dynamics Terms

1.5.7.1 Load Levels

The weight of the vehicle varies through usage. For many vehicle dynamic functions, it is important to specify this load level.

Kerb weight is the total weight of a vehicle with standard equipment, all necessary operating consumables (e.g., motor oil and coolant), a full tank of fuel, while not loaded with either passengers or cargo. Kerb weight definition differs between different governmental regulatory agencies and similar organizations. For example, many European Union manufacturers include a 75 kg driver to follow European Directive 95/48/EC.

Payload is the weight of carrying capacity of vehicle. Depending on the nature of the mission, the payload of a vehicle may include cargo, passengers or other equipment. In a commercial context, payload may refer only to revenue-generating cargo or paying passengers.

Gross Vehicle Weight/Mass (GVW/GVM) is the maximum operating weight/mass of a vehicle as specified by the manufacturer including the vehicle's chassis, body, engine, engine fluids, fuel, accessories, driver, passengers and cargo but excluding that of any trailers.

Other load definitions exist, such as:

- *"**Design Weight**"* (for passenger vehicles, this is typically Kerb weight plus 1 driver and 1 passenger, 75 kg each, in front seats)
- *"**Instrumented Vehicle Weight**"* (includes equipment for testing, e.g. out-riggers)
- ***"Road-allowed GVW/GVM"*** is the maximum GVW/GVM for a certain road, limited by the strength of the road and bridges. It is applicable for heavy trucks.

For vehicle dynamics it is often also relevant to specify where in the vehicle the load is placed because it influences how vertical forces under the wheels/axles distribute as well as moments of inertia.

1.5.7.3 Open-Loop and Closed-Loop Test Manoeuvres

Two expressions used in vehicle dynamics are "Open-loop" and "Closed-loop" test manoeuvres.

An **open-loop** manoeuvre refers to the case where the driver controls (steering wheel, brake pedal and accelerator pedal) are operated in a specific sequence, i.e. as functions of time. A typical case is a sine wave excitation of the steering wheel. The time history of the steering wheel angle is defined as a function that is independent of the road environment or driver input. This type of manoeuvre can be relevant to design for, and it tells some but not all about the real-world driving cases. Theoretical simulation and real testing with a steering robot are examples of how such studies can be made.

A **closed-loop** manoeuvre refers to the case when (human) driver feedback via driver controls is included. This represents real-world driving better. In real vehicle or driving simulator testing, a real driver is used. This enables collection of the drivers' subjective experience. In cases of simulation, a "driver-model" is needed. A driver-model can have varying levels of complexity but in all cases simulates the response of a human driver to different effects, such as lateral acceleration, steering wheel torque, various objects appearing outside the vehicle, etc.

A test with real vehicle, carried out with a steering-robot (and/or pedal robot) can also be called closed-loop if the robot is controlled with a control algorithm which acts differently depending on the vehicle states, i.e. if the algorithm is a driver model.

With increasing level of automation, there is sometimes a need for distinguishing between closed/open loop with respect to human driver or automated driver.

1.5.7.4 Objective and Subjective Measures

Two main categories of finding measures are:

- *An **Objective*** measure is a physical measure calculated in a defined and unique way from data which can be logged in a simulation or from sensors in a real test.
- *A **Subjective*** assessment is a rating measure set by a test driver (e.g. on a scale 1-10) in a real-vehicle test or driving simulator test.

One generally strives for objective measures. However, many relevant functions are so difficult to capture objectively, such as Steering feel and Comfort in transient jerks, so subjective assessments are needed and important.

1.5.7.5 Path, Path with Orientation and Trajectory

A ***path*** can be $x(y)$ or $y(x)$ for centre of gravity where x and y are coordinates in the road plane. To cope with all paths, it is often necessary to use a curved path coordinate instead, s, i.e. $x(s)$ and $y(s)$. A path do have an orientation of itself φ_{rz}, defined through $\arctan(\varphi_{rz}) = dy/dx = (dy/ds) \cdot (1/(dx/ds)) = y'/x'$;. However, a vehicle following the path does not need to point along the path.

The vehicle also has a varying orientation, $\varphi_z(x)$ or $\varphi_z(s)$, which often is often relevant, but the term "path" does necessarily include this. In those cases, it might be good to use an expression "***path with orientation***" instead.

A ***(time) trajectory*** is a more general term than a path and it brings in the dependence of time, t. One typical understanding is that trajectories can be $[x(t);\ y(t);\ \varphi_z(t)]$. But also, other quantities, such as steer angle or vehicle propulsion force can be called trajectory: $\delta(t)$ and $F_x(t)$, respectively. The word "trace" is sometimes used interchangeably with trajectory.

1.5.7.5.1 Path with Orientation

The path and path with orientation was introduced in 1.5. The path, in global coordinate system, is related to vehicle speeds, in vehicle fix coordinates, as given in Figure 1-26 and Equation [1.4].

Knowing $(v_x(t), v_y(t), \omega_z(t))$, we can determine "path with orientation" $(x(t), y(t), \varphi_z(t))$, by time integration of the right-hand side of the equation. Hence, the positions are typically "state variables" in lateral dynamics models.

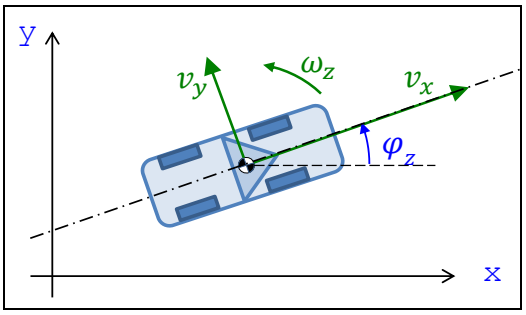

Figure 1-26: Model connecting "path with orientation" to velocities in vehicle coordinate system.

$$\begin{bmatrix}\dot{x}\\ \dot{y}\end{bmatrix} = \begin{bmatrix}\cos(\varphi_z) & -\sin(\varphi_z)\\ \sin(\varphi_z) & \cos(\varphi_z)\end{bmatrix} \cdot \begin{bmatrix}v_x\\ v_y\end{bmatrix};$$
$$\dot{\varphi}_z = \omega_z; \qquad [1.4]$$

It should be noted that in some problems, typically manoeuvring at low speed, the real time scale is of less interest. Then, the problem can be treated as time independent, e.g. by introducing a coordinate, s, along the path, as in Equation [1.5].

$$x' = \frac{v_x}{\dot{s}} \cdot \cos(\varphi_z) - \frac{v_y}{\dot{s}} \cdot \sin(\varphi_z);$$
$$y' = \frac{v_y}{\dot{s}} \cdot \cos(\varphi_z) + \frac{v_x}{\dot{s}} \cdot \sin(\varphi_z);$$
$$\varphi_z{}' = \frac{\omega_z}{\dot{s}};$$
where prime notes differentation with respect to s [1.5]

Here, $\dot{s}$ can be thought of like an arbitrary time scale, with which all speeds are scaled. One can typically choose $\dot{s} = 1\ [m/s]$. However, in this compendium we will keep notation t and the dot notation for derivative.

1.5.7.6 Stable and Unstable

Often, in the automotive industry and vehicle dynamics, the words "stable" and "unstable" have a broad meaning, describing whether high lateral slip on any axle is present or not. Sometimes it is used for roll-over instability. Also, the articulation angle can be unstable when reversing in low speed with a trailer. Stability analysis in a stricter physics/mathematical meaning is touch upon in 0.

It is useful to know about this confusion of words. An alternative expression for the wider meaning is "loss of control" or "loss of tracking" or "directional unstable", which can include that vehicle goes straight ahead, but road bends.

1.5.7.7 Subject and Object Vehicle

The ***subject vehicle*** is the vehicle that is studied. Often this is a relevant to have a name for it, since one often studies one specific vehicle, but it may interact with other in a traffic situation. Alternative names are ***host vehicle***, ***ego vehicle*** or simply ***studied vehicle***.

Other vehicles are called ***object vehicles*** or ***opponent vehicles***. A special case of object vehicle is ***lead vehicle*** which is ahead of, and travels in same direction as, subject vehicle. Another special case is ***oncoming vehicle*** which is ahead of, and travels in opposite direction as, subject vehicle.

1.5.7.8 Active Safety, ADAS and AD

The expression *Active Safety* is used in Automotive Engineering with at least two different meanings:

- Active Safety can refer to the vehicle's ability to avoid accidents, including both functions where the driver is in control (such as ABS and ESC, but also steering response) and functions with automatic interventions based on sensing of the vehicle surroundings (such as AEB and LKA). See http://en.wikipedia.org/wiki/Active_safety. Active Safety can even include static design aspects, such as designing the wind shield and head light for good vision/visibility.
- Alternatively, Active Safety can refer to only the functions with automatic interventions based on sensing of the vehicle surroundings. In those cases it is probably more specific to use Advanced Driver Assistance Systems (ADAS) instead, see http://en.wikipedia.org/wiki/Advanced_Driver_Assistance_Systems. ADAS does not only contain safety functions, but also comfort functions like CC and ACC.

Functions that off-load the driver the direct tasks during driving can be sorted under Automated Driving, AD. Fully automated driving, e.g. transportation without human driver on-board, is probably a far future vision. On the other hand, it is already a reality that some portion of the driving tasks are automated in the latest vehicle on the market, such as Adaptive cruise control, see 3.5.2.2, and Lane Keeping Aid, see 4.6.2.1. If both those are active at the same time, we have already automated driving. Definitions of automation levels 0-5 is found in Reference (SAE_J3016, 2016). Today's version of these systems normally has a way to hand-back responsibility to driver rather immediately in hazardous situations. Future automated driving functions will need to always have a safe-stop function. The way to compete between vehicle manufacturers will probably be to avoid hand-backs (maximize up-time) and to allow as long "hand-back times" as possible. So, vehicle dynamics will be important in the development, especially for safety reasons for automated driving in higher speeds; hazardous situations where human driver selects to take back the driving.

1.5.8 Architectures

Vehicles are often designed in platforms, i.e. parts of the design solutions are reused in several variants. Typical variants may be different model years or different propulsion system. To be able to reuse solutions, the vehicles have to be built using the same *architecture*.

A **mechanical** (or geometric) architecture may include design decisions about certain type of wheel suspension on front and rear axle. An **electrical and electronic** architecture may include design decisions about electric energy supply system (battery voltage etc.) and electronic hardware for computers (Electronic Control Units, ECUs) and how they are connected in networks, such as Controller Area Network, CAN.

The mechanical architecture influences vehicle dynamics functions. However, it is noteworthy that also the electronic architecture also is very important for the vehicle dynamics, through all electronic sensors, actuators and control algorithms. One example of this importance is the ABS control of the friction brake actuators. Architectures for functions are therefore motivated, see 1.5.8.2.

1.5.8.1 Subsystems

The architectures are dependent on the business model for how to purchase and integrate subsystems to a vehicle. Hence, it is relevant to define the subsystems. For vehicle motion functionality, the relevant subsystems (or "motion support devices") are typically:

- Propulsion system
- Brake system
- Wheel suspension
- Wheels and tyres
- Steering system
- Environment sensing system

Each of these can typically be purchased as one subsystem. Each typically have mechanical and signal interface to the remaining vehicle. Different vehicle manufacturers can have different strategies for signal interface and how much the subsystems are allowed to be dependent of each other.

1.5.8.2 Vehicle Function Architecture

As the number of electronically controlled functions increase, an architecture for vehicle functionality, or "Function Architecture", becomes necessary to meet fast introduction of new functionality and to manage different variety of vehicle configurations. A function architecture is a set of design rules for how functions interact with each other (e.g. signalling between control functions). Also, the decomposition in subsystems should be reflected in this architecture, see 1.5.8.1. An older expression which is related to function architecture is cybernetics. Examples (from Vehicle Dynamics/Vehicle motion function domain) of modern expressions which are related are Integrated Chassis Control (GM), Integrated Vehicle Dynamics Control (Ford), Complete Vehicle Control (Volvo) and Vehicle Dynamics Integrated Management (Toyota). There is no exact and generally well accepted definition of such architecture. However, it becomes more and more essential, driven by increasing content of electronic control in vehicles. One way to visualize a reference architecture is given in Figure 1-27 and Figure 1-28.

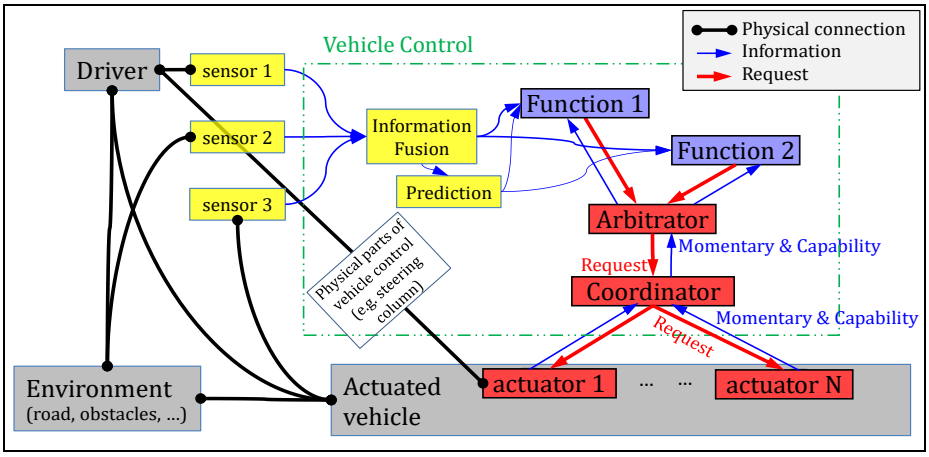

Figure 1-27: Concepts of a vehicle motion function architecture. Arbitrators, Coordinators and Actuators are the most important architectural objects for vehicle dynamics (vehicle motion).

In order to be able to formulate design rules in reference architecture of functionality the following are relevant questions:

- Which physical quantities should be represented on the interface between Devices (Sensors and Actuators) and Vehicle Level Functionality?
- Partitioning within a reference architecture of vehicle motion functionality could be realised as shown in Figure 1-28. Different Layers/Domains are defined:
  - **Human Machine Interface** Domain: This includes the sensors/buttons which the driver uses to request services from the vehicle's embedded motion functionality.
  - **Vehicle Environment** Domain: Includes surrounding sensors mounted on vehicle but also communication with other vehicles (V2V) and infrastructure (V2I) and map information.
  - **Route** Layer: Planning the whole transport mission, horizon 10..1000 km. These functions exist mainly for commercial traffic and might be done outside the subject vehicle.
  - **Traffic Situation** Layer: Interpret the immediate surrounding traffic which the vehicle is in, road/lanes and other road users, horizon ≈100..300 m. Example of functions: adaptive cruise control, collision avoidance, and lane steer support.
  - **Vehicle Motion** Layer: This includes the Energy management, powertrain coordination, brake distribution, and vehicle stability such as ESC, ABS. Horizon ≈10..30 m This layer also estimates the vehicle states e.g. v_x, v_y, ω_z. In addition, this layer would be able to give vehicle level capability of max/min acceleration and their derivative.

        - **Motion Support Device** Layer: This includes the devices/actuators that can generate vehicle motion. This layer is also consisting sensors which could include the capability and status of each device e.g. max/min wheel torque.
- Formalisation of different types of:
    - Blocks, e.g. **Controller**, **Information Fusion**, **Arbitrator** and **Coordinator**.
        - Both arbitrators and coordinators have inputs and outputs as requests, typically expressed in same physical quantity. An arbitrator has more requests in that out and a coordinator has more requests out than in.
    - Signals, e.g. **Request**, **Actual** (or Status) and **Capability**.
    - **Parameters** used in Functional blocks. One can differ between Physical parameters (or Model parameters) and Tuning parameters. Some parameters can be common across the whole vehicle, which enables a kind of communication between blocks without normal signals, but instead exchanging values during start-up of the system.

Each signal should have a definition of which physical quantity and unit it refers to. For signals of Actual type, there also needs a concept to handle how accurate they are; e.g. as a tolerance or sending an upper and lower value between the physical quantity shall be. The definition of physical quantity is very important, not the least for Request signals. An example is, if using tyre longitudinal slip as quantity, sender and receiver of signal have to agree on slip definition. Since there are many slip definitions around, it might suggest using wheel rotational speed instead, which is less ambiguous.

The functionality is then allocated to ECUs, and signals allocated to network communication. The reference architecture can be used for reasoning where the allocation should be done. Which functionality is sensitive for e.g. time delay and thus should be allocated in the same ECU? Detailed control algorithm design is not stipulated by a reference architecture. Instead the reference architecture assists how detailed control algorithms be managed in the complete problem of controlling the vehicle motion. Whether representation of solutions of Functional Safety (ISO 26262, etc.) is represented in a reference architecture of functionality can vary.

Vehicles consisting of several units add special challenges, especially if the units are actuated. A heavy truck trailer is always actuated with at least brakes.

1.5.8.3 Virtual Vehicle Architecture

Virtual vehicle architecture, VVA, here refers to how to organize complete vehicle models, which can replace some real vehicle pre-series. VVA is a set of rules how a vehicle model should be modularized, such as variable/signal interfaces, parameterization, format- and tool-chains. The vision is that a whole project organisation, within an OEM and its suppliers, could deliver modules to virtual pre-series and that these modules would fit together. The FMI format, see 1.5.4.11, is one example of what could facilitate this.

1.5.9 Verification Methods with Real Vehicle

1.5.9.1 In Traffic

Driving on public roads in real traffic is the most realistic way to verify how well a vehicle fulfils the requirements during real use. It can be used for completely new vehicle models; or new systems, mounted on old models. The drivers can be either ordinary drivers (FOT=Field Operational Test) or test drivers (expeditions). A general existing vehicle population can also be studied by collecting data, e.g. as Accident Statistics Databases.

1.5.9.2 On Test Track

For vehicles and systems which are not yet allowed on public roads, or tests which are very severe or need a high degree of repeatability, test are carried out at test tracks. There are specialized test tracks for certain conditions, such as hot climate or slippery surfaces.

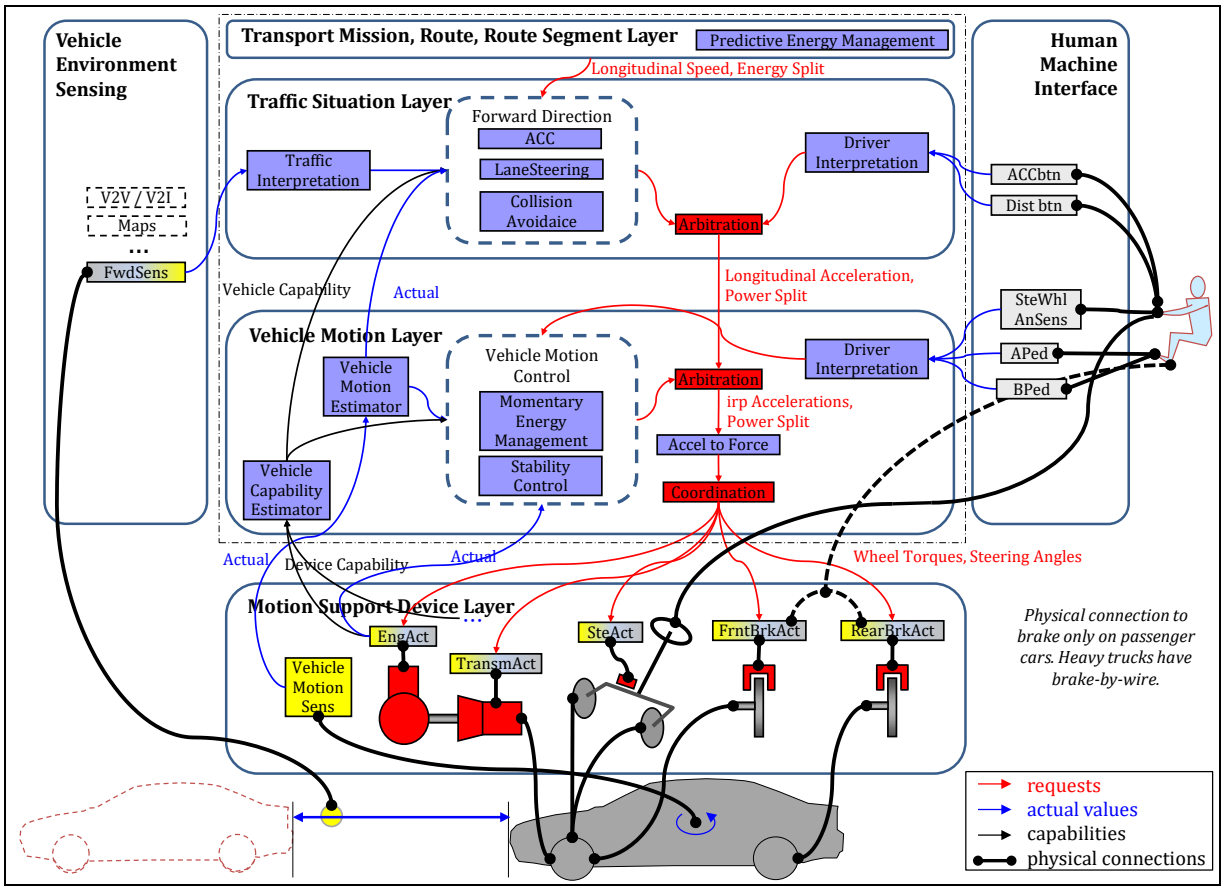

Figure 1-28: One example of reference architecture of vehicle motion functionality. Red arrows: Requests, Blue arrow: Information, Black lines with dot-ends: physical connection.

1.5.9.3 Augmented Reality, AR or Manipulated Environment

This is a new method. A typical example is: A real driver drives a real vehicle on a real road/test track. Some additional (virtual/simulated) traffic objects are presented to driver, e.g. on a head-up display. The same objects can be fed into the control functions, as if they were detected by the vehicle's camera/radar, which enables functions such as automatic braking to be triggered.

1.5.9.4 Objective Measures and Subjective Assessment

The vehicle can be instrumented so that measurements can be logged and later compared with requirements. Also, the tests can be performed with driving robot, so that the manoeuvres are well repeated.

However, driving also with human driver has its own value; the subjective assessments can be registered via interviews and debriefing after performed tests. A typical scale used for subjective rating or assessment is shown in Figure 1-29.

Rating Scale		Event Type: Disturbance	Event Type: Control
10	Desirable	Imperceptible	Excellent
9	Desirable	Trace	
8	Desirable	A Little	Good
7	Desirable	Some	
6	Desirable	Moderate	Fair
5	Borderline		
4	Undesirable	Annoying	Poor
3	Undesirable	Strong	
2	Undesirable	Severe	Very Poor
1	Undesirable	Not Acceptable	

Figure 1-29: Subjective rating scale from (SAE J1441, 2016.)

1.5.10 Verification Methods with Virtual Vehicle

1.5.10.1 Testing with Real Driver

1.5.10.1.1 DIL =Driver in the Loop Simulation

Verification with a driving simulator (or DIL) is when a real human, not a driver model, uses real driver devices (pedals, steering wheel) to influence a simulation model of the remaining system (vehicle and environment). The loop is closed by giving the human feedback through display of what would be visible from driver seat, including views outside wind-screen.

Feedback can be further improved by adding a motion platform to the driver's seat, sound, vibrations in seat, steering wheel torque, etc. The vehicle model run in the simulator can utilize HIL, SIL and MIL, from 1.5.10.1, for some part of the vehicle model. Driving simulator can be compared to other verification methods, see Table 1.2.

Subjective scale from Figure 1-29 can be used.

Table 1.2: Comparison of verification methods for complete vehicle functions.

			Alternative verification methods		
			Office simulation	Driving simulator	Real vehicle test
Requirements	Test new technology before it is built (save time and money)		+	-	- -
	Design parameter sweep/optimization		+!	-	- -
	Repeatable and Parallelized testing		+	+	-
	Safe testing		+	+	-
	Representative integration in vehicle		-	+!	++
	Representative behaviour	w.r.t. to vehicle	-	-	+!
		w.r.t. driver	-	+!	+
		w.r.t. to surroundings (road & traffic)	- - (env. sens)	- (env. sens)	+!

1.5.10.2 Testing using Driver Model

Generally, this means that driver, vehicle and environment are modelled and simulated. To perform a serious test there is also need to put effort on test scripts so that the model is run in the intended test manoeuvre and result is pre-processed. For verification of functions involving with algorithms, the HIL, SIL and MIL below are different ways to represent the algorithm in the vehicle model.

1.5.10.2.1 HIL = Hardware in the Loop Simulation

The hardware is often one or several ECUs (Electronic Control Units). If several ECUs are tested, the hardware can also contain the communication channel between them, e.g. a CAN bus. The hardware is run with real-time I/O to simulation model of the remaining system (vehicle, driver and environment).

In some cases, there is also mechanical hardware involved, such as if the ECU is the brake system ECU, the actual hydraulic part of the brake system can also be included in the HIL set-up, a so called "wet brake ECU HIL".

1.5.10.2.2 SIL = Software in the Loop Simulation

The software is often one or several computer programs (intended for download in electronic control units). The software is run with synchronized time-discrete I/O to a simulation model of the remaining system (vehicle, driver and environment).

The software is often used in compiled format (black box format) so that the supplier of the software can retain his intellectual property.

1.5.10.2.3 MIL = Model in the Loop Simulation

The model, or more correctly, a control algorithm, is a conceptual form of the computer programs (intended for download in electronic control units). The control algorithm is run with I/O to a simulation model of the remaining system (vehicle, driver and environment).

The control algorithms can appear in compiled format so that the supplier of the control algorithms can retain his intellectual property. Then it is hard to tell the difference between MIL and SIL.

1.6 Heavy Trucks

The following section describes heavy trucks, mainly as compared to passenger vehicles.

1.6.1 General Differences

Trucks are normally bought and owned by companies, not private persons. Each truck is bought for a specialized transport task. Life, counted in covered distance, for trucks is typically 10 times passenger cars. The life time cost of fuel is normally 5 times the vehicle cost, compared to passenger car where these costs are about equal. The cost for driver salary is a part of mileage cost, typically same magnitude as fuel cost. If investment cost for vehicle and repairs are distributed over travelled distance, these are typically also of same magnitude. So, the cost for a transport typically comes from one third fuel, one third driver salary and one third vehicle investment and repairs.

1.6.2 Vehicle Dynamics Differences

A truck has 5..10 times less power installed per vehicle weight. Trucks have their centre of gravity much higher, meaning that roll-over occurs at typically 4 m/s^2 lateral acceleration, as compared to around 10 m/s^2 for passenger cars. Trucks have centre of gravity far behind mid-point between axles, where passenger cars have it approximately symmetrical between the axles. Trucks are often driven with more units after, see Figure 1-30. The weight of the load in a truck can be up to 2..4 times the weight of the empty vehicle, while the maximum payload in passenger cars normally are significantly lower than the empty car weight. Trucks often have many steered axles, while passenger cars normally are only steered at front axle. The view for the driver (and environment sensors) is from higher up and without inner rear mirror. The lateral margins in lane are much smaller.

1.6.3 Definitions

In Figure 1-30, we can find the following units:

- Towing units: Tractor or Rigid (Truck)
- Towed units: Full trailer (FT), Semi-trailer (ST), Centre-axle trailer (CAT), (Converter) Dolly
- The couplings between the units can of 2 types:
    - **Fifth-wheel coupling** (e.g. between Tractor and Semi-trailer). Designed to take significant force in all 3 directions. Furthermore, it is designed to be roll-rigid, but free in pitch and yaw.
    - A **Turn-table** is similar to a fifth wheel but has a rolling bearing instead of a pitch-hinged greased surface, which leads to less yaw friction and no pitch degree of freedom. In converter dollies, one often sees both, fifth wheel on top of turntable.
    - **Hitch coupling** or **Drawbar coupling** (e.g. between Rigid and Full trailer). Designed to take significant forces in longitudinal and lateral directions, but only minor in vertical direction. Furthermore, it is rotationally free in all 3 directions. A full-trailer has pitch-moment-free rear end of drawbar. A converter dolly or centre-axle-trailers have pitch-rigid rear end of drawbar.
- There is often a need for several axles close to each other, to manage a high vertical force. Such group of axles is called “axle group”, “axle arrangement” or “running gear”.

1.7 Smaller Vehicles

This section is about smaller vehicles, meaning bicycles, electric bicycles, motorcycles and car-like vehicles for 1..2 persons. The last vehicle type refers to vehicles which are rare today, but there are reasons why they could become more common: Increasing focus on energy consumption and congestion in cities can be partly solved with such small car-like vehicles, of which the Twizy in Figure 1-31 is one example. All vehicles in Figure 1-31 can be referred to as Urban Personal Vehicle (UPVs), because they

enable personalised transport in urban environments. The transport can be done with low energy consumption per travelled person and distance, compared to today's passenger cars. The transport will also give higher levels of flexibility and privacy for the travelling persons, compared to today's public transportation. If such vehicles also could be shared between users, this concept will even more help congestion in cities but might require automation of booking and maybe even automation of driving.

Beside UPVs there could be considered smaller Urban Freight Vehicles (UFVs), but driver salary costs would then be very high per transported mass (or volume) of goods. So, UFVs might need to wait for automation of driving.

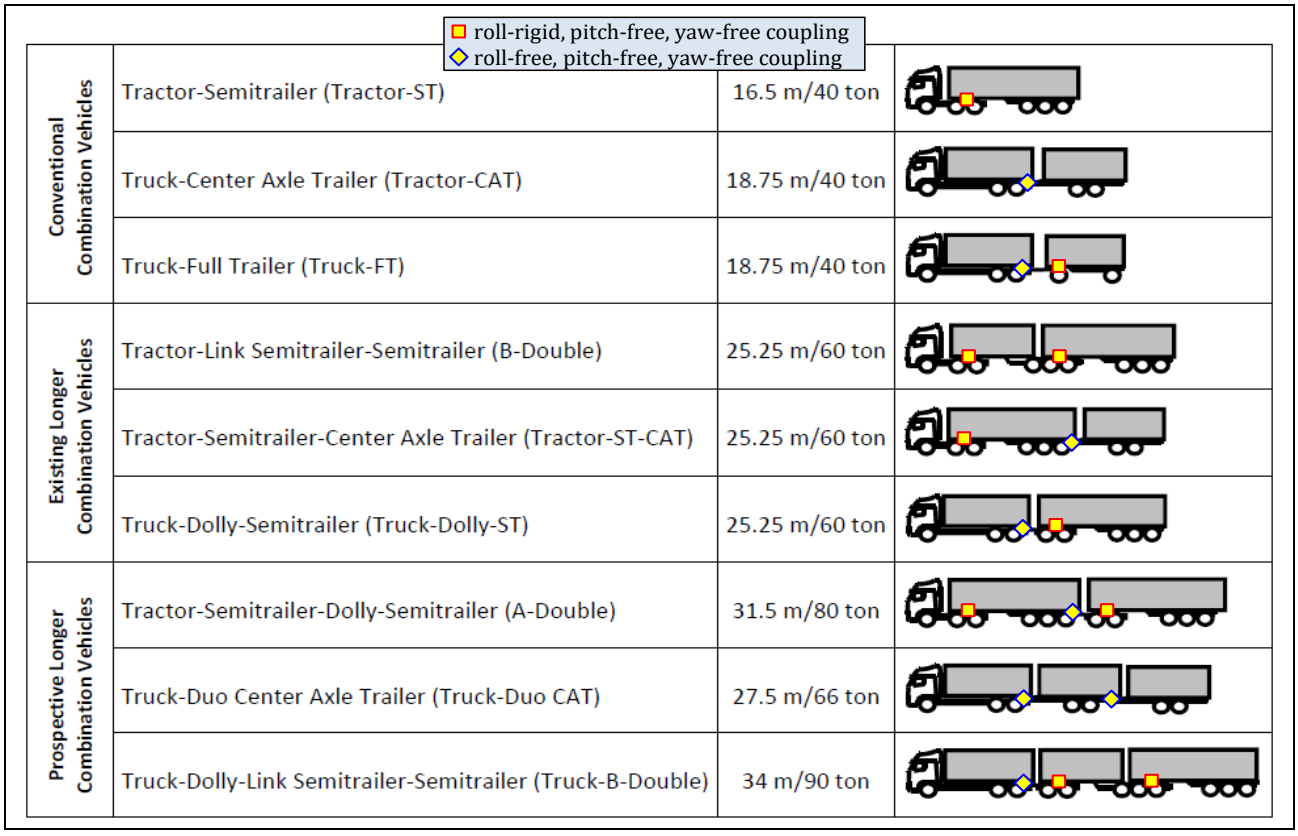

Figure 1-30: An overview over conventional and longer combinations. From (Kharrazi , 2012). The two-unit sequence "Dolly-Semitrailer" can be replaced by one "Full Trailer".

Figure 1-31 show some UPVs. UPVs/UFVs may require some categorizations:

- Climate and user type: Sheltered **or** open.
- Transport and user type: Short travels (typically urban, 5-10 km, 50 km/h) **or** long travels (typically inter-urban, 10-30 km, 100 km/h).
- Chassis concept:
  - Narrow (e.g. normal bicycles and motorcycles) **or** wide (at least one axle with 2 wheels, resulting in 3-4 wheels on the vehicle). Note that UPVs in both categories are typically still less wide than passenger cars.
  - Roll moment during cornering carried by suspension roll stiffness or roll moment during cornering avoided by vehicle cambering. The first concept can be called "Roll-stiff vehicle". The second concept can be called "Cambering vehicle" or "Leaning vehicle". 1-tracked are always Cambering vehicles. 2-tracked are normally Roll-stiff, but there are examples of Cambering such (see upper right in Figure 1-31). See Figure 1-32.
  - (This compendium does only consider vehicles which are "Pitch-stiff", i.e. such that can take the pitch moment during acceleration and braking. Examples of vehicles not considered, "Pitching vehicles", are: one-wheeled vehicles as used at circuses and two-wheeled vehicles with one axle, such as Segways.)
- Note that also Roll-stiff Vehicles camber while cornering, but **outwards** in curve and only **slightly**, while Cambering Vehicles cambers **inwards** in curve and with a **significant** angle.

Cambering Vehicles is more intricate to understand when it comes to how wheel steering is used. In a Roll-stiff Vehicle, the wheel suspension takes the roll-moment (maintains the roll equilibrium), which means that driver can use wheel steering solely for making the vehicle steer (follow an intended path). In Cambering Vehicles, the driver has to use the wheel steering for both maintaining the roll equilibrium and following the intended path. A model is given in **4.5.2.3**. Figure 1-32 shows some possible conceptual design of a cambering vehicle. It is not possible to do a partly roll-stiff and partly cambering vehicle, unless one uses suspension springs with negative stiffness, i.e. the suspension would need to consume energy to tilt the vehicle inward in curve.

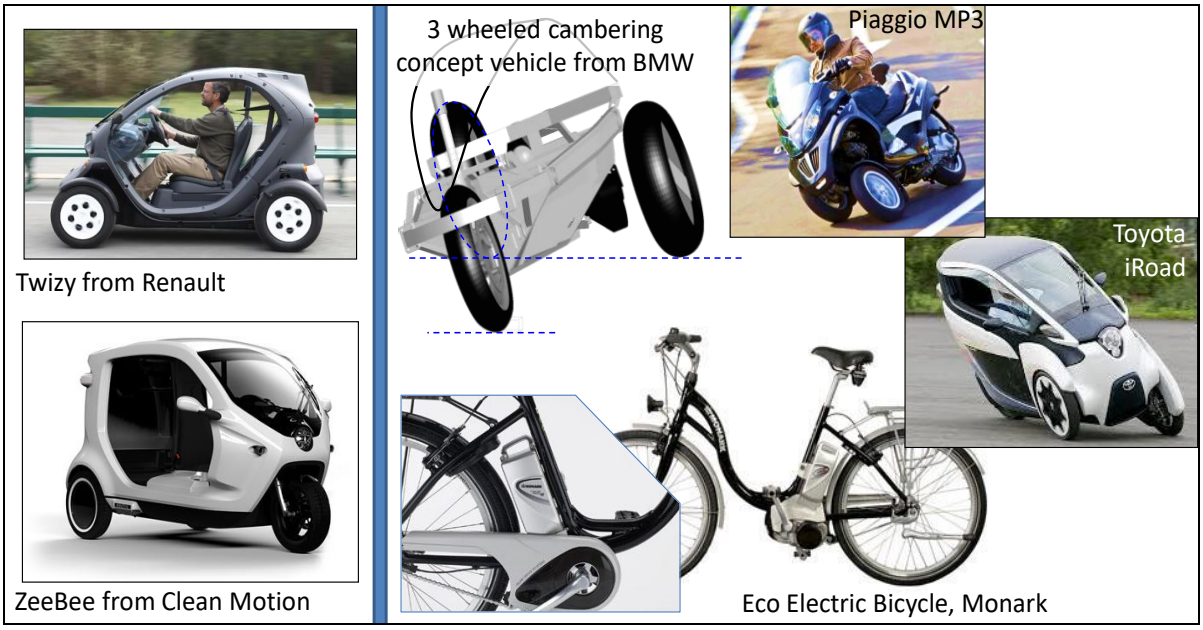

Figure 1-31: Examples of Urban Personal Vehicles. Left: "Roll-stiff". Right: "Cambering". From www.motorstown.com, www.cleanmotion.se, www.monarkexercise.se, www.nycscootering.com.

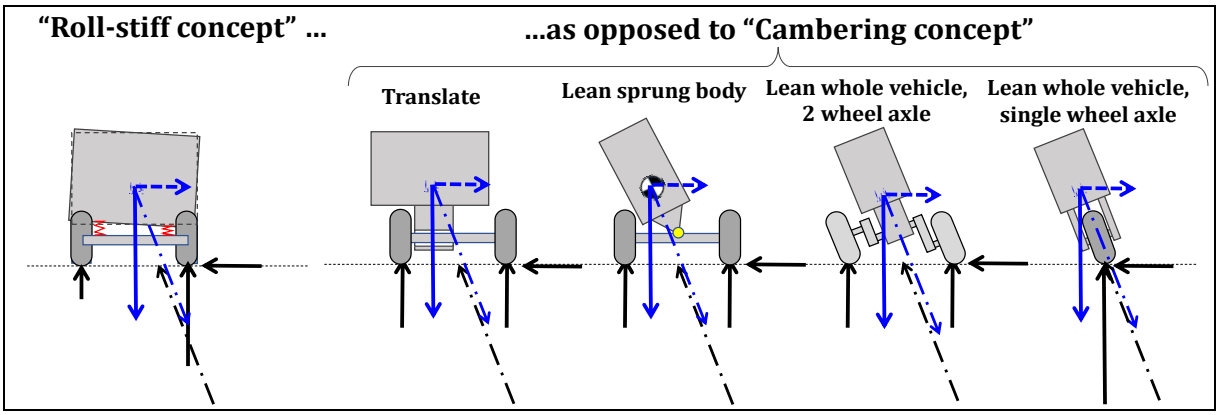

Figure 1-32: How Cambering vehicles avoid taking the roll moment while cornering. The vehicles are viewed from rear and turns to the left. The dash-dotted arrows mark the resulting forces which are equal between the 5 concepts.

1.8 Notation and Notation List

Table 1.3 shows notation of parameters, variables and subscripts used in this compendium. The intention of this compendium is to follow International Standards (ISO 8855), but deviations from this is sometimes used, especially motivated by conflicts with areas not covered by (ISO 8855). Some alternative notations are also shown, to prepare the reader for other frequently used notation in other literature.

The list does not show the order of subscripting. For example, it does not show whether longitudinal (x) force (F) on rear axle (r) should be denoted F_{rx} or F_{xr}. The intention in this compendium is to order subscript with the physical vehicle part (here rear axle) as 1st subscript and the specification (longitudinal, x) as 2nd, leading to F_{rx}. If there are further detailed specifications, such as coordinate system, e.g. wheel coordinate (w), it will be the 3rd subscript, leading to F_{rxw}. Further additional specifications, such as case, e.g. without (0) or with (1) a certain technical solution, will be the 4th subscript, leading to F_{rxw0} and F_{rxw1}. If subscripts have >1 token, it can sometimes be good to use comma, e.g. $F_{rear,x,wheel,with}$.

Naming of variables (signals), parameters and function components (blocks) is often important in large products as vehicles. Some naming needs to be readable for many engineers, such as CAN signals. Hence, companies developing their own naming standards. But also, the standardization organisation AUTOSAR has released a naming standard, with intention to be accepted by both vehicle manufacturers and system suppliers.

Table 1.3: Notation

Categorization			Notation				
			Recommended		Alternatives		
		Subject for notation	in code	*by hand*		Unit	Description / Note
1. General	Basic	(Shaft) Torque	T	T	M	Nm	
	Basic	Coefficient of friction	mu	μ	mue, muh	1=N/N	
	Basic	Damping coefficient	d	d	c,k,D	N/(m/s) or Nm/(rad/s)	
	Basic	Density	roh	ρ			
	Basic	Efficiency	eta	h η		1=W/W	Ratio between useful/output power and used/input power
	Basic	Energy	E	E	W	Nm=J	
	Basic	Force	F	F	f	N	
	Basic	Gravity	g	g		m/s^2	9.80665 average on Earth
	Basic	Height	h	h	H		
	Basic	Imaginary unit	j	j	i	-	j*j=-1
	Basic	Mass	m	m	M	kg	
	Basic	Mass moment of inertia	J	J	I	$kg*m^2$	Subscript can be given to denote around which axis
	Basic	Moment (of forces)	M	M	T	Nm	Not for shaft torque
	Basic	Power	P	P		W=Nm/s=J/s	
	Basic	Ratio	r	r	u, i (ISO8855)	Nm/(Nm) or (rad/s)/(rad/s)	Ratio between input and output rotational speed, or output and input torque, in a transmission
	Basic	Rotational speed	w	ω	ω	rad/s	
	Basic	Shear stress	tau	τ		N/m^2	
	Basic	Stiffness coefficient	c	c	C, k, K	N/m or Nm/rad	
	Basic	Strain	eps	ε		m/m	
	Basic	Translational speed	v	v	V	m/s	
	Basic	Wave length	lambda	λ		m	
	Basic	Width	W	W	w	m	Can be track width, vehicle width, tyre width, ...
	Dynamics	(Time) Frequency	f	f		1/s=periods/s	
	Dynamics	Angular (time) frequency	w	ω	ω	rad/s	
	Dynamics	Angular spatial frequency	W	Ω		rad/m	
	Dynamics	Dependent variables in a dynamic system	z	z		<various>	Both state variables and output variables
	Dynamics	Input variables in a dynamic system	u	u		<various>	
	Dynamics	Mean Square value	MS	MS			
	Dynamics	Output variables in a dynamic system	y	y		<various>	
	Dynamics	Power spectral density	G	Φ	PSD		
	Dynamics	Root Mean Square value	RMS	RMS			
	Dynamics	Spacial frequency as radians per travelled distance	W	Ω		rad/m	
	Dynamics	Spatial frequency	fs	f_s		1/m=periods/m	
	Dynamics	States variables in a dynamic system	x	x		<various>	
	Dynamics	Time	t	t	τ, T	s	The independent variable in a dynamic system
	Operators	Transfer function	H	H			
2. Vehicle	1. General	Air resistance coefficient	cd	c_d	Cd	1	
	1. General	Cornering stiffness or lateral tyre stiffness	Cy	C_y	C_α	N/rad or N/1	$dF_y/da = dF_y/ds_y$ at $a=s_y=0$
	1. General	Longitudinal tyre stiffness	Cx	C_x		N/1	df_{yw}/ds_x at $s_x=0$

Categorization			Notation				
			Recommended		Alternatives		
		Subject for notation	in code	*by hand*		Unit	Description / Note
2. Vehicle	1. General	Mass	m	m	M	kg	
	1. General	Rolling resistance coefficient	f	f		1=N/N	
	1. General	Track width	W	W		m	
	1. General	Tyre stiffness	C	C	c	N/1	*dF/ds at s=0*
	1. General	Understeer gradient	Ku	K_u	Kus, kus, U (ISO8855)	N/(N/rad) = rad/(m/s^2)	
	1. General	Vehicle side slip angle	b	β	β	rad	If no subscript, undefined or CoG
	1. General	Wheel base	L	L	l, lf+lr, WB	m	
	1. General	Wheel radius	R	R	r, Rw	m	
	2. Road	Curvature	kappa	κ	roh, ρ	rad/m=1/m	road or path
	2. Road	Curve radius	R	R	r, roh, ρ	m	road or path
	2. Road	Road bank angle	pxr	φ_{xr}			Positive when right side of ground is lower than left side ground
	2. Road	Road inclination angle	pyr	φ_{yr}		rad	Positive downhill
	2. Road	Vertical position of road	zr	z_r	z, Z	m	
	3. Motion	Vehicle acceleration, in interial system	ax, ay, az	a_x, a_y, a_z		m/(s^2)	decomposed in vehicle coordinates direction
	3. Motion	Time derivatives of each component v_x, v_y, v_z	dervx, dervy, dervz	$\dot{v}_x, \dot{v}_y, \dot{v}_z$	der(vx), der(vy), der(vz)	m/(s^2)	decomposed in vehicle coordinates direction
	3. Motion	Vehicle position	x,y,z	x, y, z	r=[rx,ry,rz] or [X,Y,Z]	m	often position of Center of Gravity, CoG
	3. Motion	Vehicle velocity, in interial system	vx,vy,vz	v_x, v_y, v_z	u,v,w	m/s	decomposed in vehicle coordinates direction
	4. Forces	Forces and moments on vehicle	Fx, Fy, Fz, Mx, My, Mz	$F_x, F_y, F_z, M_x, M_y, M_z$		[N, N, N, Nm, Nm, Nm]	From ground, air, towed units, colliding objects, etc. May appear also for in road plane: F=[Fx, Fy, Mz]
	4. Forces	Forces on one wheel, axle or side from ground	Fix,Fiy,Fiz	F_{ix}, F_{iy}, F_{iz}	lowercase f	N	Subscript "i" is placeholder for particular wheel, axle or side. May appear also extended with moments: [Fx, Fy, Fz, Mx, My, Mz]
	4. Forces	Forces on one wheel, axle or side from ground	Fixv, Fiyv,Fizv	$F_{ixv}, F_{iyv}, F_{izv}$	lowercase f	N	in vehicle coordinate system
	4. Forces	Forces on one wheel, axle or side from ground	Fixw,Fiyw ,Fizw	$F_{ixw}, F_{iyw}, F_{izw}$	lowercase f	N	in wheel coordinate system
	5. Angles	Camber angle	g	γ	γ	rad	Sign convention positive when either of "rotated as wheel roll angle" or "top leaning outward vs vehicle body".
	5. Angles	Low speed or Ackermann speed steering wheel angle	dswA	δ_{swA}		rad	The angle required for a certain vehicle path curvature at low speeds
	5. Angles	Euler rotations		ψ, θ, φ		rad	Order: yaw, pitch, roll
	5. Angles	Roll, pitch, yaw angle	px, py, pz	$\varphi_x, \varphi_y, \varphi_z$	φ, θ, ψ	rad	Angles, not rotations. Roll and Pitch normally small
	5. Angles	Vehicle angular velocity, in interial system	wx, wy, wz	$\omega_x, \omega_y, \omega_z$	$[\dot{\varphi}, \dot{\theta}, \dot{\psi}]$.$[\dot{\varphi}, \dot{\theta}, \Omega]$	rad/s	decomposed in vehicle coordinates direction (roll, pitch, yaw)
	5. Angles	Steering angle	d	δ	delta	rad	May refer to steering wheel, road wheel or axle
	5. Angles	Steering angle of road wheels	drw	δ_{rw}	RWA	rad	Normally an average of angles on front axle

Categorization			Notation				
			Recommended		Alternatives		
		Subject for notation	in code	by hand		Unit	Description / Note
2. Vehicle	5. Angles	Steering angle of steering wheel	dsw	δs_w	SWA	rad	
	6. Slip	Tyre (lateral) slip angle	a	α	alpha	rad	a=arctan(sy)
	6. Slip	Tyre lateral slip	sy	s_y		1= (m/s)/(m/s)	sy=tan(a)
	6. Slip	Tyre longitudinal slip	sx	s_x	κ, $-\kappa$		
	6. Slip	Tyre slip	s	s			
	7. Subscript	axle	a	a			used e.g. as Ca=cornering stiffness for any axle
	7. Subscript	centre of gravity	CoG	CoG	COG, cog, CG, cg		
	7. Subscript	front	f	f	F, 1		Often used as double subscript, e.g. fr=front right
	7. Subscript	inner	i	i			Often means with respect to curve
	7. Subscript	left	l	l	L		Often used as double subscript, e.g. fl=front left
	7. Subscript	outer	o	o			Often means with respect to curve
	7. Subscript	rear	r	r	R, 2		Often used as double subscript, e.g. fr=rear right
	7. Subscript	road	r	r			
	7. Subscript	road wheel	rw	rw	RW		E.g. drw=road wheel steering angle
	7. Subscript	sprung mass	s	s			
	7. Subscript	steering wheel	sw	sw	SW, H (ISO8855)		E.g. dsw=steering wheel angle
	7. Subscript	unsprung mass	u	u	us		
	7. Subscript	vehicle	v	v			used e.g. as F1v to denote wheel force on wheel 1 in vehicle coordinates
	7. Subscript	wheel	w	w			used e.g. as F1w to denote wheel force on wheel 1 in wheel coordinates
3. Subsystem in vehicles	1. Propulsion	Engine torque	Te	T_e		Nm	
	1. Propulsion	Propulsion torque	Tprop	T_{prop}		Nm	often expressed at wheel
	2. Brake	Brake torque	Tbrk	T_{brk}		Nm	
	3. Steering	Steering wheel torque	Tsw	T_{sw}	SWT	Nm	
	4. Suspension	Caster angle	CA			rad	
	4. Suspension	Caster offset	c			m	
	4. Suspension	Kingpin inclination angle	KPI			rad	
	4. Suspension	Pneumatic trail	t			m	
	4. Suspension	(Wheel) Camber angle		φ_{Camber}		rad	

1.9 Typical Numerical Data

The purpose of the tables in this section is to give approximate numerical values of parameters. Vehicle parameters are often dependent on each other; changing one leads to that it is suitable to change others. The parameters are given with the intention to be consistent with each other, for each vehicle example. The tables balance between being generic and specific, which is difficult. Therefore, please consider the table as very approximate.

1.9.1 For Passenger Vehicle

Table 1.3 gives typical numerical data for a medium sized passenger car.

Table 1.4: Typical values of parameters, common for typical passenger cars and heavy trucks

Parameter	Notation	Typical Value		Unit
		Passenger car	Heavy truck	
Air density	roh	1		kg/(m^3)
Earth gravity	g	9.80665		m/(s*s)
Road friction, at dry asphalt	mu	1.0		N/N
Road friction, at wet asphalt		0.6		
Road friction, at snow		0.3		
Road friction, at wet ice		0.1		
Tyre Cornering Coefficient (lateral slip coefficient), i.e. slip stiffness normalized with vertical load	CCy	10..15	5..10	(N/rad)/N = (N/1)/N
Ratio of tyre longitudinal and lateral slip coeffcient stiffness	CCx/CCy	1.5..2		1

Table 1.5: Typical data for a passenger vehicle

Group/Type	Parameter	Notation	Typical Value	Unit	Note / Typical / Range / Relation to other
Vehicle	Length, bumper to bumper		5.00	m	
Vehicle	Longitudinal distance from CoG to front axle	lf	1.3	m	40-50% of wheel base: lf=0.55*L;
Vehicle	Mass	m	1700	kg	
Vehicle	Moment of inertia for yaw rotation	Jzz	2900	kg*m*m	Radius of gyration is sligthly less (0.9) than half wheel base: =m*(0.9*L/2)^2
Vehicle	Unsprung mass	mus	200	kg	Sum of 4 wheels with suspensions
Vehicle	Track width	W	1.70	m	
Vehicle	Wheel base	L	2.90	m	
Vehicle	Projected area in a transversal view	Afront	2	m^2	For calculation of air resistance. Examples: Volvo XC90 has 2.78 m^2, Volvo S60 has 2.27 m^2
Vehicle	Aerodynamic coefficients	cd, clf, clr	0.31, 0.10, 0.07	1	For calculation of longitudinal resistance and lift force over front and rear axle
Wheel and Tyre	Rolling resistance		0.01	N/N	
Wheel and Tyre	Wheel radius		0.30	m	
Wheel and Tyre	Wheel rotational inertia		0.5	kg*m*m	For one wheel
Wheel and Tyre	Tyre vertical stiffness	ct	250 000	N/m	For one wheel
Propulsion	Engine inertia		0.5	kg*m*m	
Propulsion	Transmission ratio, highest gear		5.00	rad/rad= Nm/Nm	Engine to wheel. In magnitude of 5.
Propulsion	Transmission ratio, lowest gear		10.00	rad/rad= Nm/Nm	Engine to wheel. In magnitude of 10.
Brake	Brake proportioning, front/rear		70/30	N/N or Nm/Nm	Often tuned so that braking both axles when braking 0.8*g
Steering	Steering ratio		16	rad/rad	Steering wheel to Road wheel
Suspension	Suspension heave stiffness (without roll)	cs	100 000	N/m	Vertical stiffness at wheel. Sum of 4 wheels. So that bounce frequency f is between 1 and 2 Hz: sqrt(c/m)=f*2*pi; Bump stop at (3..4)*g when fully loaded.
Suspension	Suspension roll stiffness, only from anti-roll-bars	carb	14 000	N/m	Vertical stiffness at wheel. Sum of both axles.
Suspension	Suspension damping	ds	13 000	N/(m/s)	Wheel rate. Sum of 4 wheels. Some 40..60% of critical damping: d = (0.4..0.6)*2*sqrt(c*m); 2..3 times softer in compression than rebound.

1.9.2 For Heavy Vehicle

Compared to passenger cars, trucks differ much more in size and configuration, see Figure 1-30. Also, a certain individual vehicle also differs much more between empty and fully loaded. Globally, "Tractor with Semitrailer" is the most common heavy vehicle, which is why it is used as example.

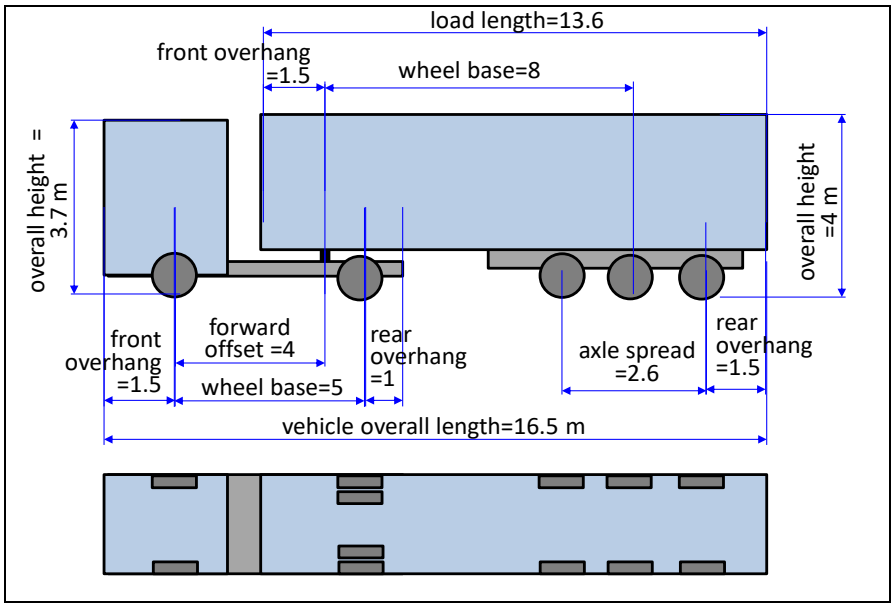

Figure 1-33: Typical data for a heavy vehicle, exemplified with "Tractor with Semi-trailer"

Table 1.6: Typical data for a heavy vehicle, exemplified with "Tractor with Semi-trailer"

Group/Type	Parameter	Typical Value Empty	Typical Value With max payload	Unit	Note / Typical / Range / Relation to other
Vehicle	Trackwidth, centre-to-centre for single tyres	2.25		m	Outer tyre edge 2.55
Vehicle	Projected area in a transversal view	10.0		m^2	For calculation of air resistance
Vehicle	Aerodynamic coefficient	0.4..0.6		1	c_d coefficient in aero dynamic resistance formula (normal truck 0.4, long combination truck 0.6)
Tractor	CoG heigth	1.00		m	
Tractor	Mass (total), tractor	7500		kg	
Tractor	Moment of yaw inertia	22500		kg*m*m	Around unit CoG
Tractor	Unsprung mass	1700		kg	Sum of all axles at unit
Semitrailer	CoG heigth	1.00	2.00	m	
Semitrailer	Mass (total), semi-trailer	10000	32500	kg	
Semitrailer	Moment of yaw inertia	150000	500000	kg*m*m	Around unit CoG
Semitrailer	Unsprung mass	2400		kg	Sum of all axles at unit
Wheel and Tyre	Wheel radius	0.50		m	0.4-0.5
Wheel and Tyre	Wheel rotational inertia	10.0		kg*m*m	For one wheel, single tyre
Wheel and Tyre	Rolling resistance	0.005		N/N	Or less, 0.003
Propulsion	Engine max power	370		kNm/s=kW	
Propulsion	Engine inertia	5		kg*m*m	
Propulsion	Transmission ratio, highest gear	3		1=rad/rad =Nm/Nm	Engine to wheel
Propulsion	Transmission ratio, lowest gear	30			Engine to wheel
Steering	Steering ratio	20		rad/rad	Steering wheel to Road wheel
Steering	Steering wheel rotational inertia	0.04		kg*m^2	Steering wheel to Road wheel

2 VEHICLE INTERACTIONS AND SUBSYSTEMS

2.1 Introduction

The study of vehicle dynamics starts with the interfaces between the vehicle and its environment, see Figure 2-1. The vehicle tyres are the primary force interface for all motion (in road plane, i.e. acceleration, steering, braking) but also undesired disturbances (out-of- road plane, i.e. road unevenness, road bumps, etc.). Additionally, the aerodynamic loads on the vehicle will create forces that are often undesirable (wind resistance, side gusts, etc.) but can sometimes be exploited for better contact with the road (down-force). An example of extreme interactions to the vehicle is the impact forces from a crash. An interaction of another kind is the driver. One often divides the whole system into 3 parts: vehicle, driver and environment, see Figure 2-1. Driver and environment can often be clustered as 2.9 Driving and Transport Application, which includes all outside subject vehicle. Some aerodynamic models are given in 2.8. Driver models are discussed with some selected example models, see 2.9.2.

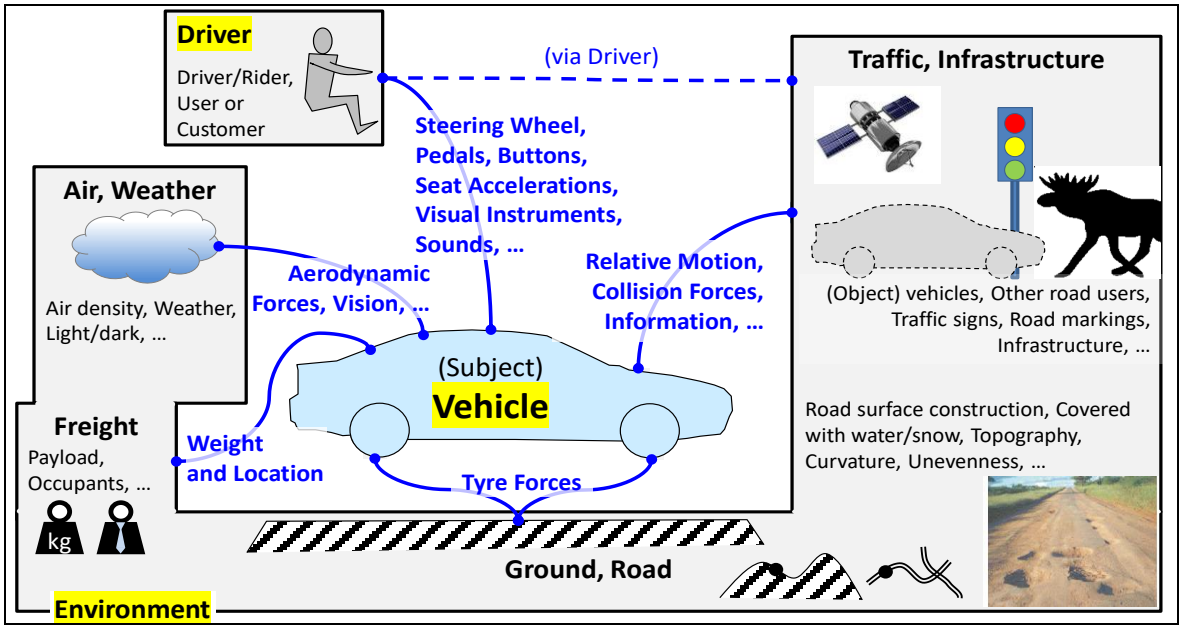

*Figure 2-1: How the **vehicle** interacts with **driver** and **environment**.*

The chapter also contains descriptions of the subsystems which are most relevant for Vehicle Dynamics, with focus on Wheels and Tyres, see Figure 2-2.

2.1.1 References for this Chapter

- Tyres: (Pacejka, 2005), (Rill, 2006), and (Michelin, 2003)
- Vehicle Aerodynamics: Reference (Barnard, 2010)
- Driver models: *"Chapter 38 Driver Models in Automobile Dynamics Application"* in Reference (Ploechl, 2013)

2.2 Wheels and Tyres

2.2.1 Introduction

The wheels and tyres of a vehicle have the following tasks:

- Carry the vertical load F_z
- Transmit longitudinal forces F_x (propulsion $F_x > 0$ and brake $F_x < 0$)
- Transmit lateral forces F_y (steering)

To minimize negative effects, we can also list these:

- Roll with minimum **energy** loss, minimum tyre **wear**, minimum **particle emissions** and **noise**
- Isolate **disturbances**, mainly vertical. This includes also to not cause disturbances, which overall means that the wheel and tyre should be round and balanced.

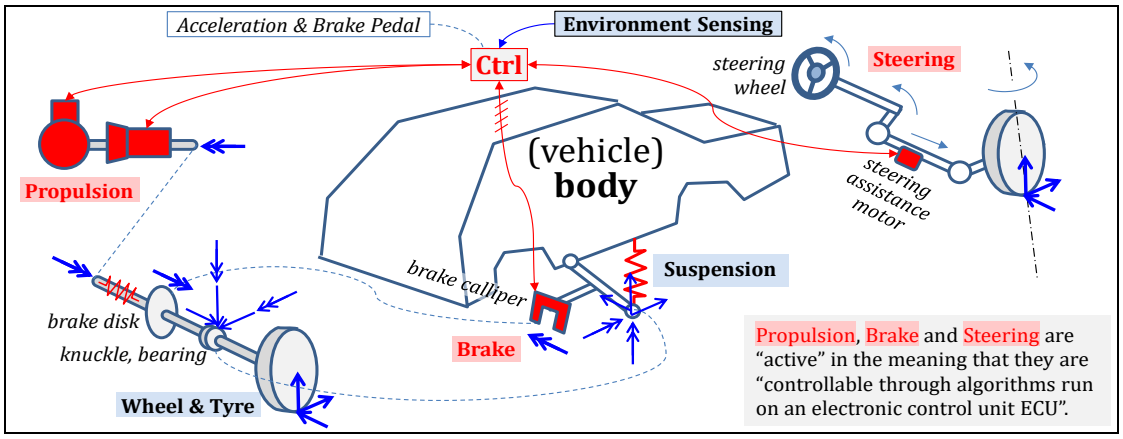

Figure 2-2: Vehicle with the 6 Vehicle Dynamics relevant subsystems: Wheels and Tyres, Suspension, Propulsion, Brake, Steering, and Environment Sensing. Towed units, with similar subsystems, are not shown.

2.2.1.1 Wheel Integration in Suspension

To understand the "force flows" of a wheel, it is good to understand the conceptual integration, regarding shaft, brake disks and wheel bearings. Cars typically have their inner bearing rings rotating with the wheel, while trucks instead have outer rings rotating, see Figure 2-3.

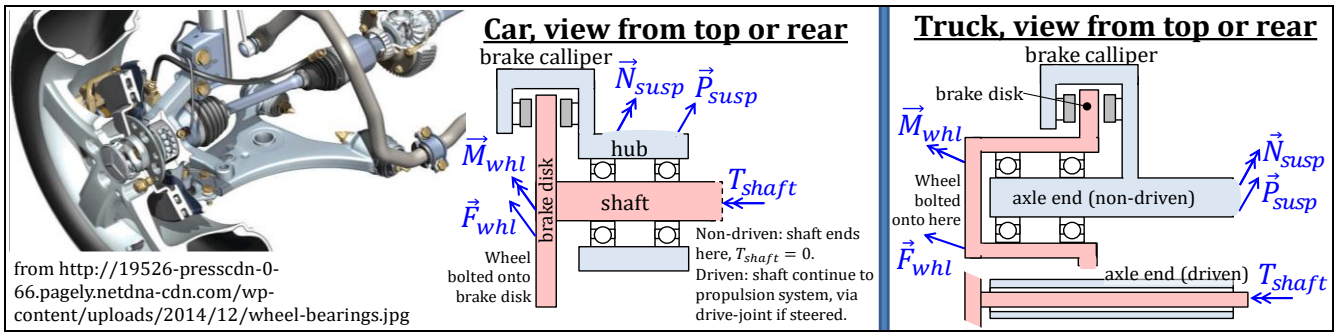

Figure 2-3: Concepts of wheels are typically integrated. All vectors are 3D, while moment $\vec{N}_{xz}$ is 2D in the wheels xz-plane and moment T_{shaft} is perpendicular to the same plane.

2.2.1.2 Tyre Design

Before discussing the mechanics of tyre and road interactions, the physical structure of the wheel assembly should be understood. Consisting of a steel rim and an inflated rubber toroid, pneumatic tyres were invented and patented by Robert William Thomson in 1845 and are essentially the only type of tyre found on motor vehicles today.

The physical construction of the tyre carcass affects the response of the tyre to different road loadings. The carcass is a network of fabric and wire reinforcement that gives the tyre the mechanical strength. The structure of the carcass can be different: Bias-ply, Bias-ply Belted, and Radial-ply, see Figure 2-4. Bias-ply tyres were the first types of pneumatic tyres to be used on motor vehicles. Radial ply tyres followed 1946 and became the standard for passenger cars and is today also dominating also on trucks.

Note how the bias-ply constructions have textile structures oriented at an angle to the tyre centreline along the x-z plane. This angle is referred to as the crown angle and is further illustrated in Figure 2-4. Note the textile orientation for the bias-ply and radial tyres. Also note the difference in crown angles

between the two tyre constructions. This difference plays an important part in the rolling resistance characteristics of the tyre which is 2.2.1.6.

The tyre components in Figure 2-4 have been constructed to provide the best tyre performance for different loading directions. Trade-offs are necessary between handling performance and comfort, between acceleration and wear, as well as between rolling resistance and desired friction for generating forces in ground plane. The rubber components and patterns incorporated in the tread are critical to the friction developed between the tyre and road under all road conditions (wet, dry, snow, etc.). Friction is most relevant in longitudinal and lateral vehicle dynamics. The belts define the circumferential strength of the tyre and thus braking and acceleration performance. The sidewall and plies define the lateral strength of the tyre and thus influence the lateral (cornering) performance of the vehicle. The sidewall as well as the inflation pressure are also significant contributors to the vertical stiffness properties of the tyre and affect how the tyre transmits road irregularities to the remainder of the vehicle. A tyre that has strong sidewalls will support vertical load well, but at the cost of vertical compliance.

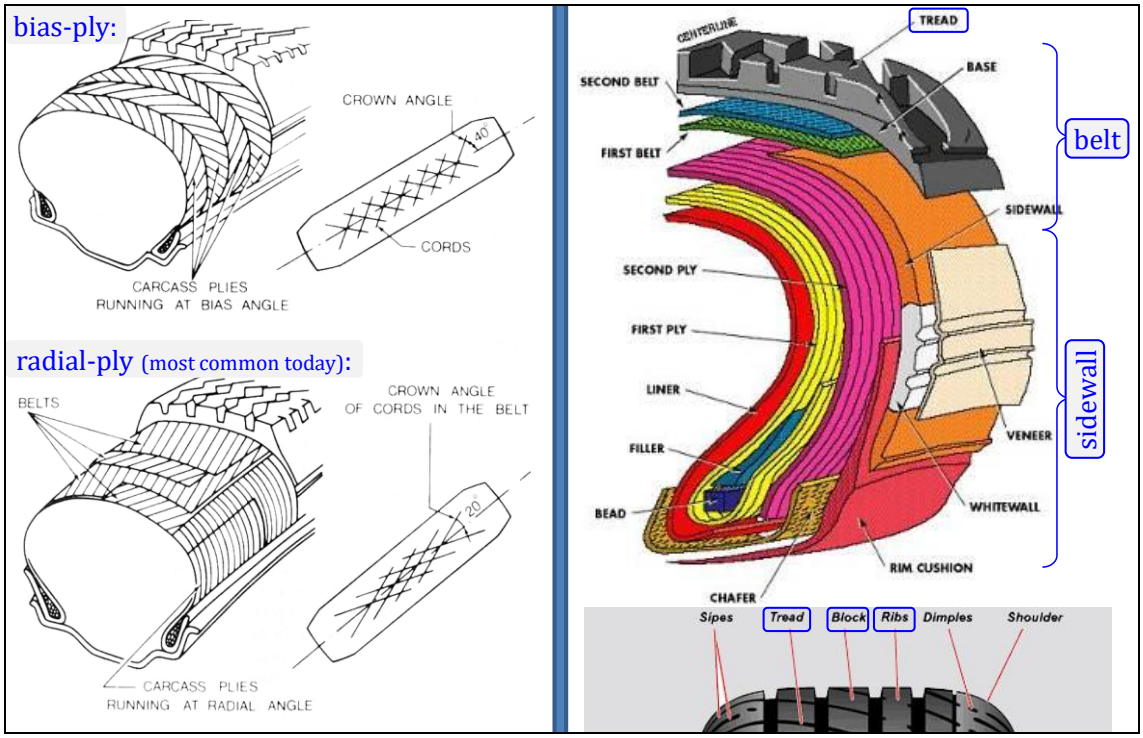

Figure 2-4: Left: Carcass Construction, (Wong, 2001). Left top: Bias-ply construction. Left bottom: Radial construction. Right: Radial Tyre Structure, (Cooper Tire & Rubber Co., 2007).

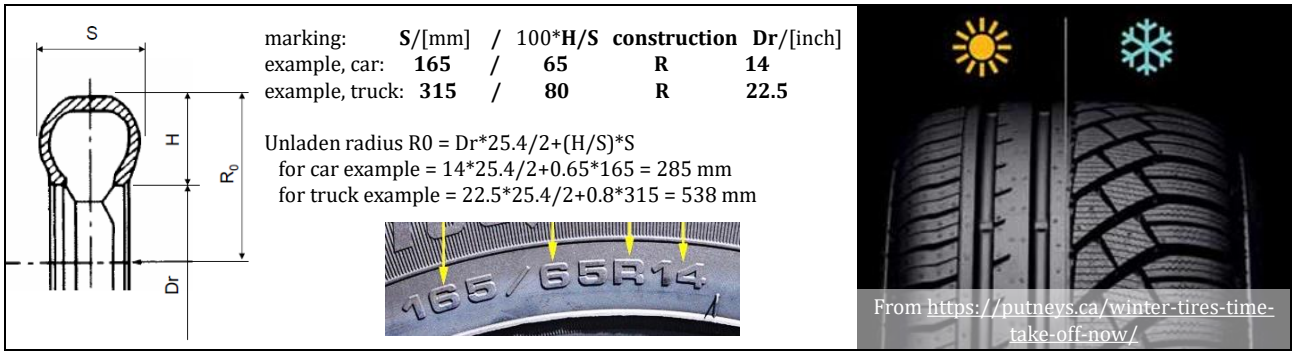

Figure 2-5: Left: Tyre marking (radial tyre). Right: Typical summer and winter tread patterns.

2.2.1.3 Wheel Angles

A wheel or a tyre is best described in its own coordinate system, see Figure 2-6. The 3 forces and 3 moments are acting on the wheel from the ground. The other quantities, such as slip angle α and camber

angle ε_w, in Figure 2-6 are examples of variables which have influence on the forces and moments in the coming chapters.

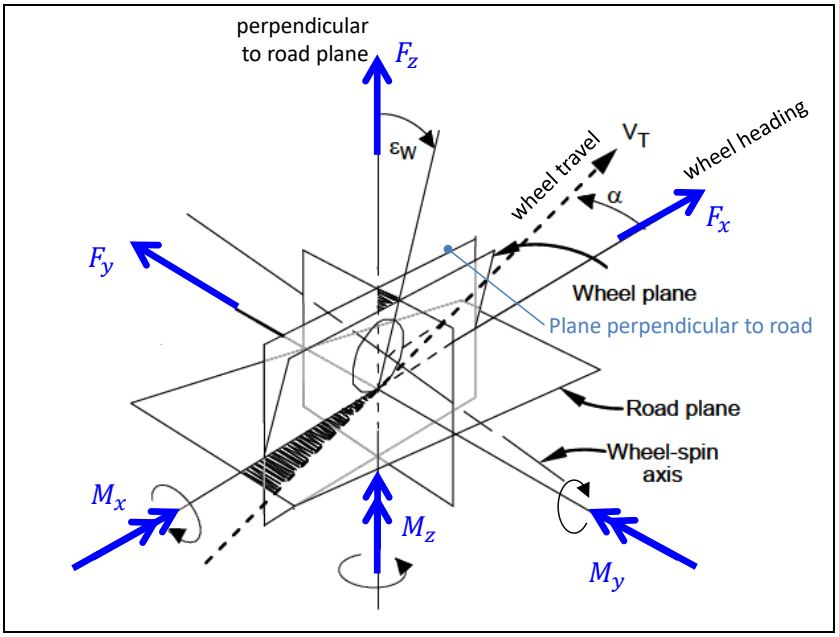

Figure 2-6: Tyre coordinate system. Forces and moments on tyre from ground. From (ISO 8855).

2.2.1.3.1 Steer Angle

A wheel on a vehicle has a *Steer angle*, δ. The Steer angle is the angle from vehicle longitudinal axis to the wheel plane about the vehicle vertical axis (ISO 8855). Assuming vehicle xy-plane is parallell to road plane, this angle is same as angle from vehicle longitudinal axis to the intersection between wheel plane and road plane.

2.2.1.3.2 Camber Angle

A wheel on a vehicle on a road surface has a *Camber angle*. The Camber angle is the angle from vehicle longitudinal axis to the wheel plane about the vehicle longitudinal axis (ISO 8855). Assuming vehicle xy-plane is parallell to road plane, this angle is same as the deviation from right angle between wheel plane and road plane. A symmetry within an axle means that camber angle typically has opposite signs on left and right wheel. However, for two-track vehicles, one can often see the sign convention that a wheel top leaning outward from vehicle body is negative, regardless of on left or right side.

2.2.1.3.3 Steer and Camber

If a wheel has both significant Steer angle and significant Camber angle at the same time, these angles alone does not define the orientation, since steering-before-cambering gives another orientation than cambering-before- steering. One way is to express the orientation in a rotational angle around the steering axis, see 2.2.1.3.5. An alternative is to use the concept of Euler rotations.

2.2.1.3.4 Castor Angle

A wheel, suspended to be steered, has a *Castor angle* (or *Caster angle*). This is the angle between the vehicle vertical axis and the projection of the steering axis (2.2.1.3.5) on the vehicle xz-plane (ISO 8855). Castor angle is positive when top of steering axis is inclined rearward. Castor angle provides an additional aligning torque, see 2.2.4.6 and 0, and changes the Camber angle when the wheel is steered.

2.2.1.3.5 Steering Axis Inclination

A wheel, suspended to be steered, has a *Steering axis inclination* (or *Kingpin inclination*).
This is the angle between the vehicle vertical axis and the projection of the steering axis (2.2.1.3.5) on the vehicle yz-plane (ISO 8855). *Steering axis inclination* is positive when top of steering axis is inclined inward. See also 0.

2.2.1.3.6 Static Toe Angle

A wheel on an axle has a *Static toe angle* (a.k.a. *Toe-in*). The Static toe angle is the angle between vehicle longitudinal axis and the wheel plane about the vehicle vertical axis, with the vehicle at rest and steering in the straight-ahead position (ISO 8855). Positive Static toe angle (a.k.a. *Toe-in* or *"−Toe-out"*) is when forward portion of the wheel is closer to the vehicle centreline than the wheel centre.

Typically, left and right wheel on same axle has same Static toe angle. Hence it measures an axle property rather than a wheel property.

One could define an "instantaneous toe angle", for an axle during arbitrary vehicle operation (non-rest and non-zero steering), as $(\delta_{right} + (-\delta_{left}))/2$. This will have a different value than Static toe angle due to suspension linkage geometry and elasticity in suspension bushings.

Toe (regardless of toe-in or toe-out) generally generates opposing lateral forces on left and right side leading to propulsion energy loss and tyre wear. Toe-out on front axle and toe-in on rear axle makes the vehicle more yaw stable (less over-steered). Tone-in on front axle makes vehicle more yaw agile but it also improves on-centre steering feel. Normal design choice for a passenger car is positive Static toe angle (Toe-in) on both axles, and more on front axle.

2.2.1.4 How Tyres Carries Vertical Load

Figure 2-7 shows how a pneumatic tyre carries the vertical load. In a traditional bicycle or motorbike wheel, the pre-tensioned spokes have a similar role as the air and rubber parts of a pneumatic tyre.

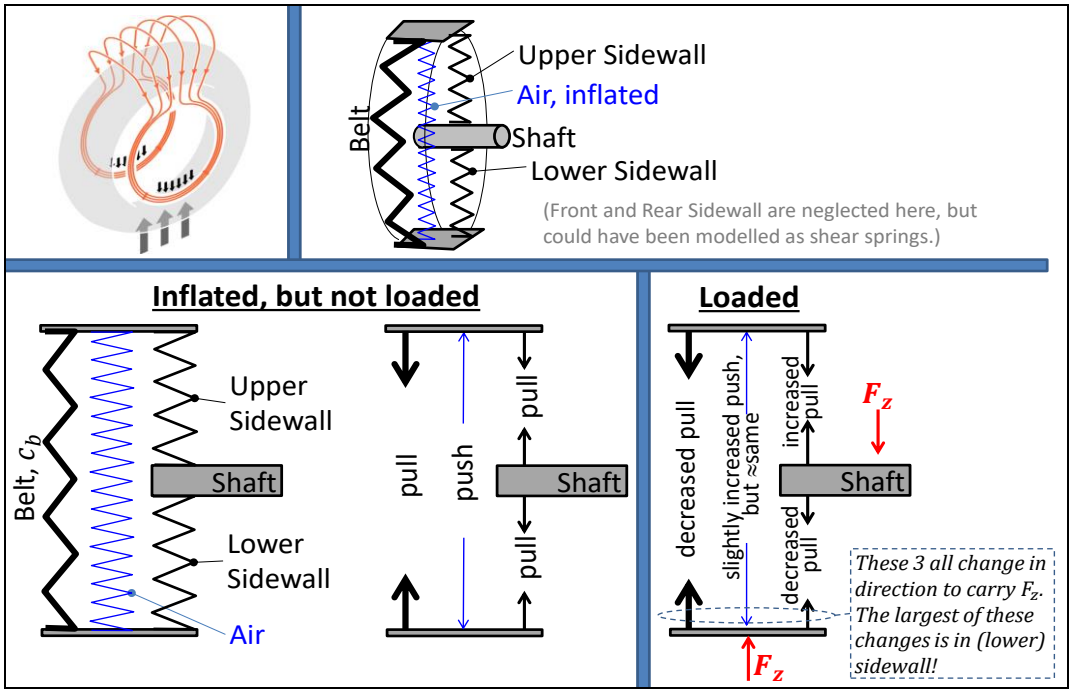

Figure 2-7: A pneumatic tyre is pre-tensioned by inflation pressure. This figure explains how the wheel and tyre takes (vertical) load without (significant) increase of inflation pressure.

2.2.1.5 Tyre Model Architecture

This section describes how a tyre model can be instantiated once per wheel and integrated in a model together with models of vehicle, driver, and environment. It is often difficult and seldom useful to distinguish exactly which is the model of the wheel and the tyre, respectively. We then need to differ between parameters and variables. The description assumes dynamic models used for simulation over time domain. Within each simulation, parameters are constant, but variables can vary. If design optimization, as opposed to simulation, the design parameters also has a role of variables (i.e. they are varied) in the optimization, but not in time domain.

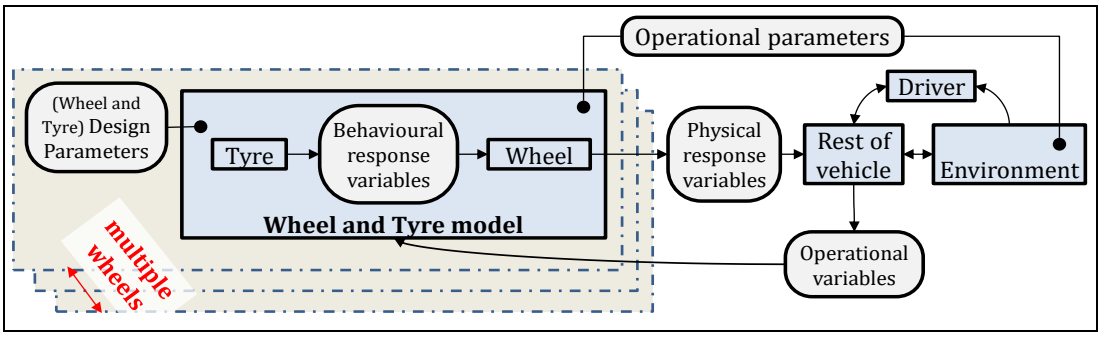

Figure 2-8: How wheel and tyre models can come into a model context.

2.2.1.5.1 (Wheel and Tyre) Design Parameters

We limit ourselves to today's traditional pneumatic tyres. Then the design is captured by:

- Carcass/Material: Rubber quality and plies arrangement.
- Tread/Grooves: Groove pattern, Groove depth, Tread depth, Spikes pattern (if spikes)
- Main dimensions: Outer radius, Width, Aspect ratio
- Installation parameters: Inflation pressure

2.2.1.5.2 Operational Parameters

These are operating conditions which vary slowly, and in this description assumed to be constant during one manoeuvre/driving cycle. These are:

- Road surface (dry/wet, asphalt/gravel/snow/ice, …)
- Road compliance and damping (hard/soft, …)
- Wear state of tyre
- Age of tyre
- Temperature

2.2.1.5.3 Operational Variables

These are operating conditions which vary quickly, and in this description assumed to be variable in time during one manoeuvre/driving cycle. These are:

- Tyre velocities (v_x, v_y, ω) or Tyre slip (s_x and s_y or α)
- Vertical tyre force, (F_z)
- Camber angle

The wheel's rotational velocity, ω, can be contained in *Wheel and Tyre model* instead of inside *Model of rest of the vehicle*, which would mean that ω will not be part of the *Operational variables* interface.

Tyre forces in road plane (F_x, F_y) can be given instead of tyre slip. Another alternative is to give the corresponding actuation, e.g. wheel shaft torque and wheel steer angle relative to wheel course angle. With those setups, the response variables in 2.2.1.5.4.

Vertical tyre force can be modelled as arbitrarily varying in time or as an offset amplitude for different frequencies where offset is from a mean value. The mean value would then be a parameter instead of a variable. The latter alternative can be more efficient if simulating a longer driving cycle, where following each road wave would be very computational inefficient.

2.2.1.5.4 Response Variables

Response refers to response to Operational variables changes.

2.2.1.5.4.1 Physical Response Variables

The variables from tyre model to model of rest of the vehicle is essential the forces and moments, see Figure 2-6:

- Longitudinal and lateral forces (F_x, F_y)
- Roll moment or Overturning moment (M_x)
- Rolling resistance moment (M_y)

- Spin moment or Aligning moment (M_z)

Other responses are:

- Wear rate [worn rubber mass or tread depth per time unit]
- Loaded radius (R_l)

2.2.1.5.4.2 Behavioural Response Variables

The Responses can be modelled as Behavioural variables:

- Slip characteristics (slip stiffnesses C_{sx}, C_{sy} $[N/1]$, peak friction coefficient, … or other parameters in physical or empirical tyre slip model, as in 2.2.3.4 and 2.2.4.3)
- Rolling resistance coefficient and Loaded radius (R_l)
- Vertical stiffness and damping coefficients
- Wear coefficient, Relaxation lengths or deformation stiffnesses $[N/m]$, …

One can select to not introduce Behavioural response variables but only use Physical response variables. If Behavioural response variables are introduced, one should consider them as special from DAE point of view, e.g. they can be difficult to differentiate. Also, they require an agreed definition to be interpreted, which is the reason to why they are not proposed as interface variables to the vehicle model.

2.2.1.6 The Wheel as a Transmission

The whole wheel, rim and tyre, can be seen as a transmission from rotational mechanical power to translational mechanical power. The shaft is on the rotating side; where we find rotational speed, ω, and the torque, T. The torque T is then the sum of torque on the propulsion shaft and torque on the brake disk or drum. The wheel hub is on the translating side of the transmission; were we find translating speed, v_x, and force, $F_{hub,x}$. See Figure 2-9. Normally, we approximate and denote $F_{ground,x} = F_{hub,x} = F_x$ and $F_{ground,z} = F_{hub,z} = F_z$.

If we neglect deformation of tyre/ground and sliding, we find the intended function of the wheel: $v_x = radius \cdot \omega$; and $F_x = T/radius$;. There will be force losses which makes F_x smaller, see rollnig resistance in 2.2.2, and speed losses which makes v_x smaller, see longitudinal force and slip in 2.2.3.

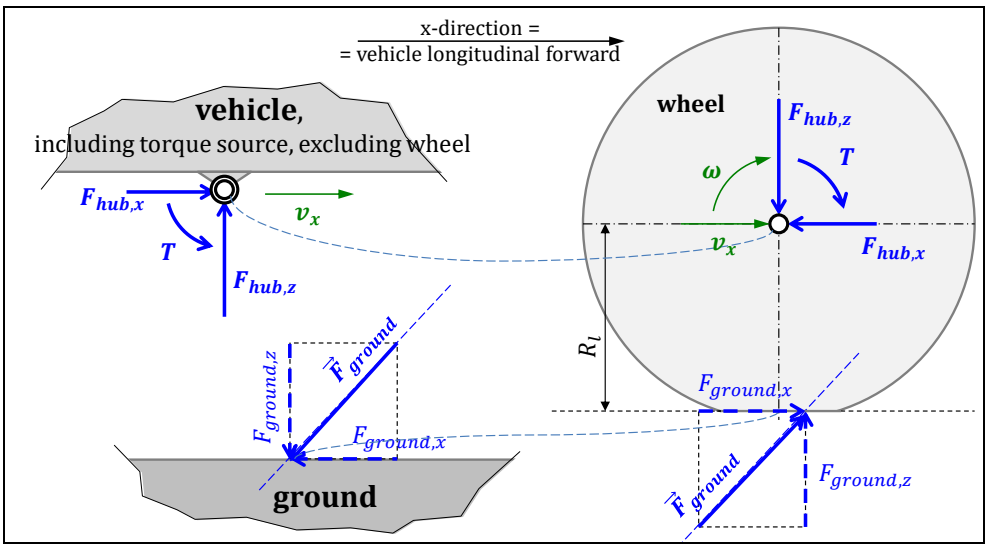

Figure 2-9: A wheel as a transmission from rotational $[\omega; T]$ to translational $[v_x; F_{hub,x}]$.

The longitudinal force in ground plane F_x, depends on the design of the tyre, the ground surface and the operational variables, such as velocities $[v_x, \omega]$ and vertical force F_z. The tyre can be under *braking*, *free rolling*, *pure rolling* or *propulsion/traction*, listed in order of increasing F_x and increasing T.

2.2.1.7 Tyre Rolling and Radii

Ideal rolling is shown in Figure 2-10 a). This relationship does not hold when the tyre is deflected as in Figure 2-10 b). Not even the deflected radius can be assumed to be a proportionality constant between

angular and translational velocity, since the tyre contact surface slides, or slips, versus the ground. Then, an even truer picture of a rolling tyre looks like Figure 2-10 c), where the deformation at the leading edge also is drawn. This means that v_x is only $\approx R \cdot \omega$ and only for limited slip levels.

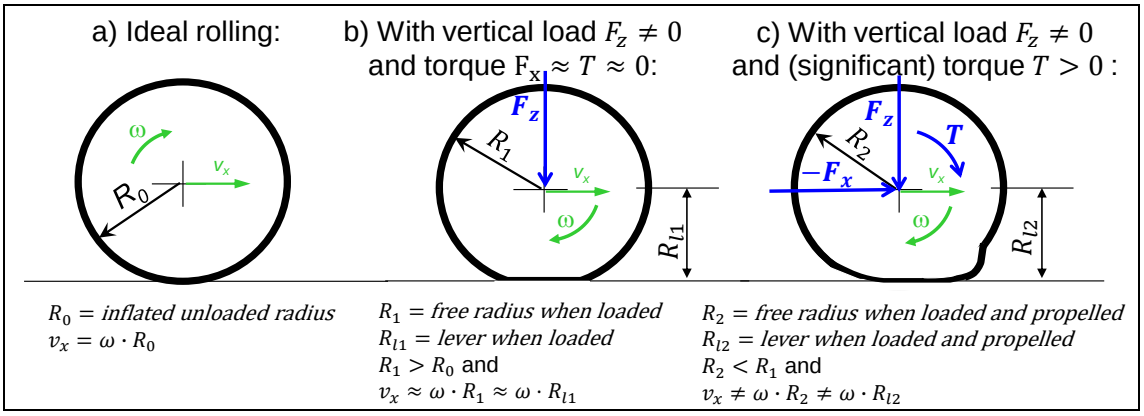

Figure 2-10: Radius and speed relations of a tyre. R_0 and R_l are not the same across a), b) and c).

There is a relative speed between tyre and the road surface. The ratio between this relative speed and a reference speed is defined as the "tyre slip". The reference speed can be the circumferential speed or the translational speed of the tyre, depending on the application. For a driven wheel, the slip definition in Eq [2.1] is often used and for braked wheels Eq [2.2] is often used. This is to avoid division by small numbers in take-off and brake tests, respectively. The physical model in 2.2.3.1 reveals that Eq [2.1] is the physically most motivated.

$$s_x = \frac{R \cdot \omega - v_x}{|R \cdot \omega|}; \quad [2.1] \qquad s_x = \frac{R \cdot \omega - v_x}{|v_x|}; \quad [2.2]$$

With the definition in Equation [2.1] and a model for how tyre longitudinal force varies with R, ω and v_x (Eq [2.20] taken as example) we get Figure 2-11, which shows cuts in Figure 2-25.

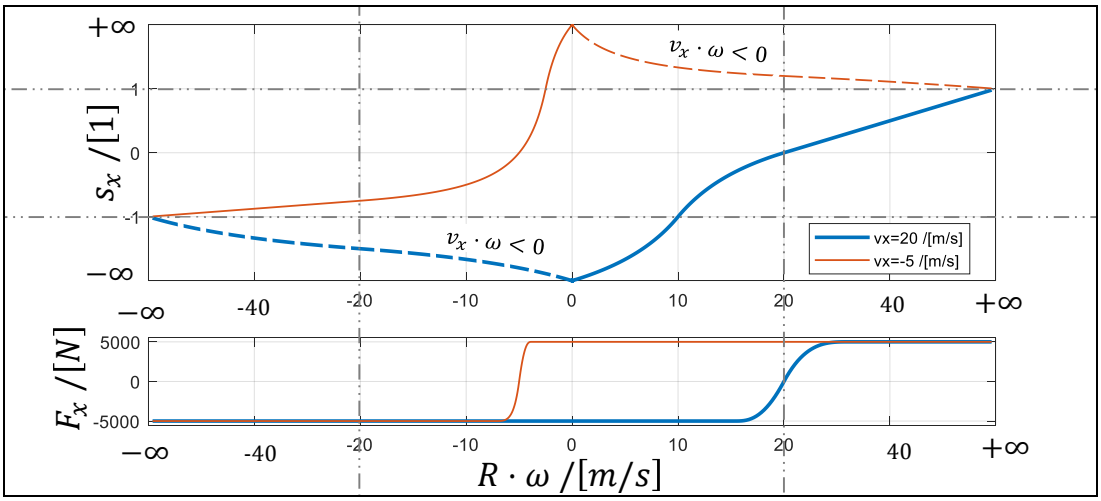

Figure 2-11: Slip s_x and force F_x as function of $R \cdot \omega$ for constant v_x. $C_x = 50$ [$kN/1$] and $\mu \cdot F_z = 5000$ [N]. Semi-inverted scales around $|R \cdot \omega| = 20$ and $|s_x| = 1$. Dashed shows where definition of s_x is not relevant, since F_x is not dependent of s_x, since $v_x \cdot \omega < 0$.

It is not obvious which R to use in Equations [2.1]..[2.2], e.g. R_0, R_1, R_2, R_{l1} or R_{l2}. However, this compendium recommends the free radius (R_1 or R_2), rather than the loaded radii (R_{l1} or R_{l2}) because the free radii are better average value of the radius around the tyre and the tyre's circumference is tangentially stiff, so speed has to be same around the circumference.

Sometimes one defines the Rolling radius $R_e = (v_x/\omega)|_{T=0}$, i.e. a speed ratio with dimension length, between translational and rotational speeds, measured when the wheel is undriven ($T = 0$). This radius can be used for relating vehicle longitudinal speed to wheel rotational speed sensors, e.g. for speedometer or as reference speed for ABS and ESC algorithms.

Yet another approach is to use the radius $(v_x/\omega)|_{F_x=0}$, i.e. the ratio when the wheel is pure rolling. Using $R = (v_x/\omega)|_{T=0}$ or $R = (v_x/\omega)|_{F_x=0}$ in the slip definitions shifts $F_x(s_x)$ curve and $T(s_x)$ curve, see more in 2.2.3.5.

The variable s_x is the longitudinal slip value, sometimes also denoted as κ or λ. When studying braking, one sometimes uses the opposite sign definition, so that the numerical values of slip becomes positive.

2.2.1.8 Tyre Contact Length

The contact length L represents the deformation shape. The L is not a design parameter, but an intermediate parameter or variable, explaining both rolling resistance and tyre forces from slip. One way to model L in a physical way is shown in Figure 2-12. The tyre belt is modelled as circumferentially rigid (constant length), which gives:

$$\begin{aligned} 2\cdot\pi\cdot R_{free} &= \frac{2\cdot\pi - 2\cdot\gamma}{2\cdot\pi}\cdot 2\cdot\pi\cdot R_{F_z} + L; \\ \left(R_{free}-\Delta z\right)^2 + (L/2)^2 &= R_{F_z}^2; \\ \frac{L/2}{R_{free}-\Delta z} &= \tan(\gamma)\,; \end{aligned} \qquad [2.3]$$

Additionally, we need a model for the vertical deformation. Simplest possible is a linear spring:

$$F_z = c_z\cdot\Delta z; \qquad [2.4]$$

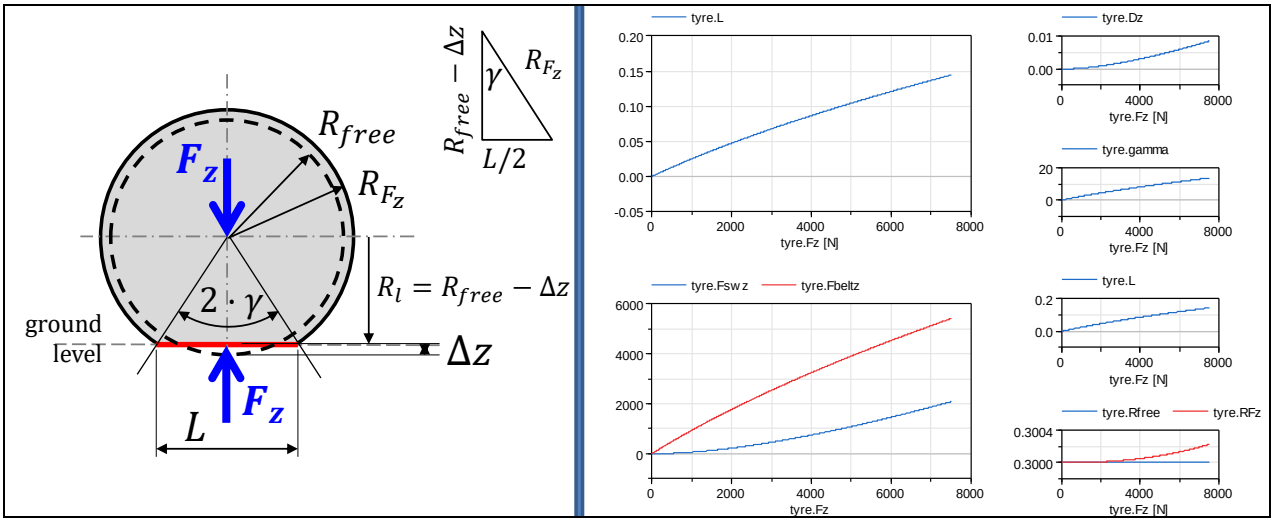

Figure 2-12: Left: Physical model. Right: Example result of model defined by Eqs [2.3] and [2.5].

A typical usage of this model is to know variable F_z and parameters R_{free} and c_z. This leaves 4 unknown variables $(\Delta z, \gamma, L, R_{F_z})$ and equally many equations. An explicit solution is easy for Δz, but difficult for the remaining 3 variables $[\gamma, L, R_{F_z}]$. For a single operation conditions, one can solve by iteration. For whole simulations, it is more computational efficient to pre-process numerically in a table for how $[\Delta z, L, R_{F_z}]$ varies with γ (for certain R_{free}, which typically not varies during a simulation). For each time instant during simulation, interpolation in this table gives $[\gamma, L, R_{F_z}]$ from known Δz.

The stiffness c_z can be found for an existing tyre with a certain inflation pressure, but it is far from a design parameter. Also, the linear model is often too simplified. To improve this, alternative vertical deformation models can be used. If studying only single operation conditions, Finite Element models are suitable. But for simulations, a more computational efficient solution is almost a necessity. The model in Eq [2.5] can replace Eq [2.4]. This is simple but indicates the mechanisms for how sidewall stiffness and inflation pressure come into play: Assume that the vertical load is carried by sidewalls $(F_{sw,z})$ and the belt area between the sidewalls $(F_{belt,z})$. Assume belt has no bending stiffness and sidewalls follow Hertz contact theory:

$$F_z = F_{sw,z} + F_{belt,z};$$
$$F_{belt,z} = p_{infl} \cdot W \cdot L; \quad (W = \text{tyre width},\ p_{infl} = \text{tyre inflation pressure})$$
$$F_{sw,z} = k_{sw} \cdot L^2;$$

[2.5]

So, Eq [2.5] can be solved for $[L, F_{sw,z}, F_{belt,z}]$. Then [2.3] can be solved for $[\gamma, \Delta z, R_{F_z}]$, using iterations or preprocessing with swept γ and interpolation, very similar as described above. The model is plotted for varying F_z in Figure 2-12.

The k_{sw} is a radial stiffness of the sidewall. The set $[W, k_{sw}, p_{infl}]$ is closer to design parameters than the parameter $[c_z]$.

When driving on soft ground, the deformation of the ground adds variables, beside L, that influences rolling resistance and forces in ground plane. Driving on soft ground is not well covered in this compendium, except shortly in 2.2.2.4.4. Present section assumes rigid ground.

2.2.2 Rolling Resistance of Tyres

2.2.2.1 Definition of Rolling Resistance

Rolling resistance on level road can be defined in two ways:

- **Energy definition**: $RRC = \frac{EnergyLoss}{F_z \cdot |Distance|} = \frac{\int |T\cdot\omega - \vec{F}_{xy} \bullet \vec{v}_{xy}| \cdot dt}{F_z \cdot \int |\vec{v}_{xy}| \cdot dt} = \begin{Bmatrix} if\ no \\ lateral \\ slip \end{Bmatrix} = \frac{\int |T\cdot\omega - F_x \cdot v_x| \cdot dt}{F_z \cdot \int |v_x| \cdot dt} = \begin{Bmatrix} if \\ steady \\ state \end{Bmatrix} = \left|\frac{T\cdot\omega - F_x \cdot v_x}{F_z \cdot v_x}\right| = \begin{Bmatrix} s_x = \frac{R\cdot\omega - v_x}{|R\cdot\omega|} \\ and\ if\ \omega > 0 \end{Bmatrix} = \left|\frac{T}{F_z} \cdot \frac{1}{R\cdot(1-s_x)} - \frac{F_x}{F_z}\right| = \begin{Bmatrix} if\ F_x = \\ = C_x \cdot s_x \end{Bmatrix} = \left|\frac{T}{F_z} \cdot \frac{1}{R\cdot\left(1-\frac{F_x}{C_x}\right)} - \frac{F_x}{F_z}\right| \approx \begin{Bmatrix} if \\ F_x \approx 0 \end{Bmatrix} \approx \left|\frac{T/R - F_x}{F_z}\right|$; This definition includes both force and slip losses.
- **Force definition**: $RRC = \frac{ForceLoss\ in\ rotation\ direction}{F_z} = \frac{T/R - F_x}{F_z} \cdot \text{sign}(\omega)$; This definition only includes force losses (relative to a nominal or expected force $F_x = T/R$); not velocity or slip losses.

Energy definition has the advantage that it does not require R. But it is not useful in most vehicle dynamics models, since it does not resolve into force and velocity. And, its RRC value varies a lot if defined for varying tyre forces in the ground plane, which makes slip vary. So, the compendium uses the force definition. It should be mentioned that (ISO28580, 2018) uses the Energy definition.

2.2.2.2 Physical Explanation of Rolling Resistance

The rolling resistance is difficult to model physically. In the following, some possible explanations are given. It focuses tyres on hard ground and moderate speeds, both positive and negative. On soft ground, there are mechanisms as in 2.2.2.4.4. At very high speeds, there are inertial impact mechanism which causes energy loss. The explanation model below mainly takes on the challenge to explain why a rolling resistance moment appears opposite to roll direction, also when speed is close to zero.

The overall explanation of rolling resistance for pneumatic tyres on hard flat surfaces is that the pressure distribution is off-set in rolling direction. Damping and friction, see Figure 2-13, is one reason for this and it is not dependent on the longitudinal force. Figure 2-13 also shows another off-set effect, which is directly influenced by the longitudinal force.

The rolling resistance coefficient is almost the same for very low speeds; even when the wheel starts rolling from zero speed, after gradually increasing the torque up to the rolling resistance moment. The radial friction in Figure 2-13 can explain that, but there is also another explanation, see Figure 2-14. It explains how the contact patch is moved ahead of wheel hub. The belt is circumferentially stiff and takes a short-cut along the corda, through the contact. This builds up shear stresses in the sidewall, τ_{sw}. The belt is flexible for bending, so belt radius is proportional to belt tension force, F_b. This is because same effect as for tension in rope around a cylinder: $force = pressure \cdot radius \cdot width$;. In our case, the pressure corresponds to the summed effects of inflation pressure p_{infl} and radial stress in sidewalls σ_{sw}. So, the radius becomes smaller than original radius in inlet and larger in outlet.

Assumption of constant contact length and geometric constraints from tensional rigid belt requires that contact patch is off-set towards the inlet, so $e = \text{sign}(\omega) \cdot |e|$;.

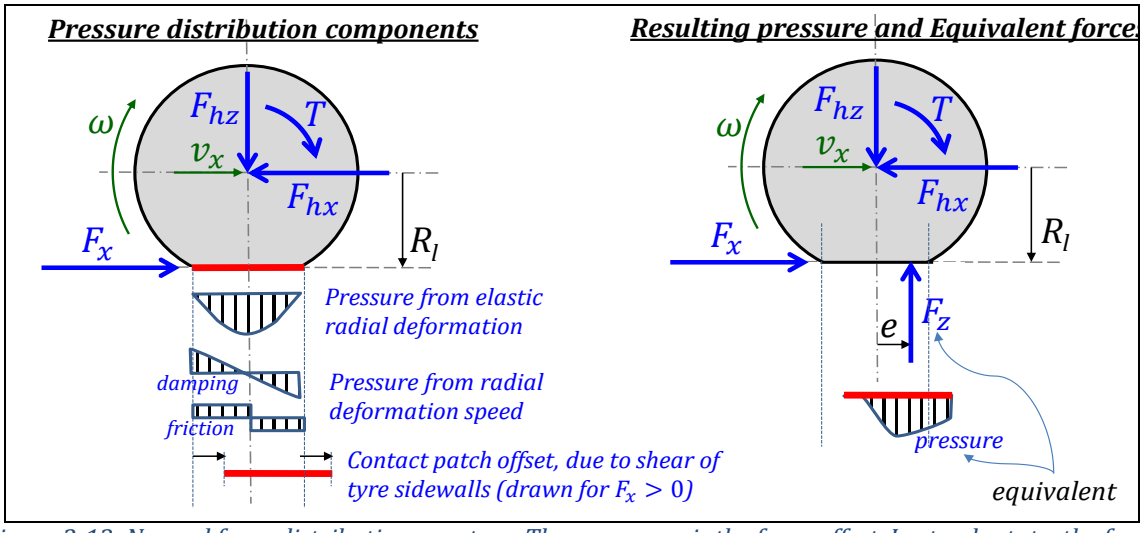

Figure 2-13: Normal force distribution on a tyre. The measure e is the force offset. In steady state, the forces in hub and contact patch are the same: $F_{hx} = F_x$ and $F_{hz} = F_z$.

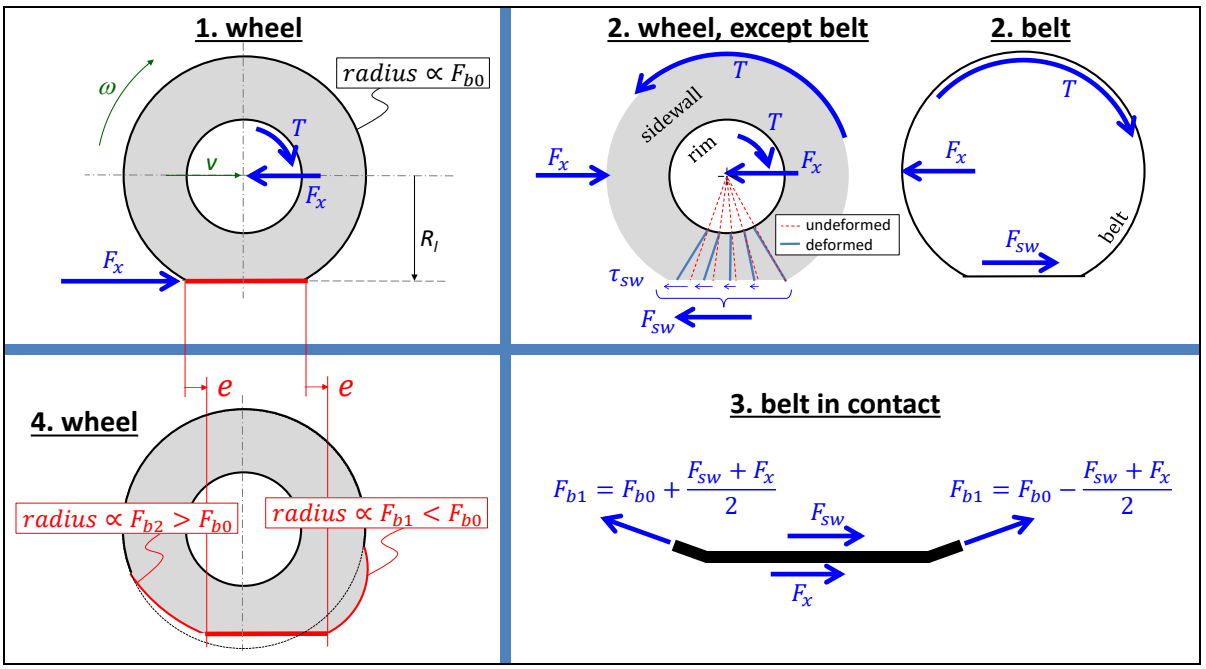

Figure 2-14: 1. Wheel at low speed (F_x small and negative). 2. Free body diagrams with belt separate. 3. How belt tension force changes before and after contact. 4. Influence of radii variation on contact patch position.

2.2.2.3 Mathematical Representation of Rolling Resistance

The rolling resistance force is defined as the loss of longitudinal force on the vehicle body, as compared to the longitudinal force which would have been transferred with an ideal wheel. The Rolling Resistance Coefficient, f_r or RRC, is the rolling resistance force divided by the normal force, F_z. Assuming force equilibria in longitudinal and vertical direction, $F_{hub,z} = F_{ground,z} = F_z$ and $F_{hub,x} = F_{ground,x} = F_x$, see Figure 2-9.

$$f_r = RRC = \left| \frac{T/R - F_x}{F_z} \right|; \qquad [2.6]$$

F_x denotes the longitudinal force on the wheel, T denotes the applied torque and R denotes the tyre radius. For a free rolling tyre, where $T = 0$, f_r becomes simply $-F_x/F_z$. One often sees definitions of f_r which assumes free rolling tyre; but Eq [2.6] is also valid when $T \neq 0$, which is useful.

A free body diagram of the forces on the wheel can be used to explain the rolling resistance. Consider Figure 2-13 which represents a free rolling wheel under steady state conditions. The inertia of the wheel is neglected.

Longitudinal and vertical force equilibria are already satisfied, due to assumptions above. However, moment equilibrium around wheel hub requires:

$$T - F_x \cdot R_l - F_z \cdot e = 0 \;\Rightarrow\; F_x = \frac{T}{R_l} - \frac{e}{R_l} \cdot F_z; \qquad [2.7]$$

This result suggests that the force F_x, which pushes the vehicle body forward, is the term T/R_l (arising from the applied torque T) minus the term $F_z \cdot e/R_l$. The term can be seen as a force F_{roll} and referred to as the rolling resistance force. We seldom know neither R_l or e, but they are rather constant and the form of Eq [2.7] is same as Eq [2.6] if:

$$f_r = RRC = |e/R|; \qquad [2.8]$$

Eq [2.8] is a definition of rolling resistance coefficient based on physical mechanisms internally in the tyre with road contact, while Eq [2.6] is based on quantities which are measurable externally, see Eq [2.6]. Sometimes one sees $f_r = -F_x/F_z$ as a definition, but that is not suitable since it assumes absence of torque.

It is not obvious which radius to use. R_l is can be motivated because R_l is the lever for F_x. However, in 2.2.1.7, we found arguments for using other radii. If same radius is used, for slip and rolling resistance, we can fully see the tyre as a transmission with the nominal ratio R and zero energy loss if $f_r = 0$ and $s_x = 0$.

It is important to refer to this phenomenon as rolling **resistance** as opposed to rolling **friction**. It is not friction in the basic sense of friction, because $F_x \neq -f_r \cdot F_z$ except for the special case when un-driven wheel ($T = 0$). Figure 2-15 shows an un-driven and pure rolling.

Rolling resistance is a torque loss. Other torque losses, which can be included or not in tyre rolling resistance, are:

- losses associated with friction in gear meshes,
- drag losses from oil in the transmission,
- wheel bearing (and bearing sealings) torque losses,
- drag from brake discs,
- drag losses from aerodynamic around the wheel, and
- uneven road in combination with suspension damping that dissipates energy.

These should, as rolling resistance, be subtracted from propulsion/brake torque. However, sometimes they are included as part of the tyres rolling resistance coefficient, which can be misleading. The wheel bearing torque loss have two torque terms: one is proportional to vertical load on the wheel (adds typically 0.0003 to rolling resistance coefficient), and the other is of constant magnitude but counter-directed to rotation speed. The former term can be included in rolling resistance coefficient. The aerodynamic losses due to wheel rotation are special since they vary with wheel rotational speed, meaning that they (for constant vertical load) are relevant to include when studying the variation of rolling resistance coefficient with vehicle speed. A summarizing comment is that one has to be careful with where to include different torque losses, so that they are included once and only once.

2.2.2.4 Variation of Rolling Resistance

Several parameters will affect the rolling resistance moment (or Rolling resistance coefficient). Design parameters, see Figure 2-8:

- Tyre material. Natural rubber often gives lower rolling resistance.
- Radial tyres have more flexible sides, giving lower rolling resistance also bias ply have a greater crown angle causing more internal friction within the tyre during deflection.
- Geometry:
  - Diameter. Large wheels often have lower coefficient of rolling resistance
  - Width
  - Groove depth

- Tread depth
- Higher inflation pressure gives lower rolling resistance on hard ground but higher rolling resistance on soft ground (and vice versa), see Figure 2-16 and Figure 2-17.

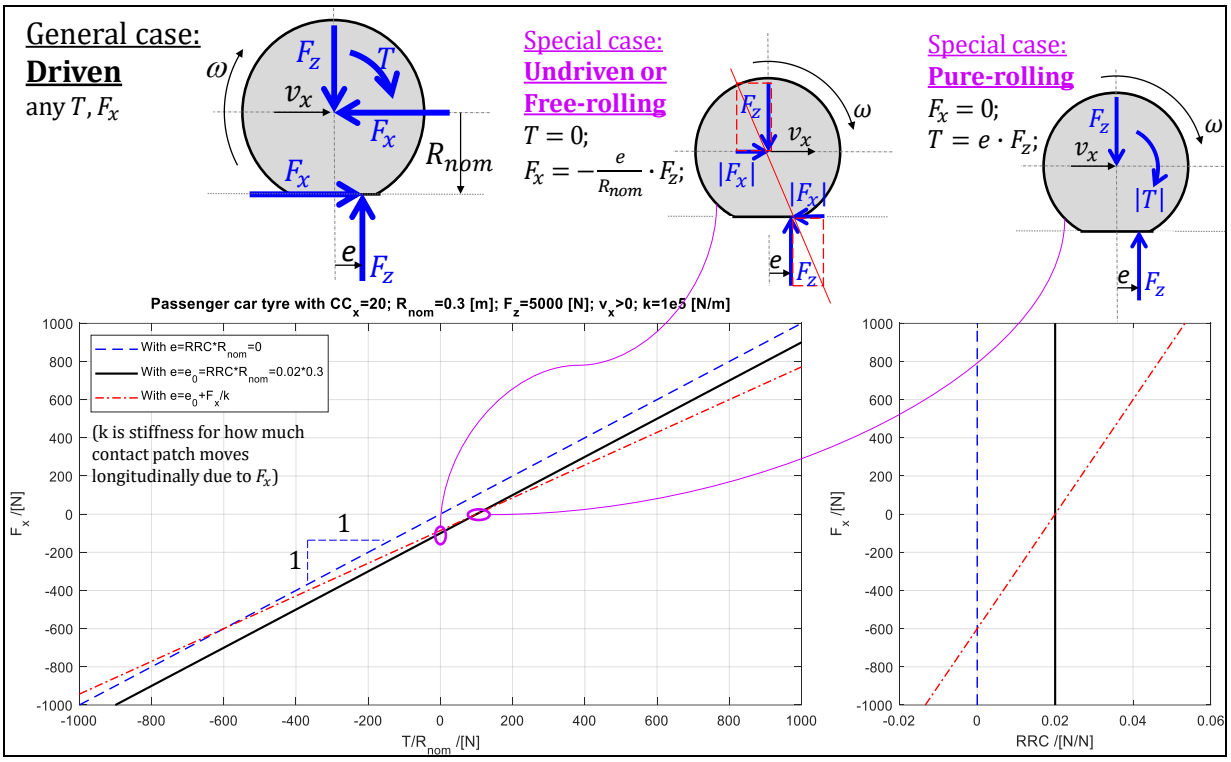

Figure 2-15: Driven wheel with rolling resistance. Special cases "Free-rolling" and "Pure rolling".

Operational parameters, see Figure 2-8:

- Elevated temperatures give low rolling resistance, via increased inflation pressure. Tyres need to roll approximately 30 km before the rolling resistance drop to their lowest values.
- Road/ground, sometimes covered: Clean asphalt, Asphalt with water/leaves/sand/…, Loose/hard gravel, Snow/ice. Soft ground or covered hard ground increases rolling resistance.
- Wear state. Worn tyres have lower rolling resistance than new ones (less rubber to deform).

Operational variables, see Figure 2-8:

- Vertical force.
- Speed. Rolling resistance increases with vehicle speed due to rubber hysteresis and air drag.
- Tyre loads (propulsion/braking and lateral forces)

2.2.2.4.1 Variation of Tyre Type

Trucks tyres have a much lower rolling resistance coefficient than passenger vehicle tyres, approximately half. Tyres have developed in that way for trucks, because their fuel economy is so critical.

2.2.2.4.2 Variation of Vertical Force

In a first approximation, the rolling resistance force is proportional to vertical force, i.e. RRC is constant. But, typically, the RRC decreases slightly with vertical force. This, and parasitic bearing losses, $torque = \text{sign}(\omega) \cdot constant$, explains why commercial vehicles lift axles when driven with low payload.

2.2.2.4.3 Variation of Speed

As an example, left part of Figure 2-16 shows the influence of tyre construction and speed on rolling resistance. The sudden increase in rolling resistance at high speed is important to note since this can lead to catastrophic failure in tyres. The source of this increase in rolling resistance is a high energy standing wave that forms at the trailing edge of the tyre/road contact.

There are some empirical relationships derived for the tyre's rolling resistance. It is advisable to refer to the tyre manufacturer's technical specifications when exact information is required. This type of information is usually very confidential and not readily available. Some general relationships have been developed, from (Wong, 2001):

Radial-ply passenger car tyres: $f_r = 0.0136 + 0.04 \cdot 10^{-6} \cdot v^2$
Bias-ply passenger car tyres: $f_r = 0.0169 + 0.19 \cdot 10^{-6} \cdot v^2$
Radial-ply truck tyres: $f_r = 0.006 + 0.23 \cdot 10^{-6} \cdot v^2$
Bias-ply truck tyres: $f_r = 0.007 + 0.45 \cdot 10^{-6} \cdot v^2$

As seen in Figure 2-16, a rule of thumb is that rolling resistance coefficient is constant up to around 100 km/h.

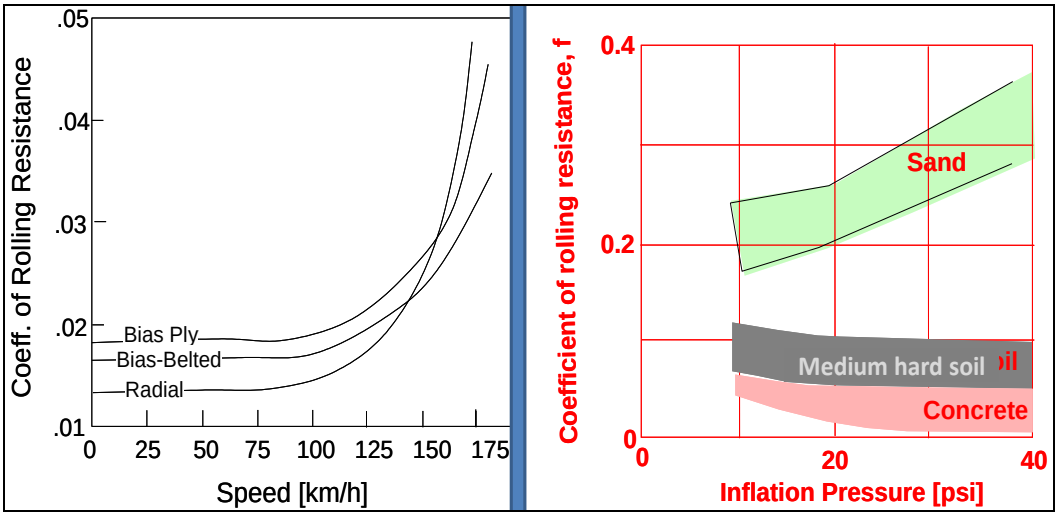

Figure 2-16 : Left: Rolling resistance coefficient variation with speed for different tyre types (Gillespie, 1992). Right: Range of Coefficient of Rolling Resistance for different road/ground material

2.2.2.4.4 Variation of Road Surface

The road or ground can mainly vary in two ways: how **rigid** and how **slippery** it is. It is not solely a question of the road, because such rigidness should be judge relative to tyre inflation pressure and such slipperiness should be judged relative to tyre tread pattern, including whether the tyre has spikes or not.

Right part of Figure 2-16 shows that the rolling resistance changes a lot due to different road/ground material and inflation pressures. As can be expected, a range of values exist depending on the specific tyre and surface materials investigated. On hard ground, the rolling resistance decreases with increased inflation pressure, which is in-line with the explanation model used above, since higher pressure intuitively reduces the contact surface and hence reduces e. On soft ground the situation is reversed, which requires a slightly different explanation model, see Figure 2-17. On soft ground, the ground is deformed so that the wheel rolls in a "wheel-local up-grade" with inclination angle φ. Intuitively, a higher inflation pressure will lead to more deformation of the ground, leading to a steeper φ.

The phenomena in Figure 2-17 is a plastic deformation of the ground, so if a vehicle has several tyres which takes the same path on ground, the rolling resistance will be different due to a memory (a state variable) in the ground.

The "wheel-local up-grade" in Figure 2-17 follows each tyre so that it is constant in time for each tyre. This is a difference to simply uneven (rigid) road, where the wheels experience alternating wheel-local up- and ground-grade. In average, the alternating up and down does not generate rolling resistance in tyre, but it can cause energy-loss in wheel suspension and consequently this contributes to energy consumption for the vehicle.

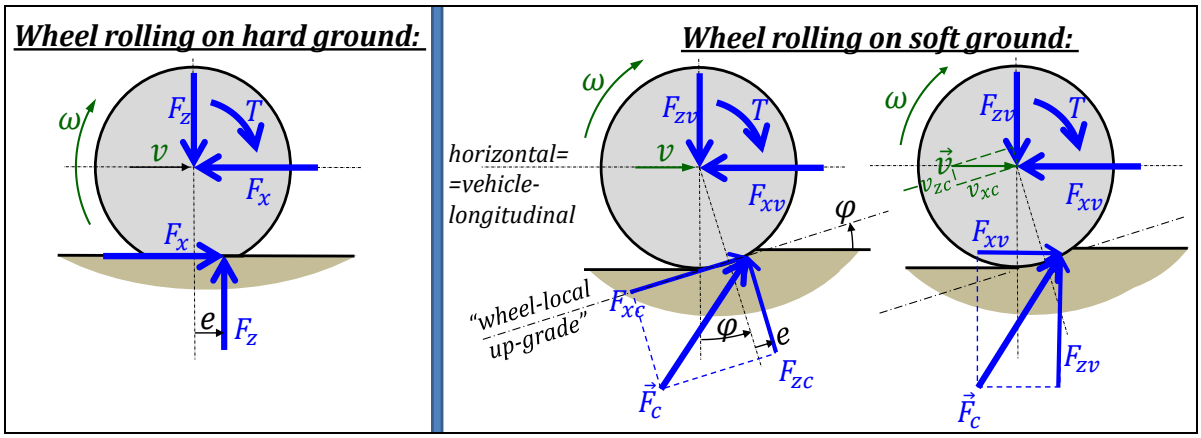

Figure 2-17 : Rolling resistance explanation for hard and soft ground. Subscripts: c=contact, v=vechile.

2.2.2.4.5 Variation of Longitudinal Force, Propulsion and Braking

Figure 2-13 shows an offset of contact patch due to longitudinal force F_x. This makes RRC dependent of F_x. The phenomena is not well studied, since RRC is often given for free-rolling tyres, but according to Figure 2-18 RRC increases with positive F_x and decreases with negative F_x. The wheel radius also decreases with magnitude of force. For negative forces, these two effects have opposite influence, so the change is less for negative force, as seen in Figure 2-18.

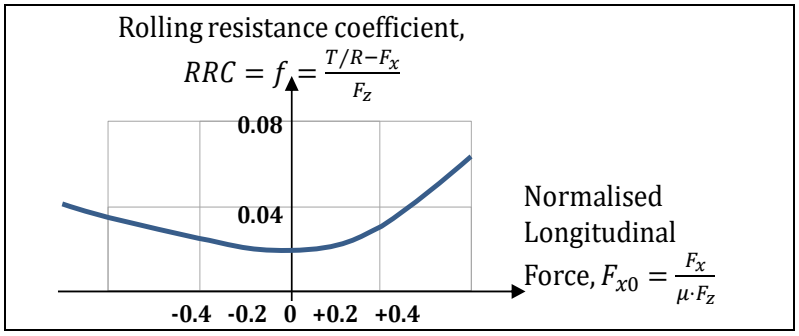

Figure 2-18 : Rolling resistance dependency of longitudinal tyre force. Inspired by (Wong, 2001)

2.2.3 Longitudinal Force due to Slip

The longitudinal force, F_x, between the tyre and ground influences the vehicle propulsion and braking performance. We can see it as a depending on the sliding between the tyre and the ground.

First, compare friction characteristics for a translating block of rubber with a rolling wheel of rubber. Figure 2-19 shows the basic differences between classical dry-friction, or Coulomb friction, of such sliding block and the basic performance of a rolling tyre. Experiments have shown that the relative speed between the tyre and the road produces a frictional force that has an initial linear region that builds to a peak value. After this peak is achieved, no further increase in the tangential (friction) force is possible. There is not always a peak value, which is shown by the dashed curve in the figure. The slope in the right diagram will be explained in 2.2.3.1, using the so called "tyre brush model".

2.2.3.1 Brush Model for Longitudinal Slip

The brush model is frequently used to explain how tyre develop forces in ground plane, see e.g. Refs (Pacejka, 2005) and (Svendenius, 2007). The brush model is a physically based model that uses shear stress and dry friction at a local level, i.e. for each contact point in the contact patch. Figure 2-20 shows the starting point for understanding the brush model.

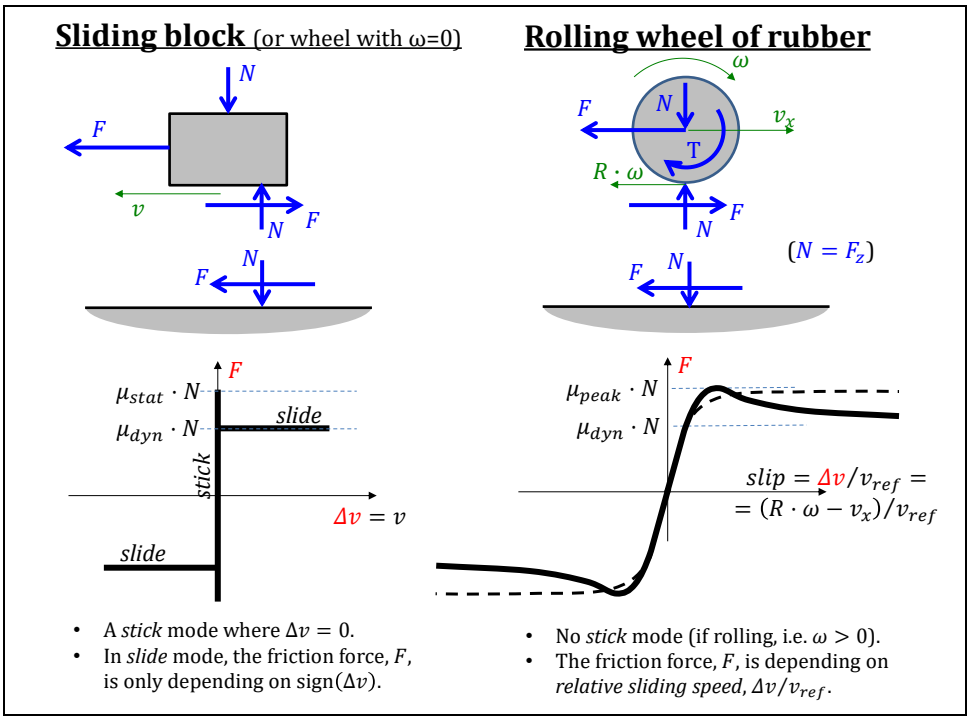

Figure 2-19: Friction characteristics.

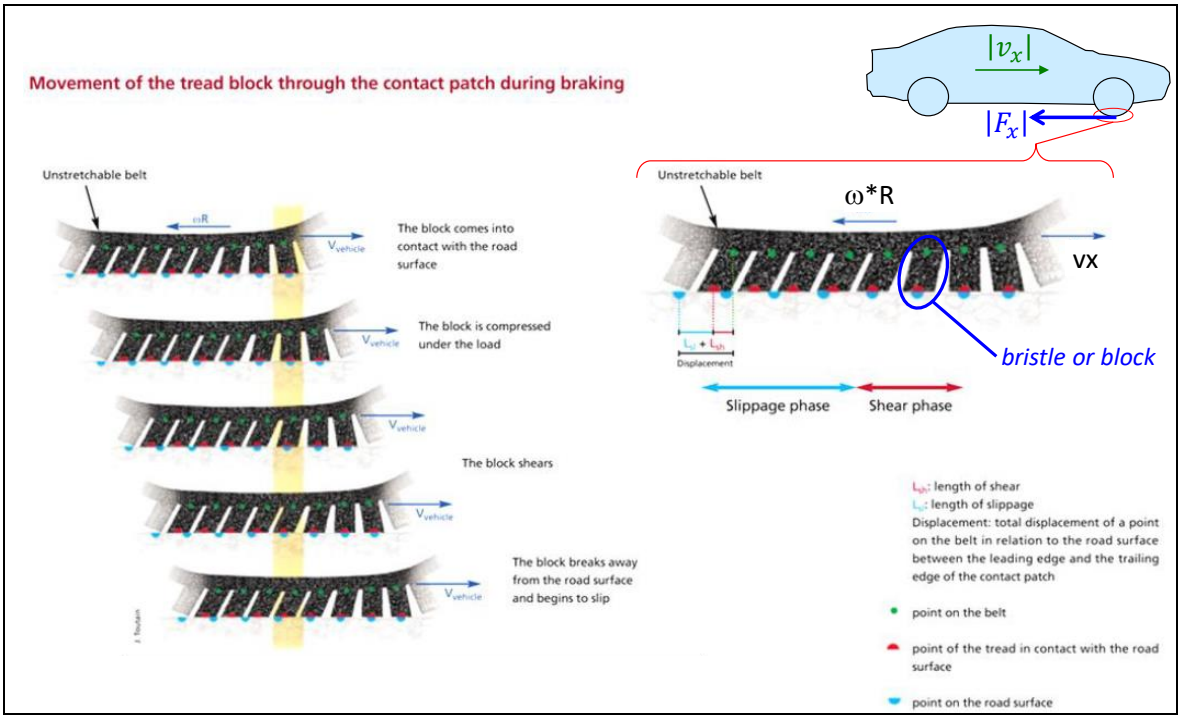

Figure 2-20: Tyre ground contact for braked tyre. Origin to the "Brush model". Picture from Michelin.

2.2.3.1.1 Uniform Pressure Distribution and Known Contact Length

A first simple variant of the brush model, uses the following assumptions:

- Sliding and shear stress only in **longitudinal** direction (as opposed to combined longitudinal and lateral)
- Uniform and known **pressure distribution** over a constant and known contact length (as opposed to using a contact mechanics-based approach, which can calculate pressure distribution and contact length L.)
- **Contact length** is known (as opposed to function of vertical force).
- No difference between **static and dynamic** coefficient of friction

- Only studying the **steady state conditions**, as opposed to including the transition between operating conditions. Here, "steady state" refers to the distributions of tyre tread shear deformation $\gamma(\xi)$ and shear stress $\tau(\xi)$, which are assumed to not vary with time.

At first, we also assume that the tread is built up of N bristles of rubber. Each bristle is assumed as a shear piece of rubber without force interaction between neighbouring bristles. The shear stress of the element develops as in Hooke's law: $F_i = \tau_i \cdot Area_i = G \cdot \gamma_i \cdot Area_i$;. The $Area_i = W \cdot L/N$, but we let $N \to \infty$, we can use a continuous model: $dF = \tau \cdot dArea = \tau \cdot W \cdot d\xi$;, where W is width of tyre and ξ a coordinate along the belt in the contact, see Figure 2-21. Figure 2-21 also shows that we assume friction contact between bristle and ground. (The bristles can alternatively be seen as bending beams fixed in the belt end or rigid beams connect with rotational springs in the belt end.)

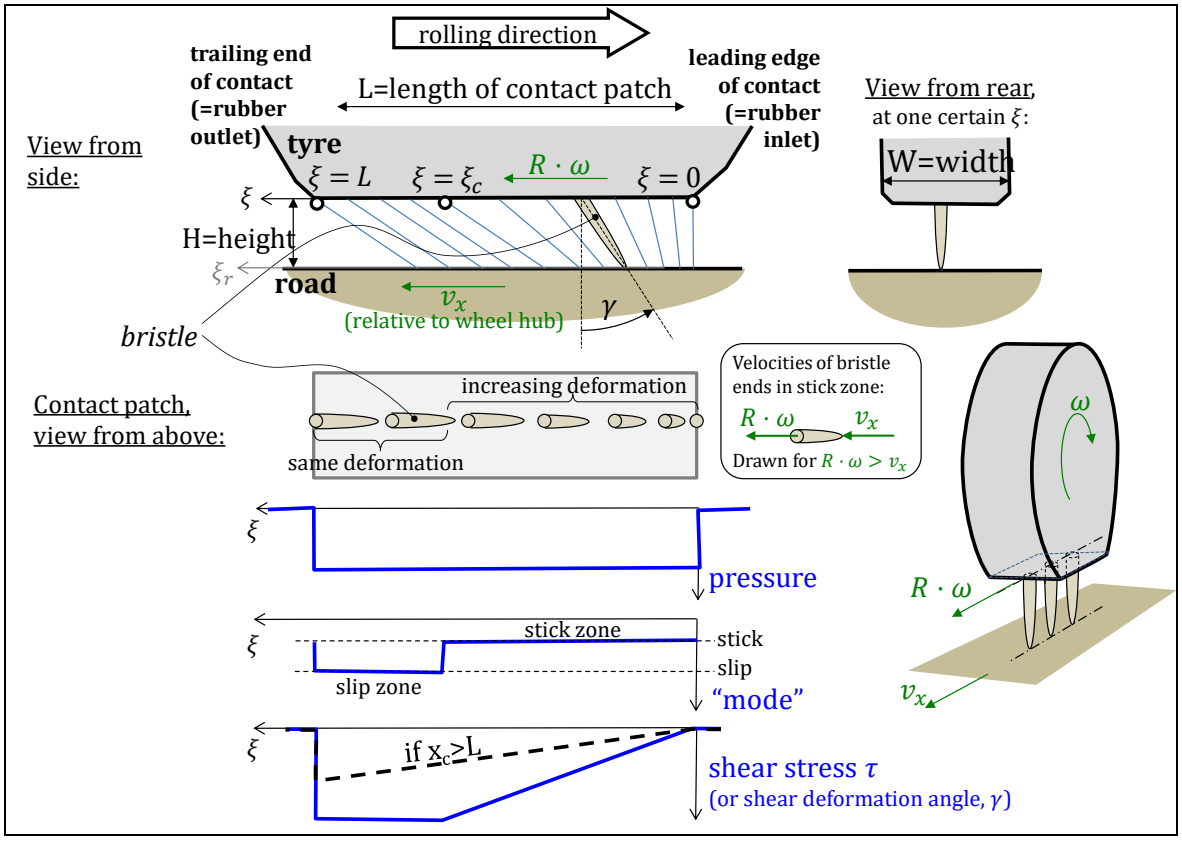

Figure 2-21: The physical model of simple brush model for longitudinal slip. Drawn for propelled tyre. The bristles represent the rubber tread, so they don't include elasticity in sidewall. Drawn for $R \cdot \omega > v_x$.

We can now state the first equation:

$$\tau = G \cdot \gamma; \quad \text{where } \tau = \text{shear stress}, G = \text{shear modulus} \text{ and } \gamma = \text{shear deformation angle}; \qquad [2.9]$$

When a bristle enters the contact patch, it lands un-deformed, i.e. with $\gamma = 0$. The further into contact, along coordinate ξ, we follow the element, the more sheared will it become. Since the ground end of the element sticks to ground, the increase becomes proportional to the speed difference Δv and the time t it takes to reach the coordinate ξ:

$$\gamma = \frac{\Delta v \cdot t(\xi)}{H} = \frac{(R \cdot \omega - v_x) \cdot t(\xi)}{H}; \quad \text{where } t(\xi) = \xi / v_{Transport} \text{ and } v_{Transport} \approx R \cdot \omega; \qquad [2.10]$$

The velocity $v_{Transport}$ is the velocity of which the brush bristles are transported through the contact. We use $v_{Transport} = R \cdot \omega$ and integrate τ from $\xi = 0$ to $\xi = L$. The initial assumption is that $\xi = 0$ in the leading edge, i.e. where the bristles are entring the contact. Hence, $v_{Transport} = |R \cdot \omega|$.

(It is possible to reach Eq [2.14] via integration over ξ_r instead. Then, one uses $v_{Transport} = |v_x|$. After a more complex derivation, the resulting slip definition $s_x = (R \cdot \omega - v_x)/|R \cdot \omega|$ falls out in the final expression for F_x, i.e. Eq [2.14]. Despite this, one often sees $s_x = (R \cdot \omega - v_x)/|v_x|$.)

Combining equations for τ and γ and identifying the slip s_x gives:

$$\tau = \frac{G}{H} \cdot \frac{R \cdot \omega - v_x}{|R \cdot \omega|} \cdot \xi = \left\{ s_x = \frac{R \cdot \omega - v_x}{|R \cdot \omega|}; \right\} = \frac{G}{H} \cdot s_x \cdot \xi; \qquad [2.11]$$

Note that this model simplifies F_x from a function of 2 variables (ω and v_x) to 1 variable (s_x). Experiments, except in odd operation conditions such as $\omega \cdot v_x < 0$, support this.

With this definition of slip, s_x, we automatically handle ω and v_x both positive and ω and v_x both negative. The case when ω and v_x have different signs will be handled below.

As long as friction limit is not reached ($|\tau| < \mu \cdot p$) within the whole contact, we can find the force as this integral:

$$F_x = \int_{W \cdot L} \tau \cdot dA = W \cdot \int_0^L \tau \cdot d\xi = W \cdot \int_0^L \frac{G}{H} \cdot s_x \cdot \xi \cdot d\xi = \frac{G \cdot W \cdot L^2}{2 \cdot H} \cdot s_x = \\ = \left\{ C_x = \frac{G \cdot W \cdot L^2}{2 \cdot H} \right\} = C_x \cdot s_x; \quad for\ s_x < \frac{\mu \cdot F_z}{2 \cdot C_x} \qquad [2.12]$$

If friction limit is reached within the contact, i.e. at the break-away point $\xi_c < L$, we have to split the integral in two. The point ξ_c is defined by $\tau(\xi_c) = \frac{G}{H} \cdot s_x \cdot \xi_c = \frac{2 \cdot C_x}{W \cdot L^2} \cdot s_x \cdot \xi_c = \mu \cdot p; \Rightarrow\ \xi_c = \frac{\mu \cdot p \cdot W \cdot L^2}{2 \cdot C_x \cdot s_x} = \frac{\mu \cdot F_z \cdot L}{2 \cdot C_x \cdot s_x}$;. For $\xi > \xi_c$, the rubber element will slide with a constant $\tau = \mu \cdot p$.

$$F_x = W \cdot \int_0^L \tau \cdot d\xi = W \cdot \int_0^{\xi_c} \frac{2 \cdot C_x}{W \cdot L^2} \cdot s_x \cdot \xi \cdot d\xi + W \cdot \int_{\xi_c}^L \mu \cdot p \cdot d\xi = \\ = \frac{2 \cdot C_x}{L^2} \cdot s_x \cdot \frac{\xi_c^2}{2} + \mu \cdot p \cdot W \cdot (L - \xi_c) = \left\{ p = \frac{F_z}{W \cdot L}; \quad and \quad \xi_c = \frac{\mu \cdot F_z \cdot L}{2 \cdot C_x \cdot s_x}; \right\} = \\ = \underbrace{\frac{\mu^2 \cdot F_z^2}{4 \cdot C_x \cdot s_x}}_{F_{x,stick}} + \underbrace{\mu \cdot F_z \cdot \left(1 - \frac{\mu \cdot F_z}{2 \cdot C_x \cdot s_x}\right)}_{F_{x,slip}} = \mu \cdot F_z \cdot \left(1 - \frac{\mu \cdot F_z}{4 \cdot C_x \cdot s_x}\right); \quad for\ s_x > \frac{\mu \cdot F_z}{2 \cdot C_x} \qquad [2.13]$$

As seen in Eq [2.13], the force terms, $F_{x,stick}$ and $F_{x,slip}$, from each of stick and slip regions are identified. These two terms are shown plotted in Figure 2-23.

The case when ω and v_x have different signs leads to that $\xi_c = 0$;, since the bristles will deform in the opposite direction; macro slip. So, the whole contact has $\tau = \mu \cdot p$, which leads to $F_z = \mu \cdot F_z$;. Hence, the total expression for F_x becomes as in [2.14], where a generalisation to cover also when ω and v_x have different signs ($\omega \cdot\ v_x < 0$) is done. We also add subscript x on G and H, to prepare for a corresponding model for lateral forces, in 2.2.4.

$$F_x = \begin{cases} = \text{sign}(R \cdot \omega - v_x) \cdot \mu \cdot F_z = \text{sign}(s_x) \cdot \mu \cdot F_z; & if\ \omega \cdot\ v_x < 0\ (macro\ slip) \\ = C_x \cdot s_x; & else\ if\ |s_x| \le \frac{\mu \cdot F_z}{2 \cdot C_x} \Leftrightarrow |F_x| \le \frac{\mu \cdot F_z}{2} \\ = \text{sign}(s_x) \cdot \mu \cdot F_z \cdot \left(1 - \frac{\mu \cdot F_z}{4 \cdot C_x} \cdot \frac{1}{|s_x|}\right); & else \end{cases} \qquad [2.14]$$

$$where\ C_x = \frac{G_x \cdot W \cdot L^2}{2 \cdot H_x};\ \ dimension: [force] \quad and\ s_x = \frac{R \cdot \omega - v_x}{|R \cdot \omega|};$$

It is important to reflect over which of the physical quantities that reasonably has to be modelled as varying. This will of course depend on the driving manoeuvre studied, but here is a typical situation:

The slip s_x and normal load F_z are typical varying and defined by the vehicle model. The quantities μ, G_x, W, H_x are often reasonably constant, so they can be parameters. However, it is often **not** reasonable to assume that the contact length L is constant. L is rather a function of F_z: $L(F_z)$;.

The case when $\omega \cdot v_x < 0$ is unusual and can only occur when $|s_x| > 1$. An example is when vehicle moves rearward with $v_x = -1\ m/s$, would be that the wheel spins forward, e.g. with $R \cdot \omega = 1\ m/s$. Then $s_x = +2$ and $F_x = \mu \cdot F_z$. Also, if increase to $R \cdot \omega = +\infty\ m/s$, we get same $F_x = \mu \cdot F_z$, but with $s_x = +\infty$. One can also note that there is another $R \cdot \omega$, for same v_x, which gives $s_x = +2$. This is $R \cdot \omega = -1/3\ m/s$ and then $F_x = \mu \cdot F_z \cdot (1 - \mu \cdot F_z/(8 \cdot C_x))$, which is $< \mu \cdot F_z$. So, F_x is uniquely defined for any (ω, v_x), but F_x has double solutions for some s_x, when $|s_x| > 1$.

If we instead hold a certain forward vehicle speed, e.g. $v_x = 1\ m/s$, and study how F_x varies with ω, we can identify 4 specific levels of ω:

- Full rearward traction: $R \cdot \omega = -\infty\ m/s$. This gives $s_x = -\infty$, with different signs on ω and v_x, and $F_x = -\mu \cdot F_z$;
- Locked wheel: $R \cdot \omega = 0\ m/s$. This also gives $s_x = -\infty$ and $F_x = -\mu \cdot F_z$;
- Pure rolling wheel: $R \cdot \omega = 1\ m/s$. This gives $s_x = 0$ and $F_x = 0$;
- Full forward traction: $R \cdot \omega = +\infty\ m/s$. This gives $s_x = +1$ and $F_x = \mu \cdot F_z \cdot (1 - \mu \cdot F_z/(4 \cdot C_x)) \approx \{typically\} \approx (0.95..0.98) \cdot \mu \cdot F_z$, which is $< \mu \cdot F_z$;

The first case is achievable, with an electric motor braking but not with friction brakes, where ω and v_x have different signs. The last case shows that we cannot reach $\mu \cdot F_z$ in the direction the vehicle moves, since there will always be a small part on the inlet side of the contact where the shear stress has not reached $\mu \cdot p$. In practice, we can see it as $\approx \mu \cdot F_z$, but when using the model mathematically, it can be good to note such small phenomena.

2.2.3.1.2 Longitudinal Tyre Slip Stiffness

In summary for many models (and tests!) the following is a good approximation for small longitudinal slip, and certain normal load and certain friction coefficient:

$$F_x = C_x \cdot s_x \qquad [2.15]$$

For the brush model, or any other model which describes $F_x(s_x, F_z, \mu, \dots)$, one can define the "Longitudinal tyre (slip) stiffness" C_x, which have the unit $N = N/1 = N/((m/s)/(m/s))$. It is the derivative of force with respect to slip. In many cases one means the derivative at $s_x = 0$:

$$C_x = \left(\frac{\partial}{\partial s_x} F_x(s_x, F_z, \mu, \dots) \right) \Bigg|_{s_x = 0} \qquad [2.16]$$

Note that C_x is not a stiffness in the conventional sense, force/deformation. The tyre also has such a deformation stiffness. Often, it is obvious which stiffness is relevant, but to be unambiguous one can use the wording: "slip stiffness" C_x [N/1=N/((m/s)/(m/s))] and "deformation stiffness" [N/m].

With the brush models with both pressure distributions, Eq [2.14] and Eq [2.20], we get the $C_x = G \cdot W \cdot L^2/(2 \cdot H)$. With $G = 0.5\ [M\,N/m^2]$ (typical shear modulus in rubber), $W = L = 0.1..0.12\ [m]$ (typical sizes of contact patch for passenger car) and $H = 0.01\ [m]$ (approximate tyre tread depth) one gets $\approx 25[kN] < C_x = G \cdot W \cdot L^2/(2 \cdot H) <\approx 40[kN/1]$. Empirically, we can measure C_x for passenger car tyres around $25..50\ [kN/1]$. This indicates that the brush model models the essential physical phenomena and that the sheared part (the bristles) is rather only the tread than the whole elastic part sidewall and tread together.

2.2.3.1.3 Influence of Vertical Load and Friction in Brush Model

The vertical load on the tyre affects the force generation, F_x. For large slip our dry friction model motivates that F_x is proportional to F_z. This is also a good approximation for small slip, via $C_x \propto F_z$. Then, one can define the Longitudinal Slip Coefficient, CC_x:

$$F_x = C_x \cdot s_x = CC_x \cdot F_z \cdot s_x; \qquad [2.17]$$

The contact length L will reasonably vary according to some deformation model. Hertz's contact theory for line contact motivates that $L \propto \sqrt[2]{F_z}$. This is implemented as $L^2 = F_z/k$, where k is a material modulus with dimension *force/area*, gives:

$$C_x = \frac{G_x \cdot W \cdot L^2}{2 \cdot H_x} = \frac{G_x \cdot W \cdot F_z/k}{2 \cdot H_x} = \underbrace{\frac{G_x \cdot W}{2 \cdot H_x \cdot k}}_{CC_x} \cdot F_z;$$

So, the assumption $L \propto \sqrt[2]{F_z}$ explains why $C_x \approx CC_x \cdot F_z \propto F_z$;. This can be verified with experiments, see Figure 2-48. A small tendency for degressive increase ($\partial^2 C_x/\partial F_z^2 < 0$) can be found.

The result is summarised in Figure 2-22. Increasing μ only increases the saturation level, while leaving the slope at lower s_x constant, or possibly slightly increased. Variation of F_z involves the contact length model. The assumption "$L \propto \sqrt[2]{F_z}$" simply scales the curve in force direction. Overall, it can be concluded that there are arguments for two conceptual ways how the tyre characteristics changes, varied vertical force and varied friction coefficient, see Figure 2-22.

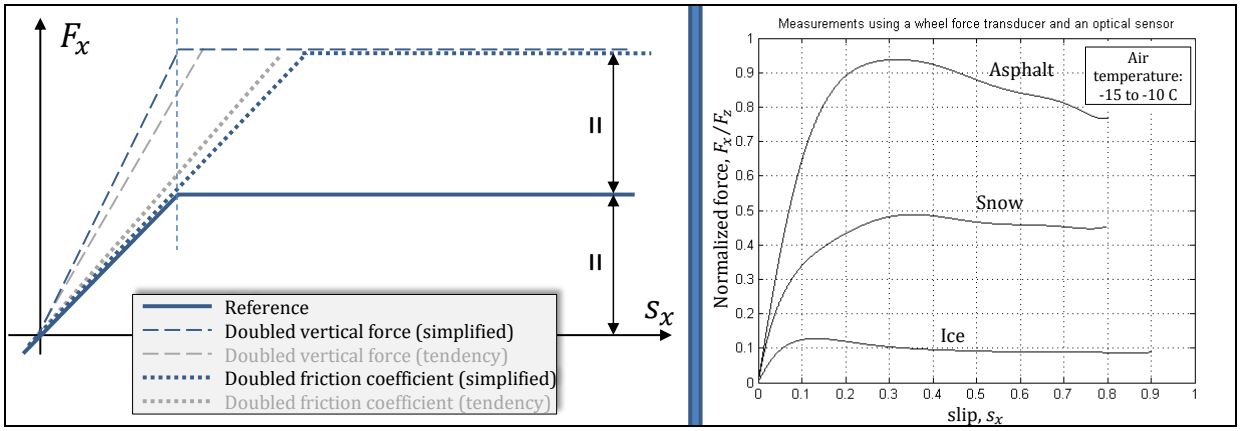

Figure 2-22: How tyre characteristics typically vary due to varying vertical force and road friction. Left: Theory. Right: Measurements with varying friction, i.e. varying surfaces, from PhD course by Ari Tuononen, Aalto university, Finland, Saariselkä, Finland 2014-03-15..22.

The influence of vertical force on C_x (and on lateral slip stiffness C_y) is further discussed in 2.2.4.3 and 2.2.5.4.

2.2.3.1.4 Influence of Different Static and Dynamic Friction

A common model for friction is that coefficient of friction to remain sticking, μ_{stick}, is higher than the coefficient of friction when slipping has started, μ_{slip}. This is sometimes called "stiction". If this is implemented in the model, the brush model can explain why the overall $F_x(s_x)$ often has a peak, as indicated already in Figure 2-19. In the derivation in Eq [2.13], the differing between μ_{stick} and μ_{slip}, affects like this: $F_{x,slip} = W \cdot \int_{\xi_c}^{L} \mu_{slip} \cdot p \cdot d\xi$; and $\xi_c = \frac{\mu_{stick} \cdot F_z \cdot L}{2 \cdot C_x \cdot s_x}$;.

$$F_x = \begin{cases} = \text{sign}(s_x) \cdot \mu_{slip} \cdot F_z; & if\ \omega \cdot\ v_x < 0\ (macro\ slip) \\ = C_x \cdot s_x; & else\ if\ |s_x| \le \frac{\mu_{stick} \cdot F_z}{2 \cdot C_x} \Leftrightarrow |F_x| \le \frac{\mu_{stick} \cdot F_z}{2} \\ = \text{sign}(s_x) \cdot \mu_{slip} \cdot F_z \cdot \left(1 - \frac{F_z}{2 \cdot C_x \cdot |s_x|} \cdot \mu_{stick} \cdot \left(1 - \frac{\mu_{stick}}{2 \cdot \mu_{slip}}\right)\right); & else \end{cases} \quad [2.18]$$

$$where\ C_x = \frac{G_x \cdot W \cdot L^2}{2 \cdot H_x};\ \ dimension: [force] \quad and\ s_x = \frac{R \cdot \omega - v_x}{|R \cdot \omega|};$$

This model only gives a peak if $\mu_{stick} > 2 \cdot \mu_{slip}$, see Figure 2-24. The model explains that a peak can occur, but the shape of the curve does not correlate well with tyre measurements. The model can work to explain some phenomena on vehicle level, but a better model can be found if assuming parabolic pressure distribution, see 2.2.3.1.5.

2.2.3.1.5 Brush Model with Parabolic Pressure Distribution

Hertz's contact theory for line contact motivate an elliptical pressure distribution. A parabolic pressure distribution approximates an elliptical and it gives an alternative brush model, as compared to the one appearing from uniform pressure. The coefficients in the parabolic pressure function have to be chosen such that $\int_0^L p(\xi)\cdot W\cdot d\xi = F_z$ and $p(0)=p(L)=0$;:

$$p(\xi)=\frac{6\cdot F_z}{W\cdot L}\cdot\frac{\xi}{L}\cdot\left(1-\frac{\xi}{L}\right); \qquad [2.19]$$

If we do the corresponding derivation as for the uniform pressure distribution, e.g. assuming a stick and slip zones, the location of where slip starts, ξ_c, becomes:

$$\tau(\xi_c)=\frac{G}{H}\cdot s_x\cdot\xi_c=\mu\cdot p(\xi_c)=\mu\cdot\frac{6\cdot F_z}{W\cdot L}\cdot\frac{\xi_c}{L}\cdot\left(1-\frac{\xi_c}{L}\right);\Rightarrow\ \xi_c=L-\frac{G\cdot W\cdot L^3\cdot s_x}{6\cdot\mu\cdot H\cdot F_z};$$

The slip where ξ_c appears outside $0<\xi_c<L$ is when ξ_c becomes <0, which is when the whole contact slips:

$$\xi_c=L-\frac{G\cdot W\cdot L^3\cdot s_x}{6\cdot\mu\cdot H\cdot F_z}=L\cdot\left(1-\frac{C_x\cdot s_x}{3\cdot\mu\cdot F_z}\right)<0;\Rightarrow s_x>\frac{3\cdot\mu\cdot F_z}{C_x};$$

Total longitudinal force, F_x, becomes:

$$F_x\cdot\mathrm{sign}(s_x)=\begin{cases}=\mu\cdot F_z & if\ \omega\cdot v_x<0\\ =\left(C_x\cdot|s_x|-\dfrac{(C_x\cdot|s_x|)^2}{3\cdot\mu\cdot F_z}+\dfrac{(C_x\cdot|s_x|)^3}{27\cdot(\mu\cdot F_z)^2}\right); & else\ if\ |s_x|<\dfrac{3\cdot\mu\cdot F_z}{C_x}\Leftrightarrow\\ & \Leftrightarrow|F_x|\le\mu\cdot F_z\\ =\mu\cdot F_z; & else\end{cases}$$

$$where\ C_x=\frac{G\cdot W\cdot L^2}{2\cdot H};\ \ dimension:[force]\quad and\ s_x=\frac{R\cdot\omega-v_x}{|R\cdot\omega|}; \qquad [2.20]$$

The shape of this curve becomes as shown in Figure 2-23. The uniform pressure distribution model is drawn as reference. Note that the parabolic pressure distribution does not give any linear part, but the derivative at $s_x=0$ is same, $C_x=G\cdot W\cdot L^2/(2\cdot H)$.

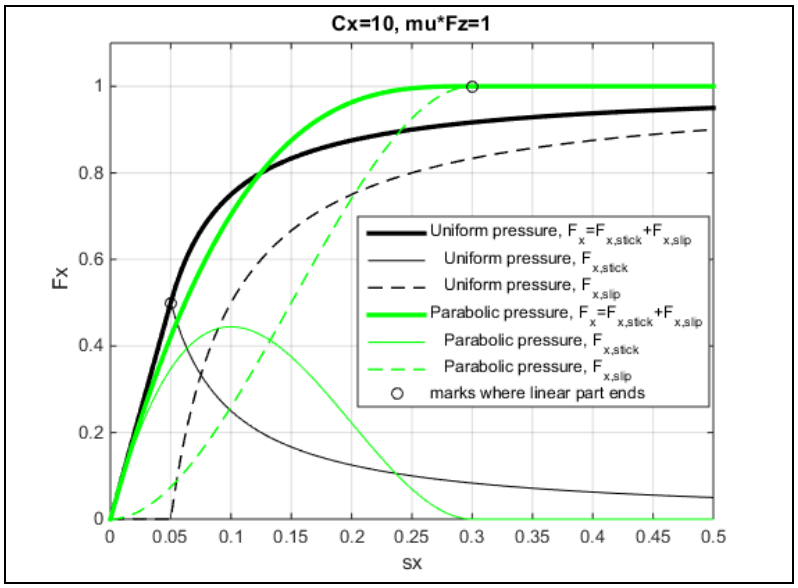

Figure 2-23: Shape of force/slip relation derived with brush model with parabolic pressure distribution and different contact length models. Also, the force terms from stick- and slip-regions are shown.

2.2.3.1.6.1 Different Static and Dynamic Friction

We now introduce different μ_{stick} and μ_{slip}. We also identify each force term, for stick and slip regions, as follows:

$$F_{x,stick} = W \cdot \int_0^{\xi_c} \tau(\xi) \cdot d\xi = W \cdot \int_0^{\xi_c} \frac{2 \cdot C_x}{W \cdot L^2} \cdot s_x \cdot \xi \cdot d\xi = \left\{ \xi_c = L \cdot \left(1 - \frac{C_x \cdot s_x}{3 \cdot \mu_{stick} \cdot F_z}\right); \right\} = \cdots =$$

$$= C_x \cdot \left(1 - \frac{C_x \cdot s_x}{3 \cdot \mu_{stick} \cdot F_z}\right)^2 \cdot s_x;$$

$$F_{x,slip} = W \cdot \int_{\xi_c}^{L} \mu_{slip} \cdot p \cdot d\xi = \mu_{slip} \cdot W \cdot \int_{\xi_c}^{L} p \cdot d\xi = \left\{ \begin{matrix} p = \frac{6 \cdot F_z}{W \cdot L} \cdot \frac{\xi}{L} \cdot \left(1 - \frac{\xi}{L}\right); \\ \xi_c = L \cdot \left(1 - \frac{C_x \cdot s_x}{3 \cdot \mu_{stick} \cdot F_z}\right); \end{matrix} \right\} = \cdots =$$

$$= \mu_{slip} \cdot F_z \cdot \left(3 - 2 \cdot \frac{C_x \cdot s_x}{3 \cdot \mu_{stick} \cdot F_z}\right) \cdot \left(\frac{C_x \cdot s_x}{3 \cdot \mu_{stick} \cdot F_z}\right)^2;$$

$$Both\ expressions\ valid\ only\ for\ s_x < \frac{3 \cdot \mu_{stick} \cdot F_z}{C_x};$$

The force terms, $F_{x,stick}$ and $F_{x,slip}$, from each of stick and slip regions are identified for $s_x < 3 \cdot \mu_{stick} \cdot F_z / C_x$. When slip is larger, $s_x > 3 \cdot \mu_{stick} \cdot F_z / C_x$, the whole contact slips, $F_{x,stick} = 0$; and $F_{x,slip} = \mu_{slip} \cdot F_z$;. If we sum to $F_x = F_{x,stick} + F_{x,slip}$ we get:

$$F_x \cdot \text{sign}(s_x) = \begin{cases} = \mu_{slip} \cdot F_z; & if\ \omega \cdot\ v_x < 0 \\ = C_x \cdot |s_x| - \left(2 - \frac{\mu_{slip}}{\mu_{stick}}\right) \cdot \frac{(C_x \cdot |s_x|)^2}{3 \cdot \mu_{stick} \cdot F_z} + \left(3 - 2 \cdot \frac{\mu_{slip}}{\mu_{stick}}\right) \cdot \frac{(C_x \cdot |s_x|)^3}{27 \cdot (\mu_{stick} \cdot F_z)^2}; & else\ if\ |s_x| < \frac{3 \cdot \mu_{stick} \cdot F_z}{C_x} \\ = \mu_{slip} \cdot F_z; & else \end{cases} \quad [2.21]$$

$$where\ C_x = \frac{G \cdot W \cdot L^2}{2 \cdot H};\ \ dimension: [force] \quad and\ s_x = \frac{R \cdot \omega - v_x}{|R \cdot \omega|};$$

Typical values of friction coefficients that give good resemblance with measurements are $\mu_{stick} / \mu_{slip} = 1.3..1.8$. In (Ludwig, o.a., 2017), the ratio μ_{stick} / μ_{slip} is experimentally found to vary approximately between 1.1 and 2.0. Note that the peak of the curve neither means $F_x / F_z = \mu_{slip}$ nor $F_x / F_z = \mu_{stick}$. For example, the curve with $[\mu_{slip}\ \ \mu_{stick}] = [1\ \ 2]$ peaks at $F_x / F_z \approx 6300/5000 \approx 1.26$, which is far from μ_{stick}.

Eq [2.21] gives same peak $F_{x,peak}$ and asymptotic $F_{x,slip}$ independent of C_x. The peak slip $s_{x,peak}$ becomes independent of $C_x / F_z = CC_x$, which is often constant:

$$F_{x,peak} = \pm F_z \cdot \mu_{stick} \cdot \frac{4 - 3 \cdot \frac{\mu_{slip}}{\mu_{stick}}}{\left(3 - 2 \cdot \frac{\mu_{slip}}{\mu_{stick}}\right)^2};\ \ \text{and}\ \ s_{x,peak} = \frac{\pm 3 \cdot F_z}{C_x} \cdot \frac{\mu_{stick}}{3 - 2 \cdot \frac{\mu_{slip}}{\mu_{stick}}} = \frac{\pm 3}{CC_x} \cdot \frac{\mu_{stick}}{3 - 2 \cdot \frac{\mu_{slip}}{\mu_{stick}}};$$

The model and analysis can be transferred to lateral slip, except that there is often a tendency that $C_y / F_z \neq CC_y$, but rather that C_y / F_z decreases with F_z. Hence, $s_{y,peak}$ increases with F_z.

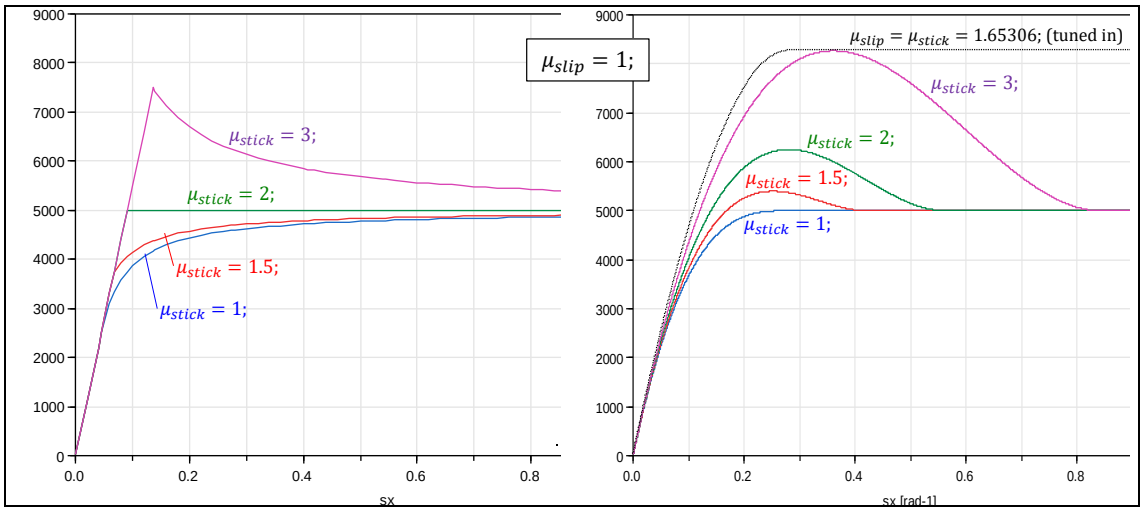

Figure 2-24: Brush model with uniform (left) and parabolic (right) pressure. Varying μ_{stick}/μ_{slip}.

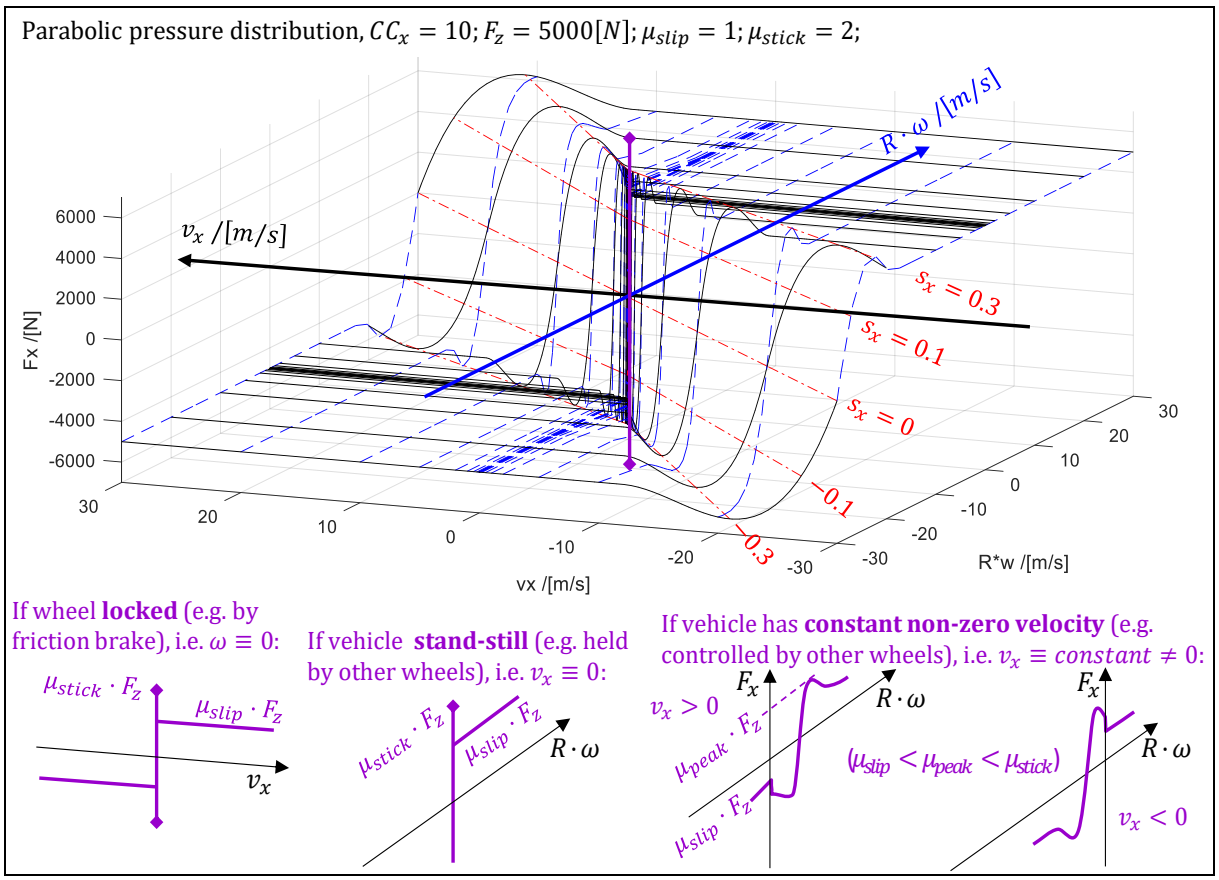

Figure 2-25: Eq [2.21] plotted over the $[R \cdot \omega, v_x]$-plane.

2.2.3.2 Measurements

Some examples of measurements are given Figure 2-26. It is important to understand that there is a big spread between different tyres (e.g. studded or not, as shown in the figure) and that the physical phenomena we try to measure and model is not only the tyre, but the contact between one certain tyre and one certain ground surface (e.g. ice, as shown in figure). Additionally, there is one certain wheel suspension which can cause different high frequency oscillations which affect the averaged measured signals. The figure shows both longitudinal and lateral grip, so both relevant for 2.2.3 and 2.2.4, but not the combined situation in 2.2.5.

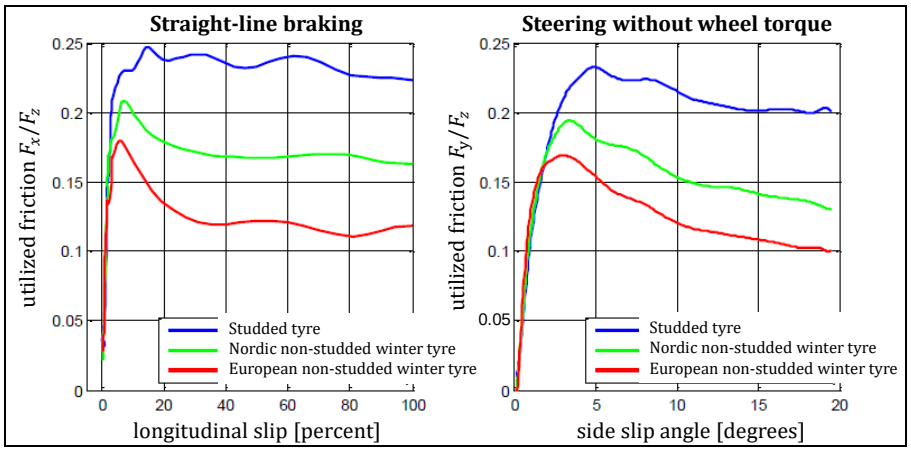

Figure 2-26: Typical measurements for passenger car tyres on ice. From Hjort and Eriksson, VTI report 875, 2015. https://www.vti.se/en/Publications .

2.2.3.3 Parameter Fitting in Physical Tyre Models

The brush model variants presented above are *physical tyre models*. They can to some extent represent changing tyre design parameters and changing ground properties. It is almost impossible to know the correct numerical values of the real design parameters, such as G_x, W, H_x in $C_x = G_x \cdot W \cdot L^2/(2 \cdot H_x)$ or μ. But if one has experimental data, one can at least fit C_x and μ, to one experiment. Changing C_x or μ then makes sense. However, L is no design parameter, but a variable dependent of F_z. So, if also changing F_z, one would need more experimental data with variation in F_z or a model for $L = L(F_z)$. The compendium argues for using slip definition from Eq [2.1] instead of Eq [2.2] when fitting parameters in physical tyre models.

2.2.3.4 Curve Fit Tyre Models

The brush model is a *physical tyre model*. However, if a model is required which is numerically accurate for one specific tyre of which one have experimental data, and there is no need for changing tyre design parameters and ground properties, one can use a *curve fit tyre model* instead.

Those "Curve Fit Tyre Models" often uses a mathematical curve approximation, such as trigonometric and exponential forms instead of models as in Eq [2.14]. Most curve fit tyre models use the "collapse from 3 to 2 independent variables", by which is meant that the fitted curves have 2 independent variables: $[F_x, F_y] = func\left(s_x(R \cdot \omega, v_x), s_y(R \cdot \omega, v_x)\right)$; instead of $[F_x, F_y] = func(\omega, v_x, v_y)$;. This selection of number of independent variables is typically the only very physical assumption in the curve fit models. The argument of physics to use slip definition from Eq [2.1] instead of Eq [2.2] are typically neglected for curve fit tyre models, and it is usual that Eq [2.2] is selected. Regardless which slip definition is used, it is important that **same** slip definition is used when numerical parameter values are fitted as when the tyre model is used, e.g. for simulation.

2.2.3.4.1 Magic Formula Tyre Model

The most well-known curve fit tyre model is probably the "Magic Formula". It was proposed by Professor Hans Pacejka, 1934-2017. It is described, e.g., in (Bakker, 1987). The curve fit has the general form:

$$Force = y(x) = D \cdot \sin\big(C \cdot \arctan\big(B \cdot x - E \cdot (B \cdot x - \arctan(B \cdot x))\big)\big) + S_V;$$
$$Slip = s = x = X + S_H; \qquad [2.22]$$

The variable $x = s_x$ is the tyre slip value. The parameters are: D $[N]$ is peak force, B $[N/1]$ is slip stiffness, C $[1]$ is shape and E $[1]$ is curvature. The parameters S_V and S_H simply shifts the curve so that it passes through the origin, which might not be the case for measurement data, since there can be errors in tyre radius and correction for rolling resistance. The relationship between these parameters and the tyre slip/friction relation is shown in Figure 2-27.

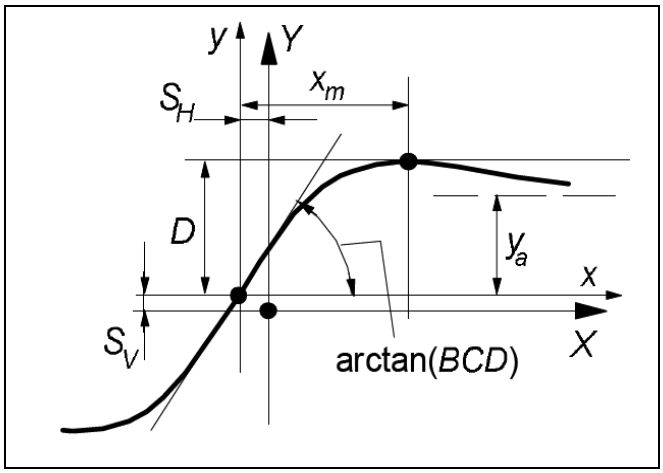

Figure 2-27: Magic Formula Tyre Parameters, (Pacejka, 2005)

2.2.3.4.2 TMsimple and TMeasy Tyre Models

TMsimple and TMeasy are two other curve fit models. TMsimple is shown in Eq [2.23] (without influence of vertical force). Both are shown in Figure 2-28. TMsimple is a simplified variant of TMeasy. For example, in TMsimple, it is not possible to set the maximum force value to a specific slip. TMeasy is described in Ref (Hirschberg, et al., 2007).

$$F(s) = F_{max} \cdot \sin\left(B \cdot \left(1 - e^{-|s|/A}\right) \cdot \text{sign}(s)\right);$$
$$where\ B = \pi - \arcsin(F_\infty / F_{max});\ and\ A = F_{max} \cdot B / \arctan(C);$$
$$with\ F_{max}, F_\infty\ and\ C\ as\ in\ Eq\ [2.29] \qquad [2.23]$$

2.2.3.4.3 More Advanced Models

There are numerous of more advanced tyre models, such as Swift and FTire. They mix physical and curve fit parameters. FTire is almost a finite element model and demands very many parameters.

2.2.3.4.4 Very Simple Tyre Models

There are many more models with different degree of curve fitting to experimental data. However, one can often have use for very simple curve fits, such as:

- Linearized: $F_x = C_x \cdot s_x$
- Linearized and saturated: $F_x = \text{sign}(s_x) \cdot min(C_x \cdot |s_x|; \mu \cdot F_z)$
- Stiff: $s_x = 0; \Leftrightarrow R \cdot \omega = v_x;$ (as if linear with $C_x \to \infty$)
- Stiff and saturated: $if\ stick\ s_x = 0;\ else\ F_x = \mu \cdot F_z;$ Discrete state switching: $when\ s_x < 0\ then\ stick \leftarrow true;\ elsewhen\ F_x > \mu\ then\ stick \leftarrow false;$ (Approximately described.)

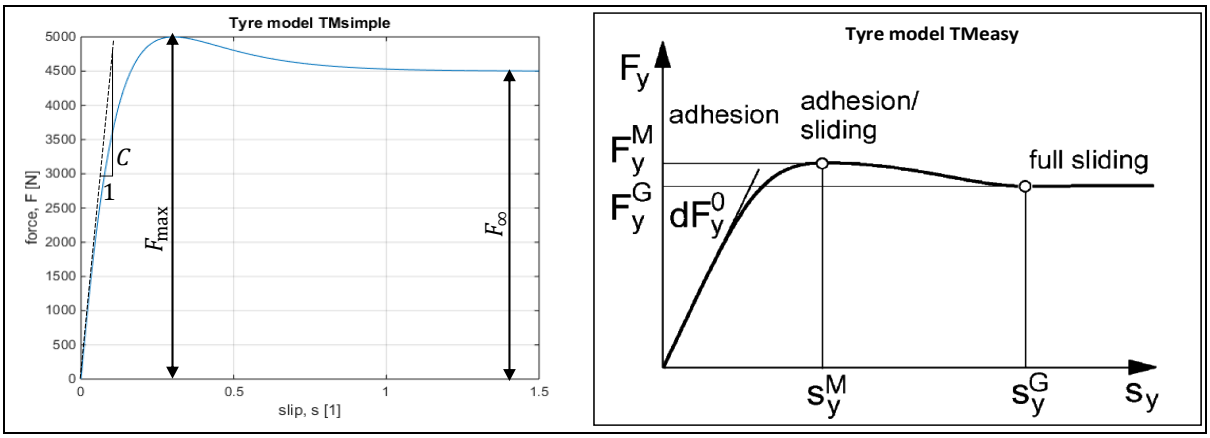

Figure 2-28: Left: TMsimple (Lex, 2015). Right: TM-Easy Tyre Model, (Hirschberg, et al., 2007).

2.2.3.5 Transients or Relaxation in Contact Patch

Both the physical and empirical tyre models assume of steady state condition in the contact patch, meaning steady state deformation pattern and steady state sliding speed distribution. Transients

between different steady state conditions take some time which is why the phenomena is called *relaxation*. Often in Vehicle Dynamics, the relaxation is such a quick process that it can be assumed to take place instantaneously, i.e. the algebraic relation $F_x = F_x(s_x)$ can be used. But sometimes it is relevant to model the transients more carefully. Transients are triggered by variations; variations in slip (v_x and/or ω), vertical force (F_z) and surface conditions (e.g. expressed in varying μ). Transients can also appear for constant conditions (constant v_x, ω, F_z, μ) if the tyre and its suspension constitute a system that comes into stick-slip oscillations.

Note that also start from stand-still and deceleration to stand-still are examples of strong transients in slip, even if vehicle acceleration/deceleration is small. We can see this in Figure 2-11 where we see that the smaller $|v_x|$, the steeper the curve $F_x(\omega)$ becomes during sign change. So, if $v_x = 0$, the $F_x(\omega)$ will have same step-form as a dry friction contact. If using slip, we experience this as a mathematical singularity; slip approaches $\pm\infty$ when ω approaches zero. Modelling transients often solve both the mentioned transients in slip, vertical force and surface conditions as well as driving situations involving/close to stand-still.

The physical phenomena to be modelled is elasticity; in tyre sidewalls and/or in contact patch.

2.2.3.5.1 Transients due to Relaxation in Contact Patch Modelled as Filter

The elasticity in the side walls, modelled in 2.2.3.5.1, explains delay; e.g. when changing ω_{rim} stepwise, the force F_x will not follow f_{SS} directly, but with a delay. Another phenomenon that causes delay is that the bristles in the contact patch needs to adopt to a new deformation pattern and sliding speed distribution. Following the brush model, the physically correct way would be to formulate the equations as a partial differential equation (*PDE*), with derivatives with respect to both time and position along the contact patch, ξ. A "quasi-physical" way to model this is to apply a 1st order time delay of force:

$$\dot{F}_x = (1/\tau) \cdot (f_{SS}(s_x, F_z, \mu, \dots) - F_x);$$

where $f_{SS}(s_x, F_z, \mu, \dots)$ is the force according to a steady state model, e.g.Eq [2.14] and the time delay, $\tau = \frac{L_r}{v_{Transport}} = \frac{L_r}{|R \cdot \omega_{rim}|}$ and L_r is the relaxation length, which often is given as a fraction ($\approx 25..50\%$) of tyre circumference. [2.24]

Alternatively, one can also express the delay as a 1st order time delay of the slip, as follows:

$$F_x = f_{SS}(s_{x,delayed}, F_z, \mu, \dots);$$

$$\dot{s}_{x,delayed} = (1/\tau) \cdot (s_x - s_{x,delayed});$$

where $f_{SS}(s_{x,delayed}, F_z, \mu, \dots)$ is the force according to a steady state model, e.g. Eq [2.14] and τ is as defined in Eq [2.24]. [2.25]

Eq [2.24] is similar to "spring in series", as in 2.2.3.5.1, if a linear tyre-to-slip-model is used. This can motivate that delaying force (Eq [2.24]) is more physical than delaying the slip (Eq [2.25]). The delay in slip rather proposes that *relative speed* as state variable, which is not physical in this context. However, the delayed force has the non-physical effect that F_x sometimes can become $> \mu \cdot F_z$ in cases when wheel is off-loaded quickly, i.e. when $\dot{F}_z$ is a large negative value. So, an extension to $F_x = \max(f_{SS}(s_{x,delayed}, F_z, \mu, \dots),\ \mu \cdot F_z)$; can be motivated.

It would make sense from physical point of view, if the relaxation length was approximately same magnitude as the contact length, or possibly the length of the sticking zone. However, commonly given size of relaxation length is 25..50% of tyre circumference, which is normally several times larger than the contact length. This can be because one measures delay due to sidewall elasticity also, but then interpreted as a relaxation length.

With $f_{SS} = C_x \cdot s_x$;, and $\omega_{rim} > 0$; and $v_x > 0$;, we can simplify Eq [2.24] to Eq [2.26]:

$$\dot{F}_x = \frac{C_x}{L_r} \cdot R \cdot \omega_{rim} - \frac{C_x}{L_r} \cdot v_x - \frac{R \cdot \omega_{rim}}{L_r} \cdot F_x; \quad \Rightarrow \left\{ s_x = \frac{F_x}{C_x}\ is\ small \right\} \Rightarrow$$

$$\Rightarrow \dot{F}_x \approx \frac{C_x}{L_r} \cdot R \cdot \omega_{rim} - \frac{C_x}{L_r} \cdot v_x;$$

[2.26]

2.2.3.5.2 Transients due to Elasticity of Sidewalls

Figure 2-29 shows a physical model which can model how the force change is delayed during quick changes in slip. The model can also handle vehicle stand-still. This type of model is often called a *rigid ring tyre model*, because the belt is modelled as a rigid ring. The ring is here massless but has mass and rotational inertia. The longitudinal and vertical support are here rigid, but they can be modelled as compliant. If no significant inertia in wheel hub, the driveshaft compliance will be series coupled with the rotational compliance, c_{sw}. The torque T_{rim} is the sum of torque from propulsion system and brake system. Damper elements can be added beside the compliances.

The mathematical model becomes as follows, where f_{SS} denotes a steady state tyre model, e.g. from 2.2.3.1:

$$\dot{F}_x = c_{sw} \cdot (R \cdot \omega_{rim} - R \cdot \omega_{belt});$$
$$F_x = f_{SS}(s_x, F_z, \mu, \ldots); \quad where \quad s_x = \frac{R \cdot \omega_{belt} - v_x}{|R \cdot \omega_{belt}|}; \qquad [2.27]$$

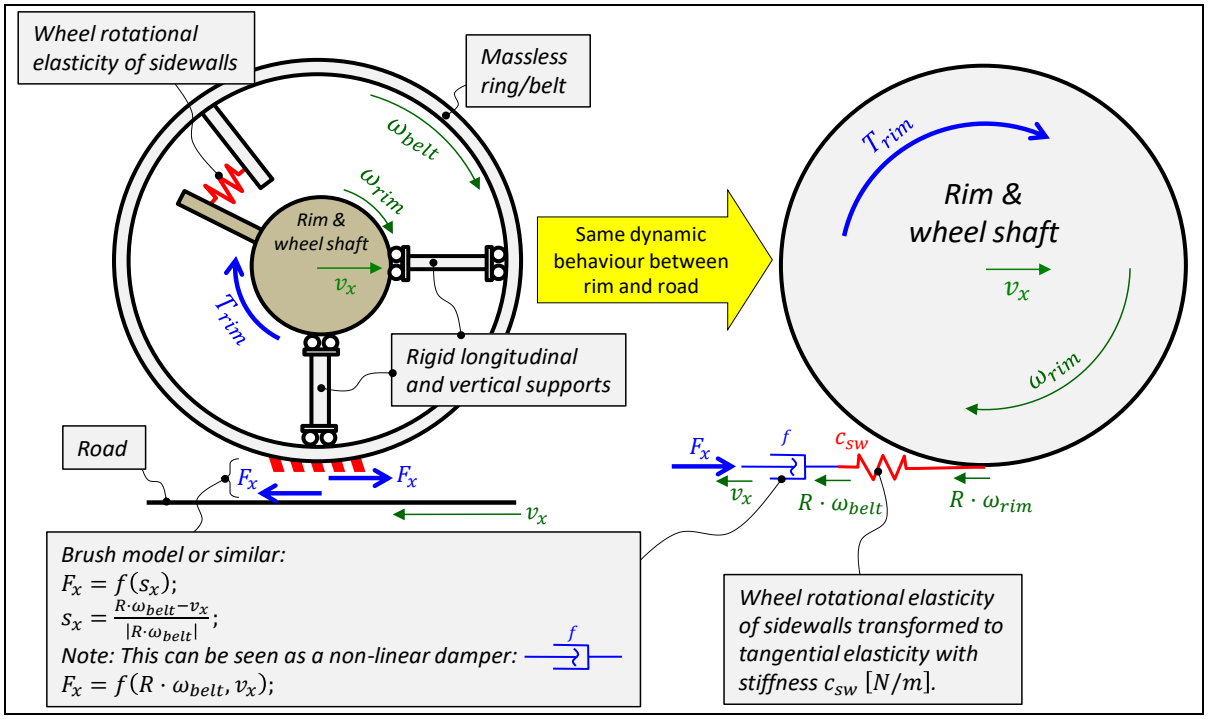

Figure 2-29: Tyre model including the rotational elasticity of tyre sidewalls.

Damping in parallel with the elasticity is often motivated also:

$$F_x = F_{xs} + F_{xd};$$
$$\dot{F}_{xs} = c_{sw} \cdot (R \cdot \omega_{rim} - R \cdot \omega_{belt});$$
$$F_{xd} = d_{sw} \cdot (R \cdot \omega_{rim} - R \cdot \omega_{belt});$$
$$F_x = f_{SS}(s_x, F_z, \mu, \ldots); \quad where \quad s_x = \frac{R \cdot \omega_{belt} - v_x}{|R \cdot \omega_{belt}|}; \qquad [2.28]$$

If used in a system where ω_{rim} and v_x are input variables to tyre, the force F_x will become a state variable. It is then not a problem that slip is undefined for $\omega = 0$, because the explicit form of equations will become as follows. Note that we simplify by only considering the case when $\omega_{belt} \cdot v_x > 0$. And the model validity is limited to $F_x, F_z, \mu, \ldots$ such that uniquely defines s_x.

$$
\begin{aligned}
&s_x \leftarrow g_{SS}(F_x, F_z, \mu, \dots);\\
&\omega_{belt} \leftarrow \frac{v_x}{R \cdot (1 - s_x \cdot \mathrm{sign}(v_x))}; \quad (only\ valid\ for\ \omega_{belt} \cdot v_x > 0)\\
&\dot{F}_x \leftarrow c_{sw} \cdot (R \cdot \omega_{rim} - R \cdot \omega_{belt});\\
&where\ g_{SS}\ is\ the\ inverse\ of\ function\ f_{SS}\ such\ that\ s_x = g_{SS}(F_x, F_z, \mu);
\end{aligned}
\qquad [2.29]
$$

With $f_{SS} = C_x \cdot s_x$;, and $\omega_{rim} > 0$; and $v_x > 0$;, we can simplify Eq [2.29]to Eq [2.30]:

$$
\begin{aligned}
&\dot{F}_x = c_{sw} \cdot R \cdot \omega_{rim} - \frac{c_{sw} \cdot v_x}{1 - \frac{F_x}{C_x}}; \quad \Rightarrow \left\{ s_x = \frac{F_x}{C_x}\ is\ small \right\} \Rightarrow\\
&\Rightarrow \dot{F}_x \approx c_{sw} \cdot R \cdot \omega_{rim} - c_{sw} \cdot v_x;
\end{aligned}
\qquad [2.30]
$$

Eq [2.29] means that we read the function f_{SS} from force F_x to slip s_x. When knowing slip, we can calculate the rotational speed ω_{belt}. Then, the state derivative $\dot{F}_x$ can be calculated, so that the state F_x can be updated in each time step.

With any reasonable tyre function f_{SS}, there is a maximum magnitude of force, $|F_x| = \mu \cdot F_z$, above which there is no slip s_x that gives that F_x. In most problems, one never ends up there in the simulations, since when approaching $|F_x| = \mu \cdot F_z$, the velocity ω_{belt} changes quickly in the direction that makes $|F_x|$ stays $<\mu \cdot F_z$. But, if $\mu \cdot F_z$ decreases stepwise, one might end up there anyway for short time intervals. In that case, it often gives physically acceptable solutions on vehicle level, to simply saturate s_x so that $|F_x|$ is saturated at a certain level, e.g. $0.95 \cdot \mu \cdot F_z$. For the brush model with uniform pressure distribution, Eq [2.14], the inverted function g becomes as follows, including such saturation:

$$
\begin{aligned}
s_x = g(F_x, F_z, \mu) = \begin{cases} = \dfrac{F_x}{C_x}; & for\ |F_x| \le \dfrac{\mu \cdot F_z}{2}; \\ = \dfrac{\mu \cdot F_z}{4 \cdot C_x} \cdot \dfrac{\mathrm{sign}(F_x)}{1 - \frac{|F_x|}{\mu \cdot F_z}}; & for\ |F_x| < 0.95 \cdot \mu \cdot F_z; \\ = \dfrac{\mu \cdot F_z}{4 \cdot C_x} \cdot \dfrac{\mathrm{sign}(F_x)}{1 - 0.95}; & else \end{cases}\\
where\ C_x = \frac{G \cdot W \cdot L^2}{2 \cdot H};\ \ dimension: [force]
\end{aligned}
\qquad [2.31]
$$

2.2.3.5.3 Relation between the two Transients Models

The models in 2.2.3.5.1 and 2.2.3.5.1 describe two different phenomena which both are present in the real world. Since it is difficult to distinguish between the two delay-creating parameters, c_{sw} and C_x/L_r, one often models only one phenomenon. But then, one adjusts the numerical value of the used parameter so that the model captures about the same delay as a real-world test. If $c_{sw} = C_x/L_r$;, the two models coincide approximately.

This compendium does not give any recommendation of which of the two models is best.

Note that, with unsaturated F_x in Eq [2.24], one has to limit the integration of $\dot{F}_x$ to $|F_x| \le \mu \cdot F_z$.

2.2.3.6 Tyre with Both Rolling Resistance and Slip

So far, the models in 2.2.3 have not included rolling resistance. As we regard rolling resistance as a torque, not a force, it does not affect the $F_x(s_x)$ curve. But the rolling resistance does move the $T(s_x)$ curve vertical. The curve moves upwards if the wheel is rolling forward and downwards if rolling rearwards, see Figure 2-30. The $F_x(s_x)$ curve is normally the suitable view for vehicle level studies, while the $T(s_x)$ curve is sometimes needed for involving a model of the propulsion and brake systems. As mentioned in 2.2.1.7, one can select different R in the slip definition. In Figure 2-30, it is assumed that one uses an R such that $F_x = 0$ for $s_x = 0$, i.e. for pure rolling. Often, for wheel slip control (ABS, TC, …), one instead uses an R such that $T = 0$ for $s_x = 0$, i.e. for free-rolling, because it is much easier to know when $T = 0$ than when $F_x = 0$.

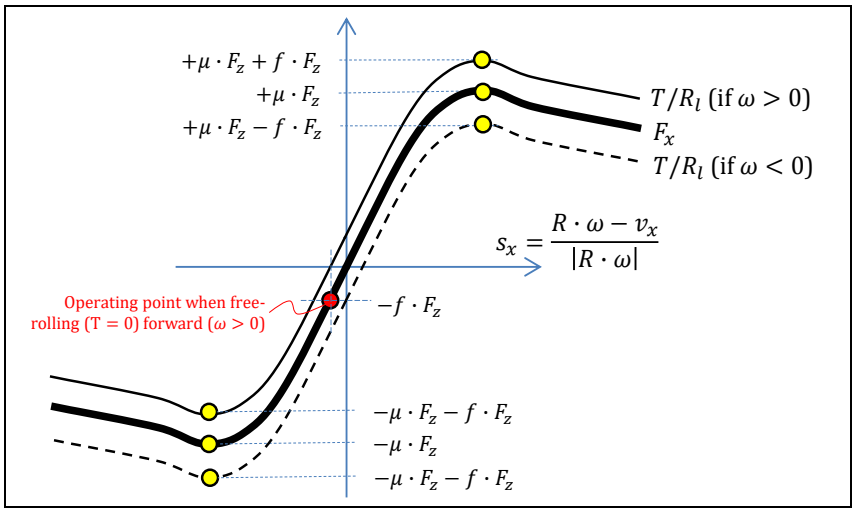

Figure 2-30: Longitudinal tyre force (F_x) and normalized wheel torque (T/R_l) for both rolling resistance and slip. Slip defined so that curve $F_x(s_x)$ passes through diagram origin, which means that $T(s_x)/R_l$ does not.

2.2.4 Lateral Force of Tyre

After a vehicle starts moving, controlling the direction of travel becomes a high priority for the operator. For wheeled vehicles, the primary mode to control travel direction is to change the orientation of the tyre, i.e. to apply a steer angle. Tyres generate a lateral force when they are oriented at an angle different to the direction of the vehicle motion. The tyre typically deforms as in Figure 2-31.

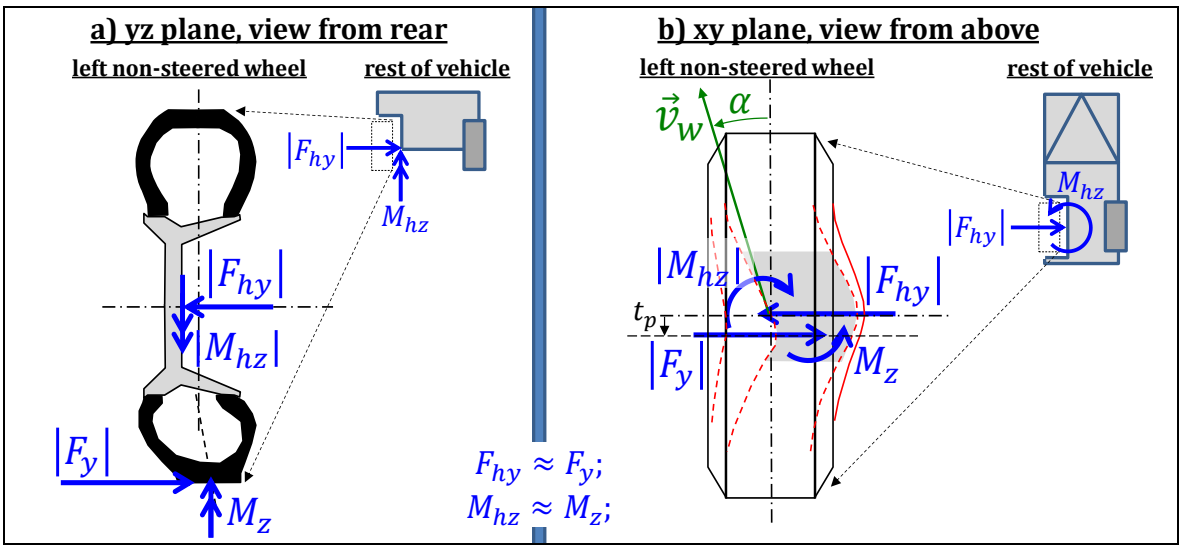

Figure 2-31: Deformation and forces of a Cornering Tyre. Wheel side slip angle is α.

It is essential to distinguish between the steer angle and wheel (lateral or side) slip angle of the tyre. Lower right part of Figure 1-20 shows this difference. The steer angle, δ or d, is the angle between vehicle longitudinal direction and tyre longitudinal direction. The wheel side slip angle, α is the angle between tyre longitudinal direction and the tyre translational velocity (=wheel hub velocity).

Assuming no longitudinal tyre slip, $R \cdot \omega = v_x$, the relation between the lateral force of a tyre and the wheel side slip angle is typically as shown in Figure 2-35. The behaviour of the curve is similar to that exhibited for longitudinal forces Figure 2-27 and Figure 2-28. It becomes even more similar if lateral slip angle is replaced by lateral wheel slip, s_y, which is $= \tan(\alpha) \approx \alpha$ for small lateral slip.

$$s_y = \frac{v_y}{|R \cdot \omega|} = \frac{v_y}{R \cdot \omega} \cdot \text{sign}(R \cdot \omega) = \left\{ \begin{matrix} if\ s_x = 0 \\ i.e.\ R \cdot \omega = v_x \end{matrix} \right\} = \tan(\alpha)\,; \qquad [2.32]$$

Using magnitude in denominator $|R \cdot \omega|$ gives same sign of s_y and F_y for all combinations of signs of ω and v_y, which leads to easier formulas.

2.2.4.1 Tyre brush Model for Lateral Slip

With corresponding simplification as in 2.2.1.6, we now use the brush model to also explain the lateral properties.

2.2.4.1.1 Model with Independent Bristles

Figure 2-32 shows the model for pure lateral slip (no longitudinal slip) and should be compared to Figure 2-21. The difference is that the model for lateral slip has the deformation of the bristles perpendicular to drawing in the upper left view in the figure.

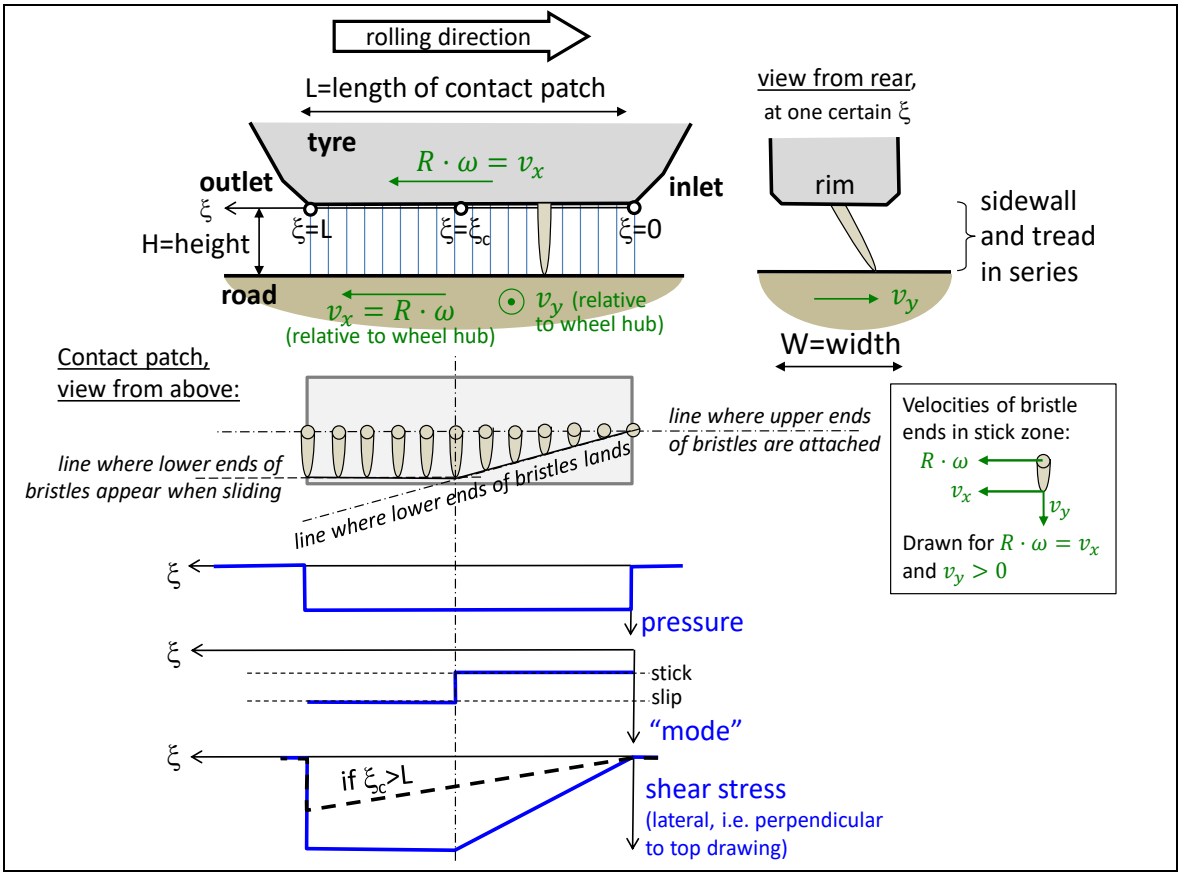

*Figure 2-32: The brush model's physical model for lateral slip. The bristles are to be thought of as the **tread in series with sidewall** lateral elasticity.*

Each bristle in Figure 2-32 is thought of as a part of the tread in series with a part of the sidewall. Further, the bristles are considered as independent of each other, which is debatable. However, it is enough for a quantitative explanation of the brush model for lateral slip. The derivation of model equations becomes similar as for the longitudinal model:

$$\tau_y = G_y \cdot \gamma_y = G_y \cdot \frac{\Delta v_y \cdot t(\xi)}{H_y} = G_y \cdot \frac{-v_y \cdot t(\xi)}{H_y} = \left\{ \begin{matrix} t(\xi) = \xi / v_{Transport}; \\ v_{Transport} \approx |R \cdot \omega|; \end{matrix} \right\} =$$

$$= G_y \cdot \frac{-v_y \cdot \xi}{H_y \cdot |R \cdot \omega|} = -\frac{G_y}{H_y} \cdot \frac{v_y}{|R \cdot \omega|} \cdot \xi = \left\{ C_y = \frac{G_y \cdot W \cdot L^2}{2 \cdot H_y};\ s_y = \frac{-v_y}{|R \cdot \omega|}; \right\} = -\frac{2 \cdot C_y}{W \cdot L^2} \cdot s_y \cdot \xi;$$

Note that subscript y has been introduced where we need to differ towards the longitudinal brush model. Correspondingly, subscript x should be used in longitudinal model. As for longitudinal model, we have to express the force differently for when friction limit is not reached within the contact and when it is. Since we assume pure lateral slip ($v_x = R \cdot \omega$), we do not have the case $v_x \cdot \omega < 0$.

$$F_y = \begin{cases} = -C_y \cdot s_y; & if\ |s_y| \le \dfrac{\mu \cdot F_z}{2 \cdot C_y} \Leftrightarrow |F_y| \le \dfrac{\mu \cdot F_z}{2} \\ = -\operatorname{sign}(s_y) \cdot \mu \cdot F_z \cdot \left(1 - \dfrac{\mu \cdot F_z}{4 \cdot C_y} \cdot \dfrac{1}{|s_y|}\right); & else \end{cases}$$

$$where\ C_y = \frac{G_y \cdot W \cdot L^2}{2 \cdot H_y};\ \ dimension: [force] \quad and\ s_y = \frac{v_y}{|R \cdot \omega|};$$

(Only valid for pure lateral slip, i.e.: $v_x = R \cdot \omega$;) [2.33]

Note that the lateral tyre slip s_y is the sliding speed of tyre over ground in lateral direction, divided by the **same** "transport speed" as for longitudinal slip, i.e. the longitudinal transport speed $R_w \cdot \omega$. Note also that the lateral force F_y and lateral tyre slip are counter-directed, which is logical since it is of friction nature.

2.2.4.1.1.1 Tyre Lateral Slip vs Wheel Slip Angle

The lateral **tyre** slip $s_y = v_y/|R \cdot \omega|$ in Eq [2.33] and Eq [2.35] can be compared with lateral **wheel** slip angle $\alpha = \arctan(v_y/v_x)$, mentioned in context of Figure 2-31:

- "Lateral **wheel** slip"$= s_{yw} = v_{yw}/v_{xw} = \tan(\alpha)$, is how wheel (hub and tyre) moves over ground and independent of wheel rotational speed.
- "Lateral **tyre** slip" $= s_{yt} = v_y/|R \cdot \omega|$, is the slip used in the constitutive relation $F_y = F_y(s_{yt})$.
- If no longitudinal tyre slip $s_x = 0$, i.e. if $R \cdot \omega = v_x$, we have $s_{yw} = s_{yt}$. Then s_{yw} can be used in the constitutive relation.

For a linearization, the most correct way is that lateral force is $F_y \propto s_y$, as opposed to $F_y \propto \alpha$. Often one finds $F_y \propto \alpha$ as starting point in the literature, but this compendium uses $F_y \propto s_y$. (In (Pacejka, 2005), pp184-185, there is also a note that s_y is more appropriate than α.)

A difference is how one linearizes a vehicle model in v_y and ω_z. A non-steered axle i modelled with $F_{iy} \propto \alpha_i$, needs to be approximated with "$\alpha_i = arctan(v_{iyv}/v_{ixv}) \approx v_{iyv}/v_{ixv}$" to make the vehicle model linear, see derivation of Eq [4.49]. However, with $F_{iy} \propto s_{iy}$; the vehicle model becomes linear without further approximations. For a steered axle it is less obvious, but it does not help the linearization to use $F_{iy} \propto \alpha_i$.

2.2.4.1.2 Model with Dependent Bristles, String Model

Opposed to the assumption in 2.2.4.1.1, the lateral deformations of the bristles are dependent on each other, especially since the tread is mounted on the belt and the belt is rather like a string. So, we assume a certain deformation of the sidewall, expressed in ε_{in} and ε_{out} for the belt="string" in Figure 2-33. This gives a slightly different model compared to 2.2.4.1.1. Models with such belt deformation are called "tyre string models". The shape of the string is dependent on the sidewall elasticity, e.g. tyre profile height, but also of the side force itself. So, the model is intrinsically implicit; the string shape influences the side force and the side force influences the string shape.

The derivation of model equations becomes similar as for the longitudinal model. Here is an intermediate result, an expression for the shear stress τ_y:

$$\tau_y = G_{y,tr} \cdot \gamma_y = G_{y,tr} \cdot \frac{\Delta v_y \cdot t(\xi)}{H_{y,tr}} = G_{y,tr} \cdot \frac{\left(R \cdot \omega \cdot \tan(\varepsilon_{in}) - v_y\right) \cdot t(\xi)}{H_{y,tr}} =$$

$$= \left\{ \begin{matrix} t(\xi) = \xi / v_{Transport}; \\ v_{Transport} \approx |R \cdot \omega|; \end{matrix} \right\} = G_{y,tr} \cdot \frac{\left(R \cdot \omega \cdot \tan(\varepsilon_{in}) - v_y\right) \cdot \xi}{H_{y,tr} \cdot |R \cdot \omega|} =$$

$$= \frac{G_{y,tr}}{H_{y,tr}} \cdot \left(\tan(\varepsilon_{in}) \cdot \operatorname{sign}(\omega) - \underbrace{\frac{v_y}{|R \cdot \omega|}}_{s_y} \right) \cdot \xi = \left\{ C_{y,tr} = \frac{G_{y,tr} \cdot W \cdot L^2}{2 \cdot H_{y,tr}} \right\} =$$

$$= -\frac{2 \cdot C_{y,tr}}{W \cdot L^2} \cdot \underbrace{\left(s_y - \tan(\varepsilon_{in}) \cdot \text{sign}(\omega)\right)}_{s_{y\varepsilon}} \cdot \xi;$$

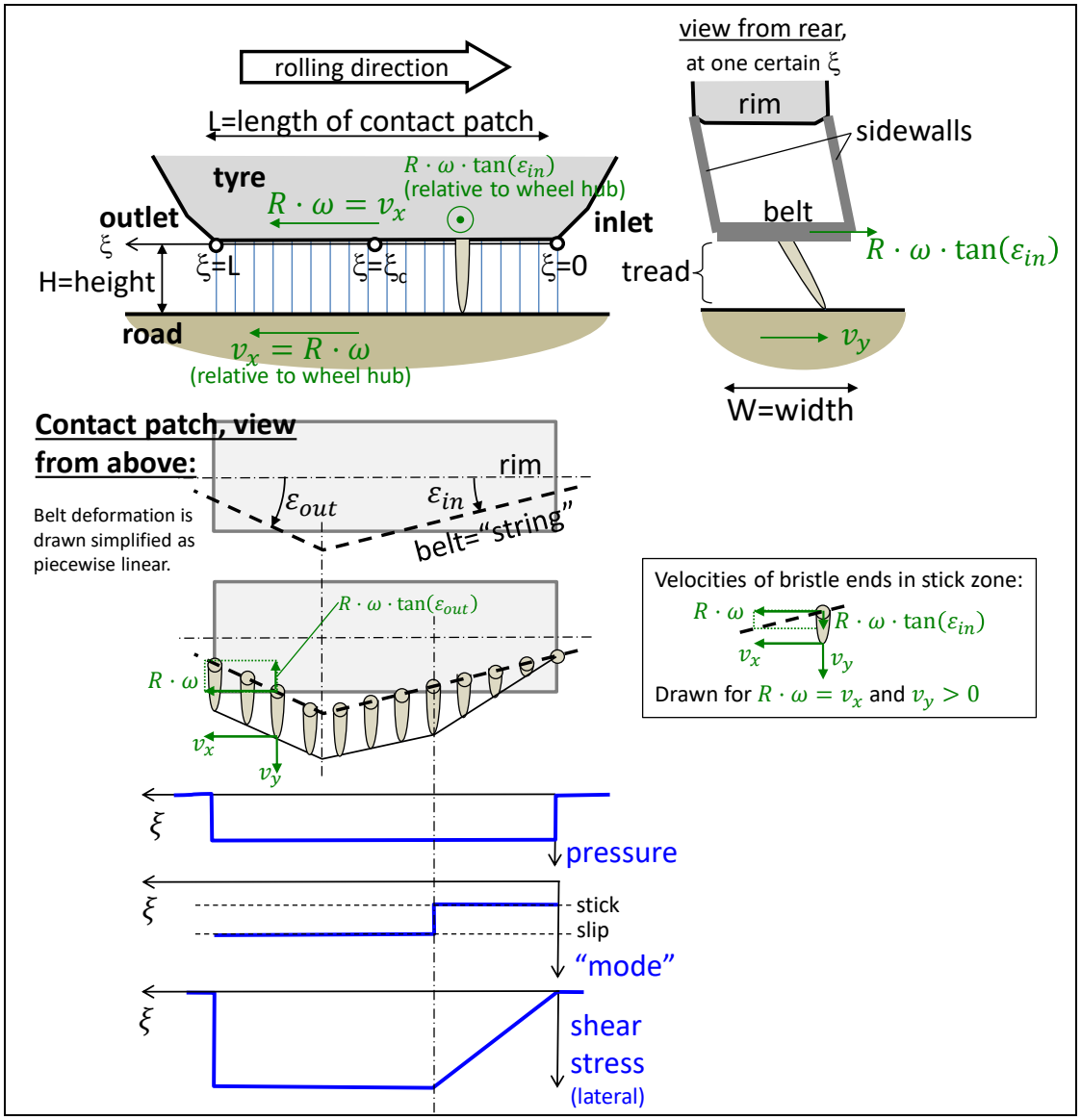

Figure 2-33: Tyre sidewall deformation and tread deformation with the belt (the "string") in between. The drawn bristles are here assumed to represent only tread parts, while the sidewall is treated as an elastic structure between rim and belt.

Comparing to 2.2.4.1.1, we can note that subscript tr is added to underline that $C_{y,tr}$ and $G_{y,tr}/H_{y,tr}$ now means only the tread, not including the sidewall. Sidewall elasticity is instead handled with ε_{in}. The variable $s_{y\varepsilon}$ is an auxiliary mathematical variable introduced only to make the expressions more manageable; it will be eliminated later.

$$F_y = \begin{cases} = -C_{y,tr} \cdot s_{y,\varepsilon}; & if\ |F_y| \le \dfrac{\mu \cdot F_z}{2} \\ = -\text{sign}(s_{y,\varepsilon}) \cdot \mu \cdot F_z \cdot \left(1 - \dfrac{\mu \cdot F_z}{4 \cdot C_{y,tr}} \cdot \dfrac{1}{|s_{y,\varepsilon}|}\right); & else \end{cases}$$

$$where\ C_{y,tr} = \frac{G_{y,tr} \cdot W \cdot L^2}{2 \cdot H_{y,tr}};\ dimension: [force]\ and\ s_y = \frac{v_y}{|R \cdot \omega|}\ \ and\ s_{y,\varepsilon} = s_y - \tan(\varepsilon_{in}) \cdot \text{sign}(\omega)\,;$$

Now, this model is still **implicit** because ε_{in} depends on $\tau(\xi)$. Introducing simplest possible (linear) constitutive equation for this dependency as in Eq [2.34]:

$$\int \tau \cdot d\xi = F_y = -C_{sw,\varepsilon,in} \cdot \tan(\varepsilon_{in})\,; \qquad [2.34]$$

Eq [2.34] makes it possible to derive the following **explicit** model:

$$F_y = \begin{cases} = -\dfrac{C_{sw,\varepsilon,in} \cdot C_{y,tr}}{C_{sw,\varepsilon,in} + C_{y,tr}} \cdot s_y; & if\ |F_y| \le \dfrac{\mu \cdot F_z}{2} \\ = -sign(s_y) \cdot \mu \cdot F_z \cdot \dfrac{1 + \dfrac{C_{sw,\varepsilon,in} \cdot |s_y|}{\mu \cdot F_z} - \sqrt{\left(1 - \dfrac{C_{sw,\varepsilon,in} \cdot s_y}{\mu \cdot F_z}\right)^2 + \dfrac{C_{sw,\varepsilon,in}}{C_{y,tr}}}}{2}; & else \end{cases} \qquad [2.35]$$

$$where\ s_y = \frac{v_y}{|R \cdot \omega|};\ \ and\ C_{y,tr} = \frac{G_{y,tr} \cdot W \cdot L^2}{2 \cdot H_{y,tr}};\ \ dimension: [force]$$

(Only valid for pure lateral slip, i.e.: $v_x = R \cdot \omega$;)

It should be noted that the constitutive relation in Eq [2.34] only states how the string is angled. It is still physically consistent to separately add, outside the tyre model, a constitutive equation for the lateral translational deformation of the sidewall; something as $F_y = c_{sw,transaltion} \cdot \delta_{tyre,y}$;, where $\delta_{tyre,y}$ would be the lateral deformation between wheel rim and contact patch. Such sidewall elasticity would appear in series with the lateral tyre slip force model, in a similar way as the torsional sidewall elasticity in 2.2.3.5.2 appeared in series with the longitudinal tyre slip force model.

2.2.4.1.3 Comparison of the Bristle Models

Eq [2.35] (dependant bristles) is to be compared to Eq [2.33] (independent bristles). Using $C_{ysw} = C_{sw,\varepsilon,in} \cdot C_{y,tr}/\left(C_{sw,\varepsilon,in} + C_{y,tr}\right)$; the models are identical up to $\mu \cdot F_z/2$ and have the same asymptote for $s \to \infty$. See Figure 2-34.

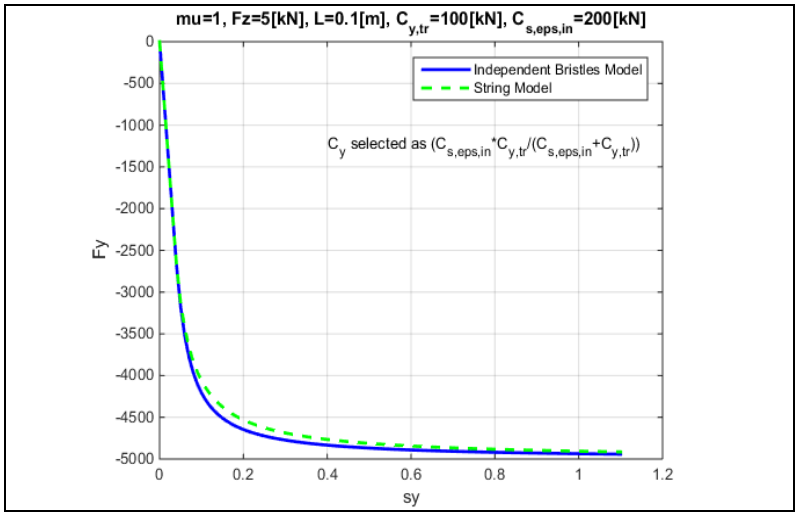

Figure 2-34: Comparison of model with independent bristles and dependent bristles (String model).

The influence of vertical load F_z was discussed in 2.2.3.1.2 but is better explained with dependent bristles. Assumes that only the tread stiffness $C_{y,tr}$ (and not $C_{sw,\varepsilon,in}$) varies with contact length, and that this variation is proportional, $C_{y,tr}(F_z) \propto F_z$;, as we found in 2.2.3.1.2. This indicates a degressive characteristics of $C_y(F_z)$, which is also observed in measurements.

The model with dependent bristles is probably more correct. Anyway, we will use the other most in this compendium, since it is much easier to combine with the longitudinal model (Eq [2.14]) to model combined (longitudinal and lateral) slip.

2.2.4.2 Lateral Tyre Slip Stiffness

In summary for many models (and tests!) the following is a good approximation for small lateral slip (and negligible longitudinal slip and constant normal load):

$$F_y = -C_y \cdot s_y; \quad \text{or} \quad F_y = -C_\alpha \cdot \alpha; \qquad [2.36]$$

For the brush model, or any other model which describes $F_y(s_y, F_z, \mu, \dots)$ or $F_y(\alpha, F_z, \mu, \dots)$, one can define the "Lateral tyre slip stiffness" or "Tyre Cornering Stiffness", C_y or C_α, which have the unit N/1 or N/rad. It is the derivative of force with respect to slip or slip angle. Reference (ISO8855) defines the cornering stiffness as C_α for slip angle $\alpha = 0$;:

$$C_\alpha = -\left(\frac{\partial}{\partial \alpha} F_y\right)\Big|_{\alpha=0} \quad = \quad C_y = -\left(\frac{\partial}{\partial s_y} F_y\right)\Big|_{s_y=0} \qquad [2.37]$$

When using only small slip, it does not matter if the cornering stiffness is defined as the slope in an F_y versus α diagram or F_y versus $s_y = tan(\alpha)$ diagram. Therefore, the notation for cornering stiffness varies between C_α and C_y. Cornering stiffness has the unit N which can be interpreted as $N = N/1 = N/((m/s)/(m/s))$ or $N = N/rad$.

The longitudinal tyre slip stiffness, C_x, is normally larger than the lateral tyre slip stiffness, C_y, which can be explained with that the tyre is less stiff in lateral direction. Since it is the same rubber one could argue that both G and H should be the same, but both due to longitudinal grooves in the tread and due to lateral deformable sidewall, it is motivated to introduce different subscripts: $(G/H)_x > (G/H)_y$. One could elaborate with different friction coefficients μ_x and μ_y, but in this compendium it is claimed that friction is well modelled as isotropic. More about this in 2.2.4.6.5.

The cornering tyre forces initially exhibit a linear relation with the slip angle. A non-linear region is then exhibited up to a maximum value. In Figure 2-35, the maximum slip angle is only 16 degrees (or $s_y = \tan(16\ deg) = 0.29$) and one can expect that the tyre forces will drop as the slip angle approaches 90 degrees.

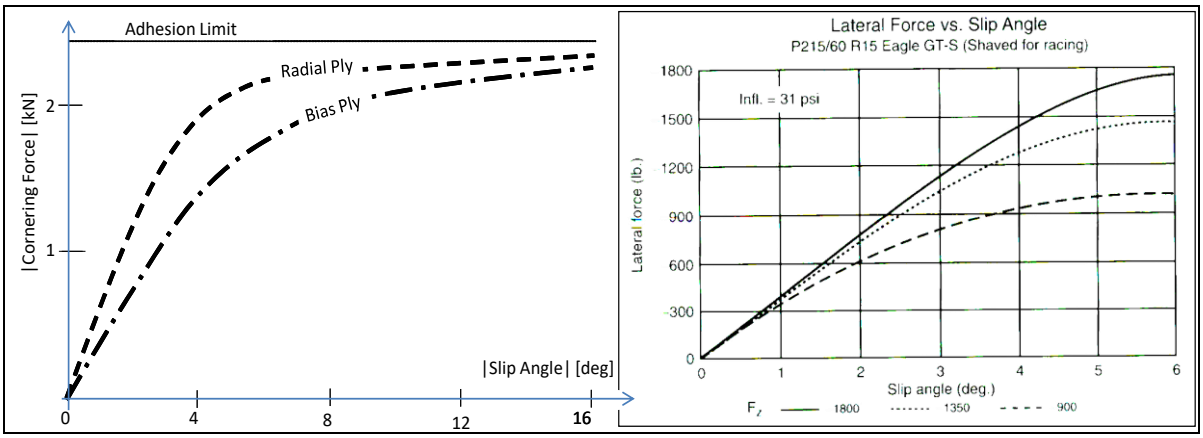

Figure 2-35: Left: Influence of tyre design. Right: Influence of inflation pressure, (Gillespie, 1992).

2.2.4.3 Influence of Vertical Load

As discussed for longitudinal slip and the rolling resistance behaviour of tyres, the vertical load on the tyre affects the force generation. The general behaviour of the tyre's cornering performance as the vertical load changes is presented in Figure 2-35. These figures show that the cornering stiffness is influenced by vertical load. A first approximation is that $C_y \propto F_z$ with proportionality coefficient $CC_y = CC_\alpha$, the Cornering Coefficient (or Lateral Slip Coefficient):

$$F_y = C_y \cdot s_y = CC_y \cdot F_z \cdot s_y; \quad \text{or} \quad F_y = C_\alpha \cdot \alpha = CC_\alpha \cdot F_z \cdot \alpha; \qquad [2.38]$$

We have the linearized in two ways: with respect to F_z and s_y. A slightly better linearization is $F_y \approx -CC_{yNom} \cdot (F_z - F_{zNom}) \cdot s_y$; where subscript *Nom* is the tyre's nominal load. Some examples are shown in Figure 2-36 and Figure 2-37. More about influence of vertical force in 2.2.5.4.

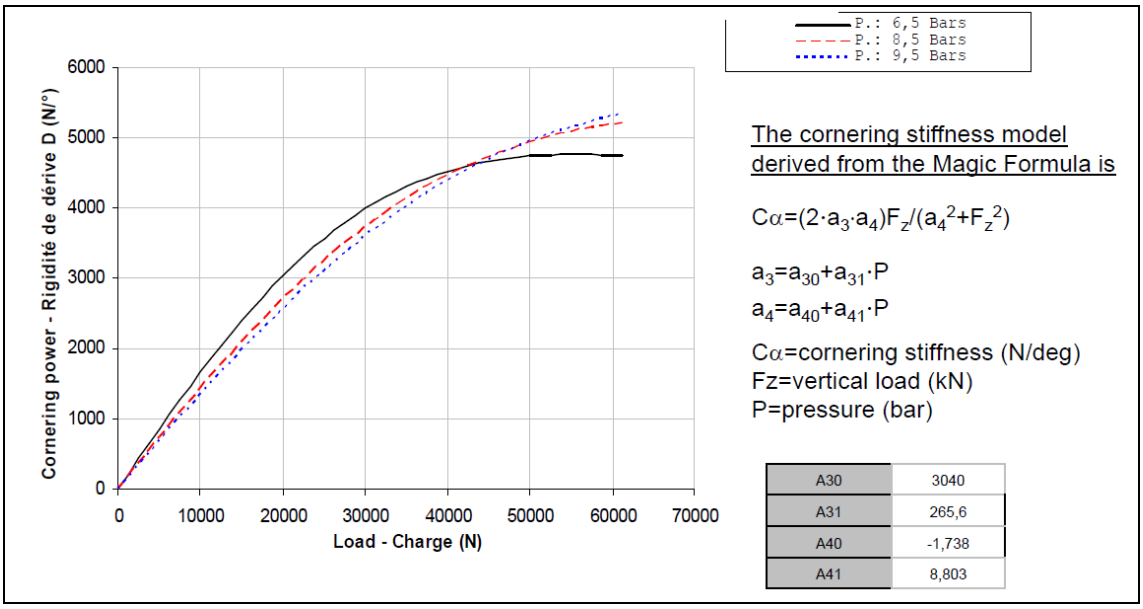

Figure 2-36: Example of cornering stiffness versus vertical load for a truck tyre 295/80R22.5.

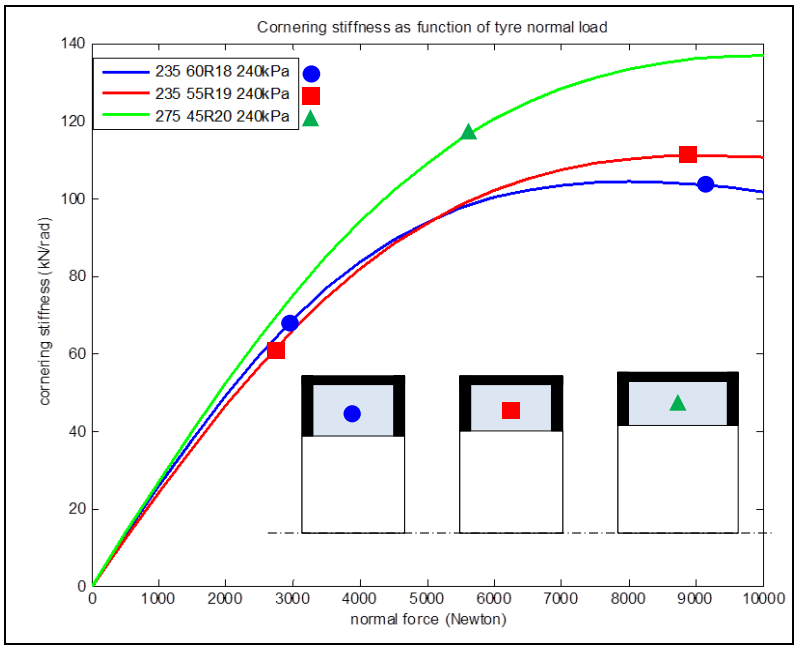

Figure 2-37: Cornering stiffness versus vertical load for some passenger car tyres. From flat track tests.

2.2.4.4 Curve Fit Tyre Models for Lateral Slip

The general form of the lateral force versus lateral slip curve is also suitable for the Magic Formula, TM-Easy, or similar curve fitting approach when sufficient test data is available.

2.2.4.5 Transients and Relaxation in Contact Patch

As for longitudinal, there is a delay in how fast the steady state conditions can be reached in contact patch, which is sometimes important to consider. A similar model, as for relaxation in longitudinal direction 2.2.3.5.1, is to add a first order delay of the force:

$$\dot{F}_y = A \cdot \left(f\left(s_y, F_z, \mu, \dots\right) - F_y \right); \quad [2.39]$$

where $f\left(s_y, F_z, \mu, \dots\right)$ is the force according to a steady state model and $A = \frac{v_{Transport}}{L_r} = \frac{|R \cdot \omega|}{L_r}$ or $A = \frac{|v_x|}{L_r}$ and L_r is the relaxation length, which is a fraction ($\approx 25..50\%$) of tyre circumference.

2.2.4.6 Other Forces and Moments in Lateral Use of Tyre

(This section has strong connection with 2.6.2.)

The deformations of the tyre during cornering are quite complex when compared to the case of pure longitudinal motion, see Figure 2-31. Hence, there are more effects than simply a lateral force. Some of these will be discussed in the following.

2.2.4.6.1 Tyre Aligning Moment due to Lateral Shear

In the lowest diagram in Figure 2-32, one can see that shear stress is concentrated to the outlet side of the contact patch for small slip angles. So, the equivalent lateral force acts behind the centre of wheel rotation for small slip angles. As seen in Figure 2-31 b) it acts at a position t_p behind the wheel's y axis. The distance t_p is called the pneumatic trail, see also Figure , and the resulting yawing moment around a vertical axis through centre of the contact patch will be $= F_y \cdot t_p$, which is often called the tyre aligning moment, M_z. The moment is named after that is normally acts to align the wheel in direction of zero side slip. Figure 2-38 shows $M_z = F_y \cdot t_p$, but also a similar moment, $F_y \cdot (t_p + c)$. Additional effects from τ_x are not drawn.

If the tyre is on a steered axle, the aligning moment influence on steering wheel torque is important. When finding that influence, the moment around the steering axis intersection with ground is the important moment $= F_y \cdot (t_p + c)$, which can be called the steering moment. The distance c is the mechanical trail, which is built into the suspension linkage design. One typically designs the suspension so that $c > 0$, which makes the whole steering moment act in the same direction as the aligning moment. If driver takes his hands from steering wheel in a curve, and/or if steering power assistance is lost, the steering will tend to steer in the direction of body motion above the steered axle, which is normally relatively smooth and safe.

Figure 2-38 shows the combined response of lateral force and slip angle. It is interesting to note that the steering torque reaches a peak before the maximum lateral force capacity of the tyre is reached. It can be used by drivers to find, via steering wheel torque, a suitable steer angle which gives a large lateral force but still does not pass the peak in lateral force. The reason why pneumatic trail can become slightly negative is because pressure centre is in front of wheel centre, see Figure 2-13.

2.2.4.6.1.1 Tyre Aligning Moment in due to Lateral Shear in Brush Model

A model for (yawing) aligning moment around a vertical axle through centre of contact point, M_z, will now be derived. Any model for lateral shear stress can be used, but we will here only use the uniform pressure distribution and independent bristles in 2.2.4.1.1. A corresponding expression as Eq [2.33] is derived, but for M_z instead of F_y.

$$M_z = -W \cdot \int_0^L \tau \cdot \left(\xi - \frac{L}{2}\right) \cdot d\xi = \cdots$$

$$= \begin{cases} = -C_y \cdot \dfrac{L}{6} \cdot s_y; & for\ F_y < \dfrac{\mu \cdot F_z}{2} \Leftrightarrow s_y < \dfrac{\mu \cdot F_z}{2 \cdot C_y} \\ = -\dfrac{\mu^2 \cdot F_z^2 \cdot L}{8 \cdot C_y \cdot s_y} \cdot \left(1 - \dfrac{\mu \cdot F_z}{3 \cdot C_y \cdot s_y}\right); & else \end{cases}$$

$$where\ C_y = \frac{G_y \cdot W \cdot L^2}{2 \cdot H_y};$$

[2.40]

The curve of Eq [2.40] is plotted in Figure 2-39.

The lateral force and the aligning torque can be used to calculate the steering forces. If also the steering assistance is known, the steering wheel torque can be calculated. It can be noted that the model does not include the moment from steering rotation itself, i.e. the torque counteracting $\dot{\delta}$.

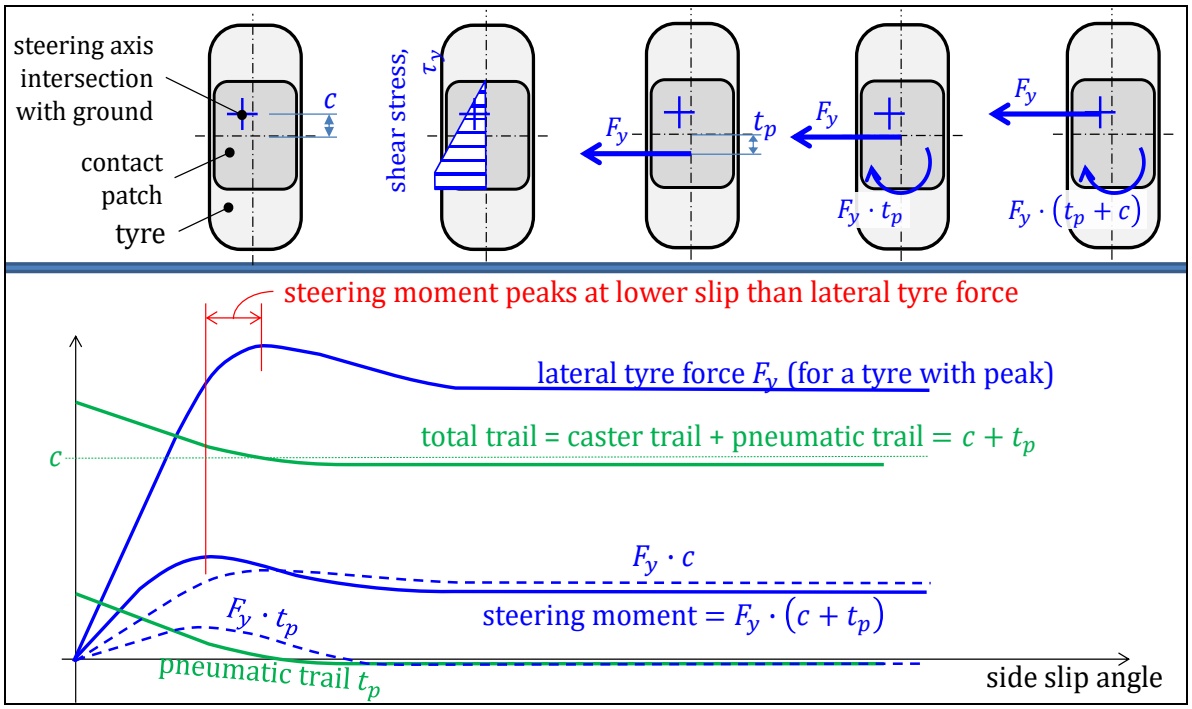

Figure 2-38: General Response of Steering torque to Side slip angle. Tyre aligning moment = $F_y \cdot t_p$ is one part of the steering moment= $F_y \cdot (t_p + c)$.

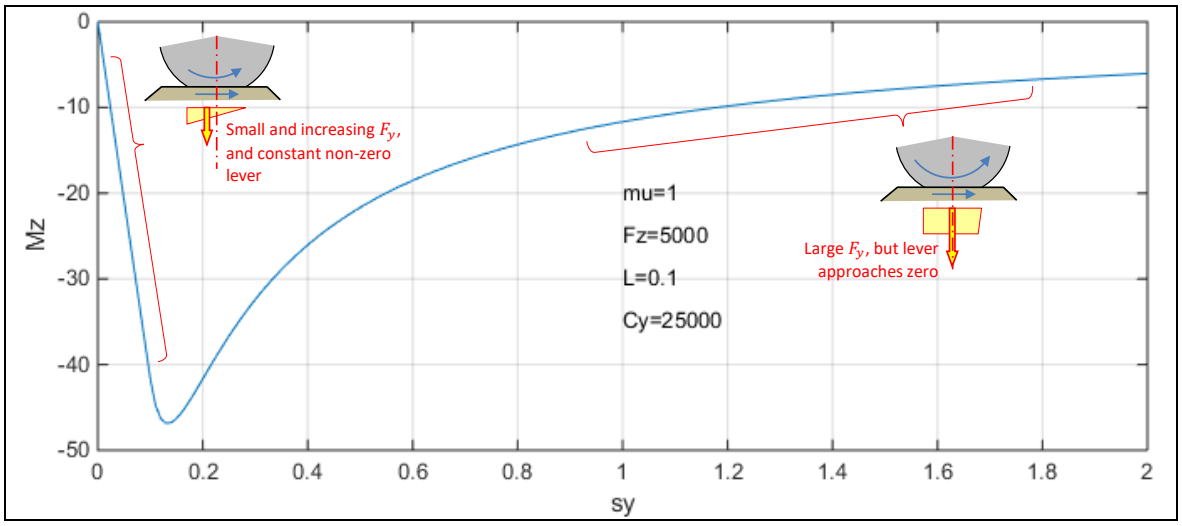

Figure 2-39: Aligning moment (M_z) around contact patch center for uniform pressure distribution.

2.2.4.6.2 Influence from Longitudinal Tyre Force

Figure 2-38 does not show effects from τ_x, but this is shown in Figure 2-40.

2.2.4.6.3 Tyre Spin Torque

The none-symmetry in shear stress around wheel centre in Figure 2-40 can appear as steady state; non-symmetry in τ_y due to brush model and in τ_x due to non-symmetric vertical pressure. But there is one additional reason to yaw moment in tyre contact patch. That is the friction yaw velocity of the wheel $\omega_{wheel,z}$. The additional moment from this effect is often called (tyre) spin torque. One way to model it is, are conceptually an elastic torsional spring in series with friction. The influence from spin torque is only important at low speed, e.g. steering in low speed, where $\omega_{wheel,z} \approx \dot{\delta}_{wheel}$.

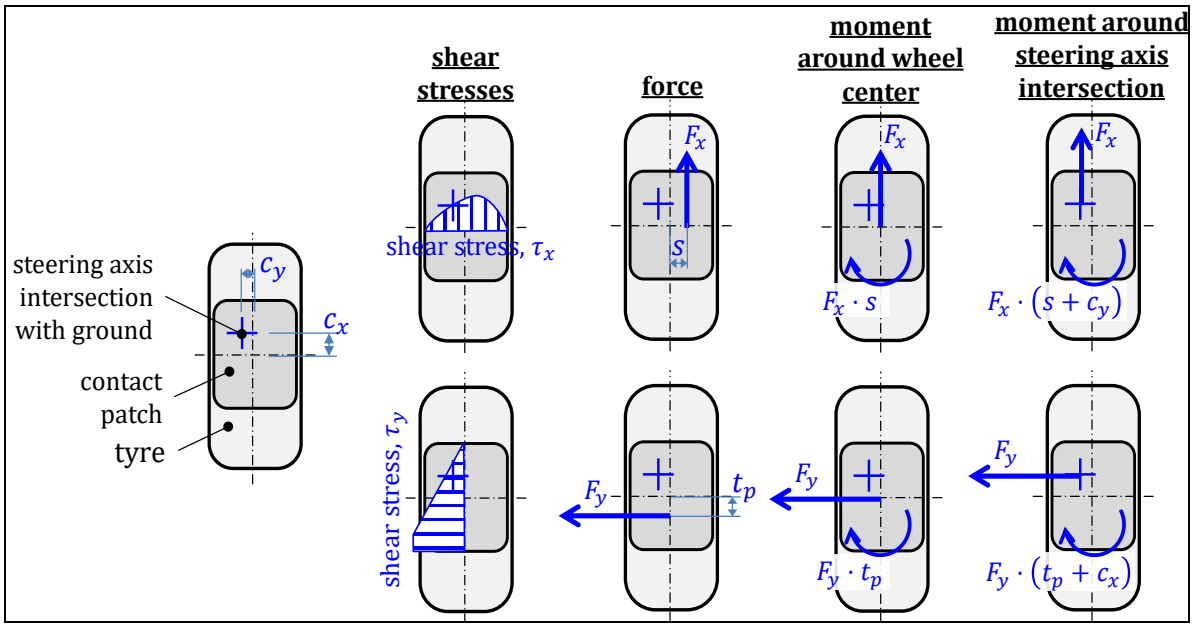

Figure 2-40: Influence from both lateral and longitudinal shear stress on aligning moment.

2.2.4.6.4 Camber Force

Camber force (also called Camber thrust) is the lateral force caused by the cambering of a wheel. Camber thrust $F_{yCamber}$ is approximately linearly proportional to camber angle φ_{wx} for small angles: Camber thrust= $F_{yCamber} = -C_{Camber} \cdot \varphi_{wx}$. The camber stiffness, C_{Camber}, is typically 5..10 % of the cornering stiffness. The tyre lateral forces due to lateral slip F_{ySlip} and due to camber $F_{yCamber}$ are superimposable when they are small:

$$F_y = F_{ySlip} + F_{yCamber} = -C_y \cdot s_y - C_\gamma \cdot \varphi_{wx}; \qquad [2.41]$$

F_{ySlip} and $F_{yCamber}$ use same friction contact to ground so the sum will be saturated by $\mu \cdot F_z$.

A physical model for camber thrust can be derived very similarly to how models in 2.2.3.1 and 2.2.4.1, see Figure 2-41: Brush modes for Camber force (or Camber thrust) $F_{yCamber}$. There action line of $F_{yCamber}$ is often ahead of contact patch centre, which is called Camber Lead.

$$\tau_y(\xi) = G_y \cdot \gamma_y(\xi) = \begin{Bmatrix} it\ takes\ time\ t_\xi \\ for\ a\ bristle \\ from\ inlet\ to\ \xi \end{Bmatrix} = G_y \cdot \frac{\int_0^{t_\xi} \left(v_{lower,y} - v_{upper,y}(\xi)\right) \cdot dt_\xi}{H_y} = G_y \cdot \frac{\int_0^{t_\xi} \left((\xi - L/2) \cdot \omega_{zg} - 0\right) \cdot dt_\xi}{H_y} =$$

$$\begin{Bmatrix} \xi = v_{transp} \cdot t_\xi = \\ = R_w \cdot \omega_w \cdot t_\xi \end{Bmatrix} = \frac{G_y}{H_y} \cdot \omega_{zg} \cdot \int_0^{t_\xi} \left(R_w \cdot \omega_w \cdot t_\xi - L/2\right) \cdot dt_\xi = \frac{G_y}{H_y} \cdot \omega_{zg} \cdot \left[R_w \cdot \omega_w \cdot \frac{t_\xi^2}{2} - \frac{L}{2} \cdot t_\xi\right]_0^{t_\xi} = \frac{G_y}{2 \cdot H_y} \cdot \omega_{zg} \cdot$$

$$\left(R_w \cdot \omega_w \cdot \frac{t_\xi^2}{2} - L \cdot t_\xi\right) = \left\{t_\xi = \frac{\xi}{R_w \cdot \omega_w};\ \omega_{zg} \approx \omega_w \cdot \varphi_{Camber}\right\} = \frac{G_y}{2 \cdot H_y} \cdot \omega_w \cdot \varphi_{Camber} \cdot \left(R_w \cdot \omega_w \cdot \left(\frac{\xi}{R_w \cdot \omega_w}\right)^2 - L \cdot \right.$$

$$\left. \frac{\xi}{R_w \cdot \omega_w}\right) = \frac{G_y}{2 \cdot H_y} \cdot \frac{1}{R_w} \cdot (\xi^2 - L \cdot \xi) \approx \frac{G_y}{2 \cdot H_y \cdot R_w} \cdot \varphi_{Camber} \cdot (\xi^2 - L \cdot \xi);$$

Integration $F_{yCamber} = \int_0^L \tau_y(\xi) \cdot d\xi$; gives:

$$F_{yCamber} = -C_{Camber} \cdot \varphi_{Camber};\quad where\ C_{Camber} = \frac{G_y \cdot W \cdot L^3}{12 \cdot H_y \cdot R_w}; \qquad [2.42]$$

Note: Only valid when no part of the contact patch is saturated by friction.

Checking with typical values for a passenger car tyre gives: $C_{Camber}/C_y = \left(G_y \cdot W \cdot L^3/(12 \cdot H_y \cdot R_w)\right)/\left(G_y \cdot W \cdot L^2/2 \cdot H_y\right) = L/6 \cdot R_w \approx 0.1/(6 \cdot 0.3) \approx 0.05 = 5\%$; which is of same magnitud as 5..10%, which was mentioned in beginning of 2.2.4.6.4.

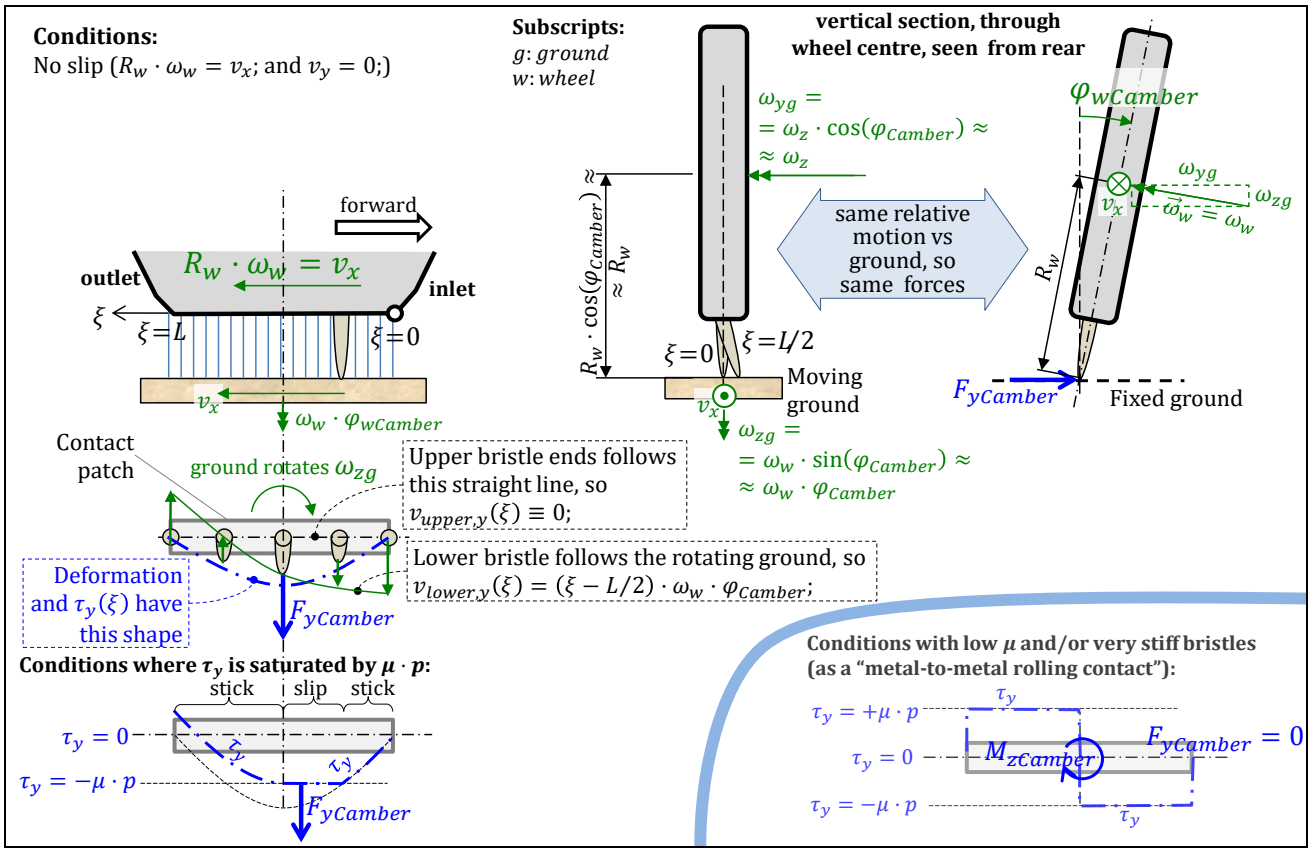

Figure 2-41: Brush modes for Camber force (or Camber thrust) $F_{yCamber}$. For intuitive understanding, note that the ground is thought of as rotating opposite to the vertical component of wheel rotation $\vec{\omega}_w$.

2.2.4.6.5 Overturning Moment

The contact patch is deflected laterally from the centre of the carcass. This creates an overturning moment M_x due to the offset position of the normal force. The lateral force F_y also contributes to the overturning moment.

2.2.5 Combined Longitudinal and Lateral Slip

Operation of vehicles often involves a combination of steering/cornering and braking/propulsion.

Generally, one can experience two causal effects of combined slip:

- Loss of sidegrip due to increased wheel torque or longitudinal tyre slip. Typically, this is when propulsion or braking **directly** cause undesired lateral vehicle motion (reduced steerability or reduced yaw stability).
- Loss of longitudinal grip due to increased lateral tyre force or tyre side slip. Typically, this is when steering cause undesired wheel rotation, and only **indirectly** causes undesired longitudinal vehicle motion (reduced acceleration or reduced deceleration).

The first effect is more directly affecting vehicle motion than the latter. So, one can say one have to be more careful when changing wheel torques in a curve than when changing steering angle while accelerating or braking. Engineering for these manoeuvres requires models of vehicle and wheels/shafts but also tyres. These tyre models have to represent combined slip, i.e. how $[F_x, F_y]$ varies with (s_x, s_y).

If the tyre has isotropic adhesion properties in the lateral and longitudinal direction, one can assume that the maximum force magnitude F_{xy} is determined by the maximum resultant friction force, $\mu \cdot F_z$.

$$F_{xy}{}^2 = F_x{}^2 + F_y{}^2 \leq (\mu \cdot F_z)^2 \Rightarrow \left(\frac{F_x}{F_z}\right)^2 + \left(\frac{F_y}{F_z}\right)^2 \leq \mu^2 \qquad [2.43]$$

Equation [2.43] can be plotted as a circle, called the "Friction Circle". Since the lateral and longitudinal properties are not isotropic (due to carcass deflection, tread patterns, camber, etc) the shape may be better described as a "Friction Ellipse" or simply "Friction limit".

When not cornering, the tyre forces are described by a position between -1 (braking) and +1 (acceleration) along the Y-axis. Note that the scales of both axes are normalized to the maximum value for friction.

The "actuation" of the wheel means the propulsion, braking and steering (and sometimes suspension control) of the wheel. An ideal actuation allows all conditions within the boundaries of the friction circle to be achieved anytime during a vehicle manoeuvre. An example of limitation in actuation is a wheel on a non-steered rear axle. They cannot access any of the lateral parts of the circle; unless the vehicle slides laterally.

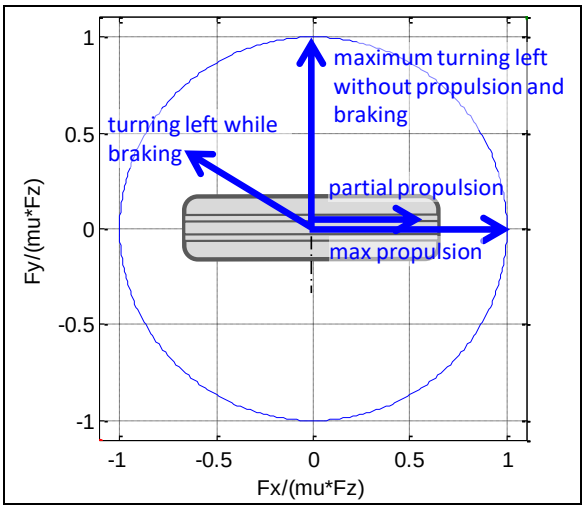

Figure 2-42: Friction Circle with some examples of utilization. View from above, forces on tyre.

At the boundary of the friction circle, tyres become more sensitive to changes in slip. It is therefore extra important to model the direction of the force in relation to shear deformation and relative slip motion in the tyre contact patch. Here, isotropic shear and friction properties are assumed:

$$\frac{lateral\ sliding\ speed}{longitudinal\ sliding\ speed} = \frac{v_y}{R\cdot\omega - v_x} = -\frac{F_y}{F_x}; \qquad [2.44]$$

When considering a combined slip model, one can establish the "total slip" $s_{xy} = s$, through the definition $s_{xy}^2 = s^2 = s_x^2 + s_y^2$;. Then, it can be tempting to look for a function $F_{xy} = f(s_{xy})$; and then decompose F_{xy} into F_x and F_y through $[F_x; F_y] = [+s_x/s_{xy}\,; -s_y/s_{xy}]\cdot F_{xy}$. This is not fully physical, which is easiest understood by looking at the brush model for uniform pressure distribution: When s_{xy} is small enough, there will be no slip in the contact, because $\tau < \mu\cdot p$ in whole contact. For such conditions and isotropic linear deformation model of the bristles, the longitudinal and lateral models from before are valid. So, F_x is independent of s_y and F_y is independent of s_x. So, going via s_{xy} would create a non-physical dependence. Anyway, such approximate models can be useful for conditions with larger slip, see 2.2.5.3.1.

For small s_x, one can still assume $F_y \propto s_y$. Then: $F_y = -C_y\cdot s_{yt} = -C_y\cdot v_y/(R_w\cdot\omega) = \{s_x = (R_w\cdot\omega - v_x)/(R_w\cdot\omega)\} = -C_y\cdot v_y\cdot(1-s_x)/v_x = -C_y\cdot(1-s_x)\cdot s_{yw}$;. Increasing s_x from 0 to small positive s_x means reduction of $|F_y|$, which should be intuitive since utilization of friction in one direction reduce force in the other. However, decreasing s_x from 0 to small negative s_x means increase in $|F_y|$, which can be counter-intuitive. However, the explanation is that the "transport speed" decreases, which means a "slip stiffer" tyre. The increase in F_y for small braking was seen already in Figure 2-43: slight brake torque on a wheel improves lateral grip!

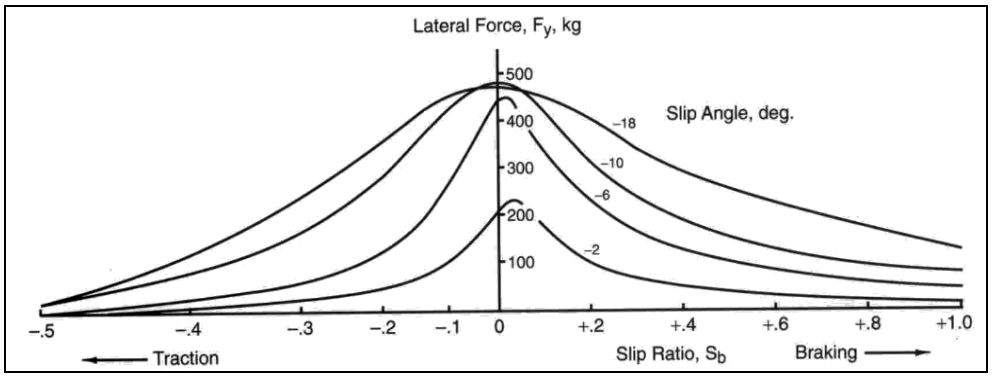

Figure 2-43: Combined Longitudinal and Lateral Slip.

2.2.5.1 Anisotropic Brush Model

The longitudinal model Eq [2.14] and the lateral model with independent bristles in 2.2.4.1.1 will now be used with the anisotropy $C_x \neq C_y$;. This is motivated by that sidewall contributes more to lateral bristle elasticity than to longitudinal bristle elasticity. With significantly different tread grooves in longitudinal and lateral direction, one could motivate also difference in friction coefficient μ, but here we assume same μ in both directions. The derivation of model equations becomes similar as for the pure longitudinal and lateral models. For the stick zone:

$$\tau_x = \frac{2 \cdot C_x}{W \cdot L^2} \cdot s_x \cdot \xi; \quad and \quad \tau_y = \frac{2 \cdot C_y}{W \cdot L^2} \cdot s_y \cdot \xi;$$

If no slip in contact:

$$F_x = W \cdot \int_0^L \tau_x \cdot d\xi = W \cdot \int_0^L \frac{2 \cdot C_x}{W \cdot L^2} \cdot s_x \cdot \xi \cdot d\xi = \frac{2 \cdot C_x}{L^2} \cdot s_x \cdot \int_0^L \xi \cdot d\xi = \frac{2 \cdot C_x}{L^2} \cdot s_x \cdot \frac{L^2}{2} = C_x \cdot s_x;$$

$$F_y = W \cdot \int_0^L \tau_y \cdot d\xi = W \cdot \int_0^L \frac{2 \cdot C_y}{W \cdot L^2} \cdot s_y \cdot \xi \cdot d\xi = \frac{2 \cdot C_y}{L^2} \cdot s_y \cdot \int_0^L \xi \cdot d\xi = \frac{2 \cdot C_y}{L^2} \cdot s_y \cdot \frac{L^2}{2} = C_y \cdot s_y;$$

Now, if there is a break-away point (ξ_c) where slip starts, we can find it from $\tau(\xi_c) = \mu \cdot p; \Rightarrow \tau_x^2 + \tau_y^2 = \mu^2 \cdot p^2;$. Introducing an auxiliary parameter, $k = C_x/C_y$;, and an auxiliary variable, $s_k = \sqrt{(k \cdot s_x)^2 + s_y^2};$, gives the following break-away point:

$$\tau(\xi_c) = \mu \cdot p; \Rightarrow \tau_x^2 + \tau_y^2 = \mu^2 \cdot p^2; \Rightarrow \cdots \Rightarrow \xi_c = \frac{\mu \cdot F_z \cdot L}{2 \cdot C_y \cdot s_k};$$

The forces, when $0 < \xi_c < L$ and $\omega \cdot v_x > 0$ becomes:

$$F_x = W \cdot \int_0^L \tau_x \cdot d\xi = W \cdot \int_0^{\xi_c} \frac{2 \cdot C_x}{W \cdot L^2} \cdot s_x \cdot \xi \cdot d\xi + W \cdot \int_{\xi_c}^L \tau_{x,slip} \cdot d\xi =$$

$$= W \cdot \int_0^{\xi_c} \frac{2 \cdot C_x}{W \cdot L^2} \cdot s_x \cdot \xi \cdot d\xi + W \cdot \int_{\xi_c}^L \mu \cdot p \cdot \frac{s_x}{s} \cdot d\xi = \cdots = \frac{C_x \cdot s_x \cdot \xi_c^2}{L^2} + \frac{\mu \cdot F_z \cdot s_x}{L \cdot s} \cdot (L - \xi_c); \quad \text{and}$$

$$-F_y = W \cdot \int_0^L \tau_y \cdot d\xi = \left\{ \begin{matrix} analogously \\ with\ x\ direction \end{matrix} \right\} = \cdots = \frac{C_y \cdot s_y \cdot \xi_c^2}{L^2} + \frac{\mu \cdot F_z \cdot s_y}{L \cdot s} \cdot (L - \xi_c);$$

Arranging for all combinations of (v_x, v_y, ω), we find Eq [2.45]. Figure 2-45 shows results from the model. It can be observed that F_x is independent of s_y and F_y is independent of s_x for $F_{xy} \leq \mu \cdot F_z/s$. This is a reasonable consequence of that no sliding occurs so that forces are purely defined by the elasticity, not the friction. At $s_y \approx 0.01..0.04$, we see that F_y increases with utilization of $|F_x|$ at some areas. This is a redistribution of force from longitudinal to lateral, due to that the tyre stiffer in longitudinal than lateral.

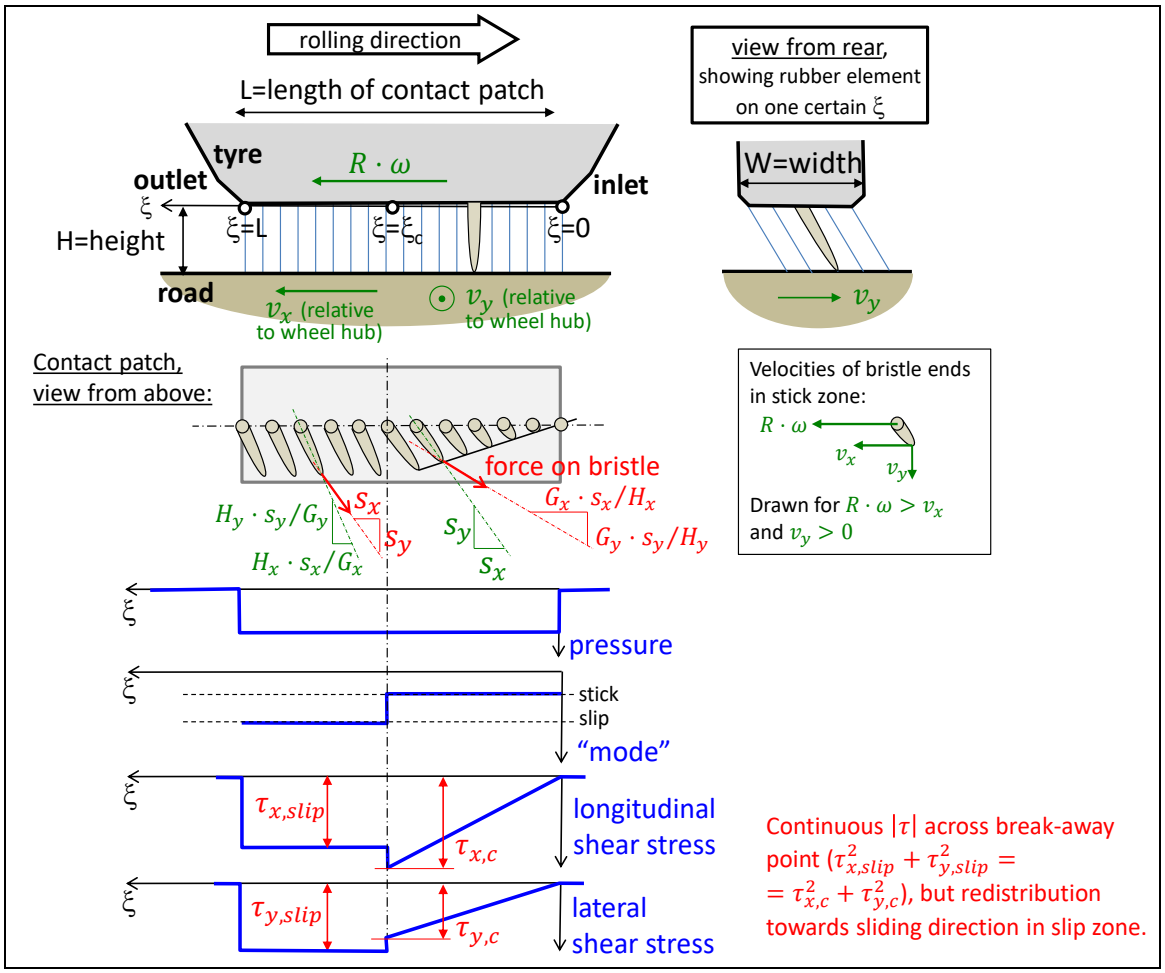

Figure 2-44: Physical model for deriving brush model for combined slip.

$$\begin{bmatrix} F_x \\ F_y \end{bmatrix} = \begin{cases} = \begin{bmatrix} +\mu \cdot F_z \cdot \frac{s_x}{s} \\ -\mu \cdot F_z \cdot \frac{s_y}{s} \end{bmatrix}; & if\ \omega \cdot v_x < 0 \\ = \begin{bmatrix} +C_x \cdot s_x \\ -C_y \cdot s_y \end{bmatrix}; \quad else\ if\ s_k \le \frac{\mu \cdot F_z}{2 \cdot C_y} \Leftrightarrow F_{xy} = \sqrt{F_x^2 + F_y^2} \le \frac{\mu \cdot F_z}{2} & \\ = \begin{bmatrix} +\left(\frac{\xi_c}{L}\right)^2 \cdot C_x \cdot s_x + \frac{\mu \cdot F_z}{L} \cdot \cos(\theta_{Fxy}) \cdot (L - \xi_c) \\ -\left(\frac{\xi_c}{L}\right)^2 \cdot C_y \cdot s_y + \frac{\mu \cdot F_z}{L} \cdot \sin(\theta_{Fxy}) \cdot (L - \xi_c) \end{bmatrix}; & else \end{cases}$$

$$where\ \theta_{Fxy} = arctan2(-v_y, R_w \cdot \omega - v_x);\ s_x = \frac{R \cdot \omega - v_x}{|R \cdot \omega|};\ s_y = \frac{-v_y}{|R \cdot \omega|};\ s = \sqrt{{s_x}^2 + {s_y}^2};\ k = \frac{C_x}{C_y};\ s_k = \sqrt{(k \cdot s_x)^2 + {s_y}^2};\ \xi_c = \frac{\mu \cdot F_z \cdot L}{2 \cdot C_y \cdot s_k};\ C_x = \frac{G \cdot W \cdot L^2}{2 \cdot H};$$

[2.45]

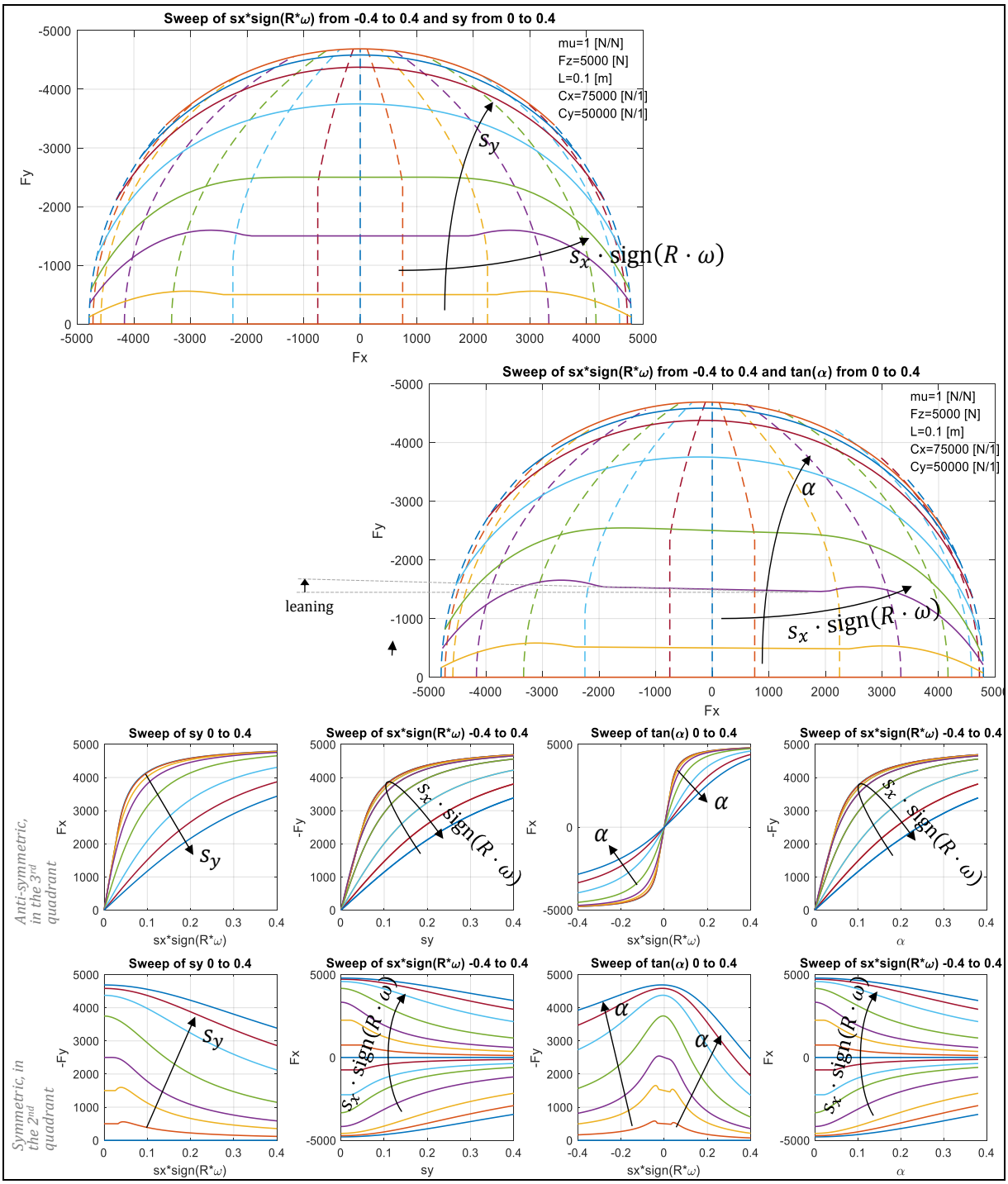

Figure 2-45: Tyre $F(s)$ with iso-curves for longitudinal slip s_x and lateral tyre slip $s_y = v_y/|R_w \cdot \omega|$ (left 5 diagrams) and for $s_x = (R_w \cdot \omega - v_x)/|R_w \cdot \omega|$ and slip angle $\alpha = arctan(v_x/v_y)$ (left 5 diagrams). Tyre model from Eq [2.45] used. Levels used for slip and $\tan(\text{slip angle})$: $0, \pm 0.01, \pm 0.03, \pm 0.05, \pm 0.1, \pm 0.2, \pm 0.3, \pm 0.4$.

2.2.5.2 Anisotropy, Parabolic Pressure, Stick and Slip Friction

Above is for uniform pressure distribution and same friction coefficient for stick and slip. We will now change to the more realistic parabolic distribution and replace μ with μ_{stick} and μ_{slip}. The model gets one more parameter and consequently becomes easier to tune to experiments, see Eq [2.46].

$$\begin{bmatrix}F_x\\F_y\end{bmatrix}=\begin{cases}=\begin{bmatrix}+\mu_{slip}\cdot F_z\cdot\frac{s_x}{s}=\mu_{slip}\cdot F_z\cdot\cos(\theta_{Fxy})\\-\mu_{slip}\cdot F_z\cdot\frac{s_y}{s}=\mu_{slip}\cdot F_z\cdot\sin(\theta_{Fxy})\end{bmatrix}; & if\ \omega\cdot v_x<0\ or\\ & s_k>\frac{3\cdot\mu_{stick}\cdot F_z}{C_y}\\ =\begin{bmatrix}+C_x\cdot s_x\cdot\left(\frac{\xi_c}{L}\right)^2+\mu_{slip}\cdot F_z\cdot\cos(\theta_{Fxy})\cdot\left(1-3\cdot\left(\frac{\xi_c}{L}\right)^2+2\cdot\left(\frac{\xi_c}{L}\right)^3\right)\\-C_y\cdot s_y\cdot\left(\frac{\xi_c}{L}\right)^2+\mu_{slip}\cdot F_z\cdot\sin(\theta_{Fxy})\cdot\left(1-3\cdot\left(\frac{\xi_c}{L}\right)^2+2\cdot\left(\frac{\xi_c}{L}\right)^3\right)\end{bmatrix}; & else\end{cases}$$

$$where\ \theta_{Fxy}=arctan2(-v_y,R_w\cdot\omega-v_x);\quad s_x=\frac{R\cdot\omega-v_x}{|R\cdot\omega|};\quad s_y=\frac{-v_y}{|R\cdot\omega|};$$

$$s=\sqrt{{s_x}^2+{s_y}^2};\quad k=\frac{C_x}{C_y};\quad s_k=\sqrt{(k\cdot s_x)^2+{s_y}^2};\quad \frac{\xi_c}{L}=1-\frac{C_y\cdot s_k}{\mu_{stick}\cdot 3\cdot F_z};$$

$$C_x=\frac{G\cdot W\cdot L^2}{2\cdot H};$$

[2.46]

Eq [2.46] assumes that tyre is rotating, so it does not reflect that break-away friction force for a locked tyre becomes $F_{xy}=\mu_{stick}\cdot F_z$. If s_x is varied while $s_y\equiv 0$ in Eq [2.46], leads exactly to the longitudinal slip model with peak (Eq [2.21]). Similar peak in F_y is found for varying s_y while $s_x\equiv 0$. The peaks in F_x and F_y are equally large, but the peak in F_y occurs at larger slip: $s_{y,peak}>s_{x,peak}$. Also for combined slip, a maximum in F_{xy}occurs, but it is found on a "2-dimensional ridge" in the "cake plot" in Figure 2-46.

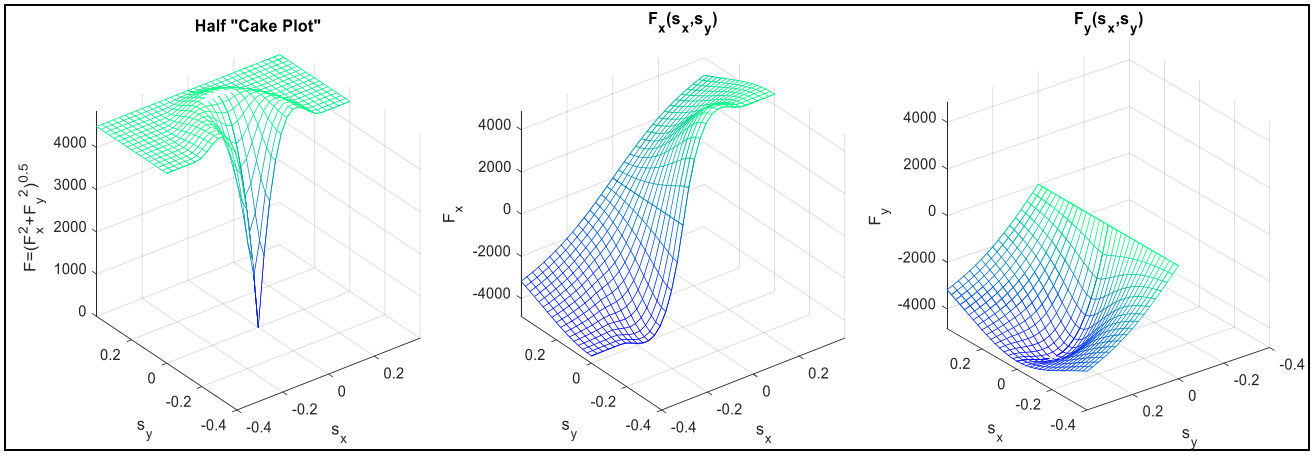

Figure 2-46: Plots of the vector field $[F_x,F_y]=f([s_x,s_y])$ or $\vec{F}=f(\vec{s})$, using the results from Figure 2-47. "Cake-plot" is an expression from (Weber, 1981).

2.2.5.3 Approximate Combined Slip Models

2.2.5.3.1 Using Scalar Force Function of Combined Slip

A simple but not fully physically consistent combined slip model can be expressed using "total slip, s_{xy}", as shown in Equation [2.47].

$$\begin{bmatrix}F_x\\F_y\end{bmatrix}=\begin{bmatrix}+s_x\\-s_y\end{bmatrix}\cdot\frac{F_{xy}}{s_{xy}}=\begin{bmatrix}R_w\cdot\omega-v_x\\-v_y\end{bmatrix}\cdot\frac{F_{xy}}{\sqrt{(R_w\cdot\omega-v_x)^2+(v_y)^2}};$$

$$where\ s_{xy}^2=s^2=s_x^2+s_y^2;\quad where\ s_x=\frac{R_w\cdot\omega-v_x}{|R_w\cdot\omega|};\quad and\quad s_y=\frac{v_y}{|R_w\cdot\omega|};$$

$$and\ F_{xy}=\begin{cases}=\mu\cdot F_z; & if\ v_x\cdot\omega<0\\ =F_z\cdot f(s_{xy}); & else\end{cases}$$

$$where, e.g.\ f(s_{xy})=\{\text{Eq [2.14], [2.18], [2.20] or [2.21]}\};\quad or$$

$$f(s_{xy})=\min(CC_{xy}\cdot s_{xy};\mu);\quad CC_{xy}\approx\{typically\}\approx 5..15\ \text{[non-dimensional]};$$

[2.47]

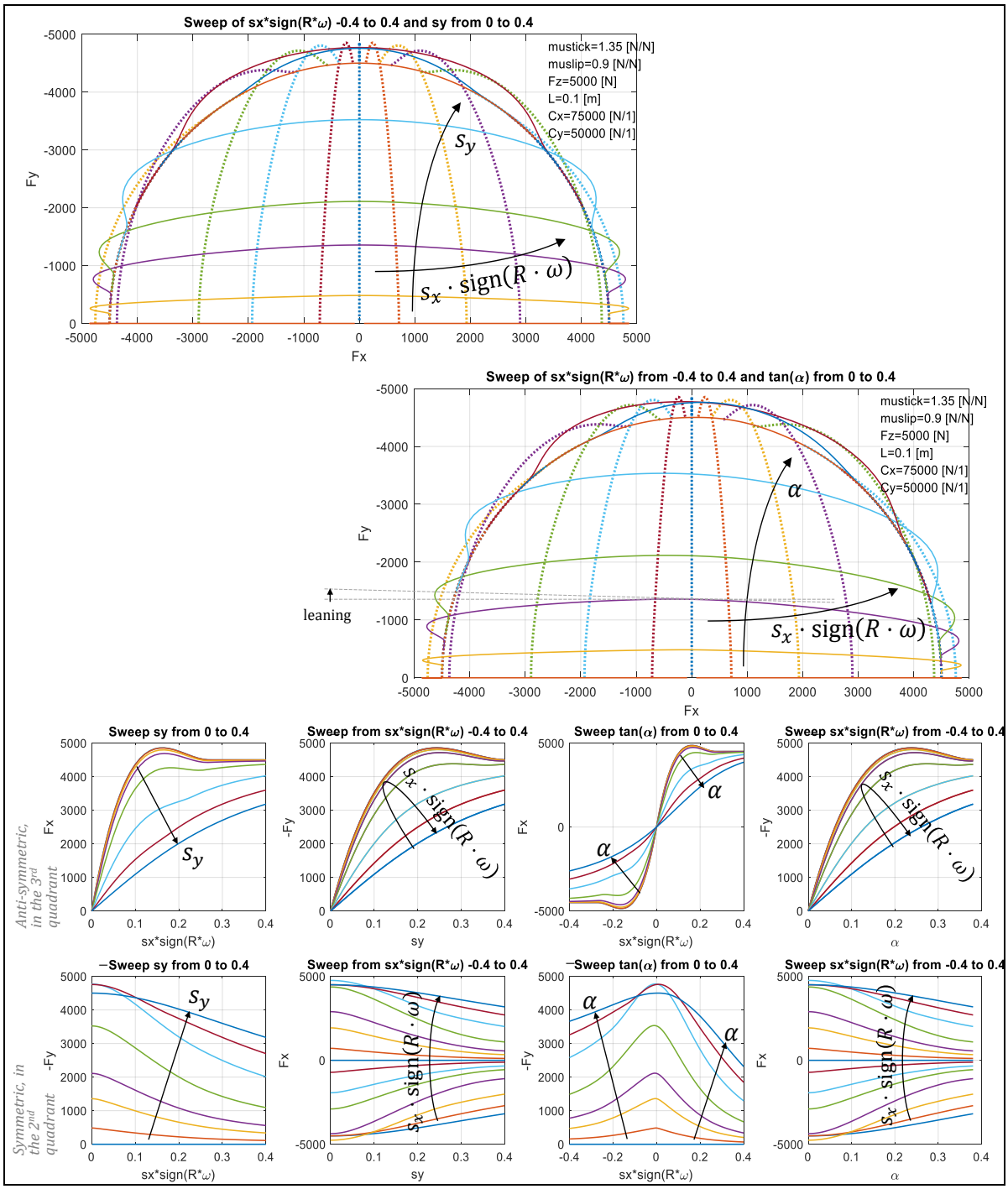

Figure 2-47: Tyre $F(s)$ with iso-curves for longitudinal slip s_x and lateral tyre slip $s_y = v_y/|R_w \cdot \omega|$ (left 5 diagrams) and for $s_x = (R_w \cdot \omega - v_x)/|R_w \cdot \omega|$ and slip angle $\alpha = arctan(v_x/v_y)$ (left 5 diagrams). Tyre model from Eq [2.46] used. Levels used for slip and tan(slip angle): $0, \pm 0.01, \pm 0.03, \pm 0.05, \pm 0.1, \pm 0.2, \pm 0.3, \pm 0.4$.

2.2.5.3.2 Friction Circle Inspired Combined Slip Model

A combined model for cases when one knows F_x without involving s_x is shown in Eq [2.48]. It can be used when we know the wheel torque, e.g. by prescribed propulsion or braking. Eq [2.48] also shows the corresponding, less usual, case when F_y is known without involving s_y. Eq [2.48] is not completely physically motivated but works relatively well if both s_x and s_y are small. One can consider Eq [2.48] as "a mathematical scaling, inspired by the friction circle".

$$F_y \approx \sqrt{1-\left(\frac{F_x}{\mu \cdot F_z}\right)^2} \cdot F_y|_{F_x=0}; \quad and \quad F_x \approx \sqrt{1-\left(\frac{F_y}{\mu \cdot F_z}\right)^2} \cdot F_x|_{F_y=0}; \qquad [2.48]$$

If this concept of scaling is applied on the slip stiffnesses instead, where $(\partial F_i/\partial s_i)|_{F_j=0}$ is the uni-directional slip stiffness:

$$C_y(F_x) = \sqrt{1-\left(\frac{F_x}{\mu \cdot F_z}\right)^2} \cdot \left.\frac{\partial F_y}{\partial s_y}\right|_{F_x=0}; \quad and \quad C_x(F_y) = \sqrt{1-\left(\frac{F_y}{\mu \cdot F_z}\right)^2} \cdot \left.\frac{\partial F_x}{\partial s_x}\right|_{F_y=0}; \qquad [2.49]$$

2.2.5.4 Influence of Vertical Force

Figure 2-48 shows experiment data on how slip stiffness varies with vertical force.

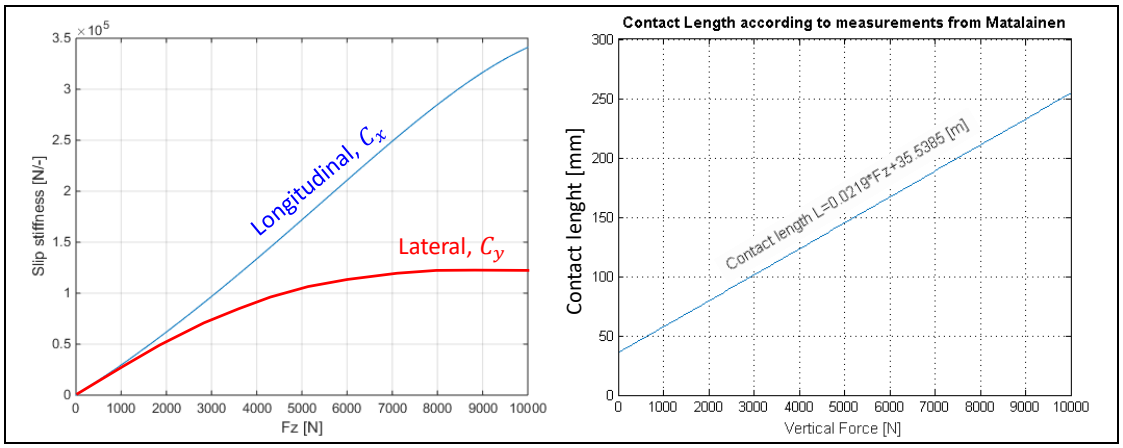

Figure 2-48: Measurements for varying vertical force. Left: Slip stiffnesses. Right: Contact length.

2.2.5.4.1 Explanation of Higher Slip Stiffness Longitudinal than Lateral

The model in 2.2.4.1.1.1 explains why tyre is more slip stiff in longitudinal than lateral direction, i.e. why $C_x > C_y$. We can then assume iso-tropic brush bristles in both friction and shear stiffness, i.e. $C_{tr,x} = C_{tr,y} = C_{tr}; \Rightarrow C_x = C_{tr}$; and $C_y = C_{sw,\varepsilon,in} \cdot C_{tr}/(C_{sw,\varepsilon,in} + C_{tr})$;. From experiments, we typically find $C_x/C_y = \{at\ nominal\ F_z = F_{zNom}\} = C_{xNom}/C_{yNom} = k_{Nom} = 1.5\,..\,2$. This could be explained with the model if $C_{sw,\varepsilon,in}/C_{tr} = 1/(k_{Nom}-1) = 2\,..\,1$. This shows that neither of $C_{sw,\varepsilon,in}$ nor C_{tr} is neglectable.

2.2.5.4.2 Model for how Lateral Slip Stiffness is Degressive with Vertical Force

The model in 2.2.4.1.1.1 can also explain why lateral slip stiffness C_y is degressive with F_z, as indicated already in 2.2.3.1.3. The C_{tr} was found to be proportional to F_z, due to that contact length increase proportional to $\sqrt{F_z}$. A very conceptional reasoning of how $C_{sw,\varepsilon,in}$ could vary with F_z follows now: We defined $C_{sw,\varepsilon,in} = \varepsilon_{in}/F_y$. For a fix lateral deformation $\varepsilon_{in} \approx\propto 1/L$ and $F_y \approx\propto L$. So, $C_{sw,\varepsilon,in} \propto 1/L^2 \propto 1/F_z$. With $C_x \propto F_z$ and $C_{sw,\varepsilon,in} \propto 1/F_z$, and given $C_x = C_{xNom}$ and $C_y = C_{yNom}$ at given nominal $F_z = F_{zNom}$, the model gives [2.50] and Figure 2-49. So, by knowing F_{zNom} and measuring C_{xNom} and C_{yNom} one can get k_{Nom} as $k_{Nom} = C_{xNom}/C_{yNom}$ and thereby get a quantified model of $C_x(F_z)$ and $C_y(F_z)$.

$$C_x = \frac{F_z}{F_{zNom}} \cdot C_{xNom}; \quad and \quad C_y = \frac{F_z}{F_{zNom} + \frac{k_{Nom}-1}{F_{zNom}} \cdot F_z^2} \cdot C_{xNom}; \qquad [2.50]$$

2.2.5.5 Transients and Relaxation in Contact Patch

The models above for combined slip assume steady state conditions. For separate longitudinal and lateral slip, there is a delay in how fast the steady state conditions can be reached, which is sometimes important to consider. A similar model, as for relaxation in longitudinal direction 2.2.3.5.1, is to add a first order delay of the force:

$$[\dot{F}_x;\ \dot{F}_y] = [A_x \cdot (f_x(s_x, s_y, F_z, \mu, \dots) - F_x);\ A_y \cdot (f_y(s_x, s_y, F_z, \mu, \dots) - F_y)];$$
where $[f_x;\ f_y]$ are the forces according to steady state models and $[A_x;\ A_y]$ are relaxation lengths, as defined in Eq [2.24] and Eq [2.39]. [2.51]

Most reasoning in 2.2.3.5 is applicable also for combined slip relaxation.

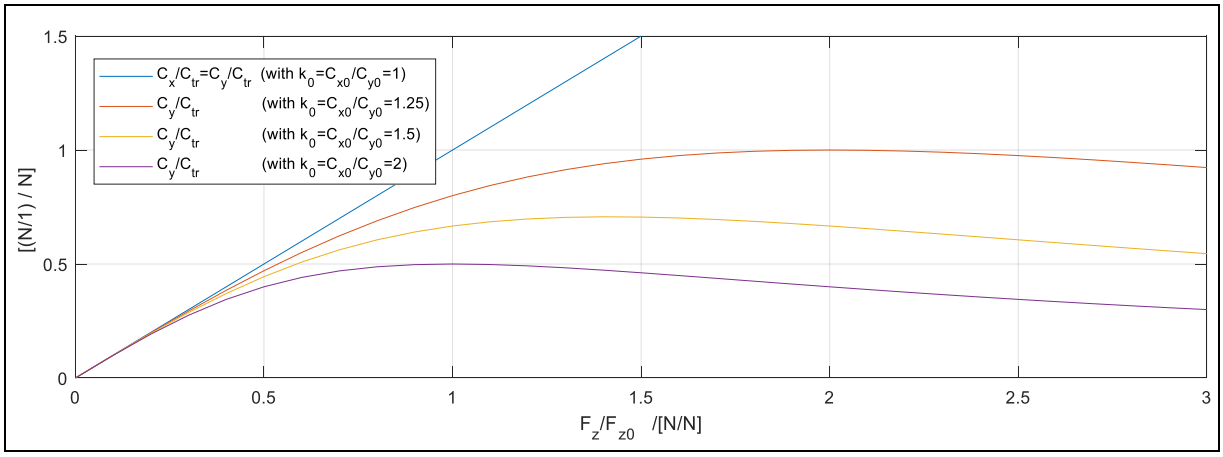

Figure 2-49: Model with Dependent Bristles explains that Lateral Slip Stiffness is degressive with F_z. The C_{tr} is (direction independent) slip stiffness due to tread (tr).

2.2.6 Summary of Tyre Force vs Slip Models

Categorization of tyre models for longitudinal force and slip:

- No lateral slip:
  - Ideally rolling ($R \cdot \omega \equiv v_x$; leaving F_x to be defined by other than the tyre)
  - Linear $F_x = +C_x \cdot s_x = +CC_x \cdot F_z \cdot s_x$;
  - Saturated due to road friction:
    - Simplest, saturated linear: $F_x = +\text{sign}(s_x) \cdot \min(C_x \cdot |s_x|,\ \mu \cdot F_z)$;
    - General: $F_x = f_x(\mu, F_z, s_x)$;
- Influence from lateral slip: $F_x = f(s_x, F_z, F_y)$;

Categorization of tyre models for lateral force and slip:

- No longitudinal slip:
  - Ideally tracking ($v_y \equiv 0$; leaving F_y to be defined by other than the tyre)
  - Linear $F_y = -C_y \cdot s_y = -CC_y \cdot F_z \cdot s_y$;
  - Saturated due to road friction:
    - Simplest, saturated linear: $F_y = -\text{sign}(s_y) \cdot \min(C_y \cdot |s_y|,\ \mu \cdot F_z)$;
    - General: $F_y = f_y(\mu, F_z, s_y)$;
- Influence from longitudinal slip: $F_y = f(s_y, F_z, F_x)$;

A general Combined force and slip model: $[F_x, F_y] = f(s_x, s_y, F_z)$; or $[F_x, F_y] = f(\omega, v_x, v_y, F_z)$;.

2.2.7 Vertical Properties of Tyres

The most important vertical property of a tyre is probably the stiffness. It mainly influences the vertical dynamics, see Chapter **5**. For normal operation, the vertical force of the tyre can be assumed to vary linearly with vertical deflection. If comparing a tyre with different pressures, the stiffness increases approximately linear with pressure. See Figure 2-50.

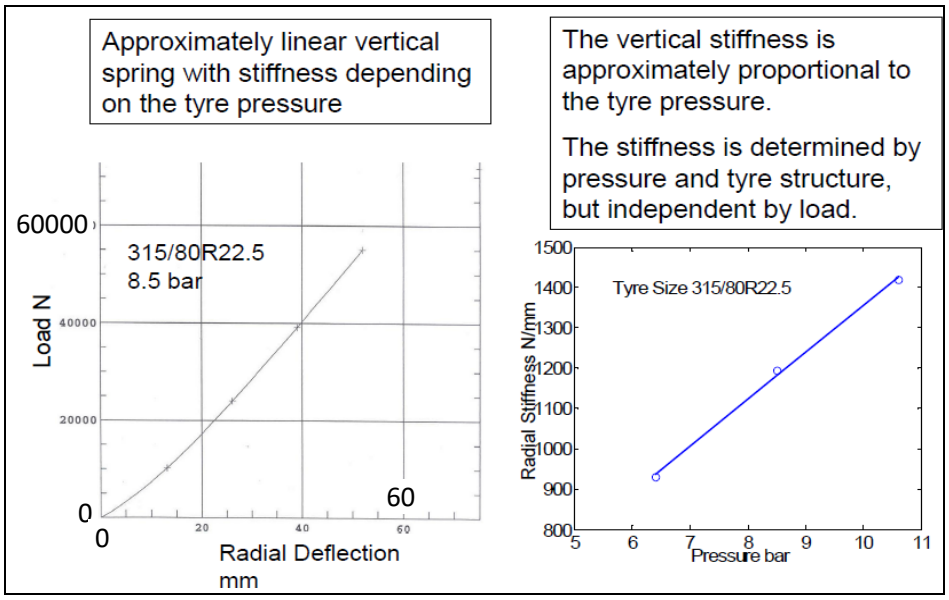

Figure 2-50: Vertical properties of a truck tyre.

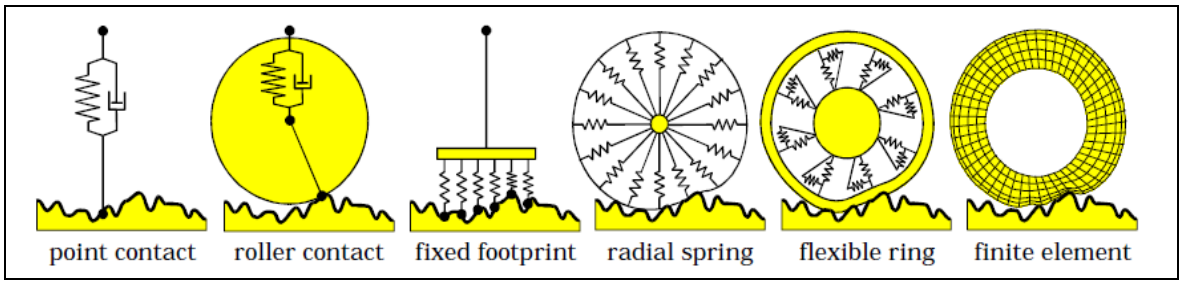

Figure 2-51: Different tyre models which will filter road irregularities differently. Picture from Peter Zegelaar, Ford Aachen.

2.2.8 Tyre Wear

There are many other aspects of tyres, for instance the wear. Wear models are often based around the Archard's (or Reye's) wear hypothesis: worn material is proportional to work done by friction, i.e. friction force times sliding distance. Wear rate (worn material per time) is therefore friction force times sliding speed. Different approaches to apply this to tyres and expanding to temperature dependency etc. is found for instance in Reference (Grosch, et al., 1961). A generalization of $WearRate$ [in mass/s or mm tread depth/s], for one certain tyre at certain temperature, becomes as follows:

$$WearRate \propto FrictionForce \cdot SlidingSpeed \Rightarrow WearRate = k_{w,av} \cdot F \cdot \Delta v \approx$$
$$\approx k \cdot F \cdot \sqrt{(R \cdot \omega - v_x)^2 + v_y^2} \approx k_{w,av} \cdot (C \cdot s) \cdot \sqrt{(R \cdot \omega - v_x)^2 + v_y^2} \approx$$
$$\approx k_{w,av} \cdot (C \cdot s) \cdot \left(s \cdot v_{Transport}\right) \Rightarrow WearRate \approx k_{w,av} \cdot C \cdot s^2 \cdot v_x; \quad [2.52]$$

where $F = \sqrt{{F_x}^2 + {F_y}^2}$; $s = \sqrt{{s_x}^2 + {s_y}^2}$; $v_{Transport}$ defined as in Eq [2.10] and $k_{w,av}$ is a constant for a certain tyre with a certain temperature, rolling on a certain road surface, which characterises the wear **averaged** over the contact patch.

2.3 Suspension System

Suspension can mean suspension of wheels (or axles), suspension of sub-frame and drivetrain and suspension of cabin (for heavy trucks). In this compendium, only wheel and axle suspension are

considered. Suspension design is explained in 2.3, but also used in complete vehicle models in 3.4.5-3.4.7, 4.3.9, and 4.5.3.

Suspension influences road grip and ride comfort, so merely all vehicle motion, Chapters 3..5. The influence is through how **vertical forces** and **camber and steer angles** on the wheels changes with **body motion** (heave, roll, pitch), **road unevenness** (bumps, potholes, waviness) and **wheel forces in ground plane** (from Propulsion, Braking and Steering subsystems). Important is also that suspension influences the material stresses (extreme values and fatigue), both in the suspension itself and other in other parts of the vehicle body. Figure 2-52 shows one way to see the suspension systems role.

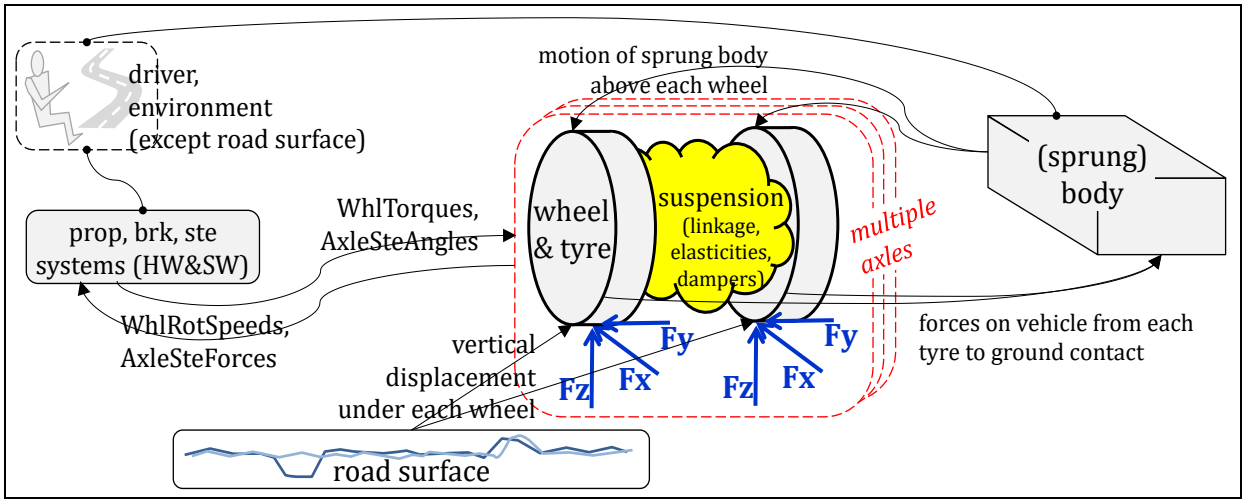

Figure 2-52: Wheel/axle suspension described as modular sub-model per axle. It may be noted that both wheel model (main geometry such as wheel radius) and tyre model (how F_x and F_y vary with tyre slip and F_z) is a part of each wheel&tyre sub-model.

The simplest view we can have of a suspension system is that it is an individual suspension between the vehicle body and each wheel, consisting of one linear spring and one linear damper in parallel. Chapter 5 uses this simple view for analysis models, because it facilitates understanding and it is enough for a first order evaluation of the functions studied (comfort, road grip and fatigue load) during normal driving on normal roads.

The full 3D aspect of suspension is not covered here in 2.3. Instead, a division into 2D is done in 2.3.3 Suspension -- Heave and Pitch and 2.3.4 Suspension -- Heave and Roll, aiming at Longitudinal and Lateral dynamics, respectively. The full 3D aspects are briefly addressed in 4.5.3.1.5 and 5.7.2.2.4.

2.3.1 Components in Suspension

Each wheel can rotate in its hub. Each hub can be individually suspended to the body or left and right hub can be mounted on a rigid beam which is suspended to the body. The suspension parts are below grouped in: Linkage, Elasticities and Dampers. One might count in additional parts in the suspension, such as bearings, shafts, brake parts, etc.

2.3.1.1 Linkage

Linkage, which has the purpose to constrain the relative motion between wheel and body via kinematics to one dof (approximately vertical translation), or, for a steered axle, also allow one more dof (approximately yaw rotation) per axle. The linkage defines how longitudinal and lateral tyre forces are brought to the body (sprung mass).

The linkage consists of links (or members) and joints; mainly ball joints, but sometimes others, such as hinge joints. The coordinates (“hard-points”) of these joints are the real design parameters, but the dynamic behaviour of a complete vehicle model can be expressed in much fewer parameters, namely the “effective pivot points”. These effective points are used in 2.3.3 and 2.3.4.

2.3.1.2 Elasticities or Compliances

Springs are examples of elasticities or compliances. The springs develop forces when the wheels are vertically displaced relative to the body. There is often one spring per wheel but also an anti-roll bar per axle. The anti-roll bar connects left and right wheel to each other to reduce body roll.

Springs often have a rather linear relation between the vertical displacement and force of each wheel, but there are exceptions:

- **Anti-roll bars** make two wheels dependent of each other (still linear). Anti-roll bars can be used on both individual wheel suspensions and rigid axle suspensions.
- The springs are intentionally designed to be non-linear in the compressed end of their stroke with **bump stops**. Bump stops at passenger cars are typically designed at $(3.5..4) \cdot g$ vertical acceleration when vehicle is fully loaded. (A somewhat opposite non-linearity appears in the rebound end of the stroke, due to wheel lift. Here it is the contact force with ground that is saturated to zero, not the spring force. The difference is the damping force.)
- The compliances can be non-linear during the whole stroke, e.g. **air-springs** and **leaf-springs**. Air-springs are non-linear due to the nature of compressing gas, e.g. assuming ideal gas: $p \cdot V = n \cdot R \cdot T;\ \Rightarrow\ \ Force = n \cdot R \cdot T/(L_0 - Compression)$;.
- The compliances can be **controllable** during operation of the vehicle. This can be to change the pre-load level to adjust for varying roads or varying weight of vehicle cargo or to be controllable in a shorter time scale for compensating in each oscillation cycle. The latter is very energy consuming and no such "active suspension" is available on market.

The springs are the main compliance, but also other smaller compliances are present and makes the effective stiffness lower: the links themselves, the bushings in the joints between the links and the brackets where the links are connected to the body. For the complete vehicle model, the tyres vertical compliance adds to the suspension compliance.

2.3.1.3 Dampers

Dampers have the purpose to dissipate energy from any oscillations of the vertical displacement of the wheel relative to the body. The most common design is the hydraulic piston type. Dampers often has a rather linear relation between the vertical deformation speed and force of each wheel, but there are exceptions:

- The dampers are normally intentionally designed to be different in different deformation direction. Typical values are about 3 times more damping in rebound (extension) than compression (bump). This can be motivated from that driving over a steep bump requires low damping to reduce upward jerk in vehicle, especially since there is a hard bump stop in the end of the spring stroke. In the other direction, driving over equally steep hole the downward jerk is limited by that the wheel cannot develop pulling forces on the ground; instead it lifts from ground if hole is too steep. So larger damping can be allowed in rebound. A reflection here is that high damping damps oscillations, but high damping also increases the shock transmittance (with this reasoning, the name "shock-absorber" is misleading).
- Damping in **leaf springs** is non-linear since they work with dry friction.
- The dampers can be designed to be **controllable** during operation of the vehicle. This can be used to change the damping characteristics to adjust for varying roads or varying weight of vehicle cargo or to be controllable in a shorter time scale for compensating in each oscillation cycle. The latter is called "semi-active suspension" and is available on some high-end vehicles on market.

2.3.2 Axle and Wheel Rates

All compliances (springs, bushings, etc) contribute to the stiffness between the body and the wheels. The wheels are not independent of each other; we have especially a connection between left and right due to the anti-roll bars. Therefore, we define both axle (compliance) rate and wheel (compliance) rate, see Figure 2-53. We can also call these *Effective stiffnesses* of the axle and wheel, respectively.

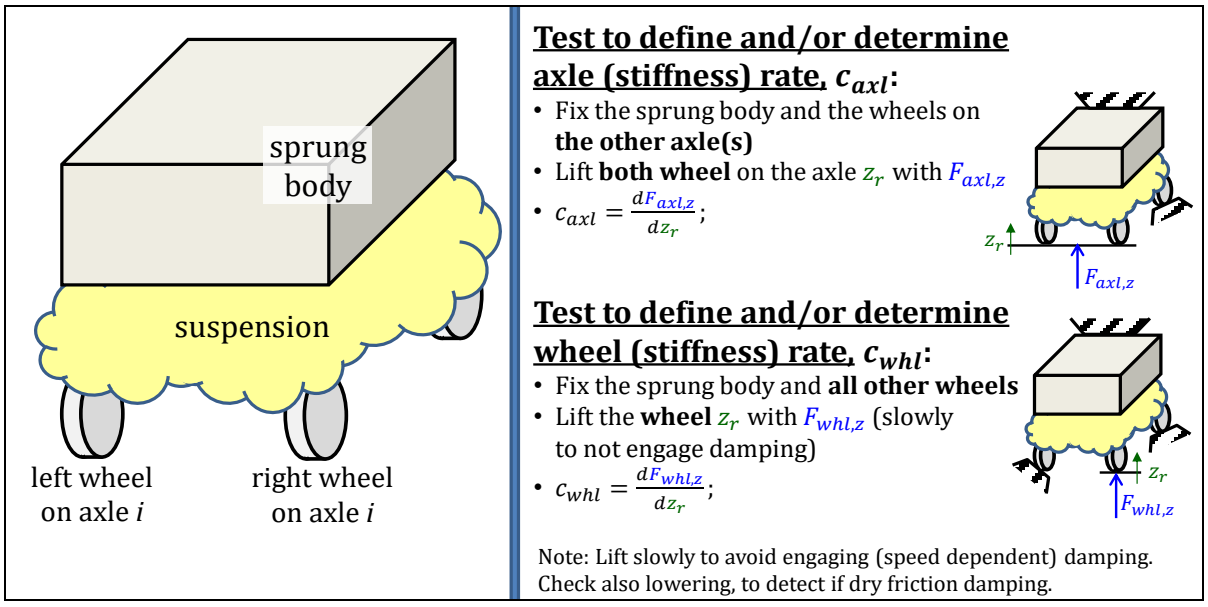

Figure 2-53: Definition of axle and wheel (stiffness) rates.

Alternatively to lifting one wheel, the axle can be rolled (without lifting the midpoint of the axle): $z_{left} = z_r = \varphi_{rx} \cdot W/2$; and $z_{right} = -z_r = -\varphi_{rx} \cdot W/2$;. It is then natural to find the measure axle roll stiffness $c_{roll}[Nm/rad] = F_{whl,z} \cdot W/\varphi_{rx}$;, instead of $c_{whl}[N/m]$. If the vehicle is symmetric and track width is known, these measures carry the same information and $c_{roll} = c_{whl} \cdot W^2/2$;.

With these definitions, the vertical wheel forces for a two-axle vehicle will be as follows. It is assumed that the vehicle is symmetrical and that there are connections between the wheels only as anti-roll bars on each axle. The body is fixed and road under the wheels are displaced with z_{rij}. Notation $c_{i,axl}$ is axle rate and $c_{i,whl}$ is wheel rate for axle i. The time derivative of spring force $\dot{F}_{sij}$ and vertical velocities are used to avoid involving pre-tension in the springs.

$$\begin{bmatrix} \dot{F}_{s1l} \\ \dot{F}_{s1r} \\ \dot{F}_{s2l} \\ \dot{F}_{s2r} \end{bmatrix} = \begin{bmatrix} \boldsymbol{C_{w1}} & \boldsymbol{0} \\ \boldsymbol{0} & \boldsymbol{C_{w2}} \end{bmatrix} \cdot \begin{bmatrix} v_{r1lz} \\ v_{r1rz} \\ v_{r2lz} \\ v_{r2rz} \end{bmatrix}; \quad where\ \boldsymbol{C_{wi}} = \begin{bmatrix} c_{i,whl} & -\left(c_{i,whl} - \frac{c_{i,axl}}{2}\right) \\ -\left(c_{i,whl} - \frac{c_{i,axl}}{2}\right) & c_{i,whl} \end{bmatrix};$$

If both body and road under the wheels is moving, we simply exchange $[v_{1lz} \quad v_{1rz} \quad v_{2lz} \quad v_{2rz}]^T$ with $[v_{r1lz} \quad v_{r1rz} \quad v_{r2lz} \quad v_{r2rz}]^T - [v_{1lz} \quad v_{1rz} \quad v_{2lz} \quad v_{2rz}]^T$. The axle roll stiffness becomes $c_{i,roll} = \left(c_{i,whl} - c_{i,axl}/4\right) \cdot W^2$; [Nm/rad] for $\dot{M}_{s1x} = c_{i,axl} \cdot \omega_{r1x}$.

Similarly, for axle i, we can define axle (damping) rate $d_{i,axl}$, wheel (damping) rate $d_{i,whl}$ and axle roll damping $d_{i,roll}$. However, $d_{i,axl}$ is often simply $2 \cdot d_{i,whl}$ since there are typically no dampers connecting left and right wheel. Corresponding 4×4 damping matrix becomes a diagonal matrix, since $d_{i,axl}$ normally is $2 \cdot d_{i,whl}$.

If we know the design parameters (stiffness and location of the actual spring) we can calculate the rates. This will be exemplified in 2D and briefly discussed for general (3D) below.

2.3.2.1 Explanation in 2D

A very simplified suspension is assumed in Figure 3-26. The stiffnesses c_f and c_r are the *effective stiffnesses* at each axle. The physical spring may have another stiffness, but its effect on vertical force is captured in the effective stiffness. An example of how the effective stiffness is found for a 2D model (heave and pitch) from a real suspension design is given in Figure 2-54.

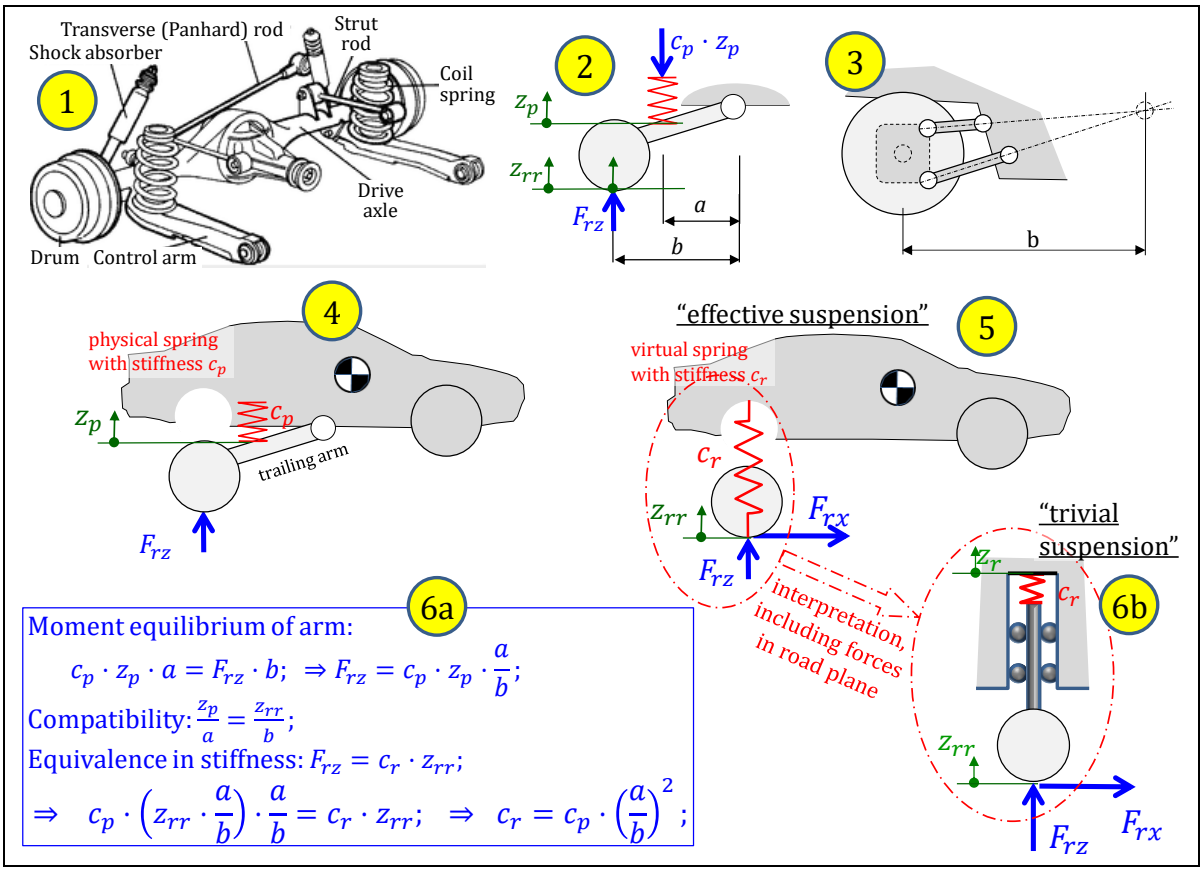

Figure 2-54: From suspension design to effective stiffness. 6a: Final Mathematical model. 6b: Interpretation ("Reverse modelling") back from Mathematical to Physical model, showing "Trivial (linkage) suspension".

Note that the factor $(a/b)^2$ is not the only difference between effective and physical stiffness, but the effective can also include compliance from other parts than just the spring, such as bushings and tyre. There will also be a need for a corresponding effective damping coefficient, see 3.4.5.2.2, or axle (damping) rate. How forces in road plane is transferred is not well captured in this model, see F_{rx} in Figure 2-54. Compared to suspension models later in compendium, Figure 2-54 ends with a "trivial (linkage) suspension model". In 3.4.5.2, the suspension linkage is better modelled, which allows validity for F_{ix} (propulsion and braking). Corresponding for F_{iy} is modelled in 4.3.9.3.

2.3.3 Suspension -- Heave and Pitch

2.3.3.1 Examples of Suspension Designs

In Figure 3-28, a "trailing arm" is drawn both for front and rear axle. For rear axle, that is a realistic design even if other designs are equally common. However, for front axle a so-called McPherson suspension is much more common, see Figure 2-55. Figure 2-56 shows a suspension for a heavy vehicle.

2.3.4 Suspension -- Heave and Roll

2.3.4.1 Examples of Suspension Designs

There are axles with dependent wheel suspensions, which basically look as the roll centre axle model in Figure 4-33 , i.e. that left right wheel are rigidly connected to each other. Then, there are axles with dependent wheel suspensions, which look more like the model with wheel pivot points in Figure 4-33. For these, there are no (rigid) connections between left and right wheel.

Many axles have a so-called anti-roll bar, which is an elastic connection between left and right side. It is connected such that if the wheel on one side is lifted, it lifts also the wheel on the other side. Note

that, if an anti-roll bar is added to an independent wheel suspension it is still called independent, because the connection is not rigid.

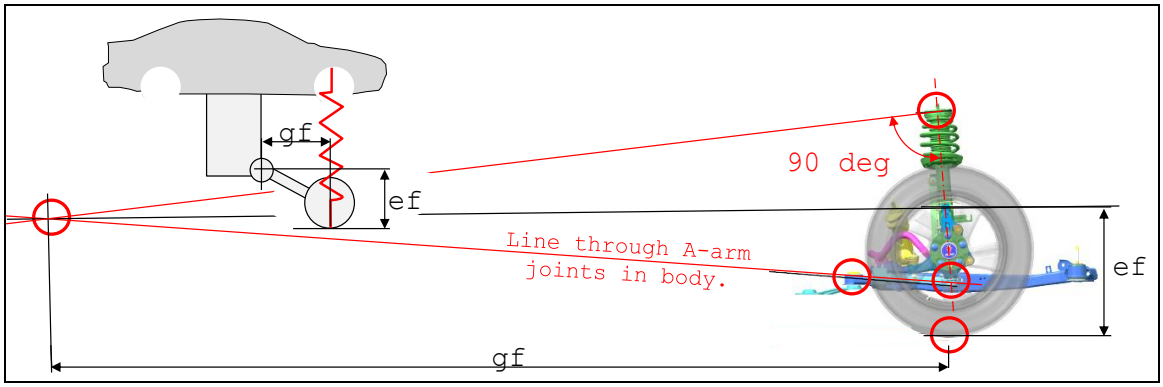

Figure 2-55: Example of typical front axle suspension, and how pivot point is found. The example shows a McPherson suspension. From Gunnar Olsson, LeanNova.

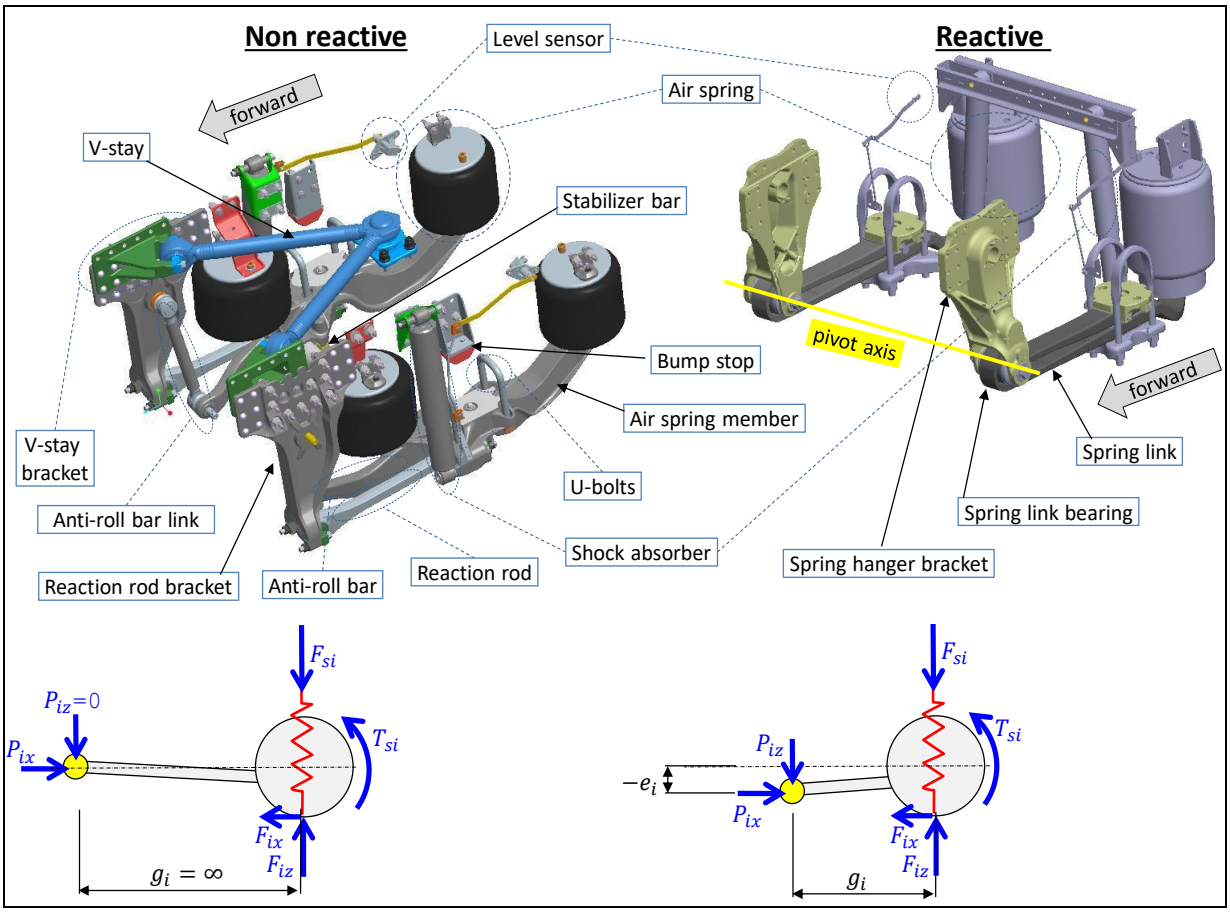

Figure 2-56: Axle suspensions/installations for double rear axle heavy vehicles.

Figure 2-57 and Figure 2-58 show design of two axles with independent wheel suspensions. Figure 2-59 shows an axle with dependent wheel suspension. These figures show how to find wheel pivot points and roll centre. In the McPherson suspension in Figure 2-58, one should mention that the strut is designed to take bending moments. For the rigid axle in Figure 2-59, one should mention that the leaf spring itself takes the lateral forces. Symmetry between left and right wheel suspension is a reasonable assumption and it places the roll centre symmetrically between the wheels, which is assumed in the previous models and equations regarding roll centre.

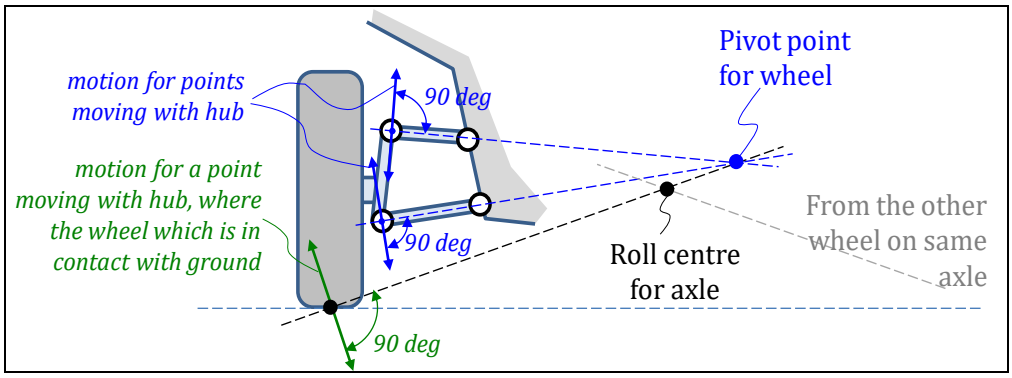

Figure 2-57: Example of how to appoint the pivot point for one wheel, and roll centre height, for an axle with double wishbone suspension.

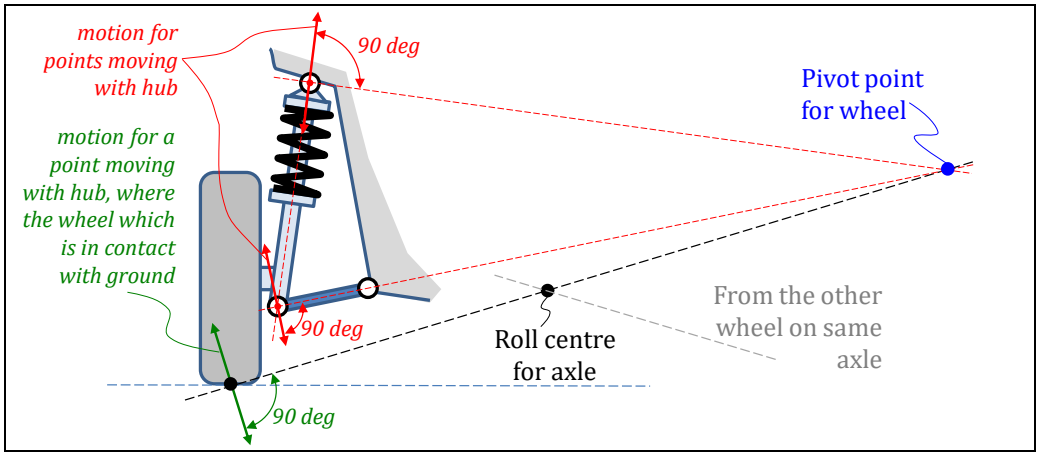

Figure 2-58: Example of how to appoint the pivot point for one wheel, and roll centre height, for axle with double McPherson suspension.

Generally, a "rigid axle" gives roll centre height on approximately the same magnitude as wheel radius, see Figure 2-59. With individual wheel suspension one has much larger flexibility, and typical chosen designs are 30..90 mm front and 90..120 mm rear.

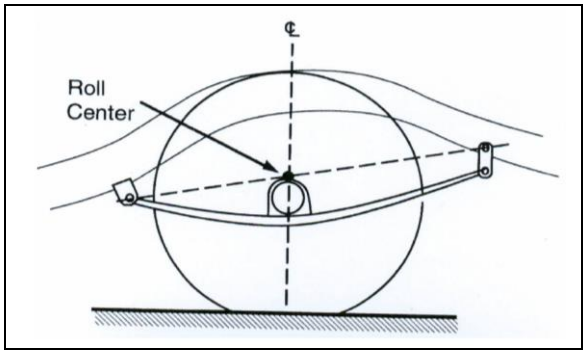

Figure 2-59: Example of how to appoint the pivot point for one wheel and roll centre for axle with rigid axle suspended in leaf springs. From (Gillespie, 1992).

The target for roll centre height is a trade-off. On one side, high roll centre is good because it reduces roll in steady state cornering. On the other side, low roll centre height is good because it gives small track width variations due to vehicle heave. Track width variations are undesired, e.g. because it makes the left and right tyre lateral force fight against each other, leaving less available friction for longitudinal and lateral grip. Roll centre is normally higher rear than front. One reason for that is that the main inertia axis leans forward, and parallelism between roll axis and main inertia axis is desired.

2.4 Propulsion System

A generalised propulsion system is shown in Figure 2-73, along with a specific example of a conventional one. There are 1+2=3 control degrees of freedom marked for the generalized one (e.g. engine power, transmission ratio and storage power) while there is only 1+1=2 for the conventional.

Note that the approach in Figure 2-60 is one-dimensional: we consider neither the differential between left and right wheel on the driven axle nor distribution between axles. Instead, we sum up the torques at all wheels and assume same rotational speed.

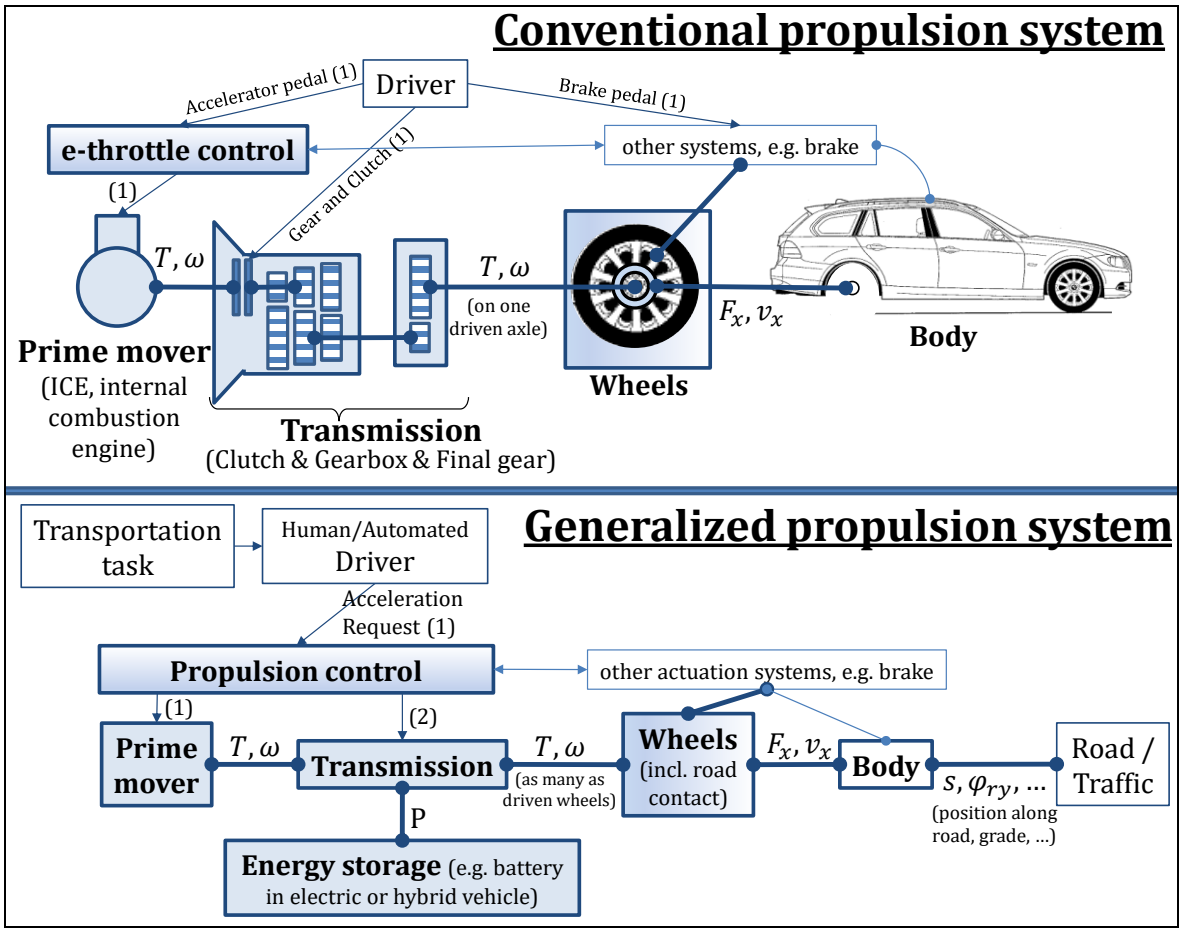

Figure 2-60: Propulsion system models, as appearing in a vehicle model

It is often suitable to model propulsion systems "connecting in nodes", see **1.5.1.9.1** and Figure 2-61.

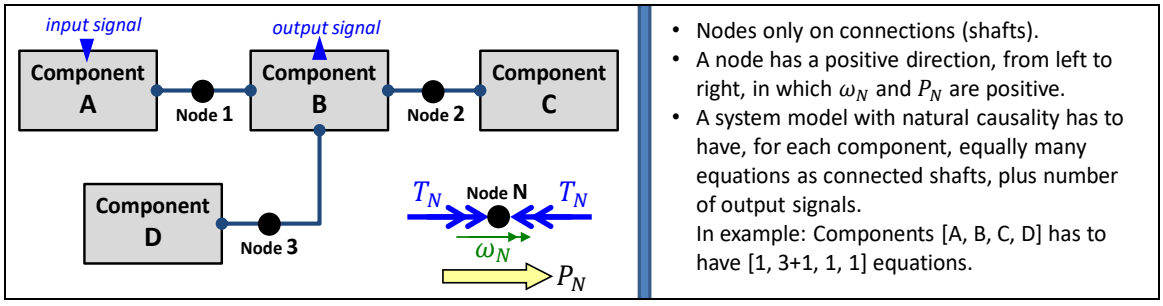

Figure 2-61: Proposed notation and sign conventions for Propulsion system models.

2.4.1 Prime movers

The conversion of stored energy to power occurs in the prime mover, see Figure 2-60. Details of the conversion processes and transmission of power to the tyres are not covered in this compendium. Some basic background is still necessary to describe the longitudinal performance of the vehicle. The

main information that is required is a description of the torque applied to the wheels over time and/or as a function of speed. Sketches of how the maximum torque varies with speed for different prime movers (internal combustion engine (ICE), electric motor or similar) are shown in Figure 2-62. The torque speed characteristics vary dramatically between electric and internal combustion engines. Also, gasoline and diesel engines characteristics vary.

The curve for electric motors in Figure 2-62 shows that the main speciality, compared to ICEs, is that their operation range is nearly symmetrical for negative speeds and torques. However, the curve should be taken as very approximate, since electric motors can work at higher torque for short periods of time. The strong time duration dependency makes electric motors very different to ICEs from a vehicle dynamics point of view. Other properties that makes them special are quick and accurate response, well known actual torque and that it is much more realistic to divide them into several smaller motors, which can operate on different wheels/axles.

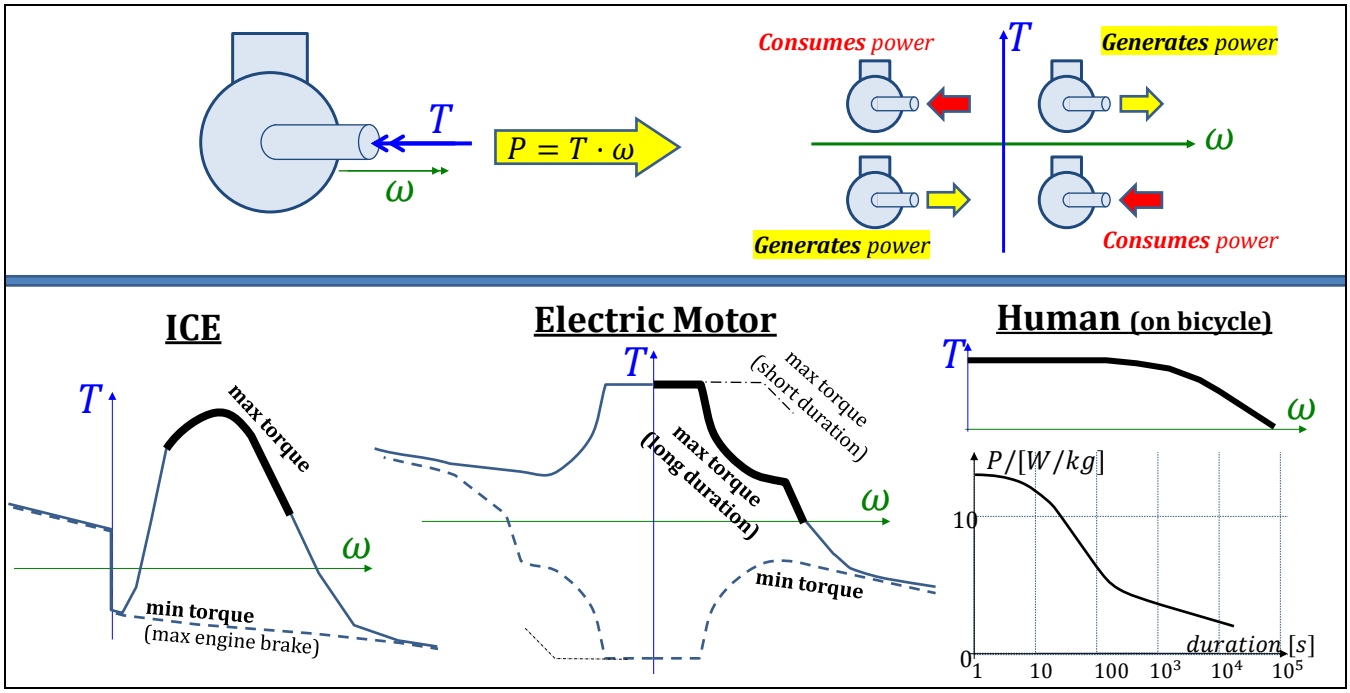

Figure 2-62: Torque Characteristics of 3 Prime Movers

A bicycle uses the human body as prime mover. It reminds of an electric motor in that it has torque from zero speed. The duration dependency is high, with maximum power ≈ 10 W/kg up to a minute duration and ≈ 2 W/kg for an hour duration.

2.4.1.1 Efficiency and Consumption

The efficiency (η) is the output power per input power. The specific consumption can be the inverted value, but often the input power is measured in fuel rate $[g/s]$ or $[litre/s]$, which makes specific consumption inversely proportional to efficiency and not the exact inverse value.

$$Efficiency = \eta = \frac{P_{out}}{P_{in}};$$

$$SpecificConsumption_1 = \frac{FuelRate}{P_{out}} \propto SpecificConsumption_2 = \frac{P_{in}}{P_{out}} = \frac{FuelRate \cdot c}{P_{out}};$$

$$where\ FuelRate\ is\ in\ [kg/s]\ or\ [litre/s]$$

$$and\ c = specific\ energy\ content\ in\ [J/kg]\ or\ [J/litre]$$

[2.53]

The efficiency is dependent on the operating point in the speed vs torque diagram, or map, for the prime mover. An example of a specific consumption map for an ICE is given in Figure 2-63. Maps with similar function can be found for other types of prime movers, such as the efficiency map for an electric motor, see Figure 2-64.

Figure 2-63 and Figure 2-64 also show that the efficiencies can be transformed to the traction diagram.

The maps for different gears partly overlap each other, which show that an operating point of the vehicle can be reached using different gears. The most fuel or energy efficient way to select gear is to select the gear which gives the lowest specific fuel consumption, or highest efficiency. Such a gear selection principle is one way of avoiding specifying the gear selection as a function over time in the driving cycle. For vehicles with automatic transmission, that principle can be programmed into the control algorithms for the transmission. However, the gear selection is often a trade-off with acceleration reserve, see 3.3.4.5, which argues for lower gear. Assuming very tightly stepped transmission, or CVT, gives that a high efficiency can be kept down to around 0.3 of maximum power.

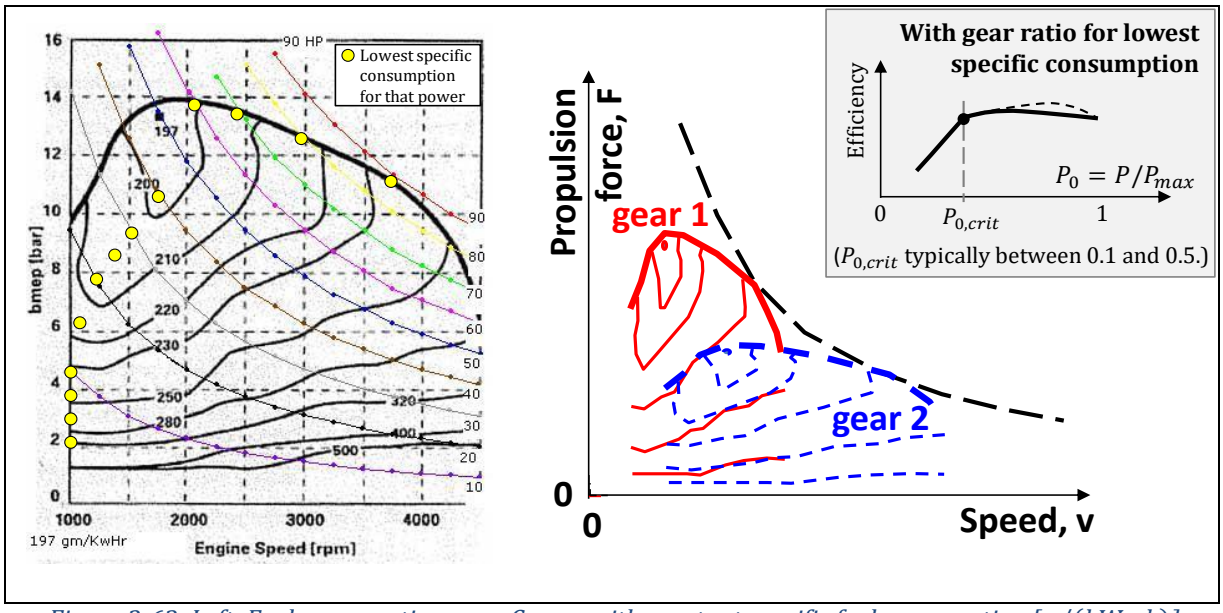

Figure 2-63: Left: Fuel consumption map. Curves with constant specific fuel consumption $[g/(kW \cdot h)]$, which is $\propto 1/efficiency$. Middle: Specific fuel consumption curves transformed to Traction Diagram, for different gears. Right: How efficiency with efficiency-optimal gear ratio drops when $P < P_{0,crit} \cdot P_{max}$.

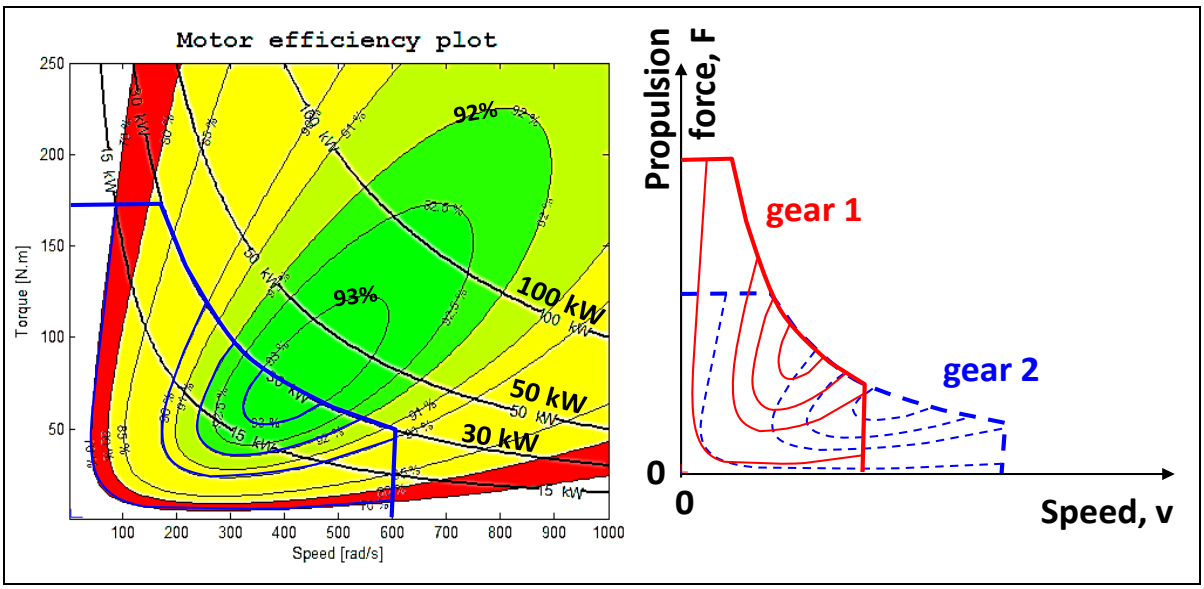

Figure 2-64: Left: Efficiency map for a typical brushless DC motor, from (Boerboom, 2012). Elliptic curves show where efficiency is constant. Right: The efficiency curves can also be transformed in Traction Diagram, for a given gear.

2.4.2 Transmissions

In some contexts, "transmission" means the 1-dimensional transmission of rotational mechanical power from an input shaft to one output shaft. Such are called "Main transmissions". In other contexts,

"transmission" means the system that distributes the energy to/from an energy buffer and to/from multiple axles and/or wheels. Such are called "Distribution transmissions".

2.4.2.1 Main Transmissions

Main transmission can be either stepped transmissions or continuously variable transmissions, CVTs. Among stepped transmissions, there are manual an automatic. Among automatic, there are those with power transmission interruption during shifting and other with powershifting, see 2.4.2.1.1. Clutches and torque converters can also be part of models of main transmissions, see 2.4.3 and 2.4.3.3. A stepped transmission, can be modelled e.g. as:

$$T_{out} = r \cdot T_{in} \cdot \eta_{CoggMeshes} - \Delta T_0 \cdot \text{sign}(\omega_{out});$$
$$\omega_{out} = \frac{\omega_{in}}{r};$$
$$where\ r = r_1, r_2, \cdots r_N; \quad r \neq 0; \qquad [2.54]$$

ΔT_0 is the "parasitic" or "load independent" losses, arising from oil, sealings and bearings. Eq [2.54] is not valid for neutral gear, because then there is no speed equation, but instead two torque equations: $T_{out} = -\Delta T_{0,out} \cdot \text{sign}(\omega_{out})$; and $T_{in} = \Delta T_{0,in} \cdot \text{sign}(\omega_{in})$;.

For any 1-dimensional transmission of rotational mechanical power between two rotating shafts, the total efficiency, $\eta_{total} = P_{out}/P_{in} = T_{out} \cdot \omega_{out}/(T_{in} \cdot \omega_{in})$;, is depending on operating condition. If assuming a nominal ratio, r, the total efficiency can be decomposed in $\eta_{total} = \eta_T \cdot \eta_\omega$;, where $\eta_T = T_{out}/(r \cdot T_{in})$; and $\eta_\omega = \omega_{out}/(\omega_{in}/r)$;.

2.4.2.1.1 Powershifting Main Transmissions

The most common powershifting transmission is using planetary gears and torque converter, see Figure 2-75. During 2000-2010, developments in mechatronics has enabled to leave out the torque converter and the planetary gears resulting in what often meant with powershifting transmissions, see concept in Figure 2-65. In practice, one can often manage with 2 clutches, and instead select different paths through gear wheels with synchronisers. An advanced design of powershifting transmission for a hybrid propulsion system is seen in Figure 2-66. A dummy sequence of shifting is simulated in Figure 2-67.

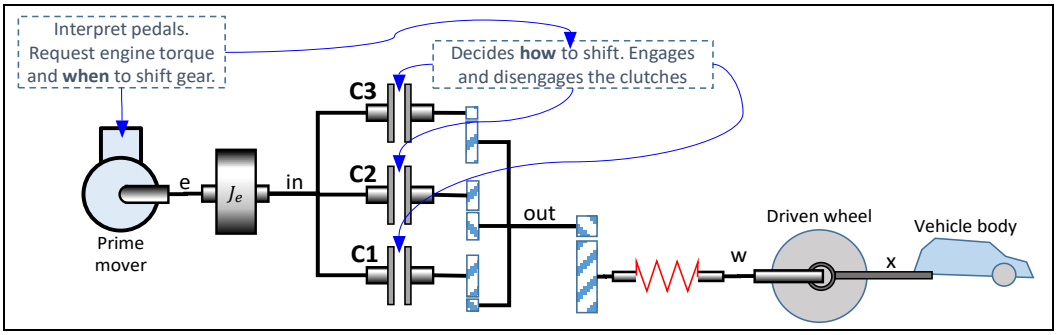

Figure 2-65: Conceptual design of powershifting transmission with 3 gears.

2.4.2.3 Distribution Transmissions

The distribution to energy buffer and multiple axles and/or wheels can basically be done in two ways:

- Distribute in certain fractions of (rotational) speed. A (rotationally) rigid shaft between left and right wheel is one example of this. We find this in special vehicles, such as go-carts, and in more common vehicles when a differential lock is engaged. There are 3 shafts in such an axle: input to the axle and two outputs (to left and right wheel). The equations will be:

$$\omega_{in} = \omega_{left};$$
$$\omega_{in} = \omega_{right};$$
$$T_{in} = T_{left} + T_{right}; \qquad [2.55]$$

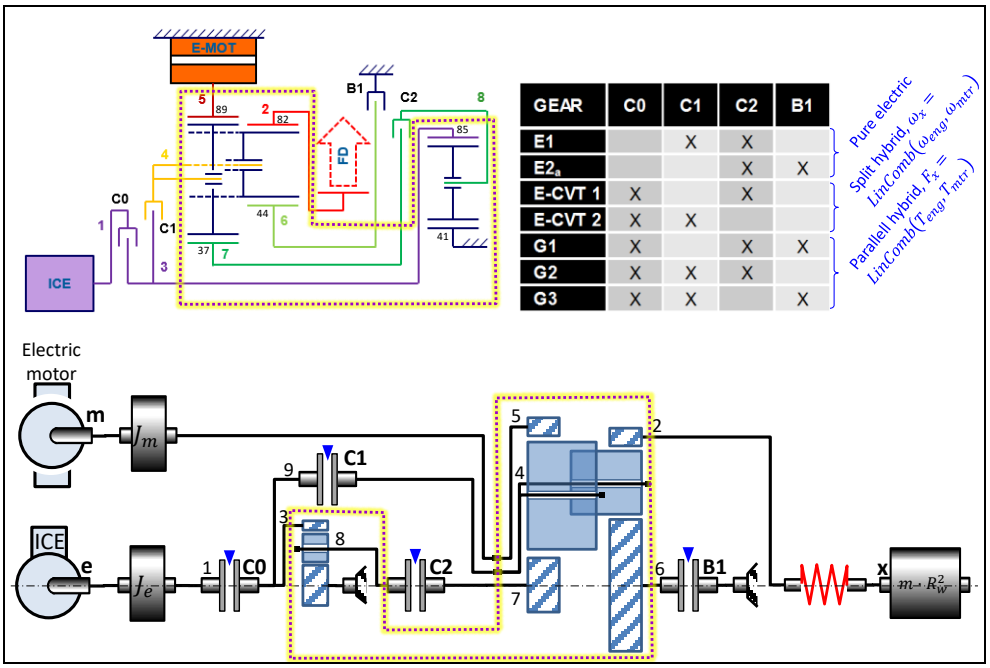

Figure 2-66: Hybrid propulsion system with powershifting, designed using planetary gears. Upper left: Design. Upper right: Gear/Clutch schedule. Lower half: Dynamic model.

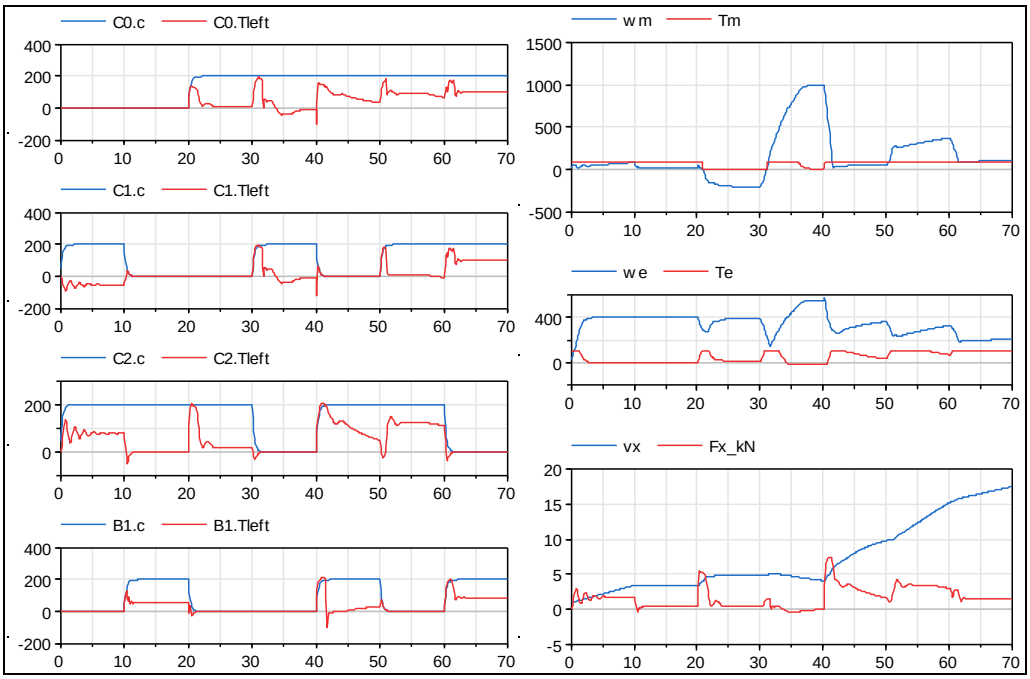

Figure 2-67: Simulation of the transmission in Figure 2-66 (with approximate clutch models from Eq [2.58]). Example sequence of shifts: Simply shift each 10th second, in order as in table in Figure 2-66.

- Distribute in certain fraction of torque. This requires some type of planetary gear arrangement. A conventional (open) differential gear is one example of this, where the equations will be:

$$\omega_{in} = \frac{\omega_{left} + \omega_{right}}{2};$$
$$T_{left} = T_{right};$$
$$T_{in} = T_{left} + T_{right};$$

[2.56]

Generally speaking, the open differential is rather straight-forward to use in most vehicle dynamics manoeuvres: The speeds are given by vehicle motion (e.g. curve-outer wheel runs faster than curve-

inner wheel, defined by vehicle yaw velocity and track width). The torques are defined by the differential, as half of the propulsion torque at each side.

Also, a locked differential, it is generally more complex to model and understand in a vehicle manoeuvre. Here, the wheels are forced to have same rotational speed, and, in a curve, that involves the tyre longitudinal slip characteristics. The solution involves more equations with shared variables.

So, open/locked differential is the basic concept choice. But there are additions to those: One can build in friction clutches which are either operated automatically with mechanical wedges or similar or operated by control functions. One can also build in electric motors which moves torque from one wheel to the other. However, the compendium does not intend to go further into these designs.

Parts of the distribution transmissions are also shafts. If oscillations are to be studied, these has to be modelled with energy storing components:

- Rotating inertias or Flywheels ($J \cdot \dot{\omega} = T_{in} - T_{out};$) and
- Elasticities, compliances or springs: ($\dot{T} = c \cdot (\omega_{in} - \omega_{out})$).

2.4.3 Clutches and Brakes in Transmission

The modelling techniques shown in this section are also applicable also for tyres (2.2) and brakes (2.5).

Seen as machine elements, brakes are special cases of clutches, specialized by that one of the clutch halves is fixed. There are brakes on the wheels, but there are also brakes inside the transmission. A tyre operates as a transmission clutch (2.2.1.6) which can stick and slip (2.10.1.2). Also, when operating between forward and rearward rolling, the rolling resistance of the tyre acts as a brake, with stick and slip.

Clutches with dry friction are difficult to model in dynamic systems since they introduce "discrete dynamics", sticking and slipping, see 1.5.1.4. The conceptual mathematical model of a controlled clutch is given in Figure 2-68 and Eq[2.57]. Here, the interface variables are T, ω_1, ω_2 and c_c. Capacity c_c $[Nm]$ is an input signal representing the magnitude of torque when the clutch slips. In the model below, a discrete state variable, $x_d = -1, 0$ *or* $+1$, is introduced to model the discrete dynamics.

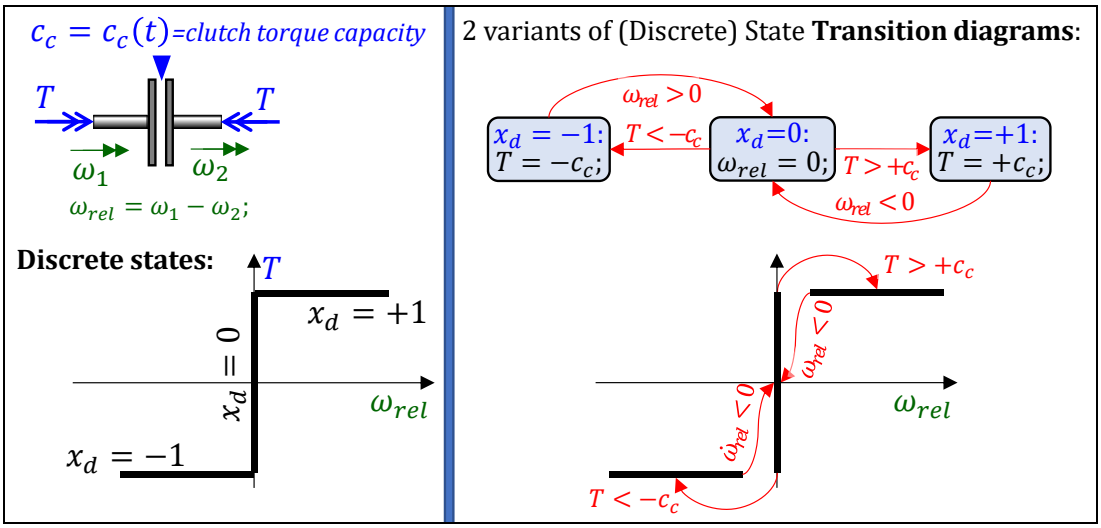

Figure 2-68: Model of a clutch. The x_d is a discrete state, declared as Integer.

$$\text{(Continuous) Equations, using the discrete state } x_d: \begin{cases} if\ x_d = -1\ then & T = +c_c; \\ elseif\ x_d = 0\ then & \omega_{rel} = 0; \\ elseif\ x_d = +1\ then & T = -c_c;\ end\ if; \end{cases}$$

$$\text{(Discrete State) Transition Equation:} \begin{cases} when\ (x_d = -1\ \ and\ \ \omega_{rel} > 0)\ then & x_d = 0; \\ elsewhen\ (x_d = 0\ \ and\ \ T < -c_c)\ then & x_d = -1; \\ elsewhen\ (x_d = 0\ \ and\ \ T > +c_c)\ then & x_d = +1; \\ ellsewhen\ (x_d = +1\ \ and\ \ \omega_{rel} < 0)\ then & x_d = 0;\ \ end\ when; \end{cases} \quad [2.57]$$

2.4.3.1 Modelling Format and Tool Aspects

A tool with discrete dynamic support should log at least two values for an event: the value before and after the event. So, there will be 2 identical time values in the time vector. Several transitions can happen during on event, e.g. switching from $x_d = -1$ to $x_d = +1$ without $x_d = 0$ in between in Figure 2-68. For this reason, the simulation tool needs to do "event iteration", which means that the whole model is evaluated repeatedly during the event until no further changes happens. It can be discussed whether intermediate values during the event iteration should be logged or not. Modelica is designed to **not** log those.

2.4.3.2 Different Surroundings for the Clutch

Different implementations can be needed for different surroundings; energy dissipating or generating components (dampers or power sources), kinetic energy storing components (flywheels) or potential energy storing components (elasticities), see examples in Figure 2-69. The challenge is to handle that the set of state variables can change between the different discrete states.

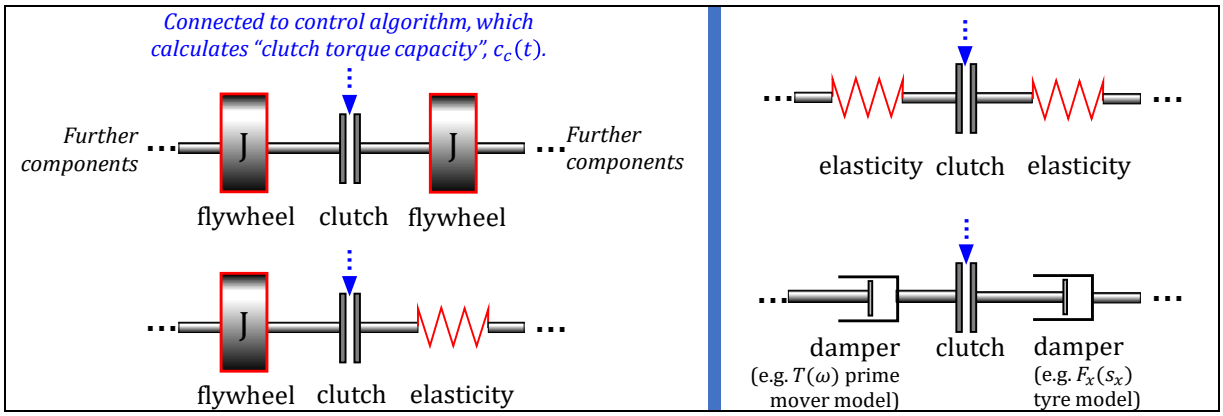

Figure 2-69: Examples of differently modelled surroundings of a clutch.

For complete main transmissions, as automatic transmissions, there are several clutches involved, the implementation of the ideal model in Eq [2.57] can be very demanding. It is modelled in Modelica. The discrete dynamics is modelled with the discrete state (`xd` declared `Integer`) and the operator "`pre(z)`", which holds the z value from last time instant or, in an event, from the last event iteration.

2.4.3.2.1 Clutch and Elasticity in Series

The easiest surrounding to a clutch is in series with elasticity, assuming velocities can be input. Figure 2-70 shows such. It also adds $stiction = st > 1$; a different static and dynamic friction, $\mu_{stick} = st \cdot \mu_{slip}$;.

2.4.3.2.2 Clutch between Inertias

When connecting 2 inertias or 2 elasticities with a clutch is more complicated. For clutch between inertias, it is proposed to use ω_{rel} as state variable, because it makes it easy to keep $\omega_{rel} \equiv 0$ during stick.be modelled, see Figure 2-71. The values $x_d = \pm 1$ are temporary during a state event; it enables a total state transition during one event between $x_d = -2$ and $x_d = +2$, without (wrongly) logging an intermediate $x_d = 0$. With $st < 1$, there is risk for chattering solutions.

2.4.3.2.3 Functional or Inverse Clutch Model

In some cases, it can be suitable to prescribe how the clutch is operates in terms of $\omega_{rel}(t)$ instead of $c_c(t)$. This means that we rather assume a successful engagement as that $\omega_{rel} \to 0$ during an assumed engagement time, than assuming a $c_c(t)$ and find out how long time it takes to engage (or fail to engage. The $\omega_{rel}(t)$ is then declared as input and the (required) torque $T(t)$ and the torque capacity $c_c(t)$ becomes an output. This can simplify the modelling. This is not further discussed in this compendium but see http://blog.xogeny.com/blog/part-2-kinematic/.

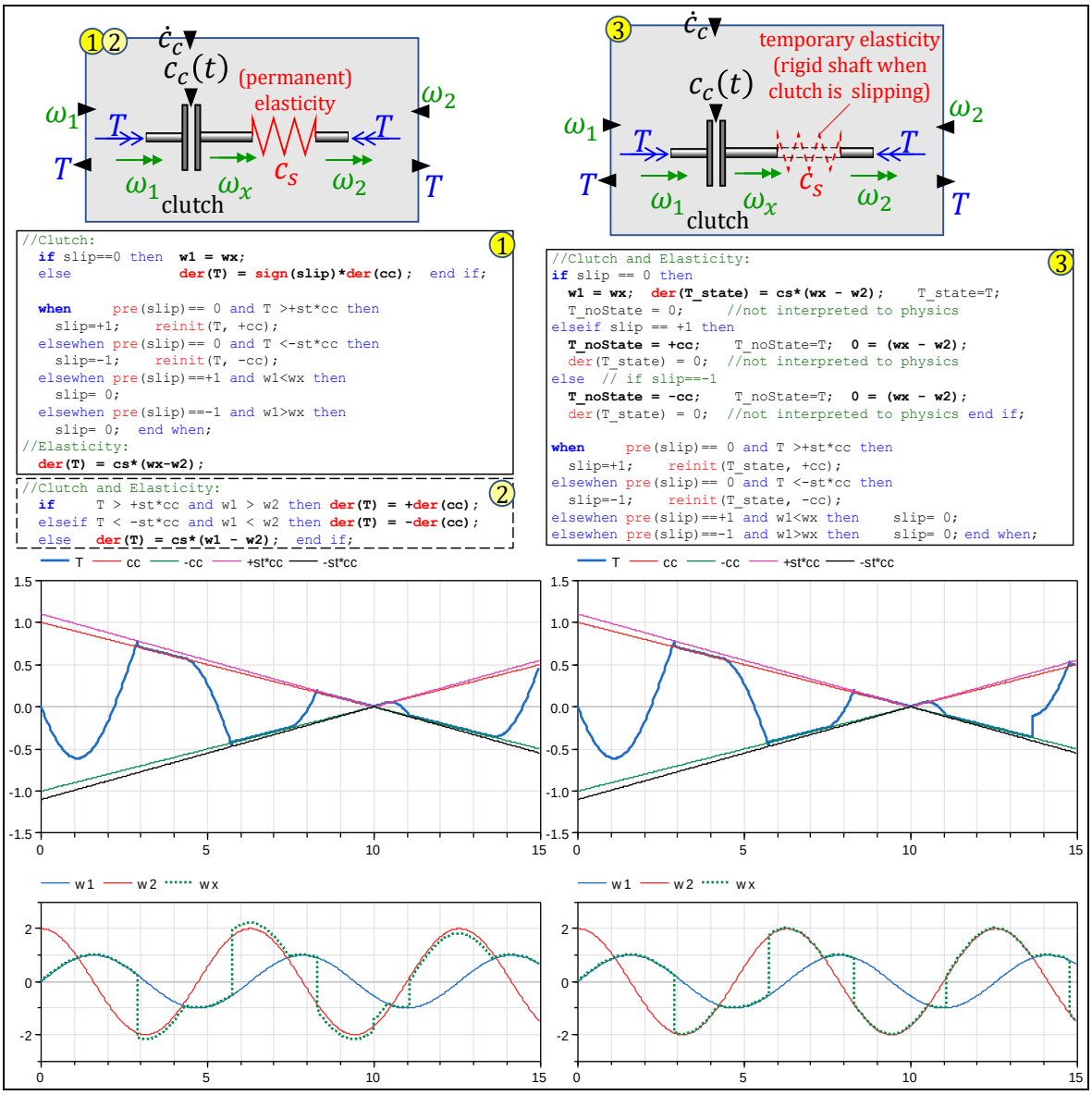

Figure 2-70: Model of clutch and elasticity in series, modelled for speed input from both sides. Implemented in Modelica. Implementation 2 (without discrete state and without `when`) only works well (without chattering) for st = 1.0. Implementation 3 uses a different physical model which has different number of states depending on the discrete state slip; elasticity is modelled only when slip = 0.

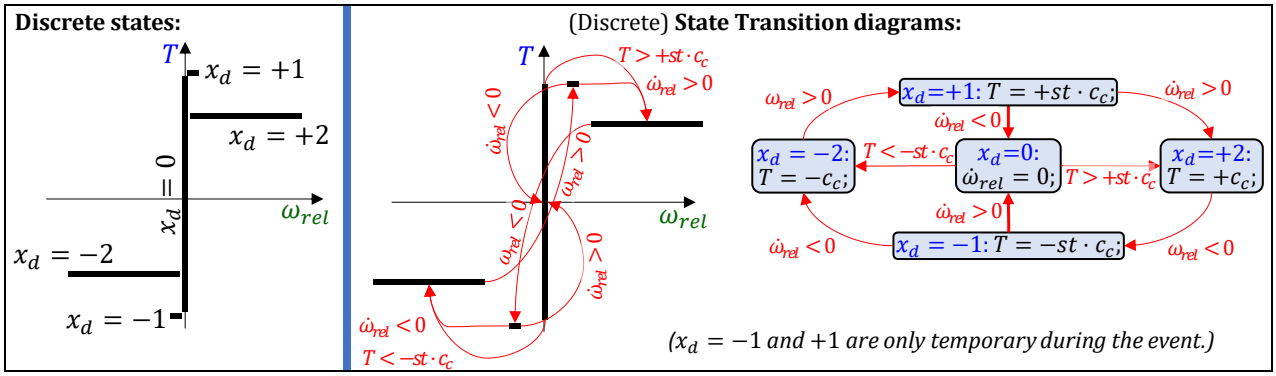

Figure 2-71: Modelica of a clutch which works to be connected between inertias.

2.4.3.3 Implementation of Clutches as Stiff Dampers

A way around model implementation problems is to use an approximate clutch model as in Eq [2.60]. The advantage is that it can handle any surrounding without leading to changing set of state variables.

The drawback is that it has a trade-off between modelling the intended physics (Eq [2.60]) and the computational efficiency in simulation; the more $d \to \infty$, the closer to the intended model we come, but the simulation time will increase towards infinity. The approximation can be seen as putting a stiff damper in direct series with an ideal clutch. There are also other approximations, which could be seen as putting a stiff spring with stiffness c in series with an ideal clutch. This will work if clutch is surrounded by inertias:

$$T_{left} = T_{right}; \quad and \quad \omega_{rel} = \omega_{left} - \omega_{right};$$

$$\frac{T_{left}}{c} \cdot \text{sign}(\omega_{rel}) =$$

$$= \begin{cases} = \min\left(\frac{1-\varepsilon}{\varepsilon} \cdot \frac{|\omega_{rel}|}{\omega_{nom}} \;\; ; \; 1 + \frac{\varepsilon}{1-\varepsilon} \cdot \left(\frac{|\omega_{rel}|}{\omega_{nom}} - 1\right)\right); & if \; \frac{|\omega_{rel}|}{\omega_{nom}} < 1 \\ = \max\left(\frac{1}{1 + \frac{\varepsilon}{1-\varepsilon} \cdot \left(\frac{\omega_{nom}}{|\omega_{rel}|} - 1\right)} \;\; ; \; \frac{\varepsilon}{1-\varepsilon} \cdot \frac{|\omega_{rel}|}{\omega_{nom}}\right); & else \end{cases}$$

[2.58]

Figure 2-73 shows an example that the ideal and approximate models can give comparable results with respect to torques and speeds. About computational efficiency, the ideal needs around 5 ms time step with Euler forward integration, while the approximate needs 100 times smaller time step. If better agreement than in Figure 2-73 is needed, ε needs to be reduced, which slows down the approximation even more. Note also that, for energy dissipation, the approximate model of course calculates a higher energy dissipation, since it assumes the clutch has to slip to transfer torque.

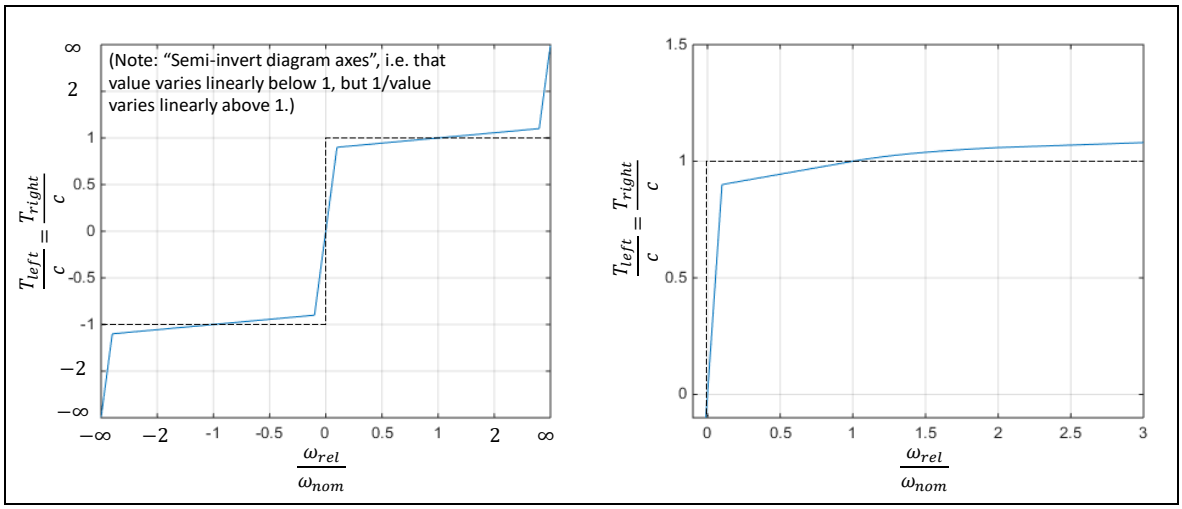

Figure 2-72: Example of approximation of clutch model. Strategies: ω_{nom} = typical slip speed of clutch, $\varepsilon \ll 1$. Dashed curve shows before approximation.

There are clutch models also in the standard Modelica (see 1.5.4.10) library, see Figure 2-74. Note that the library is built such that the "small inertia" is needed, which forces down computational efficiency during clutch slip.

Brakes, one-way clutches and backlashes often causes similar difficulties and can be modelled similarly as clutches.

2.4.4 Hydrodynamic Torque Converters

Hydrodynamic torque converters serve almost same purpose as a clutch, but it is much less complex to model as a member of a dynamic system. Such converters have a pump in input side and turbine on output side. They can operate with substantial slip, and when slip, there is a torque amplification, which leads to that a vehicle with converter have typically good acceleration performance and driveability also without the corresponding lowest gear needed on same vehicle without converter.

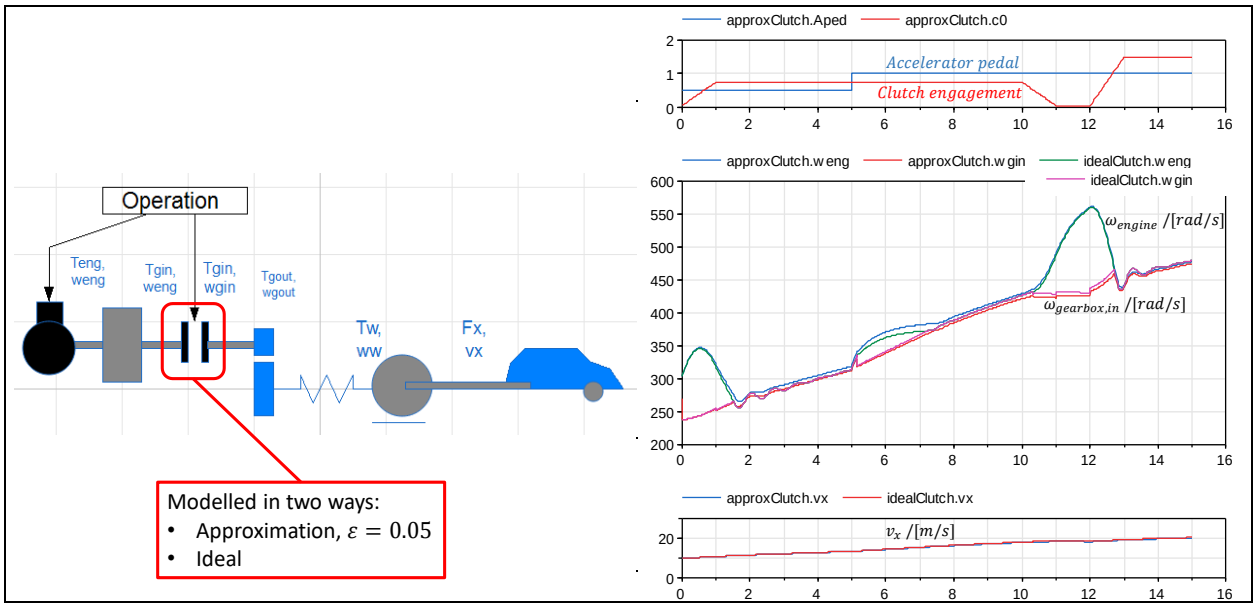

Figure 2-73: Example with clutch, modelled in two ways

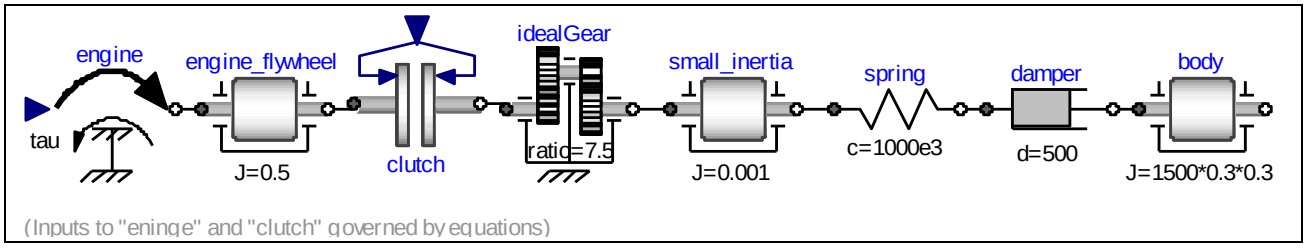

Figure 2-74: Model example with clutch, using standard Modelica library "Modelica.Mechanics.Rotational"

The following model gives the steady state characteristics of a hydrodynamic torque converter. Steady state characteristics are often enough but combined with that hydrodynamic torque converters often are possible to lock-up with a clutch, mounted in parallel to the impellers.

$$\frac{T_{out}}{T_{in}} = \mu(\nu);\ \frac{T_{in}}{\omega_{in}^2} = \lambda(\nu);\quad where\ \mu\ and\ \lambda\ are\ functions\ and\ \nu = \frac{\omega_{out}}{\omega_{in}};$$

But if locked-up: $\frac{T_{out}}{T_{in}} = 1;\ \ and\ \frac{\omega_{out}}{\omega_{in}} = 1;$

The moment capacity, λ, is often given on a dimensionless form $\lambda = T_{in}/\left(\omega_{in}^2 \cdot\ OilDensity \cdot OuterRadius^5\right)$.

[2.59]

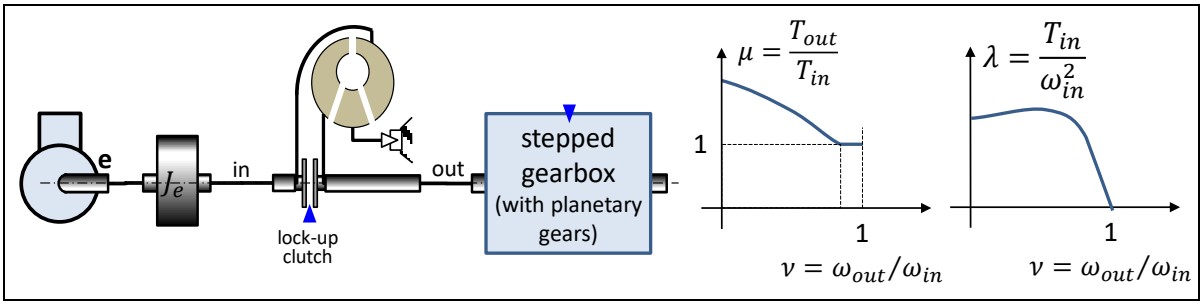

Figure 2-75: Left: Traditional automatic transmission. Right: Conceptual curves of the torque converter.

2.4.5 Energy Storages

Fuel tank and battery are two examples of energy storages. An "energy buffer" often refers to an energy storage that can not only be emptied (during propulsion), but also refilled by regenerating energy from the vehicle during deceleration. A fuel tank is an energy storage, but not an energy buffer. Also, a

battery which can only be charged from the grid, and not from regenerating deceleration energy, is not an energy buffer.

Energy buffers in vehicles are today often electro-chemical batteries. However, other designs are possible, such as flywheels and hydrostatic accumulators. A simple model of a buffer is as follows:

$$\dot{E} = \begin{cases} = (P_{in} - P_{out}) \cdot \eta_{charge}; & for\ P_{in} > P_{out}; \\ = (P_{in} - P_{out}) / \eta_{use}; & else; \end{cases}$$
$$where\ P_{in} = T_{in} \cdot \omega_{in}; and\ P_{out} = T_{out} \cdot \omega_{out};$$

[2.60]

Including how the buffer is connected, one more equation can be found: Typically, $\omega_{in} = \omega_{out}$; or $T_{in} = T_{out}$;.

The model uses stored energy, E. For batteries, one often uses state of charge, SoC, instead. Conceptually, $SoC = E/E_{max}$;, where E_{max} is a nominal maximum charge level.

A first approximation of the efficiencies, can be $\eta_{charge} = \eta_{use} = constant < 1$, but typically the efficiency is dependent of many things, such as $P_{in} - P_{out}$. The model above does not consider any leakage when buffer is "resting": $P_{in} = P_{out}$.

2.5 (Wheel) Braking System

Braking can refer to either wheel braking which means adding wheel torques from (wheel) braking system or vehicle braking which can be achieved with negative wheel torques from propulsion system. Seldom used, it would also be possible to apply unusual wheel steering angles, e.g. steer left and right wheel in different directions. Other ways are possible such as raise brake shields on the vehicle body to increase longitudinal aerodynamic resistance.

There are several systems that can brake a vehicle:

- Service brake system (brake pedal and ABS/ESC controller, which together applies brake pads to brake discs/drums)
- Parking brake (lever/button that applied brake pads to brake discs/drums, normally on rear axle on cars but all axles on heavy vehicles)
- Prime mover brakes:
    - Engine braking (ICE operates at "engine brake" as marked in Figure 2-62)
    - Electric machines (machines can be used symmetrical, i.e. both for positive and negative torques, see Figure 2-62)
- Heavy vehicles often have *Retarders*. They normally use hydraulic or Eddy current to dissipate engine, as opposed to dry-friction. So, they cannot brake at low speeds or stand-still.
- Large steer angles will decelerate the vehicle, see 3.2.2.2.

This section is about Friction brakes, meaning Service brakes and Parking brake. In vehicle dynamics perspective, these have the following special characteristics:

- Friction brakes are almost unlimited in force for a limited time since they can lock the wheels for most driving situations and road friction (ICE and electric motors are often limited by their maximum power, since it is often smaller than available road friction.) However, if the friction brakes are used for a long time, the brake lining will start to fade. This means friction coefficient is lowered due to high temperature (oxidation and melting of pad/lining material).
- Friction brakes can only give torque in opposite direction to wheel rotation. (Electric motors can brake so much that wheel spins rearwards.)
- Friction brakes can hold the vehicle at exact standstill. (If using electric machines for holding stand-still in a slope, a closed loop control would be necessary, resulting in that vehicle "floats" a little.)

The basic design of a passenger car brake system is a hydraulic system is show in Figure 2-76. Here, the brake pedal pushes a piston, which causes a hydraulic pressure (pressure = pedal force/piston area). The hydraulic pressure is then connected to brake callipers at each wheel, so that a piston at each wheel pushes a brake pad towards a brake disc ($DiscForce = Pressure \cdot PistonArea$). The brake torque on each wheel is then simply: $T = NumberOfFrictionSurfaces \cdot DiscCoefficientOfFriction \cdot$

DiscRadius · *DiscForce*. (Normally, there are 2 friction surfaces, since double-acting brake calipers.) By selecting different piston area and disc radii at front and rear, there is a basic hydro mechanical brake distribution ratio between front and rear axle. There are normally two circuits for redundancy. It should be mentioned that *DiscCoefficientOfFriction* varies a lot; during one strong brake event, it can typically drop 10..25% due to temperature rise and sliding velocity decrease.

Brake systems for heavy trucks are generally based on pneumatics, as opposed to hydraulics, see Figure 2-78. Ref (Tagesson, 2017), has a good descriptive chapter about brake systems for heavy vehicles.

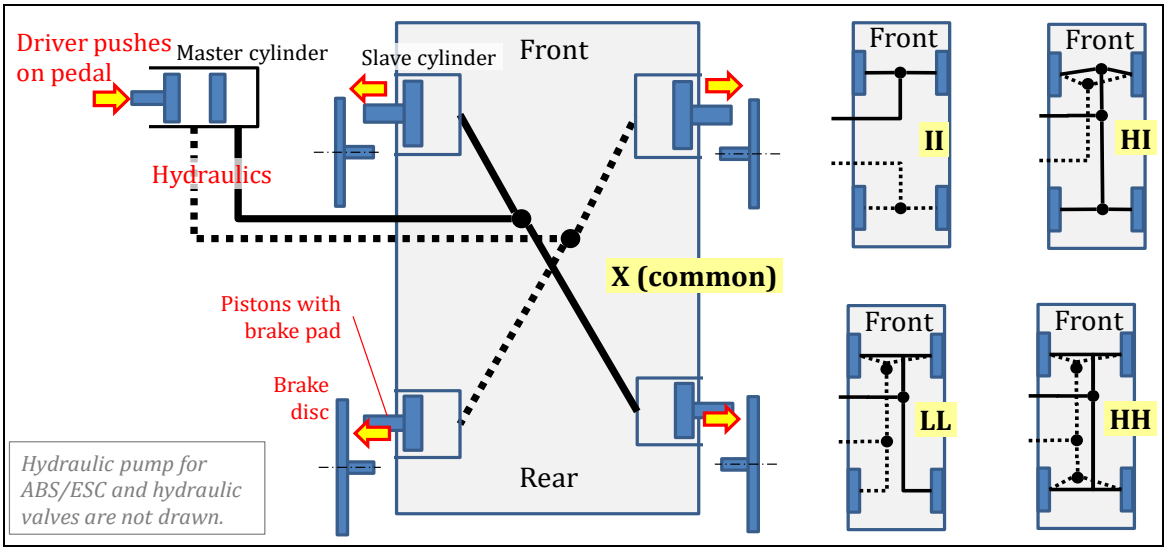

Figure 2-76: Layouts of a hydraulically applied brake system, which is conventional on passenger cars.

Brake systems for modern road vehicles are almost always mechatronic systems, i.e. they contain both mechanical parts and control algorithms. As minimum, one can include the wheel slip control, see 4.6.2.1.4, or ABS/EBD, see 3.5.2.3/3.5.2.4.

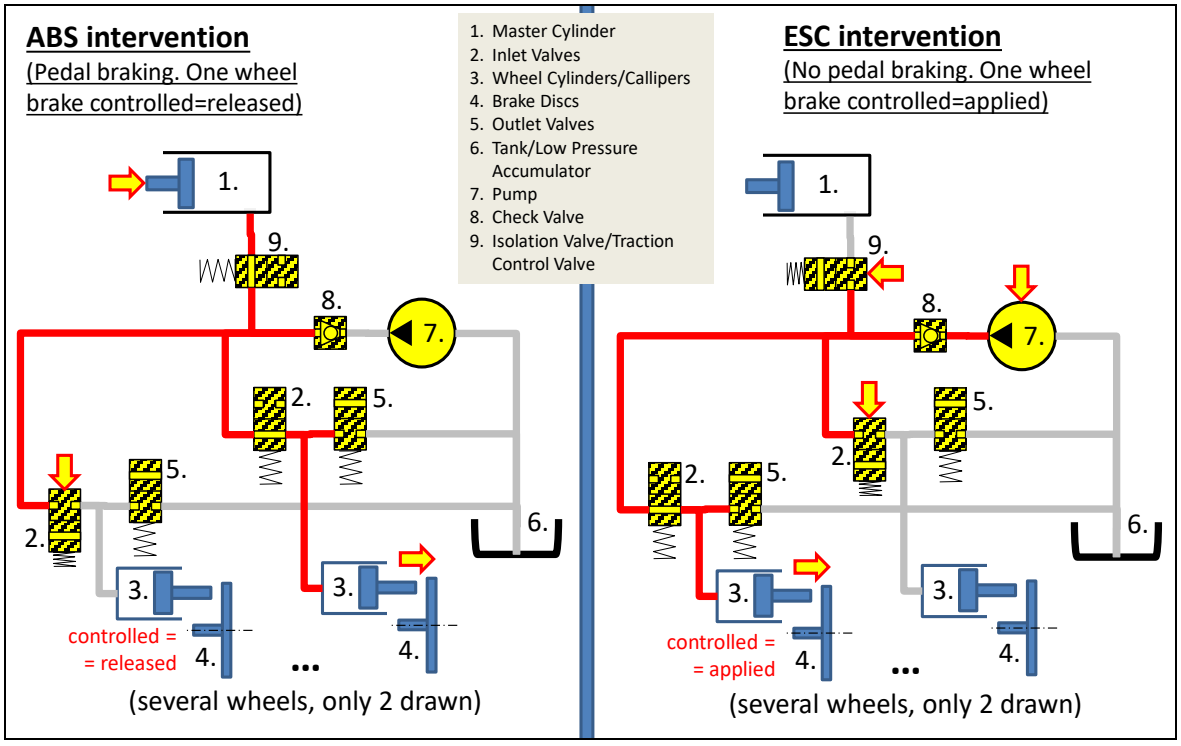

Figure 2-77: Concept of hydraulically applied brake system for ABS and ESC functions.

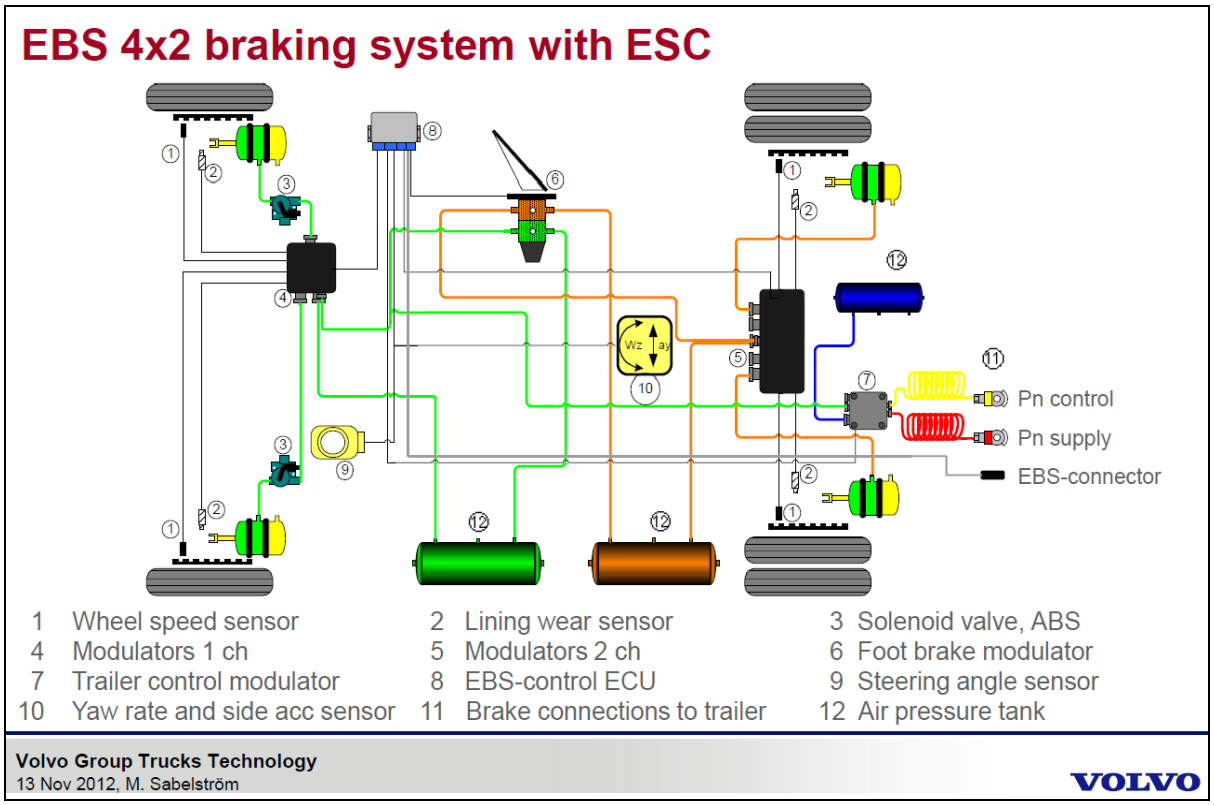

Figure 2-78: Pneumatically applied brake system for heavy vehicles. Electronics Brake System, EBS, from Volvo GTT, Mats Sabelström.

2.6 (Wheel) Steering System

Steering can refer to either wheel steering which means adding yaw angles to the wheels relative to the vehicle body or vehicle steering which can be achieved with wheel steering but also other actuators, such as propelling or braking the wheels on side.

The steering system is here referred to the link between steering wheel and the road wheel's steering, on the steered axle. It is normally the front axle that is steered. Driver's interaction is two-folded, both steering wheel angle and torque, which is introduced in 2.9. In present section, we will focus on how wheel steer angles are distributed between the wheels.

2.6.1 Chassis Steering Geometry

The most basic intuitive relation between the wheels steer angles is probably that all wheels' rotation axes always intersect in one point. This is called Ackermann geometry and is shown in Figure 2-79. The condition for having Ackermann geometry is, for the front axle steered vehicle that:

$$\left.\begin{aligned}\frac{1}{\tan(\delta_i)} &= \frac{R_r - w/2}{L};\\ \frac{1}{\tan(\delta_o)} &= \frac{R_r + w/2}{L};\end{aligned}\right\} \Rightarrow \frac{1}{\tan(\delta_o)} = \frac{1}{\tan(\delta_i)} + \frac{w}{L}; \qquad [2.61]$$

The alternative to Ackermann steering geometry is parallel steering geometry, which is simply that $\delta_i = \delta_o$. Note that Ackermann geometry is defined for a vehicle, while parallel steering is defined for an axle. This means that, for a vehicle with 2 axles, each axle can be parallel steered, which means that the vehicle is non-Ackermann steered. However, the vehicle can still be seen as Ackermann steered with respect to mean steer angles at each axle.

For low-speed, Ackermann gives best manoeuvrability and lowest tyre wear. For high-speed, Parallel is better in both aspects. This is because vehicles generally corner with drift outwards in curves, which

means that the instantaneous centre is further away than Ackermann geometry assumes, i.e. more towards optimal for parallel. Hence the chosen geometry is normally somewhere between Ackermann and parallel.

Practical arrangement to design the steering geometry is shown in Figure 2-80. The design of linkage will also make the transmission from steering wheel angle to road wheel steer angle non-linear. This can lead to different degrees of Ackerman steering for small and large steering wheel angles.

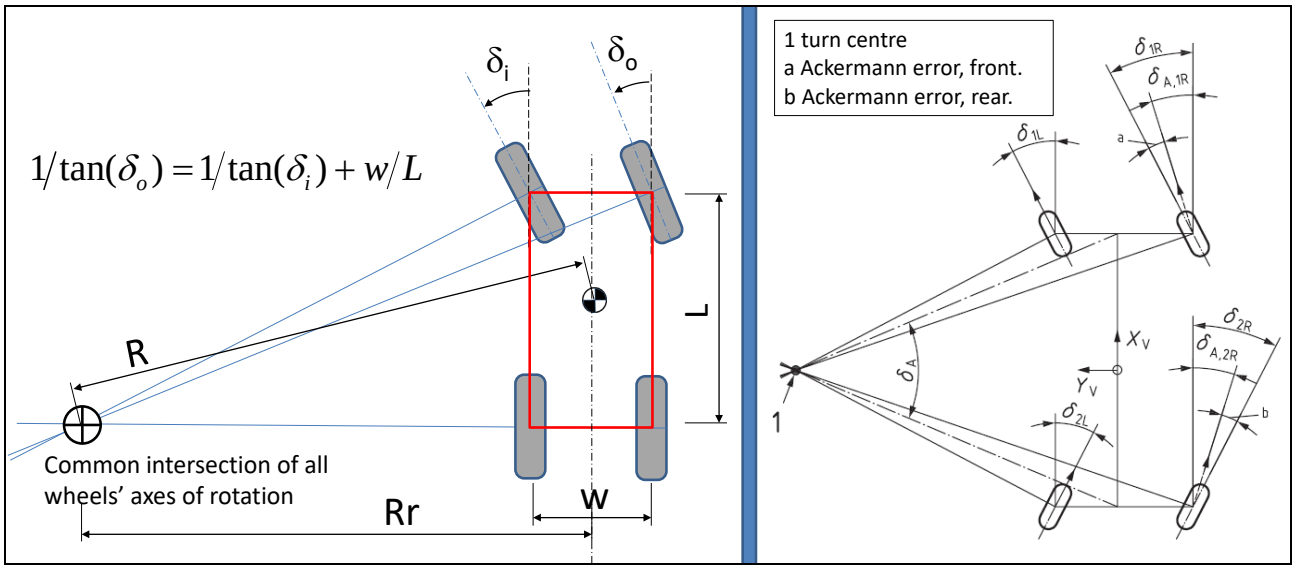

Figure 2-79: Ackermann steering geometry. Left: One axle steered. Right: Both axles steered and including "Ackermann errors". From (ISO 8855).

In traditional steering systems, the steering wheel angle has a monotonically increasing function of the steer angle of the two front axle road wheels. This relation is approximately linear with a typical ratio of 15..17 for passenger cars. For trucks the steering ratio is typically 18..22. In some advanced solutions, steering on other axles is also influenced (multiple-axle steering, often rear axle steering). There are also solutions for dynamically adding steer angle through a planetary gear and electric angle-controlled motor on the steering shaft, so called Active Front Steering (AFS). In reference (Tagesson, 2017), there is a good descriptive chapter about steering systems for heavy vehicles.

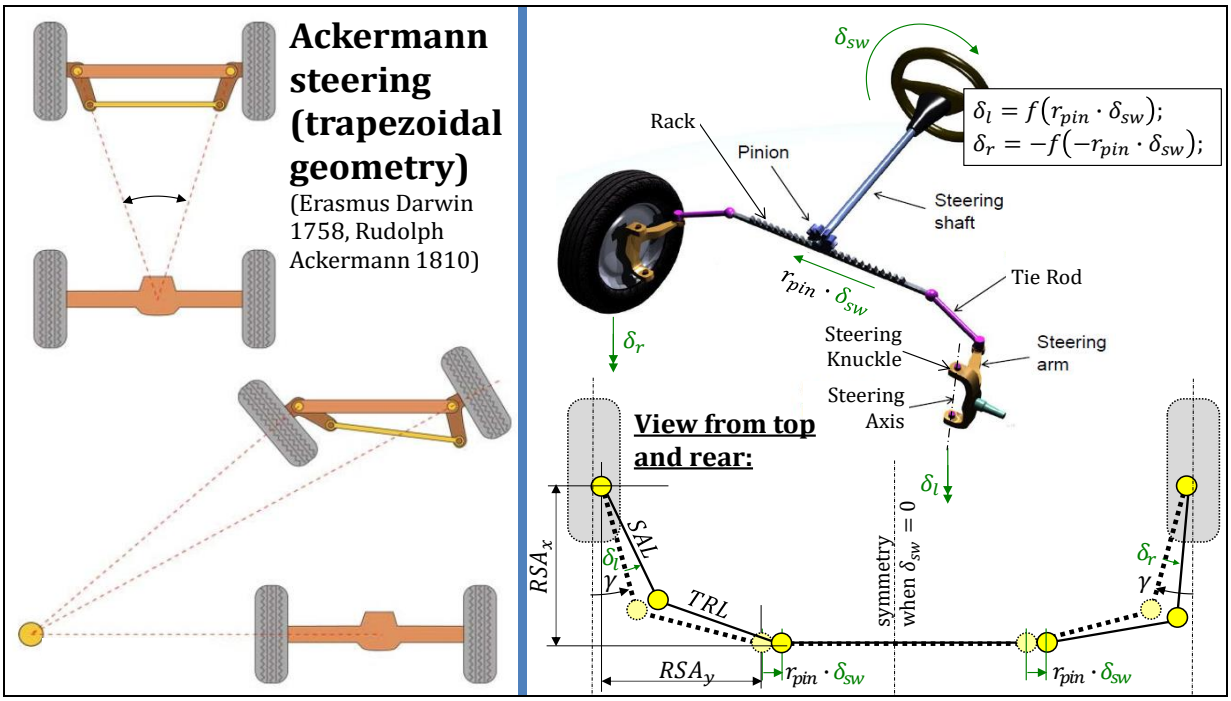

Figure 2-80: Left: Ackermann (Trapezoidal) Steering. Right: Rack Steering, common on passenger cars.

Eq [2.62] shows the relation between steering angles for rack steering, with TRL=Tie Rod Length, SAL=Steering Arm Length, RSA=Rack to Steering Axis lengths.

$$TRL^2 = (RSA_x - SAL \cdot \cos(\gamma + \delta_l))^2 + \left(RSA_y - SAL \cdot \sin(\gamma + \delta_l) + r_{pin} \cdot \delta_{sw}\right)^2;$$
$$TRL^2 = (RSA_x - SAL \cdot \cos(\gamma - \delta_r))^2 + (RSA_y - SAL \cdot \sin(\gamma - \delta_r) - r_{pin} \cdot \delta_{sw})^2; \quad [2.62]$$

The TRL determines a toe-in. To get $\delta_{\text{toe-in}}$, design (or adjust) the TRL to:

$$TRL = \sqrt{(RSA_x - SAL \cdot \cos(\gamma - \delta_{\text{toe-in}}))^2 + (RSA_y - SAL \cdot \sin(\gamma - \delta_{\text{toe-in}}))^2};.$$

2.6.2 Steering System Forces

(This section has large connection with 2.2.4.6Other Forces and Moments in Lateral.)

The steering wheel torque, T_{sw}, should basically be a function of the tyre/road forces, mainly the wheel-lateral forces. This gives the driver a haptic feedback of what state the vehicle is in. The torque/force transmission involves a servo actuator, which helps the driver to turn the steering system, typically that assists the steering wheel torque with a factor varying between 1 and 10, but less for small T_{sw} (highway driving) than large T_{sw} (parking), see Figure 2-81. Here, the variation in assistance is assumed to be hydraulic and follows a so-called boost curve. At $T_{sw} = 0$, the assistance is $\approx 0.45/0.55 \approx 1$ and for $T_{sw} = 4$ Nm, it is $\approx 0.9/0.1 \approx 10$.

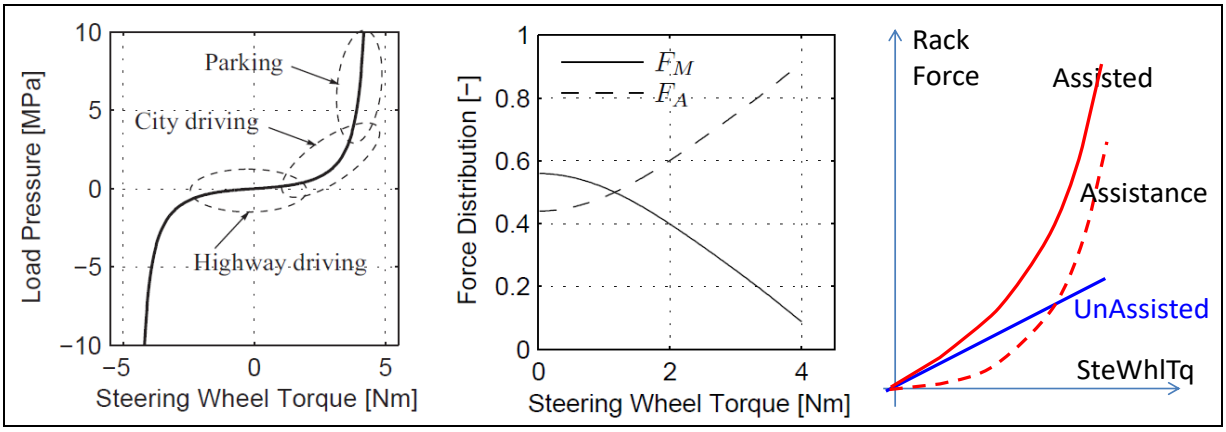

Figure 2-81: Left: Boost Curve with different working areas depending on the driving envelope. Middle: Torque distribution between manual torque, FM, and assisting torque, FA, depending on applied steering wheel torque. From Reference (Rösth, 2007). Right: Unassisted and assisted steering wheel torque.

2.7 Environment Sensing System

This subsystem has to be mentioned since it is maybe the most important new enabler for today's development of automated driving. The technology to sense (radar, camera, lidar, GPS, etc) is not typically part of vehicle dynamics, but many vehicle dynamics control functions can be invented or improved through usage of the information from the subsystem. Some typically available information is listed in 3.5.1 and 4.6.1. Another vehicle dynamics aspect is that some sensor fusion, but primarily some predictions, can be made using vehicle dynamics models.

2.8 Vehicle Aerodynamics

The flow of air around the vehicle body produces different external forces and moments acting on the vehicle. The fluid mechanics will not be covered in this course. However, practical first order models for aerodynamic forces have been established and are presented here.

2.8.1 Longitudinal Relative Wind Velocity

The most relevant aerodynamic force of interest in this course is the resistance force to forward motion, $F_{air,x}$, which is proportional to the square of the longitudinal component of the wind speed relative to the vehicle, $v_{x,rel}$. For aerodynamic loads resisting forward motion of the vehicle, the Equation [2.63] can be used. The parameters c_d, ρ and A_{front} represent the drag coefficient, the air density and a reference area of the vehicle, respectively. The A_{front} is the area of the vehicle projected on a vehicle transversal plane.

$$-F_{air,x} = \frac{1}{2} \cdot c_d \cdot \rho \cdot A_{front} \cdot {v_{x,rel}}^2; \qquad [2.63]$$

Typical values of drag coefficients (c_d) for cars can be found from sources such as: (Robert Bosch GmbH, 2004), (Barnard, 2010), (Hucho, 1998), and (Schuetz, 2015). These coefficients are derived from coast down tests, wind tunnel tests or CFD (Computational Fluid Dynamics) calculations. The air resistance can often be neglected for city speeds, but not at highway speeds.

Since a car structure moving through the air is not unlike an aircraft wing, there are also an aerodynamic lift force and pitch moment. This affects the vertical forces on front and rear axle, and consequently the tyre to road grip. Hence, it affects the lateral stability.

$$F_{air,z} = \frac{1}{2} \cdot c_l \cdot \rho \cdot A_{front} \cdot {v_{x,rel}}^2;$$
$$M_{air,y} = \frac{1}{2} \cdot c_{pm} \cdot L_c \cdot \rho \cdot A_{front} \cdot {v_{x,rel}}^2; \qquad [2.64]$$

The coefficient c_l represents the lift characteristics of the vehicle. For extreme vehicle, such as racing cars, one can achieve negative c_l, but often by sacrificing with higher c_d. The forces $F_{air,x}$ and $F_{air,z}$ are assumed to act through the same reference point, often centre of gravity (CoG), which defines $M_{air,y}$.

One can replace $[F_{air,x}, F_{air,z}, M_{air,y}]$ with equivalent $[F_{air,x}, F_{air,fz,CoG}, F_{air,rz,CoG}]$ or $[F_{air,x}, F_{air,fz}, F_{air,rz}]$, Figure 2-82 and Eq [2.65].

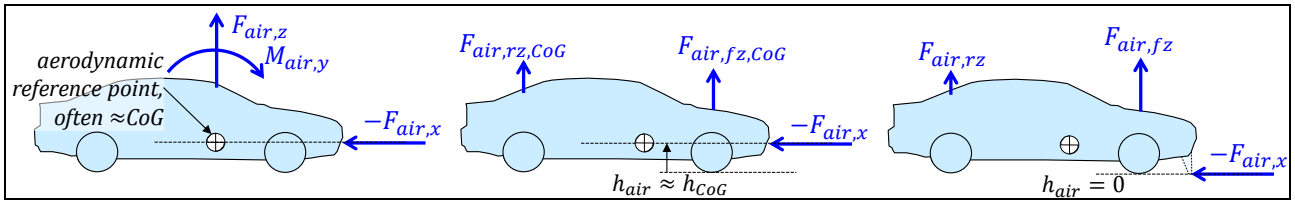

Figure 2-82: Force-equivalent ways to model longitudinal-wind aerodynamic forces in xz-plane. $F_{air,fz}$ and $F_{air,rz}$ differs between mid and right figure but $F_{air,x}$ is the same for all 3 figures.

$$F_{air,fz} = \frac{1}{2} \cdot c_{lf} \cdot \rho \cdot A_{front} \cdot {v_{x,rel}}^2;$$
$$F_{air,rz} = \frac{1}{2} \cdot c_{lr} \cdot \rho \cdot A_{front} \cdot {v_{x,rel}}^2;$$
For a reference height h_{air}, often CoG heigth. [2.65]

2.8.2 Lateral Relative Wind Velocity

When the wind comes from the side, there can be direct influences on the vehicle lateral dynamics. Especially sensitive are long but light vehicles (such as buses or vehicles with unloaded trailers). The problem can be emphasized by sudden winds (e.g. on bridges or exiting a forested area). Besides direct effects on the vehicle lateral motion, side-winds can also disturb the driver through disturbances in the steering wheel feel.

Similar expressions to the longitudinal loads are derived for lateral forces and from side-winds.

$$F_{air,y} = \frac{1}{2} \cdot c_s \cdot \rho \cdot A \cdot {v_{y,rel}}^2;$$
$$M_{air,z} = \frac{1}{2} \cdot c_{ym} \cdot \rho \cdot A \cdot L_c \cdot {v_{y,rel}}^2; \qquad [2.66]$$

The speed $v_{y,rel}$ is the lateral component of the vehicle velocity relative to the wind. Note that A and L_c may now have other interpretations and values than in Equations [2.63]-[2.65], e.g. A_{front} or A_{side}.

2.9 Driving and Transport Application

The driver drives and experiences the vehicle in the short time scale through pedals, steering wheel and seat. But the drivers'/users' choice of load (cargo weight and position) and choice of route is important on the longer time scale. One can differ between, Ref (Pettersson, 2019):

- ***Transport Application*** is how the vehicle is used by one user/owner during its lifetime. It can be commuting 2 × 15 km/day, 5 days/week (e.g. for passenger car) or loading and transporting timber on 10 km forest road + 300 km high way, twice per day (e.g. for a truck).
- ***Transport Operation*** is how the vehicle is used along a specific route. It is typically 10 min to 10 h driving. Driving Cycles, $v(t)$, mentioned in 3.3.1.1 have the purpose to describe approximately the same.
- ***Transport Mission*** is the purpose of one Transport Operation, such as where to stop and load/unload a certain payload.

2.9.1 Mission, Road and Traffic

This section is kept very short, but it is included for completeness, beside 2.9.2. See more in 3.3.1.

2.9.2 Driver

To study how different vehicle designs work in a vehicle operation a driver model is needed. In its easiest form, a driver model can be steering wheel angle $\delta_{stw} \equiv 0$;. Another extreme interpretation of what can be called a driver model is an implicit/inverse statement, like "driver will push accelerator pedal so that speed $v_x \equiv 20\ [m/s]$ during the manouvre", which leads to that accelerator pedal position becomes an output, as opposed to input, to the vehicle model. Beyond those very simple driver models, there is often need for a driver model which react on vehicle states **in relation to an environment or traffic**. In this section, driver models are primarily thought of as models of the driver of the subject vehicle, but when modelling surrounding traffic carefully, each object vehicle can also use a driver model.

The driver interacts with the vehicle mainly through steering wheel, accelerator pedal and brake pedal. In addition to these, there are clutch pedal, gear stick/gear selector, and various buttons, etc., see Figure 2-83, but we focus here on the first 3 mentioned.

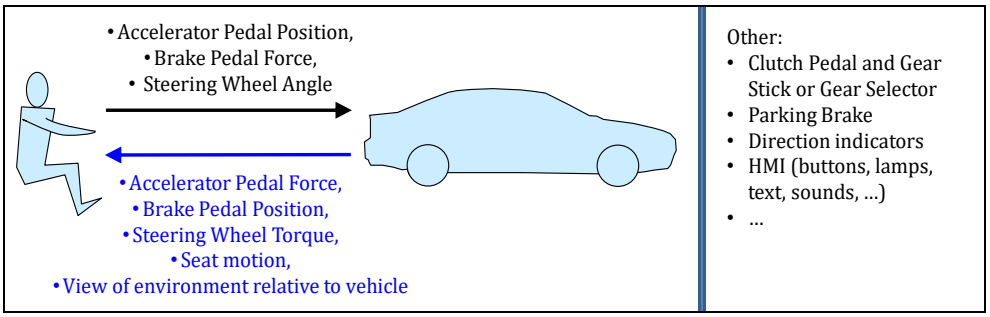

Figure 2-83: Interface of driver, and some commonly assumed causality.

Driver's control of vehicle dynamics, or vehicle motion including position, can be discussed in longitudinal (mainly pedals) and lateral (mainly steering wheel).

Driver reacts on several stimuli, such as motion (mainly through seat), sounds, and optical. Among motion, it is primarily the accelerations (and their time derivative, jerk) that is sensed by the driver, but also rotational velocity in yaw can be sensed by human. Among the optical there is looming (optical expansion of an object in the driver's field of view $[deg/s]$) is often used as a cause for how driver uses the pedals. The optical flow (the pattern of apparent motion of objects, surfaces, and edges in the driver's field of view) is often used as a cause for highest comfortable speed and yaw velocity.

Driver models are here discussed as models of the "human driver" for use in vehicle verification simulations. However, driver models can also be understood as models of "virtual driver", and then they are actually implemented as algorithms in the vehicle product, e.g. as prediction algorithms or automated driving controllers. In the first context, it is often important to vary the driver model (at least its parameters, maybe even its equations) for robustness, as mentioned in Figure 1-3. In the latter context, the driver model of the subject vehicle is rather varied for optimization/satisficing, see Figure 1-3 again.

An important aspect of driver modelling is how the user (driver or occupant) **experiences** the vehicle. This is often referred to as subjective evaluation, but for some cases one can establish methods to objectively calculate a measure of how good or bad the experience is. The measure can sometimes be a physical quantity but often it has to be a rating or grading without unit. Examples are "driveability [rating 0-10, high is good]", "steering effort [deg/s, low is good]" and "ride comfort [m/s^2, low is good]".

2.9.2.1 Driver Modelling

As in all modelling, it is important to model, or select model, after what the model should be used for. Driver modelling for "**verification of vehicle functions**" and for implementation in "**driving automation functions**" are similar in that they should react on the vehicle's environment, but there are also differences. Driver models for verification of vehicle functions should be as human-like as possible. They should also judge feedback to driver, such as assessing steering effort. Driver models for use in driving automation functions should also be human-like to facilitate cooperation between human and automated driving, such as hand-over/take-back or simultaneous control. However, there are also reasons to not mimic all aspects from a human driver, such as the human's inability to watch in several directions simultaneously.

A categorization of modelling concept is whether the model uses equations that reflect the **biological** processes human's perception, cognition and neuro-muscular or equations from a **vehicle model**. The first concept (exemplified in 2.9.2.3.3) would rather use angle to obstacle as opposed to distance to obstacle, since humans rather see angles than distances. The latter concept (exemplified in 2.9.2.2.1) assumes that driver has adapted to the specific vehicle and (subconsciously) operates the vehicle in a good way; a kind of inverse model thinking. Overall, both concepts can reflect approximately the same driving, but they are differently parameterized; typically, in biological parameters and vehicle parameters, respectively.

Driver can be modelled in 2 parts: Strategic and Operative. A division in Longitudinal and Lateral is also relevant. One can think of different ways of arranging these dimensions on each other; one possible way is shown in Figure text.

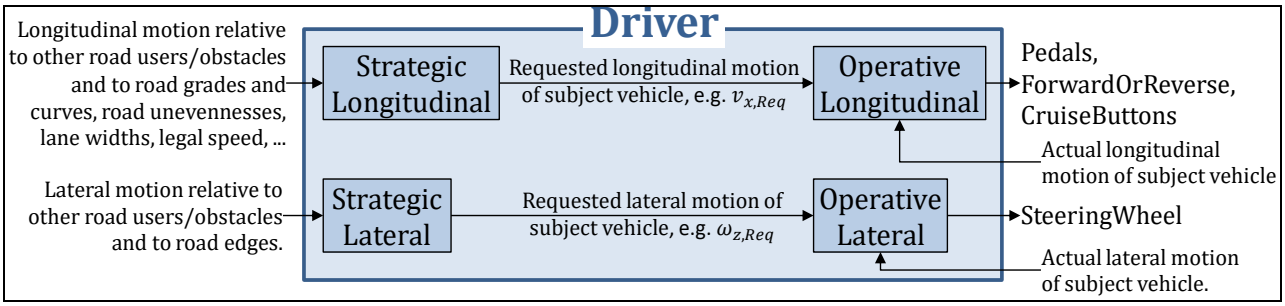

Figure 2-84: One possible arrangement of Strategic vs Operative and Longitudinal and Lateral.

3 LONGITUDINAL DYNAMICS

3.1 Introduction

The primary purpose of a vehicle is transportation, which requires longitudinal dynamics. The chapter is organised with one group of functions in each section as follows:

- 3.2 Steady State Function
- 3.3 Functions Over (Long)
- 3.4 Functions in (Short) Events
- 3.5 Control Functions

3.1.1 References for This Chapter

- 2.4 Propulsion System and *"Chapter 23. Driveline"* in Ref (Ploechl, 2013)
- 2.5 (Wheel) Braking System *"Chapter 24. Brake System Dynamics"* in Ref (Ploechl, 2013)
- *"Chapter 27 Basics of Longitudinal and Lateral Vehicle Dynamics"* in Ref (Ploechl, 2013)
- *"Chapter 6: Adaptive Cruise Control"* in Ref (Rajamani, 2012)

3.2 Steady State Functions

Functions as top speed and grade-ability are relevant without defining a certain time period. For such functions, it is suitable to observe the vehicle in steady state, i.e. independent of time. Those functions are therefore called steady state functions, in this compendium. The main subsystems that influences here are the propulsion system, see 2.4, and the (Friction) Brake system, see 2.5.

3.2.1 Traction Diagram

The force generated in the prime mover is transmitted through a mechanical transmission to the wheel which then generates the propulsive forces in the contact patch between tyre and road. In an electric in-wheel motor, the transmission can be as simple as a single-step gear. In a conventional vehicle, it is a stepped transmission with several gear ratios (i.e. a gearbox). Then, the drivetrain can be drawn as in Figure 3-1. The torque and rotational speed of the engine is transformed into force and velocity curves via the mechanical drivetrain and driven wheel. The result is a Traction diagram. The transformation follows the following formula, if losses are neglected:

$$F = ratio \cdot \frac{T}{WheelRadius}; \quad and \quad v = WheelRadius \cdot \frac{\omega}{ratio}; \qquad [3.1]$$

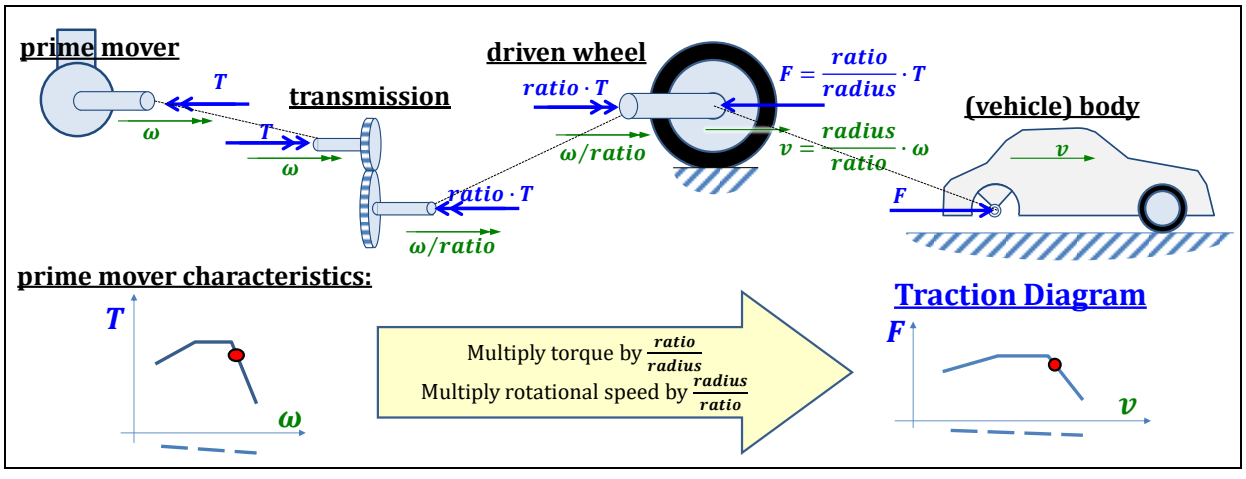

Figure 3-1: Construction of Traction Diagram.

A traction diagram for a truck is given in Figure 3-2, which also shows that there will be one curve for each gear.

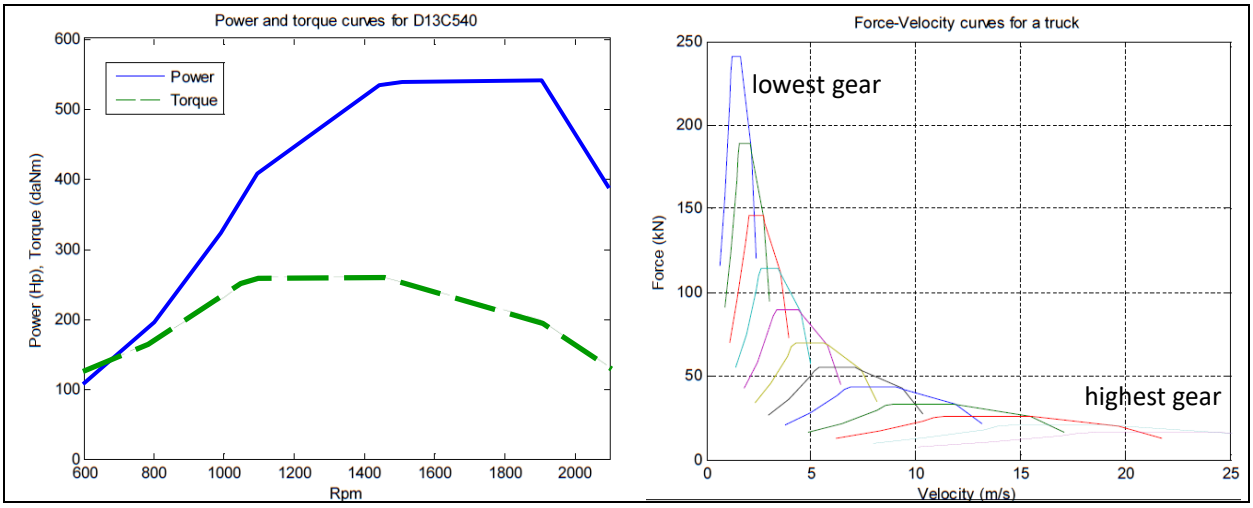

Figure 3-2: Example of engine map and corresponding traction diagram map from a truck. (D13C540 is an I6 diesel engine of 12.8-litre and 540 hp for heavy trucks.)

Losses in transmission can be included by loss models for transmission, such as:

$$F = \eta_T \cdot ratio \cdot \frac{T}{radius};\ where\ \eta_T \leq 1;$$
$$v = \eta_\omega \cdot radius \cdot \frac{\omega}{ratio};\ where\ \eta_\omega \leq 1;$$
$$where \quad \eta_T \cdot \eta_\omega = \eta_{total} = \frac{P_{vehicle}}{P_{engine}} = \frac{F \cdot v}{T \cdot \omega} \leq 1; \qquad [3.2]$$

This will move the curves in the first quadrant downwards due to $\eta_T < 1$ and to the left due to $\eta_\omega < 1$. Tyre rolling friction is a torque loss mechanism, which on its own yields $\eta_\omega = 1$ and $\eta_T < 1$. Tyre longitudinal slip is a speed loss mechanism, which on its own yields $\eta_\omega < 1$ and $\eta_T = 1$. See 2.2.1.6. The multiplication with η is only demonstrative and should be seen more generic: in many cases the losses are additional instead of multiplicative, e.g. for rolling resistance: $F = ratio \cdot (T - \Delta T)/radius = ratio \cdot (T - f \cdot F_z)/radius$;. Which wheels' F_z to use is discussed in 3.2.2.

A traction diagram is a kind of "one degree of freedom graphical model". The traction diagram is on complete vehicle level, so the force axis represents the sum of forces from all wheels. This can include more than one propulsion system and also brakes.

3.2.2 Power and Energy Losses

There are power losses P_{loss} (and energy losses $E_{loss} = \int P_{loss} \cdot dt$) which causes an energy consumption E_{cons} for a transport operation. If the operation starts and stops at same speed (often zero) and same altitude, $E_{cons} = E_{loss}$. And $E_{loss} = \sum E_{lossi} = \sum(\int P_{loss} \cdot dt) = \int(\sum P_{lossi}) \cdot dt = \int P_{loss} \cdot dt$ where i denotes different losses. One can count the energy consumption per distance $EPD = E_{cons}/x = (\int P_{loss} \cdot dt)/\int v_x \cdot dt\ \ [J/m = Nm/m = N]$. The EPD can be seen as a time-averaged resistance force, summed over all "parts", $\forall i$, where there are losses. If the operation has same character (hilliness, speed, etc) lover a long distance, $\sum EPD_i \rightarrow EPD$ when $x \rightarrow \infty$ and $t \rightarrow \infty$. See also 3.3.4.1.

3.2.2.1 Driving Resistance Force

Some losses can be identified as true forces, visible directly in a free body diagram, i.e. we don't need to go via a "Energy loss per distance, EPD". Such are forces from gravity due to road grade and aerodynamic resistance.

Another way to approach this is to study Figure 3-2 and extrapolate that a very low transmission ratio, i.e., a very high gear, we would enable infinite speed, which of course is not realistic. This is because

"driving resistance force" is missing in Figure 3-2. Such force can be added to traction diagram as a curve that typically increases with speed. The top speed is found as the intersection between propulsion curve and driving resistance force curve, see Figure 3-3.

One part of the driving resistance force comes from driving uphill: the grade or gravitational load on the vehicle. This is negative when driving down-hill. There is also aerodynamic driving resistance force, see Eq [2.63]. Grade and aero-dynamic resistance are (vehicle) **body forces**.

Also rolling resistance is, often, counted as a resistance force. However, it is **not** a body force, but instead it acts as a torque on the wheel, not a longitudinal force, on each wheel i: $F_{ix} = T_i - f \cdot F_{iz}$;. But for a non-driven wheel, the rotational equilibrium of the wheel leads to a small negative longitudinal force in tyre-to-road contact. So, rolling resistance can be included in traction diagram in either the "supply" or resistance curve. If one want to use the traction diagram to show the friction limit where a wheel start to spin, $F_{ix} > \mu \cdot F_{iz}$ as in 3.2.6, it can be suitable to include rolling resistance in supply curve for that wheel, but in the resistance curve for the other wheels. In the following, rolling resistance is represented as a torque on driven wheels (which lowers the supply curve) and a longitudinal force on non-driven wheels (which lifts the resistance curve). The traction diagram can then also host a curve for friction limit for spinning driven wheels, as in Figure 3-8.

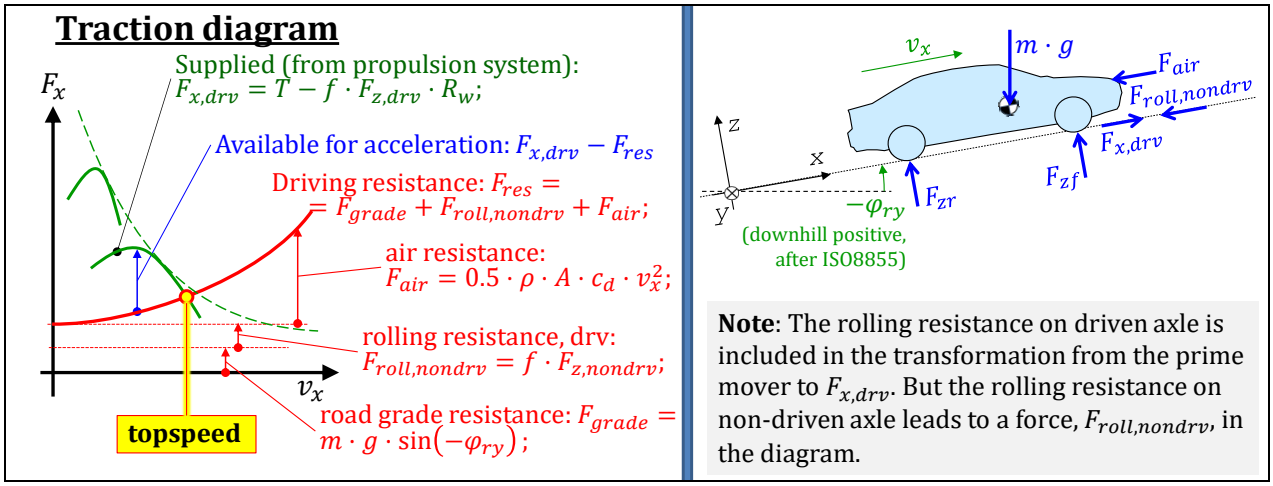

Figure 3-3: Traction diagram. Head wind speed, $v_{wind,x}$, is assumed to be zero. See also Figure 3-8.

$$F_{res} = F_{roll} + m \cdot g \cdot \sin(-\varphi_y) + \frac{1}{2} \cdot c_d \cdot \rho \cdot A \cdot (v_x - v_{wind,x})^2;$$

$$F_{roll} = \sum_{\text{non-driven wheels}} f \cdot F_{wheel,z};$$

$$if\ all\ wheels\ are\ undriven: F_{roll} = f \cdot m \cdot g \cdot \cos(\varphi_y);$$

[3.3]

As seen in Figure 3-3, the supply and resistance curves are drawn in same diagram. The resulting intersection identifies the top speed of the vehicle. This is a stable point in the diagram, so the vehicle condition at top speed is for steady state (no acceleration).

Figure 3-3 also shows that the acceleration can be identified as a vertical measure in the traction diagram, divided by the mass. However, one should be careful when using the traction diagram for more than steady state driving. We will come back to acceleration performance later, after introducing the two effects "Load transfer" and "Rotating inertia effect".

3.2.2.2 Losses due to Longitudinal Tyre Slip

Consider a vehicle with $N \geq 3$ wheels. Assume a certain vehicle speed v_x and a certain desired propulsion force $F_x = \sum_{i=1..N}(T_i/R_w)$. Also assume that wheel torques T_i can be distributed according to $N - 1$ equations, e.g. $T_1 = T_2; T_3 = T_4 = 0$; for a conventional front axle driven 4 wheeled car. Also assume same longitudinal stiffness coefficient CC_x on all wheels and that out-of-road-plane equilibria and suspension equations defines the vertical forces $F_{1z}..F_{Nz}$. The, the power loss due to longitudinal tyre slip can be calculated as:

$$P_{loss} = \sum_{i=1:N} \left(T_i \cdot (R \cdot \omega_i - v_x)\right) = \sum_{i=1:N} (T_i \cdot s_{ix} \cdot |R \cdot \omega_i|) = \sum_{i=1:N} \left(\frac{F_{ix}}{R} \cdot \frac{F_{ix}}{C_{ix}} \cdot |R \cdot \omega_i|\right) =$$
$$= \frac{1}{R} \cdot \sum_{i=1:N} \left(\frac{F_{ix}^2}{CC_{ix} \cdot F_{iz}} \cdot |R \cdot \omega_i|\right) \approx \frac{v_x}{R \cdot CC_{ix}} \cdot \sum_{i=1:N} \frac{F_{ix}^2}{F_{iz}};$$

An example with a fore-aft-symmetric 2-axle vehicle, propelled on one axle gives:

$$P_{loss} \approx \frac{v_x}{R \cdot CC_{ix}} \cdot \left(\frac{0^2}{m \cdot g/2} + \frac{F_x^2}{m \cdot g/2}\right) = \frac{2 \cdot v_x \cdot F_x^2}{R \cdot CC_{ix} \cdot m \cdot g};$$

The same vehicle, but propelled equally much on both axles gives:

$$P_{loss} \approx \frac{v_x}{R \cdot CC_{ix}} \cdot \left(\frac{(F_x/2)^2}{m \cdot g/2} + \frac{(F_x/2)^2}{m \cdot g/2}\right) = \frac{v_x \cdot F_x^2}{R \cdot CC_{ix} \cdot m \cdot g};$$

So, twice as much energy is lost due to longitudinal tyre slip if propelling on 1 instead of 2 axles.

When negative wheel torque, one can brake with friction brakes and then there is no energy loss. However, if braking with electric propulsion, the loss can be negative, meaning that energy is regenerated to electric energy storage. If braking so much with electric propulsion that wheel rotates rearwards, there would again be an energy loss, $P_{loss} = T_i \cdot \omega_i = negative \cdot negative > 0$.

3.2.2.3 Losses due to Lateral Tyre Slip

(This section might require some studying of Chapter 4 for full understanding.)

There are more driving-resistance effects than covered in Equation [3.3]. One example is that none-Ackermann steering geometry (toe or parallel steering on an axle, or two non-steered axles).

Another effect, which appears also for Ackermann steering geometry, is that power is lost due to lateral axle slip. Now, we use the same simple model as in Figure 4-18, but additionally use $a_y = v_x/\omega_z$; and define power losses P_{loss} as sliding velocity counterdirected to force:

$P_{loss} = -F_{fy} \cdot v_{fy} - F_{ry} \cdot v_{ry} = -F_{fy} \cdot s_{fy} \cdot v_x - F_{ry} \cdot s_{ry} \cdot v_x;$.

We also define a Cornering Resistance Coefficient, CRC:

$$CRC = \frac{P_{loss}/v_x}{m \cdot g} = \frac{m \cdot a_y^2}{g} \cdot \left(\left(\frac{l_f}{L}\right)^2 \cdot \frac{1}{C_r} + \left(\frac{l_r}{L}\right)^2 \cdot \frac{1}{C_f}\right) \approx \frac{1}{CC_y} \cdot \left(\frac{a_y}{g}\right)^2; \qquad [3.4]$$

CRC is such that the additional propulsion force due to cornering is $\approx CRC \cdot m \cdot g$ or the additional power is $\approx CRC \cdot m \cdot g \cdot v_x$. During a transport operation, the cornering in each time instant is typically described by two variables, e.g. (v_x, R_p), but only the combined scalar measure $a_y = v_x^2/R_p$ influences CRC. Hence, we can plot the following graph:

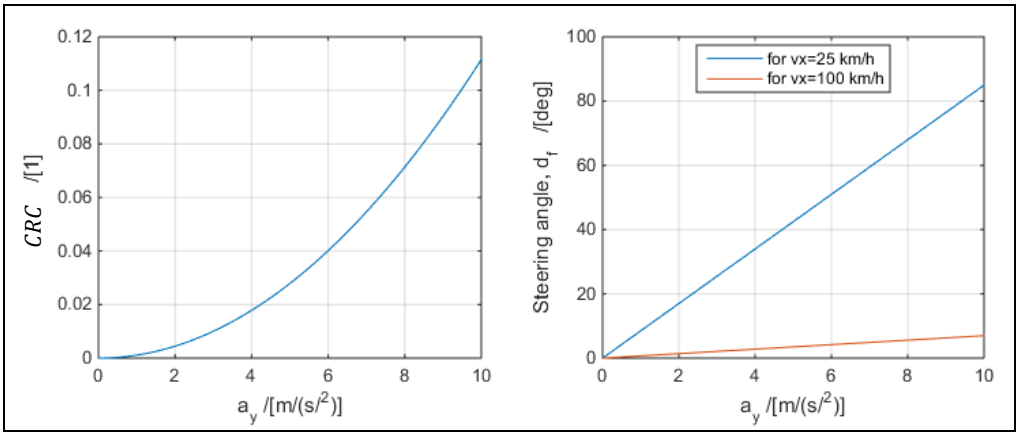

Figure 3-4: Left: Cornering Resistance Coefficient. Right: Required steer angle. Vehicle data: $m = 1500\ kg$; $L = 3$; $l_f = 1.25$; $C_f = 60\ [kN/1]$; $C_r = 80\ [kN/1]$.

Notes:

- The model used above is not advanced enough to differ between which axle is driven. For such purpose, one would need e.g. the model in Figure 4-15.
- Normal driving is often below 2 or 3 m/s^2, so the coefficient typically stays below 0.01. So, the influence on energy consumption, during such "maximum normal" negotiation of corners, is still of the same magnitude as rolling resistance coefficient $RRC \approx 0.005..0.010$.
- For ideally tracking axles, see 2.2.6, $C_f \to \infty$ and $C_r \to \infty$, which gives that $f_{CRC} \to 0$ and consequently no power loss and no required propulsion force. Therefore, high cornering stiffness is fuel efficient when cornering.
- When driving extreme cornering, such as driving as fast as possible in a circle on a test-track, one will experience that the top speed is much lower than driving straight ahead. That is NOT explained by [3.4]. It would require inclusion of a combined tyre slip model.

3.2.3 Functions After Start

Figure 3-5 shows how the functions can be found in a traction diagram.

3.2.3.1 Top Speed *

*Function definition: **Top speed** is the maximum longitudinal forward speed the vehicle can reach and maintain on level and rigid ground without head-wind.*

Top speed is the speed where the sum of all driving resistance terms is equal to the available propulsion forces.

3.2.3.2 Grade-ability *

*Function definition: **Grade-ability** is the maximum grade that a vehicle is capable to maintain the forward motion on an uphill road at a certain constant speed, at a certain road friction level and with a certain load. (from Reference (Kati, 2013))*

For vehicles with high installed propulsion power per weight, the road friction can be limiting, but this is not visualised in Figure 3-5. Since the speeds are higher than for start-ability, the air resistance cannot be neglected.

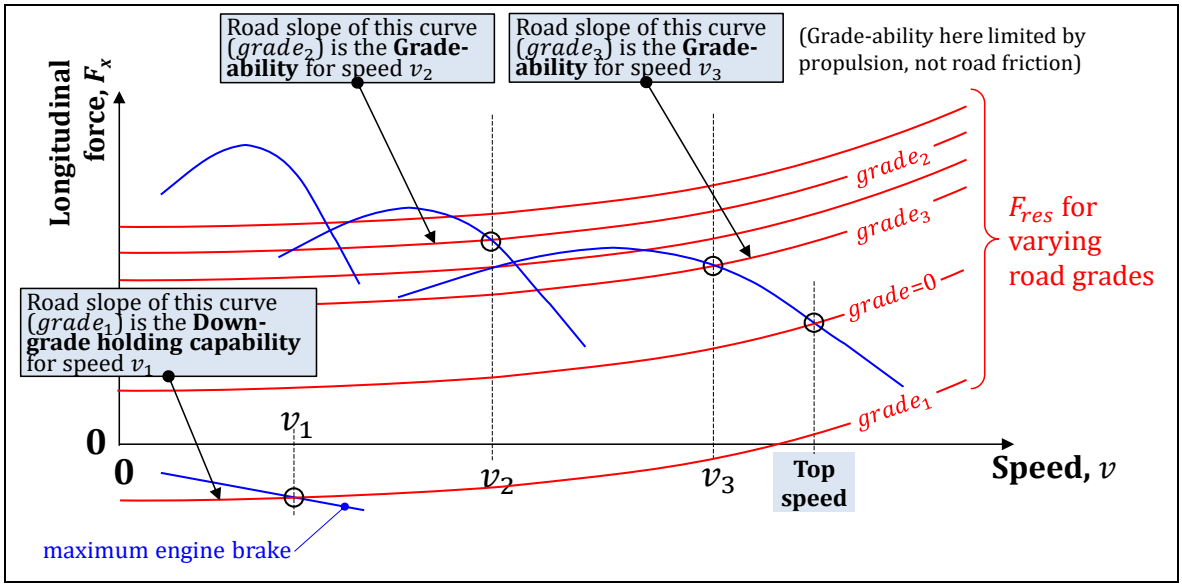

Figure 3-5: How Top speed, Grade-ability and Down grade holding capability is read-out from Traction diagram.

3.2.3.3 Down-grade Holding Capability *

*Function definition: **Down-grade holding capability** is defined as the maximum down-grade in which the vehicle with certain weight is able to maintain a certain speed without using friction brakes.*

The function is typically of interest for heavy trucks and certain typical certain weight and certain speed is payload corresponding to maximum allowed weight and 80 km/h downhill.

The function is defined assuming there are clear friction brakes and other brakes, where the other brakes are typically engine brake and retarders. For newer vehicle concepts having electric propulsion, also regenerative braking via reversed electric propulsion motors can be discussed to be allowed. However, because sometimes the energy storage will be full so that regenerative braking cannot be applied. Also, a small energy storage will have a limited downhill length, which might call for also prescribing a certain downhill distance.

3.2.4 Starting with Slipping Clutch

As seen in previous traction diagrams, there is no available positive propulsion force at zero speed. This means that the diagram can still not explain how we can start a vehicle from stand-still.

The concepts in Figure 3-1 were used to create the force-velocity diagram in

Figure 3-6. It shows the smooth curve of a Continuously Variable (ratio) Transmission (CVT) in comparison to the stepped transmission. The CVT is the ideal situation for the engine since it can always let the engine work at a maximum power or minimum fuel consumption (minimum for the momentarily required power). If the CVT has unlimited high ratio, it can actually have a non-zero propulsion force at zero vehicle speed. Without losses, this force would be infinite, but in reality, it is limited, but still positive, so the vehicle can start from stand-still.

A stepped transmission, as well as a CVT with limited ratio range, instead needs a clutch to enable starting from vehicle stand-still. This is shown in Figure 3-6. The highest force level on each curve can be reached at all lower vehicle speeds, because the clutch can slip. It requires the clutch to be engaged carefully to the torque level just below the maximum the engine can produce. In traditional automatic transmissions, the slipping clutch is replaced with a hydrodynamic torque converter, to enable start from stand-still.

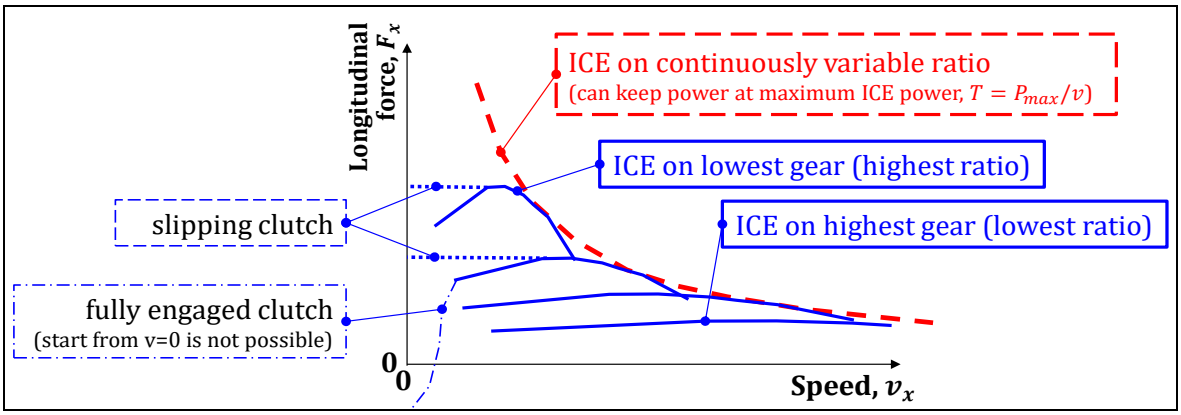

Figure 3-6: Force/Speed Curves for a Multiple Gear Transmission and for CVT.

3.2.5 Steady State Vertical Force Distribution between Axles

The vehicle performance discussed previously does not rely on knowing the distribution of (vertical) load between the axles. To be able to introduce limitations due to road friction, this distribution must be known. Hence, we set up the free-body diagram in Figure 3-7.

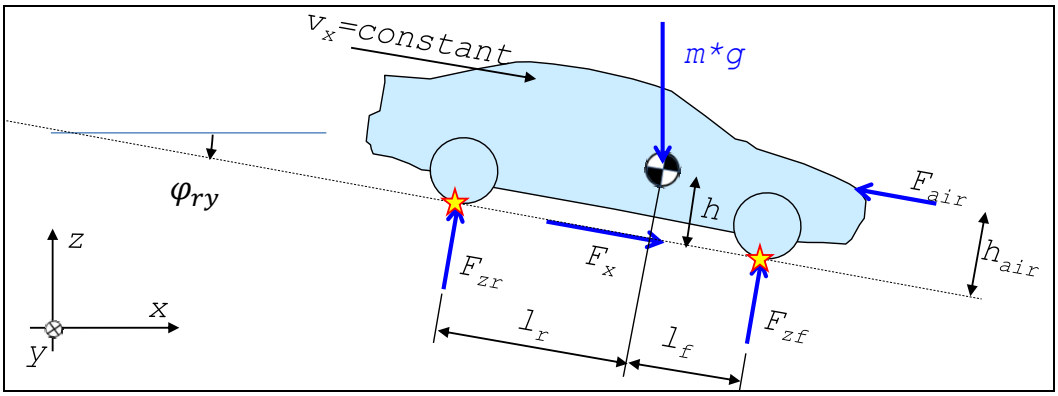

Figure 3-7: Free Body Diagram for steady state vehicle. With ISO coordinate system, the road gradient is positive when downhill. (Rolling resistance force on non-driven axles is included in F_x.)

From the free-body diagram we can set up the equilibrium equations as follows and derive the formula for load on front and rear axle:

Moment equilibrium, around rear contact with ground (✯):

$$m \cdot g \cdot \left(l_r \cdot \cos(\varphi_{ry}) + h \cdot \sin(\varphi_{ry})\right) - F_{air} \cdot h_{air} - F_{zf} \cdot \left(l_f + l_r\right) = 0; \Rightarrow$$

$$\Rightarrow F_{zf} = m \cdot g \cdot \frac{l_r \cdot \cos(\varphi_{ry}) + h \cdot \sin(\varphi_{ry})}{l_f + l_r} - F_{air} \cdot \frac{h_{air}}{l_f + l_r}$$

Moment equilibrium, around front contact with ground (✯):

$$F_{zr} \cdot \left(l_f + l_r\right) - m \cdot g \cdot \left(l_f \cdot \cos(\varphi_{ry}) - h \cdot \sin(\varphi_{ry})\right) - F_{air} \cdot h_{air} = 0; \Rightarrow$$

$$\Rightarrow F_{zr} = m \cdot g \cdot \frac{l_f \cdot \cos(\varphi_{ry}) - h \cdot \sin(\varphi_{ry})}{l_f + l_r} + F_{air} \cdot \frac{h_{air}}{l_f + l_r}$$

[3.5]

For most vehicles and reasonable gradients, one can neglect $h \cdot \sin(\varphi_{ry})$ since it is $\ll \left|l_f \cdot \cos(\varphi_{ry})\right| \approx \left|l_r \cdot \cos(\varphi_{ry})\right|$.

3.2.6 Friction Limit

With a high-powered propulsion system, there is a limitation to how much the vehicle can be propelled, due to the road friction limit. It is the normal load and coefficient of friction, which limits this. For a vehicle which is driven only on one axle, it is only the normal load on the driven axle, $F_{z,driven}$, that is the limiting factor:

$$F_x = \min\left(F_{x,PropSyst}\ ;\ \mu \cdot F_{z,driven}\right) \qquad [3.6]$$

One realises, from Figure 2-15, that the rolling resistance on the driven axle works as a torque loss and that the road friction limitation will be limiting $T_{eng} \cdot ratio - e \cdot F_{z,driven}$ rather than limiting $T_{eng} \cdot ratio$. Expressed using the rolling resistance coefficient, f_{roll}, gives:

$$F_x = \min\left(F_{x,PropSyst}\ ;\ \mu \cdot F_{z,driven}\right) = \min\left(\frac{T_{eng} \cdot ratio}{radius} - f_{roll} \cdot F_{z,driven}\ ;\ \mu \cdot F_{z,driven}\right) \qquad [3.7]$$

This is shown in the traction diagram in Figure 3-8, where it should also be noted that the rolling resistance curve only consists of the rolling resistance on the non-driven axles. See also Figure 2-15.

3.2.7 Start Functions

3.2.7.1 Start-ability *

*Function definition: **Start-ability** is the maximum grade that a vehicle is capable to start in and maintain the forward motion at a certain road friction level and a certain load. (Reference (Kati, 2013))*

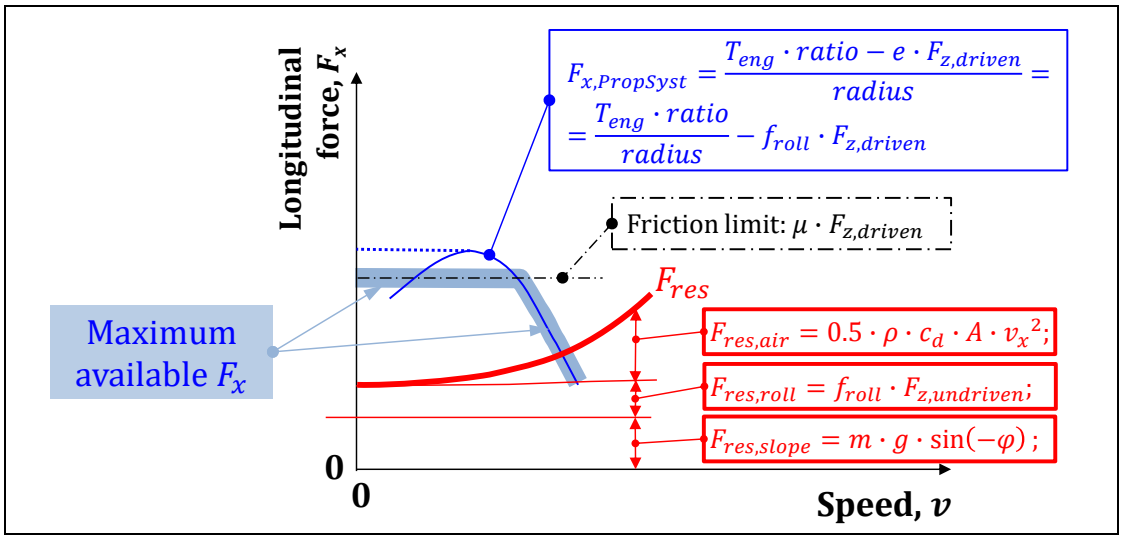

Figure 3-8: Traction diagram with Road Friction limitation and Driving Resistance curves.

Figure 3-9 shows how we find the start-ability in the traction diagram. There are two phenomena that can limit start-ability: propulsion system or road friction. Also, in each case, we can theoretically reach somewhat higher start-ability by allowing clutch or tyre to slip. However, in practice the start-ability has to require "forward motion without significant slip in clutch or tyre", because there will be a lot of wear and heat in the slipping clutch or tyre. Hence, the lower curves in Figure 3-9 are used. The reduction is however very small, since the resistance curves does not change very much in this speed interval (the resistance curves in the figure have exaggerated slope; the air resistance can typically be neglected for start-ability).

However, the energy loss (heat, wear) in clutch and tyre should be limited also **during the starting sequence**. This can limit the start-ability more severely than the slope of the resistance curves, but it cannot be shown in the traction diagram, since it is limited by energy losses in clutch or tyre, which is a time integral of $T \cdot \omega_{clutch}$ and $T_{wheel} \cdot \omega_{wheel}$. There can also be quite other limitations of start-ability, such as deliberately limited engine torque at low gears, to save drive shafts.

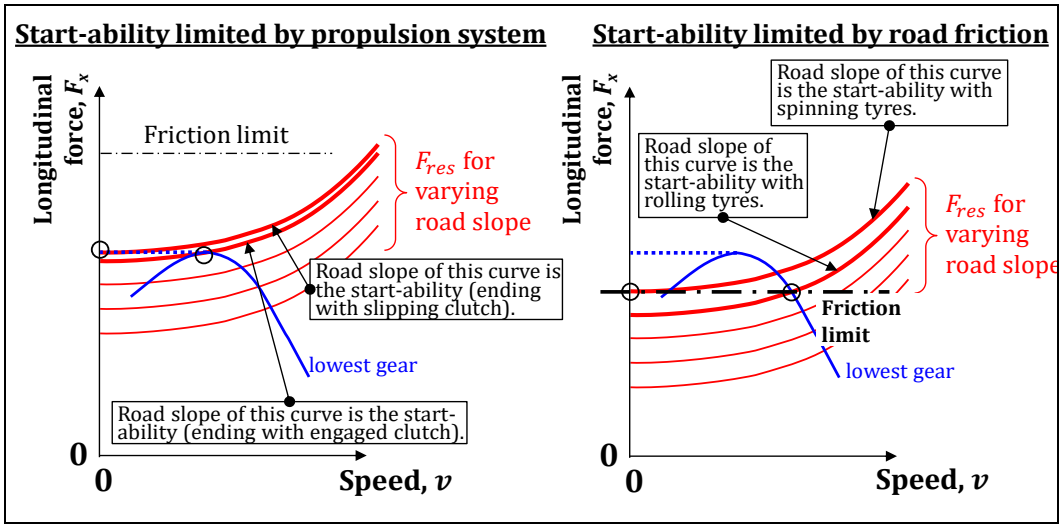

Figure 3-9: How Start-ability is read-out from Traction diagram.

3.2.7.2 Towing Capacity *

*Function definition: **Towing capacity** is the maximum vehicle-external longitudinal force the vehicle can have on its body and start and maintain a certain forward speed at a certain road friction and a certain up-hill gradient.*

The driving situation for defining towing capacity is similar to the one for defining grade-ability. Towing capacity describes how much load the vehicle can tow, P_x in Figure 3-10, on a certain up-hill gradient. Since towing a load is more relevant as part of a longer transport mission, it is normally also for a

particular constant speed, typically in range 80 to 100 km/h. Since the speed is that large, the air resistance may not be neglected. It is also important consider air resistance of the trailer and that axle loads can change, which changes both friction limitation and rolling resistance. A free-body diagram is shown in Figure 3-10. It is noticeable, that there can also be an additional air resistance of the trailer which will influence in a test of Towing capacity.

For pure off-road vehicles and agriculture tractors, the term "towing" can mean the maximum pulling force at very low forward speeds at level ground. This is related but different to the above described towing capacity for road vehicles.

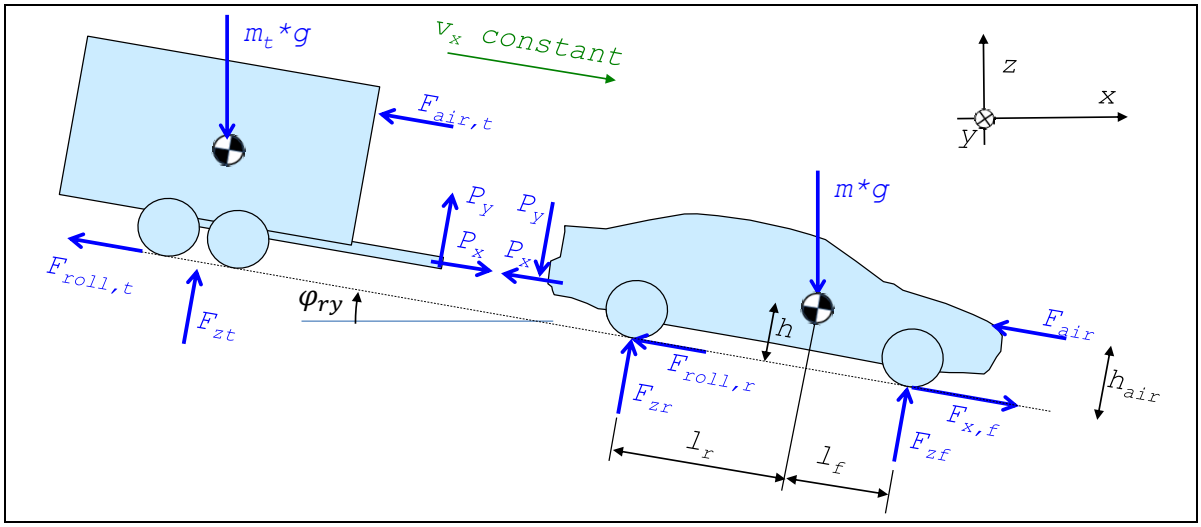

Figure 3-10: Towing Loads. The towing vehicle is front axle driven.

3.3 Functions Over (Long) Cycles

Functions as fuel or energy consumption and emissions are relevant only over longer periods of driving, typically some minutes to hours of driving. A collective name for this kind of driving can be cycles. There are different ways of defining such cycles.

3.3.1 Description Formats of Vehicle Operation

This section is about how to describe "all except the vehicle", e.g. road, traffic, driver and payload. The overall idea is to model the vehicle operation as *independent of the vehicle*, so that different vehicles, or different designs or configurations of a certain vehicle, can be compared in a fair way.

3.3.1.1 (Traditional) Driving Cycles

One way to model vehicle operation is a so-called driving cycle; where the relevant variables are prescribed as function of time. At least on defines speed as a function of time. Examples of commonly used driving cycles are given in Figure 3-11 to Figure 3-12. In addition, it can also be relevant to give road inclination as function of time. Engine temperature and selected gear as functions of time may also be defined. For hybrid vehicles, the possibility to regenerate energy via electric machines is limited in curves, so curvature radius can also be prescribed as function of time. For heavy vehicles, the weight of transported goods can be another important measure to prescribe.

FTP and HFTP are examples of cycles derived from logging actual driving, mainly used in North America. NEDC is an example of a "synthetically compiled" cycle, mainly used in Europe. Worldwide harmonized Light duty driving Test Cycle (WLTC) is a work with intention to be used world-wide, see Figure 3-14. WLTC exists in different variants for differently powered vehicle [power/weight].

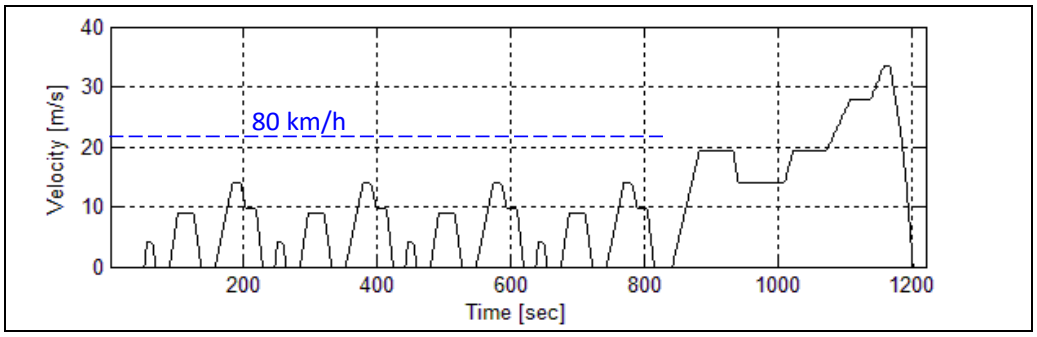

Figure 3-11: New European Driving Cycle (NEDC). From (Boerboom, 2012)

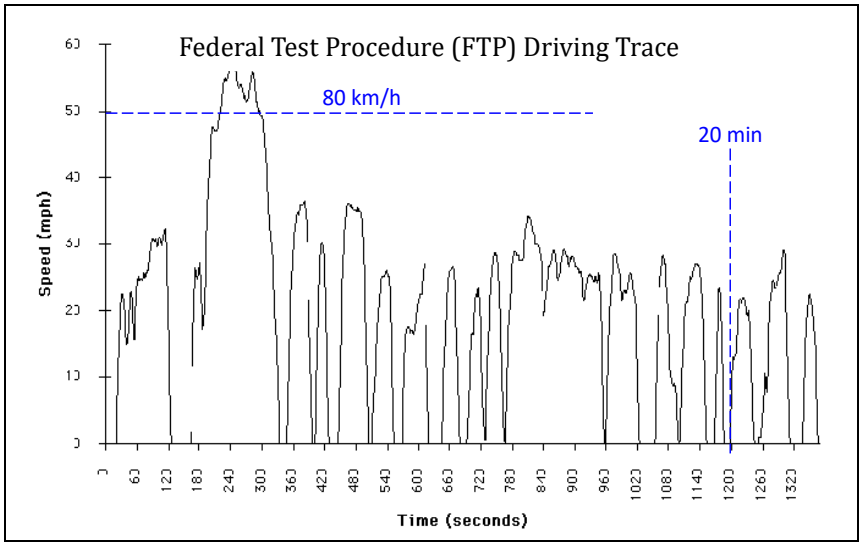

Figure 3-12: FTP cycle from http://www.epa.gov/oms/regs/ld-hwy/ftp-rev/ftp-tech.pdf

3.3.1.2 Driving Pattern

A driving cycle can be condensed into a Driving pattern, i.e. a 2-dimensional function of speed and acceleration, as shown in Figure 3-15. Note that the chronological order is no longer represented in such representation; it is not a dynamic model. Figure 3-15 shows simply a scatter plot of time-sampled combinations of speed and acceleration. Using the same diagram axis, such information can also be shown as durations (in seconds or fractions of total time or frequency). A Driving pattern can only be combined with a steady state model of the vehicle, such as "*fuel consumption=function(speed, acceleration)*", as opposed to a dynamic model of the vehicle. The Driving pattern itself includes the driver, so no driver model is needed.

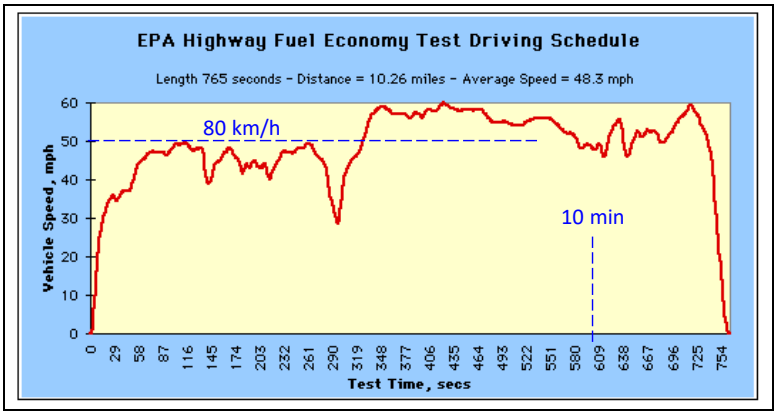

Figure 3-13: HFTP cycle from http://www.epa.gov/nvfel/methods/hwfetdds.gif

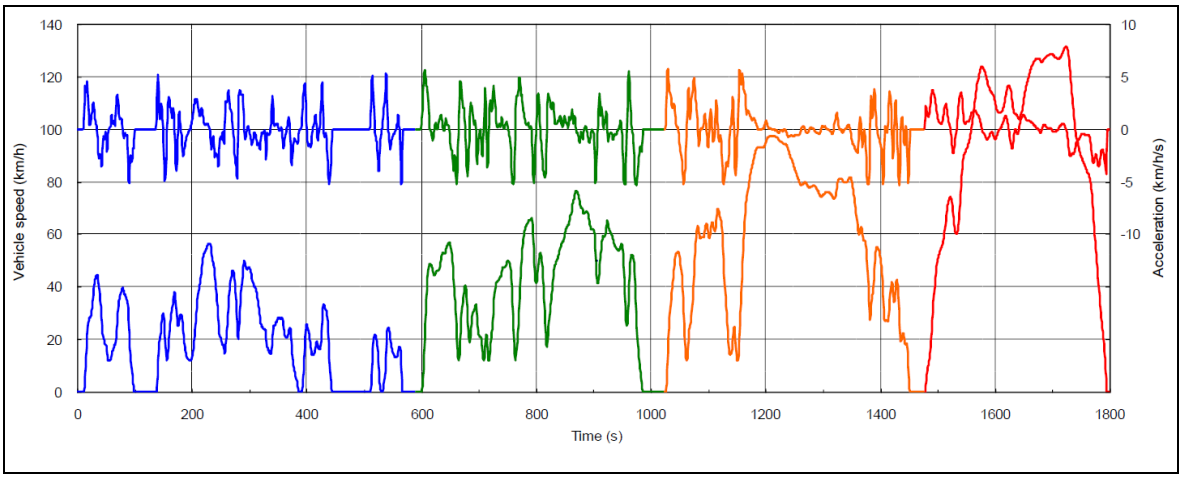

Figure 3-14: WLTC cycle from http://www.unece.org.

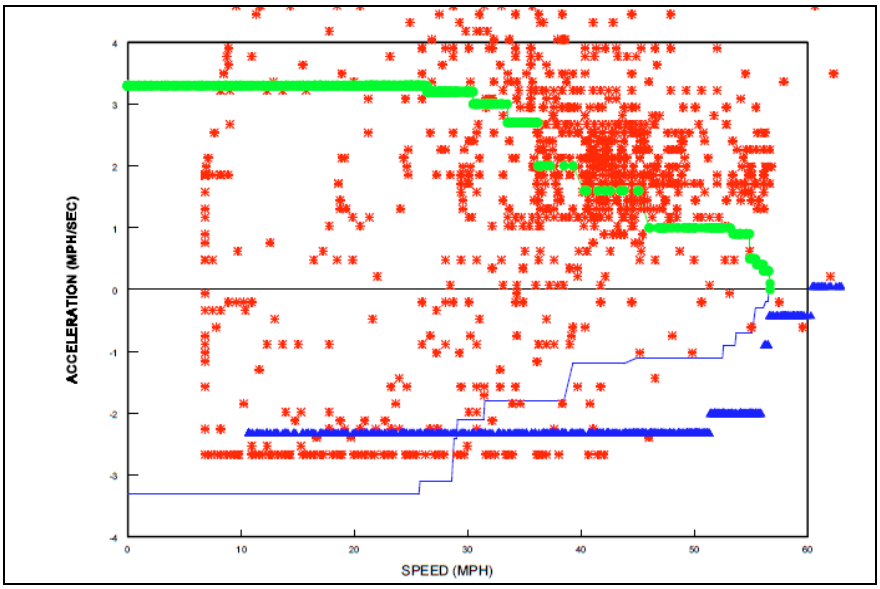

Figure 3-15: FTP cycle converted to a Driving pattern, i.e. a distribution of operating duration in speed and acceleration domain. From http://www.epa.gov/oms/regs/ld-hwy/ftp-rev/ftp-tech.pdf.

Driving patterns can use more than 2 dimensions, such as [speed, acceleration, road gradient]. In principle, they can also use less than 2 dimensions, maybe only [speed]. The (steady state) vehicle model has to reflect the corresponding dimensions.

3.3.1.3 Operating Cycle

A vehicle independent description uses legal speed rather than actual speed, and it varies with position along the route, *s*, rather than time. Also other parameters, like road grade, weight of transported goods etc. are defined in position rather than time. For stops along the route, the stop duration or departure time then has to be separately defined. This leads to a more realistic description (model) of the vehicle usage, here called Operating cycle. Important is that an Operating cycle becomes vehicle independent, so that different vehicles or different vehicle configurations can be fairly compared. See (Pettersson, 2017).

Simulation with an Operating cycle requires some kind of driver model. A consequence is that different driver models will give different results, e.g., different fuel consumption due to different driver preferred acceleration. Hence, the driver model itself can be seen as a part of the vehicle usage definition.

3.3.2 Rotating Inertia Influence on Acceleration

In Figure 3-3 it was shown that the acceleration cannot be found directly as a force difference (distance between curves) divided by vehicle mass. This is because the Traction Diagram does not contain

any dynamics, and dynamics are more complicated than accelerating the vehicle mass. The phenomenon that occurs is referred to here as "Rotating Inertia Influence on Acceleration". If no velocity losses, the rotating part of the propulsion system, e.g. engine and wheels, must be synchronically accelerated with the vehicle mass. This "steals" some of the power from the propulsion system. This affects the required propulsion force when following accelerations in a driving cycle.

Consider a wheel rolling which is ideally rolling (no slip), with a free-body diagram and notations as in Figure 3-16. Setting up 2 equilibrium equations and 1 compatibility equation gives Eq [3.8].

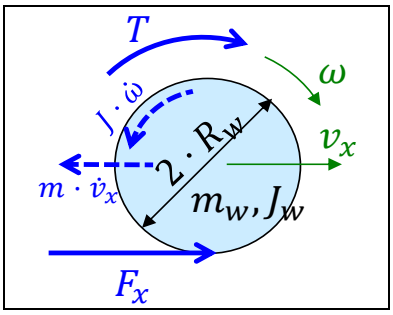

Figure 3-16: Rolling wheel

$$m_w \cdot \dot{v}_x = F_x;$$
$$J_w \cdot \dot{\omega} = T - F_x \cdot R_w;$$
$$v_x = R_w \cdot \omega \Rightarrow \dot{v}_x = R_w \cdot \dot{\omega};$$

[3.8]

Eliminate ω and F_x gives:

$$(m_w + J_w/R_w^2) \cdot \dot{v}_x = T/R_w; \quad \text{or}$$
$$k \cdot m_w \cdot \dot{v}_x = T/R_w; \quad where \quad k \cdot m_w = m_w + J/R_w^2;$$

[3.9]

Note that we can keep ω and F_x: $\omega = v_x/R_w$; and $F_x = T/(k \cdot R_w)$;.

So, the rotating inertia makes the mass m_w appear a factor k larger and the reaction force F_x (expressed in T) correspondingly lower. We call the factor k the "rotational inertia coefficient".

A vehicle with total mass m will appear to have larger mass due to inertias in the propulsion system. There are rotational inertias at two places: before transmission, i.e. rotating with same speed as engine: J_e and after transmission, i.e. rotating with same speed as the wheel: J_w. The appearant mass, $k \cdot m$, will be dependent on the main transmission ratio r as well:

$$k \cdot m \cdot \dot{v}_x = F_{x,*} = T_e \cdot \frac{r}{R_w}; \quad where\ k \cdot m = m + \frac{J_w}{R_w^2} + \frac{J_e \cdot r^2}{R_w^2};$$

[3.10]

Typically for a passenger car with traditional ICE propulsion, $k = 1.3..1.4$ in the first gear and $k = 1.1$ in the highest gear ($J_e \approx 0.2\ [kg \cdot m^2], r \approx\ 4 \cdot 4 = 16, R_w = 0.3\ [m]$). So, the phenomena is significant! Typically for electrical propulsion of same vehicle, J is smaller and there are fewer gears, so k is lower for low speed and higher for high speed.

When the clutch is slipping, there is no constraint between engine speed and vehicle, so the term with J_e disappears from Equation [3.10]. If the wheel spins, both terms J_e and J_w disappear.

We can now learn how to determine acceleration from the Traction Diagram, see Figure 3-17.

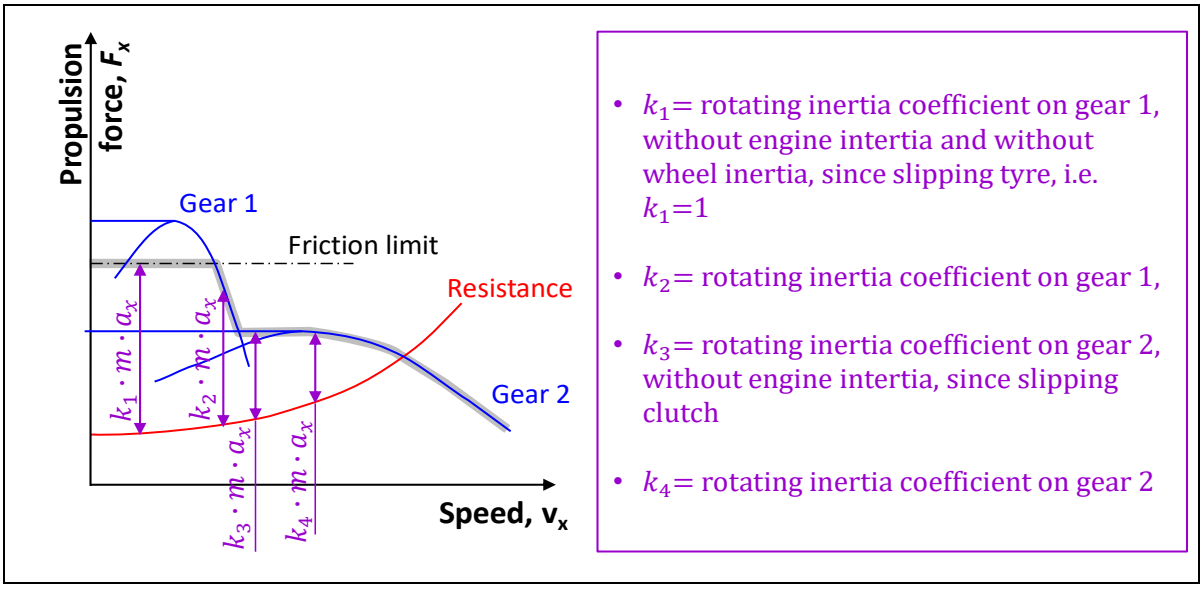

Figure 3-17: Acceleration in Traction Diagram. Rotating inertia effects are shown assuming that the engine is run on its maximum curve and the gear (or slipping clutch) for highest acceleration is selected.

It should be noted that, if tyre slip is modelled, the effect of rotating inertia is regarded without using the k factor above. That is, if the mathematical model in [3.11] is used instead of [3.8]. Eq [3.11] gives an explicit form model with two states $[v, \omega]$ and it becomes increasingly computational demanding the larger C_x is. (Similar decoupling between inertias J_e and J_w happens if torque converter or elastic driveshafts are modelled between engine inertia and wheel.)

$$\begin{aligned} & m \cdot \dot{v} = F_x; \\ & J \cdot \dot{\omega} = T - F_x \cdot R_w; \\ & F_x = C_x \cdot s_x; \quad where \quad s_x = \frac{R_w \cdot \omega - v_x}{|R_w \cdot \omega|}; \end{aligned} \qquad [3.11]$$

3.3.3 Four Quadrant Traction Diagram

When the driving cycle shows a deceleration, which is larger than can be achieved with resistance force, we need to brake with a combination of engine braking and friction brakes. If only friction braking is used, it can be with engaged or disengaged clutch. That influences the rotating inertia coefficient by using or not using the J_e term in Equation [3.10], respectively. The traction diagram can be extended to also cover engine braking and friction braking. However, the friction brake system is seldom limiting factor for how negative the longitudinal force can be. But the road friction is, see Figure 3-18.

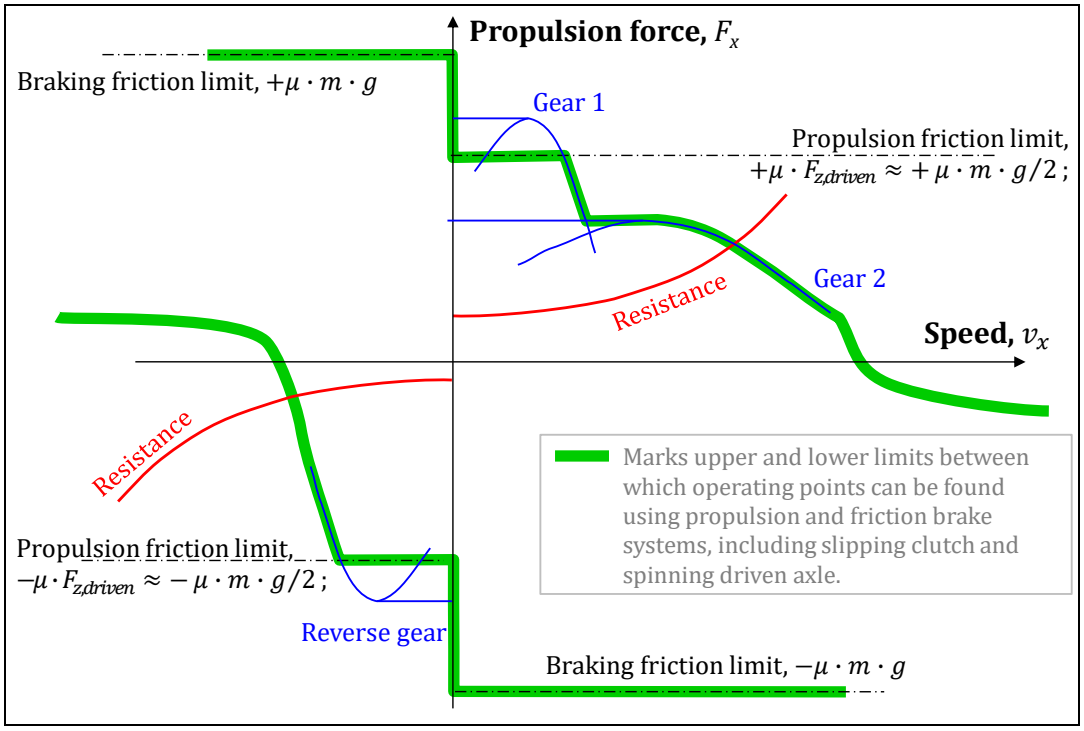

Figure 3-18: Traction Diagram in 4 quadrants. One of two axles is assumed driven, which limits propulsion to ≈half of braking friction limit. Up-hill slope is assumed, which is seen as asymmetric resistance.

3.3.4 Functions Over Cycles

3.3.4.1 Energy Consumption *

Function definition: ***Energy (or Fuel) Consumption*** *is the amount of energy* $[J]$ *(or fuel* $[kg]$ *or* $[litre]$*) consumed by the vehicle per performed transportation amount. Transportation amount can e.g. be measured in km,* $km, person \cdot km, ton \cdot km,$ *or* $m^3 \cdot km$*. The vehicle operation has to be defined, e.g. with a certain driving cycle (speed as function of time or position), including road gradient, cargo load, road surface conditions, etc.*

The consumption arises in the prime mover, see Figure 2-63 and Figure 2-64, but as a cycle measure it is dependent of the overall vehicle operation.

Driving cycles are used for legislation and rating for passenger cars. For commercial vehicles, the legislation has been for the engine alone, and not for the whole vehicle. CO2-rating for commercial vehicles is newly introduced, see http://ec.europa.eu/clima/events/docs/0096/vecto_en.pdf.

1.1.1.1 Assessing Energy Consumption and Other Cycle Measures

The measures of all functions mentioned in 3.3.4 can be assessed in some sort of driving cycle/operation cycle computation. Such computations are described in the following, as exemplified by only one measure, the Energy Consumption.

How to predict the consumption for a vehicle during a certain driving cycle is rather straight-forward using what has been presented earlier in this chapter. Since a driving cycle is a prediction of how the vehicle is moving, it actually stipulates the acceleration of a mass, which calls for an "inverse dynamic analysis". In such one assumes that the driving cycle is met exactly, which means that both required wheel speed and required wheel torque can be calculated for each time instant. Then, via a propulsion and brake system model, the corresponding fuel consumption in the engine can also be found for each time instant. A summary of such an inverse dynamic algorithm for prediction of fuel or energy consumption is given in Equation [3.12].

```
For each time step in the driving cycle:
  • Calculate operating point for vehicle (speed and acceleration) from
    driving cycle. Acceleration is found as slope of v(t) curve. Other quan-
    tities, such as road slope, also needs to be identified;
  • Select gear (and clutch state, tyre spin, friction brake state, etc) to
    obtain this operating point. Select also friction brake, especially for
    operating points which can be reached using only friction brake. If the
    vehicle has an energy buffer, regenerative braking is also an option;
  • Calculate required actuation from propulsion system on the driven wheel,
    i.e. rotational speed and shaft torque;
  • Calculate backwards through propulsion system, from wheel to prime mo-
    tor. It gives the operating point for prime mover (rotational speed and
    torque);
  • Read prime mover consumption [in kg/s or W=J/s, not specific consump-
    tion, not efficiency] from prime mover consumption map;
  • Sum up consumption [in kg or J] with earlier time steps, e.g. using the
    Euler forward integration method: AccumulatedConsumption =
    AccumulatedConsumption + Consumption*TimeStepLength;
end;
```

[3.12]

The final accumulated consumption [in kg or J] is often divided by the total covered distance in the driving cycle, which gives a value in kg/km or J/km. If the fuel is liquid, it is also convenient to divide by fuel density, to give a value in litre/(100*km). It can also be seen as a measure in m^2, which is the area of the "fuel pipe" which the vehicle "consumes" on the way.

For hybrid vehicles (with energy buffers) the same driving cycle can be performed (same $v(t)$) but ending with different level of energy in the buffer. Also, the level when starting the driving cycle can be different. This makes it unfair to compare energy consumption only as fuel consumption, one should rather weight it to energy cost, €/km or €/(ton·km).

3.3.4.1.1 Forward and Backward Simulation

We should note that the calculation scheme in Equation [3.12] does not always guarantee a solution. An obvious example is if the driving cycle prescribes such high accelerations at such high speeds that the propulsion system is not enough, i.e. we end up outside maximum torque curve in engine diagram. This is often the case with "inverse dynamic analysis", i.e. when acceleration of inertial bodies is prescribed, and the required force is calculated. An alternative is to do a dynamic analysis, which means that a driver model calculates the pedals in order to follow the driving cycle speed approximately, but not exactly. Inverse dynamic analysis is often more computational efficient, but limits what can phenomena that can be modelled in the propulsion and brake system. The computational benefit is especially large if state variables can be omitted, which is often the case but not always. Inverse dynamics

and dynamic simulations are sometimes referred to as backward and forward simulation, respectively; see Reference (Wipke, o.a., 1999).

3.3.4.1.2 Stepped, CVT and Energy Buffering Main Transmissions

For a given driving cycle $v_x(t)$ there is a certain $[F_x, v_x]$ for each time instant. For different types of main transmissions, one can select operating point $[T_e, \omega_e]$ in prime mover diagram differently, see Figure 3-19.

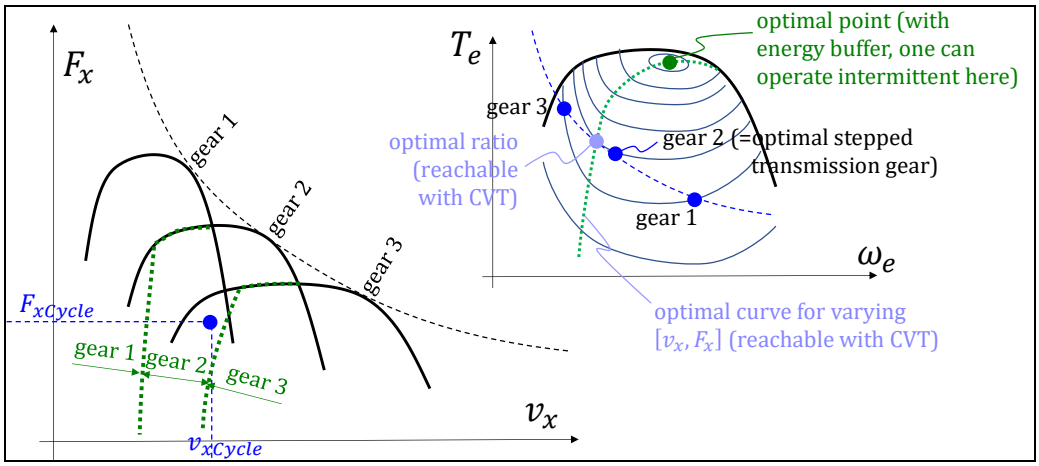

Figure 3-19: Conceptual difference between Stepped, Continuously Variable and Energy Buffering transmission. Operating intermittent would only follow the driving cycle with same average speed.

1.1.1.2 Transport time *

*Function definition: **Transport Time** is the time* $[s]$ *or* $[h]$ *for the vehicle to perform a certain transportation mission. Transportation mission can e.g. be defined in terms of distance, payload, road topography, etc.*

Transport Time is often in conflict with Energy Consumption. Either, one have independent requirements (constraints), but one can also formulate the total transport cost and minimize it, e.g.: $Cost = EnergyCost[€/J] \cdot EnergyConsumption[J] + TimeCost[€/h] \cdot TransportTime[h]$;. (That cost model is for exemplification and very simplified. Important other costs are investment and maintenance.)

For commercial freight traffic, $TimeCost$ is mainly the driver salary, so it can be quantified. For person transport, especially private travels, it is much more difficult to motivate a number. One can typically find studies which uses around$\approx 120\ SEK/h \approx 12\ €/h$ for private travels in Sweden.

3.3.4.2 Emissions *

Function definition: As Energy consumption but amount of certain substance instead of amount of energy.

There are emission maps where different emission substances (NOx, HC, etc.) per time or per produced energy can be read out for a given speed and torque. This is conceptually the same as reading out specific fuel consumption or efficiency from maps like in Figure 2-63 and Figure 2-64. A resulting value can be found in mass of the emitted substance per driven distance.

Noise is also sometimes referred to as emissions. It is not relevant to integrate noise over the time for the driving cycle, but maximum or mean values can have relevance. Noise emissions are very peripheral to vehicle dynamics.

3.3.4.3 Tyre Wear *

*Function definition: **Tyre wear** is the worn-out tyre tread depth on a vehicle per performed transportation amount. Transportation amount can be measured as for Energy consumption. Tyre wear as a vehicle function has to consider all tyres on the vehicle, e.g. as maximum over the wheels (assuming that all tyres are changed when one is worn out) or average (assuming that single tyres are exchanged when worn out).*

There are models for tyre wear (e.g. outputting "worn tread depth per time"), see Equation [2.52]. For a certain driving cycle, we can integrate the $WearRate$ [in mass/s or mm tread depth/s], over time similar to energy consumption rate, which becomes worn material [in mass or mm tread depth]. The

wear rate per wheel is a function of the total slip, so it can include both longitudinal slip (propulsion and brake) and lateral slip (from cornering and toe angles).

Generally, the worn material will be different for different axles, or wheels, so a tyre change strategy might be necessary to assume to transform the worn material on several axles into one cost. The cost will depend on whether one renews all tyres on the vehicle at once or if one change per axle. The tyre wear is a cost which typically sums up with energy cost and cost of transport time (e.g. driver salary, for commercial vehicles).

3.3.4.4 Range *

Function definition: ***Range*** *[km] is the inverted value of Energy consumption [kg/km, litre/km or J/km], and multiplied with fuel tank size [kg or litre] or energy storage size [J].*

The range is how far the vehicle can be driven without refilling the energy storage, i.e. filling up fuel tank or charging the batteries from the grid. This is in principle dependent on how the vehicle is used, so the driving cycle influences the range. In principle, the same prediction method as for energy consumption and substance emissions can be used. In the case of predicting range, you have to integrate speed to distance, so that you in will know the travelled distance.

3.3.4.5 Acceleration Reserve *

Function definition: ***Acceleration reserve*** *is the additional acceleration the vehicle will achieve within a certain time (typically 0.1..1 s) without manual gear-shifting by pressing accelerator pedal fully, when driving in a certain speed on level ground without head-wind. For vehicles with automatic transmissions or CVTs the certain time set can allow automatic gear-shift (or ratio-change) or not. The reserve can also be measured in propulsion force.*

In general terms, the lowest consumption is found in high gears. However, the vehicle will then tend to have a very small reserve in acceleration. It will, in practice, make the vehicle less comfortable and less safe to drive in real traffic, because one will have to change to a lower gear to achieve a certain higher acceleration. The gear shift gives a time delay.

Figure 3-20 shows one way of defining a momentary acceleration reserve. The reserve becomes generally larger the lower gear one selects. A characteristic of electric propulsion systems is that an electric motor can be run at higher torque for a short time than stationary, see Figure 2-62. On the other hand, the stationary acceleration reserve is less gear dependent, since an electric motor can work at certain power levels in large portions of its operating range.

One can calculate the acceleration reserve at each time instant over a driving cycle. However, integration of acceleration reserve, as we did with fuel, emissions and wear, makes less sense. Instead, a mean value of acceleration reserve tells something about the vehicle's driveability. Minimum or maximum values can also be useful measures.

Acceleration reserve was above described as limited by gear shift strategy. Other factors can be limiting, such as energy buffer state of charge for parallel hybrid vehicles or how much overload an electric machine can take short term, see right part of Figure 3-20.

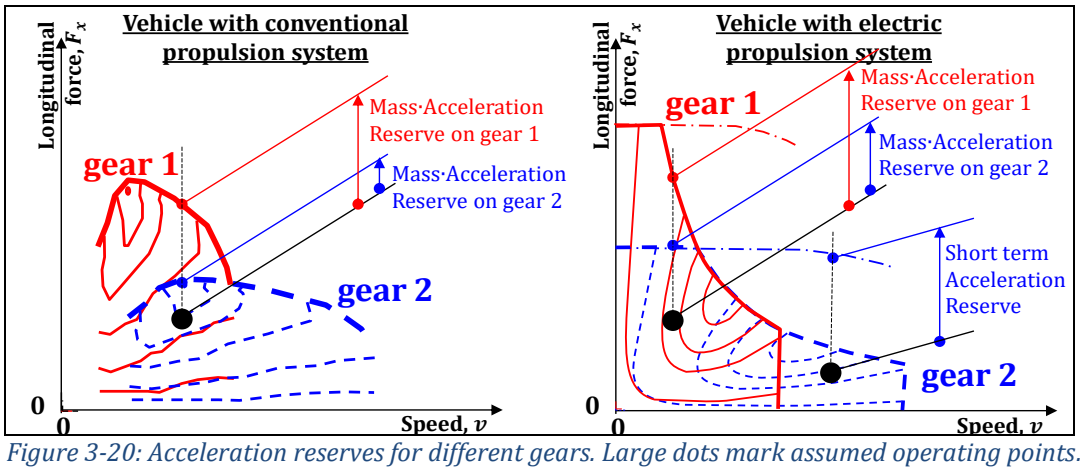

Figure 3-20: Acceleration reserves for different gears. Large dots mark assumed operating points.

3.3.5 Load Transfer with Rigid Suspension

Longitudinal load transfer redistributes vertical force from one axle to the other. The off-loaded axle can limit the traction and braking. This is because the propulsion and brake systems are normally designed such that axle torques cannot always be ideally distributed.

For functions over longer events it is often reasonable to consider the suspension as rigid. We start with the free-body diagram in Figure 3-21, which includes acceleration, a_x.

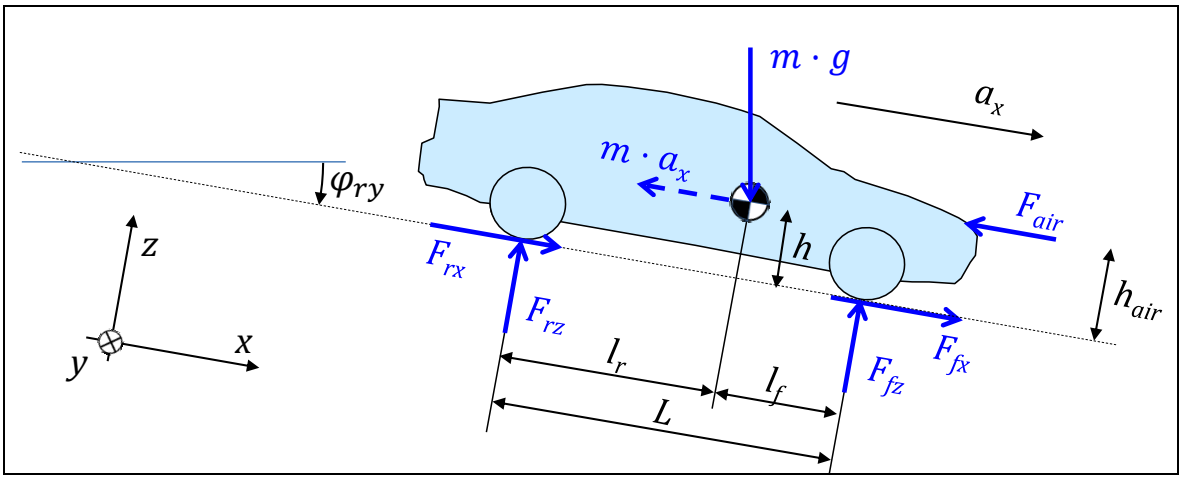

Figure 3-21: Free Body Diagram for accelerating vehicle. Rolling resistance in F_{fx} and F_{rx}.

Note that the free-body diagram and the following derivation is very similar to the derivation of Equation [3.5], but we now include the fictive force $m \cdot a_x$.

Moment equilibrium, around rear contact with ground:

$$-F_{fz} \cdot L + m \cdot g \cdot \left(l_r \cdot cos(\varphi_{ry}) + h \cdot sin(\varphi_{ry})\right) - F_{air} \cdot h_{air} - m \cdot a_x \cdot h = 0; \Rightarrow$$

$$\Rightarrow F_{fz} = m \cdot \left(g \cdot \frac{l_r \cdot cos(\varphi_{ry}) + h \cdot sin(\varphi_{ry})}{L} - a_x \cdot \frac{h}{L}\right) - F_{air} \cdot \frac{h_{air}}{L};$$

Moment equilibrium, around front contact with ground:

$$+F_{rz} \cdot L - m \cdot g \cdot \left(l_f \cdot cos(\varphi_{ry}) - h \cdot sin(\varphi_{ry})\right) - F_{air} \cdot h_{air} - m \cdot a_x \cdot h = 0; \Rightarrow$$

$$\Rightarrow F_{rz} = m \cdot \left(g \cdot \frac{l_f \cdot cos(\varphi_{ry}) - h \cdot sin(\varphi_{ry})}{L} + a_x \cdot \frac{h}{L}\right) + F_{air} \cdot \frac{h_{air}}{L};$$

[3.13]

These equations confirm what we know from experience, the front axle is off-loaded under acceleration with the load shifting to the rear axle. The opposite occurs under braking.

The load shift has an effect on the tyre's grip. If one considers the combined slip conditions of the tyre (presented in Chapter 2), a locked braking wheel limits the amount of lateral tyre forces. The same is true for a spinning wheel. This is an important problem for braking as the rear wheels become off-loaded. This can cause locking of the rear wheels if the brake pressures are not adjusted appropriately. See more in 3.4.4.

3.3.5.1 Varying Road Pitch

The model in 3.4.4..3.4.5.2 assumes flat but not level road, i.e. φ_{ry} is constant. An example where φ_{ry} varies is when passing a *crest* or a *sag*, see Figure 3-22. If negotiating a curve at the same time as a crest, a vehicle can lose vertical force under tyres so that lateral grip is affected.

Moment equilibrium, around rear and front wheel contact with ground gives:

$$F_{zf} = m \cdot \left((g + z'' \cdot v_x^2) \cdot \frac{l_r \cdot \cos(\varphi) + \mathrm{h} \cdot \sin(\varphi)}{L} - a_x \cdot \frac{h}{\mathrm{L}} \right) - F_{air} \cdot \frac{h_{air}}{\mathrm{L}};$$
$$F_{zr} = m \cdot \left((g + z'' \cdot v_x^2) \cdot \frac{l_f \cdot \cos(\varphi) - \mathrm{h} \cdot \sin(\varphi)}{L} + a_x \cdot \frac{h}{L} \right) + F_{air} \cdot \frac{h_{air}}{L};$$

[3.14]

Assuming that we have the road as $z(s)$, then $\varphi = -\arctan\left(\frac{dz}{ds}\right) \approx -\frac{dz}{ds}$; and $z'' = \frac{d^2z}{ds^2}$;.

Note that this model is assuming that vertical variations of road are larger than wheel base and track width and same on left and right side of the road/vehicle. Else the variation would be called road unevenness, which will be more treated in Chapter **5**.

If models with body vertical and pitch motion and suspension springs, such as in 3.4.5 and 3.4.5.2 it is often suitable to express the vertical fictive force, $m \cdot \ddot{z}$, with $v_x \cdot \omega_y$ instead of $m \cdot z'' \cdot v_x^2$. The fictive force downwards will then be $-m \cdot v_x^2 \cdot \kappa_y = -m \cdot v_x \cdot \omega_y$ instead. This can be understood from basic geometry, $z'' \approx -\kappa_y$, where κ_y is the road pitch curvature $[1/length]$, see Figure 3-22.

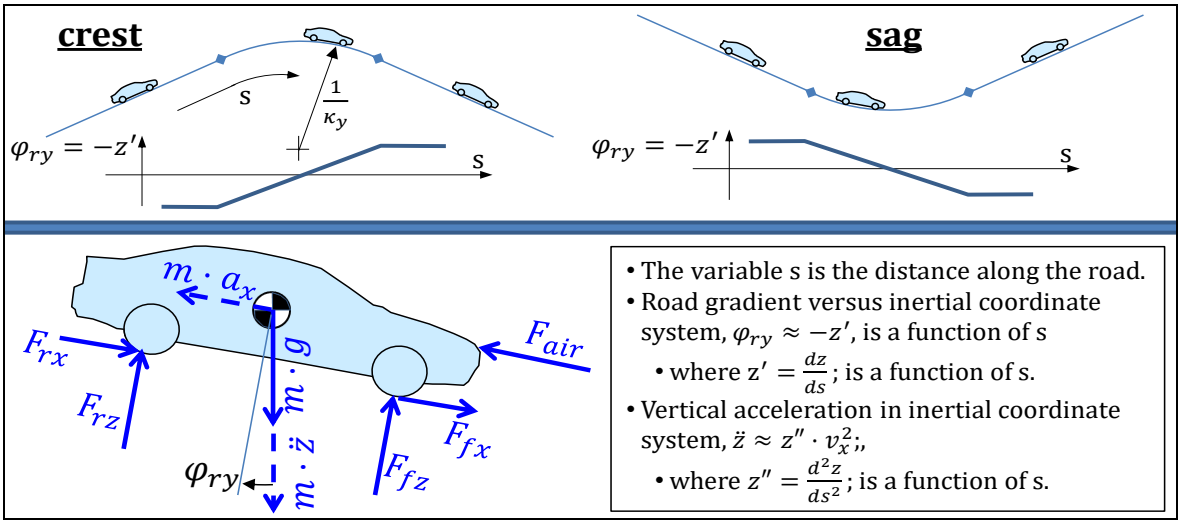

Figure 3-22: Free Body Diagram for driving over non-flat vertical road profile.

3.3.6 Acceleration

Acceleration performance like, typically, 0-100 km/h over 5..10 s, will be addressed in this section. These accelerations are relatively steady state (vehicle pitch and heave are relatively constant), so the suspension compliance is not considered.

Accelerations will also be covered in 3.4, as being shorter events. The vehicle pitch and heave vary more and, consequently, the suspension compliance becomes important to model. This modelling is also more suited for braking, which typically involve suspension more than propulsion.

3.3.6.1 Acceleration Performance *

*Function definition: **Acceleration performance** is the time needed to, with fully applied accelerator pedal, increase speed from a certain speed to another certain higher speed, at certain road friction on level ground without head-wind and certain load.*

3.3.6.2 Solution using Integration over Time

A front-wheel-drive passenger car with a stepped gearbox should accelerate from 0 to 100 km/h. A Matlab code is given in Equation [3.15], which simulates the acceleration uphill from stand-still, using simple numerical integration. The code calculates the possible acceleration in each of the gears, and one mode with slipping clutch. In each time step it selects that which gives the highest acceleration. The numerical data and results are not given in the code, but some diagrams are shown in Figure 3-23. The code is not fully documented, only using equations so far presented in this compendium.

```
dt=0.1; t_vec=[0:dt:10]; vx_vec(1)=0;
for i=1:length(t_vec)
    vx=vx_vec(i);
    Fres=m*g*sin(p)+froll*m*g*cos(p)+0.5*roh*A*cd*vx*vx;

    %if gear 1 (clutch engaged)
    ratio=ratios(1);
    we=vx*ratio/radius;
    Te=interp1(Engine_w,Engine_T,we);
    Fx=Te*ratio/radius;
    ax=(Fx-Fres)/(m+(Jw+Je*(ratio^2))/(radius^2));
    Ffz=m*(g*lr/L-ax*h/L);
    if Fx>mu*Ffz
        Fx=mu*Ffz;
        ax=(Fx-Fres)/m;
    end
    ax1=ax;

    %if gear 2 (clutch engaged)
    ratio=ratios(2);
    … then similar as for gear 1
    ax2=ax;

    %if gear 3 (clutch engaged)
    ratio=ratios(3);
    … then similar as for gears 1 and 2
    ax3=ax;

    %if clutch slipping on gear 2
    ratio=ratios(2);
    wc=vx*ratio/radius; %speed of output side of clutch
    Te=max(Engine_T);
    we=Engine_w(find(Engine_T>=Te)); %engine runs on speed where max torque
    Fx=Te*ratio/radius;
    ax=(Fx-Fres)/(m+Jw/(radius^2));
    Ffz=m*(g*lr/L-ax*h/L);
    if Fx>mu*Ffz
        Fx=mu*Ffz;
        ax=(Fx-Fres)/m;
    end
    if wc>we %if vehicle side (wc) runs too fast, we cannot slip on clutch
        ax=-inf;
    end
    ax0=ax;

    [ax,gear_vec(i)]=max([ax0,ax1,ax2,ax3]);  vx_vec(i+1)=vx+ax*dt;
end
```

[3.15]

Phenomena that are missing in this model example are:

- Gear shifts are assumed to take place instantly, without any duration
- The option to use slipping clutch on 1st and 3rd gear is not included in model
- The tyre slip is only considered as a limitation at a strict force level, but the partial slip is not considered for simplification. The code line "`we=vx*ratio/radius;`" is hence not fully correct. Including the slip, the engine would run at somewhat higher speeds, leading to that it would lose its torque earlier, leading to worse acceleration performance.
- Load transfer is assumed to take place instantly quick; delays due to Suspension compliance, as described in 3.3, are not included.

3.3.6.3 Solution using Integration over Speed

An alternative way to find the relation between v and t is to separate the differential equation:

$$m \cdot a_x = m \cdot \frac{dv_x}{dt} = F_x(v_x) - F_{res}(v_x); \Rightarrow \frac{m \cdot dv_x}{F_x(v_x) - F_{res}(v_x)} = dt \Rightarrow$$

$$\Rightarrow \int_0^{v_{x,end}} \frac{m \cdot dv_x}{F_x(v_x) - F_{res}(v_x)} = \int_0^{t_{end}} dt \Rightarrow \quad t_{end} = \int_0^{v_{x,end}} \frac{m \cdot dv_x}{F_x(v_x) - F_{res}(v_x)};$$

[3.16]

The time t_{end} is calculated through integration over speed, as opposed to integration over time. If simple mathematic functions are used to describe $F_x(v_x)$ and $F_{res}(v_x)$ the solution can be on closed form. However, but integration over time is more general and works for more advanced models.

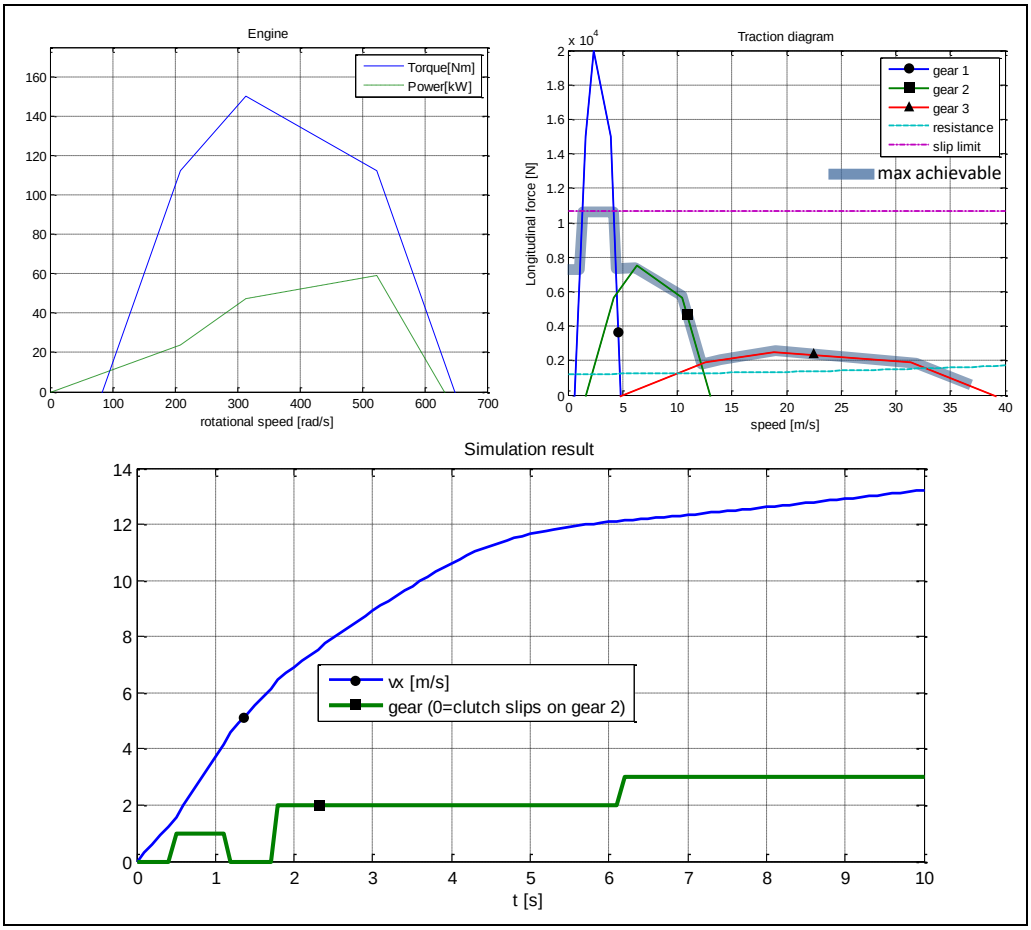

Figure 3-23: Example of simulation of acceleration, using the code in Equation [3.15].

3.4 Functions in (Short) Events

This section targets models and methods to define and verify functions in a certain and shorter time frame, typically 0.5 to 5 seconds. It can be both acceleration and deceleration. (Friction) Brake system and phenomena as load transfer then becomes important, why these are presented early. But first, some typical driving manoeuvres are presented.

3.4.1 Typical Test Manoeuvres

When applying the longitudinal actuator systems (propulsion system and brake system) there are a couple of different situations which are typical to consider:

- Straight line maximum braking from, typically 100 km/h to stand-still for passenger cars.
- Braking in curve with significant lateral acceleration, see References (ISO, 2006) and (ISO, 2011).
- Straight line acceleration, typically 0 to 100 km/h and 80-100 km/h.
- Accelerating in curve with significant lateral acceleration.

For these four main situations, one can also vary other, typically:

- At high road friction and at low friction, often called “hi-mu” and “lo-mu”
- At different road friction left and right, often called “split-mu”
- At sudden changes in road friction, called “step-mu” or “step-up” and “step-down” when going to higher and lower friction, respectively.

- At high speed, typically 200 km/h, for verifying lateral stability
- At different up-hill/down-hill gradients
- At different road banking (slope left to right)

A propelled or braked wheel or axle develops a longitudinal force, F_x, counter-acting the rotation. F_x is limited by the road friction: $|F_x|_{max} = \mu \cdot F_z$;. (**not** $|F_x|_{max} = \mu \cdot F_z - f_r \cdot F_z$, see Figure 2-15).

Braking Coefficient $= -F_x/F_z$, is a property defined for an axle or a single wheel. It can be seen as the utilized friction coefficient, μ_{util} = brake force/normal load. The μ_{util} should not be mixed up with (available) friction coefficient, μ; the relation between them is $\mu_{util} \leq \mu$.

3.4.2 Deceleration Performance

There are some different functions that measures braking performance or deceleration performance.

3.4.2.1 Braking Efficiency *

Function definition: ***Braking Efficiency*** *is the ratio of vehicle deceleration and the best brake-utilized axle (or wheel), while a certain application level of the brake pedal at a certain speed straight ahead, at certain road friction on level ground without head-wind and certain load at a certain position in the vehicle.*

In equation form, the Braking Efficiency becomes $= (-a_x/g)/\left(\max_{\forall axles}(\mu_{util})\right)$;. If Braking Efficiency = 1 = 100%, the distribution of braking is optimal.

3.4.2.2 Braking Distance *

Function definition: ***Braking Distance*** *is the distance travelled during braking with fully applied brake pedal from a certain speed straight ahead to another certain lower speed, at certain road friction on level ground without head-wind and certain load at a certain position in the vehicle.*

For passenger cars one typically brakes fully from 100 km/h and then the braking distance is typically around 40 m (average $a_x = -9.65\ m/s^2$). For a truck it is typically longer, 51..55 m ($-7.5..-7\ m/s^2$).

3.4.2.3 Stopping Distance *

Function definition: ***Stopping Distance*** *is the distance travelled from that an obstacle becomes visible to driver have taken the vehicle to stand-still. Certain conditions, as for Braking Distance, have to be specified, but also a certain traffic scenario and a certain driver to be well defined.*

Stopping Distance is the braking distance + the "thinking/reaction distance", which depends on the speed and the reaction time. The reaction time of a driver is typically 0.5..2 seconds.

3.4.3 Pedal Functions

3.4.3.1 Pedal Response *

Function definition: ***Accelerator pedal response*** *is how vehicle acceleration varies with accelerator pedal position, for a certain vehicle speed and possibly certain gear, on level ground without pressing the brake pedal.*

Function definition: ***Brake pedal response*** *is how vehicle deceleration varies with brake pedal force, for a certain vehicle speed, on level ground without pressing the accelerator pedal.*

These functions, together with the functions in 3.4.3.2, enable the driver to operate the vehicle longitudinally with precision and in an intuitive and consequent way. The requirements based on above function definitions, are typically that the translation of pedal position (or force) to vehicle acceleration (or deceleration) should be consistent, progressive and oscillation-free.

For accelerator pedal steps, there should be enough acceleration, but also absence of "shunt and shuffle" (driveline oscillations). When accelerator pedal is suddenly lifted off, there shall be certain deceleration levels, depending on vehicle speed and gear selected.

3.4.3.2 Pedal Feel *

Function definition: ***Accelerator pedal feel*** *is the pedal's force response to pedal position.*

Function definition: ***Brake pedal feel*** *is the pedal's position response to pedal force.*

These functions, together with the functions in 3.4.3, enable the driver to operate the vehicle longitudinally with precision and in an intuitive and consequent way.

3.4.4 Brake Proportioning

For brake performance it is important that both axles are used as much as possible during braking. But one also should consider that, in most driving situations, it is preferred that the front wheels lock first, because:

- A vehicle with **locked front** wheels ($\omega_f = 0$) tends to be yaw **stable**. However, steering ability is lost, so vehicle continues straight, incapable of curving its path.
- A vehicle with **locked rear** wheels ($\omega_r = 0$) tends to be yaw **unstable**. It turns around and ends up sliding with the rear first.

Hence, there are trade-offs when designing the wheel torque distribution. Same reasoning works for propulsion, if "locked" is replaced by "spin", meaning large positive longitudinal tyre slip. Spin at front makes vehicle more yaw stable than spin rear. The yaw stability then has a trade-off with acceleration performance.

Wheel torques is influenced simultaneously by both propulsion system and (friction) brake system, especially if regenerative braking with electric propulsion system. So, coordination of brake and propulsion systems might be needed.

The basic function of a brake system is that brake pressure (hydraulic on passenger cars and pneumatic on trucks) is activated so that it applies brake pads towards brake discs or drums. In a first approximation, the pressure is distributed with a certain fraction on each axle. For passenger cars this is typically 60..70% of axle torque front. In heavy trucks, the proportioning varies a lot, e.g. 90% for a solo tractor and 30% for heavy off-road construction rigid truck. The intention is to utilize road friction in proportion to the normal load, but not brake too much rear to avoid yaw instability.

If neglecting air resistance and road grade in Eq [3.13], the vertical axle loads can be calculated as function of deceleration ($-a_x$). An ideal brake distribution would be if each axle always utilize same fraction of available friction: $\frac{F_{fx}}{\mu_f \cdot F_{fz}} = \frac{F_{rx}}{\mu_r \cdot F_{rz}} \Rightarrow \left\{\begin{matrix} Assume \\ \mu_f = \mu_r; \end{matrix}\right\} \Rightarrow \frac{F_{fx}}{F_{rx}} = \frac{F_{fz}}{F_{rz}} \Rightarrow \frac{F_{fx}}{F_{rx}} = \frac{m \cdot \left(g \cdot \frac{l_r}{L} - a_x \cdot \frac{h}{L}\right)}{m \cdot \left(g \cdot \frac{l_f}{L} + a_x \cdot \frac{h}{L}\right)} = \frac{g \cdot l_r - a_x \cdot h}{g \cdot l_f + a_x \cdot h}$; Combining with $F_{fx} + F_{rx} = m \cdot a_x$; gives the optimal F_{fx} and F_{rx}:

$$F_{fx} = m \cdot a_x \cdot \left(\frac{l_r}{L} - \frac{a_x}{g} \cdot \frac{h}{L}\right); \text{ and } F_{rx} = m \cdot a_x \cdot \left(\frac{l_f}{L} + \frac{a_x}{g} \cdot \frac{h}{L}\right);$$

$$\text{or, if eliminating } a_x\text{: } F_{rx} = \frac{m \cdot g \cdot l_r}{2 \cdot h} - F_{fx} - \frac{m \cdot g}{2 \cdot h} \cdot \sqrt{l_r^2 - 4 \cdot h \cdot L \cdot \frac{F_{fx}}{m \cdot g}};$$

$$\text{or: } F_{fx}/F_x = \frac{l_r}{L} - \frac{h}{m \cdot g \cdot L} \cdot F_x; \text{ and } F_{rx}/F_x = \frac{l_f}{L} + \frac{h}{m \cdot g \cdot L} \cdot F_x; \qquad [3.17]$$

If including non-zero F_{air} and non-zero (but small) φ_{ry}: $F_{fx}/F_x = l_r/L - F_x \cdot h/(m \cdot g \cdot L) + F_{air} \cdot (h - h_{air})/(m \cdot g \cdot L)$; and $F_{rx}/F_x = l_f/L + F_x \cdot h/(m \cdot g \cdot L) - F_{air} \cdot (h - h_{air})/(m \cdot g \cdot L)$;. Air resistance F_{air} and road gradient φ_{ry}, of course, influences so that we need to adjust F_x to reach a certain a_x. However, road gradient does not influence the distribution of longitudinal tyre force between axles and air resistance only if $h \neq h_{air}$.

Eq [3.17] is plotted for variation in centre of gravity height and longitudinal position in Figure 3-24.

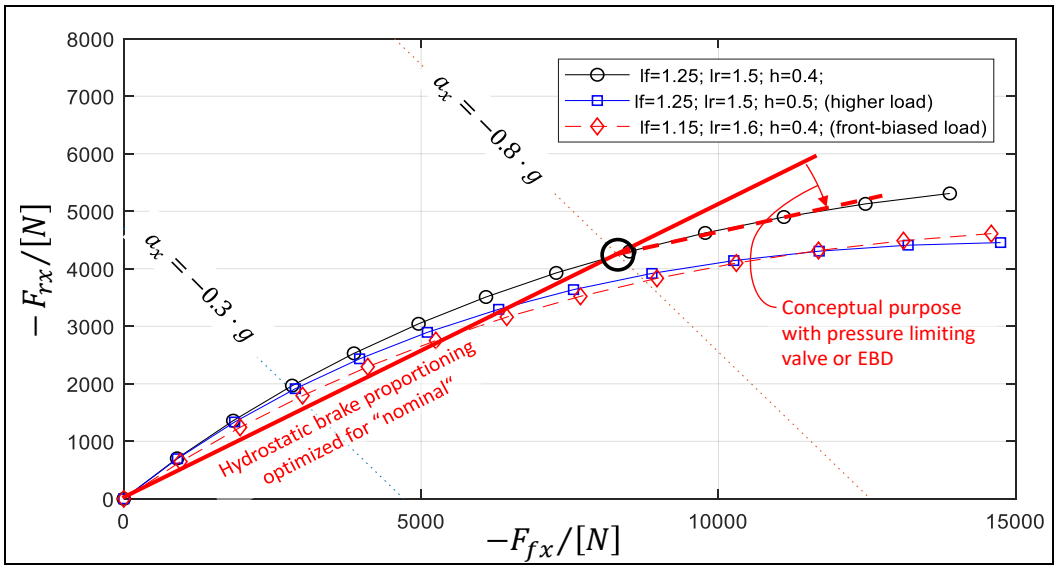

Figure 3-24: Brake Proportioning diagram. The curved curves mark optimal distribution for some variation in position of centre of gravity.

The proportioning is done by selecting pressure areas for brake calipers, so the base proportioning will be a straight line, marked as "Hydrostatic brake proportioning". For passenger cars, one typically designs this so that front axle locks first for friction below 0.8 for lightest vehicle load and worst variant. For heavier braking than $0.8 \cdot g$, or higher (or front-biased) centre of gravity, rear axle will lock first, if only designing with hydrostatic proportioning.

To avoid rear axle lock-up, one restricts the brake pressure to the rear axle. This is done by pressure limiting valve, brake pads with pressure dependent friction coefficient or Electronic Brake Distribution (EBD). In principle, it bends down the straight line as shown in Figure 3-24. With pressure dependent values one gets a piece-wise linear curve, while pressure dependent friction coefficient gives a continuously curved curve. EBD is an active control using same mechatronic actuation as ABS. EBD is the design used in today's passenger cars, since it comes with ABS, which is now a legal requirement on most markets.

On heavy vehicles with EBS (Electronic Brake System) and vertical axle load sensing, the brake pressure for each axle can be tailored. For modest braking (corresponding to deceleration $\leq 2\ m/s^2$) all axles are braked with same brake torque, to equal the brake pad wear which is importance for vehicle maintenance. When braking more, the brake pressure is distributed more in proportion to each axle's vertical load.

3.4.5 Heave and Pitch

So far, in 3.3.5 and 3.4.4, we modelled transfer of vertical forces between axles, but neither heave and pitch motion nor displacement. This will be added in 3.4.5. In 3.4.5.1, the load transfer is steady state and the linkage "trivial". In 3.4.5.2, the load transfer is transient and the linkage "non-trivial".

3.4.5.1 Steady State Load Transfer and Trivial Linkage

Additional to that the axle vertical loads change due to acceleration a_x, there are also change in out-of-road-plane motion (heave and pitch). In the following section, we study constant acceleration, e.g. when mild braking for a long time. We propose the steady state model in Figure 3-26. The model differs between the "unsprung mass" (wheels and the part of the suspension that does not heave) and the "sprung mass" or "body" (parts that heaves and pitches as one rigid body). The wheels are assumed to be linked to the body through "trivial linkage" as in Figure 2-54.

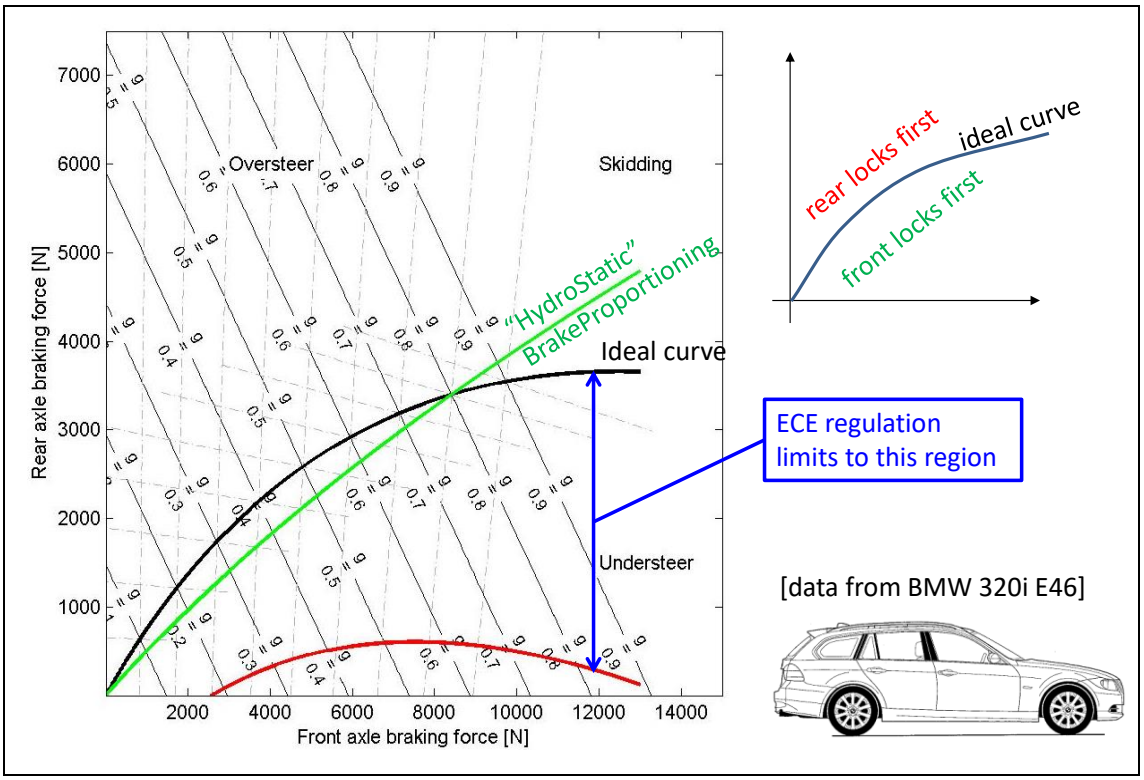

Figure 3-25: Brake Proportioning. From (Boerboom, 2012). If looking carefully, the "HydroStatic" curve is weakly degressive, thanks to brake pad material with pressure dependent friction coefficient.

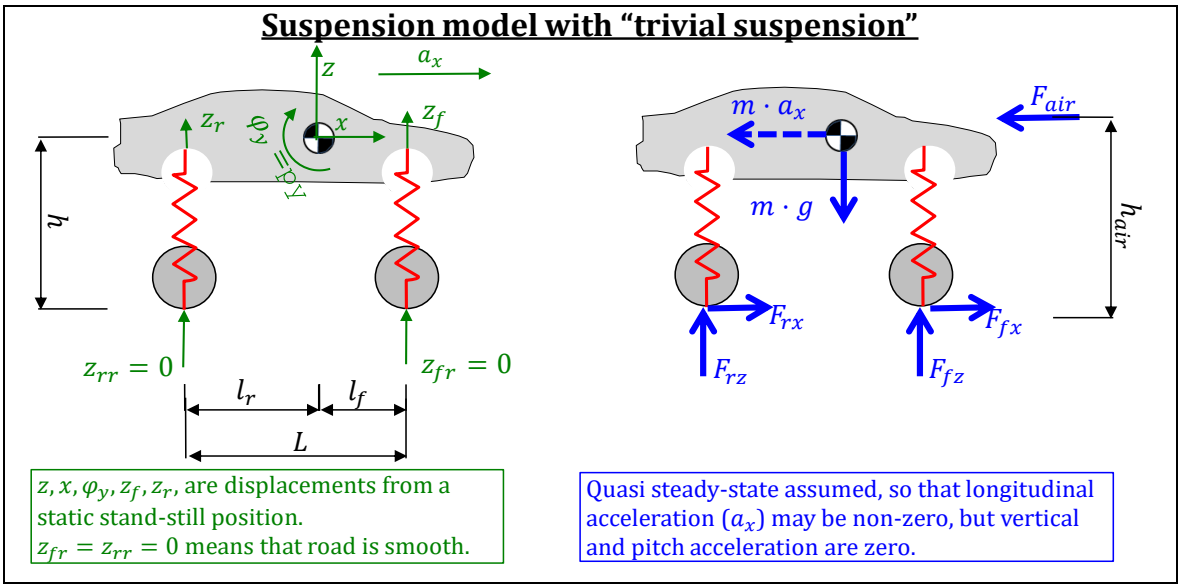

Figure 3-26: Model for steady state heave and pitch due to longitudinal wheel forces.

There is no damping included in model, because their forces would be zero, since there is no displacement velocity, due to the steady-state assumption. As **constitutive equations** for the compliances (springs) we assume that displacements are measured from a static condition and that the compliances are linear. The road is assumed to be smooth, i.e. $z_{fr} = z_{rr} = 0$.

$$F_{fz} = F_{fz0} + c_f \cdot (\cancel{z_{fr}} - z_f); \quad and \quad F_{rz} = F_{rz0} + c_r \cdot (\cancel{z_{rr}} - z_r);$$
$$where\ F_{fz0} + F_{rz0} = m \cdot g; \quad and \quad F_{fz0} \cdot l_f - F_{rz0} \cdot l_r = 0; \qquad [3.18]$$

We see already in free-body diagram that F_{fx} and F_{rx} always act together, so we rename $F_{fx} + F_{rx} = F_{wx}$, where w refers to wheel. The assumption of "trivial linkage" explains how longitudinal forces are transferred between wheels and body. **Equilibrium** then gives:

$$-F_{air} - m \cdot a_x + F_{wx} = 0;$$
$$m \cdot g - F_{fz} - F_{rz} = 0;$$
$$F_{rz} \cdot l_r - F_{fz} \cdot l_f - F_{wx} \cdot h - F_{air} \cdot (h_{air} - h) = 0;$$

[3.19]

Compatibility, to introduce body displacements, z and p_y, gives:

$$z_f = z - l_f \cdot \varphi_y; \quad and \quad z_r = z + l_r \cdot \varphi_y;$$

[3.20]

Solving constitutive relations, equilibrium, compatibility using Matlab Symbolic toolbox gives:

```
>> clear, syms zf zr Ffz Frz Ffz0 Frz0 ax z py
>> sol=solve( ...
    'Ffz=Ffz0-cf*zf', ...
    'Frz=Frz0-cr*zr', ...
    'Ffz0+Frz0=m*g', ...
    'Ffz0*lf-Frz0*lr=0', ...
    '-Fair-m*ax+Fxw=0', ...
    'm*g-Ffz-Frz=0', ...
    'Frz*lr-Ffz*lf-Fxw*h-Fair*(hair-h)=0', ...
    'zf=z-lf*py', ...
    'zr=z+lr*py', ...
    zf, zr, Ffz, Frz, Ffz0, Frz0, ax, z, py);
```

The solution is given in Eq [3.21]:

$$a_x = \frac{F_{wx} - F_{air}}{m};$$
$$z = -\frac{c_f \cdot l_f - c_r \cdot l_r}{c_f \cdot c_r \cdot L^2} \cdot \left(F_{wx} \cdot h + F_{air} \cdot (h_{air} - h)\right)$$
$$p_y = -\frac{c_f + c_r}{c_f \cdot c_r \cdot L^2} \cdot \left(F_{wx} \cdot h + F_{air} \cdot (h_{air} - h)\right)$$

[3.21]

In agreement with intuition and experience the body dives (positive pitch) when braking (negative F_{xw}). Further, the body centre of gravity is lowered (negative z) when braking and weaker suspension front than rear ($c_f \cdot l_f < c_r \cdot l_r$), which is normally the chosen design for cars.

The air resistance force is brought into the equation. It can be noted that for a certain deceleration, there will be different heave and pitch depending on how much of the decelerating force that comes from air resistance and from longitudinal wheel forces. But, as already noted, heave and pitch does not depend on how wheel longitudinal force is distributed between the axles.

3.4.5.2 Transient Load Transfer and Non-Trivial Linkage

Compared to 3.4.5.1, we will now model also the transients of load transfer. If we study longer events when the wheel force is applied and then kept constant for a longer time (1-5 s), it is often a good enough model. But if the wheel forces vary more, we need to capture the transients better. Then it is important to consider that the linkage can transfer some of the wheel longitudinal forces. When studying the transients, it is also relevant to consider the damping.

There are basically two modelling ways to include the suspension linkage in the load transfer: through a pitch centre or through a pivot point for each axle, see Figure 3-27.

3.4.5.2.1 Model with Pitch Centre

This model will not be deeply presented in this compendium. It has drawbacks in that it has only one suspended degree of freedom. Also, it does not take the distribution of longitudinal wheel forces between the axles into account. These short-comings is not very important for studying dive and squat, but they are essential when studying rapid individual wheel torque changes in time frames of 0.1 s, such as studying ABS or traction control. So, since the model with axle pivot points is more generally useful and not much more computational demanding (and probably easier intuitively), that model is prioritized in this compendium.

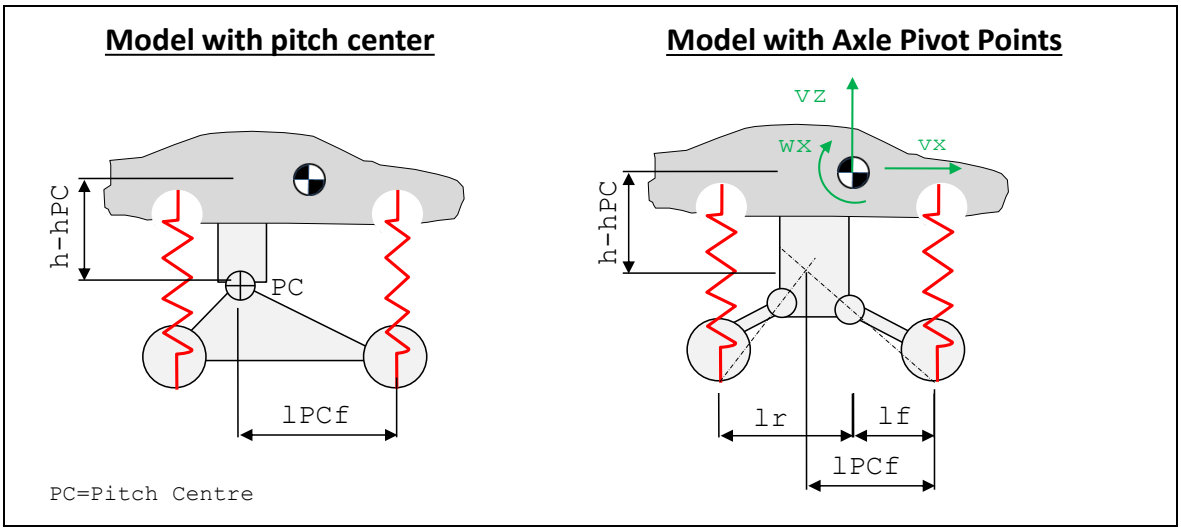

Figure 3-27: Models for including suspension effects in longitudinal load transfer

3.4.5.2.2 Model with Axle Pivot Points

Behold the free-body diagram in Figure 3-28. The road is assumed to be flat, $z_{fr} = z_{rr} \equiv 0$. The force play in the rear axle is shown in more detail. P_{xr} and P_{zr} are reaction forces in the pivot point. The F_{sr} is the force in the elasticity, i.e. where potential spring energy is stored. The torque T_{sr} is the shaft torque, i.e. from the propulsion system. Both torque from propulsion and brake system contribute to F_{xr}. But torque from friction brake $T_{reac,r}$ is not visible in free-body diagram, unless decomposed in suspension and wheel, as in the right-most part of Figure 3-28. This is because the friction braking appears as internal torque (or, depending on the brake design, probably forces) between brake pad and brake calliper. Any part of the longitudinal wheel force that is applied via reaction torque to unsprung parts will not add to shaft torque, such as an electric motor mounted on unsprung parts or propulsion via longitudinal propeller shaft to a final gear (as usual for rigid propelled axles).

The term $\omega_y \cdot v_x$ is easy to forget, but it does influence especially when v_x is large. The term can be explained as the other centripetal accelerations (giving centrifugal (fictive) forces) in 4.4.2.2.3. The term $\omega_y \cdot v_z$ is generally much smaller. Both the terms appear due to that velocities and accelerations are expressed as components in the vehicle fix (and hence rotating) coordinate system. We could introduce also velocities and accelerations in ground fix coordinate system, with subscripts differing between $[v_{xv}, v_{yv}]$ and $[v_{xg}, v_{yg}]$ and between $[a_{xv}, a_{yv}]$ and $[a_{xg}, a_{yg}]$, in a similar way shown in 4.4.2.3.3 for yaw rotation where it is much more important to differ between vehicle and ground fix.

We assume that displacements are measured from the forces F_{sf0} and F_{sr0}, respectively, and that the compliances are linear. The total constitutive equations become:

$$F_{sf} = F_{sf0} + c_f \cdot (\cancel{z_{fr}} - z_f); \quad and \quad F_{sr} = F_{sr0} + c_r \cdot (\cancel{z_{rr}} - z_r); \qquad [3.22]$$

Now, there are two ways of representing the dynamics in spring-mass systems: Either as second order differential equations in position or first order differential equations in velocity and force. We select the latter, because it is easier to select suitable initial values. Then we need the differentiated versions of the compliance's constitutive equations:

$$\dot{F}_{sf} = 0 + c_f \cdot (\cancel{\dot{z}_{fr}} - \dot{z}_f) = -c_f \cdot v_{zf}; \quad and \quad \dot{F}_{sr} = 0 + c_r \cdot (\cancel{\dot{z}_{rr}} - \dot{z}_r) = -c_r \cdot v_{zr}; \qquad [3.23]$$

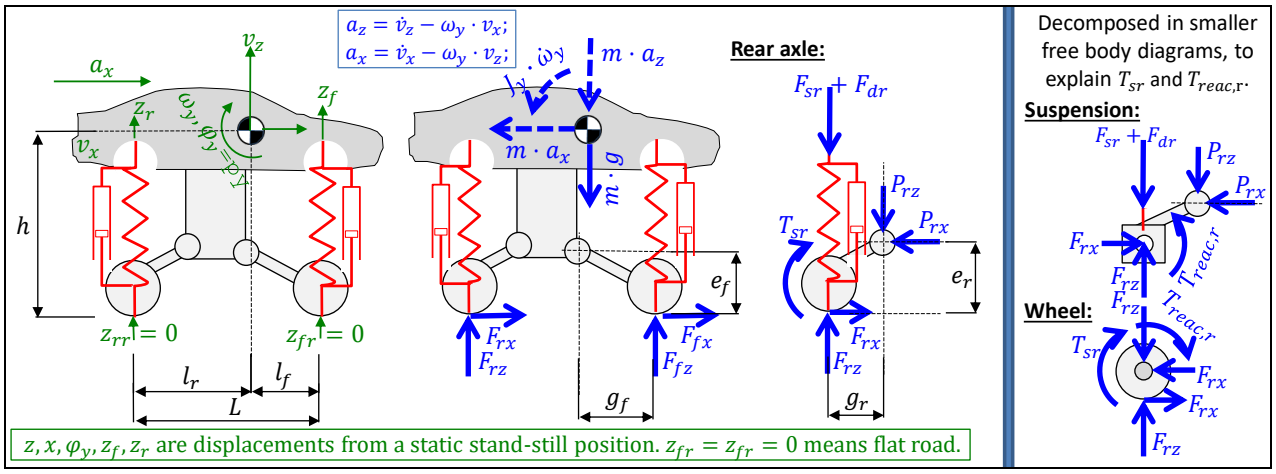

Figure 3-28: Free-body diagram for model with Axle Pivot Points. (The model assumes drive shafts from propulsion system mounted on body. If rigid shaft with longitudinal propeller shaft, $T_{sr} = 0$.)

The damper forces are denoted F_{df} and F_{dr}. They will appear in the equilibrium equations quite similar to F_{sf} and F_{sr}. Note that the damping coefficients, d_f and d_r, are the effective ones, i.e. the ones defined at the wheel contact point with ground, as opposed to the physical ones defined for the actual physical damper. C.f. effective stiffness in 3.4.5.

$$F_{df} = d_f \cdot \left(\dot{z}_{fr} - \dot{z}_f\right) = -d_f \cdot v_{zf}; \quad and \quad F_{dr} = d_r \cdot (\dot{z}_{rr} - \dot{z}_r) = -d_r \cdot v_{zr}; \qquad [3.24]$$

Now, 3 equilibria for whole vehicle and one moment equilibria around pivot point for each axle gives:

$$\begin{aligned}
&-m \cdot a_x + F_{xf} + F_{xr} = 0; \quad (with\ a_x = \dot{v}_x - \omega_y \cdot v_z \approx \dot{v}_x;)\\
&-m \cdot a_z - m \cdot g + F_{zf} + F_{zr} = 0; \quad (with\ a_z = \dot{v}_z - \omega_y \cdot v_x;)\\
&-J_y \cdot \dot{\omega}_y + F_{zr} \cdot l_r - F_{zf} \cdot l_f - \left(F_{xf} + F_{xr}\right) \cdot h = 0;\\
&(F_{zr} - F_{sr} - F_{dr}) \cdot g_r - F_{xr} \cdot e_r + T_{sr} = 0;\\
&\left(F_{sf} + F_{df} - F_{zf}\right) \cdot g_f - F_{xf} \cdot e_f + T_{sf} = 0;
\end{aligned} \qquad [3.25]$$

It can be noted that a "trivial suspension model" (as used in Eq [3.18] and see also Figure 2-54) falls out of the equations if we let $g_r \to \infty$ and $g_f \to \infty$. With such trivial model, there is no difference if the vehicle is actuated with a F_{xi} via shaft torque T_{si} or via reaction to unsprung parts, $T_{reac,i}$.

Compatibility, to connect to body displacements, z and φ_y, gives:

$$\begin{aligned}
&z_f = z - l_f \cdot \varphi_y; \quad and \quad z_r = z + l_r \cdot \varphi_y;\\
&v_{zf} = v_z - l_f \cdot \omega_y; \quad and \quad v_{zr} = v_z + l_r \cdot \omega_y;\\
&\dot{z} = v_z; \quad and \quad \dot{\varphi}_y = \omega_y;
\end{aligned} \qquad [3.26]$$

By combining constitutive relations, equilibrium and compatibility we can find explicit function so:

- $StateDerivatives = ExplicitFormFunction(States, Inputs);$
- $States = [v_x \quad v_z \quad \omega_y \quad F_{sf} \quad F_{sr} \quad z \quad \varphi_y];$
- $StateDerivatives = \left[\dot{v}_x \quad \dot{v}_z \quad \dot{\omega}_y \quad \dot{F}_{sf} \quad \dot{F}_{sr} \quad \dot{z} \quad \dot{\varphi}_y\right];$
- $Inputs = [F_{xf} \quad F_{xr} \quad T_{sf} \quad T_{sr}];$

The *ExplicitFormFunction* can be integrated with well-established methods for numerical ODE. Such simulation of is shown in 3.4.8.1. Note that the model is linear.

3.4.5.2.3 Additional Phenomena

It is relevant to point out the following, which are not modelled in this compendium:

- **Stiffness** and **damping** may be dependent of **wheel (vertical) displacement** and **wheel steer angle**. One way of inserting this in the model is to make the coefficients varying with spring force, which is a measure of how much compressed the suspension is. Here, non-linearity within spring working range, as well as bump stops, can be modelled. Also, **position of pivot points (or pitch and roll centres)** can be dependent of wheel displacement steer angle.

- Dampers are often **deformation direction dependent**, i.e. different damping coefficients are suitable to use for compression and rebound. Typical is 2..4 times softer (smaller d [N/(m/s)]) in compression than in rebound.

3.4.6 Steady State Heave and Pitch, Non-Trivial Linkage

If we study long term steady state for the model described in 3.4.5.2.2 we will find a steady state model comparable with the model in 3.4.5. So, Equations [3.22] to [3.26] are combined. We also neglect air resistance force for clarity of equations. Equation [3.22] becomes, in Matlab format:

```
sol=solve( ...
    F_sf==F_sf0-c_f*z_f, F_sr==F_sr0-c_r*z_r, ...
    F_sf0+F_sr0==m*g,    F_sf0*l_f-F_sr0*l_r==0, ...
    -m*a_x+F_fx+F_rx==0, ...
    -m*0-m*g+F_fz+F_rz==0, ...
    -J*0+F_rz*l_r-F_fz*l_f-(F_fx+F_rx )*h==0, ...
    (F_rz-F_sr-0 )*g_r-F_rx*e_r+T_sr==0,   ...
    (F_sf+0-F_fz )*g_f-F_fx*e_f+T_sf==0, ...
    z_f==z-l_f*p_y, z_r==z+l_r*p_y, ...
    F_sf0,F_sr0, F_fz, F_rz, z_f,z_r, a_x, F_sf,F_sr, z,p_y)

%results:
% ax = (F_xf + F_xr)/m
% z  = -(Tsr*cf*gf*lf^2 - Tsf*cr*gr*lr^2 + Tsr*cf*gf*lf*lr -
      Tsf*cr*gr*lf*lr - Fxr*cf*er*gf*lf^2 + Fxf*cr*ef*gr*lr^2 +
      Fxf*cf*gf*gr*h*lf + Fxr*cf*gf*gr*h*lf - Fxf*cr*gf*gr*h*lr -
      Fxr*cr*gf*gr*h*lr - Fxr*cf*er*gf*lf*lr +
      Fxf*cr*ef*gr*lf*lr)/(cf*cr*gf*gr*(lf + lr)^2)
% py = -(Tsr*cf*gf*lf + Tsr*cf*gf*lr + Tsf*cr*gr*lf +
      Tsf*cr*gr*lr + Fxf*cf*gf*gr*h + Fxr*cf*gf*gr*h +
      Fxf*cr*gf*gr*h + Fxr*cr*gf*gr*h - Fxr*cf*er*gf*lf -
      Fxf*cr*ef*gr*lf - Fxr*cf*er*gf*lr -
      Fxf*cr*ef*gr*lr)/(cf*cr*gf*gr*(lf + lr)^2)
% F_fz = -(F_fx*h + F_rx*h - g*l_r*m)/(l_f + l_r)
% F_rz =  (F_fx*h + F_rx*h + g*l_f*m)/(l_f + l_r)
```

[3.27]

The solution can be compared with corresponding solution in Equation [3.21]. The a_x is exactly the same. Then, a general reflection is that the displacement, z and py, in Equation [3.27] follows a complex formula, but that they are dependent on how the $F_{xw} = F_{xf} + F_{xr}$ is applied: both dependent on distribution between axles and dependent on how much of the axle forces (F_{xf} and F_{xr}) that are actuated with shaft torques (T_{sf} and T_{sr}, respectively). In Figure 3-29, dashed lines show the solutions from Equation [3.21].

3.4.7 Pitch Functions at Transient Wheel Torques

3.4.7.1 Dive at Braking *

*Function definition: **Dive at braking** is pitch angle of the vehicle body when applying a step in deceleration request to a certain level. Either peak pitch or quasi-steady state pitch angle can be addressed.*

Now, study the suspension at front axle in Figure 3-28. When the axle is braked, F_{xf} will be negative and push the axle rearwards, i.e. in under the body. The front of the vehicle will then be lifted as in pole jumping. This means that this design counter-acts the (transient) dive of the front. (Only the transient dive will be reduced, while the dive after a longer time of kept braking is dependent only on the stiffnesses according to Equation [3.21].) The design concept for front axle suspension to place the pivot point behind axle and above ground is therefore called “anti-dive”.

If the braking is applied without shaft torque T_{sf}, a good measure of the Anti-dive mechanism is e_f/g_f. This is the normal way for braking, since both the action and reaction torque acts on the axle. For inboard brakes, or braking via propulsion shaft, the reaction torque is not taken within the axle, but the reaction torque is taken by the vehicle body. The action torque T_{sf} then appears in the equilibrium equation for the axle, as shown in Equation [3.25]. If we neglect the wheel rotational dynamics for a while, we can insert $T_{sf} = F_{xf} \cdot R_w$ in the equation with T_{sf} in Equation [3.25]:

$$\begin{aligned}&\left(F_{sf} + F_{df} - F_{fz}\right) \cdot g_f - F_{fx} \cdot e_f + T_{sf} = 0; with\ T_{sf} = F_{fx} \cdot R_w;\ \Rightarrow \\ &\Rightarrow \left(F_{sf} + F_{df} - F_{fz}\right) \cdot g_f - F_{fx} \cdot e_f + F_{fx} \cdot R_w = 0; \Rightarrow \\ &\Rightarrow \left(F_{sf} + F_{df} - F_{fz}\right) \cdot g_f - F_{fx} \cdot \left(e_f - R_w\right) = 0;\end{aligned} \qquad [3.28]$$

We can then see that a good measure of the Anti-dive mechanism is $\left(e_f - R_w\right)/g_f$ instead.

3.4.7.2 Squat at Propulsion *

Function definition: ***Squat at propulsion*** *is pitch angle of the vehicle body when applying a step in acceleration request to a certain level. Either peak pitch or quasi-steady state pitch angle can be addressed.*

Now, study the suspension at rear axle in Figure 3-28. When the axle is propelled, F_{xr} will push the axle in under the body. This means that this design reduces the rear from squatting (transiently). The design concept for rear axle suspension to place the pivot point ahead of axle and above ground is therefore called "anti-squat".

3.4.7.3 Anti-dive and Anti-Squat Designs

With Anti-dive front and Anti-squat rear, we avoid front lowering at braking and rear lowering at acceleration, respectively. But how will the designs influence the parallel tendencies: that rear tend to lift at braking and front then to lift at propulsion? Well, they will luckily counteract also these: Braking at rear axle will stretch the rear axle rearwards and upwards relative to the body. When propelling the front axle, the propulsion force will stretch the front axle forwards and upwards relative to the body. (If one brakes at one axle and propels at the other, the reasoning is not valid. This mode can be desired for a hybrid vehicle with ICE on front axle and electric motor on rear axle, if one would like to charge batteries "via the road".)

In summary: Anti-dive and anti-squat refer to the front diving when braking and the rear squatting when acceleration. Anti-dive and anti-squat can be measured in fractions: Anti-dive for $=e_f/g_f$ or $= \left(e_f - R_w\right)/g_f$ and Anti-squat$=e_r/g_r$ or $= (e_r - R_w)/g_r$. Normal values are typically 0.05..0.15.

3.4.8 Acceleration and Deceleration

Acceleration performance like, typically, 0-100 km/h over 5..10 s, was addressed in 3.3.6. In present Section we address the similar functionality but include larger transients, such as when wheel longitudinal wheel force is changed more rapidly, typically changing $\pm\mu \cdot F_z/2$ during 0.2-0.5 s.

3.4.8.1 Deceleration Performance *

Function definition: See 3.4.2.2.

Deceleration performance can now be predicted, including the suspension mechanisms. It is a very important function, and every decimetre counts when measuring braking distance in standard tests like braking from 100 to 0 km/h. The active control of the brake torques (ABS function) is then very important, and this is so fast dynamics that the suspension mechanisms of Anti-lift and Anti-dive influences. The position of the load in the vehicle will influence, since it influences the load transfer.

We will now set up a mathematical model, see Equation [3.29], which shows how the normal forces change during a braking event. It is based on the physical model in Figure 3-28. Driving resistance contributes normally with a large part of the deceleration, but we will neglect this for simplicity, just to show how the suspension mechanism works. The equations in the model are presented in the dynamic modelling standardized format "Modelica", and are hence more or less identical to Equation [3.23] to [3.26]. (The term $\omega_y \cdot v_z$ is included but makes no visible difference.)

```
Ffx = if 1 < time and time < 3 then -0.4*m*g else 0;
Frx = if 3 < time and time < 7 then -0.4*m*g else 0;
Tsf/Rw = 0;
Tsr/Rw = if 5 < time and time < 7 then -0.4*m*g else 0;

// Motion equations:
der(z) = vz;
der(py) = wy;

// Constitutive equations for the springs:
der(Fsf) = -cf*vfz;
der(Fsr) = -cr*vrz;

// Constitutive equations for the dampers:
Fdf = -df*vfz;
Fdr = -dr*vrz;

//(Dynamic) Equilibrium equations:
-m*(der(vx)-vz*wy) + Ffx + Frx = 0;
-m*(der(vz)-vx*wy) - m*g + Ffz + Frz = 0;
-Jy*der(wy) + Frz*lr - Ffz*lf - (Ffx + Frx)*h = 0;
(Frz - Fsr - Fdr)*gr - Frx*er + Tsr = 0;
(Fsf + Fdf - Ffz)*gf - Ffx*ef + Tsf = 0;

//Compatibility:
zf = z - lf*py;
zr = z + lr*py;
vfz = vz - lf*wy;
vrz = vz + lr*wy;
```

[3.29]

The simulation results are shown in Figure 3-29. It shows a constant deceleration, but it is changed how the decelerating force is generated. At time=3 s, there is a shift from braking solely on front axle to solely on rear axle. The braking is, so far, only done with friction brakes, i.e. generating torque by taking reaction torque in the axle itself. At time=5 s, there is a shift from braking with friction brakes to braking with shaft torque. It should be noted that if we shift axle or shift way to take reaction torque, gives transients even if the deceleration remains constant.

One can also see, at time=1 s, that the normal load under the braked axle first changes in a step. This is the effect of the Anti-dive geometry. Similar happens when braking at rear axle, due to the Anti-squat geometry. Since brake performance is much about controlling the pressure rapidly, the transients are relevant, and the plots should make it credible that it is a control challenge to reach a high braking efficiency.

3.4.8.2 Acceleration Performance *

Function definition: See 3.3.6.1.

The model presented in Equation [3.29] can also be used to predict acceleration performance in a more accurate way compared to 3.3.6. Especially, the more accurate model is needed when propelling or braking on the limit of tyre to road adhesion, since the normal load of each tyre then is essential. It is a challenge to control the propulsion and brake wheel torques to utilize the varying normal loads under each axle.

3.4.9 Other Functions

There are many more longitudinal functions, originating from the attribute Driving dynamics, which could have fitted in 3.4. Examples of such:

- Off-road accessibility: Ability to pass obstacles of different kind, such as uneven ground, extreme up- and down-hills, mud depth, snow depth, etc.
- Shift quality: Quick and smooth automatic/automated gear shifts
- Shunt & shuffle: Absence from oscillation for quick pedal apply, especially accelerator pedal.

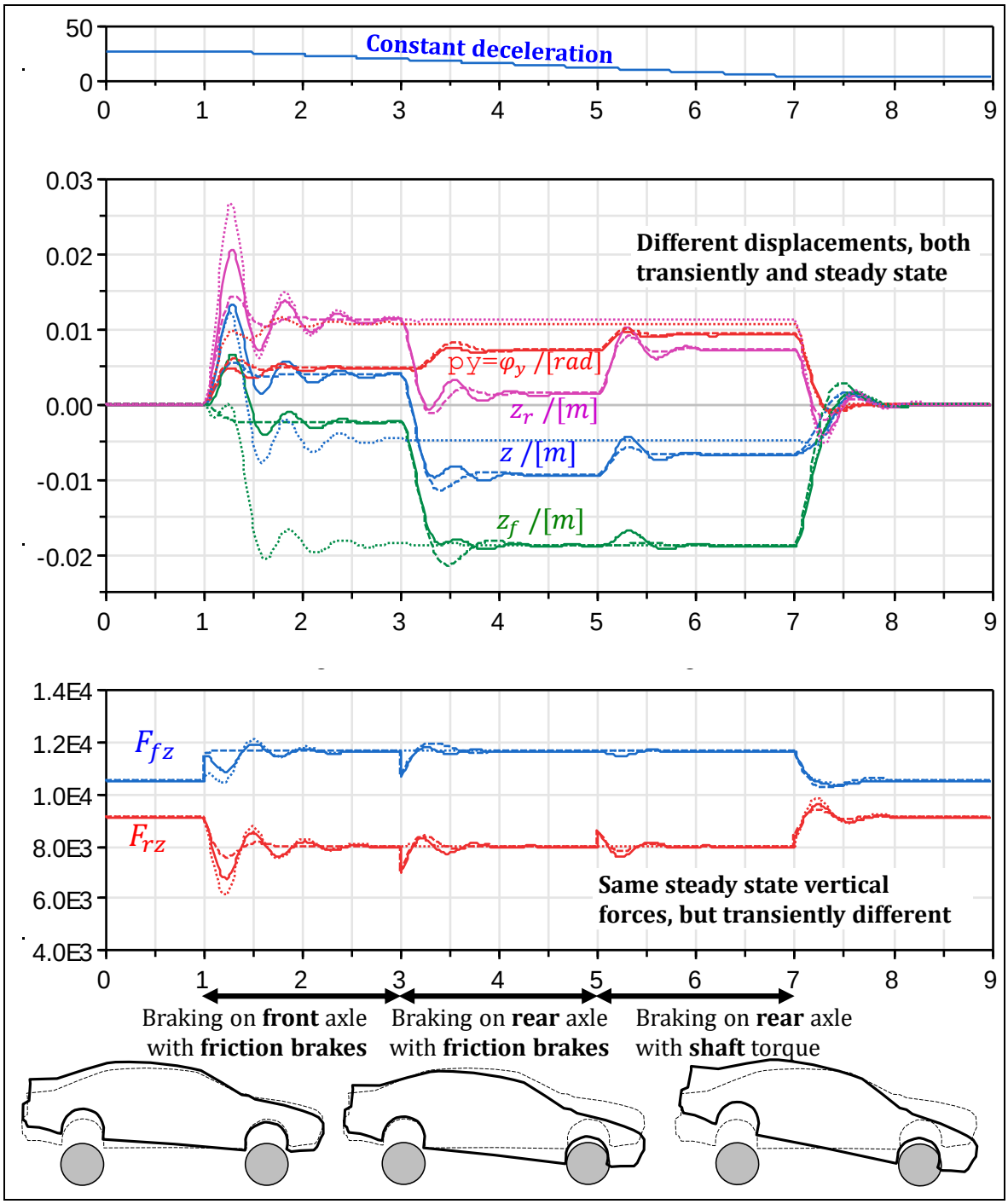

Figure 3-29: Deceleration sequence with constant vehicle deceleration but changing between different ways of actuation. (With the centripetal term $\omega_y \cdot v_x$ (solid) and without (dashed). Dotted shows without anti-dive/-squat geometry, i.e. $g_f = g_r = \infty$. The term $\omega_y \cdot v_z$ makes no visible difference.)

3.5 Control Functions

Some control functions will be described. First, some general aspects on control are given.

3.5.1 Longitudinal Control

Some of the most important sensors available in production vehicles and used mainly for longitudinal control are listed below. (Sensors for instrumented vehicles for testing can be many more.)

- **Wheel Speed Sensors**, WSS. For vehicle control design, one can often assume that "sensor-close" software also can supply information about longitudinal vehicle speed.
- **Vehicle body inertial sensors.** There is generally a yaw velocity gyro and a lateral accelerometer available, but sometimes also a longitudinal accelerometer. The longitudinal accelerometer is useful for longitudinal control and longitudinal velocity estimation.
- **Pedal sensors**. Accelerator pedal normally has a position sensor and brake pedal force can be sensed via brake system main pressure sensor. Heavy vehicles often have both a brake pedal position and brake pressure sensors.
- Today's vehicles have **environment sensors** (camera, radar, GPS with electronic map, etc.) that can give information (relative distance and speed, etc.) about objects ahead of subject vehicle. It can be both fixed objects (road edges, curves, hills, …) and moving objects (other road users, animals, …). See also *2.7* Environment Sensing System.
- Information about what actuation that is **actually applied at each time instant** is available, but it should be underlined that the confidence in that information often is questionable. Information about axle propulsion torque is generally present, but normally relies on imprecise models of the whole combustion process and torque transmission, based on injected amount of fuel and gear stick position. (Electric motors can typically give better confidence in estimation, especially if motor is close to the wheel without too much transmission in between.) Wheel individual friction brake torque is available, but normally rely on imprecise models of the brake systems hydraulic/pneumatic valves and disc friction coefficient, based on brake main cylinder pressure.
- Information about what **actuation levels that are possible** upon request (availability or capability) is generally not so common. It is difficult to agree of general definitions of such information, because different functions have so different needs, e.g. variations in accepted time delay for actuation.
- Sometime **wheel/axle forces** can be sensed. One case is when pneumatic suspension. More extreme variants are under development, such as sensors in the wheel bearings which can sense forces (3 forces and roll and yaw moment) and sensors in shafts.

3.5.2 Longitudinal Control Functions

3.5.2.1 Pedal Driving *

Function definition: See 3.4.3.

These functions, Pedal Functions

Pedal Response *, are often not seen as comparable with other control functions, but they become more and more relevant to define as such, since both accelerator and brake pedals tend to be electronically controlled, and hence they become increasingly tuneable. Also, more and more functions, such as those below in 3.5.2, will have to be arbitrated with the pedals.

In modern passenger vehicles, Accelerator pedal is normally electronically controlled but the Brake pedal is basically mechanical. In modern heavy commercial vehicles, both functions are electronically controlled.

The functions in "3.4.3.2 Pedal Feel *" are normally not actively controlled, but in there are concept studies with active pedals, where also the pedal feel can be actively changed to give feedback to driver.

3.5.2.2 Cruise Control and Adaptive Cruise Control (CC, ACC) *

Function definition: ***Cruise Control, CC,*** *controls the vehicle's longitudinal speed. Driver can activate the function and decide desired speed.*

Function definition: ***Adaptive Cruise Control, ACC,*** *is an addition to CC. ACC controls the vehicle's time gap to a lead vehicle. Driver can activate the function and decide desired gap. When there is no lead vehicle, CC controls the vehicle's speed.*

The purpose of CC is to keep the vehicle at a driver selected longitudinal speed, while driver not pushes the accelerator pedal. The actuator used is the propulsion system. In heavy vehicles, also the braking system (both retarders and service brakes) is used to maintain or regulate the vehicle speed.

ACC is an addition to CC. The purpose of ACC is to keep a safe distance to the lead vehicle (vehicle ahead of subject vehicle). ACC uses also friction brake system as actuator, but normally limited to a deceleration of 2..4 m/s^2.

The safe distance which ACC aims for, is often expressed as a time gap, driver adjustable in the range 2..3 s. A model behind this is that the time gap is the driver reaction time and the subject vehicle can decelerate as much as the object vehicle. More advanced models can allow smaller time gap in certain situations. This is desired because it reduces the risk that other vehicles cut in between subject and leading object vehicle. Such models can consider, e.g., acceleration of the object vehicle, pedal operation of subject vehicle, road gradient, road curvature, road friction and deceleration capabilities of subject and object vehicles.

Pedals and CC/ACC has to be arbitrated. Typically, accelerator pedal wins temporarily if pressed to higher request than CC/ACC, while any use of brake pedal turns off (wins permanently over) the CC/ACC .

CC is normally only working down to 30.. 40 km/h. ACC can have same limitation, but with automatic transmission, good forward-looking environment sensors, brake actuators and speed sensing, ACC can be allowed down to stand-still.

3.5.2.2.1 Topography adapted CC

A development of CC has varying set speed which is optimized for a predicted road topography about a minute ahead. Such products are on the market, e.g. Volvo iSee and Scania Active Prediction.

3.5.2.3 Anti-Lock Braking System, ABS *

Function definition: ***Anti-lock Braking System, ABS****, prohibits driver to lock the wheels while braking. The wheel brake torques requested are limited by ABS in a way that each individual wheel's longitudinal slip stays above a certain (negative) value. An extended definition of ABS also includes vehicle deceleration requested by other functions than pedal braking, such as AEB.*

The purpose of ABS is to avoid losing vehicle brake force due to that the tyre force curve drops at high slips AND to leave some friction for steering and cornering, see 2.2.1.6 and 2.2.4.6.5. ABS is a wheel slip closed loop control, active when driver brakes via brake pedal. It keeps the slip above a certain value, typically -15..-20 %. ABS uses the friction brakes as actuator.

Each wheel is controlled individually, but all wheels' speed sensors contribute to calculation of vehicle longitudinal speed, for calculation of actual slip. In the ABS function, it may be included how slip are distributed between the wheels, such as normally the front axle is controlled to a slip closer to locking than the rear axle. Also, a sub-function called "select-low" which makes the wheel closest to locking decide the pressure also for the other wheel at the same axle. Select-low is typically used at rear axles.

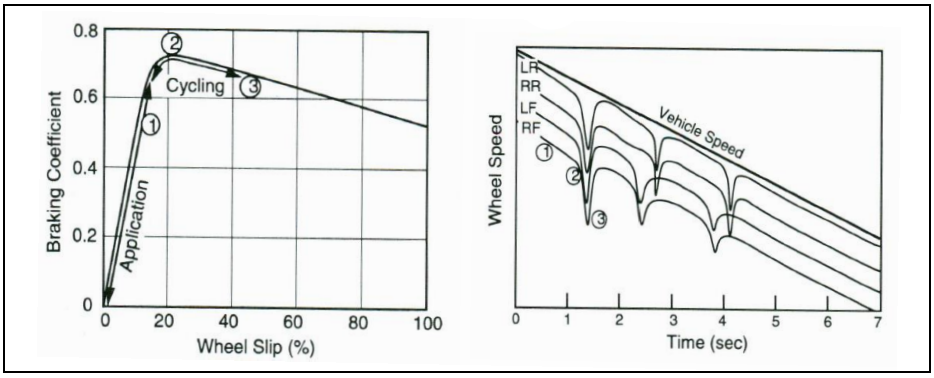

Figure 3-30: ABS control. Principle and control sequence, from Ref (Gillespie, 1992)

3.5.2.4 Electronic Brake Distribution, EBD *

Function definition: ***Electronic Brake Distribution*** *prohibits driver to over-brake the rear axle while braking. An extended definition of EBD also includes vehicle deceleration requested by other functions than pedal braking, such as AEB. EBD only uses friction brake as actuator.*

With a fix proportioning between front and rear axle braking, there is a risk to over-brake rear axle when friction is very high, since rear axle is unloaded so much then. Before electronic control was available, it was solved by hydraulic valves, which limited the brake pressure to rear axle when pedal force became too high. In today's cars, where electronic brake control is present thanks to legislation of ABS, the software base function EBD fulfils this need. EBD is primarily a feedforward control of $a_{x,Request}$ and $v_{x,Actual}$. Good estimates of mass, CoG location in x and z direction would be useful, but these are seldom available. EBD can also have feedback of longitudinal slip difference between axles. In heavy vehicles, pneumatic valves are used that limits the brake pressure in relation to the rear axle load (deflection of mechanical spring suspension or air pressure in air suspension).

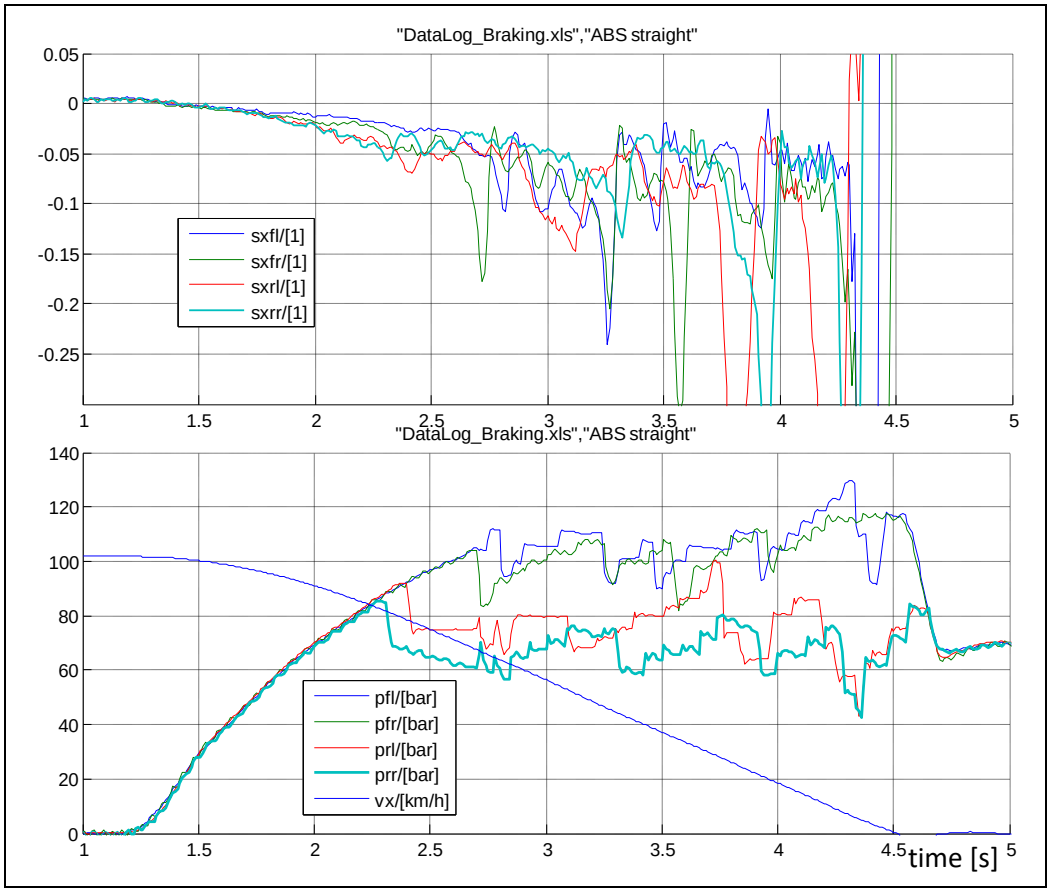

Figure 3-31: ABS control, Data log from passenger car test.

There are other side functions enabled by having ABS on-board. Such are "select low", which means that the brake pressure to both wheels on an axel is limited by the one with lowest pressure allowed from ABS. So, if one wheel comes into ABS control, the other gets the same pressure. This is most relevant on rear axle (to reduce risk of losing side grip) but one tries to eliminate the need of it totally, because it reduces the brake efficiency when braking in curve or on different road friction left/right.

It is often difficult to define strict border between functions that is a part of ABS and which is part of EBD, which is why sometimes one say ABS/EBD as a combined function.

3.5.2.5 Traction Control, TC *

Function definition: ***Traction Control*** *prohibits driver to spin the driven axle(s) in positive direction while accelerating. An extended definition of TC also includes vehicle acceleration requested by other functions than pedal braking, such as CC. TC uses both friction brakes and propulsion system as actuators.*

The purpose of Traction Control is to maximise traction AND to leave some friction for lateral forces for steering and cornering. Traction control is similar to ABS, but for keeping slip below a certain value, typically +(15..20)%.

Traction control can use different ways to control slip, using different actuators. One way is to reduce engine torque, which reduces slip on both wheels on an axle if driven via differential. Another way is to apply friction brakes, which can be done on each wheel individually. Vehicles with propulsion on several axles can also redistribute propulsion from one axle to other axles, when the first tends to slip. Vehicles with transversal differential clutch or differential lock can redistribute between left and right wheel on one axle.

3.5.2.6 Engine Drag Torque Control, EDC *

Function definition: ***Engine Drag Torque Control*** *prohibits over-braking of the driven axle(s) while engine-braking. EDC uses both friction brakes and propulsion system as actuators.*

The purpose of Engine Drag Torque Control is as the purpose of ABS, but the targeted driving situation is when engine braking at low road friction, when engine drag torque otherwise can force the wheels to slip too much negative. Similarly to ABS, it keeps the slip above a certain negative value. However, it does it by increasing the engine torque from negative (drag torque) to zero (or above zero for a short period of time).

3.5.2.7 Automatic Emergency Brake, AEB *

Function definition: ***Automatic Emergency Brake*** *decelerates vehicle without driver having to use brake pedal when probability for forward collision is predicted as high.*

The purpose of AEB is to eliminate or mitigate collisions where subject vehicle collides with a lead vehicle. AEB uses friction brake system as actuator, up to full brake which would be typically 10 m/s2. An AEB system is often limited by not trigger too early, because driver would be disturbed, or it could actually cause accidents. Therefore, in many situations, AEB will rather mitigate than avoid collisions.

Conceptually, an AEB algorithm can be assumed to know physical quantities as marked in Figure 3-32. The quantity time-to-collision, TTC, can then be defined as $TTC = x_o/(v_{sx} - v_{ox})$, which means the time within a collision will appear if no velocities changes. Subscript s and o means subject and object vehicle, respectively.

Also, one can define enhanced time-to-collision measure, eTTC, which considers the present accelerations of the lead vehicle. TTC shall not be mixed up with “time gap” (TG), which is the time when subject vehicle will reach the present position of the lead vehicle, $TG = x_o/v_{sx}$;.

AEB function shall, continuously, decide whether or not to trigger AEB braking. AEB shall intervene by braking when driver can be assumed to collide without intervention. If no other information, this can be predicted as when driver can NOT avoid by normal driving. Avoidance manoeuvres that have to be considered are (normal) deceleration and (normal) lateral avoidance to the left and to the right. What to assume as normal driving is a question of tuning; here the following limits are used $|\dot{v}_{sx}| < a_{sxn} = e.g. 4\ m/s^2$ and $|\dot{v}_{sy}| < a_{syn} = e.g. 6\ m/s^2$. The concept of a physical model-based algorithm is this:

- Normal **deceleration** ($\dot{v}_{sx} = -a_{sxn} = -4\ m/s^2$) leads to **collision if**:
  $\min_{t>0}(x_o(t)) < 0 \quad \Rightarrow \quad \min_{t>0}(x_o + v_{ox}\cdot t - (v_{sx}\cdot t + a_{sxn}\cdot t^2/2)) < 0 \quad \Rightarrow$
  $\Rightarrow \quad (x_o + v_{ox}\cdot t - (v_{sx}\cdot t + a_{sxn}\cdot t^2/2))\big|_{t=\frac{v_{ox}-v_{sx}}{a_{sxn}}} < 0 \quad \Rightarrow$
  $\Rightarrow \quad x_o - \frac{1}{2\cdot(-a_{sxn})}\cdot(v_{sx}-v_{ox})^2 < 0 \quad \Rightarrow \quad \frac{x_o}{v_{sx}-v_{ox}} < \frac{v_{sx}-v_{ox}}{2\cdot(-a_{sxn})} \quad \Rightarrow \quad \boldsymbol{TTC < \frac{v_{sx}-v_{ox}}{8}}$;
- Normal **avoidance to the left** ($\dot{v}_{sy} = a_{syn} = 6\ m/s^2$) leads to **collision if**:
  $\left(y_{ol}(t) + \frac{w}{2}\right)\Big|_{x_o=0} < 0 \quad \Rightarrow \quad \left(y_{ol} - a_{syn}\cdot\frac{t^2}{2} + \frac{w}{2}\right)\Big|_{t=\frac{x_o}{v_{sx}-v_{ox}}} < 0 \quad \Rightarrow$
  $\Rightarrow \quad \frac{x_o}{v_{sx}-v_{ox}} < \sqrt{2\cdot\frac{y_{ol}+w/2}{a_{syn}}} = \{e.g.\} = \sqrt{\frac{0.6+1.8/2}{3}} \approx 0.4\ s \quad \Rightarrow \quad \boldsymbol{TTC < 0.4\ s}$;

- Normal **avoidance to the right** ($\dot{v}_{sy} = -a_{syn} = -6\ m/s^2$) leads to **collision if**:
  $\cdots \Rightarrow \frac{x_o}{v_{sx}-v_{ox}} < \sqrt{2 \cdot \frac{-y_{or}-w/2}{a_{syn}}} = \cdots \Rightarrow \boldsymbol{TTC < 0.4\ s}$;
- Assuming that the AEB intervention decelerates the vehicle with $-\dot{v}_{sx} = a_{sxAEB} = -8\ m/s^2$, a forward collision can be avoided if AEB intervenes AND if:
  $\cdots \Rightarrow \frac{x_o}{v_{sx}-v_{ox}} > \frac{\boldsymbol{v_{sx}-v_{ox}}}{\boldsymbol{2\cdot(-a_{sxAEB})}} = \frac{v_{sx}-v_{ox}}{16} \Rightarrow \boldsymbol{TTC > \frac{v_{sx}-v_{ox}}{16}}$;

Figure 3-32 shows a diagram where different condition areas are marked. The sectioned area shows where AEB will be triggered, using above rules. The smaller of the sectioned areas shows where it also will be possible to trigger AEB so timely that a collision is actually avoided; with the assumed numbers, this is for speeds up to 6.4 m/s≈23 km/h.

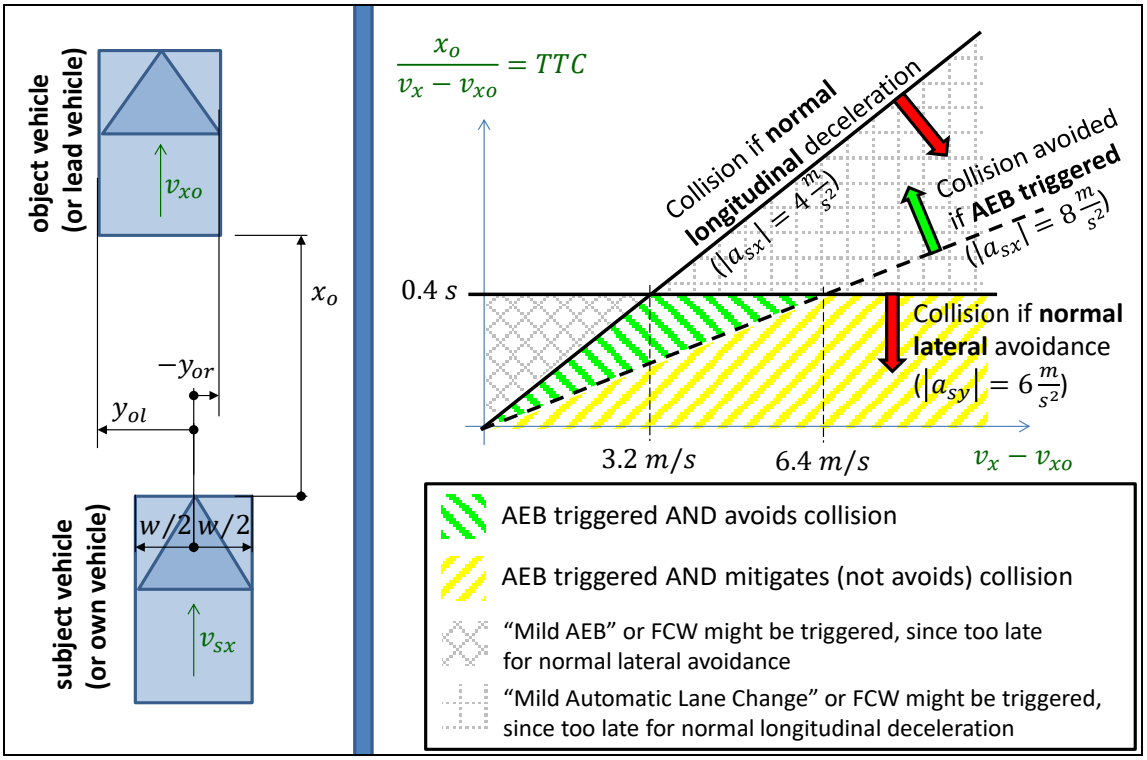

Figure 3-32: Left: Quantities known for an AEB algorithm in the subject vehicle, assuming "symmetrically behind" ($y_{ol} = -y_{or}$). Right: Model based decision of triggering AEB and effectiveness of AEB if triggered.

The reasoning above is very simplified. Additional information can improve effectiveness of AEB, such as knowing if a lateral avoidance on one side of object vehicle is blocked, the acceleration of the object vehicle, pedal operation of subject vehicle, road gradient, road curvature and road friction is. The vehicle dynamics model used is simply a point mass with predicted constant velocity and certain assumed acceleration capability, which of course can be extended a lot; both with taking actual accelerations into account and more advanced vehicle dynamics models. The decision to intervene is dependent of many pieces of information and simple models; vehicle dynamics and driver behaviour (in both subject and object vehicles) as well as road characteristics. AEB function has to be designed together with other similar functions, such as ACC and Forward Collision Warning (FCW).

AEB is on market and legal requirement for both passenger vehicles and heavy vehicles (ISO19377, 2017).

Related functions are, e.g. extra force assistance in brake pedal when driver steps quickly onto brake. Another related function is automatic braking triggered by a first impact and intended to mitigate or avoid secondary accident events, starts to appear at market, see Reference (Yang, 2013). In semantic meaning, this could be seen as AEB, but they are normally not referred to as AEB; AEB normally refers to functions that use environment sensors (forward directed radar, camera, etc.).

When designing and evaluating AEB, it is important to also know about the function Forward Collision Warning, FCW. FCW is a function that warns the driver via visual and/or audio signals when a forward collision is predicted. FCW is typically triggered earlier than AEB.

AEB as described above could be called “Rear-end AEB”. Another similar functionality, not included in today’s AEB, could be called “Intersection AEB” and include braking for intersecting traffic, see (Sander, 2018).

3.5.3 Longitudinal Motion Functionality in a Reference Architecture

All control functions controls have to cooperate, and they have to be transferable between platforms and vehicle variants. It is very complex to take all functions into consideration, but with a scope limited to the longitudinal Motion functionality

Figure 3-33 can be drawn as a solution within the reference architecture.

By using a reference architecture, it can be illustrated that Adaptive Cruise control and cruise control can be seen as part of Traffic Situation Layer (ACC=CC if no vehicle ahead). The Traffic Situation Layer has the purpose and scope to understand the ego vehicle’s surrounding traffic by looking at e.g. Forward Sensors. The forward-looking sensor is in this case part of Vehicle Environment sensors.

Vehicle Motion and Coordination Layer would include the arbitration of Driver’s Acceleration and Brake pedal input and Traffic functionality, see Figure 3-33. In addition, Vehicle Motion and Coordination Layer would perform the powertrain coordination and brake distribution. The coordinated requests are then sent to Motion Support Device Layer.

The Human Machine Interface would include the services available for the driver to activate or request, E.g. ACC activation to Traffic Situation or Deceleration by pressing the brake pedal.

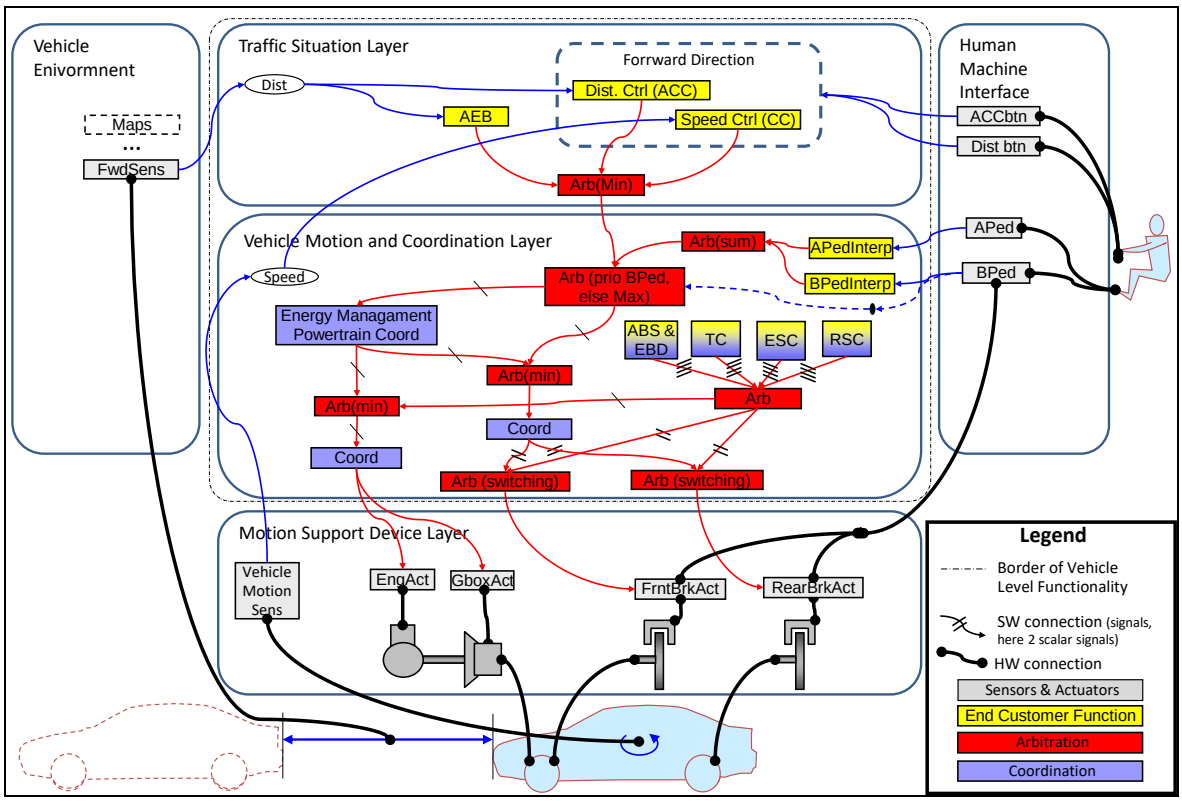

Figure 3-33: Functional architecture for conventional front axle driven passenger car. Mainly longitudinal functions (plus ESC, RSC) are shown, e.g. no steering. Cf. ***Figure 1-28****.*

If a reference architecture is used, it can assist function developers from OEM’s Electrical, Powertrain, and Chassis departments and suppliers to have a common view of how vehicle’s embedded motion

functionality is intended to be partitioned and to understand how different functions relate and interact with each other and what responsibilities they have.

4 LATERAL DYNAMICS

4.1 Introduction

The lateral motion of a vehicle is needed to follow the road curves, select route in intersections and laterally avoid obstacles, which all involve steering. Vehicle steering is studied mainly through the vehicle degrees of freedom: yaw rotation ω_z and lateral translation v_y.

A vehicle can be steered in different ways:

- Applying steer angles on road wheels. Normally both of front wheels are steered with approximately same angle. Steering system described in 0.
- Applying longitudinal forces on road wheels; directly by unsymmetrical between left and right side of vehicle, e.g. one-sided braking, or indirectly by deliberately use up much friction longitudinally on one axle in a curve, so that that axle loses lateral force.
- Articulated steering, where the axles are fixed mounted on the vehicle body, but the vehicle itself can bend.

The turning manoeuvres of vehicles encompass two sub-attributes. Handling is the driver's perception of the vehicle's response to the steering input. Cornering is the physical response (open-loop) of the vehicle independent of how it influences the driver.

The lateral dynamics of vehicles is often experienced as the most challenging for the new automotive engineer. Longitudinal dynamics is essentially motion in one plane and rectilinear. Vertical dynamics may be 3 dimensional, but normally the displacements are small and in this compendium the vertical dynamics is mainly studied in one plane as rectilinear. However, lateral dynamics involves motion in the vehicle coordinate system which introduces curvilinear motion since the coordinate system is rotating as the vehicle yaws.

The chapter introduces the models, more or less, in order of increasing number of states. For some readers, it might be comprehensive to start with a look-ahead on the "linear 1-track model" in 4.4.2. This is the simplest model which yet captures the essential lateral motion quantities v_y and ω_z as states. The models earlier in the chapter can then be seen as simplifications.

4.1.1 Lateral Model Categorization

The chapter is organised as shown in Table 4.1. The table also shows a high-level categorization of functions/models in the sections. Generally speaking, the input is steer angle δ and the output is yaw rate ω_z and lateral velocity v_y. The longitudinal speed v_x is often treated as a parameter ($\dot{v}_x \equiv 0$).

Table 4.1: Approximate high-level categorization of lateral functions/models

Section	Longitudinal velocity v_x	Typical input variables or parameters	Typical output variables
4.2 Low Speed	Parameter, $v_x \equiv 0^+ \; or \; 0^- \; [m/s]$	Path limitations, like road width and radius	Path $x(s), y(s), \varphi_z(s)$, i.e. v_x, v_y, ω_z integrated over the manoeuvre
4.3 Steady State Cornering at High Speed	Parameter, $v_x = 10..30 \; [m/s]$	v_x and Path radius R_p	Steady states $\delta(R_p, v_x)$, $v_y(\delta, v_x), \omega_z(\delta, v_x)$ and $a_y(\delta, v_x)$
4.4 Stationary Oscillating Steering	Parameter, $v_x = 10..30 \; [m/s]$	v_x, Steering amplitude $\hat{\delta}$, Frequency f	Stationary oscillating responses $\hat{\omega}_z(\hat{\delta}, f)$ and $\hat{a}_y(\delta, v_x)$
4.5 Transient Driving	Variable, $\dot{v}_x \neq 0$	Initial v_{x0}, Steering $\delta(t)$, Wheel torques ($\boldsymbol{T}(t)$)	<Numerous and various>
	Parameter, $v_x = 0..30 \; [m/s]$	Pure and simplified handling manoeuvres, such as "4.5.3.4 #Draft: (Example Step Steering Response *"	

There are other categorizations in 1.5.6, such as *irp/oorp* and *1-track/2-track*. Categorization of *tyre* models is found in 2.2.6.

4.1.2 References for this Chapter

- **0** and *"Chapter 25 Steering System"* in Ref (Ploechl, 2013).
- *"Chapter 27 Basics of Longitudinal and Lateral Vehicle Dynamics"* in Ref (Ploechl, 2013).
- *"Chapter 8: Electronic Stability Control"* in Ref (Rajamani, 2012)

4.2 Low Speed Manoeuvres

This section is about operating vehicles in low speeds, including stand-still and reverse. Specific for low speed models is that inertia effects can be neglected, i.e. one can neglect $m \cdot a_y$ in equilibrium equation. In low speed, one often needs to find the path $[x(s), y(s)]$ of the vehicles body edges, which can be obtained from CoG path with orientation, see 1.5.7.5.

4.2.1 Low Speed Model, Ackermann, without Forces

Low speed manoeuvres are characterised by that the inertial forces are neglected, i.e. $m \cdot a = 0$. If the geometry is according to Ackermann and the forces on the vehicle are small, it is reasonable to assume that the tyre forces also are small, and we can use *ideally tracking* tyre model for wheels or axles, see 2.2.6. We can see this as Eq [2.36] with infinite cornering stiffness: Eq [2.36] $\Rightarrow F_y = -C_y \cdot s_y \to \infty \cdot s_y; \Rightarrow s_y = 0; \Rightarrow v_{yw} = 0;$. The tyre force F_y can be any (finite) value, determined by other part of the system than the tyre. This tyre model can be seen as a compatibility relation (or "kinematic model"), since it relates velocities to eachother without involving any force. However, in this compendium we still consider it as a constitutive model, keeping in mind that it is definitely invalid if $F_y > \mu \cdot F_z;$.

The effects of ideal tracking are that the intersection point of the wheels rotational axes coincides with the instantaneous centre of vehicle rotation in ground plane. This directly relates steer angles and path radius to each other. For the one-track model in Figure 1-25 this relation becomes:

$$\left.\begin{aligned} \tan(\delta_f) &= \frac{L}{R_r}; \\ R^2 &= {R_r}^2 + {l_r}^2; \end{aligned}\right\} \Rightarrow \delta_f = \arctan\left(\frac{L}{\sqrt{R^2 - {l_r}^2}}\right) \cdot \text{sign}(R) \approx \frac{L}{\sqrt{R^2 - {l_r}^2}} \cdot \text{sign}(R) \approx \frac{L}{R}; \quad [4.1]$$

$$where\ R > 0\ means\ that\ instantaneous\ centre\ of\ rotation\ is\ left\ of\ the\ vehicle$$

4.2.2 Low Speed Functions

4.2.2.1 Turning Diameter *

Function definition: ***Turning diameter*** *is the diameter of the smallest possible circular path obtained steady state at low speed, measured to a certain point at the vehicle. The certain point can be either outer-most point on wheel (Kerb Turning diameter) or outer-most point on body (Wall Turning diameter).*

The end of the simulation in Figure 4-5 is made with constant steer angle. If we assume that it is the maximum steer angle, the circle actually shows the turning circle for centre of gravity. If we add the path for the outermost wheels, we get the kerb turning diameter, see Figure 4-1. If we add the path for the outermost point at the vehicle body we get the wall turning diameter, also shown in Figure 4-1. The outermost point at the vehicle body is normally the front outer corners of the vehicle body.

4.2.2.2 Swept Path Width, SPW *

Function definition: ***Swept path width*** *is the distance between the outermost and innermost paths of wheels (or body points). The paths are then from a certain turning or lane change manoeuvre at a certain speed.*

For manoeuvrability, there is a function which is complementary to turning diameter. It is "Swept Path Width" (SPW), see Figure 4-1. It can be defined for circle driving with maximum steering angle, as Turning diameter, but also for any other certain manoeuvre. It can be defined for kerb and wall; distance between wheels or body points. The SPW should be small for good manoeuvrability.

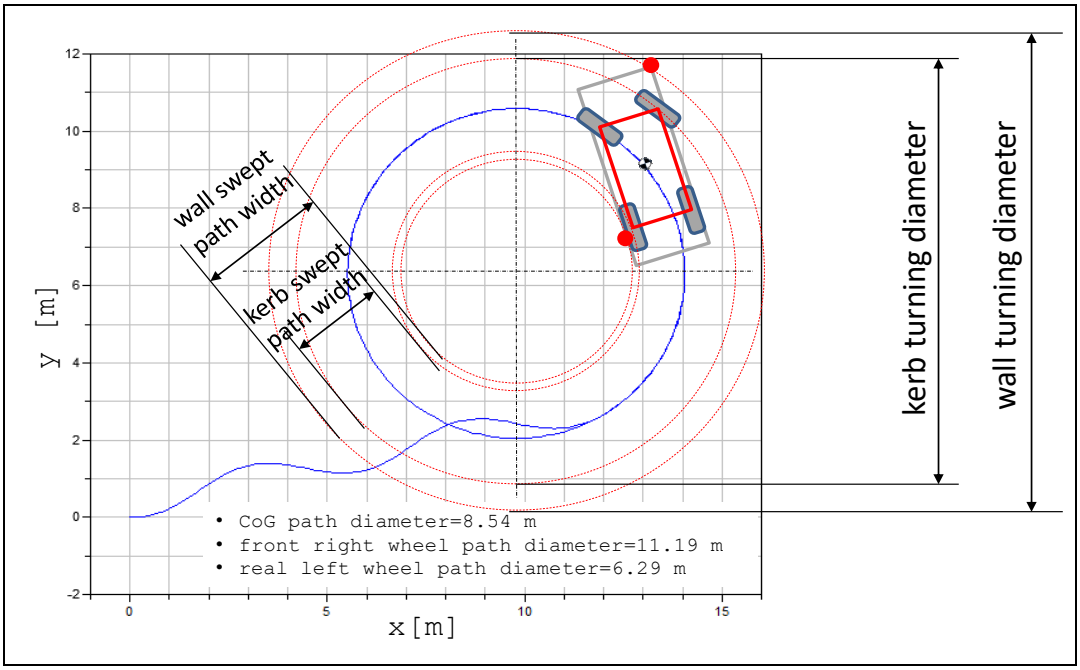

Figure 4-1: Paths for wheels and body points (added to result in Figure 4-5).

4.2.2.3 Low Speed Off-Tracking, LSOT *

*Function definition: **Off-tracking** is the distance between the outermost and innermost paths of mid-points of axles. The paths are then from a certain turning or lane change manoeuvre at a certain speed.*

Another measure of manoeuvrability is "Off-tracking", see Figure 4-2. It is like Swept Path Width, but for the mid points of the axles. It is also used for higher speeds, and then the rear axle often tracks on a larger radius than front axle. A variant of definition of Off-Tracking uses (lateral) midpoints of body and it can be much larger than the first definition for vehicles with long front or rear overhangs.

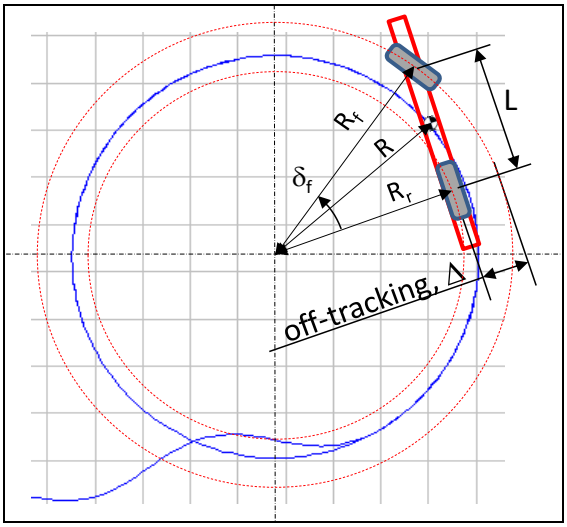

Figure 4-2: Off-tracking (added to result in Figure 4-5).

4.2.2.4 Circle and Manoeuvre Measures

SPW and Off-tracking is most relevant for vehicles with several units, such as truck with trailer. They can be defined for driving several rounds in a circle with constant steering angle ("**Circle** SPW/Off-tracking"). It is a well-defined measure since it is a steady state with respect to articulation angle. However, circle driving is seldom the most relevant manoeuvre. So, one often set requirements on "**Manoeuvre** SPW/Off-tracking", e.g. when driving from straight, via curve with certain outer radius, to a new straight in a certain angle from the first straight, e.g. 12.5 m and 90 deg is common. A way to

predict SPW/Off-tracking for such a manoeuvre is to simulate with time integration, see 4.2.5.2. One can integrate in travelled distance s instead of time, but time is often easier and allows stand-still parts in the manoeuvre. The states in the simulation are the path coordinates with orientation (x, y, φ_z) and articulation angles $(\theta_1, \theta_2, \ldots)$.

The steady state is typically approached asymptotically, so the corresponding circle values requires either long simulations or inserting state derivatives zero and algebraic solution. From geometry in Figure 4-2 on can find an expression for (Circle) Off-tracking Δ:

$$\Delta(R_f, L) = R_f - R_r = R_f - \sqrt{R_f^2 - L^2};$$
$$\Delta(\delta_f, L) = R_f - R_r = L/\sin(\delta_f) - L/\tan(\delta_f);$$

[4.2]

4.2.2.5 Steering Effort at Low Speed *

Function definition: ***Steering effort at low speed*** *is the steering wheel torque needed to turn the steering wheel a certain angle at a certain angular speed at vehicle stand-still on high road friction.*

At low or zero vehicle speed, it is often difficult to reach a low steering wheel torque, due to:

- Castor offset in Figure gives the wheel a side slip when steering and hence a tyre lateral force is developed. Tyre lateral forces times castor offset increases the steering wheel torque.
- Additionally, there is a spin moment in the contact patch, M_{ZT} in Figure 2-6. It does not influence very much, except for at very low vehicle speed. Quantitative models for M_{ZT} are not presented in this compendium.

A critical test for steering effort at low speed is to steer a parked vehicle with a certain high steering wheel rotational speed, typically some hundred deg/s. The steering wheel torque is then required to stay under a certain design target value, normally a couple of Nm. The torque needed will be dependent on lateral force, spin moment and steering geometry and dependent on the capability of the power steering system (which is dependent on steering, due to delays in the steering assistance actuator). A failure in this test is called “catch-up”, referring to that driver catches up with the power steering system. It can be felt as a soft stop and measured as a step in steering wheel torque.

4.2.3 Low Speed Model, Ackermann, with Forces

4.2.3.1 Implications of Forces on Turning Circle

If we have a vehicle with Ackermann geometry, it is tempting to model without involving forces, using Eq [4.1]. But forces can influence low speed paths. When introducing rolling resistance, the force equilibrium is obtained by counter-directed tyre-longitudinal forces on the two axles. Due to the steer angle, a lateral force on the front wheel is required, which gives a lateral tyre slip, $\alpha_f \neq 0$, see Figure 4-3. This changes the motion compared to **Figure 1-25**. Road grade resistance influences in same way and superimposes on rolling resistance.

For heavy combination vehicles, these effects can be significant, adding also rolling resistance from towed units and non-Ackermann effects of several non-steered axles on some units. Then, the function to turn can be quantified by required road friction on steered and driven axle, as opposed to radius at maximum steer angle.

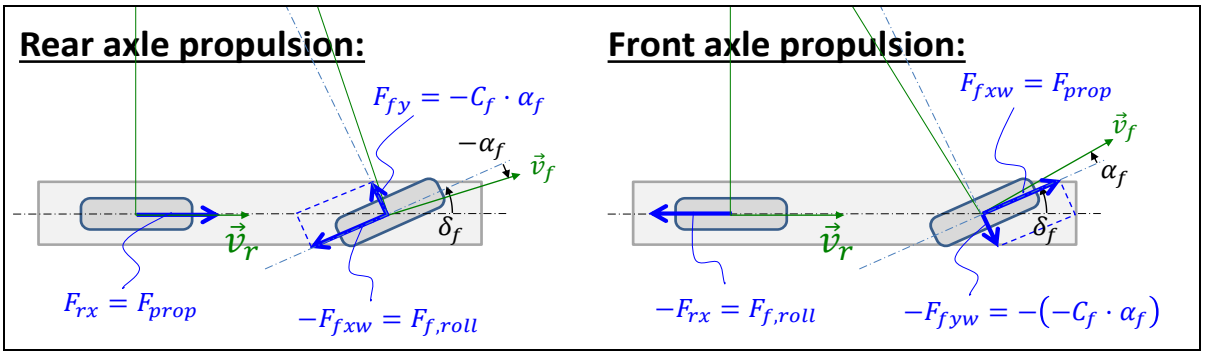

Figure 4-3: Smaller turning circle diameter for front axle propulsion, as compared to rear axle propulsion due to rolling resistance on the un-driven axle.

4.2.3.2 Model

The model in Eq [4.1] predicts a motion without involving forces, or actually assuming forces are zero. To get a more complete model, where more variables can be extracted, we can set up the model in Figure 4-4.

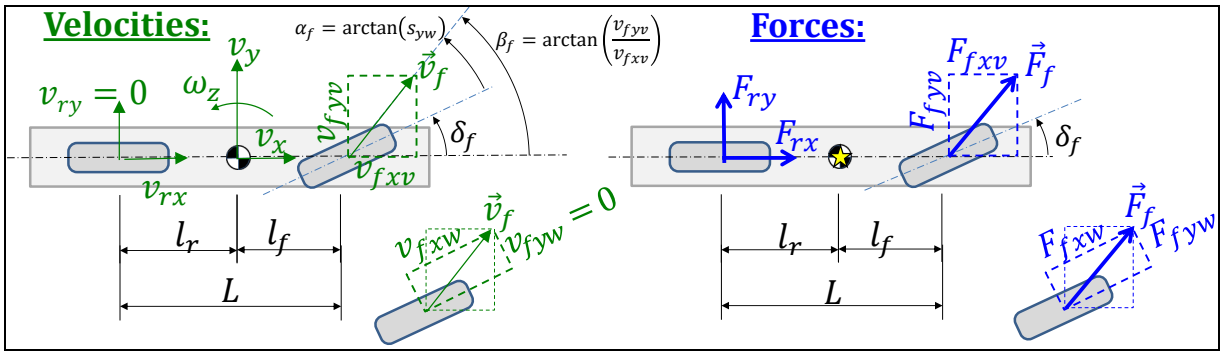

Figure 4-4: One-track model with ideally tracking axles. Lower view of front wheel shows conversion between wheel and vehicle coordinate systems.

The "physical model" in Figure 4-4 gives the following "mathematical model":

Equilibrium (longitudinal, lateral and yaw around CoG):

$$0 = F_{fxv} + F_{rx};$$
$$0 = F_{fyv} + F_{ry};$$
$$0 = F_{fyv} \cdot l_f - F_{ry} \cdot l_r;$$

Transformation between vehicle and wheel coordinate systems:

$$F_{fxv} = F_{fxw} \cdot \cos(\delta_f) - F_{fyw} \cdot \sin(\delta_f);$$
$$F_{fyv} = F_{fxw} \cdot \sin(\delta_f) + F_{fyw} \cdot \cos(\delta_f);$$
$$v_{fxv} = v_{fxw} \cdot \cos(\delta_f) - v_{fyw} \cdot \sin(\delta_f);$$
$$v_{fyv} = v_{fxw} \cdot \sin(\delta_f) + v_{fyw} \cdot \cos(\delta_f);$$

Compatibility between CoG and axles:

$$v_{fxv} = v_x; \quad and \quad v_{fyv} = v_y + l_f \cdot \omega_z;$$
$$v_{rx} = v_x; \quad and \quad v_{ry} = v_y - l_r \cdot \omega_z;$$

Ideal tracking (Constitutive relation, but without connection to forces):

$$v_{fyw} = 0; \quad and \quad v_{ry} = 0;$$

Path with orientation (compatibility), from Eq [1.4]:

$$\dot{x} = v_x \cdot \cos(\varphi_z) - v_y \cdot \sin(\varphi_z);$$
$$\dot{y} = v_y \cdot \cos(\varphi_z) + v_x \cdot \sin(\varphi_z);$$
$$\dot{\varphi}_z = \omega_z;$$

Controls (driver or actuation):

$$\delta_f = \begin{cases} = (35 \cdot \pi/180) \cdot \sin(0.5 \cdot 2 \cdot \pi \cdot t); & if\ t < 4.5; \\ = 35 \cdot \pi/180; & else \end{cases}$$

[4.3]

Constitution (Rear axle undriven, which gives drag from roll resistance):

$$F_{rx} = -100 \cdot \text{sign}(v_x);$$

Note that, since we have Ackermann geometry, we can (mathematically) use the ideal tracking tyre model ($v_{iyw} = 0$;) even if forces are now introduced. For some engineering problems, it might be motivated to use $F_{iyw} = -C_{iy} \cdot s_{iy} = -C_{iy} \cdot v_{iyw}/|R \cdot \omega| \approx -C_{iy} \cdot v_{iyw}/|v_{ixw}|$;, but we leave this to 4.2.4.

The compatibility in Eq [4.3] neglects the influence of steering axis offsets at ground, see 0. The terms neglected are of the type $LateralOffset \cdot \dot{\delta}$; in the equation for v_{fxv} and $LongitudinalOffset \cdot \dot{\delta}$ in the equation for v_{fyv}. This is generally well motivated for normal road vehicles, except for very quick steering when vehicle is close to stand-still.

Equation [4.3] is written in Modelica format in Equation [4.4]. Comments are marked with //. The subscripts v and w refer to vehicle coordinate system and wheel coordinate system, respectively. The actual assumption about ideal tracking lies in that $v_{fyw} = v_{ry} = 0$. Global coordinates from Figure 1-26 is also used. A driving resistance of 100 N is assumed on the rear axle ($F_{rx} = -100$;) to exemplify that forces do not need to be zero.

```
//Equilibrium:
  0 = Ffxv + Frx;
  0 = Ffyv + Fry;
  0 = Ffyv*lf - Fry*lr;
//Ideal tracking (Constitutive relation, but without connection to forces):
  vfyw = 0;     vry = 0;
//Compatibility:
  vfxv = vx;    vfyv = vy + lf*wz;
  vrx = vx;     vry = vy - lr*wz;
//Transformation between vehicle and wheel coordinate systems:
  Ffxv = Ffxw*cos(df) - Ffyw*sin(df);
  Ffyv = Ffxw*sin(df) + Ffyw*cos(df);
  vfxv = vfxw*cos(df) - vfyw*sin(df);
  vfyv = vfxw*sin(df) + vfyw*cos(df); //or atan(vfyv/abs(vfxv))=df+atan(sfy); sfy=0;
//Path with orientation:
  der(x) = vx*cos(pz) - vy*sin(pz);
  der(y) = vy*cos(pz) + vx*sin(pz);
  der(pz) = wz;
// Prescription of actuation:
  df = if time < 4.5 then (35*pi/180)*sin(0.5*2*pi*time) else 35*pi/180;
//Rear axle undriven, which gives drag from roll resistance:
  Frx = -100;
```

[4.4]

4.2.3.3 Simulation

The longitudinal speed is a parameter, $v_x = 10\ km/h$. A simulation result from the model is shown in Figure 4-5. It shows the assumed steer angle function of time, which is an input. It also shows the resulting path, $y(x)$.

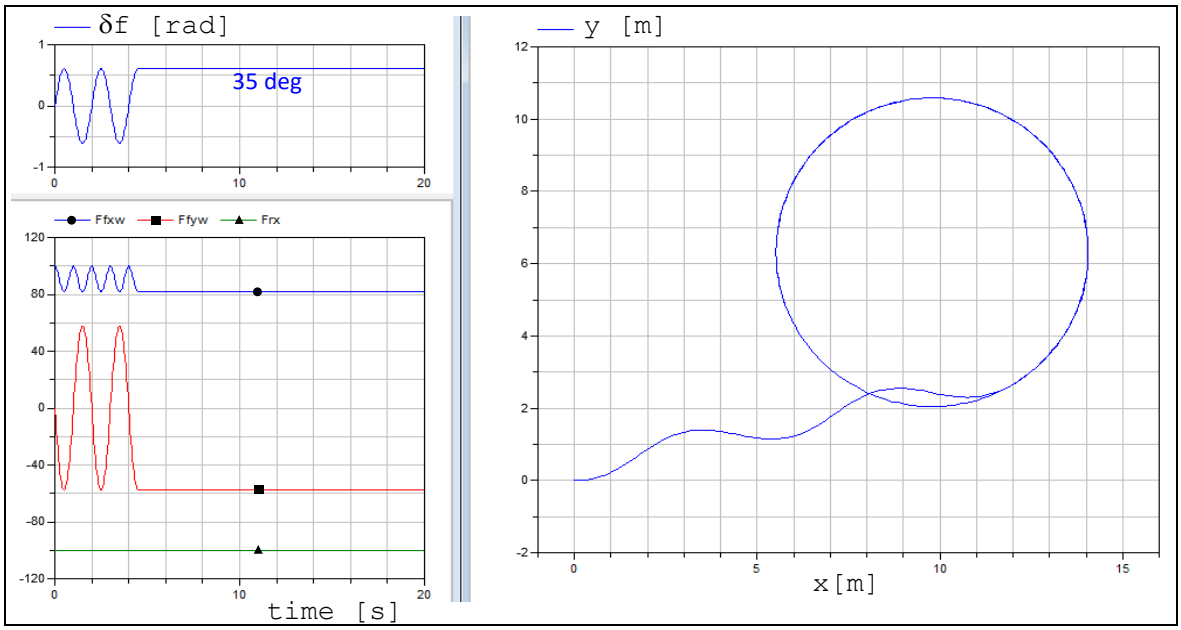

Figure 4-5: Simulation results of one-track model with ideal tracking tyres.

The variables $x, y, p_z = \varphi_z$ are the only state variables of this simulation. If not including the path model (Eq [1.4]), the model would be only an algebraic system of equations. That system of equations could be solved isolated for any value of steer angle without knowledge of time history.

4.2.4 Low Speed Model, Non-Ackermann

If Non-Ackermann geometry, we have to include the forces. Non-Ackermann geometry can be seen as lateral wheel or tyre forces fight each other; either between left and right wheels or between axles. Examples are a two-axle vehicle which has parallel steering and truck with 3 axles, whereof the two rear are non-steered, respectively.

4.2.4.1 Non-Ackermann between Axles

We will go through model changes needed for the latter example. In order to compare the models as closely as possible, we simply split the rear axle into two rear axles, in the example in 4.2.1. The physical model becomes as in Figure 4-6. The measures appear in Figure 4-8, and you see that it is not a typical truck, but a very unconventional vehicle of passenger car size but with two rear axles.

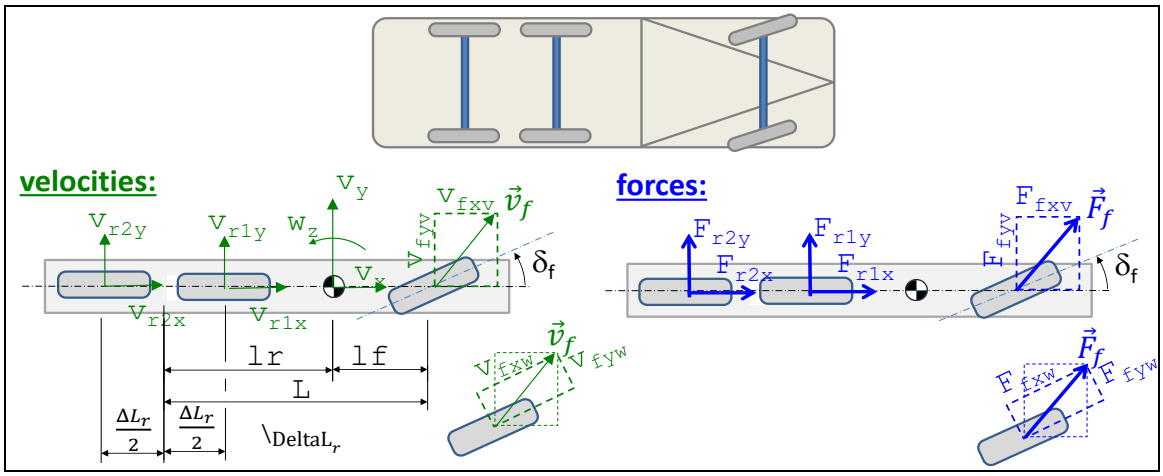

Figure 4-6: Non-Ackermann geometry, due to un-steered rear axles.
Top: Rigid Truck with 3 axles, whereof only the first is steered. Bottom: One-track model.

The changes we have to do in the model appear as underlined in Equation [4.5]. There has to be double variables for v_{rx}, v_{ry}, F_{rx}, F_{ry}, denoted 1 and 2 respectively. Also, we cannot (mathematically) use $v_{fyw} = v_{ry} = 0$ anymore, but instead we introduce a lateral tyre force model, as described in 2.2.4.

```
//Equilibrium:
  0 = Ffxv + Fr1x + Fr2x; //grade resistance could be added here, e.g. "+500"
  0 = Ffyv + Fr1y + Fr2y;
  0 = Ffyv*lf - Fr1y*(lr - DLr/2) - Fr2y*(lr + DLr/2);
//Constitutive relation (with slip, as opposed to Ideal tracking):
  Ffyw = -Cf*sfy;     sfy = vfyw/abs(vfxw);
  Fr1y = -Cr1*sr1y;   sr1y = vr1y/abs(vr1x);
  Fr2y = -Cr2*sr2y;   sr2y = vr2y/abs(vr2x);
//Compatibility:
  vfxv = vx;
  vfyv = vy + lf*wz;
  vr1x = vx;
  vr2x = vx;
  vr1y = vy - (lr - DLr/2)*wz;
  vr2y = vy - (lr + DLr/2)*wz;
//Transformation between vehicle and wheel coordinate systems:
  Ffxv = Ffxw*cos(df) - Ffyw*sin(df);
  Ffyv = Ffxw*sin(df) + Ffyw*cos(df);
  vfxv = vfxw*cos(df) - vfyw*sin(df);
  vfyv = vfxw*sin(df) + vfyw*cos(df);
//Path with orientation:
  der(x) = vx*cos(pz) - vy*sin(pz);
  der(y) = vy*cos(pz) + vx*sin(pz);
  der(pz) = wz;
// Prescription of steer angle:
  df = if time < 4.5 then (35*pi/180)*sin(0.5*2*pi*time) else 35*pi/180;
//Rear axles undriven, which gives drag from rolling resistance:
  Fr1x = -100/2*sign(vx);
  Fr2x = -100/2*sign(vx);
```

[4.5]

The new result is shown in Figure 4-7, which should be compared to Figure 4-5. The radius in the circle increases a little, which is intuitive, since the double rear axle makes turning less easy.

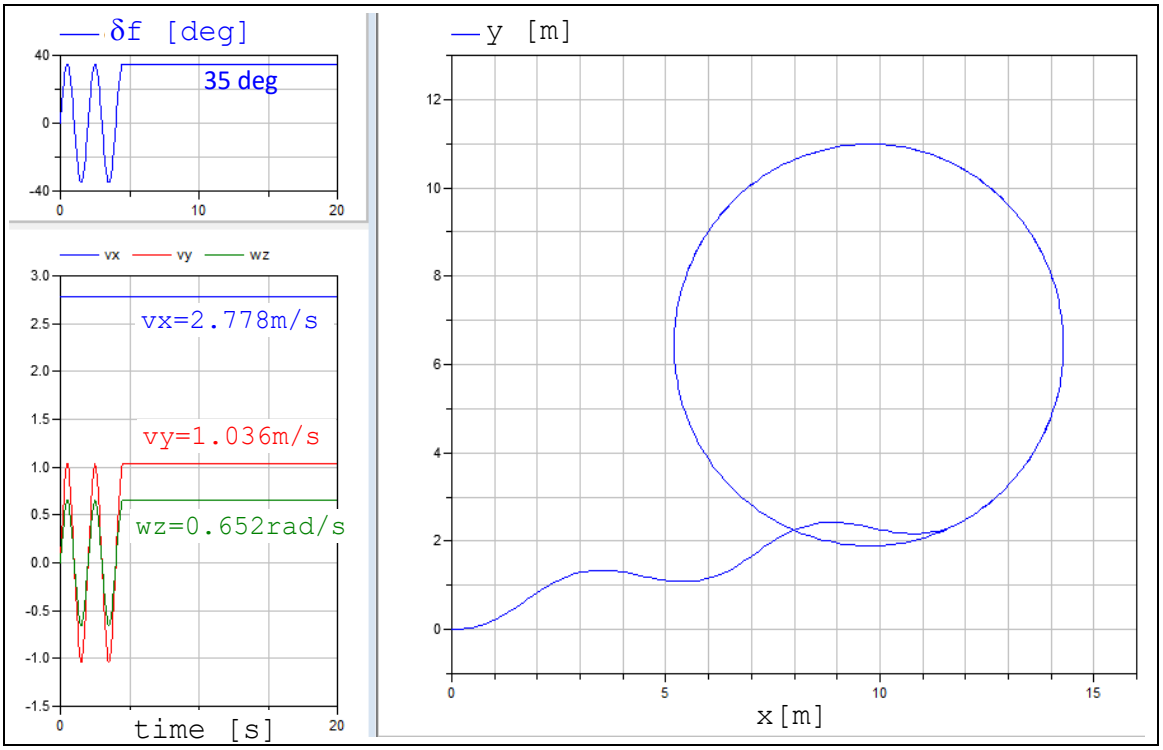

Figure 4-7: Simulation results of one-track model. Non-Ackermann geometry due to two non-steered rear axles. Tyres models are linear, as opposed to ideally tracking.

4.2.4.2 Equivalent Wheel Base

We can also draw the different locations of the instantaneous centre for both cases. This is shown, in scale, in Figure 4-8.

We could tune the steer angle required to reach exactly the same path radius as for the 2-axle reference vehicle. Then, we would have to steer a little more than the 35 degrees used, and we could find a new instantaneous centre, and we could identify a so-called Equivalent wheelbase. This leads us to a definition: The equivalent wheel base of a multi-axle vehicle is the wheel base of a conventional two-axle vehicle which would exhibit the same turning behaviour as exhibited by the multi-axle vehicle, given same steer angle and similar axle cornering stiffnesses. In 4.2.4 it is shown that ideally tracking tyre model is not enough for non-Ackermann geometry; at least a linear tyre model is needed with $C_y \neq \infty$.

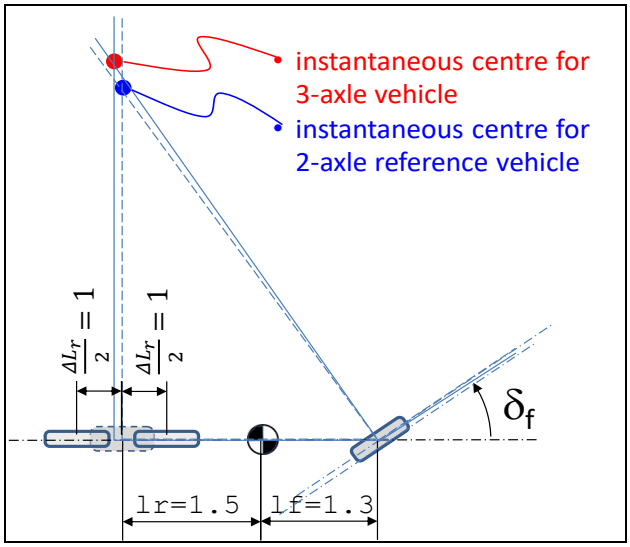

Figure 4-8: Instantaneous centre with a 3-axle vehicle, with corresponding 2-axle vehicle as reference.

Figure text: Two-track model with arbitrary angles δ_{ij}, so that non-Ackermann steering can be modelled.

Figure text: Simulation result showing Low Speed Manoeuvrability. The model from 4.2.4.3.1 is used.

4.2.5 Low Speed Manoeuvres, Articulated Vehicles

4.2.5.1 Ackermann Geometry for Articulated vehicles

For vehicle without articulation, there has to be one common instantaneous centre for all points on the vehicle body. For articulated vehicles, each unit can have its own instantaneous centre. But these are dependent of each other through the coupling points. So, adding units with one axle does not disqualify the Ackermann property of the resulting combination vehicle. See “transient state” in Figure 4-9.

4.2.5.2 Transients in Articulation Angle

For articulated vehicles, also the low speed case has transients in the sense that the articulation angles change transiently. The models are steady state with respect to velocities, but transient with respect to articulation angle, see “transient state” in Figure 4-9. Consider the case of instantaneous step steer. For a vehicle without articulation, a steady state is reached directly, since inertia is not considered. But for an articulated vehicle it takes some time (or travelled distance, since it can be studied independent of speed and time) before a steady state articulation angle is achieved, see “steady state” in Figure 4-9.

So, for articulated vehicles, a scalar requirement on turning radius is not so relevant as for two axle vehicles. The functions “4.2.2.2 Swept Path Width, SPW *” and “4.2.2.3 Low Speed Off-Tracking, LSOT *” are better, assuming one defines a certain road geometry, e.g. through outer radius and total angle of turning.

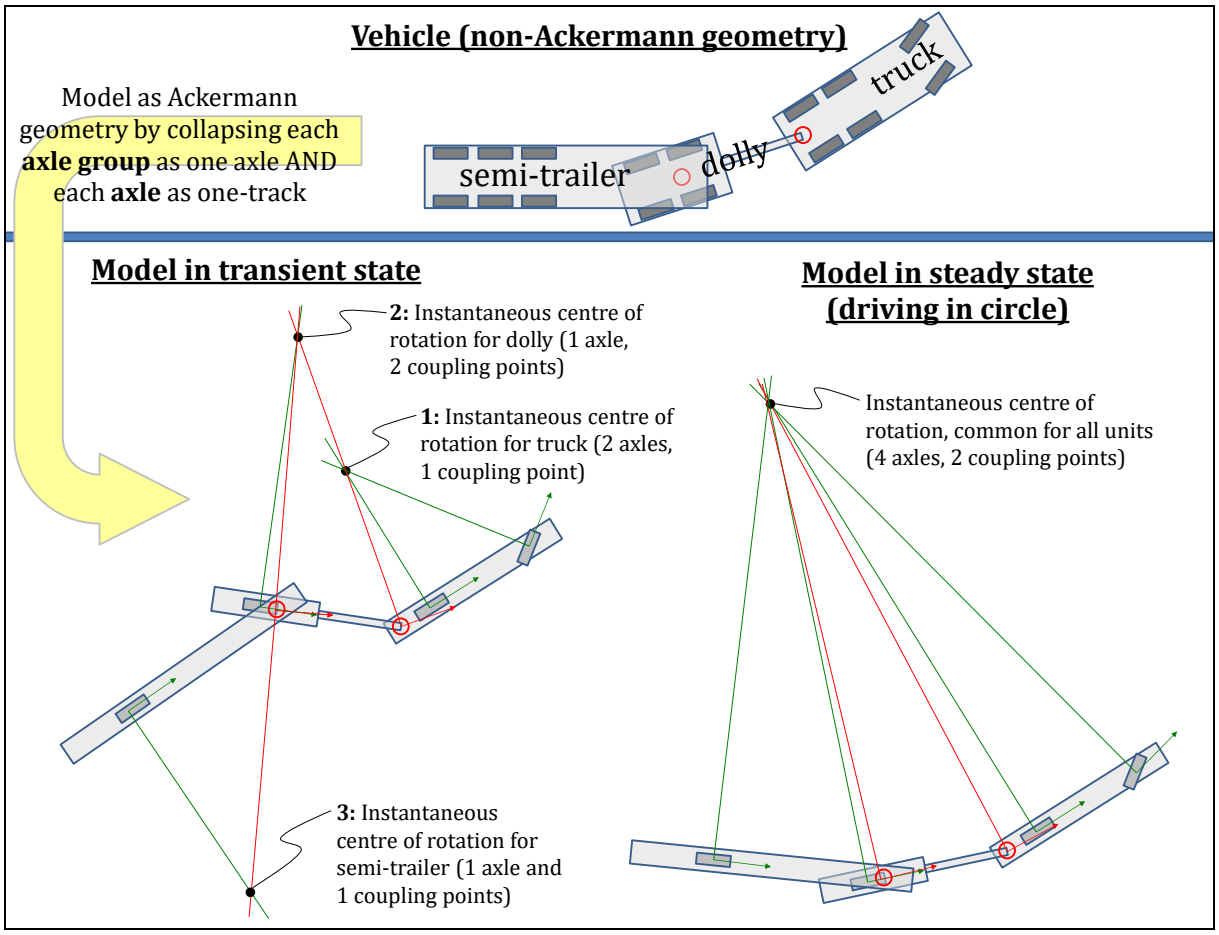

Figure 4-9: Instantaneous centre of rotation for truck with trailer.

4.2.6 Reversing

Low speed manoeuvring is often about both driving forward and reversing. The derived models work formally also for $v_x < 0$. Assume that, after some driving forward, v_x is changed to a negative value. Assume that steering is same for same position along the path, $\delta = \delta(s)$. The vehicle will then reverse in approximately same path as it first drove forward. If ideal tracking tyres, such as Eq [4.1], the paths will be identical. If adding forces to the model, the reverse path can deviate from forward path. A small such deviation can be seen in Figure text due to a large rolling resistance coefficient ($RRC = 0.10$).

In reality, the reverse path for an articulated vehicle often differs more from the forward path. This is mainly due to back-lash in couplings; even if only some centimetre backlash it can influence a lot. The backlash can be modelled by letting coupling point position be dependent of sign(*coupling force*).

4.2.6.1 Stability when Reversing

Single unit vehicles do not become unstable in low speed, neither for forward nor reverse driving. But articulated vehicles do, when reversing. To study this, we derive a linear model, by assuming small angles. Note that the stability analysis for low speed differs from stability analysis at higher speeds, see 4.4.4, in that the low speed models do not include inertial terms $mass \cdot acceleration$.

4.2.6.2 Linear Low Speed Model for Tractor with Semi-trailer

Figure 4-10 shows a physical model for tractor with trailer, assuming small angles φ_{1z}, δ and θ.

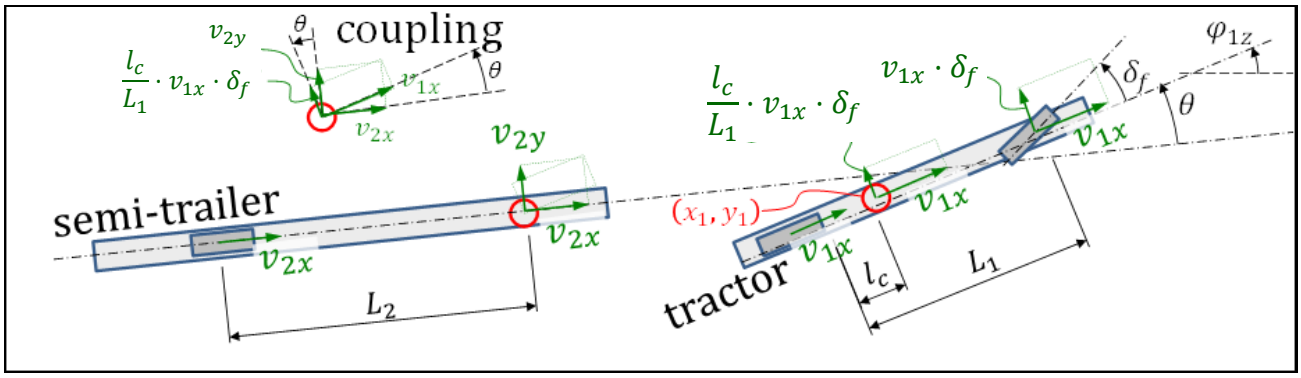

Figure 4-10: A low speed model of tractor with semi-trailer. Small angles $\varphi_{1z}, \theta, \delta_f$ are assumed.

The mathematical model for lateral position variables $(y_1, \varphi_{1z}, \theta)$ becomes:

$\dot{y}_1 = \frac{l_c}{L_1} \cdot v_{1x} \cdot \delta_f + v_{1x} \cdot \varphi_{1z}$; (from Eq **[1.4]**, with small φ_{1z})

$\dot{\varphi}_{1z} = \frac{v_{1x} \cdot \delta}{L_1}$; (rotational velocity = tangential speed / radius to instantaneous centre)

$\dot{\theta} = \frac{v_{1x} \cdot \delta}{L_1} - \frac{v_{2y}}{L_2}$; (articulation angle is difference between units)

$v_{2y} = v_{1x} \cdot \theta + \frac{l_c}{L_1} \cdot v_{1x} \cdot \delta$; (units have same velocity in coupling point, small θ, small δ_f)

Eliminating v_{2y} gives:

$$\begin{bmatrix} \dot{y}_1 \\ \dot{\varphi}_{1z} \\ \dot{\theta} \end{bmatrix} = \underbrace{\begin{bmatrix} 0 & v_{1x} & 0 \\ 0 & 0 & 0 \\ 0 & 0 & -v_{1x}/L_2 \end{bmatrix}}_{\boldsymbol{A}} \cdot \begin{bmatrix} y_1 \\ \varphi_{1z} \\ \theta \end{bmatrix} + v_{1x} \cdot \begin{bmatrix} l_c/L_1 \\ 1/L_1 \\ 1/L_1 - l_c/(L_1 \cdot L_2) \end{bmatrix} \cdot \delta_f;$$

The eigenvalues to $\boldsymbol{A}$ becomes $\lambda_{1,2} = \pm 0; \lambda_3 = -v_{1x}/L_2$;. So, the system is unstable when $v_{1x} < 0$, because it makes $\mathrm{Re}(\lambda_3) > 0$. It is probably intuitive for may readers that the vehicle is unstable, as the semi-trailer pushed rearwards via a moment-free joint. However, the analysis was included in the compendium to show how stability appears for low speed models, i.e. without inertial terms $mass \cdot acceleration$. The model can be extended with other multiple-unit vehicles, multiple axles in axle groups and driver models. The state variables will remain as y_1, φ_{1z} and one articulation angle θ_i for each coupling.

4.3 Steady State Cornering at High Speed

Steady state cornering refers to that all time derivatives of vehicle speeds (v_x, v_y, ω_z) are zero. The physical understanding is then that the vehicle drives on a circle with constant yaw velocity, see Figure 4-11. Alternatively, this can be described as driving with constant tangential speed (v), on a constant path radius (R) and with a constant side slip angle (β).

4.3.1 Steady State Driving Manoeuvres

When testing steady state function, one usually runs on a so called "skid-pad" which appears on most test tracks, see Figure 1-25. It is a flat circular surface with typically 100 m diameter and some concentric circles marked. A general note is that tests in real vehicles are often needed to be performed in simulation also, and normally earlier in the product development process.

Typical steady state tests are:

- Constant path radius. Driven for different longitudinal speeds.
- Constant longitudinal speed. Driven for different path radii.
- Constant steering wheel angle. Then increase accelerator pedal (or apply brake pedal) gently. (If too quick, the test would fall under transient handling instead.)

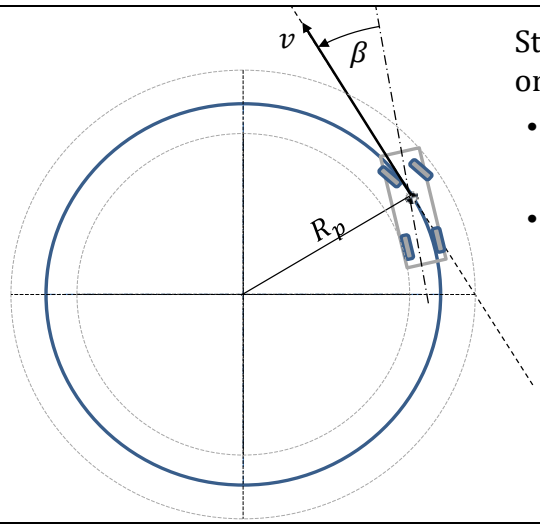

Steady state cornering can be defined by either 3 or 2 quantities, depending on assumptions:

- For a **general vehicle** it is fully defined only by all **3 quantities**, e.g. $[v_x, v_y, \omega_z]$ or $[v, \beta, R_p]$.
- For a **certain vehicle** it is often considered as fully defined by **2 inputs from driver**: accelerator pedal and steering wheel. (Then, one have neglected other inputs from driver, such as brake pedal and parking brake. One have also neglected other possible automatic actuation, such as all wheel drive distribution and ESC-braking one wheel.)

Figure 4-11: Steady state cornering. (β will be negative for larger v_x, i.e. vehicle will point inwards.)

Relevant standards for these test manoeuvres are: References (ISO 4138) and (ISO 14792).

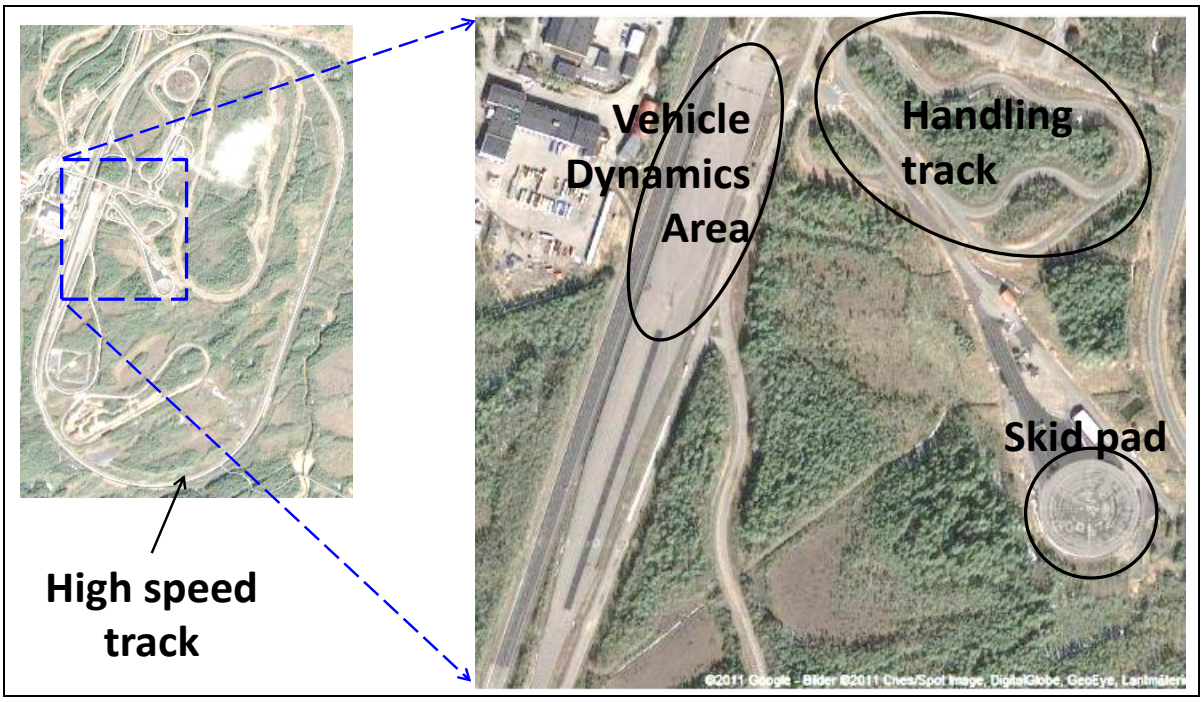

Figure 4-12: An example of test track and some parts with special relevance to Vehicle Dynamics. The example is Hällered Proving Ground, Volvo Car Corporation.

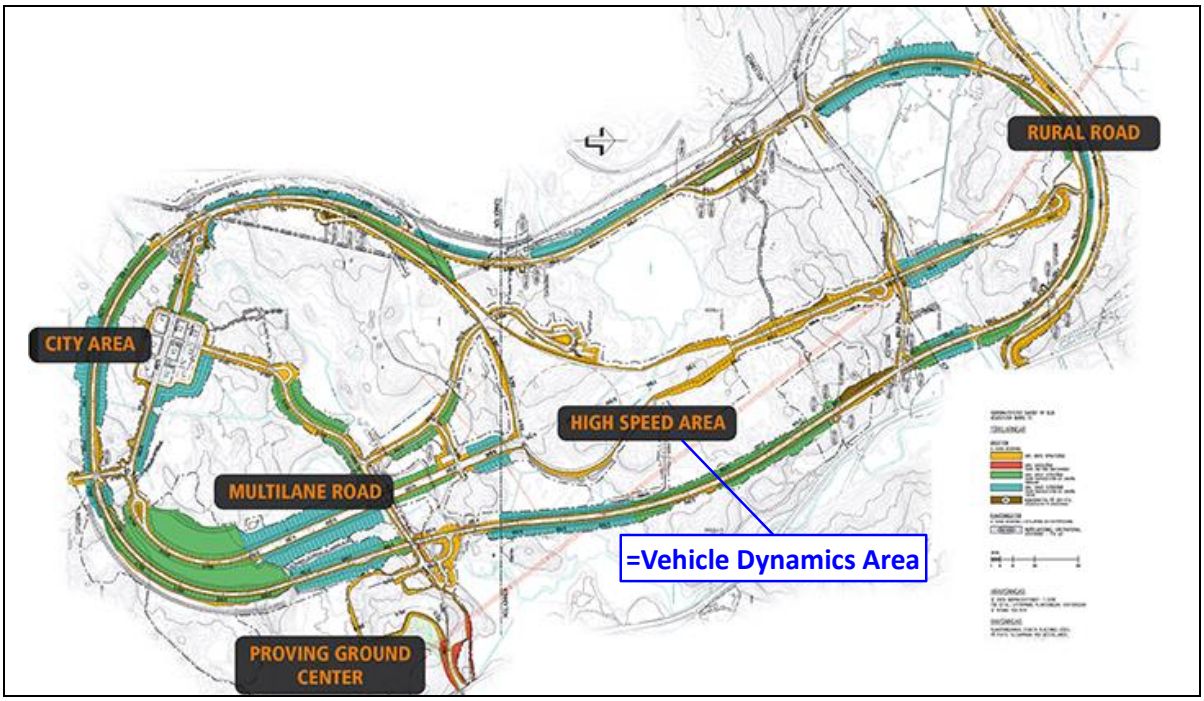

Figure 4-13: An example of test track. The example is AstaZero (Active Safety Test Arena), owned by Research Institute of Sweden (RISE) and Chalmers University of Technology.

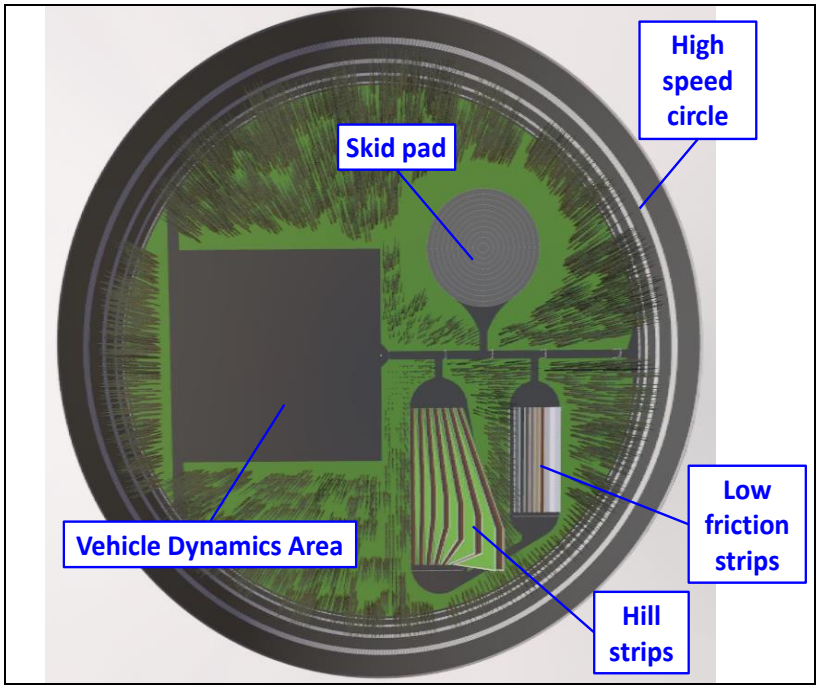

Figure 4-14: An example of test track. The example is CASTER's (virtual) test track. Used for CASTER's driving simulator at Chalmers University of Technology.

4.3.2 Steady State 1-Track Model

In steady state we have neither inertial effect from changing the total vehicle speed ($v = \sqrt{v_x^2 + v_y^2} = constant$) nor from changing the yaw velocity ($w_z = constant$). However, the inertial "centrifugal" effect of the vehicle must be modelled. The related acceleration is the centripetal acceleration, $a_c = R_p \cdot {\omega_z}^2 = v^2/R_p = \omega_z \cdot v$.

A vehicle model for this is sketched in Figure 4-15. The model is a development of the model for low-speed in Figure 4-4 and Equation [4.4], with the following changes:

- Longitudinal and lateral accelerations are changed from zero to components of centripetal acceleration, ac, as follows (see Figure 4-15):
  - $a_x = -a_c \cdot \sin(\beta) = -\omega_z \cdot v \cdot \sin(\beta) = -\omega_z \cdot v_y$;
  - $a_y = +a_c \cdot \cos(\beta) = +\omega_z \cdot v \cdot \cos(\beta) = +\omega_z \cdot v_x$;
- The constitutive relations for the axles are changed from ideal tracking to a (linear) relation between lateral force and lateral slip:
  - $F_{fyw} = -C_f \cdot s_{fy}$; where $s_{fy} = v_{fyw}/|R_w \cdot \omega_f| \approx v_{fyw}/|v_{fxw}|$;
  - $F_{ry} = -C_r \cdot s_{ry}$; where $s_{ry} = v_{ry}/|R_w \cdot \omega_r| \approx v_{ry}/|v_{rx}|$;

The constitutive relations above capture the slip characteristics for the tyres, see **2.2.4**, but they can also capture steering system compliance, side force steering, and roll steering (see 4.3.6.3).

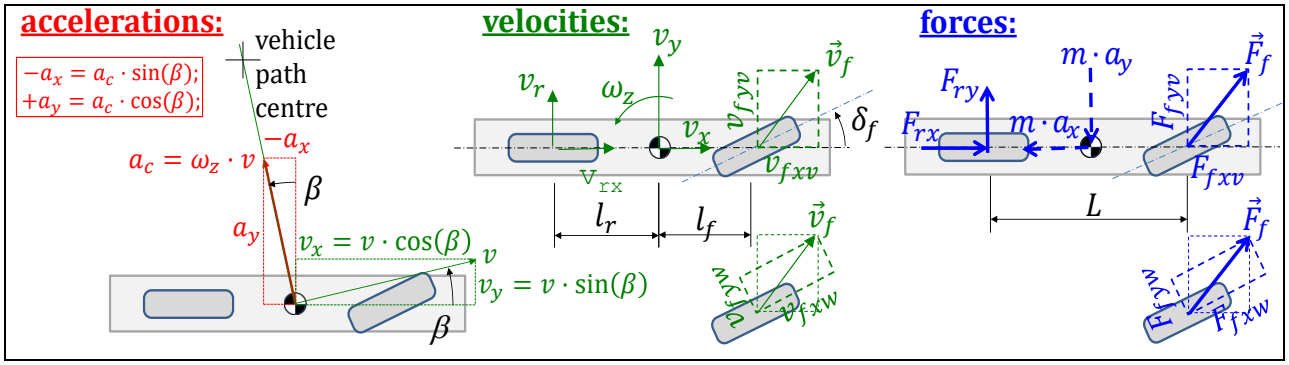

Figure 4-15: One-track model. Dashed forces and moment are fictive forces.

The model in Figure 4-15 is documented in mathematical form in Equation [4.6] (in Modelica format). Longitudinal speed v_x is assumed to be positive. The subscripts *v* and *w* refer to vehicle coordinate system and wheel coordinate system, respectively. A driving resistance of 100 N is assumed on the rear axle (`Frx=100;`). The longitudinal speed is a parameter, $v_x = 100\ km/h$.

```
//Equilibrium:
  m*ax = Ffxv + Frx;    //Air and grade resistance neglected
  m*ay = Ffyv + Fry;    Jz*0 = Ffyv*lf - Fry*lr;    // der(wz)=0
  -ax = wz*vy;    +ay = wz*vx;
//Constitutive relation, i.e. Lateral tyre force model:
  Ffyw = -Cf*sfy;   sfy = vfyw/vfxw;
  Fry = -Cr*sry;    sry = vry/vrx;
//Compatibility:
  vfxv = vx;    vfyv = vy + lf*wz;
  vrx = vx;     vry  = vy - lr*wz;
//Transformation between vehicle and wheel coordinate systems:
  Ffxv = Ffxw*cos(df) - Ffyw*sin(df);
  Ffyv = Ffxw*sin(df) + Ffyw*cos(df);
  vfxv = vfxw*cos(df) - vfyw*sin(df);
  vfyv = vfxw*sin(df) + vfyw*cos(df);
//Path with orientation (from Eq [1.4]):
  der(x) = vx*cos(pz) - vy*sin(pz);
  der(y) = vy*cos(pz) + vx*sin(pz);
  der(pz) = wz;
// Prescription of steer angle:
  df = if time < 2.5 then (5*pi/180)*sin(0.5*2*pi*time) else 5*pi/180;
// Rear axle undriven, which gives drag from roll resistance:
  Frx = -100;
```

[4.6]

A simulation result from the model is shown in Figure 4-16. Note that steering start to the left, but vehicle path starts bending to the right. This comes from that it is a steady state model but used in a transient manoeuvre. The steady state cornering condition is found directly and turning left has the steady state v_y directed outwards, to the right, due to centrufugal force.

Now, the validity of a model always has to be questioned. There are many modelling assumptions which could be checked, but in the following we only check the assumption $a_y = \omega_z \cdot v_x$; instead of the more correct $a_y = \dot{v}_y + \omega_z \cdot v_x$;, which we will learn in "4.4.2 Linear 1-Track Model". Comparison of

the terms gives $|\dot{v}_y|_{max} \approx |\omega_z \cdot v_x|_{max} \approx 10\,m/s^2$, so $|\omega_z \cdot v_x|$ is large and this jeopardizes the validity. Large $|\omega_z \cdot v_x|$ happens during $0 < t <\approx 2\ s$, so the model is not very valid there. But, at $t >\approx 2\ s$, the model is valid, at least in this aspect, since there $|\dot{v}_y| \approx 0 \ll |\omega_z \cdot v_x|$. So, the model is not so valid during the initial sinusoidal steering. This shows that a steady state *models* should not be thrusted outside steady state *conditions*.

Equation [4.6] is a complete model suitable for simulation, but it does not facilitate understanding very well. We will reformulate it assuming small δ_f (i.e. $\cos(\delta_f) = 1$, $\sin(\delta_f) = 0$, and $\delta_f^2 = 0$). Eliminate slip, all forces that are not wheel longitudinal, and all velocities that are not CoG velocities:

$$
\begin{aligned}
&-m \cdot \omega_z \cdot v_y \cdot \left(v_x + \left(v_y + l_f \cdot \omega_z\right) \cdot \delta_f\right) = \\
&\quad = F_{fxw} \cdot \left(v_x + \left(v_y + l_f \cdot \omega_z\right) \cdot \delta_f\right) + C_f \cdot \left(v_y + l_f \cdot \omega_z\right) \cdot \delta_f + F_{rx} \cdot \left(v_x + \left(v_y + l_f \cdot \omega_z\right) \cdot \delta_f\right); \\
&m \cdot \omega_z \cdot v_x \cdot \left(v_x + \left(v_y + l_f \cdot \omega_z\right) \cdot \delta_f\right) = \\
&\quad = -C_f \cdot \left(-v_x \cdot \delta_f + \left(v_y + l_f \cdot \omega_z\right)\right) + F_{fxw} \cdot \delta_f \cdot v_x - C_r \cdot \frac{v_y - l_r \cdot \omega_z}{v_x} \cdot \left(v_x + \left(v_y + l_f \cdot \omega_z\right) \cdot \delta_f\right); \\
&C_f \cdot \left(-v_x \cdot \delta_f + \left(v_y + l_f \cdot \omega_z\right)\right) \cdot l_f - F_{fxw} \cdot \delta_f \cdot l_f \cdot v_x = \\
&\quad = C_r \cdot \frac{v_y - l_r \cdot \omega_z}{v_x} \cdot l_r \cdot \left(v_x + \left(v_y + l_f \cdot \omega_z\right) \cdot \delta_f\right);
\end{aligned}
\qquad [4.7]
$$

Equation [4.7] is a complete model, which we can see as a dynamic system without state variables.

- Actuation: Steering and wheel torque on each axle: $\delta_f, F_{fxw}, F_{rx}$.
- Motion quantities: v_x, v_y, ω_z

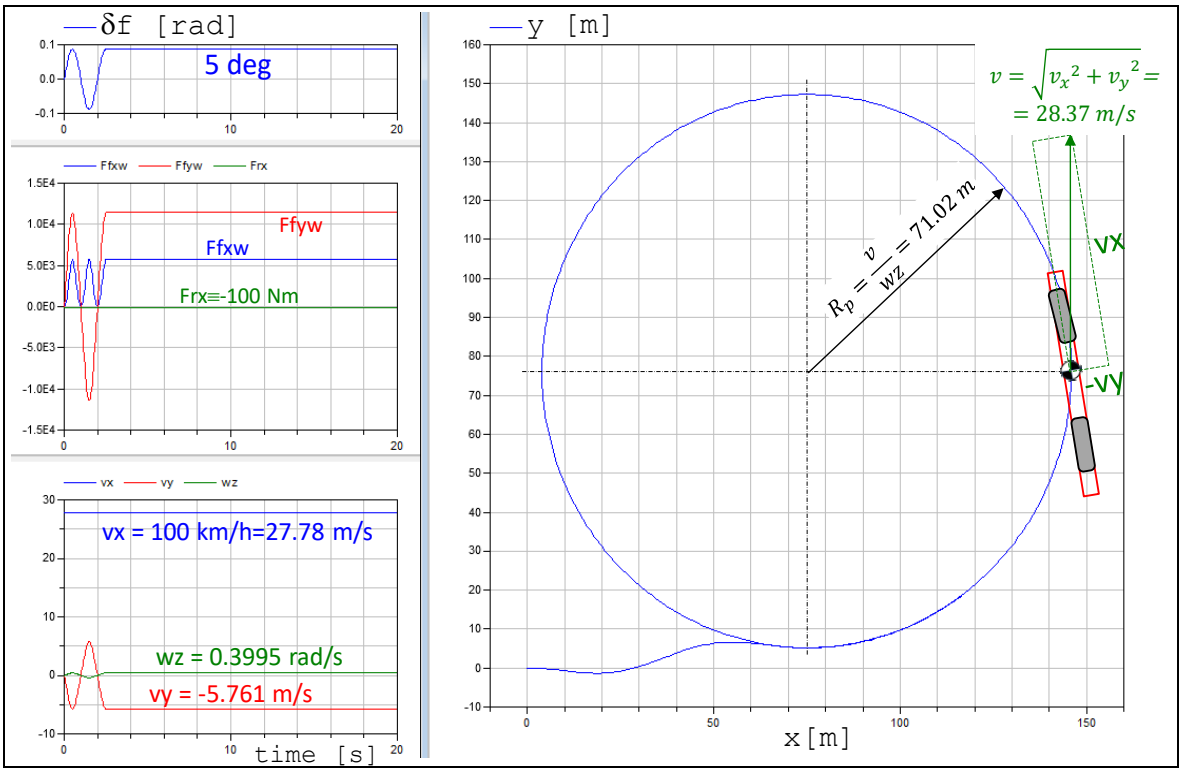

Figure 4-16: Simulation results of steady state one-track model. The vehicle sketched in the path plot is not in scale, but correctly oriented.

For propulsion on both axles, it can be a reasonable case that we know δ_f, F_{fxw}, v_x and want to calculate F_{rx}, v_y, ω_z. Eq [4.8] is a rearrangement of Eq [4.7] for this purpose. It can be used for rear axle drive using $F_{fxw} = 0$ and calculating how large F_{rx} needs to be. Front axle drive requires more rearrangements.

$$\omega_z = \frac{C_f \cdot C_r \cdot L + C_r \cdot L \cdot F_{fxw}}{C_f \cdot C_r \cdot L^2 + \left(C_r \cdot l_r - C_f \cdot l_f\right) \cdot m \cdot v_x^2} \cdot v_x \cdot \delta_f;$$

$$v_y = \frac{C_f \cdot \left(C_r \cdot L \cdot l_r - l_f \cdot m \cdot v_x^2\right) + \left(C_r \cdot L \cdot l_r - l_f \cdot m \cdot v_x^2\right) \cdot F_{fxw}}{C_f \cdot C_r \cdot L^2 + \left(C_r \cdot l_r - C_f \cdot l_f\right) \cdot m \cdot v_x^2} \cdot v_x \cdot \delta_f;$$

$$F_{rx} = -m \cdot \omega_z \cdot v_y - F_{fxw} - \frac{C_f \cdot \left(v_y + l_f \cdot \omega_z\right) \cdot \delta_f}{\left(\left(v_y + l_f \cdot \omega_z\right) \cdot \delta_f + v_x\right)};$$

[4.8]

4.3.2.1 Relation δ_f, v_x and R_p

Solving the first equation in Equation [4.8] yields:

$$\delta_f = \frac{C_f \cdot C_r \cdot L^2 + \left(C_r \cdot l_r - C_f \cdot l_f\right) \cdot m \cdot v_x^2}{C_f \cdot C_r \cdot L + \left(C_r \cdot l_f + C_r \cdot l_r\right) \cdot F_{fxw}} \cdot \frac{\omega_z}{v_x} \approx \left\{\begin{matrix} assume\ small\ v_y \Rightarrow \\ \Rightarrow v_x/\omega_z \approx R_p \end{matrix}\right\} \approx$$

$$\approx \frac{1}{1 + F_{fxw}/C_f} \cdot \frac{L}{R_p} + \frac{C_r \cdot l_r - C_f \cdot l_f}{\left(C_f + F_{fxw}\right) \cdot C_r \cdot L} \cdot \frac{m \cdot v_x^2}{R_p} \approx \left\{\begin{matrix} assume: \\ F_{fxw}/C_f \approx 0 \end{matrix}\right\} \approx$$

$$\approx \frac{L}{R_p} + \frac{C_r \cdot l_r - C_f \cdot l_f}{C_f \cdot C_r \cdot L} \cdot \frac{m \cdot v_x^2}{R_p} = \left\{use: K_u = \frac{C_r \cdot l_r - C_f \cdot l_f}{C_f \cdot C_r \cdot L} = \frac{l_r}{C_f \cdot L} - \frac{l_f}{C_r \cdot L}\right\} =$$

$$= \frac{L}{R_p} + K_u \cdot \frac{m \cdot v_x^2}{R_p};$$

[4.9]

The coefficient K_u is the *understeer gradient* and it will be explained more in 4.3.3.

4.3.2.2 Relation δ_f, v_x and β

Solving the second equation in Equation [4.8] yields:

$$\delta_f = \frac{C_f \cdot C_r \cdot L^2 + \left(C_r \cdot l_r - C_f \cdot l_f\right) \cdot m \cdot {v_x}^2}{C_f \cdot \left(C_r \cdot L \cdot l_r - l_f \cdot m \cdot {v_x}^2\right) + \left(C_r \cdot L \cdot l_r - l_f \cdot m \cdot v_x^2\right) \cdot F_{fxw}} \cdot \frac{v_y}{v_x} \approx$$

$$\approx \left\{use: F_{fxw} = 0\right\} \approx \frac{C_f \cdot C_r \cdot L^2 - \left(C_f \cdot l_f - C_r \cdot l_r\right) \cdot m \cdot {v_x}^2}{C_f \cdot C_r \cdot l_r \cdot L - C_f \cdot l_f \cdot m \cdot {v_x}^2} \cdot \frac{v_y}{v_x} \approx$$

$$\Rightarrow \begin{cases} \delta_f \xrightarrow[v_x \to 0]{} \frac{L}{l_r} \cdot \frac{v_y}{v_x}; \\ \delta_f \xrightarrow[v_x \to \infty]{} \frac{C_f \cdot l_f - C_r \cdot l_r}{C_f \cdot l_f} \cdot \frac{v_y}{v_x} = -K_u \cdot C_r \cdot \frac{L}{l_f} \cdot \frac{v_y}{v_x}; \end{cases}$$

[4.10]

We can see that there is a speed dependent relation between steer angle and side slip, $\frac{v_y}{v_x}$. The side slip can also be expressed as a side slip angle, $\beta = \arctan\left(\frac{v_y}{v_x}\right)$. Since normally $K_u > 0$, the side slip changes sign, when increasing speed from zero to sufficient high enough. This should feel intuitively correct, if agreeing on the conceptually different side slip angles at low and high speed, as shown in Figure 4-17. We will come back to this equation in context of Figure 4-26.

4.3.2.3 Relation v_x, R_p and β

If we approximate $F_{fxw} = 0$ and use both equations in Equation [4.8] to eliminate δ_f we get:

$$\frac{C_r \cdot L \cdot l_r - l_f \cdot m \cdot v_x^2}{C_r \cdot L} = l_r - \frac{l_f \cdot m \cdot v_x^2}{L \cdot C_r} = \frac{v_y}{\omega_z} = \frac{v_x}{\omega_z} \cdot \frac{v_y}{v_x} \approx R_p \cdot \tan(\beta); \Rightarrow$$

$$\Rightarrow \frac{v_y}{v_x} = \tan(\beta) = \left(l_r - \frac{l_f \cdot m \cdot v_x^2}{L \cdot C_r}\right) \cdot \frac{1}{R_p};$$

[4.11]

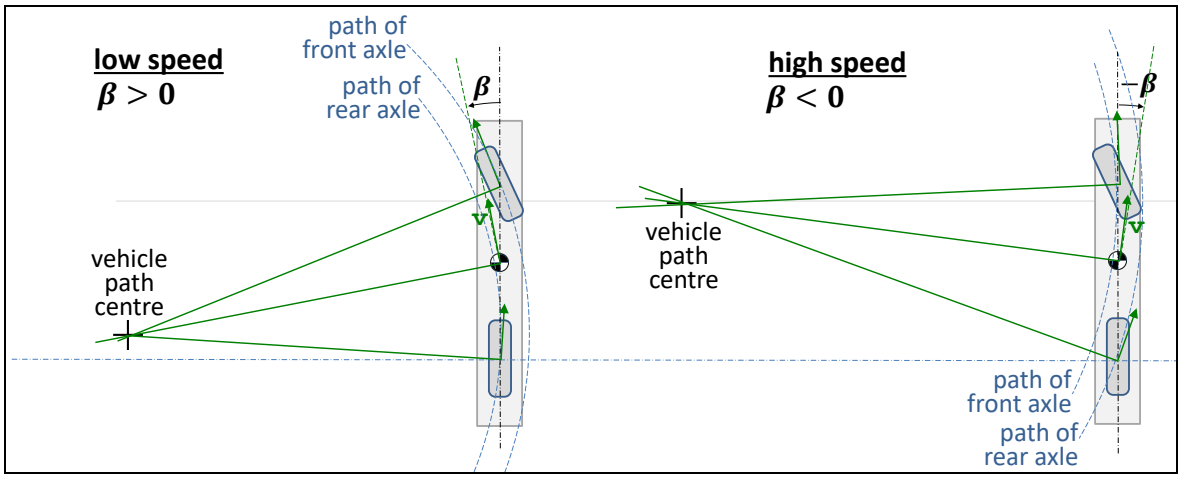

Figure 4-17: Body Slip Angle for Low and High Speed Steady State Curves

4.3.2.4 Simpler Derivation of Model

A simpler way to reach almost same expression as first expression in Eq [4.8] is given in Figure 4-18. Here, the simplifications are introduced earlier, already in physical model, which means e.g. the influence of F_{fxw} is not captured. The simpler compatibility from 1.5.5.3 is used and $v_x > 0$ is assumed.

Physical model:

- Path radius >> the vehicle. Then, all forces (and centripetal acceleration) are approximately co-directed.
- Small tyre and vehicle side slip. Then, angle=sin(angle)=tan(angle). (Angles are not drawn small, which is the reason why the forces not appear co-linear in figure.)

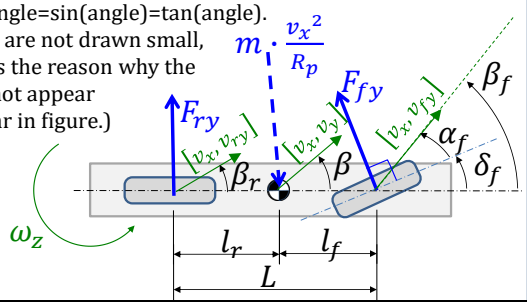

Mathematical model:

Equilibrium: $m \cdot \frac{v_x^2}{R} \approx F_{fy}+F_{ry}; \quad 0 \approx F_{fy} \cdot l_f - F_{ry} \cdot l_r;$

Constitution: $F_{fy} = -C_f \cdot s_{fy}; \quad F_{ry} = -C_r \cdot s_{ry};$

Compatibility:

$s_{fy} \approx (v_y + l_f \cdot \omega_z)/v_x - \delta_f;$

$s_{ry} \approx (v_y - l_r \cdot \omega_z)/v_x;$

$\omega_z \approx v_x/R_p;$

Eliminate $F_{fy}, F_{ry}, s_{fy}, s_r, \omega_z, v_y$ yields:

$$\delta_f \approx \frac{L}{R_p} + K_u \cdot \frac{m \cdot {v_x}^2}{R_p}; \quad where\ K_u = \frac{C_r \cdot l_r - C_f \cdot l_f}{C_f \cdot C_r \cdot L};$$

Figure 4-18: Simpler derivation final step in Equation [4.9].

4.3.2.5 Steady State Cornering for Non-Ackermann Geometry

Ackermann geometry has been assumed above. We will now try a vehicle like in 4.2.4 and Figure 4-6. Further on, we assuming $F_{fxw} = 0;, l_r = (l_{r1} + l_{r2})/2;, \ \Delta L_r = l_{r2} - l_{r1};, L = l_f + l_r;, and\ C_{r1} = C_{r2} = C_{ra}/2;$. This gives an equation, comparable with Eq [4.9], as follows:

$$\delta_f = \underbrace{\frac{L}{R_p} + \left(\frac{\Delta L_r}{2 \cdot L}\right)^2 \cdot \left(1 + \frac{C_{ra}}{C_f}\right) \cdot \frac{L}{R_p}}_{\delta_A} + K_u \cdot \frac{m \cdot v_x^2}{R_p}; \quad where\ and\ K_u = \frac{C_{ra} \cdot l_r - C_f \cdot l_f}{C_f \cdot C_{ra} \cdot L}; \qquad [4.12]$$

Note: We can still identify an K_u, but the reference angle δ_A, see also 4.3.3, is not as simple as L/R_p.

4.3.2.6 Model Validity

The validity of the steady state models described in 4.3.2, is of course limited by if the manoeuvre is transient which would mean that steady state is not reached, e.g. if driving above critical speed. But it is also limited by if the assumption of linear tyre characteristics, $F_y = -C \cdot s_y;$, is violated. Therefore, one should check if some axle uses too much of available friction, $F = \sqrt{F_x^2 + F_y^2} > fraction \cdot \mu \cdot F_z;$.

Referring to the tyre brush model with uniform pressure distribution one can argue for using 0.5 as this limiting fraction, since the tyre force is linear with slip up to this value.

4.3.3 Under-, Neutral- and Over-steering *

Function definition: ***Understeering (gradient)*** *is the additional steer angle needed per increase of lateral force (or lateral acceleration) when driving in high speed steady state cornering on level ground and high road friction. Additional refers to low speed. The gradient is defined at certain high-speed steady state cornering conditions, including straight-line driving. Steer angle can be either road wheel angle or steering wheel angle.*

The first term in Eq [4.9], L/R, can be seen as a reference steer angle δ_A, which is the Ackermann steer angle. The (ISO 8855) defines δ_A as the steer angle which would be needed to give same instantaneous centre of rotation if the vehicle would have had two axles, perfect Ackermann steering and no tyre side slip. So, δ_A corresponds to L/R for a two-axle vehicle. An extended definition of δ_A is the steering angle needed for a certain curvature $1/R_p$ at low speed. The understeer gradient is then understood as a measure of how this is changed with increasing speed v_x.

The understeering gradient, K_u, is normally positive, which means that most vehicles require more steer angle for a given curve, the higher the speed is. Depending on the sign of K_u a vehicle is said to be oversteered (if $K_u < 0$), understeered (if $K_u > 0$) and neutral steered ($if\ K_u = 0$). In practice, all vehicles are designed as understeered, because over steered vehicle would become unstable and difficult to control.

The K_u in Eq [4.9] is called "understeer gradient" and has hence the unit rad/N or 1/N. Sometimes one can see slightly other definitions of what to include in definition of understeer gradient, which have different units, see K_{u2} and K_{u3} in Eq [4.13].

$$\delta_f = \frac{L}{R} + \frac{C_r \cdot l_r - C_f \cdot l_f}{C_f \cdot C_r \cdot L} \cdot \frac{m \cdot g \cdot {v_x}^2}{g \cdot R} = \left\{ K_{u2} = m \cdot g \cdot \frac{C_r \cdot l_r - C_f \cdot l_f}{C_f \cdot C_r \cdot L} [1\ or\ rad] \right\} = \frac{L}{R} + K_{u2} \cdot \frac{{v_x}^2}{g \cdot R};$$

$$\delta_f = \frac{L}{R} + \frac{C_r \cdot l_r - C_f \cdot l_f}{C_f \cdot C_r \cdot L} \cdot \frac{m \cdot {v_x}^2}{R} = \left\{ K_{u3} = m \cdot \frac{C_r \cdot l_r - C_f \cdot l_f}{C_f \cdot C_r \cdot L} \left[\frac{1}{m/s^2}\ or\ \frac{rad}{m/s^2} \right] \right\} = \frac{L}{R} + K_{u3} \cdot \frac{{v_x}^2}{R};$$

[4.13]

K_{u3} is the definition used in (ISO 8855). For K_{u3}, one can sometimes see the unit "rad/g" used, which present compendium recommended to not use.

If vertical loads on axles are only due to gravity ($F_{iz} = m \cdot g \cdot (L - l_i)/L$) and tyres linear with vertical load ($C_{iy} = CC_{iy} \cdot F_{iz}$) we can express $K_{u2} = 1/CC_f - 1/CC_r$;.

4.3.3.1 Understeering as a Fix Built-In Measure

The understeering gradient K_u can be understood as how much additionally to the reference steer angle one has to steer, to reach a certain centrifugal force, $F_c = m \cdot {v_x}^2/R$ (or, if using K_{u3}, a certain acceleration $a_c = {v_x}^2/R$):

$$\delta_f = \delta_A + K_u \cdot F_c = \delta_A + K_u \cdot \frac{m \cdot {v_x}^2}{R};\quad \Rightarrow \quad K_u = \frac{\delta_f - \delta_A}{F_c} = \frac{\Delta\delta_f}{F_c};\quad or\quad K_{u3} = \frac{\Delta\delta_f}{a_c}$$

Understeering is a steady state property and does depend on which axle is steered, see Figure 4-19.

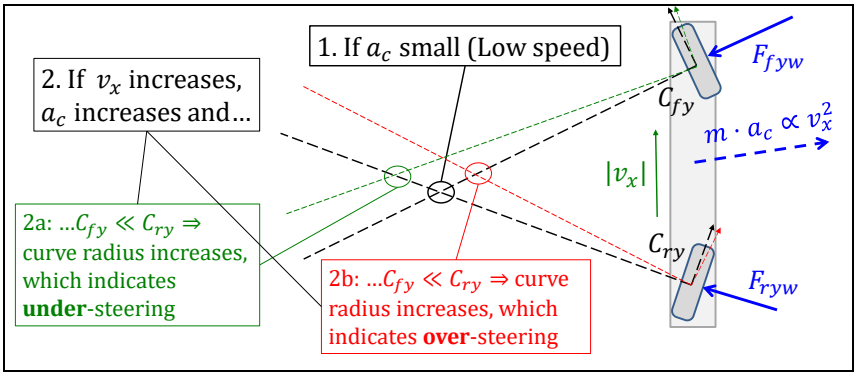

Figure 4-19: Under- and over-steering for a two-axle vehicle with $l_f = l_r$. It does not depend on which axle is steered, but which axle is first in the direction of motion. Figure drawn for vehicle driving forward.

4.3.3.2 Understeer Gradient as Varying with Steady State Lateral Acceleration

So far, the understeering gradient is presented as a fix vehicle parameter. There is nothing that says that a real vehicle behaves linear, so in order to get a well-defined value of K_u, the $\Delta\delta_f$ and the F_c should be small. However, if we accept that K_u can change with F_c, K_u can be defined as a differential quantity. K_u can also be understood as how much the additional steer angle, $\Delta\delta_f$, has to increase per increased centrifugal force, F_c, or per centrifugal acceleration, a_c:

$$K_u = \frac{\partial(\Delta\delta_f)}{\partial F_c} = \frac{\partial}{\partial F_c}(\delta_f - \delta_A) = \frac{\partial \Delta\delta_f}{\partial F_c}; \quad or \quad K_{u3} = \frac{\partial(\Delta\delta_f)}{\partial a_c} = \frac{\partial \delta_f}{\partial a_c}; \qquad [4.14]$$

Equation [4.14] shows the understeering gradient as a function of a_c, rather than a scalar parameter. But it is still fix and built-in in the vehicle. If assessing understeering for a lateral forces up to near road friction limit, Equation [4.14] is more relevant than Equation [4.9], because it reflects that understeering gradient changes.

4.3.3.3 Understeering as a Varying Quantity during a Transient Manoeuvre

A third understanding of the word understeering is quite different and less strictly defined. It is to see the understeering as a variable during a transient manoeuvre. For instance, a vehicle can be said to understeer if tyre side slip is larger on front axle than on rear axle, $|\propto_f| > |\propto_r|$, and over-steer if opposite, $|\propto_r| > |\propto_f|$. This way of defining understeering and oversteering is not built-in in vehicle but varies over time through a (transient) manoeuvre. E.g., when braking in a curve a vehicle loses grip on rear axle due to temporary load transfer from rear to front. Then the rear axles can slide outwards significantly, and the vehicle can be referred to as over-steering at this time instant, although the built-in understeering gradient is >0. This "instantaneous" under-/over-steering (binary, not an understeer gradient) can be approximately found from log data with this simple approximation:

$$\delta_{neutral} = \frac{L}{R} \approx \{v_x \approx R \cdot \omega_z\} \approx \frac{L \cdot \omega_z}{v_x} \approx \{a_y \approx v_x \cdot \omega_z\} \approx \frac{L \cdot a_y}{v_x^2}; \qquad [4.15]$$

If the actual vehicle has $|\delta_f| < |\delta_{neutral}|$ the vehicle oversteers, and vice versa. This is often very practical since it only requires simply logged data, δ_f, v_x and a_y. Note that when δ_f and $\delta_{neutral}$ have different signs, neither understeer or oversteers is suitable as classification, but it can sometimes be called "counter-steer". An example of applying Eq [4.15] is shown in Figure 4-20, where one also see that the ESC system does not follow the Eq [4.15] when deciding ESC interventions; ESC has more advanced "reference models", see 4.6.2.1.

A second look at Equation [4.9] tells us that we have to assume absence of propulsion and braking on front axle, $F_{fxw} = 0$, to get the relatively simple final expression. When propulsion on front axle ($F_{fxw} > 0$), the required steer angle, δ_f, will be smaller; the front propulsion pulls in the front end of the vehicle. When braking on front axle ($F_{fxw} < 0$), the required steer angle, δ_f, will be larger; the front braking hinders the front end to turn in. To keep v_x constant, which is required within definition of steady state, one have to propel the vehicle because there will always be some driving resistance to overcome. Driving fast on a small radius is a situation where the driving resistance from tyre lateral forces becomes significant, which is a part of driving resistance which was only briefly mentioned in 3.2.

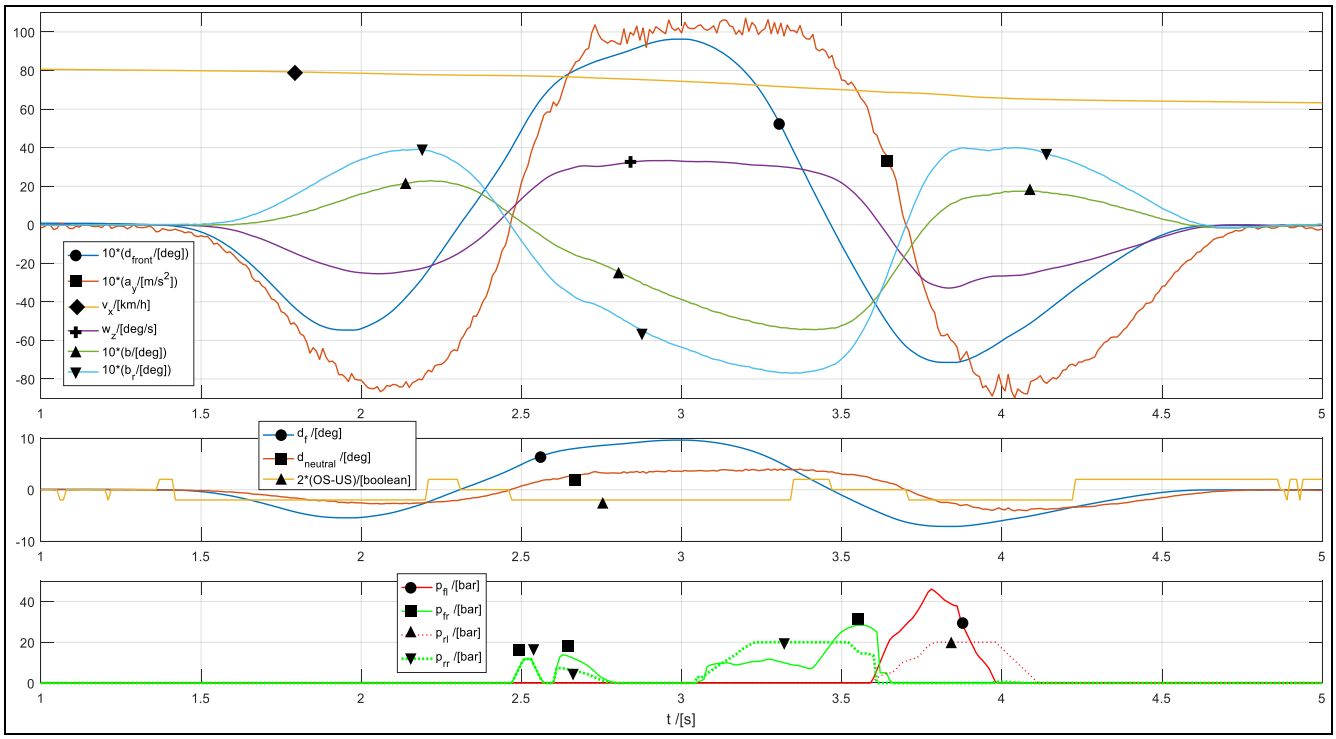

Figure 4-20: Log data from passenger car with ESC in a double lane change. Upper: Vehicle motion. Middle: $\delta_{neutral}$ from Eq [4.15] used to define "instantaneous under-/over-steering" (US/OS). Lower: Pressure to each wheel brake.

4.3.3.4 Neutral Steering Point

An alternative measure to understeering coefficient is the longitudinal position of the *neutral steering point*. The point is defined for lateral force disturbance during steady state **straight-ahead** driving, as opposed to steady state cornering without lateral force disturbance. The point is where a vehicle-external lateral force, such as wind or impact, can be applied on the vehicle without causing a yaw velocity ($\omega_z = 0$), i.e. only causing lateral velocity ($v_y \neq 0$). From this definition, we can derive a formula for calculating the position of the neutral steering point, see Figure 4-21.

The result is condensed in Eq [4.16].

$$l_s = \frac{C_r \cdot l_r - C_f \cdot l_f}{C_f + C_r} = K_u \cdot \frac{C_f \cdot C_r}{C_f + C_r} \cdot L; \quad where\ K_u = \frac{C_r \cdot l_r - C_f \cdot l_f}{C_f \cdot C_r \cdot L}; \qquad [4.16]$$

We can see that the understeer gradient from steady state cornering model appears also in the formula for neutral steering point position, l_s. Since $C_f, C_r\ and\ L$ are positive, the neutral steering point is behind of CoG for understeered (two-axle) vehicles, and in front of CoG for oversteered (two-axle) vehicles. This is why l_s and K_u can be said to be alternative measures for the same vehicle function/character, the yaw balance.

4.3.4 Required Steer Angle

A fundamental property of the vehicle is what steer angle that is required to negotiate a certain curvature (=1/path radius $= 1/R_p$). This value can vary with longitudinal speed and it can be normalized with wheel base, L. From Equation [4.9], we can conclude:

$$\boldsymbol{Normalized\ required\ steering\ angle} = \frac{\delta_f \cdot R_p}{L} = 1 + K_u \cdot \frac{m \cdot {v_x}^2}{L}; \qquad [4.17]$$

The normalized required steer angle is plotted for different understeering gradients Figure 4-22. It is the same as the inverted and normalized curvature gain, see 4.3.5.2.

Physical model:

- Steady state ($\dot{v}_x = \dot{v}_y = \dot{\omega}_z = 0$)
- Straight ahead driving ($\omega_z = 0$)
- No steering
- Small tyre and vehicle side slip. Then, angle=sin(angle)=tan(angle).

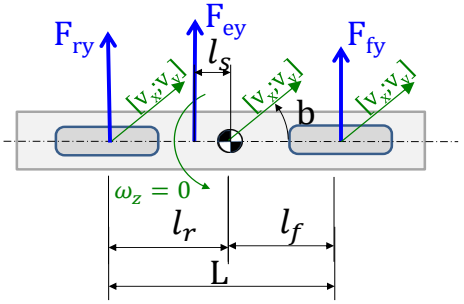

Mathematical model:

Equilibrium:

$$0 = F_{fy} + F_{ry} + F_e;$$

$$0 = F_{fy} \cdot l_f - F_{ry} \cdot l_r - F_e \cdot l_s;$$

Constitution: $F_{fy} = -C_f \cdot s_{fy}; and\ F_{ry} = -C_r \cdot s_{ry};$

Compatibility: $s_{fy} = s_{ry} = \frac{v_y}{v_x};$

Eliminate $F_{fy}, F_{ry}, s_{fy}, s_{ry}, F_e$ yields: $l_s = \frac{C_r \cdot l_r - C_f \cdot l_f}{C_f + C_r};$

Identify understeering gradient, $K_u = \frac{C_r \cdot l_r - C_f \cdot l_f}{C_f \cdot C_r \cdot L}$

Then:

$$l_s = K_u \cdot \frac{C_f \cdot C_r}{C_f + C_r} \cdot L;$$

Figure 4-21: Model for definition and calculation of neutral steering point.

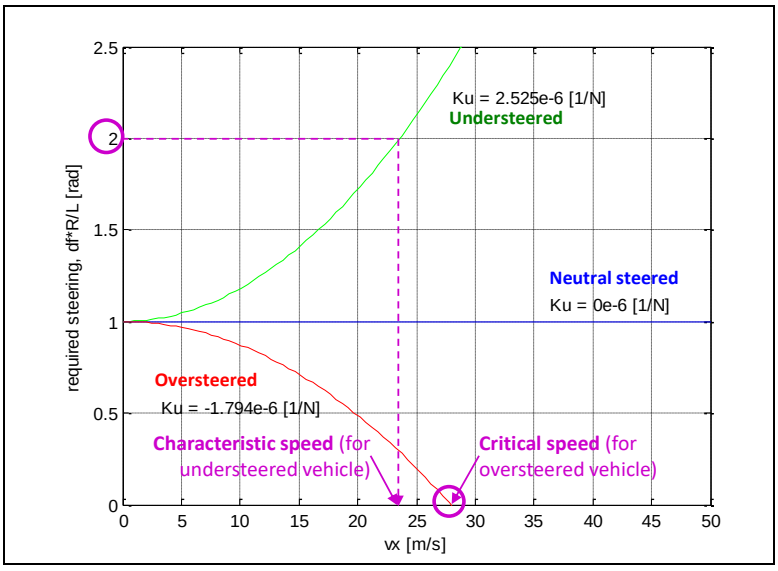

Figure 4-22: Normalized steer angle ($\delta_f \cdot R/L$) for Steady State Cornering

4.3.4.1 Critical and Characteristic Speed *

*Function definition: **Critical speed** is the speed above which the vehicle becomes unstable in the sense that the yaw velocity grows largely for a small disturbance in, e.g., steer angle.*

*Function definition: **Characteristic speed** is the speed at which the vehicle requires twice as high steer angle for a certain path radius as required at low speed (Figure 4-22). (Alternative definitions: The speed at which the yaw velocity gain reaches maximum (Figure 4-23). The speed at which the lateral acceleration gain per longitudinal speed reaches its highest value. (Figure 4-25).)*

We can identify that zero steer angle is required for the over-steered vehicle at 28 m/s. This is the so-called Critical Speed, which is the speed where the vehicle becomes unstable. It should be noted here, that there are stable conditions also above critical speed, but one has to steer in the opposite direction then. Normal vehicles are built understeered, which is why a Critical speed is more of a theoretical definition. However, if studying (quasi-steady state) situations where the rear axle is heavily braked, the cornering stiffness rear is reduced, and a critical speed can be relevant.

For understeered vehicles, we can instead read out another measure, the Characteristic Speed. The understanding of Characteristic Speed is, so far just that required steering increases to over twice what is needed for low speed at the same path radius. A better feeling for Characteristic Speed is suggested in 4.3.5.3.

The vehicle is unstable for speeds above the critical speed. Instability is further discussed in 4.4.4. From Equation [4.9], we can find a formula for critical and characteristic speeds:

$$\delta_f = \frac{L}{R_p} + K_u \cdot \frac{m \cdot {v_{x,crit}}^2}{R_p} = 0 \;\Rightarrow\; v_{x,crit} = \sqrt{\frac{L}{-K_u \cdot m}} = \sqrt{\frac{C_f \cdot C_r \cdot L^2}{(C_f \cdot l_f - C_r \cdot l_r) \cdot m}};$$

$$\delta_f = \frac{L}{R_p} + K_u \cdot \frac{m \cdot {v_{x,char}}^2}{R_p} = 2 \cdot \frac{L}{R_p} \;\Rightarrow\; v_{x,char} = \sqrt{\frac{L}{K_u \cdot m}} = \sqrt{\frac{C_f \cdot C_r \cdot L^2}{(C_r \cdot l_r - C_f \cdot l_f) \cdot m}}; \quad [4.18]$$

4.3.5 Steady State Cornering Gains *

Function definition: ***Steady state cornering gains*** *are the amplification from steer angle to certain vehicle response measures for steady state cornering at a certain longitudinal speed.*

From Equation [4.9], we can derive some interesting ratios. We put steer angle in the denominator, so that we get a gain, in the sense that the ratio describes how much of something we get "per steer angle". If we assume $F_{fxw} = 0$, we get Equation [4.19].

$$\textbf{\textit{Yaw velocity gain}} = \frac{\omega_z}{\delta_f} = \left\{use: \frac{\omega_z}{v_x} \approx \frac{1}{R_p}\right\} \approx \frac{v_x / R_p}{\frac{L}{R_p} + K_u \cdot \frac{m \cdot {v_x}^2}{R_p}} = \frac{v_x}{L + K_u \cdot m \cdot {v_x}^2};$$

$$\textbf{\textit{Curvature gain}} = = \frac{\kappa}{\delta_f} = \frac{1/R_p}{\delta_f} = \frac{1/R_p}{\frac{L}{R} + K_u \cdot \frac{m \cdot {v_x}^2}{R_p}} = \frac{1}{L + K_u \cdot m \cdot {v_x}^2};$$

$$\textbf{\textit{Lateral acceleration gain}} = = \frac{a_y}{\delta_f} = \left\{\begin{matrix} use: \\ a_y = \omega_z \cdot v_x; \\ and\ \frac{\omega_z}{v_x} \approx \frac{1}{R_p}; \end{matrix}\right\} \approx \frac{\frac{{v_x}^2}{R_p}}{\frac{L}{R_p} + K_u \cdot \frac{m \cdot {v_x}^2}{R_p}} = \frac{{v_x}^2}{L + K_u \cdot m \cdot {v_x}^2}; \quad [4.19]$$

Yaw velocity gain is also derived for $F_{fxw} \neq 0$, and then we get Equation [4.20].

$$\textbf{\textit{Yaw velocity gain}}\ (with\ F_{fxw}\ taken\ into\ account) = = \frac{\omega_z}{\delta_f} = \left(1 + \frac{F_{fxw}}{C_f}\right) \cdot \frac{v_x}{L + K_u \cdot m \cdot {v_x}^2}; \quad [4.20]$$

4.3.5.1 Yaw Velocity Gain

The yaw velocity gain gives us a way to understand Characteristic Speed. Normally one would expect the yaw velocity to increase if one increases the speed along a circular path. However, the vehicle will also increase its path radius when speed is increased. At the Characteristic Speed, the increase in radius cancel out the effect of increased speed, so that yaw velocity in total decrease with increased speed. One can find the characteristic speed as the speed where one senses or measures the highest value of yaw velocity for a fix steer angle. The curves for $F_{fxw} = +0.25 \cdot F_{fz}$ and $F_{fxw} = -0.25 \cdot F_{fz}$ in Figure 4-23 are generated using Eq [4.20]. Note that critical and characteristic speed is independent of F_{fxw}.

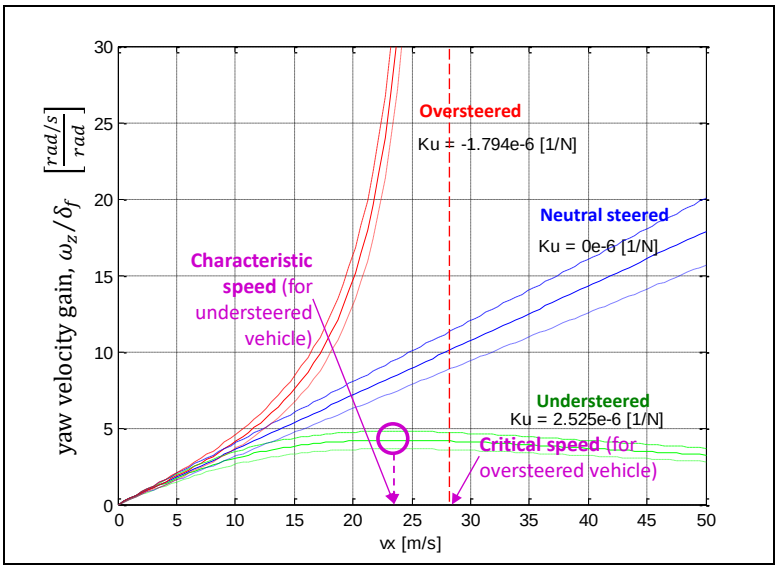

Figure 4-23: Yaw velocity gain (ω_z/δ_f) for Steady State Cornering. Each "cluster of 3 curves": Mid curve $F_{fxw} = 0$. Upper $F_{fxw} = +0.5 \cdot F_{fz}$. Lower $F_{fxw} = -0.5 \cdot F_{fz}$.

4.3.5.2 Curvature Gain

If driving on a constant path radius, and slowly increase speed from zero, an understeered vehicle will require more and more steer angle ("steer-in"), to stay at the same path radius. For an over-steered vehicle, one has to steer less ("open up steering") when increasing the speed.

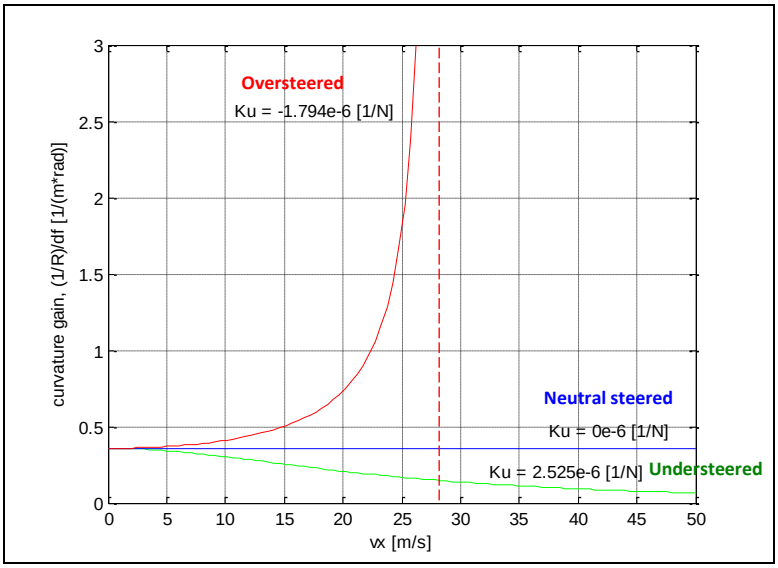

Figure 4-24: Curvature gain ($\frac{1/R}{\delta_f}$) for Steady State Cornering

4.3.5.3 Lateral Acceleration Gain

Figure 4-26 shows the lateral acceleration gain as function of vehicle speed. The characteristics speed is once again identified in this diagram, and now as the speed when lateral acceleration per longitudinal speed ($(a_y/\delta_f)/v_x$) reaches its highest value. This is an alternative definition of characteristic speed, c.f. 4.3.4.1.

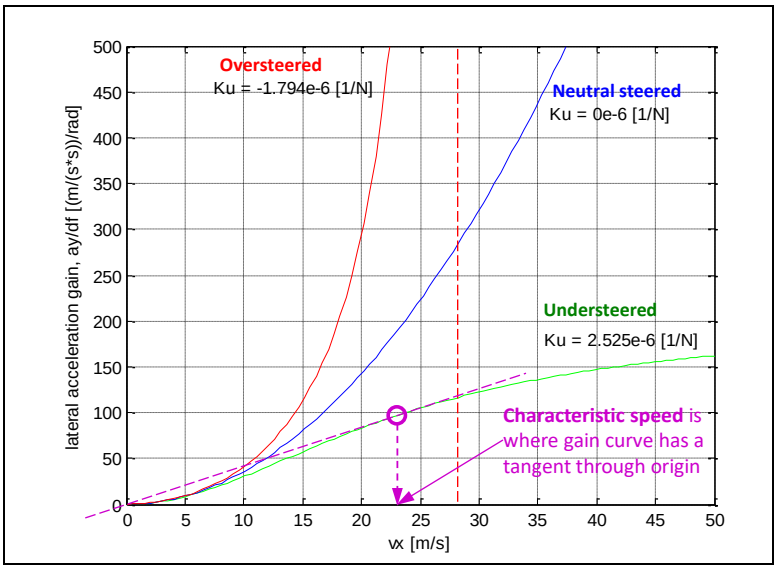

Figure 4-25: Lateral acceleration gain ($\frac{a_y}{\delta_f}$) for Steady State Cornering

From the previous figures the responsiveness of the vehicle can be identified for different understeer gradients. In all cases the vehicle which is understeered is the least responsive of the conditions. Both the yaw velocity and lateral acceleration cannot achieve the levels of the neutral steered or over-steered vehicle. The over-steered vehicle is seen to exhibit instability when the critical speed is reached since small changes in the input result in excessive output conditions. In addition, the over-steered vehicle will have a counter-intuitive response for the driver. To maintain a constant radius curve, an increase in speed requires that the driver turns the steering wheel opposite to the direction of desired path. The result of these characteristics leads car manufacturers to produce understeered vehicles that are close to neutral steering to achieve the best stability and driver feedback.

4.3.5.4 Side Slip Gain as Function of Speed

All gains above can be found from solving ω_z from Eq [4.9]. If instead solving the other unknown, v_y, we can draw "side slip gain" instead. Eq [4.21] shows the formula for this.

$$\frac{v_y}{v_x \cdot \delta_f} = \frac{C_f \cdot C_r \cdot l_r \cdot L - C_f \cdot l_f \cdot m \cdot {v_x}^2}{C_f \cdot C_r \cdot L^2 - \left(C_f \cdot l_f - C_r \cdot l_r\right) \cdot m \cdot {v_x}^2} \qquad [4.21]$$

It is not solely the understeering gradient that sets the curve shape, but we can still plot for some realistic numerical data, which are under-, neutral and over-steered, see Figure 4-26.

All cases in Figure 4-26 goes from positive side slip to negative when speed increases. This is the same as we expected already in Figure 4-17.

We can also calculate and plot the longitudinal location of the motion centre, i.e. $x_{MC} = -v_y/\omega_z$, by combining Eqs [4.21] and [4.19]. Note that R_x is independent of δ_f, while the longitudinal location of the motion centre, $y_{MC} = v_x/\omega_z$, is not.

4.3.5.5 Limitations due to Road Friction

The formulas with the gains in Eq [4.19] does not include the limitation due to maximum road friction, i.e. the peak of the tyres' $F_{iy}\left(s_{iy}\right)$ curves. This limitation is a lateral acceleration $a_{y,max}$ where on of the axles reach friction limit. Yaw and lateral equilibrium requires $F_{fy} = m \cdot a_y \cdot l_r/L$; and $F_{ry} = m \cdot a_y \cdot l_f/L$;, so the limit due to front axle is $m \cdot a_{y,max,f} \cdot l_r/L = \mu_f \cdot F_{fz} = \mu_f \cdot m \cdot g \cdot l_r/L \Rightarrow a_{y,max,f} = \mu_f \cdot g$; and corresponding for rear axle. The total limit is $a_{y,max} = \min\left(\mu_f, \mu_r\right) \cdot g$; Inserting this in Eq [4.19] and eliminate δ_f, one finds:

$$v_{x,max} = \sqrt{a_{y,max} \cdot R_p} = \sqrt{\min\left(\mu_f, \mu_r\right) \cdot g \cdot R_p}; \qquad [4.22]$$

For example, if negotiating a curve with $R = 100\ m$ and $\mu_f = \mu_r = 1$ gives $v_{x,max} \approx 31\ m/s \approx 113\ km/h$ and if either (or both) of μ_f and μ_r are just 0.5, $v_{x,max} \approx 22\ m/s \approx 80\ km/h$. So, we should see the curves in Figure 4-22 and in Figure 4-23 to Figure 4-26 as invalid over certain speed $v_{x,max}$, which depends on max road friction and curvature.

Reaching $v_{x,max}$ means loss of steerability if $\mu_f < \mu_r$, and loss of yaw stability if $\mu_r < \mu_f$. So, also an under-steered vehicle becomes unstable, if $\mu_r < \mu_f$ and driving faster than $v_{x,max}$. And, an oversteered vehicle might be limited from reaching its critical speed if $\mu_f < \mu_r$ and driving on a certain radius R.

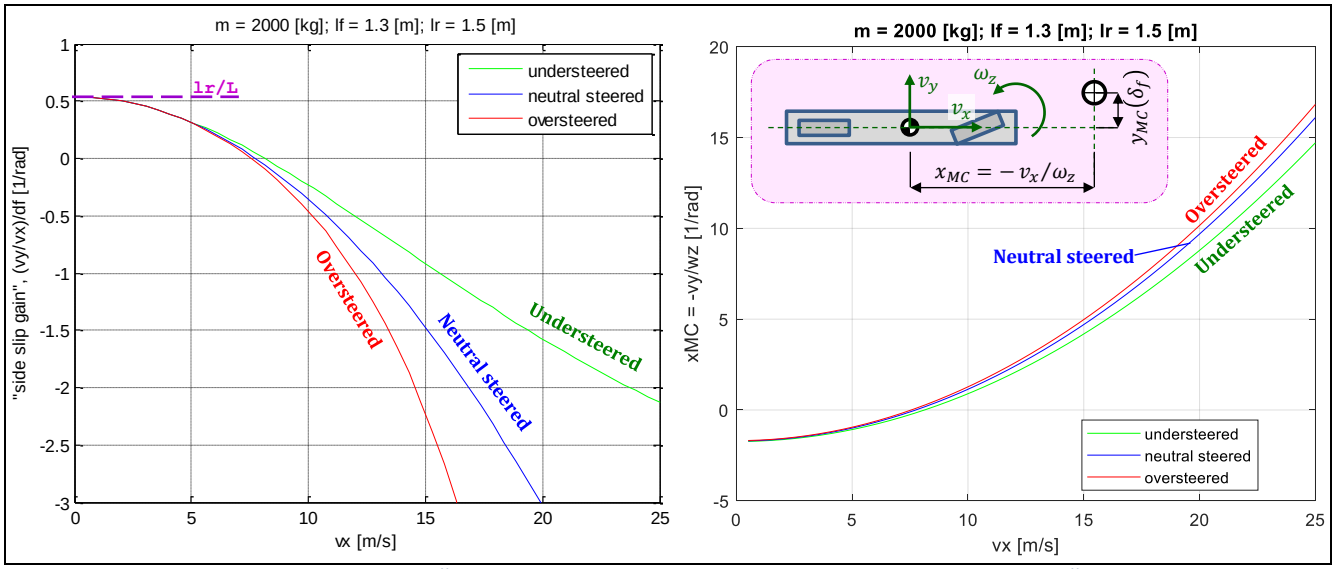

Figure 4-26: Left Side slip gain ($\frac{v_y}{v_x \cdot \delta_f}$). Right: Motion centre longitudinal location ($x_{MC} = \frac{-v_y}{\omega_z}$). For Steady State Cornering.

4.3.6 How Design Influences Steady State Gains

The cornering stiffness for each axle are only abstract design parameters which influence steady state gains. The cornering stiffness is a combined effect from various, more concrete, design parameters. Such more concrete design parameters are presented in 4.3.6. Also, some vehicle operation which affects understeering gradient, such as hard braking in 4.3.6.1, is mentioned.

4.3.6.1 Tyre Design, Inflation Pressure and Number of Tyres

The cornering stiffness of each tyre is an obvious parameter which influences the axle cornering stiffness. The cornering stiffness of an axle is influenced by the sum of cornering stiffness for all tyres. There are normally two tyres per axle, but there are also vehicles with one tyre (e.g. bicycles) or 4 (e.g. 2 double mounted tyres on each side in heavy trucks).

Tyre design influences, which is geometrical dimensions and material selection. Inflation pressure is in this context very close to a design parameter.

In a first approximation, tyre cornering stiffness is approximately proportional to vertical load: $C_{iy} = CC_{iy} \cdot F_{iz}$. For a vehicle with equally many and same tyres front and rear, this means that it will be neutral steered, neglecting body forces (air and grade). This is because, in steady state cornering, vertical loads are distributed over the axles in the same relation as lateral loads. Using definition of understeer gradient:

$$K_u = \frac{l_r}{C_f \cdot L} - \frac{l_f}{C_r \cdot L} = \frac{l_r}{CC_f \cdot F_{fz} \cdot L} - \frac{l_f}{CC_r \cdot F_{rz} \cdot L} = \begin{Bmatrix} longitudinal \\ load\ transfer \\ m \cdot a_x \cdot h/L \end{Bmatrix} =$$
$$= \frac{l_r}{CC_f \cdot \left(m \cdot g \cdot \frac{l_r}{L} - m \cdot a_x \cdot \frac{h}{L}\right) \cdot L} - \frac{l_f}{CC_r \cdot \left(m \cdot g \cdot \frac{l_f}{L} + m \cdot a_x \cdot \frac{h}{L}\right) \cdot L} =$$
$$= \frac{1}{m \cdot g} \cdot \left(\frac{l_r}{CC_f \cdot \left(l_r - \frac{a_x}{g} \cdot h\right)} - \frac{l_f}{CC_r \cdot \left(l_f + \frac{a_x}{g} \cdot h\right)} \right) = \begin{Bmatrix} if\ CC_f = \\ = CC_f = CC_y \end{Bmatrix} =$$
$$= \frac{1}{m \cdot g \cdot CC_y} \cdot \left(\frac{1}{\left(1 - \frac{a_x}{g} \cdot \frac{h}{l_r}\right)} - \frac{1}{\left(1 + \frac{a_x}{g} \cdot \frac{h}{l_f}\right)} \right) = \begin{Bmatrix} if \\ a_x = 0 \end{Bmatrix} = 0; \quad [4.23]$$

Longitudinal load transfer (influence of a_x in the equations) show that braking increases over-steering tendency. It is actually so, that the critical speed $v_{x,crit} = \sqrt{L/(-K_u \cdot m)}$ (see Equation [4.18]) can come down to quite reachable levels when braking hard; i.e. hard braking at high speed may cause instability. This is especially so for front biased CoG location. See Figure 4-27, inspired by Reference (Drenth, 1993).

However, the cornering stiffness varies degressively, e.g. $C_i = k_{ip} \cdot F_{iz} - k_{id} \cdot {F_{iz}}^2$. This is further studied in Reference (Drenth, 1993).

If taking the degressiveness of tyre cornering stiffness into account, the weight distribution plays a role also without longitudinal load transfer; front biased weight distribution gives under-steered vehicles and vice versa. Also, the number of wheels per axle influence stronger; single wheel front (or double-mounted rear) gives under-steered vehicles and vice versa.

It should be noted that if the longitudinal acceleration is due to wheel torques, as opposed to road grade or aerodynamic forces, the tyre combined slip effects will influence the curves which is not considered in Figure 4-27; the cornering stiffness of an axle will decrease with increased longitudinal force.

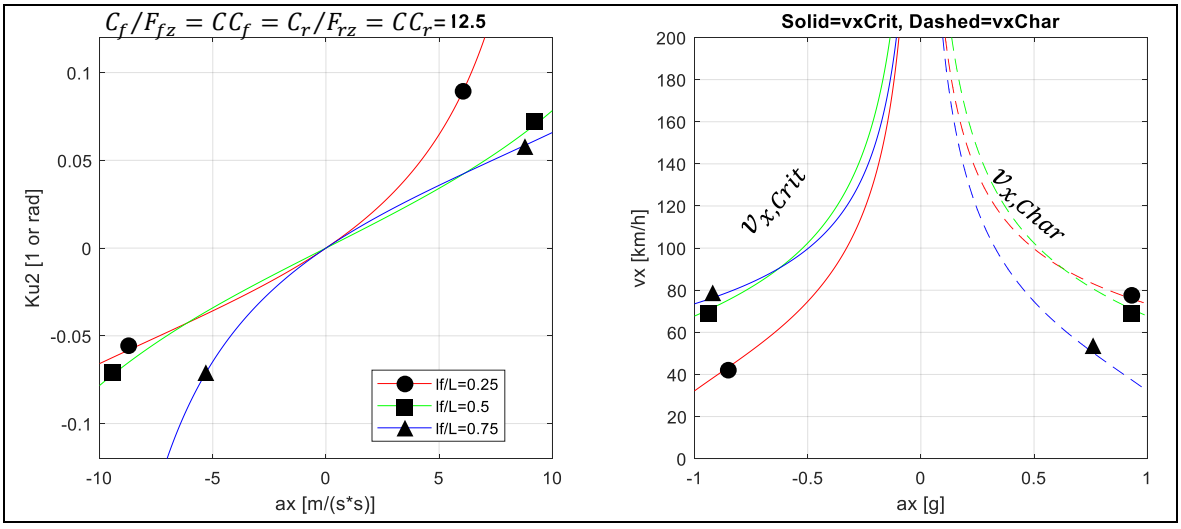

Figure 4-27: Left: Under-steering gradient as function of longitudinal acceleration, a_x, and static load distribution, l_f/L. Right: Critical and characteristic velocity as function of acceleration and load distribution.

4.3.6.2 Roll Stiffness Distribution between Axles

During cornering, the vertical load is shifted towards the outer wheels. Depending on the roll stiffness of each axle, the axles take differently much of this lateral load transfer. This also influences the yaw balance. The more roll stiff an axle is, the more of the lateral load shift it takes. Tyre cornering stiffness

varies degressively with vertical load. Together, this means that increasing the roll stiffness on the front axle, leads to less front cornering stiffness, see Figure 2-35, and consequently more understeered vehicle. Increasing roll stiffness on rear axle makes the vehicle more oversteered. The total roll stiffness of the vehicle does not influence the understeering gradient. Normally one makes the front axle more roll stiff than the rear axle. This means that vehicle becomes more and more understeered for increased lateral acceleration, e.g. more steer angle is needed to maintain a certain path radius if speed increases. One can change the roll stiffness of an axle by changing roll centre height, wheel stiffness rate and anti-roll bar stiffness.

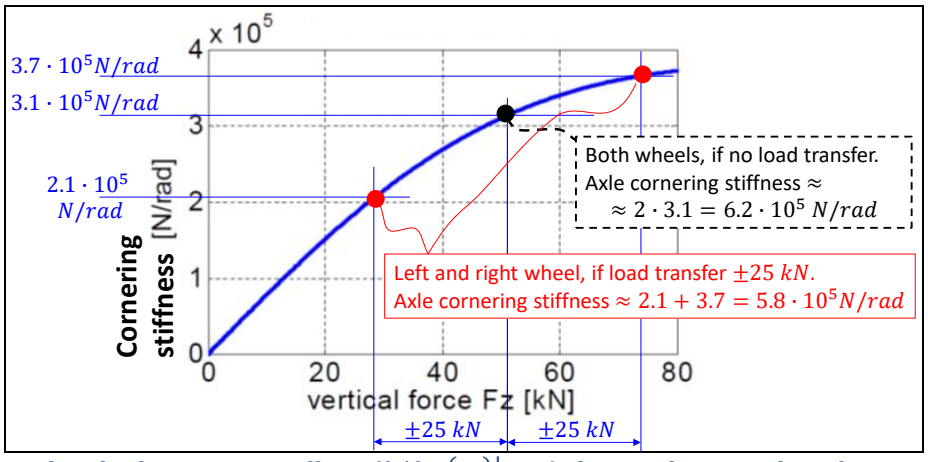

Figure 4-28: The wheels cornering stiffness ($\partial/\partial\alpha\,(F_y)|_{s_y=0}$) changes degressively with vertical load. The axle cornering stiffness therefore decreases with increased load transfer.

4.3.6.3 Steering and Suspension Compliances

4.3.6.3.1 Side-Force Steer Gradient

Side-force steer gradient, c_{iSFS}, is defined for an axle and it is how much the wheels on an axle steers [deg] negatively per lateral force [N]. Negative is chosen since the normal case is that pivot point is ahead of wheel, so that wheel steers negative for a positive force. Also, a non-steered axle steers due to side force steering, which depends on the compliance of the suspension bushings.

It can be modelled as an extra compliance, with the constitutional equations: $F_{fy} = -c_{fSFS} \cdot \Delta\delta_f$; and $F_{ry} = -c_{rSFS} \cdot \Delta\delta_r$;, where the Δ marks additional steer angle due to the lateral force. These extra compliances come into play as series connected with the tyre cornering compliances. If we update Equation [4.9] with side force steering it becomes:

$$\delta_f = \frac{L}{R} + K_u \cdot \frac{m \cdot {v_x}^2}{R};$$

$$where\ K_u = \frac{l_r}{C_{f,tot} \cdot L} - \frac{l_f}{C_{r,tot} \cdot L} = \frac{C_{r,tot} \cdot l_r - C_{f,tot} \cdot l_f}{C_{f,tot} \cdot C_{r,tot} \cdot L};$$

$$where\ C_{f,tot} = \frac{1}{\frac{1}{C_f} + \frac{1}{c_{fSFS}}} \quad and \quad C_{r,tot} = \frac{1}{\frac{1}{C_r} + \frac{1}{c_{rSFS}}};$$

[4.24]

For vehicles with largely varying vertical axle load (such as heavy trucks), one has to consider that the contribution from tyre to axle cornering stiffness is rather proportional to vertical axle load, while the contribution from side-force steering comes from suspension elasticities and is rather constant. So, utilizing side-force steering makes the vehicles lateral manoeuvrability inconsistent with vertical load.

4.3.6.3.2 Roll Steer Gradient

Roll steer gradient, k_{iRS}, is defined for an axle and it is how much the wheels on an axle steers [deg] per vehicle roll angle [deg]. Also, a non-steered axle can steer due to roll-steering. Roll-steering depends on the suspension linkage geometry. The added steer angle can be expressed: $\Delta\delta_i = k_{iRS} \cdot \varphi_x$;.

We will now derive the influence on steady state cornering. Add steering on rear axle to Eq [4.9]:

$$\delta_f - \delta_r \approx \frac{L}{R_p} + K_{u,noRS} \cdot \frac{m \cdot {v_x}^2}{R_p}; K_{u,noRS} = \frac{C_r \cdot l_r - C_f \cdot l_f}{C_f \cdot C_r \cdot L};$$ (subscript "*noRS*" means "*no Roll-Steer*")

If we see δ_i as built up by one angle from the steering system δ_{i0} and one part coming from the suspension, via roll-steering $\Delta\delta_i$:

$$\delta_{f0} + \Delta\delta_f - (\delta_{r0} + \Delta\delta_r) \approx \frac{L}{R_p} + K_{u,noRS} \cdot \frac{m \cdot {v_x}^2}{R_p};$$

Then, we can express $\Delta\delta_i$ in φ_x:

$$\Delta\delta_i = \{\Delta\delta_i = k_{iRS} \cdot \varphi_x\} = k_{iRS} \cdot \varphi_x; \quad for\ i = f, r.$$

We can also express the relation between a_y and φ_x:

$$\Delta\delta_i = k_{iRS} \cdot \varphi_x = \begin{Bmatrix} m \cdot a_y \cdot h = \\ = c_x \cdot \varphi_x \end{Bmatrix} = k_{iRS} \cdot \frac{m \cdot a_y \cdot h}{c_x} = \left\{a_y = \frac{v_x^2}{R}\right\} = \frac{h \cdot k_{iRS}}{c_x} \cdot \frac{m \cdot v_x^2}{R_p}; \quad for\ i = f, r.$$

Insertion identifying an understeering gradient with roll-steering gives:

$$\delta_{f0} - \delta_{r0} \approx \frac{L}{R_p} + K_{u,RS} \cdot \frac{m \cdot v_x^2}{R_p}; K_{u,RS} = K_{u,noRS} + \frac{h \cdot \left(k_{rRS} - k_{fRS}\right)}{c_x}; \qquad [4.25]$$

4.3.6.3.3 Quantified Combined Effect

Side force steering and roll-steering are similar but have different time scales. Roll-steering requires that sprung body changes roll angle, which takes significantly longer time; typically roll eigen-frequency is 1..2 Hz. Side force steering does not require a roll angle change, so side-force steering has much less time delay. Roll-steering also comes into play for one-sided road unevenness, i.e. also without cornering and without body roll.

The combined effect from steering system (0), side force steering (4.3.6.3.1) and roll-steering (4.3.6.3.2) often represent a significant part of the front axle cornering compliance, e.g. reduces compliance with 20..40% compared to tyre cornering compliance only, Reference (Wedlin, o.a., 1992). Most of this is due to steering system compliance.

On rear axles on passenger cars, the influence is typically less and in opposite direction, e.g. increase 1..5% compared to tyre cornering compliance only.

Rear axles on heavy vehicles are typically designed without significant side-force steering. However, the frame compliance can cause a relevant amount of side-force oversteering due to that the whole frame steers curve-outwards rear and curve-inwards front. The frame compliance is especially influential on a tractor with fifth wheel ahead of rear axle(s); clearly larger than sideforce compliance on a single axle and on a rigid truck about the same, depending on the body-build on the frame.

Patents exist for making the rear axle suspension on heavy vehicle's trailers sideforce steering so that axle becomes less cornering compliant, reducing compliance with typically 1/3 compared to tyre cornering compliance only. This increases yaw stability, which is very much same concept as using sideforce understeering rear at a two-axle vehicle. Using this concept can lead to very yaw stable vehicles. The drawback is reduced yaw agility. If really exaggerated, it can take the rear axle to effectively negative cornering stiffness, which makes vehicle unstable.

4.3.6.4 Camber Steer

Negative camber (wheel top leaning inwards) increases the cornering stiffness. One explanation to this is that curve outer wheel gets more vertical load than the curve inner wheel. Hence, the inwards directed camber force from outer wheel dominates over outwards directed camber force from the inner wheel. Negative camber is often used at rear axle at passenger cars. Drawback with non-zero camber is tyre wear.

4.3.6.5 Toe Angle

Toe has some, but limited effect on an axle's cornering stiffness. Non-zero toe increases tyre wear. Toe-angle: When rolling ahead, tyre side forces pre-tension bushes.

If toe (=toe-in) is positive there are tyre-lateral forces on each tyre already when driving straight ahead, even if left and right cancel out each other: $F_{ay} = \left(C_{left} - C_{right}\right) \cdot \frac{toe}{2} = 0;$. Then, if the axle

takes a side force, the vertical loads of the wheels are shifted between left and right wheel, which also changes the tyre cornering stiffnesses. The outer wheel will get more cornering stiffness. Due to positive toe, it will also have the largest steer angle. So, the axle will generate larger lateral force than with zero toe. For steady-state cornering vehicle models, this effect comes in as an increased axle cornering stiffness, i.e. a linear effect.

4.3.6.6 Wheel Torque Effects

Wheel torque give tyre longitudinal force, directed as the wheel is directed. If the wheel is steered, the wheel longitudinal forces can influence the yaw balance, see also F_{fxw} in Equation [4.9].

Unsymmetrical wheel torques (left/right) will give a **direct yaw moment** in the yaw equilibrium in Equation [4.6]. The actuated yaw moment around CoG is then of the magnitude of wheel longitudinal wheel force times half the track width. ESC and Torque vectoring interventions have such effects.

High longitudinal utilization of friction on an axle leads to that lateral grip is reduced on that axle. The changed yaw moment, compared to what one would have without using friction longitudinally, can be called an **indirect yaw moment**. The actuated change in yaw moment around CoG is then of the magnitude of change in wheel lateral wheel force times half the wheel base. It influences the yaw balance. That is the reason why a front axle driven vehicle may be more understeered than a rear axle driven one. On the other hand, the wheel-longitudinal propulsion force on the front axle does also help the turn-in, which acts towards less understeering.

4.3.6.7 Transient Vehicle Motion Effects on Yaw Balance

The effects presented here are not so relevant for steady state understeering coefficient. However, they affect the yaw balance in a more general sense, why it is relevant to list them in this section.

- Longitudinal load transfer changes normal forces. E.g. strong deceleration by wheel forces helps against under-steering, since front axle gets more normal load. This effect has some delay. Also, it vanishes after the transient.
  (This effect can be compared with the effect described in 4.3.6.2, which is caused by tyre cornering stiffness varying degressively with vertical load, while the longitudinal load transfer effect can be explained solely with the proportional variation.)
- Change of longitudinal speed helps later in manoeuvre. E.g. deceleration early in a manoeuvre makes the vehicle easier to manoeuvre later in the manoeuvre. It is the effect of the term $\omega_z \cdot v_x$ that is reduced.

4.3.6.8 Some Other Design Aspects

High cornering stiffness is generally desired for controllability.

Longer wheel base (with unchanged yaw inertia and unchanged steering ratio) improves the transient manoeuvrability, because the lateral forces have larger levers to generate yaw moment with.

4.3.7 Manoeuvrability and Stability

The overall conclusion of previous section is that all gains become higher the more over-steered (or less understeered) the vehicle is. Higher gains are generally experienced as a sportier vehicle and they also improves safety because they improve the manoeuvrability. A higher manoeuvrability makes it easier for the driver to do avoidance manoeuvres. This motivates a design for low understeering gradient.

However, there is also the effect that a vehicle with too small understeer gradient becomes very sensitive to the steering wheel angle input. In extreme, the driver would not be able to control the vehicle. This limits how small the understeering gradient one can design for. Generally, vehicles are built understeered.

It is not impossible for a driver to keep an unstable vehicle ($K_u < 0$ and $v_x > v_{x,crit}$) on an intended path, but it requires an active compensation with steering wheel. If adding support systems, such as yaw damping by steering support or differentiated propulsion torques, it can be even easier. If one

could rely on a very high up time for such support systems, one could move today's trade-off between manoeuvrability and stability. This conceptual design step has been taken for some airplanes, which actually are designed so that they would be unstable without active control. See also 4.4.4.

4.3.8 Handling Diagram

There are many frequently used graphical tools or diagrams to represent vehicle characteristics. One is the "handling diagram". A handling diagram is useful for comparing yaw stability. A handling diagram is essential a plot of same data as in Lateral Acceleration gain in Figure 4-25, but the curve $a_y(\delta_f)$ for one v_x instead of $a_y/\delta_f\ (v_x)$. For the linear model it would be a straight line, with $da_y/d\delta_f = constant = {v_x}^2/(L + K_u \cdot m \cdot {v_x}^2)$. But for a more advanced model, or a real vehicle test, it becomes more interesting.

A handling diagram is constructed as follows. Same simplifying assumptions are done as in Figure 4-18, with the exception that we don't assume linear tyre models.

Equilibrium:

$$\left\{ m \cdot \frac{{v_x}^2}{R} = m \cdot a_y = F_{fy} + F_{ry};\quad 0 = F_{fy}\ \cdot l_f\ - F_{ry} \cdot l_r; \right\} \Rightarrow F_{fy} = \frac{l_r}{L} \cdot m \cdot a_y;\ F_{ry} = \frac{l_f}{L} \cdot m \cdot a_y;$$

Constitution:

$$F_{fy} = F_{fy}(\alpha_f) \Rightarrow \alpha_f = {F_{fy}}^{-1}(F_{fy});\quad F_{ry} = F_{ry}(\alpha_r) \Rightarrow \alpha_r = {F_{ry}}^{-1}(F_{ry});$$

Solving for $\alpha_f - \alpha_r$ yields:

$$\alpha_r - \alpha_f = {F_{ry}}^{-1}(F_{ry}) - {F_{fy}}^{-1}(F_{fy}) = {F_{ry}}^{-1}\left(\frac{l_f}{L} \cdot m \cdot a_y\right) - {F_{fy}}^{-1}\left(\frac{l_r}{L} \cdot m \cdot a_y\right);$$

So, we can plot $\alpha_r - \alpha_f$ as function of a_y. This relation is interesting because compatibility ($\delta_f + \alpha_f - \alpha_r = L/R$;) yields $\alpha_r - \alpha_f = \delta_f - L/R = \delta_f - \delta_A$. And $\delta_f - \delta_A$ is connected to one of the understandings of K_u in Equation [4.14], ($K_u = \frac{\partial}{\partial a_y}(\delta_f - \delta_A)$;). If we plot $\alpha_r - \alpha_f = \delta_f - \delta_A$ on abscissa axis and a_y on ordinate axis, we get the most common way of drawing the handling diagram, see Figure 4-29. The axle's constitutive relations can be used as graphical support to construct the diagram, but then the constitutive relations should be plotted as: $a_{yi}(\alpha_i) = \frac{L}{L-l_i} \cdot \frac{1}{m} \cdot F_{iy}(\alpha_i)$;. The quantity a_{yi} can be seen as the lateral force scaled with a certain fraction of vehicle mass, where the certain fraction is such that both axles' values correspond to the same vehicle lateral acceleration.

Figure 4-29 shows the construction of a handling diagram from axle slip characteristics. Figure 4-30 show examples of handling diagrams constructed via tests with simulation tools. Handling diagrams can be designed from real vehicle tests as well. The slope in the handling diagram corresponds to understeering gradient K_{u3} in Equation [4.13].

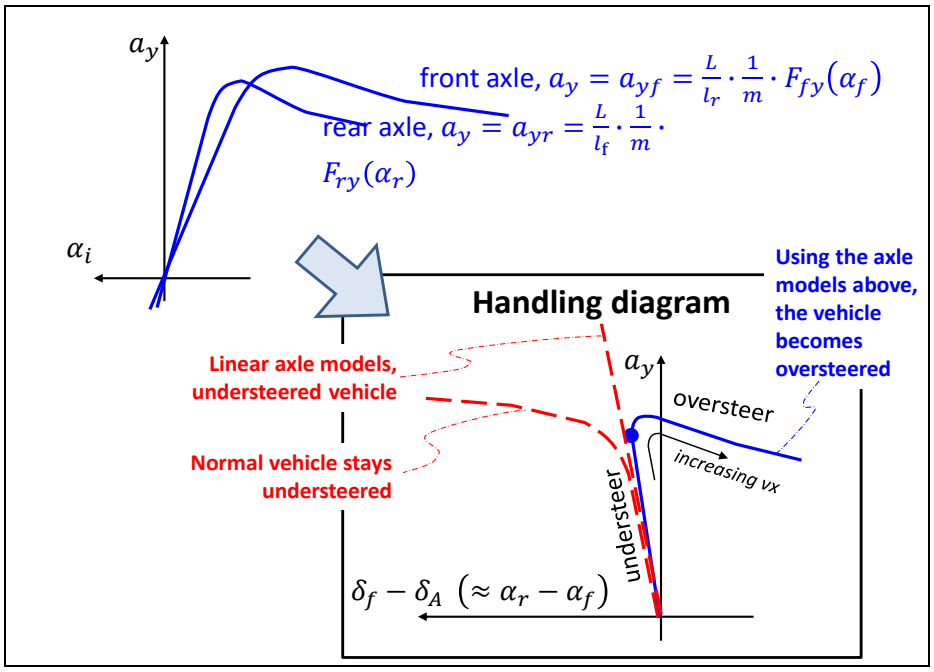

Figure 4-29: Construction of the "Handling diagram". The axle's slip characteristics (upper diagram) are chosen so that vehicle transits from understeer to over-steer with increased longitudinal speed, v_x. The dashed shows two other slip characteristics.

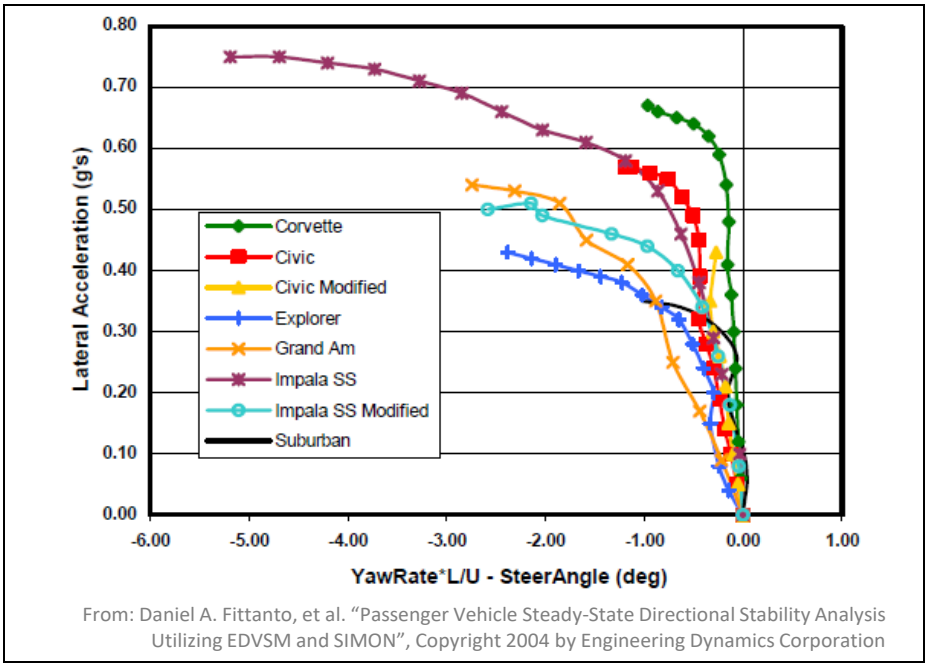

From: Daniel A. Fittanto, et al. "Passenger Vehicle Steady-State Directional Stability Analysis Utilizing EDVSM and SIMON", Copyright 2004 by Engineering Dynamics Corporation

Figure 4-30: Example of handling diagram.

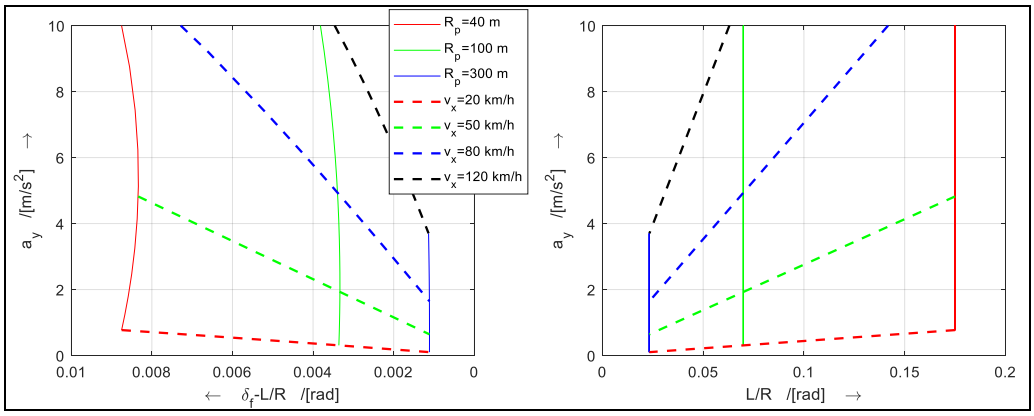

4.3.9 Lateral Load Transfer in Steady State Cornering

In the chapter about longitudinal dynamics we studied (vertical tyre) load transfer between front and rear axle. The corresponding issue for lateral dynamics is load transfer between left and right side of the vehicle. Within the steady state lateral dynamics, we will cover some of the simpler effects, but save the more complex suspension linkage dependent effects to 4.4.4.

The relevance to study the load transfer during steady state cornering is to limit the roll during cornering (for comfort) and yaw balance (understeering gradient, see 4.3.6.2). Additionally, the load transfer influence the transient handling; see 4.4 and 4.4.4.

4.3.9.1 Load Transfer between Vehicle Sides

Without resolving into front and rear, we do not need to involve suspension in model:

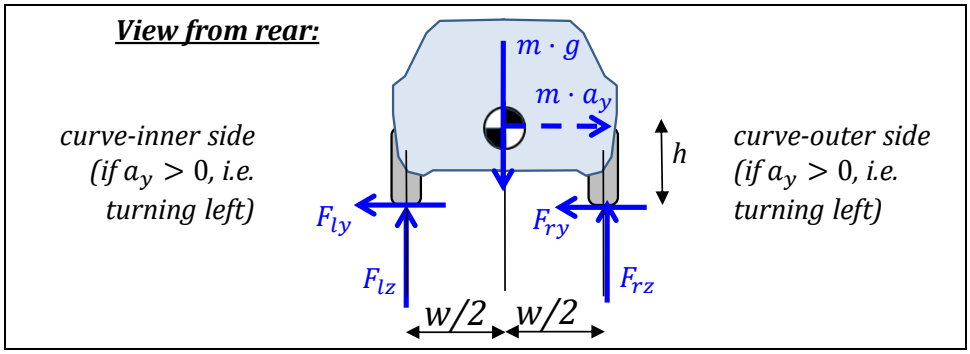

Figure 4-31: A cornering vehicle. The $m \cdot a_y$ is a fictive force. Subscript l and r mean left and right.

Moment equilibrium, around left contact with ground: ⇒

$$\Rightarrow m \cdot g \cdot \frac{w}{2} + m \cdot a_y \cdot h - F_{rz} \cdot w = 0 \Rightarrow F_{rz} = m \cdot \left(\frac{g}{2} + a_y \cdot \frac{h}{w}\right);$$

Moment equilibrium, around right contact with ground: $\Rightarrow F_{lz} = m \cdot \left(\frac{g}{2} - a_y \cdot \frac{h}{w}\right);$ [4.26]

These equations confirm what we know from experience, the curve-inner side if off-loaded.

4.3.9.2 Body Heave and Roll Due to Lateral Wheel Forces

Now, we shall find out how much the vehicle rolls and heaves during steady state cornering. First, we decide to formulate the model in "effective stiffnesses", in the same manner as for longitudinal load transfer in previous chapter.

There is no damping included in model, because their forces would be zero, since there is no displacement velocity, due to the "quasi-steady-state" assumption. As constitutive equations for the compliances (springs) we assume that displacements are measured from a static condition and that the compliances are linear. The road is assumed to be smooth, i.e. $z_{lr} = z_{rr} = 0$ (2nd subscript means *road*).

$$F_{lz} = F_{lz0} + c_{side} \cdot (z_{lr} - z_l) + c_{arb} \cdot \big((z_{lr} - z_l) - (z_{rr} - z_r)\big) = \\ = \{z_{lr} = z_{rr} = 0\} = F_{lz0} - (c_{side} + c_{arb}) \cdot z_l + c_{arb} \cdot z_r;$$
$$F_{rz} = \cdots = F_{rz0} - (c_{side} + c_{arb}) \cdot z_r + c_{arb} \cdot z_l;$$
$$where\ F_{lz0} + F_{rz0} = m \cdot g; \quad and \quad F_{lz0} \cdot w/2 - F_{rz0} \cdot w/2 = 0;$$

[4.27]

The stiffnesses c_{side} and c_{arb} (arb means *anti-roll bar*) are effective stiffnesses as measurable under the wheels. The physical springs are mounted inside in some kind of linkage and have different stiffness values, but their effect is captured in the effective stiffnesses. Some examples of different physical spring and linkage design are given in 2.3.3.1 and 2.3.4.1.

We see already in free-body diagram in Figure 4-32 that F_{yl} and F_{yr} always act together, so we rename $F_{yl} + F_{yr} = F_y$. We see in Figure 2-54 that we have to assume something about how the lateral forces are transferred from road to body. The "trivial linkage" from Figure 2-54 is assumed. **Equilibrium** then gives:

$$F_y - m \cdot a_y = 0;$$
$$m \cdot g - F_{zl} - F_{zr} = 0;$$
$$F_{zl} \cdot (w/2) - F_{zr} \cdot (w/2) + F_y \cdot h + m \cdot g \cdot (-y) = 0;$$

[4.28]

The term $m \cdot g \cdot (-y)$ is taken as $m \cdot g \cdot (h - h_{RC}) \cdot \sin(\varphi_x) \approx m \cdot g \cdot (h - h_{RC}) \cdot \varphi_x$. It assumes a height for the point where the roll takes place, h_{RC}. We don't know the value of it, until below where we study the suspension design, but it can be mentioned already here that most vehicles have an $h_{RC} \ll h$. This causes a "pendulum effect", especially significant for heavy commercial vehicles due to their large h..

Compatibility, to introduce body displacements, z and φ_x, gives:

$$z_l = z + (w/2) \cdot \varphi_x; \quad and \quad z_r = z - (w/2) \cdot \varphi_x;$$

[4.29]

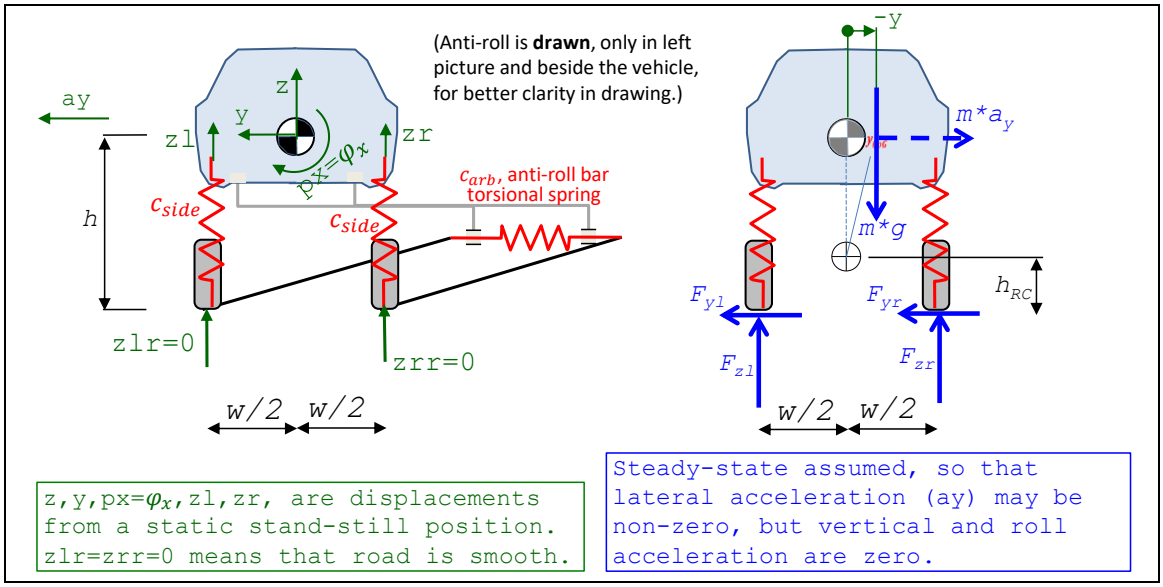

Figure 4-32: Model for steady state heave and roll due to lateral acceleration. Suspension model is no linkage (or "trivial linkage") and without difference front and rear.

Combining constitutive relations, equilibrium and compatibility, gives, as Matlab script:

```
syms …; sol=solve( ...
    Flz==Flz0-(cside+carb)*zl+carb*zr, ...
    Frz==Frz0-(cside+carb)*zr+carb*zl, ...
    Flz0+Frz0==m*g,  Flz0*w/2-Frz0*w/2==0, ...
    Fy-m*ay==0, ...
    m*g-Flz-Frz==0', ...
    Flz*(w/2)-Frz*(w/2)+Fy*h+m*g*(h-hRC)*px==0, ...
    zl==z+(w/2)*px,  zr==z-(w/2)*px, ...
    Fzl1==-1/((Fzl/m-g/2)*w/(ay*h)), ...
    zl, zr, Flz, Frz, Flz0, Frz0, Fy, z, px);
```

[4.30]

The results from the Matlab script in Equation [4.30]:

$$
\begin{aligned}
&F_y = m \cdot a_y; \;\; z = 0; \\
&p_x = \varphi_x = \frac{2 \cdot m \cdot a_y \cdot h}{(c_{side} + 2 \cdot c_{arb}) \cdot w^2 - 2 \cdot m \cdot g \cdot (h - h_{RC})}; \\
&F_{lz} = m \cdot \left(\frac{g}{2} - \frac{a_y \cdot h}{w} \Big/ \left(1 - \frac{2 \cdot m \cdot g}{c_{side} + 2 \cdot c_{arb}} \cdot \frac{h - h_{RC}}{w^2} \right) \right); \\
&F_{rz} = m \cdot \left(\frac{g}{2} + \frac{a_y \cdot h}{w} \Big/ \left(1 - \frac{2 \cdot m \cdot g}{c_{side} + 2 \cdot c_{arb}} \cdot \frac{h - h_{RC}}{w^2} \right) \right);
\end{aligned}
\qquad [4.31]
$$

In agreement with intuition and experience the body rolls with positive roll when steering to the left (positive F_{yw}). Further, the body centre of gravity is unchanged in heave (vertical motion, z). The formula uses h_{RC} which we cannot estimate without modelling the suspension. Since front and rear axle normally are different, we could expect that h_{RC} is expressed in some similar quantities for each of front and rear axle, which also is the case, see Equation [4.38].

4.3.9.2.1 Steady-State Roll-Gradient *

Function definition: ***Steady state roll-gradient*** *is the body roll angle per lateral acceleration for the vehicle during steady state cornering with a certain lateral acceleration and certain path radius on level ground.*

4.3.9.3 Lateral Load Transfer Models of Suspension Linkage

For longitudinal load transfer, during purely longitudinal dynamic manoeuvres, the symmetry of the vehicle makes it reasonable to split vertical load on each axle equally between the left and right wheel of the axle. However, for lateral dynamics it is not very realistic to assume symmetry between front and rear axle. Hence, the suspension has to be considered separately for front and rear axle. The properties that are important to model for each axle is not only left and right elasticity (as we modelled the whole vehicle in Figure 4-32). It is also how the lateral tyre forces are transmitted from road contact patches to the vehicle body. We end up with conceptually the same two possible linkage modelling concepts as we found for longitudinal load transfer, see Figure 3-27. Either we can introduce 1 roll centre heights for each axle (c.f. pitch centre in 3.4) or we can introduce two pivot points for each axle (1 per wheel if individually suspended wheels or 2 per axle if rigid axle) (c.f. axle pivot points in 3.4). A difference for lateral load transfer, compared to longitudinal load transfer, is that it is significant also at steady state (due to centrifugal force). The two modelling ways to include the suspension in the lateral load transfer are shown in Figure 4-33. Generally speaking, they can be combined, so that one is used on front axle and the other on rear axle. In this compendium, we will select the roll-centre model when modelling.

One should differ between roll-centre heights and roll-centres. One can say that roll-centre heights exists while roll-centres is only a model concept. If a vehicle was actually designed with a roll-centre as being a real pivot point between axle and body, that vehicle would be totally rigid in vertical direction.

4.3.9.3.1 Load Transfer Model with Two Pivot Points per Axle

This model will not be deeply presented in this compendium. However, it should be mentioned as having quite a few advantages:

- The model has both heave and roll degree of freedom. (Roll centre model is restricted to roll around roll centre.)
- If wheel independent suspension, the distribution of lateral wheel forces between left and right side is considered. (Roll centre model only uses the sum of lateral forces per axle and needs involvement of tyre model to resolve into individual left and right side forces.)

Generally spoken, this model is more accurate and not much more computational demanding and probably easier to intuitively understand, since it does not constrain heave motion.

Note that non-individual, rigid axles or beam axles, the pivot-point model does not have one pivot point for each wheel, but instead two pivot points for the whole axle: heave and roll. The roll-centre height affects as the height where lateral force is transferred between axle and body.

Cases when this model is recommended as opposed to the model with roll centres are:

- Steady state and transient manoeuvres where the heave displacement is important.

- When large differences between lateral load on left and right wheels are present, such as:
  - Large load transfer, i.e. high CoG and large lateral accelerations. One example is when studying wheel lift and roll-over tendencies.
  - Large differences between longitudinal slip, while axle skids sideways. Then one wheel might have zero lateral force, due to that friction is used up longitudinally, while the other can have a large lateral force.
  - If individual steering within an axle would be studied. One could think of an extreme case if actuating a sudden toe-in or toe-out, which would cause large but counter-directed lateral forces on left and right wheel.

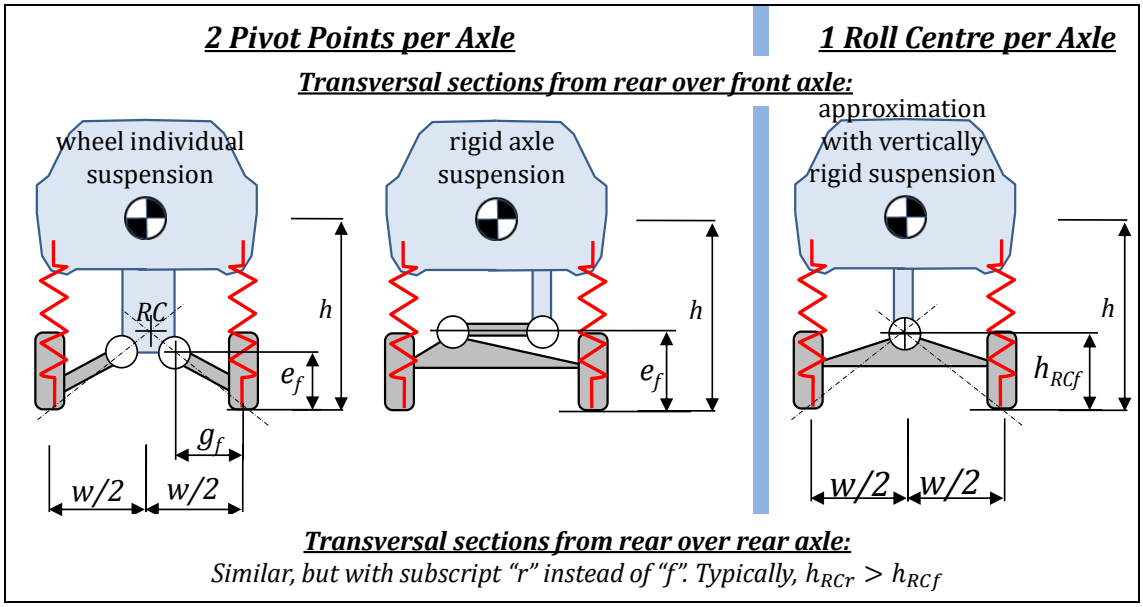

Figure 4-33: Two alternative models for including suspension linkage effects (kinematics) in lateral load transfer. Anti-roll bars not drawn.

4.3.9.3.2 Load Transfer Model with Roll Centre (One Pivot Point) per Axle

The model with 1 roll centres has some drawback as listen before. To mention some advantages, it is somewhat less computational demanding. However, the main reason why the compendium uses this model is to cover two different concepts with longitudinal and lateral load transfer.

Study the free-body diagrams in Figure 4-34.

The road is assumed to be flat, $z_{flr} = z_{frr} = z_{rlr} = z_{rrr} = 0$. In free-body diagram for the front axle, P_{fz} and P_{fy} are the reaction force in the rear roll-centre. Corresponding reaction forces are found for rear axle. Note that roll centres are free of roll moment, which is the key assumption about roll centres. The $F_{sfl}, F_{sfr}, F_{srl}$ and F_{srr} are the forces in the compliances, i.e. where potential spring energy is stored. One can understand the roll-centres as also unable to take vertical force, as opposed to constraining vertical motion (as drawn). Which of vertically force-free or vertically motion-free depends on how one understands the concept or roll-centre, and it does not influence the equations.

Note carefully that the "pendulum effect" is NOT included here, in 4.3.9.3, as it was in 4.3.9.2. The motivation is to get simpler equations for educational reasons.

There is no damping included in model, because their forces would be zero, since there is no displacement velocity, due to the steady-state assumption. As constitutive equations for the compliances (springs) we assume that displacements are measured from a static condition and that the compliances are linear. Note that there are two elasticity types modelled: springs per wheel (c_{fw} per front wheel and c_{rw} per rear wheel) and anti-roll bars per axle (c_{af} front and c_{ar} rear). The road is assumed to be smooth, i.e. $z_{flr} = z_{frr} = z_{rlr} = z_{rrr} = 0$. The stiffnesses c_{fw}, c_{rw}, c_{af} and c_{ar} are effective stiffnesses per wheel. We see already in free-body diagram that F_{fly} and F_{fry} always act together, so we rename $F_{fly} + F_{fry} = F_{fy}$ and $F_{rly} + F_{rry} = F_{ry}$.

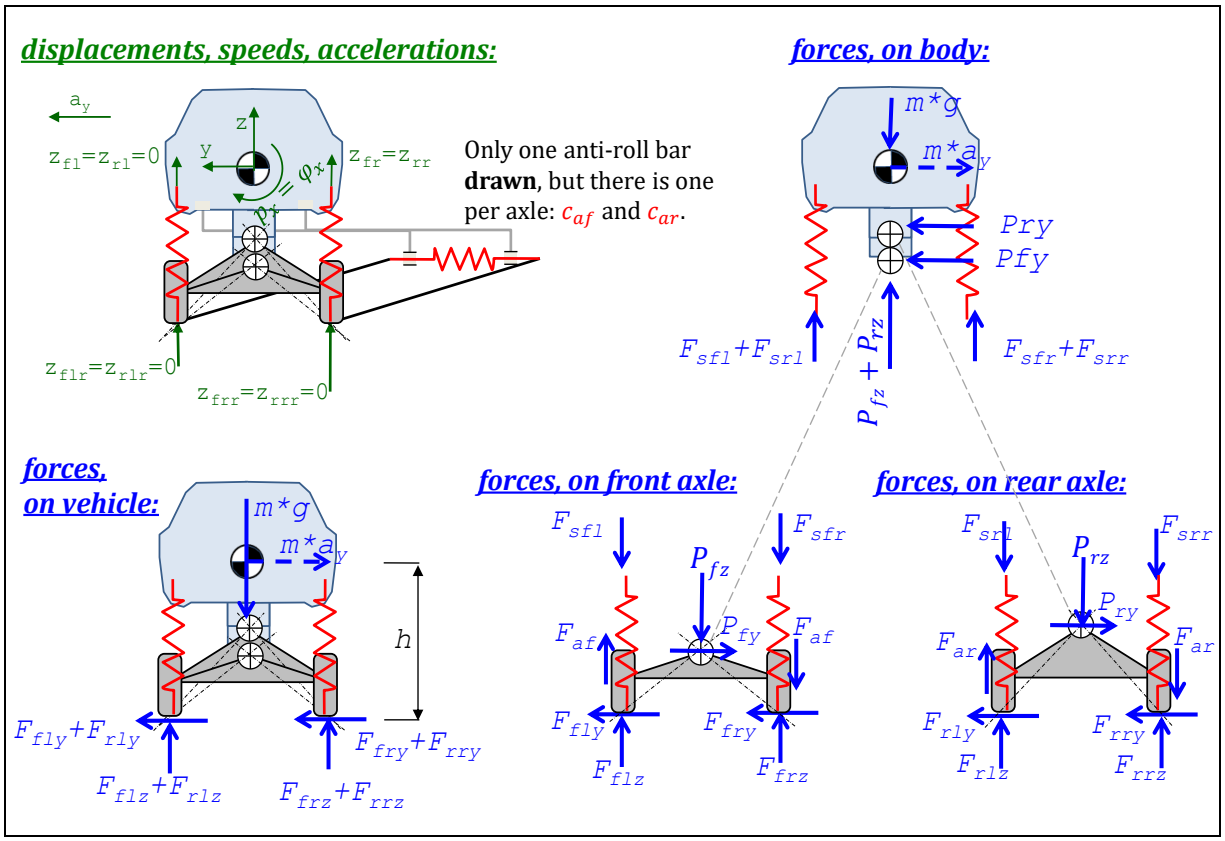

Figure 4-34: Model for steady state heave and roll due to lateral acceleration, using roll centres, which can be different front and rear.

$$
\begin{aligned}
F_{sfl} &= F_{sfl0} + c_{fw} \cdot (\cancel{z_{flr}} - z_{fl});\\
F_{sfr} &= F_{sfr0} + c_{fw} \cdot (\cancel{z_{frr}} - z_{fr});\\
F_{srl} &= F_{srl0} + c_{rw} \cdot (\cancel{z_{rlr}} - z_{rl});\\
F_{srr} &= F_{srr0} + c_{rw} \cdot (\cancel{z_{rrr}} - z_{rr});\\
F_{af} &= 0 + c_{af} \cdot \left((\cancel{z_{flr}} - z_{fl}) - (\cancel{z_{frr}} - z_{fr})\right);\\
F_{ar} &= 0 + c_{ar} \cdot \left((\cancel{z_{rlr}} - z_{rl}) - (\cancel{z_{rrr}} - z_{rr})\right);\\
\text{where } F_{sfl0} &= F_{sfr0} = \frac{m \cdot g \cdot l_r}{2 \cdot L};\ \text{and}\ \ F_{srl0} = F_{srr0} = \frac{m \cdot g \cdot l_f}{2 \cdot L};
\end{aligned}
\qquad [4.32]
$$

Equilibrium for whole vehicle (vertical, lateral, yaw, pitch, roll) neglecting body forces (air resistance and gravity components in road plane) gives:

$$
\begin{aligned}
&F_{flz} + F_{frz} + F_{rlz} + F_{rrz} = m \cdot g;\\
&m \cdot a_y = F_{fy} + F_{ry};\\
&0 = F_{fy} \cdot l_f - F_{ry} \cdot l_r;\\
&-(F_{flz} + F_{frz}) \cdot l_f + (F_{rlz} + F_{rrz}) \cdot l_r = 0;\\
&(F_{flz} + F_{rlz}) \cdot \frac{w}{2} - (F_{frz} + F_{rrz}) \cdot \frac{w}{2} + (F_{fy} + F_{ry}) \cdot h = 0;
\end{aligned}
\qquad [4.33]
$$

Equilibrium for each axle (roll, around roll centre):

$$
\begin{aligned}
&(F_{flz} - F_{sfl} + F_{af}) \cdot \frac{w}{2} - (F_{frz} - F_{sfr} - F_{af}) \cdot \frac{w}{2} + F_{fy} \cdot h_{RCf} = 0;\\
&(F_{rlz} - F_{srl} + F_{ar}) \cdot \frac{w}{2} - (F_{rrz} - F_{srr} - F_{ar}) \cdot \frac{w}{2} + F_{ry} \cdot h_{RCr} = 0;
\end{aligned}
\qquad [4.34]
$$

Compatibility, to introduce body displacements, z, φ_x and φ_y, gives:

$$z_{fl} = z + \frac{w}{2} \cdot \varphi_x - l_f \cdot \varphi_y; \quad and \quad z_{fr} = z - \frac{w}{2} \cdot \varphi_x - l_f \cdot \varphi_y;$$
$$z_{rl} = z + \frac{w}{2} \cdot \varphi_x + l_r \cdot \varphi_y; \quad and \; z_{rr} = z - \frac{w}{2} \cdot \varphi_x + l_r \cdot \varphi_y;$$
$$z_{fl} + z_{fr} = 0; \quad and \quad z_{rl} + z_{rr} = 0; \qquad [4.35]$$

The measure Δh is redundant and can be connected to the other geometry measures as follows. The geometrical interpretation is given in Figure 4-35.

$$\Delta h = h - \frac{l_r \cdot h_{RCf} + l_f \cdot h_{RCr}}{L}; \qquad [4.36]$$

Combining Equations [4.32] to [4.36] gives, as Matlab script and solution:

```
syms …; sol=solve( ...
    Fsfl==Fsfl0-cfw*zfl,  Fsfr==Fsfr0-cfw*zfr, ...
    Fsrl==Fsrl0-crw*zrl,  Fsrr==Fsrr0-crw*zrr, ...
    Faf==0-caf*(-zfl+zfr),  Far==0-car*(-zrl+zrr), ...
      Fsfl0==(1/2)*m*g*lr/L,  Fsfr0==(1/2)*m*g*lr/L, ...
      Fsrl0==(1/2)*m*g*lf/L,  Fsrr0==(1/2)*m*g*lf/L, ...
    Fflz+Ffrz+Frlz+Frrz==m*g, ...
    m*ay==Ffy+Fry, ...
    0==Ffy*lf-Fry*lr, ...
    -(Fflz+Ffrz)*lf+(Frlz+Frrz)*lr==0, ...
    (Fflz+Frlz)*w/2-(Ffrz+Frrz)*w/2+(Ffy+Fry)*h==0, ...
      (Fflz-Fsfl+Faf)*w/2-(Ffrz-Fsfr-Faf)*w/2+Ffy*hRCf==0, ...
      (Frlz-Fsrl+Far)*w/2-(Frrz-Fsrr-Far)*w/2+Fry*hRCr==0, ...
    zfl==z+(w/2)*px-lf*py,  zfr==z-(w/2)*px-lf*py, ...
    zrl==z+(w/2)*px+lr*py,  zrr==z-(w/2)*px+lr*py, ...
      zfl+zfr==0,  zrl+zrr==0, ...
    dh==h-(lr*hRCf+lf*hRCr)/(lf+lr), ...
    zfl, zfr, zrl, zrr, Fsfl, Fsfr, Fsrl, Fsrr, ...
    Faf, Far, Fsfl0, Fsfr0, Fsrl0, Fsrr0, ...
    Fflz, Ffrz, Frlz, Frrz, Ffy, Fry, z, px, py, h);
```

[4.37]

The result from the Matlab script in Equation [4.37], but in a prettier writing format:

$$F_{fy} = m \cdot a_y \cdot \frac{l_r}{L}; \quad and \quad F_{ry} = m \cdot a_y \cdot \frac{l_f}{L};$$
$$z = 0; \quad and \quad p_x = \frac{m \cdot a_y \cdot \Delta h}{c_{vehicle,roll}} = \frac{(F_{fy}+F_{ry}) \cdot \Delta h}{c_{vehicle,roll}}; \quad and \quad p_y = 0;$$
$$F_{flz} = m \cdot \left(\frac{g \cdot l_r}{2 \cdot L} - a_y \cdot \left(\frac{h_{RCf} \cdot l_r}{L \cdot w} + \frac{\Delta h}{w} \cdot \frac{c_{f,roll}}{c_{vehicle,roll}} \right) \right);$$
$$F_{frz} = m \cdot \left(\frac{g \cdot l_r}{2 \cdot L} + a_y \cdot \left(\frac{h_{RCf} \cdot l_r}{L \cdot w} + \frac{\Delta h}{w} \cdot \frac{c_{f,roll}}{c_{vehicle,roll}} \right) \right);$$
$$F_{rlz} = m \cdot \left(\frac{g \cdot l_f}{2 \cdot L} - a_y \cdot \left(\frac{h_{RCr} \cdot l_f}{L \cdot w} + \frac{\Delta h}{w} \cdot \frac{c_{r,roll}}{c_{vehicle,roll}} \right) \right);$$
$$F_{rrz} = m \cdot \left(\frac{g \cdot l_f}{2 \cdot L} + a_y \cdot \left(\frac{h_{RCr} \cdot l_f}{L \cdot w} + \frac{\Delta h}{w} \cdot \frac{c_{r,roll}}{c_{vehicle,roll}} \right) \right);$$

where, roll stiffnesses are:

$$c_{f,roll} = 2 \cdot (c_{fw} + 2 \cdot c_{af}) \cdot \left(\frac{w}{2}\right)^2 \quad \left[\frac{Nm}{rad}\right];$$
$$c_{r,roll} = 2 \cdot (c_{rw} + 2 \cdot c_{ar}) \cdot \left(\frac{w}{2}\right)^2 \quad \left[\frac{Nm}{rad}\right];$$
$$c_{vehicle,roll} = c_{f,roll} + c_{r,roll} \quad \left[\frac{Nm}{rad}\right];$$

[4.38]

The axle roll stiffnesses, $c_{f,roll}$ and $c_{r,roll}$ are identified beside vehicle roll stiffness $c_{vehicle,roll}$. We should compare Equation [4.38] with Equation [4.31]. Eq [4.31] considers the "pendulum effect", but not the differentiation between front and rear suspension. Eq [4.38] does the opposite.

Assume $h = h_{RC}$ and look at the sum of vertical force on one side, F_{lz} in Eq [4.31]. Compare F_{zl} in Eq [4.31] and $F_{flz} + F_{rlz}$ in Eq [4.38]; the equations agree if:

$$F_{flz} + F_{rlz} = F_{zl} \Rightarrow m \cdot \left(\frac{g}{2} - a_y \cdot \left(\frac{h_{RCf} \cdot l_r + h_{RCr} \cdot l_f}{L \cdot w} + \frac{\Delta h}{w}\right)\right) = m \cdot \left(\frac{g}{2} - a_y \cdot \frac{h}{w}\right) = F_{zl} \Rightarrow$$

$$\Rightarrow \frac{h_{RCf} \cdot l_r + h_{RCr} \cdot l_f}{L \cdot w} + \frac{\Delta h}{w} = \frac{h}{w} \Rightarrow h_{RCf} \cdot l_r + h_{RCr} \cdot l_f = (h - \Delta h) \cdot L;$$

This is exactly in agreement with the definition of the redundant geometric parameter Δh, see Eq [4.36]. This means that a consistent geometric model of the whole model is as drawn in Figure 4-35. Here the artefact roll axis is also defined.

The terms of type $h_{RCi} \cdot l_j/(L \cdot w)$ in Eq [4.38] can be seen as the part of the lateral tyre forces that goes via the stiff linkage. The terms of type $(\Delta h/w) \cdot \left(c_{iw}/\left(c_{iw} + c_{jw}\right)\right)$ in Eq [4.38] can be seen as the part of the lateral tyre forces that goes via the compliance. The latter part is distributed in proportion to roll stiffness of the studied axle, as a fraction of the vehicle roll stiffness. This should agree with intuition and experience from other preloaded mechanical systems (load distributes as stiffness).

Body rolls with positive roll when steering to the left, as long as CoG is above roll axle. Further, the body centre of gravity is unchanged in heave (vertical z) because the model does not allow any vertical displacements, which is a drawback already mentioned.

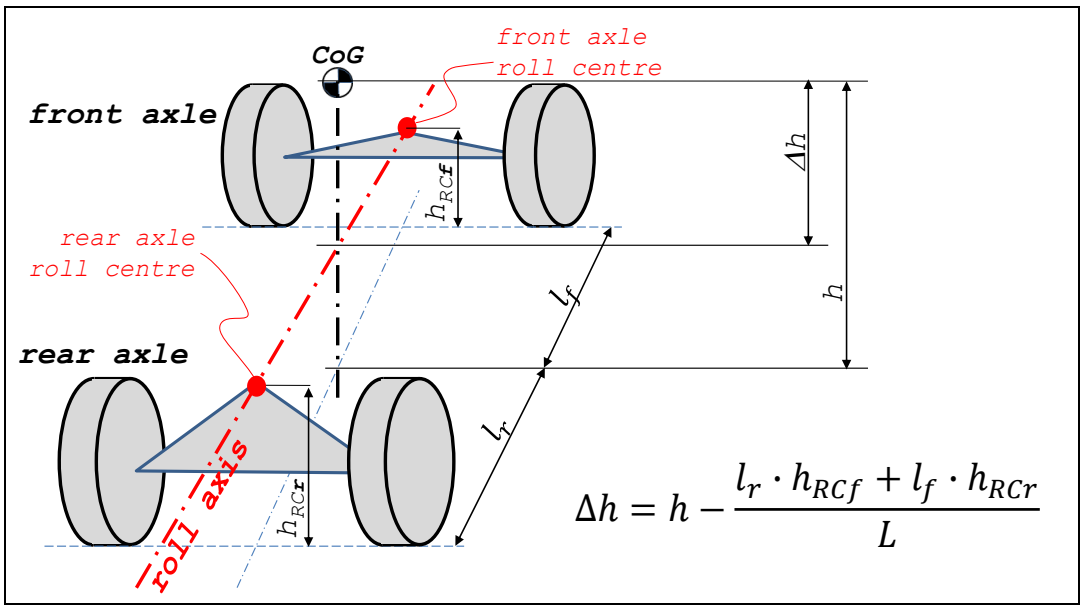

Figure 4-35: Roll axis for a two-axle vehicle. (Note that the picture may indicate that the roll centres and roll axis are above wheel centre, but this is normally not the case.)

Eq [4.44] was derived as a *steady state out-of-road-plane* model, but only the ratio between roll stiffnesses influence the lateral load transfer. So, if the roll stiffnesses are large, they can be neglected (considered infinite), if the ratios are given. Then, Eq [4.44] works also for transient manoeuvres.

4.3.9.3.3 Steady State Longitudinal and Lateral Distribution

If the vehicle has a steady state acceleration with combined a_x and a_y, we can combine Eqs [4.38]and [3.27] (with $\left(F_{fx} + F_{rx}\right) = m \cdot a_x$) to Eq [4.39]. Note that body forces (air resistance and gravity components in road plane) are neglected.

$$F_{flz} = m \cdot \left(\frac{g \cdot l_r}{2 \cdot L} - a_x \cdot \frac{h}{2 \cdot L} - a_y \cdot \left(\frac{h_{RCf} \cdot l_r}{L \cdot w} + \frac{\Delta h}{w} \cdot \frac{c_{f,roll}}{c_{vehicle,roll}}\right)\right);$$

$$F_{frz} = m \cdot \left(\frac{g \cdot l_r}{2 \cdot L} - a_x \cdot \frac{h}{2 \cdot L} + a_y \cdot \left(\frac{h_{RCf} \cdot l_r}{L \cdot w} + \frac{\Delta h}{w} \cdot \frac{c_{f,roll}}{c_{vehicle,roll}}\right)\right); \qquad [4.39]$$

$$F_{rlz} = m \cdot \left(\frac{g \cdot l_f}{2 \cdot L} + a_x \cdot \frac{h}{2 \cdot L} - a_y \cdot \left(\frac{h_{RCr} \cdot l_f}{L \cdot w} + \frac{\Delta h}{w} \cdot \frac{c_{r,roll}}{c_{vehicle,roll}} \right) \right);$$

$$F_{rrz} = m \cdot \left(\frac{g \cdot l_f}{2 \cdot L} + a_x \cdot \frac{h}{2 \cdot L} + a_y \cdot \left(\frac{h_{RCr} \cdot l_f}{L \cdot w} + \frac{\Delta h}{w} \cdot \frac{c_{r,roll}}{c_{vehicle,roll}} \right) \right);$$

4.3.10 High Speed Steady State Vehicle Functions

4.3.10.1 Steering Feel *

Function definition: ***Steering feel*** *is the steering wheel torque response to steering wheel angle. The function is used in a very wide sense; on a high level, it is a measure of steering wheel torque, or its variation, for certain driving situations. Often, it can only be subjectively assessed.*

At steady state driving at high speed, there are basically three aspects of steering feel:

- Lateral steering feel feedback at cornering. The steering wheel torque is normally desired to increase monotonously with lateral forces on the front axle. This is basically the way the mechanics work due to castor trail. Some specifications on steering assistance system is however needed to keep the steering wheel torque low enough for comfort.
- Steering torque drop when cornering at low-friction. It is built into the mechanics of the castor trail and the pneumatic trail that steering wheel torque drops slightly when one approaches the friction limit on front axle. This is normally a desired behaviour because it gives driver feedback that the vehicle is approach the limits.
- On-centre feel in straight line driving. When the vehicle is driven in straight line, the steering wheel is normally desired to return to centre position after small perturbations. This is a comfort function, which OEMs works a lot with, and it is often rather subjectively assessed.

4.3.10.2 High Speed Steady-State Off-tracking *

Function definition: ***High speed steady-state off-tracking*** *is the lateral offset between the paths of the centre of the front axle and the centre of the most severely off-tracking axle of any unit in a steady turn at a certain friction level and a certain constant longitudinal speed. From Reference [(Kati, 2013)].*

The function is mainly of interest for long combination vehicles, as illustrated in Figure 4-36. Off-tracking was also mentioned in 4.2. It measures the lateral road space required. High speed Off-tracking, which is an outboard off-tracking, can be either determined in a steady state turn or in a transient manoeuvre such as lane change; the latter is termed as high speed transient off-tracking, see 4.5.6.2.

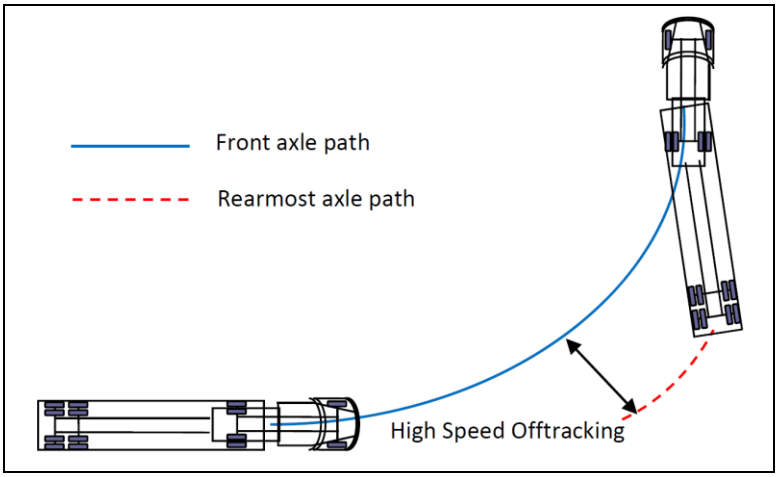

Figure 4-36: Illustration of high speed off-tracking. From (Kharrazi , 2012).

4.3.10.3 Tracking-Ability on Straight Path *

Function definition: ***Tracking-ability on straight path*** *is the swept width between outer-most axle centres when driving at a road with certain cross-fall and certain road friction at a certain speed.*

The axles on any vehicle driving at a road with cross-fall will not track exactly in each other's trajectories. This is especially pronounced if long vehicles with many articulation points. The driving situation is straight steady state low or high speed.

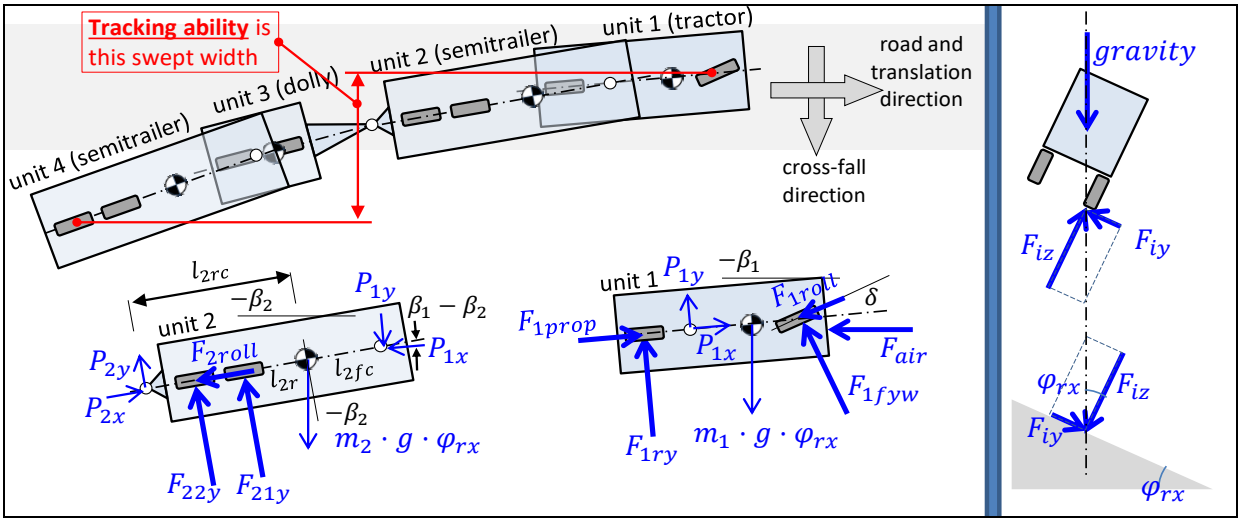

Figure 4-37: Tracking ability on straight path for an "A-double" (Tractor-SemiTrailer-Dolly-SemiTrailer).

An example is seen in Figure 4-37. If we neglect longitudinal forces and combined tyre slip effects, and assume same cornering coefficient, CC, on all axles we can derive these equations:

- $F_{1fyw} = -CC \cdot F_{1fz} \cdot (\beta_1 - \delta)$;
- $F_{1ry} = -CC \cdot F_{1rz} \cdot \beta_1$;
- $F_{iy} = -CC \cdot F_{iz} \cdot \beta_i; \quad for\ i = 2..4$

Since the levers for moment equilibria in road x-y-plane and in road x-z-plane are equal, the distribution of the axles' vertical forces and lateral forces becomes identical. So, relation between lateral force and vertical force becomes $\frac{F_{iy}}{F_{iz}} = \tan(\varphi_{rx}) \approx \varphi_{rx}$ for all axles:

- $\varphi_{rx} = -CC \cdot (\beta_1 - \delta)$;
- $\varphi_{rx} = -CC \cdot \beta_i; \quad for\ i = 1..4$

Solving for steer angle and side slip angles:

- $\beta_i = -\frac{\varphi_{rx}}{CC} = \beta; \quad for\ i = 1..4$;
- $\delta = \beta_1 + \frac{\varphi_{rx}}{CC} = 2 \cdot \frac{\varphi_{rx}}{CC}$;

The swept width becomes: $SweptWidth = (l_{1f} + l_{1rc}) \cdot \frac{\varphi_{rx}}{CC} + (l_{2fc} + l_{2rc}) \cdot 2 \cdot \frac{\varphi_{rx}}{CC} + (l_{3fc} + l_{3rc}) \cdot 3 \cdot \frac{\varphi_{rx}}{CC} + (l_{4fc} + l_{4rc}) \cdot 4 \cdot \frac{\varphi_{rx}}{CC}$; This can be expressed as:

$$SweptWidth = \frac{\varphi_{rx}}{CC} \cdot \left((l_{1f} + l_{1rc}) + \sum_{i=2}^{4} \left((l_{ifc} + l_{irc}) \cdot i \right) \right); \qquad [4.40]$$

There is no influence of longitudinal speed. There is influence of cornering coefficient CC. Model assumes that the influence of longitudinal force is small. These will affect via articulation angles and via combined tyre slip effects. So, the model will be less valid if low road friction and if strong up- or downhill.

4.3.11 Roll-Over in Steady State Cornering

When going in curves, the vehicle will have roll angles of typically some degrees. At that level, the roll is a comfort issue. However, there are manoeuvres which can cause the vehicle to roll-over, i.e. roll ≥ 90 deg so that vehicle body crashes into ground. Roll-over can be seen as a special event, but if sorting into the chapters of this compendium it probably fits best in present chapter, about lateral dynamics.

One can categorize roll-overs in e.g. 3 different types:

- **Tripped roll-over**. This is when the car skids sideways and hits an edge, which causes the roll-over. It can be an uprising edge, e.g. pavement or refuge. It can be the opposite, a ditch or loose gravel outside road. In both these cases, it is strong lateral forces on the wheels on one side of the vehicle that causes the roll-over. Tripped roll-over can also be when the vehicle is exposed to large one-sided vertical wheel forces, e.g. by running over a one-sided bump. A third variant of tripped roll-over is when the vehicle is hit by another vehicle so hard that it rolls over.
- **Un-tripped roll-over** or on-road roll-overs. These happen on the road and triggered by high tyre lateral forces. This is why they require high road friction. For sedan passenger cars, these events are almost impossible, since road friction seldom is higher than approximately 1. For SUVs, un-tripped roll-overs can however occur but require dry asphalt roads, where friction is around 1. For trucks, un-tripped roll-over, can happen already at very moderate friction, like 0.4, due to their high CoG in relation to track width. Within un-tripped roll-overs, one can differ between:
  - **Steady state roll-over**. If lateral acceleration is slowly increased, e.g. as running with into a hairpin curve or a highway exit, the vehicle can slowly lift off the inner wheels and roll-over. This is the only case of roll-over for which a model is given in this compendium.
  - **Transient roll-over**. This is when complex manoeuvres, like double lane changes or sinusoidal steering, are made at high lateral accelerations. This can trigger roll eigen-modes, which can be amplified due to unlucky timing between the turns. Models from 4.4.4 can be used as a start, but it is required that load transfer is modelled carefully and includes wheel lifts, suspension end-stops and bump stops.

4.3.11.1 Roll-Over Threshold Definitions

An overall requirement on a vehicle is that the vehicle should not roll-over for certain manoeuvres. Heavy trucks will be possible to roll-over on high-mu conditions. The requirement for those is based on some manoeuvres which not utilize the full road friction. For passenger cars, it is often the intended design that they should be impossible to roll-over, even at high mu. Any requirement needs a definition of what exactly roll-over is, i.e. a Roll over threshold definition. Candidates for Roll over threshold definition are:

- **One wheel** lifts from ground
- All wheels on **one side** lift from ground
- Vehicle **CoG** reaches its **highest point** (point of no-return towards roll $\geq$ 90 deg)

Note that:

- It is the 3rd threshold which really is the limit, but other can still be useful in requirement setting. To use the 3rd for requirement setting makes the verification much more complex, of course in real vehicles but also in simulation.
- The 1st is not a very serious situation for a conventional vehicle with 4 wheels. However, for a 3-wheeled vehicle, such as small "Tuctucs" or a 3-wheel moped, it is still a relevant threshold.
- The 2nd threshold is probably the most useful threshold for two-tracked vehicles, because it defines a condition from which real roll-over is an obvious risk, and still it is relatively easy to test and simulate. For 3-wheeled vehicle, 2nd and 3rd threshold generally coincide. The 2nd threshold will be used in this compendium.

Figure 4-38 shows how the inner wheels lift off subsequently during a slowly increasing lateral force (or lateral acceleration) build-up. Before any wheel is lifted, the load transfer is proportional to roll-centre heights and roll stiffnesses, as shown in Equation [4.38]. But every time a wheel lifts, the distribution changes, so that a "knee" on the curves appears, see Figure 4-38. So, the relation of type as Equation [4.38] is no longer valid. For instance, it is not physically motivated to keep the roll-centre model for an axle which has lifted one side. So, the prediction of critical lateral acceleration for roll-over is not trivial, especially for heavy vehicles which has many axles, and often also a fifth wheel which can transfer roll-moment to a certain extent. There are approximate standards for how to

calculate steady state roll-over thresholds for such vehicle, e.g. UN ECE 111 (http://www.unece.org/fileadmin/DAM/trans/main/wp29/wp29regs/r111e.pdf).

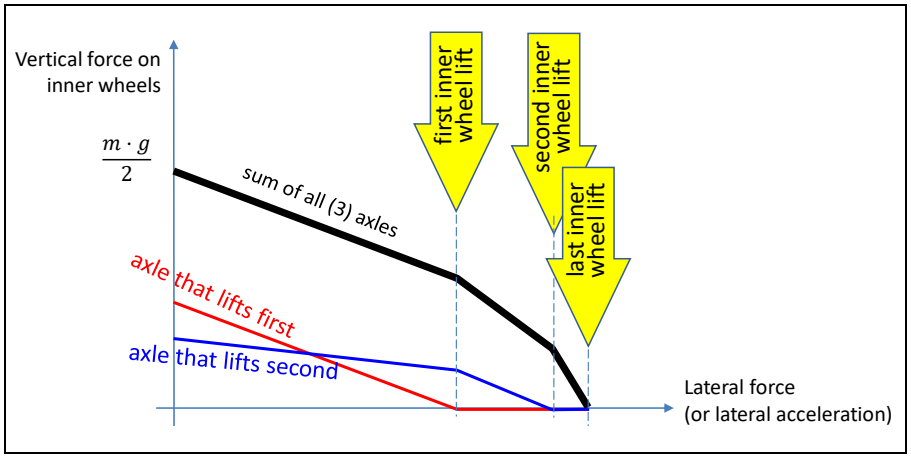

Figure 4-38: Example of 3-axle vehicle steady state roll-over wheel lift diagram.

4.3.11.2 Static Stability Factor, SSF

One very simple measure of the vehicles tendency to roll-over is the Static Stability Factor, SSF. It is proposed by NHTSA, http://www.nhtsa.gov/cars/rules/rulings/roll_resistance/, and it is simply defined as:

$$\text{SSF} = \frac{Half\ TrackWidth}{HeigthOfCoG} = \frac{w/2}{h}; \qquad [4.41]$$

A requirement which requires *SSF>number* cannot be directly interpreted in terms of certain manoeuvre and certain roll-over threshold. It is not a *performance-based requirement*, but a *design-based* (or *prescriptive*) *requirement*. However, one of many possible performance-based *interpretations* is that the vehicle shall not roll-over for steady-state cornering on level ground with an enough friction coefficient. Another is that it should not roll-over in a tilt-table. Since the requirement is not truly performance based, each interpretation will also stipulate a certain verification method; here it would be theoretical verification using a rigid suspension model. Such model and threshold are shown in Figure 4-39.

The derivation of the SSF based requirement looks as follows:

$$\left.\begin{array}{l} Model: \begin{cases} F_{iz} \cdot w + m \cdot a_y \cdot h = m \cdot g \cdot \frac{w}{2}; \\ F_{iz} + F_{oz} = m \cdot g; \\ m \cdot a_y = F_y = \mu \cdot (F_{iz} + F_{oz}); \end{cases} \Rightarrow F_{iz} = m \cdot g \cdot \left(\frac{1}{2} - \frac{h \cdot \mu}{w}\right); \\ Requirement: F_{iz} \geq 0; \end{array}\right\} \Rightarrow$$

$$\Rightarrow Requirement: \frac{1}{2} > \frac{h \cdot \mu}{w} \Rightarrow \frac{w}{2 \cdot h} = SSF > \mu; \qquad [4.42]$$

Maximum road friction, μ, is typically 1, which is why SSF>μ=1 would be a reasonable. However, typical values of SSF for passenger vehicles are between 0.95 and 1.5. For heavy trucks, it can be much lower, maybe 0.3..0.5, much depending on how the load is placed. There are objections to use SSF as a measure, because SSF ignores suspension compliance, handling characteristics, electronic stability control, vehicle shape and structure.

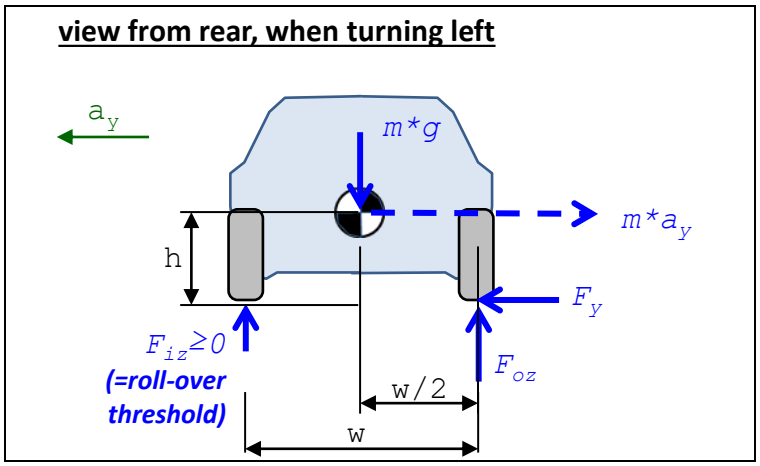

Figure 4-39: Model for verification of requirement based on Static Stability Factor, SSF.

4.3.11.3 Steady-State Cornering Roll-Over *

A function defined for requirement setting can be:

> *Function definition:* ***Steady state cornering roll-over acceleration*** *is the maximum lateral acceleration the vehicle can take in steady state cornering without lifting all inner wheels. On level ground with enough road friction and certain weight and position of payload.*

For a long combination-vehicle with several articulation points, one often need to drive a long distance after a steer angle change before steady state values on articulation angles are reached. Hence, it can be more relevant to formulate a corresponding roll-over function in terms of curvature to follow, total yaw angle for turn and longitudinal speed. A common way is also the, somewhat artificial, tilt-table test, which means that one measure steady-state roll-over with a (real or virtual) tilt-table where the maximum road pitch angle before wheel lift on one side is the measure to set requirement on. An even simpler way to handle steady-state roll-over is to set requirement on the SSF.

Consider a roll-stiff vehicle in steady state cornering. Assume lateral acceleration is subsequently increased. If the vehicle is a two-axle vehicle, Eq [4.38] is valid until first axle lifts its inner wheel, since for larger lateral accelerations, the constitutive equation Eq [4.32] is invalid for the inner wheel, since the lifted inner wheel has zero force from ground. We can identify the terms of one of the inner wheels (if $a_y > 0$) equations in Eq Eq [4.38] as follows:

$$F_{flz} = m \cdot \left(\frac{g \cdot l_r}{2 \cdot L} - a_y \cdot \left(\frac{h_{RCf} \cdot l_r}{L \cdot w} + \frac{\Delta h}{w} \cdot \frac{c_{f,roll}}{c_{roll,vehicle}} \right) \right) =$$

$$= \frac{1}{2} \cdot \underbrace{\frac{m \cdot g \cdot l_r}{2 \cdot L}}_{VerticalForceOnAxle} - \underbrace{m \cdot a_y \cdot \frac{l_r}{L}}_{LateralForceOnAxle} \cdot \frac{h_{RCf}}{w} - \underbrace{m \cdot a_y}_{LateralForceOnVehicle} \cdot \frac{\Delta h}{w} \cdot \underbrace{\frac{c_{f,roll}}{c_{roll,vehicle}}}_{RollStiffnessFractionOnAxle} =$$

$$= \frac{F_{iz}}{2} - F_{iy}(a_y) \cdot \frac{h_{RCi}}{w} - F_y(a_y) \cdot \frac{\Delta h}{w} \cdot \frac{c_{i,roll}}{c_{roll,vehicle}};$$

If the vehicle has more axles, Eq [4.38] is generalized to Eq [4.43], which also is valid until first inner wheel lifts from ground.

For axle i of a roll-stiff vehicle:

$$F_{ilz} = \frac{F_{iz}}{2} - F_{iy}(a_y) \cdot \frac{h_{RCi}}{w} - F_y(a_y) \cdot \frac{\Delta h_i}{w} \cdot \frac{c_{i,roll}}{c_{roll,vehicle}}; \qquad [4.43]$$

For a vehicle with >2 axles, the parameter Δh_i can not be calculated from Eq [4.36], but can still be understood as the vertical distance between roll axis and the axles roll centre. It should be noted that the pendulum effect is **not** included in Eq [4.43], and this is often a significant approximation if applied on high CoG vehicles, like heavy trucks.

4.3.11.3.1 Model Assuming All Inner Wheels Lift at the Same Lateral Acceleration

An approximation of Steady state cornering roll-over acceleration $a_{y,crit}$ (lateral acceleration when all inner wheels lifted) can be found for vehicles where Eq [4.43] gives $F_{ilz} = 0$ for all axles at same a_y. Then, summing the Eq [4.43] for all axles leads to the Eq [4.44] which is the same $a_{y,crit}$ as the simple SSF model in Figure 4-39 and 4.3.11.2 gives.

$$a_{y,crit} = \frac{w \cdot g}{2 \cdot h}; \qquad [4.44]$$

In the following, we will elaborate with 4 additional effects, which marked in Figure 4-40.

- The tyre will take the vertical load on its **outer edge** in a roll-over situation. This suggests a change of performance and requirement to: $\frac{a_y}{g} < \frac{w+w_{tyre}}{2 \cdot h}$ and $\frac{w+w_{tyre}}{2 \cdot h} > \mu$. This effect is accentuated when low tyre profile and/or high inflation pressure. This effect **decreases** the risk for roll-over.
- Due to suspension and tyre **lateral deformation**, the body will translate laterally outwards, relative to the tyre. This could motivate $\frac{a_y}{g} < \frac{w-Def_y}{2 \cdot h}$ and $\frac{w-Def_y}{2 \cdot h} > \mu$. This effect **increases** the risk for roll-over.
- Due to suspension linkage and compliances, the **body will roll**. Since the CoG height above roll axis, Δh, normally is positive, this could motivate $\frac{a_y}{g} < \frac{w-\Delta h \cdot \varphi_x}{2 \cdot h}$ and $\frac{w-\Delta h \cdot \varphi_x}{2 \cdot h} > \mu$. This effect **increases** the risk for roll-over. At heavy vehicle this "pendulum effect" is large.
- Due to suspension linkage and compliances, the body will also heave. This requires a suspension model with pivot points per wheel, as opposed to roll-centre per axle. The heave is normally positive. This could motivate $\frac{w}{2 \cdot (h+z)} > \mu$ and $\frac{a_y}{g} < \frac{w}{2 \cdot (h+z)}$. The effect is sometimes called "jacking" and it **increases** the risk for roll-over.
- Road leaning left/right (road banking) or driving with one side on a different level (e.g. outside road or on pavement) also influence the roll-over performance.

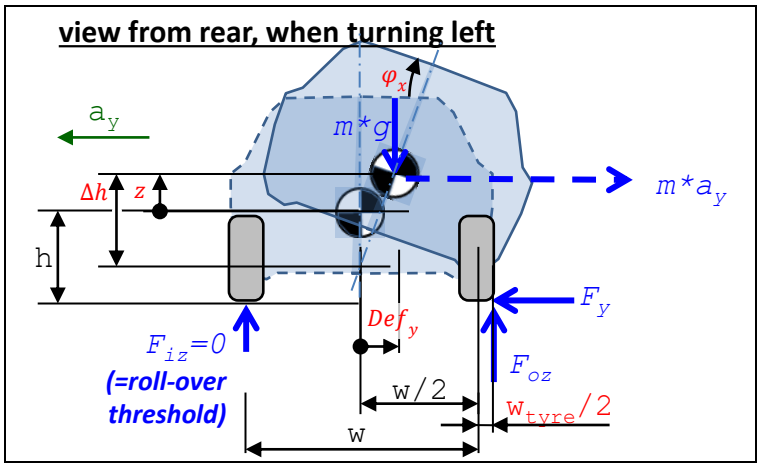

Figure 4-40: Steady-state roll-over model, with fore/aft symmetry. The measures w_{tyre}, Def_y, $\Delta h \cdot \varphi_x$ and z mark effects additional to what is covered with a simple SSF approach.

4.3.11.3.2 Model with Sequential Lifts of Inner Wheels

A model which does not assume wheel lift at same lateral acceleration will be sketched. For each axle that has lifted, the equations have to be changed. Instead of simply the constitutive equation $(F_{ilz} - F_{irz}) \cdot w/2 = c_{i,roll} \cdot \varphi_x$; one need to assure $F_{ilz} = 0$;. The axle will then position itself so that it keeps $F_{ilz} + F_{irz} = F_{iz,static}$;. That means both roll and vertical translation of the axle centre, why also the vertical suspension compliance needs to be modelled. A new position variable has to be declared, e.g. the lift distance of the inner wheel, $lift_{ilz}$. This variable is constrained to $lift_{ilz} = 0$; before lift, but after lift the constraint is $F_{ilz} = 0$;. So, the model is suitably implemented as a state event model with

the event "*when* F_{ilz} *becomes* < 0". If a_y is swept from zero and upwards, the result will be something like shown in Figure 4-38.

4.3.11.3.3 Using a Transient Model for Steady-State Roll-Over

Another work-around to avoid complex algebra is to run a fully transient model, including suspension, and run it until a steady state cornering conditions occur. If then, the lateral acceleration is slowly increased, one can identify when or if the roll-over threshold is reached. Lateral acceleration increase can be through either increase of longitudinal speed or steer angle. It should be noted that the model should reasonably be able to manage at least lift of one wheel from the ground. This way of verifying steady state cornering roll-over requirements has the advantage that, if using tyre models with friction saturation, the limitation discussed in 4.3.11.3.2 does not have to be checked separately.

4.3.11.4 Roll-Over and Understeering/Propulsion

With the above formulas for roll-over there will always be a certain lateral acceleration that leads to roll-over, because neither limitation due to road friction nor propulsion power modelled yet. Since vehicles generally are understeered, they are limited to develop lateral acceleration, see Figure 4-25. For propulsion-weak vehicles, there is also the limitation of lateral acceleration due to limited longitudinal speed, which in turn is due to driving resistance from the steered wheels (=wheel lateral force * sin(steer angle)) and loosing propulsion power due to longitudinal wheel slip. However, one should consider that the propulsion limitation is less in down-hill driving, which increases the roll-over risk again. Also, if the vehicle goes relatively quickly into steady state cornering, the longitudinal speed will not have time to decelerate to its real (longitudinal) steady state value.

For heavy trucks, the critical lateral acceleration is typically $(0.3..0.4) \cdot g$, which is quite possible to reach during normal road conditions, because road friction is around 1. For passenger cars, the critical lateral acceleration is typically in the region of 1, so it is often not possible to reach the roll-over-critical lateral acceleration. This is also the case for heavy trucks on low road friction.

4.4 Stationary Oscillating Steering

In between steady state and transient manoeuvres, one can identify stationary oscillations as an intermediate step. Generally, a mechanical system can be excited with a stationary oscillating excitation. The response of the system is, after possible transients are damped out, a stationary oscillation. How this response vary with excitation frequency will be called Frequency Response. If staying within the linear region for the system and the excitation is harmonic (sinus and cosine), the ratio between the response amplitude and the excitation amplitude is only dependent of the frequency. The ratio is called transfer function.

For lateral vehicle dynamics, the excitation is typically steering wheel angle and the response is amplitudes of yaw velocity, curvature or lateral acceleration. The corresponding transfer functions are a frequency version of the gains defined in Equation [4.19]. Also, there will be a delay between excitation and response. This is another important measure, beside the amplitude ratio.

4.4.1 Stationary Oscillating Steering Tests

When testing stationary oscillating steering functions, one usually drives on a longer part of the test track. It might be a high-speed track, see Figure 1-25, because the track rather needs to be long than wide, since one is often not too close to lateral grip limits. If the available Vehicle Dynamics Area, see Figure 1-25, is long enough this is of course a safer option. A Vehicle Dynamics Area is a flat surface with typically 100..300 m diameter. It normally has entrance roads for accelerating up to a certain speed.

Typical tests for Stationary oscillating steering functions:

- Sweeping frequency (chirp) and/or amplitude
- Random frequency and amplitude

There are ISO standards for sweeping and random tests. The Frequency Response will be very dependent of the vehicle longitudinal speed, why the same tests are typically done at different such speeds.

4.4.2 Linear 1-Track Model for 2-axle Vehicle for Transient Dynamics

The model needed for stationary oscillation is only a linearization of the model needed for fully transient handling, in 4.4.4. However, a model will be derived then approximated to linear. The resulting linear model is in Eq [4.50] and a less general derivation of it is found in Figure 4-44.

The vehicle model is sketched in Figure 4-42. The model is similar to the model for steady state cornering in Figure 4-15, with the following changes:

- Longitudinal and lateral accelerations have both components of centripetal acceleration ($\omega_z \cdot v_y$ and $\omega_z \cdot v_x$) and the derivatives $\dot{v}_x$ and $\dot{v}_y$:

$$a_x = \dot{v}_x - \omega_z \cdot v_y;$$
$$a_y = \dot{v}_y + \omega_z \cdot v_x;$$
(Often, $v_y \ll v_x$, why $\omega_z \cdot v_y$ is more neglectable than $\omega_z \cdot v_x$.) [4.45]

- The yaw acceleration, $\dot{\omega}_z$, is no longer zero.
- The speed v_x is no longer defined as a parameter, but a variable. Then, one more prescription is needed to be a consistent model. For this purpose, an equation that sets front axle propulsion torque to 1000 Nm is added.

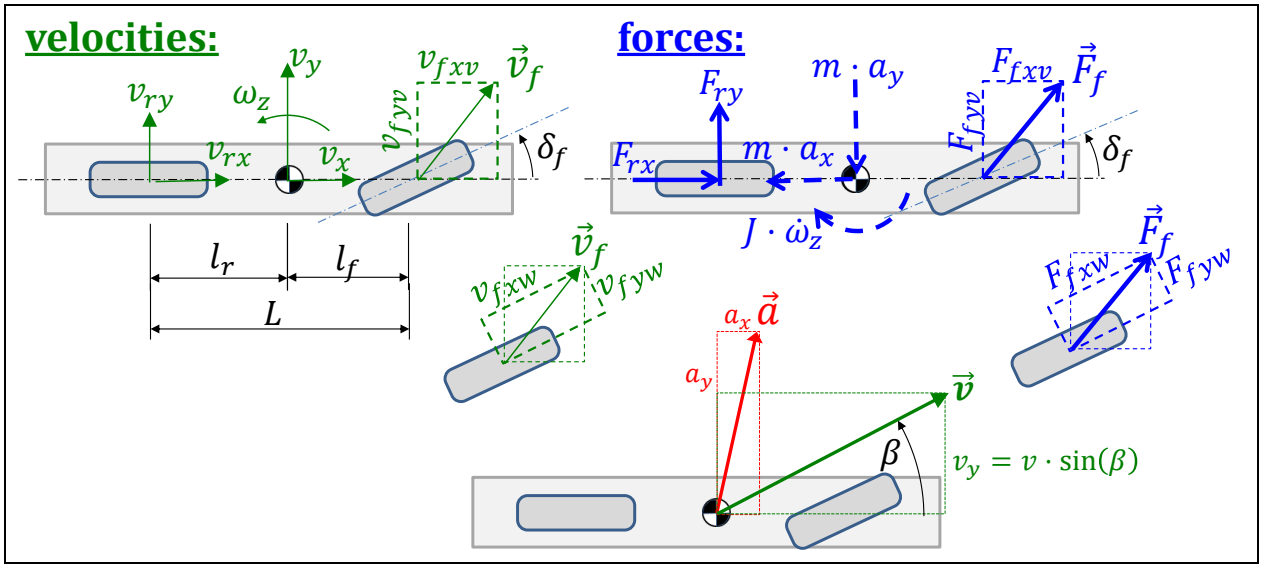

Figure 4-42: One-track model for transient dynamics. Dashed show fictive forces. Compare to Figure 4-15.

It is assumed that the longitudinal tyre forces and slips are small, so $F_{iyw}(s_{iyt}) \approx F_{iyw}(s_{iyw})$. It is also assumed that lateral tyre forces are far below road friction saturation, $F_{iyw}(s_{iyw}) \approx C_{iy} \cdot s_{iyw}$.

It can be difficult to understand the difference between acceleration $[a_x; a_y]$ and derivatives $[\dot{v}_x; \dot{v}_y]$ of velocities $[v_x; v_y]$. Some explanations are proposed in 4.4.2.3.

The Mathematical model shown in Eq [4.46] in Modelica format. The subscript v and w refers to **v**ehicle coordinate system and **w**heel coordinate system, respectively. The model is developed from the model for low-speed in Eq [4.6], with the changes marked with yellow and underlined text.

```
//(Dynamic) Equilibrium:
m*ax = Ffxv + Frx;    m*ay = Ffyv + Fry;    J*der(wz) = Ffyv*lf - Fry*lr;
ax=der(vx)-wz*vy;    ay=der(vy)+wz*vx;

//Constitutive relation (Lateral tyre force model):
Ffyw=-Cf*sfyw;    Fry=-Cr*sryw;
```
[4.46]

```
sfyw=vfyw/vfxw;    sryw=vry/vrx;

//Compatibility:
vfxv = vx;    vfyv = vy + lf*wz;
vrx = vx;     vry = vy - lr*wz;

//Transformation between vehicle and wheel coordinate systems:
Ffxv = Ffxw*cos(df) - Ffyw*sin(df);
Ffyv = Ffxw*sin(df) + Ffyw*cos(df);
vfxv = vfxw*cos(df) - vfyw*sin(df);
vfyv = vfxw*sin(df) + vfyw*cos(df); //can be exactly replaced with
       // atan2(vfyv,vfxv)=df+atan(sfyw); or approximately with vfyv/vfxv=df+sfyw;

//Path with orientation:
der(x)  = vx*cos(pz) - vy*sin(pz);
der(y)  = vy*cos(pz) + vx*sin(pz);
der(pz) = wz;

// Prescription of steer angle:
df = if time < 2.5 then (5*pi/180)*sin(0.5*2*pi*time) else 5*pi/180;
//Shaft torques:
Ffxw = +1000; // Front axle driven.
Frx  = -100; // Rolling resistance on rear axle.
```

Position variables $[x, y, \varphi_y{=}\text{pz}]$ and speed variables $[v_x, v_y, \omega_z{=}\text{wz}]$ are selected state variables. The input variables are $\delta_f, F_{fxw}, F_{rx}$. The only non-zero initial value is $v_x = 100\ km/h$. Simulation result is shown in Figure 4-43. The manoeuvre selected is same steering wheel function of time as in Figure 4-16, for better comparison of the different characteristics of the models.

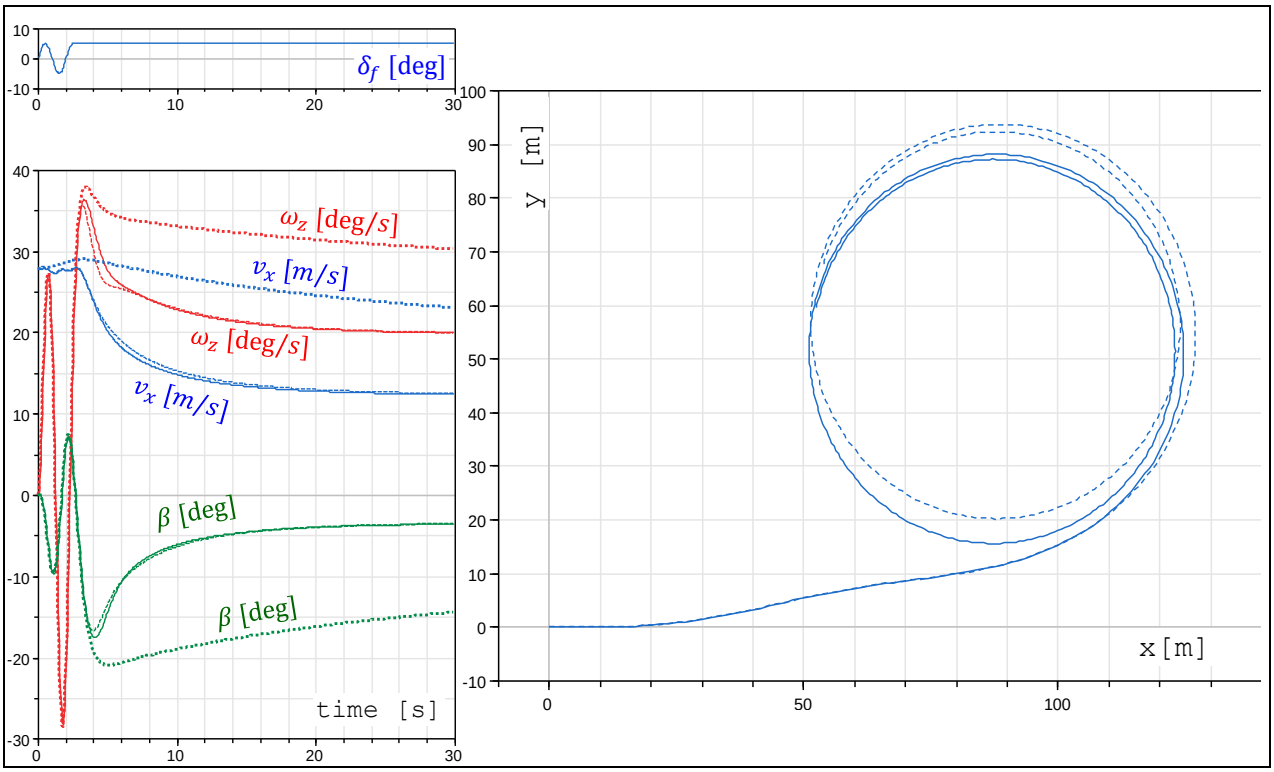

Figure 4-43: Simulation results of transient one-track models. Solid: Eq [4.46] or [4.47]. Dashed: Eq [4.48], which employs the small angle approximation. Dotted: Eq [4.46] or [4.47], which is without the $v_x \cdot \omega_z$ term.

Eq [4.46] is a complete model suitable for simulation. Removing $[x, y, \varphi_y{=}\text{pz}]$ and the 3 equations for "path with orientation", eliminating some variable and rewrite (no added approximations) gives:

$$\begin{aligned}
&\text{Equilibrium: } m\cdot\left(\dot{v}_x-\omega_z\cdot v_y\right)=F_{fxw}\cdot\cos\left(\delta_f\right)-F_{fyw}\cdot\sin\left(\delta_f\right)+F_{rx};\\
&\qquad m\cdot\left(\dot{v}_y+\omega_z\cdot v_x\right)=F_{fxw}\cdot\sin\left(\delta_f\right)+F_{fyw}\cdot\cos\left(\delta_f\right)+F_{ry};\\
&\qquad J\cdot\dot{\omega}_z=\left(F_{fxw}\cdot\sin\left(\delta_f\right)+F_{fyw}\cdot\cos\left(\delta_f\right)\right)\cdot l_f-F_{ry}\cdot l_r;\\
&\text{Constitution: }\quad F_{fyw}=-C_f\cdot s_{fyw};\quad F_{ry}=-C_r\cdot s_{ryw};\\
&\text{Compatibility: }\quad s_{fyw}=v_{fyw}/\left|v_{fxw}\right|;\blacksquare\quad\text{and}\quad s_{ryw}=\left(v_y-l_r\cdot\omega_z\right)/|v_x|;\\
&\text{Transformation from vehicle to wheel coordinate system on front axle:}\\
&\qquad v_{fxw}=\left(v_y+l_f\cdot\omega_z\right)\cdot\sin\left(\delta_f\right)+v_x\cdot\cos\left(\delta_f\right);\ \blacksquare\\
&\qquad v_{fyw}=\left(v_y+l_f\cdot\omega_z\right)\cdot\cos\left(\delta_f\right)-v_x\cdot\sin\left(\delta_f\right);\ \blacksquare
\end{aligned}\qquad [4.47]$$

Typically, this model is used for simulation, where δ_f, F_{fxw} and F_{rx} are input variables. Suitable state variables are v_x, v_y and ω_z. It is a non-linear model suitable for arbitrary transient manoeuvres and we will come back to this in 4.4.4.

4.4.2.1 Known Longitudinal Velocity and Small Angles

Model in Eq [4.47] is not linear, but we will derive a linear model from it now, through some approximations. The angle sum approach from 1.5.5.3 is used to replace the 3 equations (■) with 2 new and replace the 2 unknowns v_{fxw}, v_{fyw} with one new β_f.

$$\begin{aligned}
&\text{Equilibrium: } m\cdot\left(\dot{v}_x-\omega_z\cdot v_y\right)=F_{fxw}\cdot\cos\left(\delta_f\right)-F_{fyw}\cdot\sin\left(\delta_f\right)+F_{rx};\\
&\qquad m\cdot\left(\dot{v}_y+\omega_z\cdot v_x\right)=F_{fxw}\cdot\sin\left(\delta_f\right)+F_{fyw}\cdot\cos\left(\delta_f\right)+F_{ry};\\
&\qquad J\cdot\dot{\omega}_z=\left(F_{fxw}\cdot\sin\left(\delta_f\right)+F_{fyw}\cdot\cos\left(\delta_f\right)\right)\cdot l_f-F_{ry}\cdot l_r;\\
&\text{Constitution: }\quad F_{fyw}=-C_f\cdot s_{fyw};\quad F_{ry}=-C_r\cdot s_{ryw};\\
&\text{Compatibility: }\quad \arctan\left(\beta_f\right)=\delta_f+\arctan\left(s_{fyw}\right);\quad \arctan\left(\beta_f\right)=\frac{v_y+l_f\cdot\omega_z}{|v_x|};\quad s_{ryw}=\frac{v_y-l_r\cdot\omega_z}{|v_x|};
\end{aligned}$$

Now, we assume small angles: steering angle δ_f, wheel side slip angles $\alpha_i\approx\arctan\left(v_{yiw}/v_{xiw}\right)=\arctan\left(s_{iyw}\right)$, and body side slip angle over steered axle $\beta_f\approx\arctan\left(v_{fy}/v_x\right)$. These are "trigonometric approximations" during the Mathematical modelling stage, motivated if not too sharp turning.

$$\begin{aligned}
&\text{Equilibrium: } m\cdot\left(\dot{v}_x-\omega_z\cdot v_y\right)=F_{fxw}-F_{fyw}\cdot\delta_f+F_{rx};\\
&\qquad m\cdot\left(\dot{v}_y+\omega_z\cdot v_x\right)=F_{fxw}\cdot\delta_f+F_{fyw}+F_{ry};\\
&\qquad J\cdot\dot{\omega}_z=\left(F_{fxw}\cdot\delta_f+F_{fyw}\right)\cdot l_f-F_{ry}\cdot l_r;\\
&\text{Constitution: }\quad F_{fyw}=-C_f\cdot s_{fyw};\quad F_{ry}=-C_r\cdot s_{ryw};\\
&\text{Compatibility: }\quad \beta_f\approx\delta_f+s_{fyw};\quad \beta_f\approx\frac{v_y+l_f\cdot\omega_z}{|v_x|};\quad s_{ryw}=\frac{v_y-l_r\cdot\omega_z}{|v_x|};
\end{aligned}\qquad [4.48]$$

(Note that $F_{iyw}=-C_i\cdot\alpha_i$; can be employed as approximation already during tyre modelling. This would not change the resulting Eq [4.48].)

Figure 4-43 shows a simulation with model in Eq [4.48], for comparison with the model without small angle approximations, i.e. from Eq [4.47].

Eliminating $F_{fyw}, F_{ry}, s_{fyw}, s_{ry}, \beta_f$ gives:

$$\begin{aligned}
&m\cdot\left(\dot{v}_x-\omega_z\cdot v_y\right)=F_{fxw}+C_f\cdot\left(\frac{v_y+l_f\cdot\omega_z}{|v_x|}-\delta_f\right)\cdot\delta_f+F_{rx};\\
&m\cdot\left(\dot{v}_y+\omega_z\cdot v_x\right)=F_{fxw}\cdot\delta_f-C_f\cdot\left(\frac{v_y+l_f\cdot\omega_z}{|v_x|}-\delta_f\right)-C_r\cdot\frac{v_y-l_r\cdot\omega_z}{|v_x|};\\
&J\cdot\dot{\omega}_z=\left(F_{fxw}\cdot\delta_f-C_f\cdot\left(\frac{v_y+l_f\cdot\omega_z}{|v_x|}-\delta_f\right)\right)\cdot l_f+C_r\cdot\frac{v_y-l_r\cdot\omega_z}{|v_x|}\cdot l_r;
\end{aligned}$$

Yet another approximation which we can do is to assume that centripetal acceleration is directed purely lateral in vehicle and hence remove the term $\omega_z\cdot v_y$. Figure 4-43 shows a simulation of Eq [4.47] without the term $\omega_z\cdot v_y$ for judging the importance of it; it has considerable influence on v_x over time. Also, the influence of the force $F_{fyw}\cdot\delta_f$ in longitudinal direction can be neglected. The resulting model then becomes:

$$
\begin{aligned}
&m \cdot \dot{v}_x = F_{fxw} + F_{rx};\\
&m \cdot \left(\dot{v}_y + \omega_z \cdot v_x\right) = F_{fxw} \cdot \delta_f - C_f \cdot \left(\frac{v_y + l_f \cdot \omega_z}{|v_x|} - \delta_f\right) - C_r \cdot \frac{v_y - l_r \cdot \omega_z}{|v_x|};\\
&J \cdot \dot{\omega}_z = \left(F_{fxw} \cdot \delta_f - C_f \cdot \left(\frac{v_y + l_f \cdot \omega_z}{|v_x|} - \delta_f\right)\right) \cdot l_f + C_r \cdot \frac{v_y - l_r \cdot \omega_z}{|v_x|} \cdot l_r;
\end{aligned}
\qquad [4.49]
$$

For stationary oscillation steering, $\dot{v}_x = 0$, so v_x can be seen as a manoeuvre-parameter. This is often a good approximation also when turning during mild acceleration and deceleration. But, instead of setting $\dot{v}_x = 0$, we keep it more generic: v_x is considered as a known function of time $v_x(t)$, i.e. v_x and $\dot{v}_x$ are known functions of time, or $\dot{v}_x$ is an input and v_x a state. So, we can continue to select v_x, v_y, ω_z as states, but inputs become $\delta_f, F_{fxw}, \dot{v}_x$:

The first scalar equation (the longitudinal equilibrium) in Eq [4.49] can be used to calculate what F_{rx} is needed to keep the prescribed $v_x(t)$: $F_{rx} = m \cdot \dot{v}_x(t) - F_{fxw};$. Note that neither aerodynamic, grade nor rolling resistance are considered.

The two latter scalar equations can be written as a linear dynamic model on matrix state-space form, with 2 states v_y, ω_z and 2 inputs $\delta_f, F_{fxw} \cdot \delta_f$, see Eq [4.50], where the output is chosen as $\boldsymbol{y^T} = \left[\omega_z, a_y\right] = \left[\omega_z, \dot{v}_y + \omega_z \cdot v_x\right]$. The $v_x(t)$ is often a scalar constant v_x.

$$
\begin{aligned}
&\begin{cases}
\begin{bmatrix}\dot{v}_y\\ \dot{\omega}_z\end{bmatrix} = \boldsymbol{A} \cdot \begin{bmatrix}v_y\\ \omega_z\end{bmatrix} + \boldsymbol{B} \cdot \begin{bmatrix}\delta_f\\ F_{fxw} \cdot \delta_f\end{bmatrix};\\
\begin{bmatrix}\omega_z\\ a_y\end{bmatrix} = \boldsymbol{C} \cdot \begin{bmatrix}v_y\\ \omega_z\end{bmatrix} + \boldsymbol{D} \cdot \begin{bmatrix}\delta_f\\ F_{fxw} \cdot \delta_f\end{bmatrix};
\end{cases}
\text{ or }
\begin{cases}
\dot{\boldsymbol{x}} = \boldsymbol{A} \cdot \boldsymbol{x} + \boldsymbol{B} \cdot \boldsymbol{u};\\
\boldsymbol{y} = \boldsymbol{C} \cdot \boldsymbol{x} + \boldsymbol{D} \cdot \boldsymbol{u};
\end{cases}\\
&\textit{Where } \boldsymbol{A} = -\begin{bmatrix}m & 0\\ 0 & J\end{bmatrix}^{-1} \cdot \begin{bmatrix}\frac{C_f + C_r}{|v_x(t)|} & \frac{C_f \cdot l_f - C_r \cdot l_r}{|v_x(t)|} + m \cdot v_x(t)\\ \frac{C_f \cdot l_f - C_r \cdot l_r}{|v_x(t)|} & \frac{C_f \cdot {l_f}^2 + C_r \cdot {l_r}^2}{|v_x(t)|}\end{bmatrix};\\
&\textit{and } \boldsymbol{B} = \begin{bmatrix}m & 0\\ 0 & J\end{bmatrix}^{-1} \cdot \begin{bmatrix}C_f & 1\\ C_f \cdot l_f & l_f\end{bmatrix};\\
&\textit{and } \boldsymbol{C} = \begin{bmatrix}0 & 0\\ 1 & 0\end{bmatrix} \cdot \boldsymbol{A} + \begin{bmatrix}0 & 1\\ 0 & v_x(t)\end{bmatrix};\ \textit{and } \boldsymbol{D} = \begin{bmatrix}0 & 0\\ 1 & 0\end{bmatrix} \cdot \boldsymbol{B};
\end{aligned}
\qquad [4.50]
$$

The model above is approximated only for driving situation where tyre forces are far from saturation and angles are small. If studying driving conditions which not fulfil this, we can still find approximate with linear models if variation from the driving condition is small. A more general method to find linear models is to use only the first terms in a Taylor series expansion of the model $\dot{\boldsymbol{x}} = \boldsymbol{f}(\boldsymbol{x}, \boldsymbol{u})$; around $[\boldsymbol{x}, \boldsymbol{u}] = [\boldsymbol{x_0}, \boldsymbol{u_0}]$:

$$
\begin{aligned}
\dot{\boldsymbol{x}} = \boldsymbol{f}(\boldsymbol{x}, \boldsymbol{u}) \approx \tilde{\boldsymbol{f}}(\boldsymbol{x}, \boldsymbol{u}) = \boldsymbol{f}(\boldsymbol{x_0}, \boldsymbol{u_0}) + \left.\frac{\boldsymbol{df}}{\boldsymbol{dx}}\right|_{\boldsymbol{x_0}, \boldsymbol{u_0}} \cdot (\boldsymbol{x} - \boldsymbol{x_0}) + \left.\frac{\boldsymbol{df}}{\boldsymbol{du}}\right|_{\boldsymbol{x_0}, \boldsymbol{u_0}} \cdot (\boldsymbol{u} - \boldsymbol{u_0}) \approx \left\{\begin{matrix}\text{if } f \text{ is close}\\ \text{to affine}\end{matrix}\right\} \approx\\
\approx \left.\frac{\boldsymbol{df}}{\boldsymbol{dx}}\right|_{\boldsymbol{x_0}, \boldsymbol{u_0}} \cdot \boldsymbol{x} + \left.\frac{\boldsymbol{df}}{\boldsymbol{du}}\right|_{\boldsymbol{x_0}, \boldsymbol{u_0}} \cdot \boldsymbol{u};
\end{aligned}
$$

Examples of where this can be useful is when studying small steering offsets from a steady state cornering.

4.4.2.2 Less General Derivation of Linear 1-Track Model

A less general and less careful derivation of Eq [4.50] is made in Figure 4-44. The approximations are introduced earlier, already in the physical model. Therefore, the influence of F_{fxw} is not reflected and the longitudinal equilibrium is neglected. It is also assumed that $v_x > 0$.

Physical model:

- Path radius >> the vehicle. Then, all forces (and centripetal acceleration) are approximately co-directed.
- Small tyre and vehicle side slip ⇒ angle=sin(angle)=tan(angle). (Angles are not drawn small, which is the reason why the forces not appear co-linear in figure.)

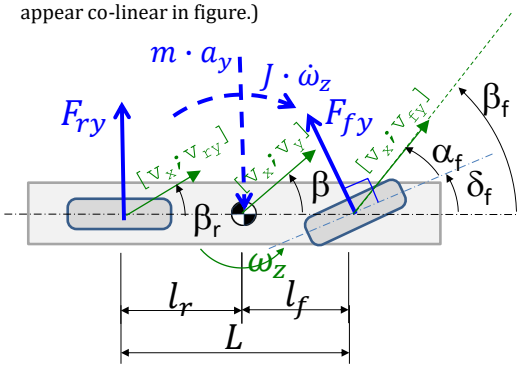

Mathematical model:

Equilibrium:

$$m \cdot (\dot{v}_y + \omega_z \cdot v_x) \approx F_{fy} + F_{ry};$$
$$J \cdot \dot{\omega}_z \approx F_{fy} \cdot l_f - F_{ry} \cdot l_r;$$

Constitution:

$$F_{fy} = -C_f \cdot s_{fy}; \quad F_{ry} = -C_r \cdot s_{ry};$$

Compatibility:

$$\delta_f + s_{fy} \approx \delta_f + \alpha_f = \beta_f \approx \frac{v_{fy}}{v_x} = \frac{v_y + l_f \cdot \omega_z}{v_x};$$
$$s_{ry} \approx \alpha_r = \beta_r \approx \frac{v_{ry}}{v_x} = \frac{v_y - l_r \cdot \omega_z}{v_x};$$

Eliminate $F_{fy}, F_{ry}, \alpha_f, \alpha_r, \beta_f, \beta_r$ yields:

$$m \cdot \dot{v}_y + \frac{C_f + C_r}{v_x} \cdot v_y + \left(\frac{C_f \cdot l_f - C_r \cdot l_r}{v_x} + m \cdot v_x\right) \cdot \omega_z \approx C_f \cdot \delta_f;$$
$$J \cdot \dot{\omega}_z + \frac{C_f \cdot l_f - C_r l_r}{v_x} \cdot v_y + \frac{C_f \cdot {l_f}^2 + C_r \cdot {l_r}^2}{v_x} \cdot \omega_z \approx C_f \cdot l_f \cdot \delta_f;$$

Figure 4-44: Less general derivation of the Linear 1-Track Model, i.e. Eq [4.50].

One can add more axles to the derivation. E.g., a truck with double rear axle will get an added term proportional to ω_z in the moment equilibrium.

4.4.2.3 Accelerations and Velocity Derivatives

See Equation [4.45]. This section provides some explanations to the difference between acceleration $[a_x; a_y]$ and derivatives $[\dot{v}_x; \dot{v}_y]$ of velocities $[v_x; v_y]$.

4.4.2.3.1 Theoretical explanation

First, think of $\vec{a}$ and $\vec{v}$ as geometric vectors (acceleration and velocity are vectors in physics). Acceleration $\vec{a}$ is acceleration in inertial frame, i.e. accelerations over ground. Velocity $\vec{v}$ is velocity in inertial frame, i.e. velocity over ground. A driver or accelerometers, attached to the vehicle body, will experience $[a_x; a_y]$. The ground, observed from the vehicle through a whole in the floor, would be experienced as moving with $[-v_x; -v_y]$.

It is suitable to decompose $\vec{a}$ and $\vec{v}$ in vehicle directions, since most equations (tyres, steering, propulsion, braking, etc) are expressed in those directions. With $\vec{u}_x$ and $\vec{u}_y$ as unit vectors in vehicle directions: $\vec{a} = a_x \cdot \vec{u}_x + a_y \cdot \vec{u}_y$ and $\vec{v} = v_x \cdot \vec{u}_x + v_y \cdot \vec{u}_y$, or shorter, $[a_x; a_y]$ and $[v_x; v_y]$, which are mathematical vectors. Now, it is important to remember that the vehicle is rotating with ω_z.

The accelerations are used in equilibrium equations, where the fictive force is $m \cdot \vec{a} = m \cdot \frac{d}{dt}\vec{v};$. Since we express $\vec{v}$ in components in vehicle coordinate system directions, the differentiation is **not** as simple as differentiation component by component, $[\dot{v}_x; \dot{v}_y]$. Instead: $[a_x; a_y] = [\dot{v}_x; \dot{v}_y] + [-\omega_z \cdot v_y;\ \omega_z \cdot v_x];$. The terms proportional to ω_z are centrifugal accelerations.

This can be mathematically shown as differentiation of the geometrical vector $\vec{v}$:

$$\vec{a} = \frac{d}{dt}\vec{v} = \frac{d}{dt}(v_x \cdot \vec{u}_x + v_y \cdot \vec{u}_y) = \left(\dot{v}_x \cdot \vec{u}_x + v_x \cdot \frac{d}{dt}\vec{u}_x\right) + \left(\dot{v}_y \cdot \vec{u}_y + v_y \cdot \frac{d}{dt}\vec{u}_y\right) =$$
$$= (\dot{v}_x \cdot \vec{u}_x + v_x \cdot \omega_z \cdot \vec{u}_y) + (\dot{v}_y \cdot \vec{u}_y - v_y \cdot \omega_z \cdot \vec{u}_x) = \underbrace{(\dot{v}_x - v_y \cdot \omega_z)}_{a_x} \cdot \vec{u}_x + \underbrace{(\dot{v}_y + v_x \cdot \omega_z)}_{a_y} \cdot \vec{u}_y;$$

The constitutive and compatibility equations are typically expressed in velocities, not accelerations. For high index models, some of the compatibility equations (a.k.a. constraint equations) also needs to be differentiated, see example in 4.5.2.2.

4.4.2.3.2 Practical Explanation

Another explanation is given in left part of Figure 4-45 and the following reasoning. We can express the velocity in direction of the x axis at time t, at two time instants:

- Velocity at time $= t$: v_x
- Velocity at time $= t + \Delta t$: $(v_x + \Delta v_x) \cdot \cos(\Delta\psi) - (v_y + \Delta v_y) \cdot \sin(\Delta\psi) = (v_x \cdot \cos(\Delta\psi) + \Delta v_x \cdot \cos(\Delta\psi)) - (v_y \cdot \sin(\Delta\psi) + \Delta v_y \cdot \sin(\Delta\psi)) \approx \{\Delta\psi\ small\} \approx (v_x + \Delta v_x) - (v_y \cdot \Delta\psi + \Delta v_y \cdot \Delta\psi) \approx \{\Delta v_y \cdot \Delta\psi\ small\} \approx (v_x + \Delta v_x) - v_y \cdot \Delta\psi$

Using these two expressions, we can express a_x as the change of that speed per time unit:

- Acceleration=Velocity change per time $= a_x = \frac{\{(v_x+\Delta v_x)-v_y\cdot\Delta\psi\}-v_x}{\Delta t} = \frac{\Delta v_x - v_y\cdot\Delta\psi}{\Delta t} = \frac{\Delta v_x}{\Delta t} - v_y\frac{\Delta\psi}{\Delta t} \approx \dot{v}_x - v_y \cdot \dot{\psi} = \dot{v}_x - v_y \cdot \omega_z$

Corresponding for the lateral direction gives the Equation [4.45]. In Equation [4.45], the term $\omega_z \cdot v_x$ is generally more important than the term $\omega_z \cdot v_y$. This is because v_x is generally much larger than v_y.

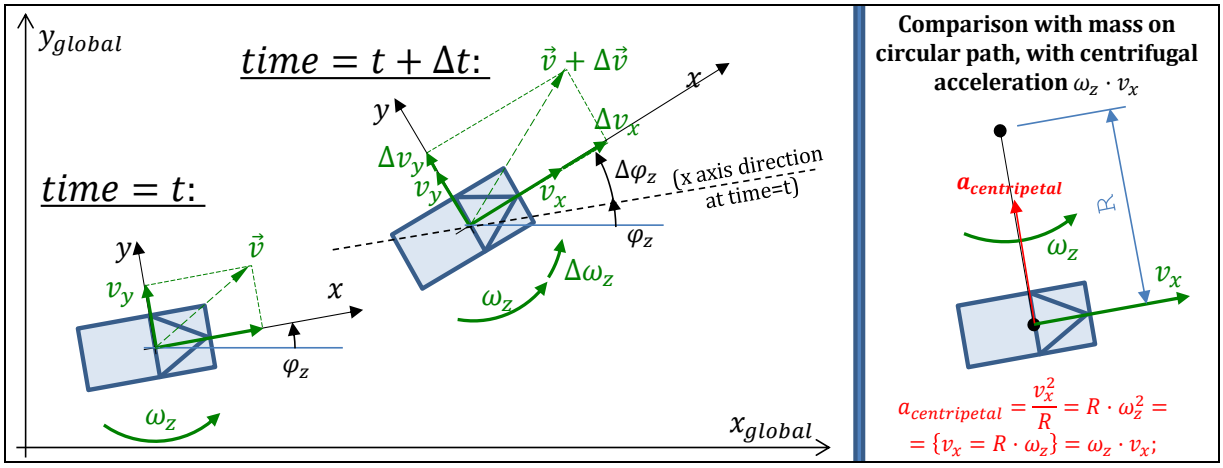

Figure 4-45: How to understand the acceleration term $\omega_z \cdot v_x$ for vehicle motion in ground plane. Left: Two consecutive time instants. Right: Comparison with circular motion, to identify the centripetal acceleration.

4.4.2.3.3 Model with Velocity Components in Ground Fixed Directions

An alternative mathematical model is to express the velocity in components in ground fix (inertial) directions ($\vec{v} = v_{xg} \cdot \vec{u}_{xg} + v_{yg} \cdot \vec{u}_{yg}$, subscript g for *ground*) instead of vehicle fix directions ($\vec{v} = v_{xv} \cdot \vec{u}_{xv} + v_{yv} \cdot \vec{u}_{yv}$, subscript v for *vehicle*). The fictive forces are till $m \cdot \frac{d}{dt}\vec{v}$, but we should express $\frac{d}{dt}\vec{v}$ in $[v_{xg}, v_{xg}]$ instead of $[v_{xv}, v_{yv}]$, which becomes: $\vec{a} = \frac{d}{dt}(v_{xg} \cdot \vec{u}_{xg} + v_{yg} \cdot \vec{u}_{yg}) = \dot{v}_{xg} \cdot \vec{u}_{xg} + \dot{v}_{yg} \cdot \vec{u}_{yg};$. This is a simpler differentiation than using the rotating unit vectors $\vec{u}_{xv}$ and $\vec{u}_{yv}$. We get $a_{yg} = \dot{v}_{yg};$ and $a_{xg} = \dot{v}_{xg};$ instead of $a_{yv} = \dot{v}_{yv} + v_{xv} \cdot \omega_z;$ and $a_{xv} = \dot{v}_{xv} - v_{yv} \cdot \omega_z;$.

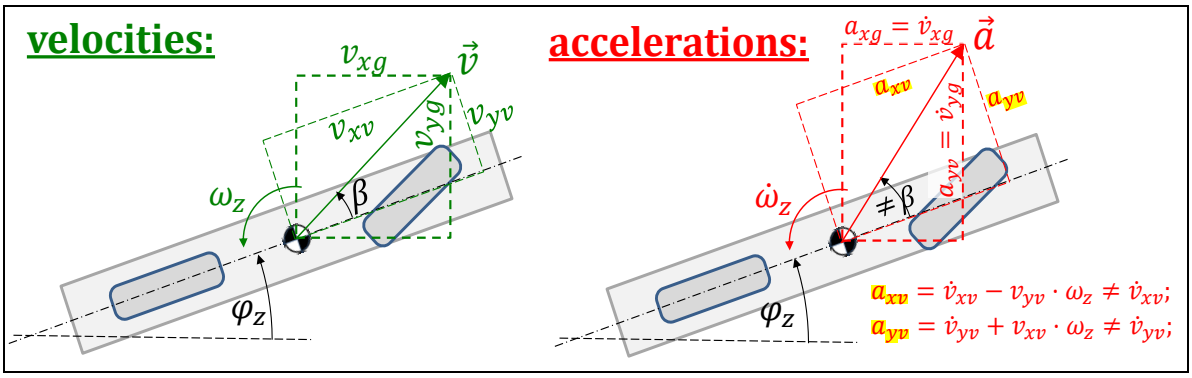

Figure 4-46: Velocity and Acceleration Components in Vehicle fix and Ground Fixed Directions.

Then, we replace the 2 translation equilibrium equations in Eq [4.47]. We also add 2 transformation equations and a compatibility in yaw. The remaining equations can be kept, but it is proposed to add subscript v to v_x, v_y and F_{rx}. The two models, side-by-side becomes as:

Table 4.2: Comparison between modelling with velocities in vehicle fixed and ground fixed directions

Model in…	**…vehicle fix directions,** Eq [4.47]	**… ground fixed directions**
Translation Equilibrium	$m \cdot (\dot{v}_{xv} - \omega_z \cdot v_{yv}) = F_{fxv} + F_{rxv};$ $m \cdot (\dot{v}_{yv} + \omega_z \cdot v_{xv}) = F_{fyv} + F_{ryv};$	$m \cdot \dot{v}_{xg} = (F_{fxv} + F_{rxv}) \cdot \cos(\varphi_z) - (F_{fyv} + F_{ryv}) \cdot \sin(\varphi_z);$ $m \cdot \dot{v}_{yg} = (F_{fxv} + F_{rxv}) \cdot \sin(\varphi_z) + (F_{fyv} + F_{ryv}) \cdot \cos(\varphi_z);$
Velocity Transformation, ground to vehicle	<not needed>	$v_{xv} = +v_{xg} \cdot \cos(\varphi_z) + v_{yg} \cdot \sin(\varphi_z);$ $v_{yv} = -v_{xg} \cdot \sin(\varphi_z) + v_{yg} \cdot \cos(\varphi_z);$
Compatibility, yaw	<not needed>	$\dot{\varphi}_z = \omega_z;$ (adds φ_z as state)
Yaw Equilibrium	$J \cdot \dot{\omega}_z = F_{fyv} \cdot l_f - F_{ryv} \cdot l_r;$	
Constitution	$F_{fyw} = -C_f \cdot s_{fyw};$ $F_{ryv} = -C_r \cdot s_{ry};$	
Compatibility	$\delta_f + s_{fyw} \approx (v_{yv} + l_f \cdot \omega_z)/\lvert v_{xv} \rvert;$ $s_{ry} = (v_{yv} - l_r \cdot \omega_z)/\lvert v_{xv} \rvert;$	
Force transformation, steered wheels to vehicle	$F_{fxv} = F_{fxw} - F_{fyw} \cdot \delta_f;$ $F_{fyv} = F_{fxw} \cdot \delta_f + F_{fyw};$	
Path with orientation:	From Eq [4.46]: $\dot{x} = v_{xv} \cdot cos(\varphi_z) - v_{yv} \cdot sin(\varphi_z);$ $\dot{y} = v_{yv} \cdot \cos(\varphi_z) + v_{xv} \cdot sin(\varphi_z);$ $\dot{\varphi}_z = \omega_z;$	$\dot{x} = v_{xg};$ $\dot{y} = v_{yg};$ $\dot{\varphi}_z = \omega_z;$

Using the velocity components in inertial directions brings heading angle φ_z into the differential equations for velocities. So, we have to add φ_z as state: we get 4 states $(v_{xg}, v_{yg}, \omega_z, \varphi_z)$ instead of 3 $(v_{xv}, v_{yv}, \omega_z)$. The need of transformation manifests that vehicle directions is more natural directions for the constitutive equations (tyre models). However, the equations for path becomes simpler with the ground fixed directions. The two models gives, of course, the same result, e.g. $v_{xg}(t) \equiv v_{xv}(t) \cdot \cos(\varphi_z(t)) - v_{yv}(t) \cdot \sin(\varphi_z(t))$, but the model in vehicle fixed directions is more frequently used.

A similar comparison between model in vehicle and ground fix v and a components can be done for pitch rotation in 3.4.5 and 5.7.2 but the difference there is less important since pitch angle is much more limited than yaw angle.

4.4.2.4 Validity of Model

When only studying the Frequency Response as yaw velocity and curvature response, it is easy to forget that one very easily comes into manoeuvres where road friction is limited, i.e. where the linear tyre model is not valid. Hence it is good to look at lateral acceleration Frequency Response, because we can roughly say that for $\lvert a_y \rvert$ in the same magnitude as $\mu \cdot m \cdot g$, it is doubtful if the model is valid. If the wheel torques are significant, the validity limit is even lower. For high CoG vehicles, another invalidating circumstance is wheel lift, which can be approximately checked by checking that $\lvert a_y \rvert \ll SSF = g \cdot w/(2 \cdot h)$.

If one needs to include nonlinear tyre models in stationary oscillation response, one can simulate using time integration (same method as usually used for transient handling) over several excitation cycles, until the response shows a clear stationary oscillation. This consumes more computational efforts and the solutions become approximate and numerical.

4.4.3 Using the 1-Track Model

Use the linear state-space-model in Eq [4.50] to study "stationary oscillating steering":

$$\begin{bmatrix} \dot{v}_y \\ \dot{\omega}_z \end{bmatrix} = A \cdot \begin{bmatrix} v_y \\ \omega_z \end{bmatrix} + B \cdot \delta(t) = A \cdot \begin{bmatrix} v_y \\ \omega_z \end{bmatrix} + B \cdot \hat{\delta} \cdot \cos(\omega \cdot t)$$

(Note similar notation for vehicle yaw velocity, ω_z, and steering angular frequency, ω.) Knowing $\hat{\delta}$ and ω, it is possible to calculate the responses $\hat{v}_y$, $\hat{\omega}_z$, φ_y and φ_z:

$$\begin{bmatrix} v_y \\ \omega_z \end{bmatrix} = \begin{bmatrix} \hat{v}_y \\ \hat{\omega}_z \end{bmatrix} \cdot \cos\left(\omega \cdot t - \begin{bmatrix} \varphi_{v_y} \\ \varphi_{\omega_z} \end{bmatrix}\right); \quad and \quad \begin{bmatrix} \omega_z \\ a_y \end{bmatrix} = \begin{bmatrix} \hat{\omega}_z \\ \hat{a}_y \end{bmatrix} \cdot \cos\left(\omega \cdot t - \begin{bmatrix} \varphi_{\omega_z} \\ \varphi_{a_y} \end{bmatrix}\right);$$

Different methods are available for calculation of the Frequency Responses:

- **Fourier** transform
- **Complex mathematics**, using $e^{j\cdot\omega\cdot t}$
- **Real trigonometry**, using $\cos(\omega \cdot t + phase)$, $\sin(\omega \cdot t + phase)$ or $\cos(\omega \cdot t) + \sin(\omega \cdot t)$.

Typically, the problem has at least dimension 2, which makes matrix algebra efficient. Matrix formulation and Fourier transform is very convenient with tools as Matlab if numerical solutions are accepted.

4.4.3.1 Single Frequency Response

4.4.3.1.1 Solution with Fourier Transform

Equation [4.50] can be transformed to the frequency domain ($\mathcal{F}$ denotes Fourier transform, i.e. $\mathcal{F}(\xi(t)) = \int_{-\infty}^{\infty} e^{-j\cdot\omega\cdot t} \cdot \xi(t) \cdot dt$):

$$\begin{cases} j \cdot \omega \cdot \boldsymbol{\mathcal{F}}\left(\begin{bmatrix} v_y \\ \omega_z \end{bmatrix}\right) = \boldsymbol{A} \cdot \boldsymbol{\mathcal{F}}\left(\begin{bmatrix} v_y \\ \omega_z \end{bmatrix}\right) + \boldsymbol{B} \cdot \mathcal{F}(\delta_f); \\ \boldsymbol{\mathcal{F}}\left(\begin{bmatrix} \omega_z \\ a_y \end{bmatrix}\right) = \boldsymbol{C} \cdot \boldsymbol{\mathcal{F}}\left(\begin{bmatrix} v_y \\ \omega_z \end{bmatrix}\right) + \boldsymbol{D} \cdot \mathcal{F}(\delta_f); \end{cases}$$

Solving for states and outputs, using $\mathcal{F}(\dot{z}) = -j \cdot \omega \cdot \mathcal{F}(z)$;, gives:

$$\begin{cases} \begin{bmatrix} v_y \\ \omega_z \end{bmatrix} = \mathcal{F}^{-1}\left(\boldsymbol{\mathcal{F}}\left(\begin{bmatrix} v_y \\ \omega_z \end{bmatrix}\right)\right) = \mathcal{F}^{-1}\left((j \cdot \omega \cdot I - \boldsymbol{A})^{-1} \cdot \boldsymbol{B} \cdot \mathcal{F}(\delta_f)\right); \\ \begin{bmatrix} \omega_z \\ a_y \end{bmatrix} = \mathcal{F}^{-1}\left(\boldsymbol{\mathcal{F}}\left(\begin{bmatrix} \omega_z \\ a_y \end{bmatrix}\right)\right) = \mathcal{F}^{-1}\left(\boldsymbol{C} \cdot \boldsymbol{\mathcal{F}}\left(\begin{bmatrix} v_y \\ \omega_z \end{bmatrix}\right) + \boldsymbol{D} \cdot \mathcal{F}(\delta_f)\right); \end{cases}$$

Expressed as transfer functions:

$$\begin{aligned} \boldsymbol{H}_{\delta_f \to \begin{bmatrix} v_y \\ \omega_z \end{bmatrix}} &= \frac{1}{\mathcal{F}(\delta_f)} \cdot \boldsymbol{\mathcal{F}}\left(\begin{bmatrix} v_y \\ \omega_z \end{bmatrix}\right) = \frac{(j \cdot \omega \cdot \boldsymbol{I} - \boldsymbol{A})^{-1} \cdot \boldsymbol{B} \cdot \mathcal{F}(\delta_f)}{\mathcal{F}(\delta_f)} = (j \cdot \omega \cdot \boldsymbol{I} - \boldsymbol{A})^{-1} \cdot \boldsymbol{B}; \\ \boldsymbol{H}_{\delta_f \to \begin{bmatrix} \omega_z \\ a_y \end{bmatrix}} &= \frac{1}{\mathcal{F}(\delta_f)} \cdot \boldsymbol{\mathcal{F}}\left(\begin{bmatrix} \omega_z \\ a_y \end{bmatrix}\right) = \boldsymbol{C} \cdot \boldsymbol{H}_{\delta_f \to \begin{bmatrix} v_y \\ \omega_z \end{bmatrix}} + \boldsymbol{D} = \boldsymbol{C} \cdot (j \cdot \omega \cdot \boldsymbol{I} - \boldsymbol{A})^{-1} \cdot \boldsymbol{B} + \boldsymbol{D}; \end{aligned} \quad [4.51]$$

We have derived the transfer functions. The subscript tells that the transfer function is for the vehicle operation with excitation=input= δ_f and response=output= $[v_y \quad \omega_z]^T$ and output= $[v_y \quad a_y]^T$. The transfer function has dimension 2x1 and is complex. It operates as follows:

$$\text{Amplitudes: } \begin{cases} \begin{bmatrix} \hat{v}_y \\ \hat{\omega}_z \end{bmatrix} = \left| H_{\delta_f \to \begin{bmatrix} v_y \\ \omega_z \end{bmatrix}} \right| \cdot \hat{\delta}_f; \\ \begin{bmatrix} \hat{\omega}_z \\ \hat{a}_y \end{bmatrix} = \left| H_{\delta_f \to \begin{bmatrix} \omega_z \\ a_y \end{bmatrix}} \right| \cdot \hat{\delta}_f; \end{cases}$$

$$\text{Phase delays: } \begin{cases} \begin{bmatrix} \varphi_{v_y} \\ \varphi_{\omega_z} \end{bmatrix} = \begin{bmatrix} \arg(v_y) \\ \arg(\omega_z) \end{bmatrix} - \begin{bmatrix} 1 \\ 1 \end{bmatrix} \cdot \arg(\delta_f) = \begin{Bmatrix} \arg(\delta_f) \\ = 0 \end{Bmatrix} = \arg\left(H_{\delta_f \to \begin{bmatrix} v_y \\ \omega_z \end{bmatrix}}\right); \\ \begin{bmatrix} \varphi_{\omega_z} \\ \varphi_{a_y} \end{bmatrix} = \begin{bmatrix} \arg(\omega_z) \\ \arg(a_y) \end{bmatrix} - \begin{bmatrix} 1 \\ 1 \end{bmatrix} \cdot \arg(\delta_f) = \begin{Bmatrix} \arg(\delta_f) \\ = 0 \end{Bmatrix} = \arg\left(H_{\delta_f \to \begin{bmatrix} \omega_z \\ a_y \end{bmatrix}}\right); \end{cases} \quad [4.52]$$

4.4.3.1.2 Solution with Complex Mathematics

This section avoids requiring skills in Fourier transform. This makes the derivation quite long to reach the final results Eqs [4.57] and [4.56]. With Fourier Transform, the expression for the Transfer Function, H, can be reached with less algebra. Knowing H, it can be used in Eq [4.56].

The fundamental situation for steering frequency response is that the excitation is: $\delta_f = \hat{\delta}_f \cdot \cos(2 \cdot \pi \cdot f \cdot t) = \{e^{j\cdot a} = \cos(a) + j \cdot \sin(a)\} = \mathrm{Re}(\hat{\delta}_f \cdot e^{j\cdot 2\cdot\pi\cdot f\cdot t})$, where f is the (time) frequency in Hz and j is the imaginary unit. We rewrite $2 \cdot \pi \cdot f$ as ω (angular frequency), which has to be carefully

distinguished from ω_z (yaw velocity). Insert this in Eq [4.50] and neglecting the longitudinal force F_{fxw}. The full (complex) equation is used:

$$\mathrm{Re}\left[\begin{bmatrix} m & 0 \\ 0 & J \end{bmatrix} \cdot \begin{bmatrix} \dot{v}_{yc} \\ \dot{\omega}_{zc} \end{bmatrix} + \begin{bmatrix} \dfrac{C_f + C_r}{v_x} & \dfrac{C_f \cdot l_f - C_r \cdot l_r}{v_x} + m \cdot v_x \\ \dfrac{C_f \cdot l_f - C_r \cdot l_r}{v_x} & \dfrac{C_f \cdot {l_f}^2 + C_r \cdot {l_r}^2}{v_x} \end{bmatrix} \cdot \begin{bmatrix} v_{yc} \\ \omega_{zc} \end{bmatrix} = \begin{bmatrix} C_f \\ C_f \cdot l_f \end{bmatrix} \cdot \hat{\delta}_f \cdot e^{j\omega \cdot t}\right]; \quad [4.53]$$

We intend to solve the complex equation, and then find the solutions as real parts: $v_y = \mathrm{Re}[v_{yc}]$; and $\omega_z = \mathrm{Re}[\omega_{zc}]$;. (Subscript c means complex.)

If only interested in the stationary solution, which is valid after possible initial value dependent transients are damped out, we can assume a general form for the solution.

$$\begin{bmatrix} v_{yc} \\ \omega_{zc} \end{bmatrix} = \begin{bmatrix} \hat{v}_{yc} \\ \hat{\omega}_{zc} \end{bmatrix} \cdot e^{j \cdot \omega \cdot t} \quad \Rightarrow \quad \begin{bmatrix} \dot{v}_{yc} \\ \dot{\omega}_{zc} \end{bmatrix} = j \cdot \omega \cdot \begin{bmatrix} \hat{v}_{yc} \\ \hat{\omega}_{zc} \end{bmatrix} \cdot e^{j \cdot \omega \cdot t}; \quad [4.54]$$

Inserting the assumption in the differential equation gives:

$$\begin{bmatrix} m & 0 \\ 0 & J \end{bmatrix} \cdot j \cdot \omega \cdot \begin{bmatrix} \hat{v}_{yc} \\ \hat{\omega}_{zc} \end{bmatrix} \cdot e^{j \cdot \omega \cdot t} + \\ + \begin{bmatrix} \dfrac{C_f + C_r}{v_x} & \dfrac{C_f \cdot l_f - C_r \cdot l_r}{v_x} + m \cdot v_x \\ \dfrac{C_f \cdot l_f - C_r \cdot l_r}{v_x} & \dfrac{C_f \cdot {l_f}^2 + C_r \cdot {l_r}^2}{v_x} \end{bmatrix} \cdot \begin{bmatrix} \hat{v}_{yc} \\ \hat{\omega}_{zc} \end{bmatrix} \cdot e^{j \cdot \omega \cdot t} = \begin{bmatrix} 1 \\ l_f \end{bmatrix} \cdot C_f \cdot \hat{\delta}_f \cdot e^{j \cdot \omega \cdot t} \Rightarrow$$

$$\Rightarrow \begin{bmatrix} \hat{v}_{yc} \\ \hat{\omega}_{zc} \end{bmatrix} =$$

$$= \left(\begin{bmatrix} m & 0 \\ 0 & J \end{bmatrix} \cdot j \cdot \omega + \begin{bmatrix} \dfrac{C_f + C_r}{v_x} & \dfrac{C_f \cdot l_f - C_r \cdot l_r}{v_x} + m \cdot v_x \\ \dfrac{C_f \cdot l_f - C_r \cdot l_r}{v_x} & \dfrac{C_f \cdot {l_f}^2 + C_r \cdot {l_r}^2}{v_x} \end{bmatrix} \right)^{-1} \cdot \begin{bmatrix} 1 \\ l_f \end{bmatrix} \cdot C_f \cdot \hat{\delta}_f =$$

$$= H_{\delta_f \to \begin{bmatrix} v_y \\ \omega_z \end{bmatrix}} \cdot \hat{\delta}_f; \quad [4.55]$$

Then, we can assume we know $\hat{v}_{yc}$ and $\hat{\omega}_{zc}$ from Equation [4.55], and consequently we know v_{yc} and ω_{zc} from Eq [4.54]. We have derived the transfer function, $H_{\delta_f \to \begin{bmatrix} v_y \\ \omega_z \end{bmatrix}}$. The subscript tells that the transfer function is for the vehicle operation with excitation=input= δ_f and response=output= $\begin{bmatrix} v_y \\ \omega_z \end{bmatrix}$ case. This transfer function has dimension 2x1 and it is complex. It operates as follows:

$$\text{Amplitudes: } \begin{bmatrix} \hat{v}_y \\ \hat{\omega}_z \end{bmatrix} = \begin{bmatrix} |v_y| \\ |\omega_z| \end{bmatrix} = \left| H_{\delta_f \to \begin{bmatrix} v_y \\ \omega_z \end{bmatrix}} \right| \cdot |\delta_f|;$$

$$\text{Phase delays: } \begin{bmatrix} \arg(v_y) \\ \arg(\omega_z) \end{bmatrix} - \begin{bmatrix} 1 \\ 1 \end{bmatrix} \cdot \arg(\delta_f) = \{\arg(\delta_f) = 0\} = \arg\left(H_{\delta_f \to \begin{bmatrix} v_y \\ \omega_z \end{bmatrix}} \right) \quad [4.56]$$

However, we can derive expressions for v_{yc} and ω_{zc} on a real (non-complex) form, $amplitude \cdot \cos(angular\ frequency \cdot t - phase\ delay)$, without involving transfer function. That is done in the following:

$$v_y = \mathrm{Re}(v_{yc}) = \mathrm{Re}(\hat{v}_{yc} \cdot e^{j \cdot \omega \cdot t}) = \cdots = |\hat{v}_{yc}| \cdot \cos(\omega \cdot t + \arg(\hat{v}_{yc}));$$

The same rewriting can be done with ω_z, so that in total:

$$\begin{bmatrix} v_y \\ \omega_z \end{bmatrix} = \begin{bmatrix} \hat{v}_y \cdot \cos(\omega \cdot t - \varphi_{vy}) \\ \hat{\omega}_z \cdot \cos(\omega \cdot t - \varphi_{\omega z}) \end{bmatrix} = \begin{bmatrix} |\hat{v}_{yc}| \cdot \cos\left(\omega \cdot t - (-\arg(\hat{v}_{yc}))\right) \\ |\hat{\omega}_{zc}| \cdot \cos(\omega \cdot t - (-\arg(\hat{\omega}_{zc}))) \end{bmatrix} \quad [4.57]$$

Equation [4.55] and Equation [4.57] now gives us the possibility to find vehicle response amplitude and phase delay. The ratios between amplitude of responses and amplitude of excitation, $\hat{v}_y/\hat{\delta}_f$ and $\hat{\omega}_z/\hat{\delta}_f$, are called gains. The difference in argument is the phase delay.

4.4.3.2 Random Frequency Response

Solutions to harmonic excitation of linear dynamic systems are superimposable. This is also why the response from a mixed frequency excitation can be spliced into separate frequencies, e.g. using Fourier transformation. Hence, a common way to measure the frequency response diagrams is to log data from a random steering test. The frequency response diagram can then be extracted from this test.

4.4.3.3 Frequency Responses on Steering *

Function definition: ***Frequency Responses on Steering*** *are amplification and delay of steer angle to vehicle responses' measures (yaw velocity, lateral acceleration etc.), for stationary oscillating harmonic steering at certain longitudinal speed and varying steering frequency.*

4.4.3.3.1 Lateral Velocity and Yaw Velocity Frequency Response *

The frequency response for the two states, Lateral Velocity and Yaw velocity, can be plotted using Eq [4.51] and only one input ($\boldsymbol{u} = \delta_f$; instead of $\boldsymbol{u} = [\delta_f \quad F_{fxw} \cdot \delta_f]^T$), see Figure 4-47. The curves show Frequency Response for same vehicle, but different speed. The yaw velocity gain curve has a knee at 0.5..1 Hz. The decrease after that is a measure of yaw damping. The curve for high speed actually has a weak peak just before the knee. This is not desired, because the vehicle might feel a bit nervous. Yaw damping can also be how fast yaw velocity decays after a step response, see 4.4.4.

From Equation [4.18] we can calculate that characteristic speed for the vehicle is 120 km/h. With another understeering coefficient, we could have calculated a critical speed. Studying Figure 4-47 to Figure 4-50, one can find these special speeds in another appearance:

- For an understeered vehicle, speeds above the characteristic speed gives a negative yaw velocity delay for low steering frequencies will be negative.
- For over-steered vehicles, speeds above the critical speed gives a yaw velocity delay larger than 180 deg and yaw velocity amplitudes which are very large for low steering frequencies.

From Equation [4.18] we can calculate that characteristic speed for the vehicle is 120 km/h.

In Figure 4-48 the curves are for same speed and constant understeering gradient, but they show the Frequency Response for different sums of cornering stiffness $C_f + C_r$. Increasing the stiffness increases the yaw velocity gain (agility) at high frequencies.

In Figure 4-49 the curves are for same speed and constant sum of cornering stiffness ($C_f + C_r$), but they show the Frequency Response for different values of understeering gradient (Ku). Increasing understeer gradient decreases the yaw velocity gain (agility) at low frequencies. But, also note that increased understeering increases the peak in YVFR at around 0.5 Hz, which means low yaw damping.

4.4.3.3.2 Lateral Acceleration Frequency Response *

The lateral acceleration Frequency Response is another useful measure to study and set requirements on. Actually, yaw velocity and lateral acceleration are the most frequently used measures, since they are easily measured, e.g. from ESC sensors in most vehicles.

The transfer function is found (here using Fourier transform and previous results):

$$\text{Amplitude: } \hat{a}_y = |a_{yc}| = \left\{use: a_y = \frac{\dot{v}_y + \omega_z \cdot v_x}{m}\right\} = \left|\frac{j \cdot \omega \cdot v_{yc} + \omega_{zc} \cdot v_x}{m}\right| =$$
$$= \left|\frac{1}{m} \cdot [j \cdot \omega \quad v_x] \cdot H_{\delta_f \to \begin{bmatrix} v_y \\ \omega_z \end{bmatrix}} \cdot \delta_f\right| = \left|[j \cdot \omega \quad v_x] \cdot H_{\delta_f \to \begin{bmatrix} v_y \\ \omega_z \end{bmatrix}}\right| \cdot \frac{\delta_f}{m};$$
$$\text{Phase delay: } \arg(a_y) - \arg(\delta_f) = \{use: \arg(\delta_f) = 0\} = \arg\left([j \cdot \omega \quad v_x] \cdot H_{\delta_f \to \begin{bmatrix} v_y \\ \omega_z \end{bmatrix}}\right); \qquad [4.58]$$

Lateral acceleration Frequency Response is plotted for different vehicle speeds in Figure 4-50.

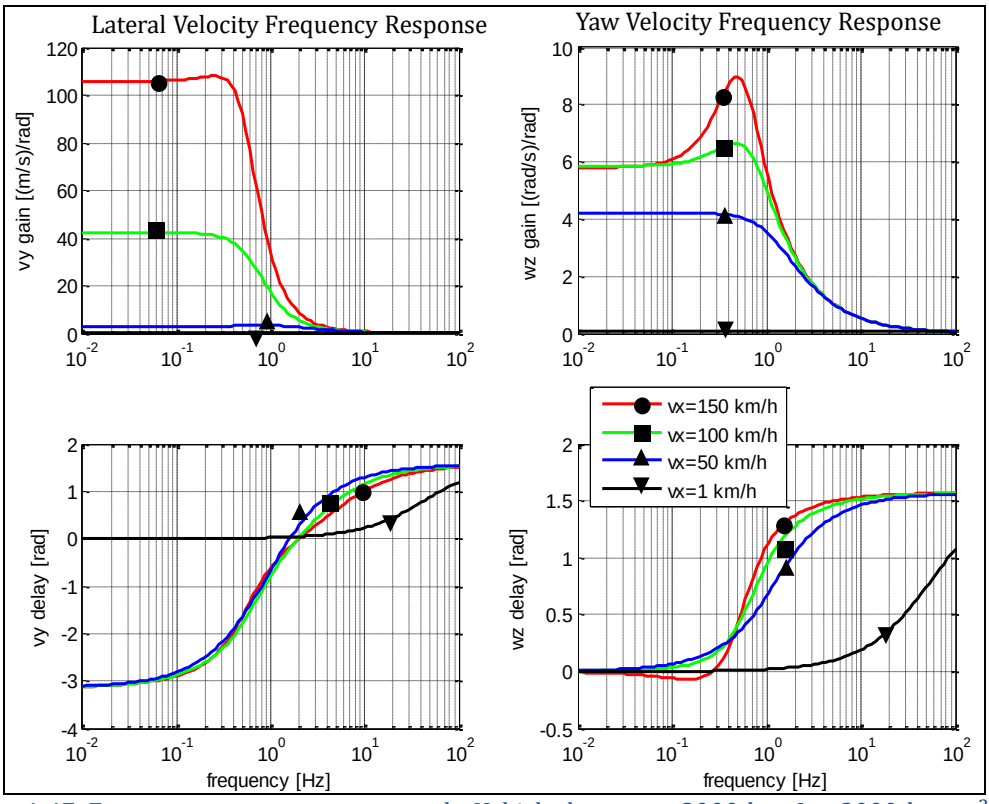

Figure 4-47: Frequency response to steer angle. Vehicle data: $m = 2000\ kg$; $J = 3000\ kg \cdot m^2$; $l_f = 1.3\ m$; $l_r = 1.5\ m$; $C_f = 81400\ N/rad$; $C_r = 78000\ N/rad$; ($K_u = 1.26\ rad/MN$).

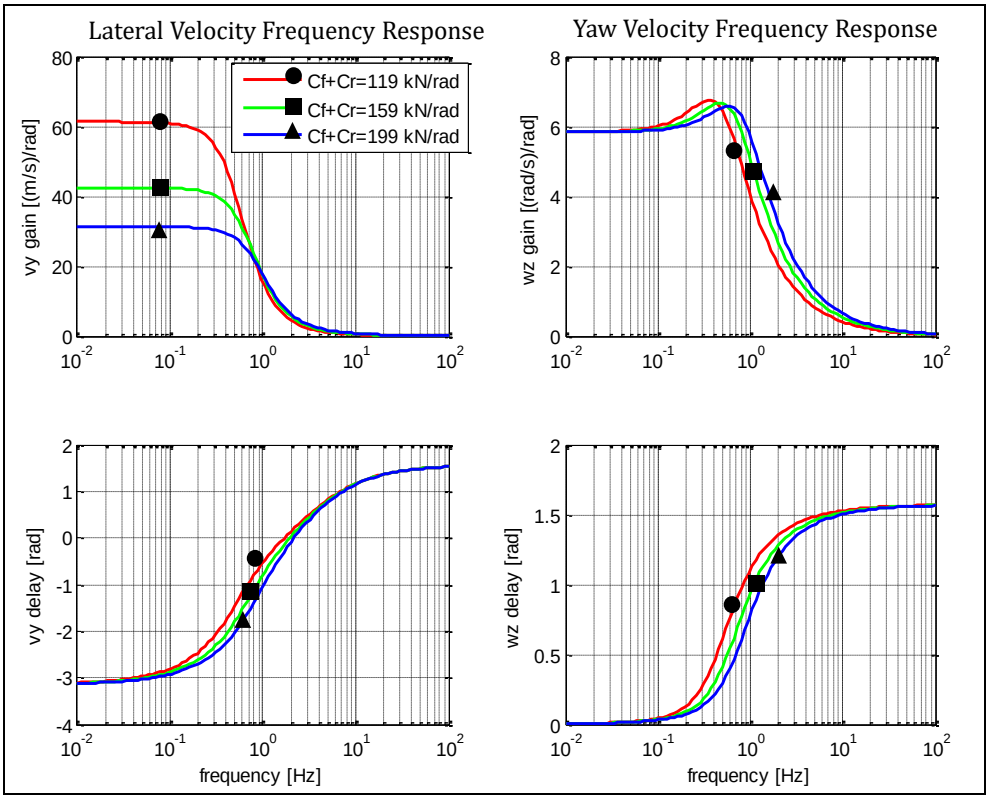

Figure 4-48: Frequency response to steer angle. Same vehicle data as in Figure 4-47, except varying C_f and C_r but keeping understeering gradient K_u constant. Vehicle speed = 100 km/h.

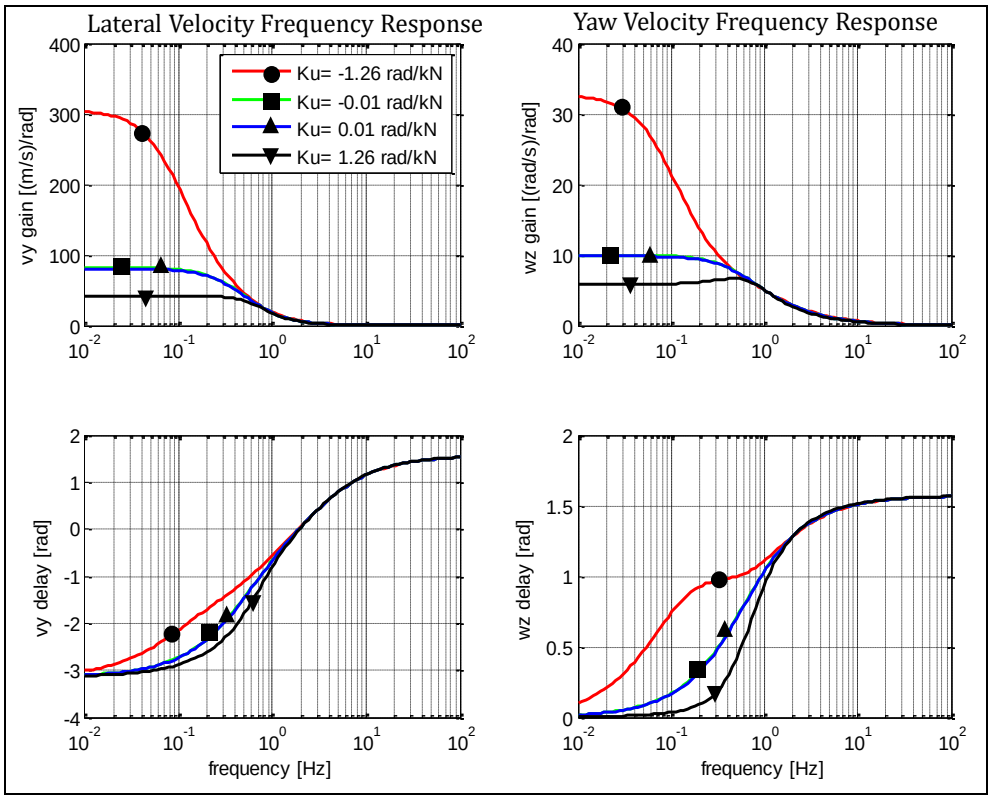

Figure 4-49: Frequency response to steer angle. Same vehicle data as in Figure 4-47, except varying understeering gradient Ku but keeping $C_f + C_r$ constant. Vehicle speed = 100 km/h.

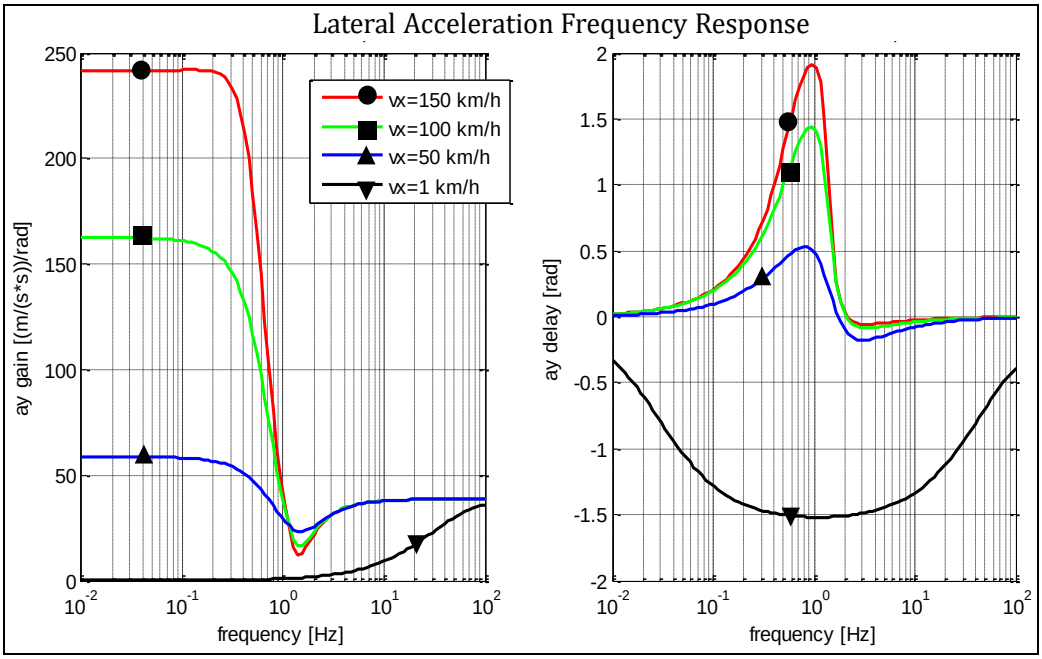

Figure 4-50: Lateral acceleration frequency response to steer angle. Vehicle data: $m = 2000\ kg$; $J = 3000\ kg \cdot m^2$; $l_f = 1.3\ m$; $l_r = 1.5\ m$; $C_f = 81400\ N/rad$; $C_r = 78000\ N/rad$; $(K_u = 1.26\ rad/MN)$.

4.4.3.4 Other Frequency Responses to Oscillating Steering *

In principle, it is possible to study a lot of other responses, such as Path Curvature Frequency Response, Side slip Frequency Response and Lateral Path Width Frequency Response etc. For combination-vehicles it is common to plot Rearward amplification (RA) as function of frequency. The compendium identifies some alternative definitions: $RA_{\omega z} = \max_i(\hat{\omega}_{iz}/\hat{\omega}_{1z})$; where i numbers the vehicle units. If the manoeuvre is not stationary oscillations, but e.g. a single lane change, we instead propose

$RA_{\omega z} = \max_i \left(\max_t |\omega_{iz}| / \max_t |\omega_{1z}| \right)$;. RA can also be defined for the worst frequency, e.g. $RA_{\omega z} = \max_f \left(\max_i (\hat{\omega}_{iz} / \hat{\omega}_{1z}) \right)$;. (Some argue for alternative definitions with a_y instead of ω_z. However, these are more difficult to agree on; which point, vertical and longitudinal, one should measure a_y in.)

4.4.4 Stable and Unstable Conditions

4.4.4.1 Locking One Axle

Locking one axle, i, can be modelled by replacing C_i with $\mu \cdot F_{iz}$;. This can be proven by linearization of Eq [4.47] with the locked axle's constitution replaced by "$F_{iy} = -\mu \cdot F_{iz} \cdot v_{iy} / |v_{ix}|$;". Since $C_i \approx CC_i \cdot F_{iz}$ and cornering compliance, CC_i, is typically 5..10 (trucks) and 10..15 (passenger cars), we can conclude that $\mu \cdot F_{iz}$ is normally $\ll C_i$. Realistic variation of road friction coefficient μ is 0.2..1. So, a locked axle can be seen as having much (typically 5..75 times) lower cornering stiffness on the locked axle. So, locking front gives extreme under-steering and locking rear gives extreme over-steering.

4.4.4.2 Frequency Responses for Varying Understeering Gradients

Eq [4.50] can explain instability. Instability means here that vehicle gets infinitely growing solutions although $\delta_f \equiv 0$. Eq [4.66] shows the explicit solution. We set $\delta_f \equiv 0$; and a small yaw disturbance as initial conditions: $[v_{y0} \quad \omega_{z0}] = [0 \quad \varepsilon]$; and get the following expression for the solution:

$$\begin{bmatrix} v_y \\ \omega_z \end{bmatrix} = \begin{bmatrix} \hat{v}_{y1} & \hat{v}_{y2} \\ \hat{\omega}_{z1} & \hat{\omega}_{z2} \end{bmatrix} \cdot \begin{bmatrix} e^{\lambda_1 \cdot t} & 0 \\ 0 & e^{\lambda_2 \cdot t} \end{bmatrix} \cdot \begin{bmatrix} \hat{v}_{y1} & \hat{v}_{y2} \\ \hat{\omega}_{z1} & \hat{\omega}_{z2} \end{bmatrix}^{-1} \cdot \begin{bmatrix} v_{y0} \\ \omega_{z0} \end{bmatrix};$$

$$where \left[\begin{bmatrix} \hat{v}_{y1} & \hat{v}_{y2} \\ \hat{\omega}_{z1} & \hat{\omega}_{z2} \end{bmatrix}, \begin{bmatrix} \lambda_1 & 0 \\ 0 & \lambda_2 \end{bmatrix} \right] = \text{eig}(\boldsymbol{A});$$

In Figure 4-51 we sweep v_x for normal passenger car data and try the following cornering stiffnesses:

- Locked front axle: $C_f \cdot l_f \approx 0.1 \cdot C_r \cdot l_r$; (extremely under-steered)
- Under-steered: $C_f \cdot l_f \approx 0.9 \cdot C_r \cdot l_r$; (moderatly under-steered
- Neutral-steered: $C_f \cdot l_f \approx 1 \cdot C_r \cdot l_r$;
- Over-steered: $C_f \cdot l_f \approx 1.1 \cdot C_r \cdot l_r$; (moderatly over-steered
- Locked rear axle: $C_f \cdot l_f \approx 10 \cdot C_r \cdot l_r$; (extremely over-steered)

In Figure 4-51 we see that only over-steered (incl. lock rear) gives an unstable vehicle. And that only under-steered vehicles (incl. lock front) gives oscillating solutions. Also, we see that all vehicles are stable for low enough speed.

Limit to instability (subscript $crit$) is when $Real(\lambda_{crit}) = 0$. Since $\lambda = \lambda(v_x)$, we can find $v_{x,crit} = \sqrt{C_f \cdot C_r \cdot L^2 / \left(C_f \cdot l_f - C_r \cdot l_r \right) \cdot m}$;. This is the same expression as we found already with the steady state model in Eq [4.18]. An advantage with using the transient model in Eq [4.50] is that we can also express how fast the solutions grows towards infinity, if they are oscillating or exponential and how the eigenmodes look.

We can express the condition for instability in other quantities. An example is when we want to limit regenerative braking with electric motor on rear axle. Then we solve for $C_{r,crit}$: $C_{r,crit} = l_f / \left(L^2 / m \cdot v_x^2 - l_f / C_f \right)$;. Together with a combined slip tyre model (e.g. Eq [2.49]), we can express instability in: $F_{x,crit} = \sqrt{(\mu \cdot F_z)^2 - \left(\mu \cdot F_z \cdot l_f / \left(\left(L^2 / m \cdot v_x^2 - l_f / C_f \right) \cdot C_{ry} \big|_{s_x = 0} \right) \right)^2}$;.

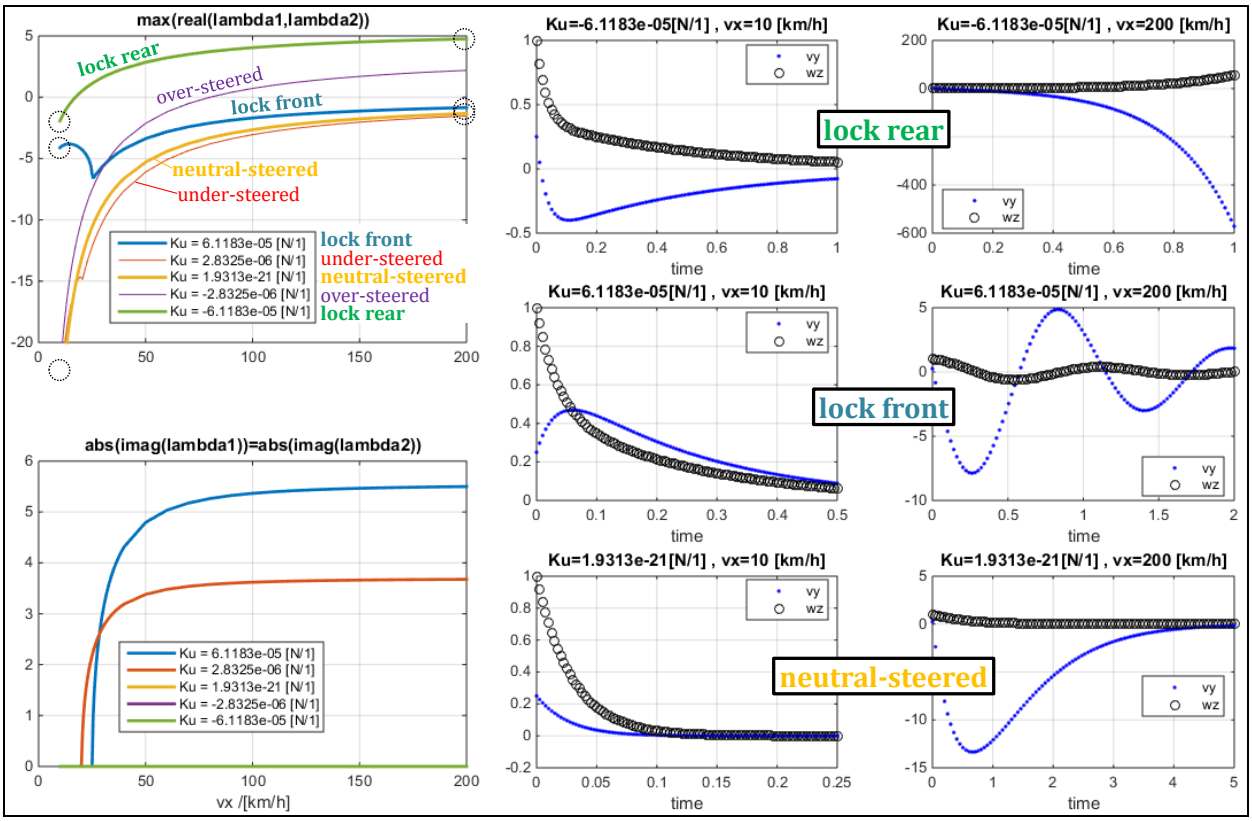

Figure 4-51: Stability analysis of passenger car with varying cornering stiffnesses.

4.4.4.2.1 Driver Influence on Stability

A driver can improve or disturb the vehicle. The gains for steady state cornering and the frequency responses for stationary oscillating steering does not measure the real stability since they do not include the dynamics of the driver, neither human nor automated driver. However, studying critical speed through a transient model enables to add a dynamic driver model and quantify the influence of driver.

A driver model can be, e.g.: $\delta_f = k \cdot (\omega_{z,Req} - \omega_z) = \left\{ \begin{matrix} assume \\ \omega_{z,Req} = 0 \end{matrix} \right\} = -k \cdot \omega_z = [0 \quad -k] \cdot \begin{bmatrix} v_y \\ \omega_z \end{bmatrix};$

Adding this equation to Eq [4.50] gives: $\begin{bmatrix} \dot{v}_y \\ \dot{\omega}_z \end{bmatrix} = \boldsymbol{A} \cdot \begin{bmatrix} v_y \\ \omega_z \end{bmatrix} + \boldsymbol{B} \cdot \delta_f = (\boldsymbol{A} + \boldsymbol{B} \cdot [0 \quad -k]) \cdot \begin{bmatrix} v_y \\ \omega_z \end{bmatrix};$

Eigenvalue analysis on matrix $(\boldsymbol{A} + \boldsymbol{B} \cdot [0 \quad -k])$ for varying speed and driver gain gives:

$l_f = 1.3\ m;$
$l_r = 1.5\ m;$
$m = 2000;$
$J = 3000;$

$C_f = 15 \cdot m \cdot g \cdot \frac{l_r}{L};$

$C_r = 10 \cdot m \cdot g \cdot \frac{l_f}{L};$

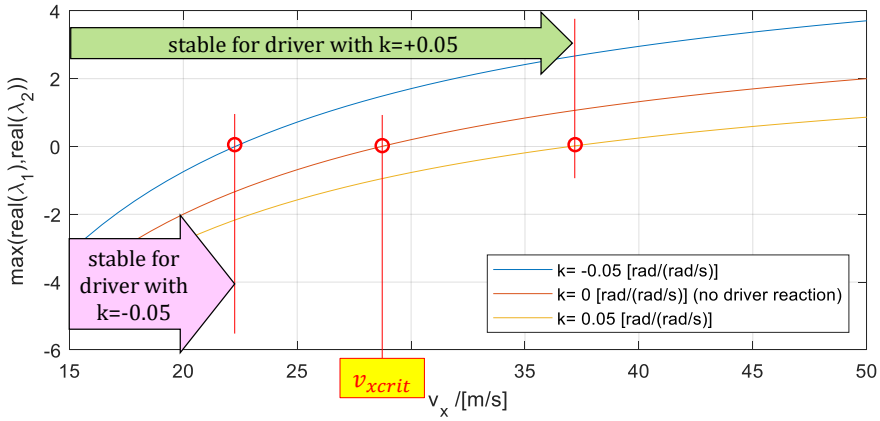

Figure 4-52: Influence of driver on stability. Driver model used: $\delta_f = k \cdot (\omega_{z,Req} - \omega_z) = -k \cdot \omega_z$.

4.5 Transient Driving

This section addresses both transient handling and arbitrary transient driving, where the first is mainly lateral, while longitudinal dynamics is added in the latter. Generally, this can be turning and braking/accelerating at the same time through a manoeuvre.

4.5.1 Transient Driving Manoeuvres *

From the manoeuvres defined in this section, there are a large number of relevant function possible to define. Here, only a few is mentioned:

> *Function definition:* ***Double Lane Change Capability*** *is the highest entry speed that a certain driver (or driver model) can manage without hitting any cones. A certain cone pattern (e.g. as Figure 4-53 or Figure 4-54) and a certain road friction has to be defined. A certain operation principle of pedals needs to be specified, e.g. release both pedals at entry or full brake pedal apply.*
>
> *Function definition:* ***Over-speed into Curve Capability*** *is the highest entry speed that a certain driver (or driver model) can manage without hitting any cones. A certain cone pattern e.g. as Figure 4-55) and a certain road friction has to be defined. A certain operation principle of pedals needs to be specified, e.g. release both pedals at entry or full brake pedal apply.*
>
> *Function definition:* ***Steer-In and Release Accelerator Pedal stability*** *is a measure (e.g. side slip rear axle peak) after a certain simultaneous steer-in and release of accelerator pedal, starting from a steady state cornering at a certain path radius and speed. A certain road friction has to be defined.*

When testing Transient driving manoeuvres, the typical part of the test track is the Vehicle Dynamics Area or a Handling Track, see Figure 1-25. A Handling Track is a normal width road, intentionally curved and with safety areas beside the curves for safety in case of run-off road during tests.

Typical transient tests are:

- Step steer, where one can measure transient versions of
  - Yaw velocity response
  - Lateral acceleration response
  - Curvature response
  - Yaw damping
- Lateral avoidance manoeuvres:
  - Single Lane Change SLC cone track
  - Double Lane Change DLC cone track, see Figure 4-20, Figure 4-53, and Figure 4-54
  - Lane change while full braking
  - Sine with dwell
  - Steering effort in evasive manoeuvres
- Tests from steady state cornering
  - Brake or accelerate in curve
  - Lift accelerator pedal and steer-in while cornering
  - Over-speeding into curve, see Figure 4-55
- Handling type tests
  - Slalom between cones
  - Handling track, general driving experience
- Roll-over tests

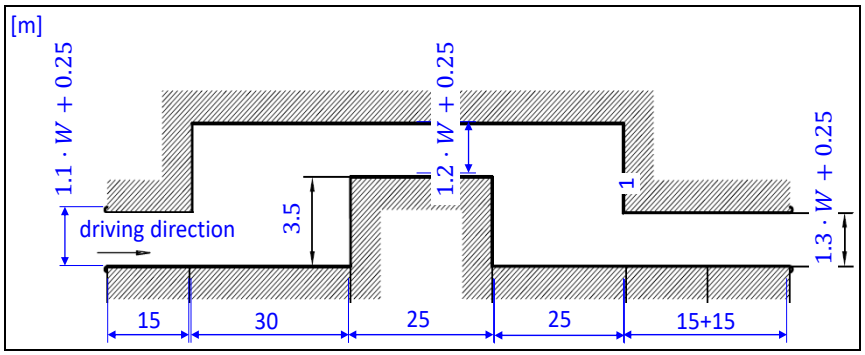

Figure 4-53: Passenger cars - Test track for a severe lane-change manoeuvre - Part 1: Double lane-change. Reference (ISO 3888).

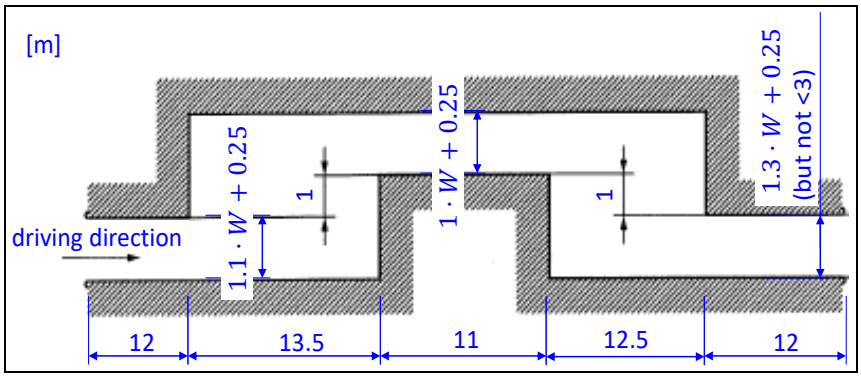

Figure 4-54: Passenger cars - Test track for a severe lane-change manoeuvre - Part 2: Obstacle avoidance. Reference (ISO 3888).

There are many standards for DLC beside ISO, such as Consumer Union. Generally speaking, the DLCs with short distance in 2nd lane is often used for ESC-like tests.

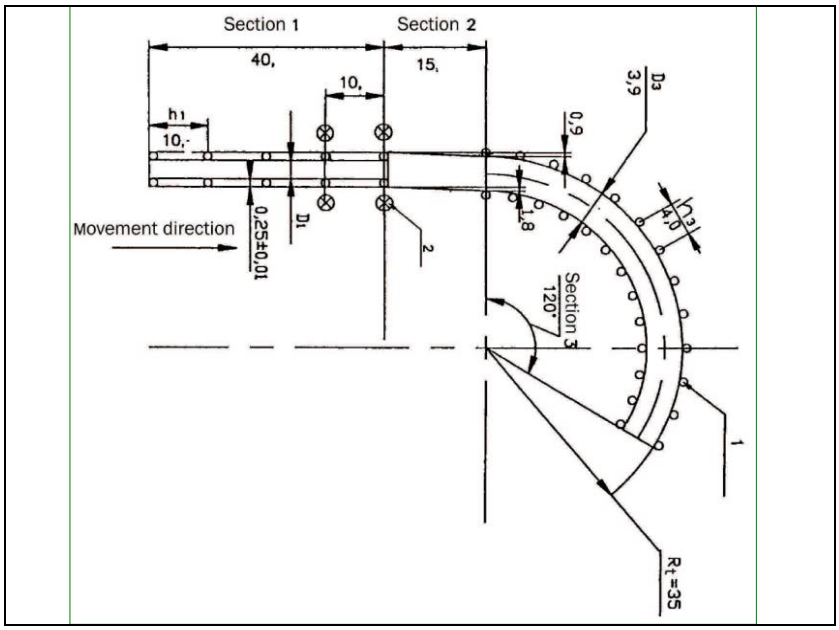

Figure 4-55: Cone track for one standardized test of Over-speeding into curve

Standards which are relevant to these test manoeuvres are, e.g. References (ISO 3888), (ISO 7401), (ISO 7975, 2006), (ISO 11026), (ISO 14791), (ISO 14793), (ISO 14794, 2011) and (NHTSA).

4.5.2 One-Track Models, without Lateral Load Transfer

4.5.2.1 Two-Axle Vehicle

This section starts from the model derived in 4.4.2 and Figure 4-42 and Equations [4.46] and [4.47]. However, in the context of transient dynamics it is more relevant to use the model for more violent manoeuvres, and also active control such as ESC interventions. Hence, we extend the model in three ways:

- The constitutive relation is saturated, to reflect that each axle may reach friction limit, friction coefficient times normal load on the axle. See max functions in Equation [4.59].
- To be able to do mentioned limitation, the longitudinal load transfer is modelled, but only in the simplest possible way using stiff suspension models. Basically, it is the same model as given in Equation [3.13].
- A yaw moment representing (left/right) unsymmetrical braking/propulsion. See the term $M_{act,z}$ in yaw equilibrium in Equation [4.59]. This is much better modelled in a two-track model, where $M_{act,z}$ does not appear, but we instead can have different longitudinal tyre forces on left and right side.

It should be noted that the model lacks lateral load transfer and the transients in longitudinal load transfer and the reduced cornering stiffness and reduced max friction due to load transfer and utilizing friction for wheel longitudinal forces.

Equilibrium in road plane (longitudinal, lateral, yaw):

$$m \cdot (\dot{v}_x - \omega_z \cdot v_y) = F_{fxw} \cdot \cos(\delta_f) - F_{fyw} \cdot \sin(\delta_f) + F_{rx};$$
$$m \cdot (\dot{v}_y + \omega_z \cdot v_x) = F_{fxw} \cdot \sin(\delta_f) + F_{fyw} \cdot \cos(\delta_f) + F_{ry};$$
$$J \cdot \dot{\omega}_z = (F_{fxw} \cdot \sin(\delta_f) + F_{fyw} \cdot \cos(\delta_f)) \cdot l_f - F_{ry} \cdot l_r + M_{act,z};$$

Equilibrium out of road plane (vertical, pitch):

$$F_{fz} + F_{rz} - m \cdot g = 0;$$
$$-F_{fz} \cdot l_f + F_{rz} \cdot l_r - (F_{fxw} \cdot \cos(\delta_f) - F_{fyw} \cdot \sin(\delta_f) + F_{rx}) \cdot h = 0;$$

Constitution:

$$F_{fyw} = -\text{sign}(s_{fy}) \cdot \min(C_f \cdot |s_{fy}|;\ \mu \cdot F_{fz});$$
$$F_{ry} = -\text{sign}(s_{ry}) \cdot \min(C_r \cdot |s_{ry}|;\ \mu \cdot F_{rz});$$

Compatibility, slip definitions:

$$s_{fy} = \frac{v_{fyw}}{v_{fxw}};\quad and\quad s_{ry} = \frac{v_y - l_r \cdot \omega_z}{v_x};$$

Compatibility, transformation from vehicle to wheel coordinate system:

$$v_{fxw} = (v_y + l_f \cdot \omega_z) \cdot \sin(\delta_f) + v_x \cdot \cos(\delta_f);$$
$$v_{fyw} = (v_y + l_f \cdot \omega_z) \cdot \cos(\delta_f) - v_x \cdot \sin(\delta_f);$$

[4.59]

A Modelica model is given in Eq [4.60]. Changes compared to Eq [4.46] are marked as underlined code.

```
//Equilibrium, in road plane:
  m*(der(vx)-wz*vy) = Ffxv + Frx;
  m*(der(vy)+wz*vx) = Ffyv + Fry;
  J*der(wz) = Ffyv*lf - Fry*lr + Mactz;
//Equilibrium, out of road plane:
  Ffz + Frz - m*g = 0;
  -Ffz*lf + Frz*lr -(Ffxv + Frx)*h = 0;
//Compatibility:
  vfxv = vx;     vfyv = vy + lf*wz;
  vrx = vx;      vry = vy - lr*wz;
//Lateral tyre force model:
  Ffyw = -sign(sfy)*min(Cf*abs(sfy), mu*Ffz);    sfy = vfyw/vfxw;
  Fry  = -sign(sry)*min(Cr*abs(sry), mu*Frz);    sry = vry/vrx;
//Transformation between vehicle and wheel coordinate systems:
  Ffxv = Ffxw*cos(df) - Ffyw*sin(df);
```

[4.60]

```
  Ffyv = Ffxw*sin(df) + Ffyw*cos(df);
  vfxv = vfxw*cos(df) - vfyw*sin(df);
  vfyv = vfxw*sin(df) + vfyw*cos(df);
//Shaft torques
  Ffxw = +1000; // Front axle driven.
  Frx  = -100; // Rolling resistance on rear axle.
  Mactz=0;
```

A simulation of this model is seen in Figure 4-56. Same steering input as used in Figure 4-43. $M_{act,z}$ is zero. Cornering stiffnesses are chosen so that the vehicle is understeered in steady state. Road friction coefficient is 1. We can see that the vehicle now gets unstable and spins out with rear to the right. This is mainly because longitudinal load transfer unloads the rear axle, since the kept steer angle decelerates the vehicle. In this manoeuvre, it would have been reasonable to model also that the rear cornering stiffness decreases with the decreased rear normal load, and opposite on front. Such addition to the model would make the vehicle spin out even more. On the other hand, the longitudinal load shift is modelled to take place immediately. With a suspension model, this load shift would require some more time, which would calm down the spin-out. In conclusion, the manoeuvre is violent enough to trigger a spin-out, so a further elaboration with how to control $M_{act,z}$ could be of interest. However, it is beyond the scope of this compendium.

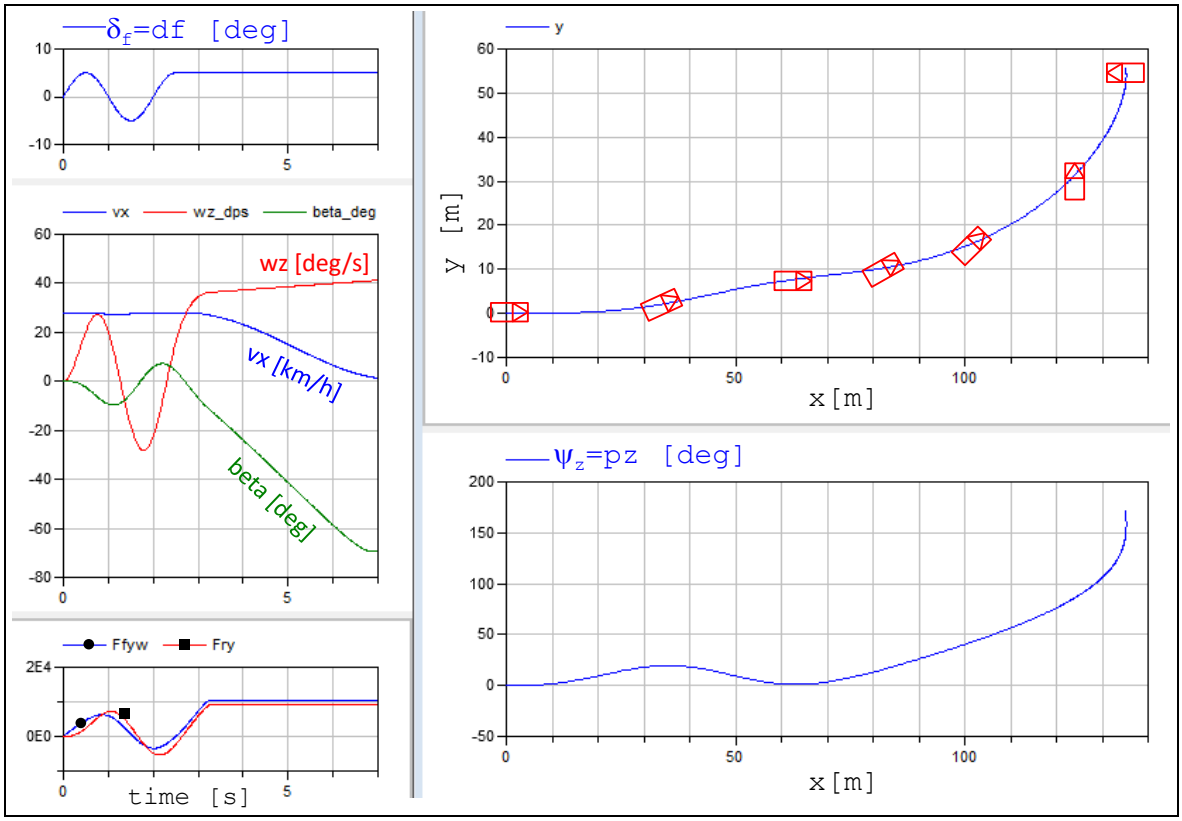

Figure 4-56: Simulation results of one-track model for transient dynamics. The vehicle drawn in the path plot is not in proper scale, but the orientation is approximately correct.

The vehicle reaches zero speed already after 7 seconds, because the wide side slip decelerates the vehicle a lot. The simulation is then stopped, because the model cannot handle zero speed. That vehicle models become singular at zero speed is very usual, since the slip definition becomes singular due to zero speed in the denominator. The large difference compared to Figure 4-43 is due to the new constitutive equation used, which shows the importance of checking validity region for any model one uses.

A simplified version of the mathematical model in Eq [4.59] follows in Eq [4.61]; assuming constant v_x and small angles and small propulsion force and no $M_{act,z}$.

Equilibrium in road plane (lateral, yaw):

$$m \cdot (\dot{v}_y + \omega_z \cdot v_x) = F_{fy} + F_{ry};$$
$$J \cdot \dot{\omega}_z = F_{fy} \cdot l_f - F_{ry} \cdot l_r;$$

Equilibrium out of road plane (vertical, pitch):

$$F_{fz} + F_{rz} - m \cdot g = 0;$$
$$-F_{fz} \cdot l_f + F_{rz} \cdot l_r = 0;$$

Constitution:

$$F_{fy} = -\text{sign}(s_{fy}) \cdot \min(C_f \cdot |s_{fy}|;\ \mu \cdot F_{fz});$$
$$F_{ry} = -\text{sign}(s_{ry}) \cdot \min(C_r \cdot |s_{ry}|;\ \mu \cdot F_{rz});$$

Compatibility:

$$\delta_f + s_{fy} = \frac{v_y + l_f \cdot \omega_z}{v_x};\quad and\quad s_{ry} = \frac{v_y - l_r \cdot \omega_z}{v_x};$$

[4.61]

4.5.2.2 Articulated Vehicles

A model for an articulated vehicle will now be derived in the same spirit as in 4.4.2. The model can represent a car with trailer or rigid truck with centre-axle trailer or tractor with semitrailer (if $l_{1c} < L_1$).

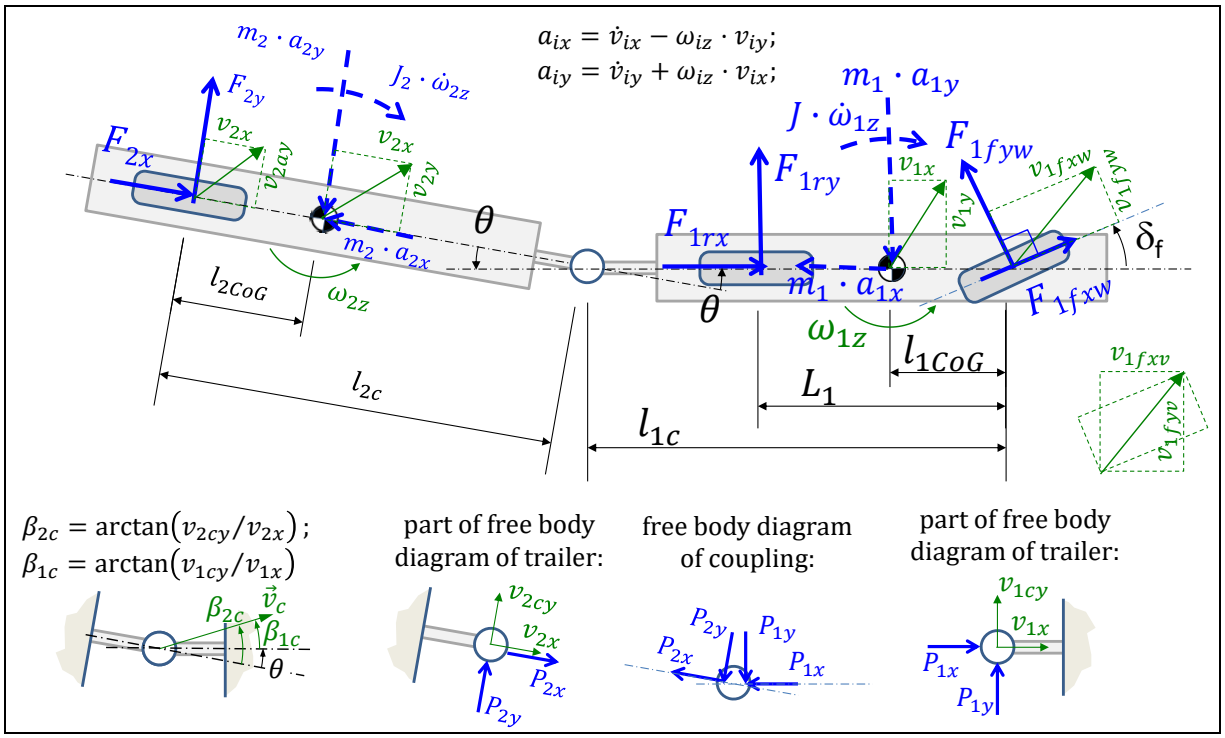

Figure 4-57: Model of two-unit articulated vehicle.

Model equations for the 1st unit:

Equilibrium of 1st unit (longitudinal, lateral, yaw around CoG):

$$m_1 \cdot (\dot{v}_{1x} - \omega_{1z} \cdot v_{1y}) = \cos(\delta_f) \cdot F_{1fxw} - \sin(\delta_f) \cdot F_{1fyw} + F_{1rx} + P_{1x};$$
$$m_1 \cdot (\dot{v}_{1y} + \omega_{1z} \cdot v_{1x}) = \sin(\delta_f) \cdot F_{1fxw} + \cos(\delta_f) \cdot F_{1fyw} + F_{1ry} + P_{1y};$$
$$J_1 \cdot \dot{\omega}_{1z} = (\sin(\delta_f) \cdot F_{1fxw} + \cos(\delta_f) \cdot F_{1fyw}) \cdot l_{1CoG} - F_{1ry} \cdot (L_1 - l_{1CoG}) +$$
$$+(-P_{1y}) \cdot (l_{1c} - l_{1CoG});$$

Constitution for axles on 1st unit:

$$F_{1fyw} = -C_{1f} \cdot s_{1fy};\quad F_{1ry} = -C_{1r} \cdot s_{1ry};$$

Compatibility, within 1st unit:

$$s_{1fy} = v_{1fyw}/|v_{1fxw}|;\quad s_{1ry} = v_{1ry}/|v_{1x}|;$$
$$v_{1fxw} = +\cos(\delta_f) \cdot v_{1x} + \sin(\delta_f) \cdot v_{1fyv};$$
$$v_{1fyw} = -\sin(\delta_f) \cdot v_{1x} + \cos(\delta_f) \cdot v_{1fyv};$$

[4.62]

$$v_{1fyv} = v_{1y} + \omega_{1z} \cdot l_{1CoG};$$
$$v_{1ry} = v_{1y} - \omega_{1z} \cdot (L_1 - l_{1CoG});$$
$$v_{1cy} = v_{1y} - \omega_{1z} \cdot (l_{1c} - l_{1CoG}); \quad \blacksquare$$

Model equations for the 2nd unit:

Equilibrium of 2nd unit (longitudinal, lateral, yaw around CoG)**:**

$$m_2 \cdot (\dot{v}_{2x} - \omega_{2z} \cdot v_{2y}) = F_{2x} + P_{2x};$$
$$m_2 \cdot (\dot{v}_{2y} + \omega_{2z} \cdot v_{2x}) = F_{2y} + P_{2y};$$
$$J_2 \cdot \dot{\omega}_{2z} = -F_{2y} \cdot l_{2CoG} + P_{2y} \cdot (l_{2c} - l_{2CoG});$$

Constitution for axles on 2nd unit:

$$F_{2y} = -C_2 \cdot s_{2y};$$

Compatibility, within 2nd unit:

$$s_{2y} = v_{2ay}/|v_{2x}|;$$
$$v_{2ay} = v_{2y} - \omega_{2z} \cdot l_{2CoG};$$
$$v_{2cy} = v_{2y} + \omega_{2z} \cdot (l_{2c} - l_{2CoG}); \quad \blacksquare$$

[4.63]

Model equations for the coupling:

Equilibrium of coupling (x, y in 1st unit's coordinates):

$$P_{1x} + \cos(\theta) \cdot P_{2x} + \sin(\theta) \cdot P_{2y} = 0;$$
$$P_{1y} - \sin(\theta) \cdot P_{2x} + \cos(\theta) \cdot P_{2y} = 0;$$

Compatibility of coupling:

$$v_{1x} = +\cos(\theta) \cdot v_{2x} + \sin(\theta) \cdot v_{2cy}; \quad \blacksquare$$
$$v_{1cy} = -\sin(\theta) \cdot v_{2x} + \cos(\theta) \cdot v_{2cy}; \quad \blacksquare$$
$$\dot{\theta} = \omega_{1z} - \omega_{2z};$$

[4.64]

Let us assume $\boldsymbol{u} = [\delta_f; F_{1fxw}; F_{1rx}; F_{2x}]^T$ are known inputs. Eqs [4.62].. [4.64] is a DAE system in with 24 equations and 24 unknowns: $v_{1x}, v_{1y}, \omega_{1z}, v_{2x}, v_{2y}, \omega_{2z}, \theta, F_{1fyw}, F_{1ry}, F_{2y}, s_{1fy}, s_{1ry}, s_{2y}, P_{1x}, P_{1y}, P_{2x}, P_{2y}, v_{1fxw}, v_{1fyw}, v_{1fyv}, v_{1ry}, v_{2ay}, v_{1cy}, v_{2cy}$. The equations can be written as they are into a Modelica tool, which can find a possible state selection (such as $v_{1x} v_{1y}, \omega_{1z}, \omega_{2z}, \theta$), an explicit form and perform simulations. The use of a Modelica tool is very motivated for articulated vehicles, since the articulation points makes the DAE system of equation to be of "high index", meaning that the Modelica tool identifies the constraints equations, i.e. the equations which have to be differentiated, cf. 3.3.2. In this case, it is the equations marked with ■ in Eqs [4.62]..[4.64].

4.5.2.2.1 Explicit Form Model without DAE Tool

It will now be explained how the explicit form model can be found using manual equation manipulations or simpler symbolic tools, unable to handle DAEs (e.g. Matlab Symbolic Toolbox). We have to differentiate the equations marked with ■ in Eqs [4.62]..[4.64]. It leads to:

$$\dot{v}_{1cy} = \dot{v}_{1y} - \dot{\omega}_{1z} \cdot (l_{1c} - l_{1CoG});$$
$$\dot{v}_{2cy} = \dot{v}_{2y} + \dot{\omega}_{2z} \cdot (l_{2c} - l_{2CoG});$$
$$\dot{v}_{1x} = (-\sin(\theta) \cdot \dot{\theta} \cdot v_{2x} + \cos(\theta) \cdot \dot{v}_{2x}) + (\cos(\theta) \cdot \dot{\theta} \cdot v_{2cy} + \sin(\theta) \cdot \dot{v}_{2cy});$$
$$\dot{v}_{1cy} = (-\cos(\theta) \cdot \dot{\theta} \cdot v_{2x} - \sin(\theta) \cdot \dot{v}_{2x}) + (-\sin(\theta) \cdot \dot{\theta} \cdot v_{2cy} + \cos(\theta) \cdot \dot{v}_{2cy});$$

So, we regard it as an ODE with 24+4=28 equations. States and inputs as above DAE. The states are regarded as known and we can count to 28 unknown variables: $\dot{v}_{1x}, \dot{v}_{1y}, \dot{\omega}_{1z}, \dot{\omega}_{2z}, \dot{\theta}, \dot{v}_{1cy}, \dot{v}_{2cy}, \dot{v}_{2y}, \dot{v}_{2x}, v_{2x}, v_{2y}, F_{1fyw}, F_{1ry}, F_{2y}, s_{1fy}, s_{1ry}, s_{2y}, P_{1x}, P_{1y}, P_{2x}, P_{2y}, v_{1fxw}, v_{1fyw}, v_{1fyv}, v_{1ry}, v_{2ay}, v_{1cy}, v_{2cy}$. The expressions for state derivatives $\dot{v}_{1x}, \dot{v}_{1y}, \dot{\omega}_{1z}, \dot{\omega}_{2z}, \dot{\theta}$ can be found through algebraic manipulations, but in this case the symbolic tools will generate huge expressions (hundreds of thousands of tokens) or even fail. Therefore, we will reformulate model and introduce approximations in 4.5.2.2.1.1.

4.5.2.2.1.1 Reformulated Model with Approximations

We will derive a model without introducing the constraint forces $P_{1x}, P_{1y}, P_{2x}, P_{2y}$. We select intuitively the 5 states $v_{1x} v_{1y}, \omega_{1z}, \omega_{2z}, \theta$ and find the equations to express their derivatives: 4 equilibria and 1 compatibility relations which involves $\dot{\theta}$. We also introduce approximations as for the two axle one-track model in 4.4.2: small angles $\delta_f, \beta_{ij}, \alpha_{ij} = \arctan\left(v_{ijyw} / \left|v_{ijxw}\right|\right)$, centrifugal acceleration perpendicular to each unit ($v_{ix} \cdot \omega_{iz} = 0$) and steered axle lateral tyre force does not influence whole vehicle longitudinally ($F_{fyw} \cdot \delta_f = 0$). Some new, but conceptually same, approximations can be done especially for articulated vehicles: small articulation angle θ and lateral tyre force on axles on 2nd unit does not influence whole vehicle longitudinally ($F_{2y} \cdot \theta = 0$).

Equilibrium of whole vehicle (longitudinal to 1st unit, lateral to 1st unit):

$$\begin{aligned} 0 = & -m_1 \cdot a_{1x} + F_{1fxw} \cdot \cos(\delta_f) - F_{1fyw} \cdot \sin(\delta_f) + F_{1rx} + (F_{2x} - m_2 \cdot a_{2x}) \cdot \cos(\theta) \\ & + (F_{2y} - m_2 \cdot a_{2y}) \cdot \sin(\theta) \\ & \approx -m_1 \cdot a_{1x} + F_{1fxw} - 0 + F_{1rx} + (F_{2x} - m_2 \cdot a_{2x}) + (0 - m_2 \cdot a_{2y}) \cdot \theta; \\ 0 = & -m_1 \cdot a_{1y} + F_{1fxw} \cdot \sin(\delta_f) + F_{1fyw} \cdot \cos(\delta_f) + F_{1ry} - (F_{2x} - m_2 \cdot a_{2x}) \cdot \sin(\theta) \\ & + (F_{2y} - m_2 \cdot a_{2y}) \cdot \cos(\theta) \\ & \approx -m_1 \cdot a_{1y} + F_{1fxw} \cdot \delta_f + F_{1fyw} + F_{1ry} - (F_{2x} - m_2 \cdot a_{2x}) \cdot \theta \\ & + (F_{2y} - m_2 \cdot a_{2y}); \end{aligned}$$

$$\begin{aligned} & where\ a_{1x} = \dot{v}_{1x} - \omega_{1z} \cdot v_{1y} \approx \dot{v}_{1x}; \quad a_{2x} = \dot{v}_{2x} - \omega_{2z} \cdot v_{2y} \approx \dot{v}_{2x}; \\ & a_{1y} = \dot{v}_{1y} + \omega_{1z} \cdot v_{1x}; \quad a_{2y} = \dot{v}_{2y} + \omega_{2z} \cdot v_{2x}; \end{aligned}$$

Equilibrium of 1st unit (yaw around coupling):

$$\begin{aligned} 0 = & + (F_{1fxw} \cdot \sin(\delta_f) + F_{1fyw} \cdot \cos(\delta_f)) \cdot l_{1c} + F_{1ry} \cdot (l_{1c} - L_1) - m_1 \cdot a_{1y} \cdot (l_{1c} - l_{1CoG}) - J_1 \cdot \dot{\omega}_{1z} \approx \\ \approx & + (F_{1fxw} \cdot \delta_f + F_{1fyw}) \cdot l_{1c} + F_{1ry} \cdot (l_{1c} - L_1) - m_1 \cdot a_{1y} \cdot (l_{1c} - l_{1CoG}) - J_1 \cdot \dot{\omega}_{1z}; \end{aligned}$$

Equilibrium of 2nd unit (yaw around coupling):

$$0 = -F_{2y} \cdot l_{2CoG} + m_2 \cdot a_{2y} \cdot (l_{2c} - l_{2CoG}) - J_2 \cdot \dot{\omega}_{2z};$$

Compatibility in coupling:

$$\dot{\theta} = \omega_{1z} - \omega_{2z};$$

(Note: The same concept works for a vehicle with *N* units: 2 translational equilibria for the whole vehicle and 2 rotational equilibria (fore and aft part) per coupling point: $2 + 2 \cdot N$ equilibria.)

Now, we realize that we have to find 2 compatibility relations that eliminate $\dot{v}_{2x}, \dot{v}_{2y}$. These may not involve any new derivatives, only $\dot{v}_{2x}, \dot{v}_{2y}$ and the state derivatives:

Differentiated Compatibility (to *eliminate* $\dot{v}_{2x}, \dot{v}_{2y}$):

$$\begin{aligned} \dot{v}_{2x} = & \frac{d}{dt}(v_{1x} \cdot \cos(\theta) - v_{1cy} \cdot \sin(\theta)) = \frac{d}{dt}\left(v_{1x} \cdot \cos(\theta) - \left(v_{1y} - \omega_{1z} \cdot (l_{1c} - l_{1CoG})\right) \cdot \sin(\theta)\right) \\ & = +\dot{v}_{1x} \cdot \cos(\theta) - v_{1x} \cdot \sin(\theta) \cdot \dot{\theta} - \left(\dot{v}_{1y} - \dot{\omega}_{1z} \cdot (l_{1c} - l_{1CoG})\right) \cdot \sin(\theta) \\ & - \left(v_{1y} - \omega_{1z} \cdot (l_{1c} - l_{1CoG})\right) \cdot \cos(\theta) \cdot \dot{\theta} \approx \\ & \approx +\dot{v}_{1x} - v_{1x} \cdot \theta \cdot \dot{\theta} - \left(\dot{v}_{1y} - \dot{\omega}_{1z} \cdot (l_{1c} - l_{1CoG})\right) \cdot \theta - \left(v_{1y} - \omega_{1z} \cdot (l_{1c} - l_{1CoG})\right) \cdot \dot{\theta}; \\ \dot{v}_{2y} = & \frac{d}{dt}\left(v_{2cy} - \omega_{2z} \cdot (l_{2c} - l_{2CoG})\right) = \frac{d}{dt}\left(v_{1cy} \cdot \cos(\theta) + v_{1x} \cdot \sin(\theta) - \omega_{2z} \cdot (l_{2c} - l_{2CoG})\right) = \\ & = \frac{d}{dt}\left(\left(v_{1y} - \omega_{1z} \cdot (l_{1c} - l_{1CoG})\right) \cdot \cos(\theta) + v_{1x} \cdot \sin(\theta) - \omega_{2z} \cdot (l_{2c} - l_{2CoG})\right) = \\ & = \left(\dot{v}_{1y} - \dot{\omega}_{1z} \cdot (l_{1c} - l_{1CoG})\right) \cdot \cos(\theta) - \left(v_{1y} - \omega_{1z} \cdot (l_{1c} - l_{1CoG})\right) \cdot \sin(\theta) \cdot \dot{\theta} + \dot{v}_{1x} \\ & \cdot \sin(\theta) + v_{1x} \cdot \cos(\theta) \cdot \dot{\theta} - \dot{\omega}_{2z} \cdot (l_{2c} - l_{2CoG}) \approx \\ \approx & \left(\dot{v}_{1y} - \dot{\omega}_{1z} \cdot (l_{1c} - l_{1CoG})\right) - \left(v_{1y} - \omega_{1z} \cdot (l_{1c} - l_{1CoG})\right) \cdot \theta \cdot \dot{\theta} + \\ & + \dot{v}_{1x} \cdot \theta + v_{1x} \cdot \dot{\theta} - \dot{\omega}_{2z} \cdot (l_{2c} - l_{2CoG}); \end{aligned}$$

Now the constitution can be involved:

Constitution for axles (to *eliminate* lateral forces $F_{1fyw}, F_{1ry}, F_{2y}$):

$$F_{1fyw} = -C_{1f} \cdot s_{1fyw};$$

$F_{1ry} = -C_{1r} \cdot s_{1ryw};$
$F_{2y} = -C_2 \cdot s_{2y};$

We now eliminate the slips $s_{1fyw}, s_{1ryw}, s_{2y}$ and express them in state variables:

Compatibility (to *eliminate* s_{fyw}):

$\arctan2(v_{1fyv}, |v_{1x}|) = \delta_f + \arctan(s_{1fyw}) \Rightarrow s_{1fyw} \approx v_{1fyv}/|v_{1x}| - \delta_f;$

where $v_{1fyv} = v_{1y} + \omega_{1z} \cdot l_{1CoG};$

Compatibility (to *eliminate* s_{1ry}):

$s_{1ry} = v_{1ry}/|v_{1x}|;$

where $v_{1ry} = v_{1y} - \omega_{1z} \cdot (L_1 - l_{1CoG});$

Compatibility (to *eliminate* s_{2y}):

$s_{2y} = v_{2ay}/|v_{2x}|;$

where $v_{2ay} = v_{2cy} - \omega_{2z} \cdot l_{2c};$

where $v_{2cy} = v_{1cy} \cdot \cos(\theta) + v_{1x} \cdot \sin(\theta) \approx v_{1cy} + v_{1x} \cdot \theta;$

where $v_{1cy} = v_{1y} - \omega_{1z} \cdot (l_{1c} - l_{1CoG});$

and $v_{2x} = +v_{1x} \cdot \cos(\theta) - v_{1cy} \cdot \sin(\theta) \approx +v_{1x} - v_{1cy} \cdot \theta;$

If we perform the *eliminations* we get 5 equations:

$$\boldsymbol{f_{DAE}}(\dot{\boldsymbol{x}}, \boldsymbol{x}, \boldsymbol{u}) = \boldsymbol{0}; \quad where\ \boldsymbol{x} = [v_{1x}; v_{1y}; \omega_{1z}; \omega_{2z}; \theta],\ \ \boldsymbol{u} = [\delta_f; F_{1fxw}; F_{1rx}; F_{2x}];$$

Using the exact (grey text) expressions, this is exactly same model as in Eqs [4.62]..[4.64].

4.5.2.2.1.2 Explicit Form Model and Linear Explicit Form Model

We can reformulate to explicit form: $\dot{\boldsymbol{x}} = \boldsymbol{f_{ODE}}(\boldsymbol{x}, \boldsymbol{u})$; but this is the same huge expression, mentioned above. Using the approximate (black text) expressions, the solution will be somewhat smaller, but still very large. However, we can linearize around an operation point $(\boldsymbol{x_0}, \boldsymbol{u_0})$:

$$\dot{\boldsymbol{x}} \approx \boldsymbol{f_{ODE}}(\boldsymbol{x_0}, \boldsymbol{u_0}) + \boldsymbol{A}(\boldsymbol{x_0}, \boldsymbol{u_0}) \cdot (\boldsymbol{x} - \boldsymbol{x_0}) + \boldsymbol{B}(\boldsymbol{x_0}, \boldsymbol{u_0}) \cdot (\boldsymbol{u} - \boldsymbol{u_0}) =$$
$$= \boldsymbol{f_0} + \boldsymbol{A_0} \cdot (\boldsymbol{x} - \boldsymbol{x_0}) + \boldsymbol{B_0} \cdot (\boldsymbol{u} - \boldsymbol{u_0});$$

The elements of the matrices $\boldsymbol{A_0}, \boldsymbol{B_0}$ is: $A_{0,ij} = \left.\frac{\partial f_{ODE,i}}{\partial x_j}\right|_{\boldsymbol{x_0}, \boldsymbol{u_0}}$; and $B_{0,ij} = \left.\frac{\partial f_{ODE,i}}{\partial u_j}\right|_{\boldsymbol{x_0}, \boldsymbol{u_0}}$;

As example of relevant operating condition to linearize around, we take straight-line without significant longitudinal tyre forces: $\boldsymbol{x_0} = [v_{1x0}; 0; 0; 0; 0]^T, \boldsymbol{u_0} = [0; 0; 0; 0]^T$. Note that we do not assume constant speed, i.e. we do **not** set $\dot{v}_{1x} = 0$, but v_{1x} is still a state variable.

Then we get symbolic expressions of only $\boldsymbol{A_0}, \boldsymbol{B_0}$ of around 15 thousand tokens, which is manageable, but not worth writing out in this compendium, except on this overviewing way:

$$\boldsymbol{A_0} = \begin{bmatrix} 0 & 0 & 0 & 0 & 0 \\ 0 & 0 & \neq 0 & \neq 0 & \neq 0 \\ 0 & 0 & \neq 0 & \neq 0 & \neq 0 \\ 0 & 0 & \neq 0 & \neq 0 & \neq 0 \\ 0 & 0 & 1 & -1 & 0 \end{bmatrix}; \quad \boldsymbol{B_0} = \begin{bmatrix} 0 & \neq 0 & \neq 0 & \neq 0 \\ \neq 0 & 0 & 0 & 0 \\ \neq 0 & 0 & 0 & 0 \\ \neq 0 & 0 & 0 & 0 \\ 0 & 0 & 0 & 0 \end{bmatrix};$$

Now, we can simulate to compare the different models:

- "*Exact*" ("Modular" Eqs [4.62]..[4.64], which is identical to the equations with black text above)
- "*Small Angles*" (the equations above, with a mixture of black and grey text so that only using the small angle approximations, but not using the "zeros")
- "*With All Physical Approximations*, except linearized" (the equations with black text above)
- "*Linearized*" ($\dot{\boldsymbol{x}} = \boldsymbol{A_0} \cdot \boldsymbol{x} + \boldsymbol{B_0} \cdot \boldsymbol{u}$; as described above)

A simulation with these 4 models is shown in Figure 4-58.

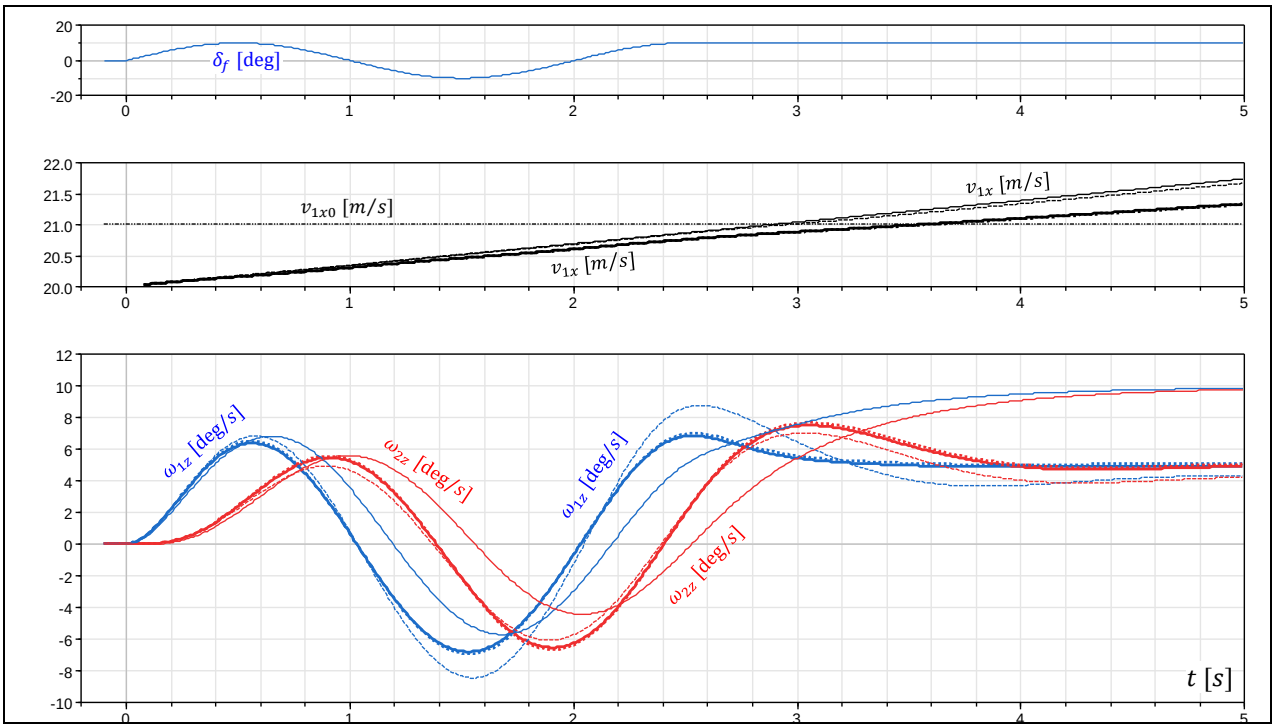

Figure 4-58: Tractor and semitrailer. Comparison of simulations with the 4 models (thick solid: "Exact", thick dotted: "Small Angles", thin dashed: "All physical approximations", thin solid: "Linearized").

A similar linearization is done for a longer combination vehicle (A-double, i.e. Tractor+Semi-trailer+Fulltrailer) in https://research.chalmers.se/publication/192958.

4.5.2.2.2 Model Library for Articulated Vehicles

The first model (Eqs [4.62].. [4.64]) for articulated vehicle is written so that each equation belongs to either a unit or a coupling. This opens up for systematic treatment of combination vehicles with more than one articulation point. There are basically two conceptual ways:

- Vectorised formulation, see Reference (Sundström, o.a., 2014).
- Modular library from which parts can be graphically dragged, dropped and connected. This is briefly visualized as implemented in the Modelica-tool Dymola in Figure 4-59.

4.5.2.2.2.1 Modular Library

A modular library is shown in Figure 4-59. Eq [4.62] is declared in "Unit" and Eq [4.64] in "Coupling".

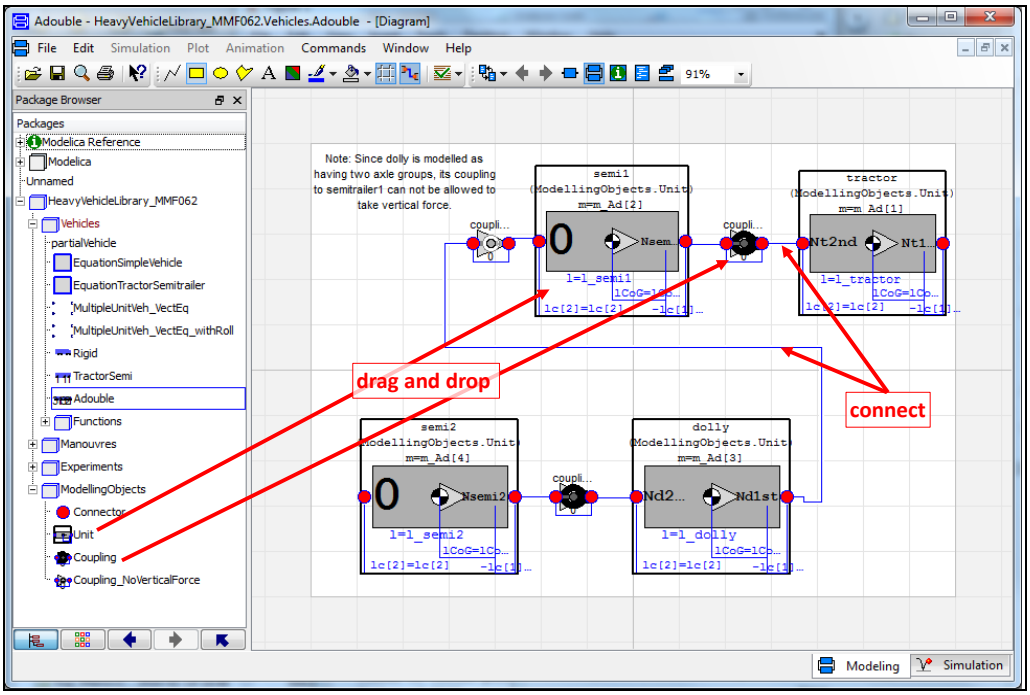

Figure 4-59: Drag, drop and connect library for heavy combination vehicles. The model example shows a so-called A-double, Tractor+SemiTrailer+Dolly+SemiTrailer.

An example of lane change manoeuvre, defined as lateral acceleration on 1st axle follows a single sine-wave, is shown in Figure 4-60. The natural input is prescribed steer angle ($\delta_f = \sin(time)$;), but since modelled in Modelica, it is as easy to prescribe something else, e.g. lateral acceleration on first axle ($a_{f1y} = \sin(time)$;).

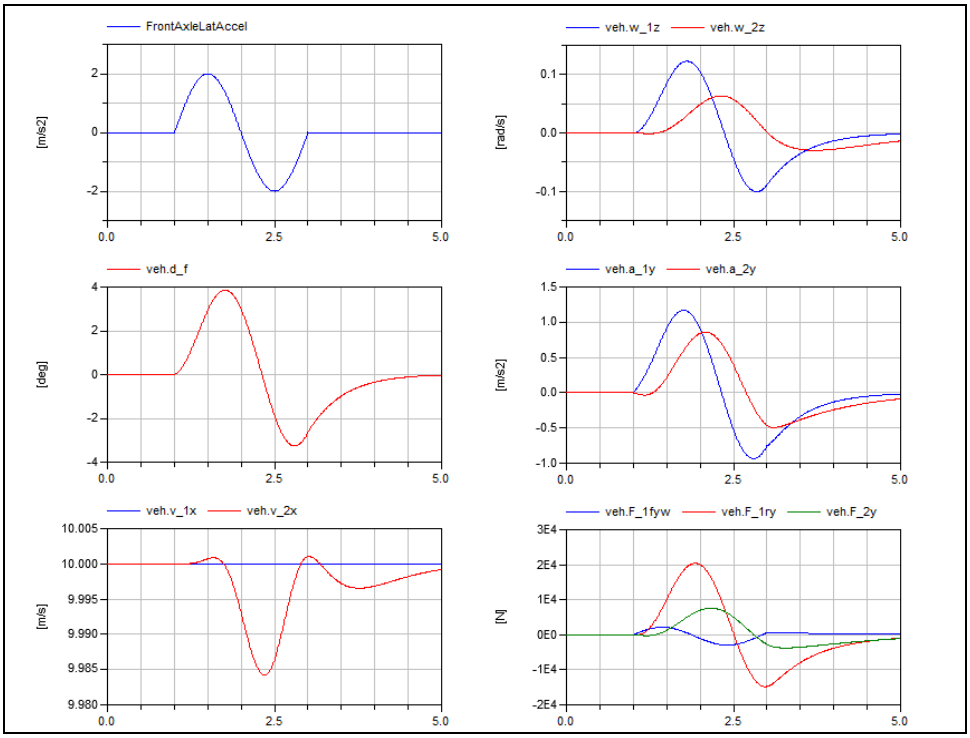

Figure 4-60: One period sinus test of a Tractor+SemiTrailer.

4.5.2.3 Cambering Vehicle Model

The model below shows how a cambering vehicle can be modelled. The model is mainly made for lateral dynamics, but it allows also longitudinal acceleration. The drawing shows a two-wheeler, but any or both of the axles could have two wheels, as long as the suspension linkage is such that the axle does

not take any roll moment. The model is shown in Eq [4.65] in Modelica format. It is not modelled that driver moves within the vehicle, which is why the inertial data is constant. Also, the chassis (frame) is modelled as stiff and steering system as massless. The model lacks two equations, which is logical since a driver model can add prescribed steer angle and prescribed F_{rx}.

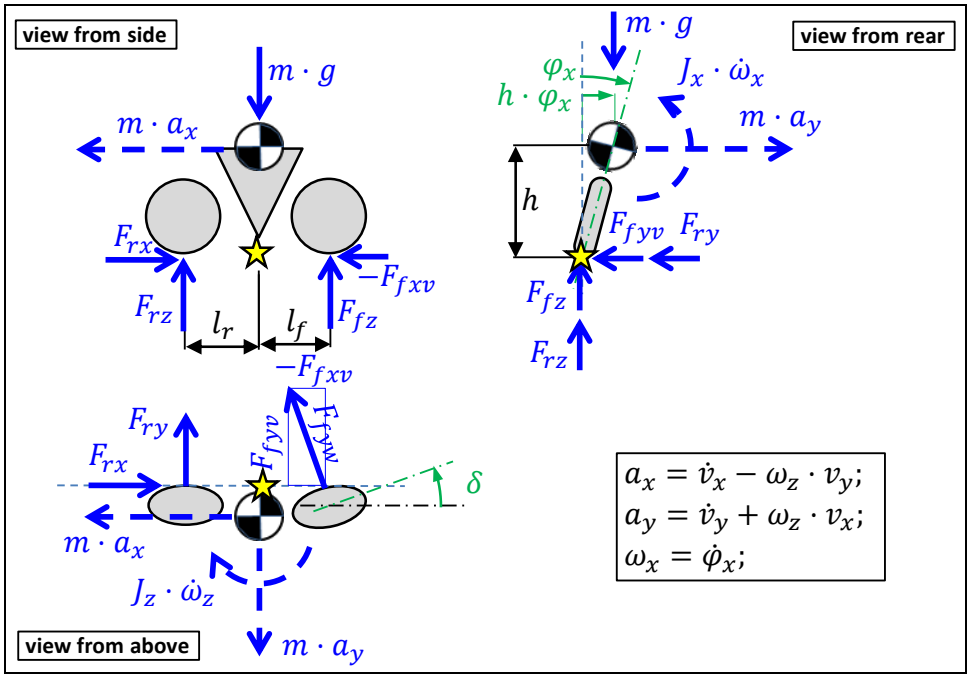

Figure 4-61: Model of cambering vehicle. (The stars marks point of moment equilibria in the "mathematical model" derived from this "physical model".)

```
//Equilibrium in road plane (x,y,rotz):
  m*ax = Ffxv + Frx;
  m*ay = Ffyv + Fry;
  Jz*der(wz) = Ffyv*lf - Fry*lr - m*ax*h*px;
  ax = der(vx) - wz*vy;
  ay = der(vy) + wz*vx;
//Equilibrium out of road plane (z, rotx, roty):
  m*g = Ffz + Frz;
  Jx*der(wx) = m*g*h*px + m*ay*h;
  0 = -Ffz*lf + Frz*lr - m*ax*h;
  wx = der(px);
//Constitution:
  Ffyw = -CC*Ffz*sfy;    Fry = -CC*Frz*sry;
//Compatibility, slip definition:
  atan(sfy) = atan2(vy + lf*wz + h*wx, vx - h*px*wz) - d;
  atan(sry) = atan2(vy - lr*wz + h*wx, vx - h*px*wz) - 0;
//Force coordinate transformation:
  Ffxv = -Ffyw*sin(d);
  Ffyv = +Ffyw*cos(d);
```

[4.65]

When entering a constant radius curve from straight driving one has to first steer out of the curve to tilt the vehicle a suitable amount for the coming path curvature, R_p. The suitable amount is hence $\varphi_{x,suitable} = -a_y/g = -\omega_z \cdot v_x/g = -v_x^2/(R_p \cdot g)$;. Then one steers with the turn and balances (closed loop controls) to the desired roll angle. Systems like this, which has to be operated in opposite direction initially is called "Non-minimum phase systems". It is generally difficult to design a controller for such systems. The two simulations shown in Figure 4-75 are done with the above model. Initial speed is $v_x = 10\ m/s$ and $F_{rx} = 0$. Path radius, $R_p(t) = step\ function\ at\ t = 0.1$, representing a suddenly curving road or path.

- One simulation (`veh_driver`) uses a closed loop driver model which first steers outwards ($\delta < 0$) and then continuously calculates the steer angle as a closed loop controller: $\delta = Gain \cdot (\varphi_{x,req} - \varphi_x)$;. It is not claimed that the driver model is representative for real drivers.

- In the other simulation (`veh_inverse`), the roll angle is prescribed as $\varphi_x = -v_x^2/(R_p \cdot g)$;. To prescribe the roll angle, instead of steer angle, is a way to avoid the "Non-minimum phase" difficulties. The system becomes a normal Minimum phase system if actuated with roll angle instead of steer angle. A price one has to pay for this is that the model equations has to go through a more advanced symbolic manipulation, e.g. differentiation, to solve for all variables, including the steer angle δ. However, with a Modelica tool the symbolic manipulation is done automatically. One can see this as a way to avoid a controller design and instead use an optimal driver; optimal in the sense that it follows the path curvature with optimal yaw agility. The road path curvature is a step function but has to be filtered twice (time constant 0.1 s is used in Figure 4-75) to become differentiable.

The latter, optimal driver, negotiates the turn without overshot in yaw velocity, so it follows a suddenly curving path better.

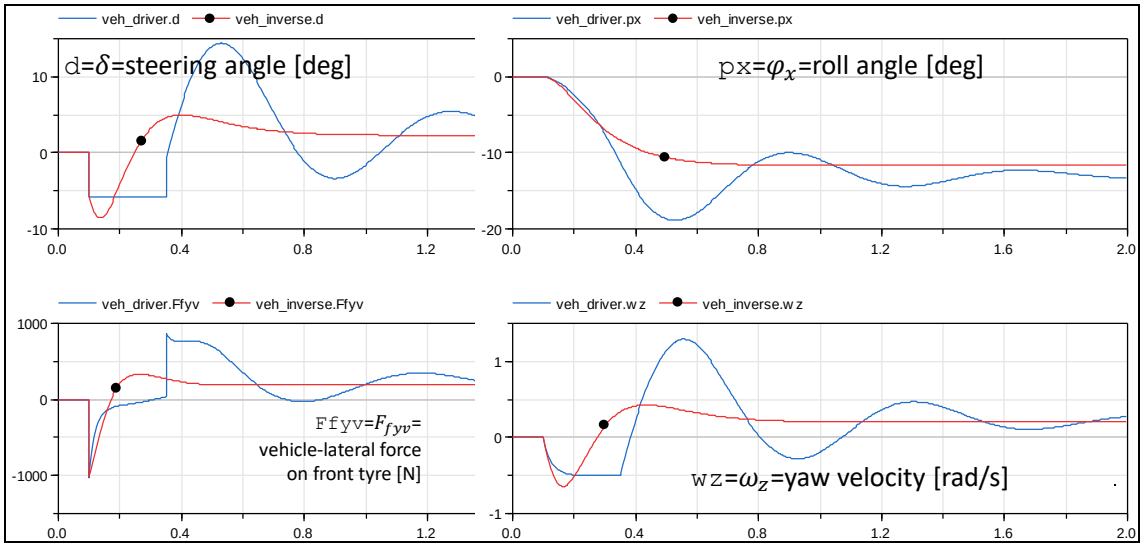

Figure 4-62: Simulations of entering a curve with a cambering vehicle. Blue solid curves without dot-marker show a closed-loop driver model which actuates δ. Red curves with dot-marker shows an optimal/inverse driver model which actuates φ_x.

Both driver models above only exemplify the low-level, roll-balancing, part of a driver. To run the model in an environment with obstacles, one would also need a high-level, path selecting, part which outputs desired, e.g., δ or φ_x. Additional driver model for longitudinal actuation is also needed.

It can be noted that the roll influences in two ways, compared to the non-cambering (roll-stiff) vehicles previously modelled in the compendium:

- The roll motion itself is a dynamic motion, where the roll velocity becomes a state variable carrying kinetic energy.
- The roll influences the tyre slip, e.g. rear: $s_{ry} = (v_y - l_r \cdot \omega_z + h \cdot \omega_x)/(v_x - h \cdot \varphi_x \cdot \omega_z)$;. The term $h \cdot \omega_x$ can generally be neglected for non-cambering vehicles, but for a cambering vehicle, such as a bike, it is essential. The term $h \cdot \varphi_x \cdot \omega_z$ is only important at large roll angles, it is for instance used as lever for longitudinal wheel forces in ESC-like control systems for motorbikes.

4.5.3 Two-Track Models, with Lateral Load Transfer

The models in this section model both transients longitudinal load transfer (as in 3.4.5.2) and transient lateral load transfer (extension from 4.3.9.3, with transients and wheel-individual suspension).

4.5.3.1 Example of Explicit Form Model; Two-Axle Vehicle, Driver and Environment

The implementation of the model in 4.5.2.3 was done in Modelica. A Modelica tool automatically transforms the model to explicit form which can be simulated, which is very efficient. But, as mentioned in

1.5.4.10, explicit form models can sometimes facilitate the understanding of the vehicle's dynamics. This is why the following model is presented. It is implemented in the data flow diagram tool Simulink. This section explains how the **states** (or state variables) together with **inputs** (or input variables), influence the **derivatives** (or state derivatives).

The example model in this section is similar, but not identical, to the model in 4.5.2.3. The aim is to model in-road-plane motion, due to transient actuation (wheel torques and wheel steer angles). Limitations in this example model are:

- Influence from vertically uneven road is NOT modelled.
- Neither wheel lift nor suspension bump stop are modelled
- Control functions (such as ABS, TC and ESC) are NOT modelled
- The pendulum effect is NOT modelled, see 4.3.9.2
- Wheel camber and steer angle change with suspension travel is NOT modelled.

The model is a typical passenger vehicle, with driver and environment, see Figure 4-63. The driver interface is the normal, 2 pedals, 1 steering wheel and a boolean request for direction of propulsion, `LongDir` (=-1 or +1). The interface to environment is motion (variable position) in surrounding world. To try out the vehicle model, driver and environment is also modelled. This includes also the interface between them, which is motion of obstacles in environment, relative to subject vehicle. The suspension is exemplified with wheel-individual suspension on both axles.

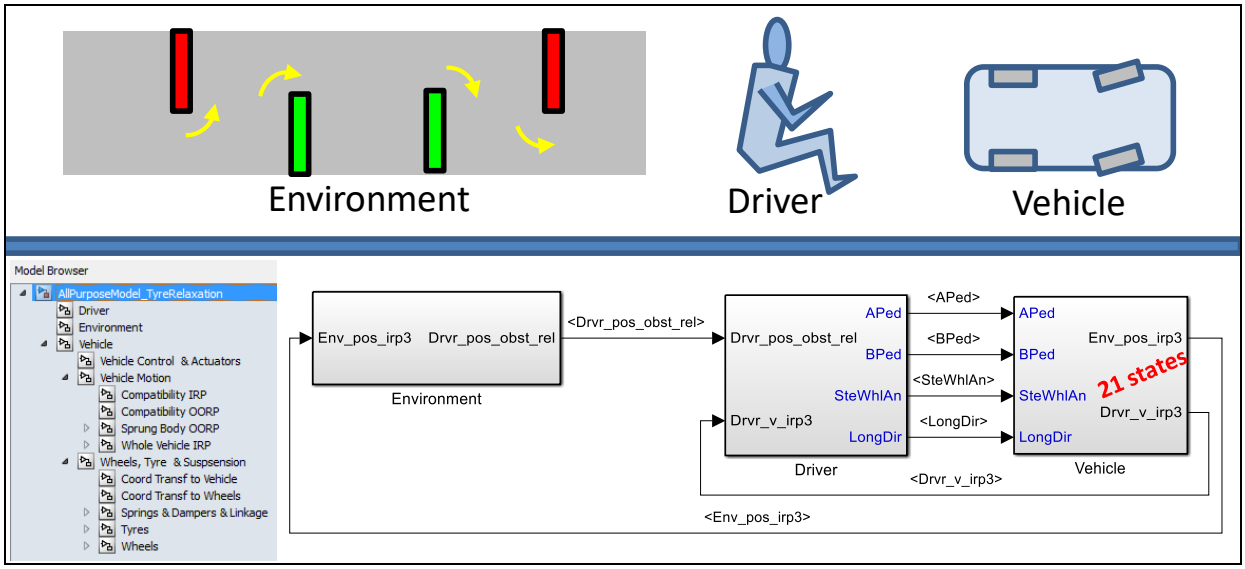

Figure 4-63: Top level of model with model tree structure. The Environment is a track test with cone walls to go left and right around. Notation "irp" and "oorp" refers to in-road-plane and out-of-road-plane, respectively.

As an initial overview, the states are presented. There are **21 states** in total, and distributed:

- Driver: 0 states
- Vehicle:
  - Vehicle Control & Actuation: 0 states
  - **Wheels, Tyres & Suspension: 12 states** (4 wheels' rotational speed, 4 Elastic parts of vertical wheel forces, 4 Longitudinal tyre forces, 4 Lateral tyre forces)
  - **Vehicle Motion: 9 states** (6 velocities and 3 positions)
- Environment: 0 states

The 4+4 tyre force states arise from modelled tyre relaxation, see 2.2.5.4.

4.5.3.1.1 Submodel Environment

Generally, the environment model is where the surrounding to the driver and the vehicle should be defined: road/road network, obstacles, other road users and the "driving task"/"driving instructions". In this example, it is very small and simple; it only captures stand-still point obstacles, each with instructions whether to be passed as obstacle left or right of the vehicle. Inputs to environment model is

the (subject) vehicles position, including orientation in global coordinates. Outputs are the relative position (x, y) to each obstacle, in (subject) vehicle coordinate system.

4.5.3.1.2 Submodel Driver

In this example, the driver model is very small and simple. Briefly described, it treats the longitudinal dynamics very simple, as closed loop control towards a constant desired speed forward. The lateral dynamics is divided into two parts:

- Driver planning: Based on how driver perceives the obstacles relative to the vehicle, one of the objects is selected to mind for, which leads to where to be aim. Basically, the nearest obstacle ahead of vehicle is selected as mind for and aim is, in principle, either half a vehicle width left (or right) of this obstacle.
- Driver operation: Based on the driver's motorics, the steering wheel angle is calculated. In the example, it is simply an inverse model of an ideally tracking two-axle vehicle which calculates which constant steering wheel angle that would be needed to make front axle run over the aim obstacle.

It can be noted that a Driver model would also be a logical model part where to include calculation of driver's perception, such as steering effort and perceived safety during manoeuvre, etc. It can also be noted that the border between Environment and Driver is sometimes not obvious, especially when it comes to modelling the "driving task" in the Environment model, which can also be seen as a "driver high-level decision" and then be a logical part of the Driver model. If Environment model includes surrounding vehicles (object vehicles), it also includes driver models for those. For automatic functionality, anything from cruise control to automated driving, there should also be a "button HMI output" from Driver model, not only pedals and steering wheel. Such interface would turn on/off such functionality in the Vehicle model.

4.5.3.1.3 Submodel Vehicle

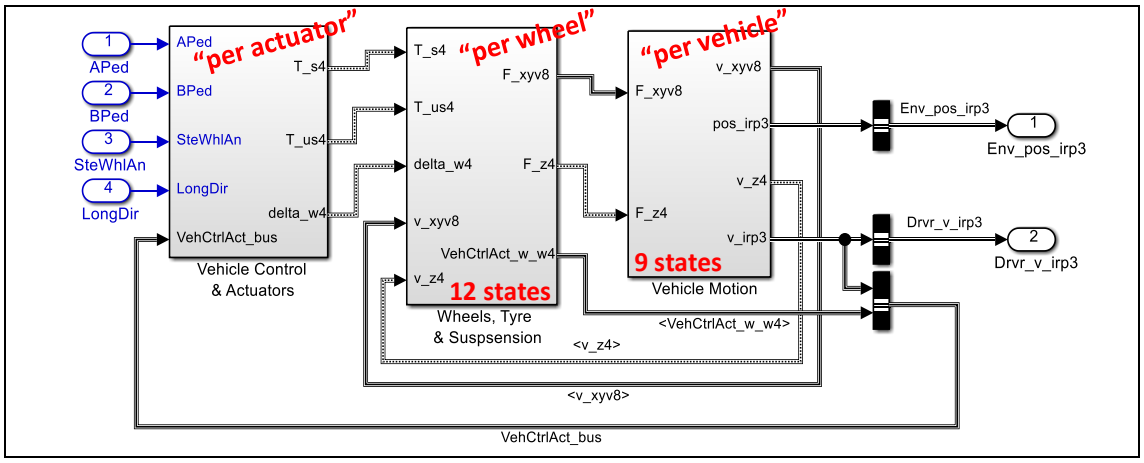

Figure 4-64: Vehicle submodel.

The figure shows the decomposition of the vehicle into 3 parts:

- Submodel **"Vehicle Control & Actuation"** models the actuators (Propulsion system, Brake system and Steering system, including "control functions") that respond on requests from the driver with wheel torques (`T_s` and `T_us`) and wheel steer angles (`delta_w`). The notation ending "4" refers to that the quantities are vectors with 4 components, one per wheel. `T_s` is shaft torque and `T_us` is torque applied from unsprung parts, e.g. friction brake torque from brake calliper. One can think of very advanced models of these actuator systems, including e.g. propulsion system dynamics and control functions (ABS, ESC, TC, …). However, in this example model it is only modelled very simple:
  - Propulsion system outputs a fraction (determined by `APed`) of a certain maximum power, distributed equally on front left and front right wheel. If brake pedal is applied, the propulsion system outputs zero torque.

  - Brake system outputs a fraction (determined by `BPed`) of a maximum brake torque ($\mu \cdot m \cdot g/R_w$), distributed in a certain fix fraction between front and rear axle (70/30). The distribution within each axle is equal on left and right wheel.
  - There are **no states** modelled in the vehicle Control & Actuator submodel.
- Submodel **"Wheels, Tyre & Suspension"** models the part which pushes the tyres towards the ground and consequently transforms the wheel torques and wheel steer angles, via the tyre, to forces on the whole vehicle. `F_xyv8` is the x and y forces in each of the 4 wheels, 2x4=8. `F_z4` is the 4 vertical forces under each wheel. Submodel "Wheels, Tyre & Suspension" is **further explained** in 4.5.3.1.5.
- Submodel "**Vehicle Motion"** models motion of whole vehicle in-road-plane and motion of sprung body out-of-road-plane. The inertial effects (mass·acceleration) of the unsprung parts are considered for in-road-plane but not for out-of-road-plane. This submodel includes integrators for the 3+3+3=9 **states**:
  - Velocities in-road-plane, v_x, v_y, ω_z: **`v_irp3`** (which is transformed to x- and y-velocities of each wheel and then fed back as `v_irpv8`)
  - Position in-road-plane, x, y, φ_z: **`pos_irp3`** (which is only fed forward to "Environment")
  - Velocities out-of-road-plane, v_z, ω_x, ω_y: **`v_oorp3`** (which is transformed to z-velocities of sprung body over each wheel and then fed back as `v_z4`)

4.5.3.1.4 Submodel Vehicle Control and Actuators

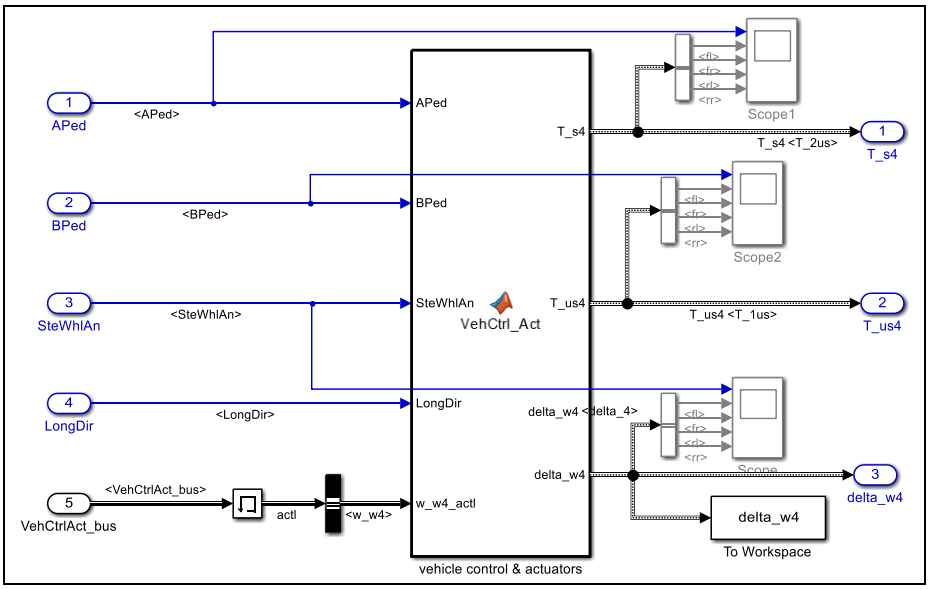

Figure 4-65: Vehicle Control & Actuators sub-model.

The example content of this sub-model is very minimalistic but can still be explained as two parts:

- **Interpret** pedals (including **arbitrate** between accelerator and brake pedal) to a sum over wheels longitudinal force request ($F_{x,req}$) and steering wheel angle to a front road wheel angle request ($\delta_{f,req}$).
- **Coordinate** and **actuate** propulsion and brake, i.e. allocate $F_{x,req}$ to 4 wheels' propulsion torques and brake torques. Also allocate $\delta_{f,req}$ to each of left and right front wheels.

Vehicle variables used for the control are wheel rotational speeds. Since front axle propulsion is assumed, the front rotational speeds are also input to the propulsion actuator modelling. No state variables are present in this minimalistic example, but in a more advanced actuation model there could typically be states such as: engine speed, gear (discrete state), delay states for brake system and elastic forces in steering system.

4.5.3.1.5 Submodel Wheels, Tyres and Suspension

This submodel is shown in Figure 4-66.

- The 2 sub-models "**Coord Transf to Vehicle**" and "**Coord Transf to Wheels**" are straight-forward coordinate transformations, see Eq [1.1].
- The sub-model "**Wheels**" is also relatively straight-forward. For each wheel, the rotational equilibrium is used as model: $J \cdot \dot{\omega} = T_{us} + T_s - F_x \cdot R_w - \text{sign}(\omega) \cdot RRC \cdot F_z \cdot R_w$; where R_w is wheel radius and RRC is rolling resistance coeeficient. The submodel will hence contain the 4 **states**: Rotational speeds of each wheel: **`w_w4.`**
- The sub-model "**Springs, Dampers & Linkage**" models the springs (incl. anti-roll-bars) and dampers and the linkage. For each wheel:
  - Four **states**: Elastic part of vertical tyre force under each wheel: **`F_s4`**
  - The derivatives are governed by the differentiated constitution of the springs: Conceptually $\dot{F}_s = -c \cdot v_z$; but involving both wheel spring and anti-roll-bar.
  - The force in damper is governed by the damper's constitutive relation: $F_d = -d \cdot v_z$;
  - The contact forces F_z are calculated in submodel "Suspension Equilibrium" in Figure 4-67. They are calculated from moment equilibrium of unsprung parts around a 3-dimensional pivot axis. The pivot axis is defined by two points, the pivot point in longitudinal load transfer (see Figure 3-27) and the pivot point in longitudinal load transfer (see Figure 4-33). The scalar equilibrium equation for one wheel can be expressed, with vector (cross) and scalar (dot) products, in $F_{xv}, F_{yv}, F_s, F_d, T_s, F_z$ and point coordinates. From this, F_z can be solved. It should be noted that the general relation should use a screw joint along the pivot axis, see https://en.wikipedia.org/wiki/Screw_theory, which is why the *lead* of the screw appears in equations.

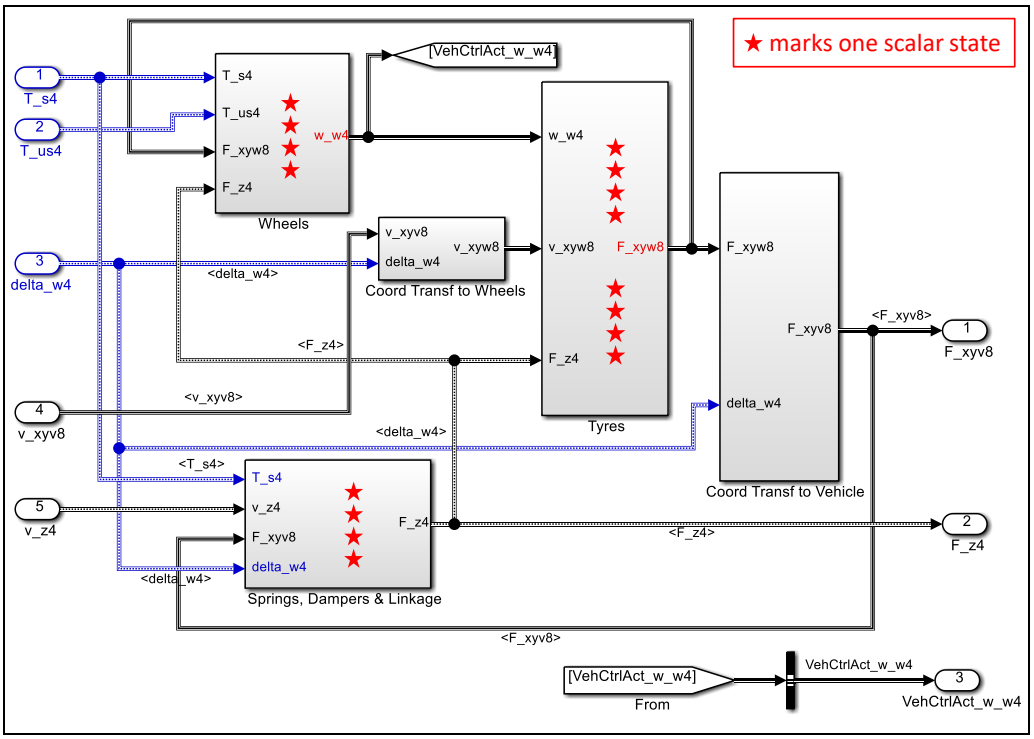

Figure 4-66: Wheels, Tyres & Suspension sub-model.

- The sub-model "**Tyres**" models the tyre mechanics, very much like the combined slip model in Equation [2.47] and the relaxation model in Eq [2.51]. For each wheel:
  - Four **states**: Magnitudes of tyre forces in ground plane (F_{xy}) for each wheel: **`F_xyw4`**
  - Unfortunately, the tyre forces F_x and F_y depend on F_z. This could easily create algebraic loops. However, since we also model relaxation, the tyre forces become state variables which breaks such algebraic loops. Another way of getting rid of the algebraic loops could have been to use "memory blocks". "Memories" are such that value from last time instant is used to calculate derivatives in present time instant. This is generally NOT a recommended way of modelling.

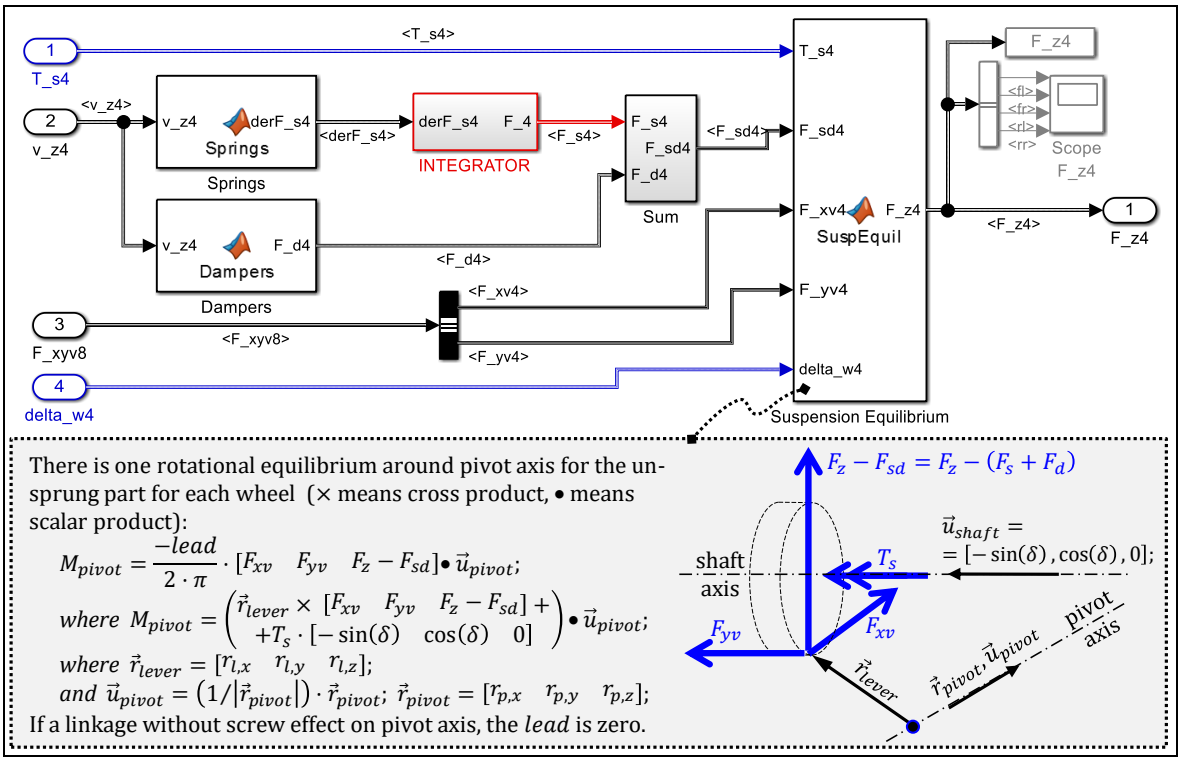

Figure 4-67: Sub-model "Springs, Dampers & Linkage".

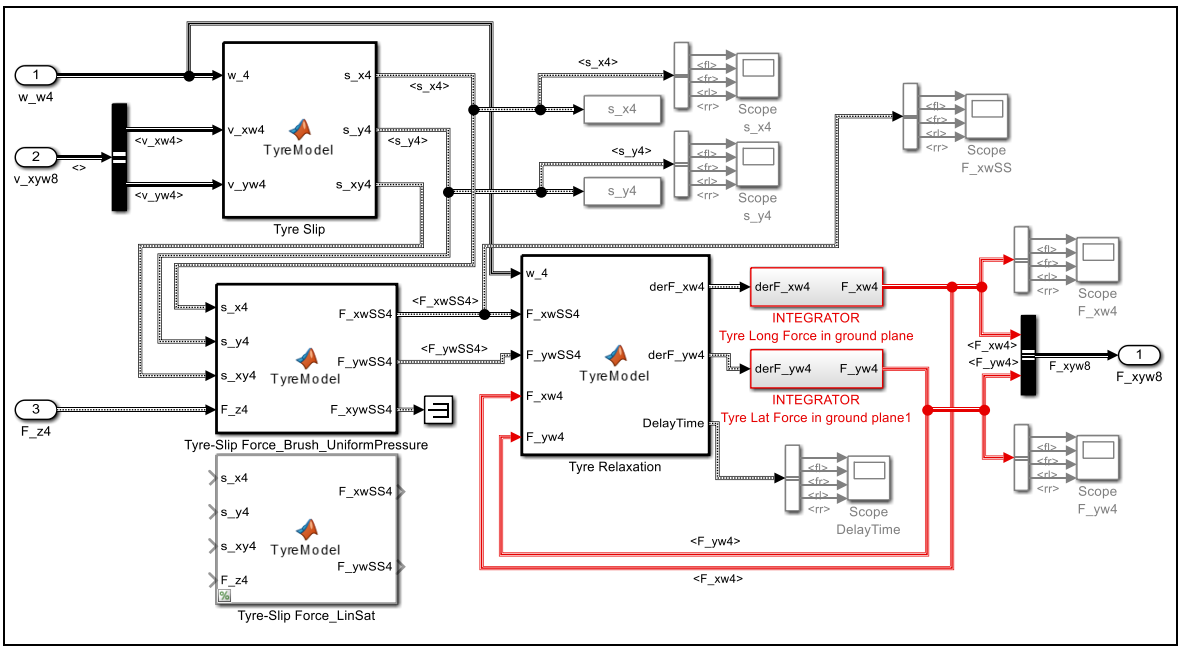

Figure 4-68: Sub-model "Tyres".

4.5.3.1.6 Sub-model Vehicle Motion

The sub-model is shown in Figure 4-69. It is divided in upper part in-road-plane (irp) and lower part out-of-road-plane (oorp). The velocities in road plane (v_irp3= $[v_x, v_y, \omega_z]$) is needed also in Sprung body OORP because of the centripetal term, $\omega_y \cdot v_x$, identified in 3.3.5.1 and used in 3.4.8.1.

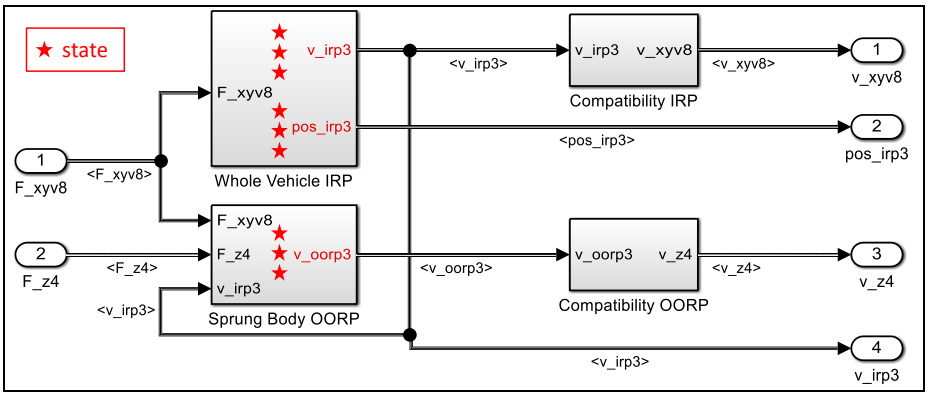

Figure 4-69: Vehicle Motion.

4.5.3.1.7 Simulation Example Double Lane Change

A double lane change between cones is used as simulation example, see Figure 4-70. The cones are run over and even passed on the wrong side because the driver model is very simple.

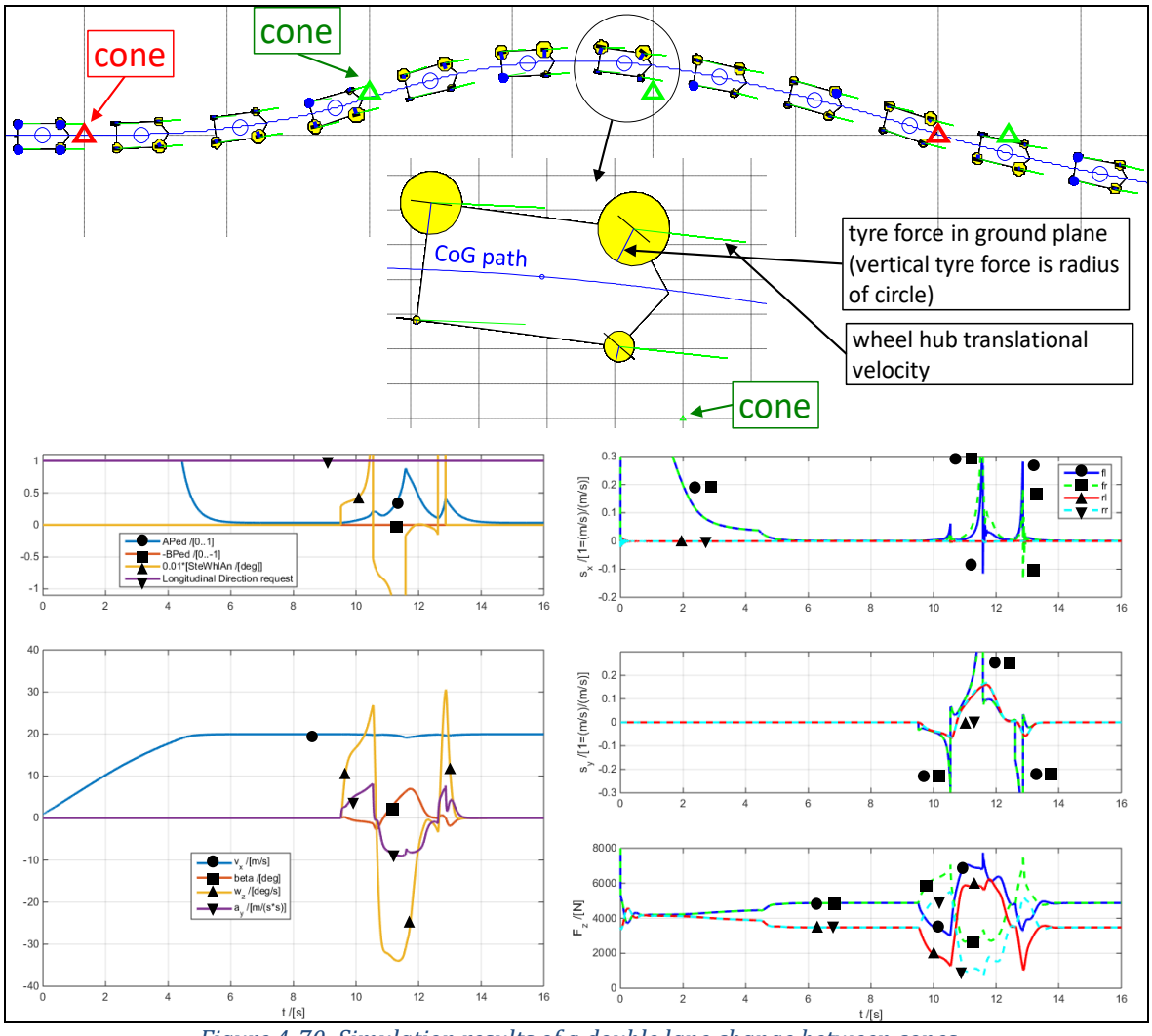

Figure 4-70: Simulation results of a double lane change between cones.

4.5.3.2 Additional Phenomena

It is relevant to point out the following, which are not modelled in this compendium:

- Same as pointed out as missing for longitudinal load transfer, see 3.4.5.2.3.
- Additionally, anti-roll arrangements (elastic connections between left and right wheel on one axle, often built as torsion bar) are not modelled in this compendium. With same modelling

concept as used above, each such would be treated as a separate spring with one state variable, e.g. F_{af} (Force-antiroll-front). This force will act in parallel with F_{sf} and F_{df} on each side. Note that it will be added on one side and subtracted on the other.

4.5.3.3 Transient Roll-Over *

Function definition: ***Transient roll-over resistance*** *is the most severe measure of a certain transient manoeuvre that the vehicle can manage without lifting all wheels on inner side. The manoeuvre is typically on level ground with high road friction and certain payload, loaded high.*

The manoeuvre can typically be a double lane change, since the double triggers roll oscillations. The severity measure of the manoeuvre can be the peak lateral acceleration, or a lane change width or longitudinal speed for given lane width.

If applying the function on articulated vehicles, it is often relevant to define the threshold as lifting all inner wheels on a roll-stiff unit. Two units connected by a fifth wheel constitutes one roll-stiff unit, since the fifth wheel is conceptually roll rigid.

The function is not relevant for cambering vehicles. These could rather roll-over inward in curve, triggered by tyre loses lateral grip, which would be a completely different situation.

4.5.4 Step Steering Response *

Function definition: ***Step steering response*** *is the response to a step in steering wheel angle measured in certain vehicle measures. The step is made from a certain steady state cornering condition to a certain steering wheel angle. The response can be the time history or certain measures on the time history, such as delay time and overshoot.*

4.5.4.1 Mild Step Steering Response

This section is to be compared with 4.5.4.2, which uses a more advanced model. In present section a less advanced model will be used, which is enough for small steering steps.

The model used for single frequency stationary oscillating steering can also be used for other purposes, as long as limited lateral accelerations. Most common interpretation is to make the steering step from an initial straight-line driving. In reality, the step will be a quick ramp. Equation [4.50] allows an explicit solution prediction of stationary oscillating steering, but also for step response:

Start from **Equation [4.50]**: $\begin{bmatrix}\dot{v}_y\\ \dot{\omega}_z\end{bmatrix} = \mathbf{A}\cdot\begin{bmatrix}v_y\\ \omega_z\end{bmatrix} + \mathbf{B}\cdot\delta_f;$

With **initial conditions**: $\begin{bmatrix}v_y(0)\\ \omega_z(0)\end{bmatrix} = \begin{bmatrix}v_{y0}\\ \omega_{z0}\end{bmatrix}$; or $\begin{bmatrix}v_{y0}\\ \omega_{z0}\end{bmatrix} = -\mathbf{A}^{-1}\cdot\mathbf{B}\cdot\delta_{f0}$; where δ_{f0} is before step.

Assume: $\begin{bmatrix}v_y\\ \omega_z\end{bmatrix} = \begin{bmatrix}v_{y\infty}\\ \omega_{z\infty}\end{bmatrix} + \begin{bmatrix}\hat{v}_{y1} & \hat{v}_{y2}\\ \hat{\omega}_{z1} & \hat{\omega}_{z2}\end{bmatrix}\cdot\begin{bmatrix}e^{\lambda_1\cdot t} & 0\\ 0 & e^{\lambda_2\cdot t}\end{bmatrix}\cdot\begin{bmatrix}a_1\\ a_2\end{bmatrix};\ \Rightarrow$

$$\Rightarrow\ \begin{bmatrix}\dot{v}_y\\ \dot{\omega}_z\end{bmatrix} = \begin{bmatrix}\hat{v}_{y1} & \hat{v}_{y2}\\ \hat{\omega}_{z1} & \hat{\omega}_{z2}\end{bmatrix}\cdot\begin{bmatrix}\lambda_1\cdot e^{\lambda_1\cdot t} & 0\\ 0 & \lambda_2\cdot e^{\lambda_2\cdot t}\end{bmatrix}\cdot\begin{bmatrix}a_1\\ a_2\end{bmatrix};$$

Insert: $\begin{bmatrix}\hat{v}_{y1} & \hat{v}_{y2}\\ \hat{\omega}_{z1} & \hat{\omega}_{z2}\end{bmatrix}\cdot\begin{bmatrix}\lambda_1\cdot e^{\lambda_1\cdot t} & 0\\ 0 & \lambda_2\cdot e^{\lambda_2\cdot t}\end{bmatrix}\cdot\begin{bmatrix}a_1\\ a_2\end{bmatrix} =$

$$= \mathbf{A}\cdot\left(\begin{bmatrix}v_{y\infty}\\ \omega_{z\infty}\end{bmatrix} + \begin{bmatrix}\hat{v}_{y1} & \hat{v}_{y2}\\ \hat{\omega}_{z1} & \hat{\omega}_{z2}\end{bmatrix}\cdot\begin{bmatrix}e^{\lambda_1\cdot t} & 0\\ 0 & e^{\lambda_2\cdot t}\end{bmatrix}\cdot\begin{bmatrix}a_1\\ a_2\end{bmatrix}\right) + \mathbf{B}\cdot\delta_f;$$

Solve for each time function term (constant, $e^{\lambda_1\cdot t}$ and $e^{\lambda_2\cdot t}$ terms):

$$\begin{bmatrix}v_{y\infty}\\ \omega_{z\infty}\end{bmatrix} = -\mathbf{A}^{-1}\cdot\mathbf{B}\cdot\delta_f;\ \ and\ \ \left[\begin{bmatrix}\hat{v}_{y1} & \hat{v}_{y2}\\ \hat{\omega}_{z1} & \hat{\omega}_{z2}\end{bmatrix},\begin{bmatrix}\lambda_1 & 0\\ 0 & \lambda_2\end{bmatrix}\right] = \mathrm{eig}(\mathbf{A})\,;$$

The function ”eig” is identical to function ”eig” in Matlab. It is defined as eigenvalues and eigenvectors for the matrix input argument.

Initial conditions: $\begin{bmatrix} v_{y0} \\ \omega_{z0} \end{bmatrix} = \begin{bmatrix} v_{y\infty} \\ \omega_{z\infty} \end{bmatrix} + \begin{bmatrix} \begin{bmatrix} \hat{v}_{y1} \\ \hat{\omega}_{z1} \end{bmatrix} & \begin{bmatrix} \hat{v}_{y2} \\ \hat{\omega}_{z2} \end{bmatrix} \end{bmatrix} \cdot \begin{bmatrix} a_1 \\ a_2 \end{bmatrix}; \Rightarrow$

$$\Rightarrow \begin{bmatrix} a_1 \\ a_2 \end{bmatrix} = \begin{bmatrix} \begin{bmatrix} \hat{v}_{y1} \\ \hat{\omega}_{z1} \end{bmatrix} & \begin{bmatrix} \hat{v}_{y2} \\ \hat{\omega}_{z2} \end{bmatrix} \end{bmatrix}^{-1} \cdot \left(\begin{bmatrix} v_{y0} \\ \omega_{z0} \end{bmatrix} - \begin{bmatrix} v_{y\infty} \\ \omega_{z\infty} \end{bmatrix} \right);$$

The solution in summary:

$$\begin{cases} \begin{bmatrix} v_y \\ \omega_z \end{bmatrix} = \begin{bmatrix} v_{y\infty} \\ \omega_{z\infty} \end{bmatrix} + \begin{bmatrix} \begin{bmatrix} \hat{v}_{y1} \\ \hat{\omega}_{z1} \end{bmatrix} & \begin{bmatrix} \hat{v}_{y2} \\ \hat{\omega}_{z2} \end{bmatrix} \end{bmatrix} \cdot \begin{bmatrix} e^{\lambda_1 \cdot t} & 0 \\ 0 & e^{\lambda_2 \cdot t} \end{bmatrix} \cdot \begin{bmatrix} a_1 \\ a_2 \end{bmatrix}; \\ a_y = \dot{v}_y + v_x \cdot \omega_z = \lambda_1 \cdot \hat{v}_{y1} \cdot e^{\lambda_1 \cdot t} \cdot a_1 + \lambda_2 \cdot \hat{v}_{y2} \cdot e^{\lambda_2 \cdot t} \cdot a_2 + v_x \cdot \omega_z; \\ \textit{where: } \begin{bmatrix} v_{y\infty} \\ \omega_{z\infty} \end{bmatrix} = -\boldsymbol{A}^{-1} \cdot \boldsymbol{B} \cdot \delta_f; \ \textit{and } \left[\begin{bmatrix} \hat{v}_{y1} \\ \hat{\omega}_{z1} \end{bmatrix} \ \begin{bmatrix} \hat{v}_{y2} \\ \hat{\omega}_{z2} \end{bmatrix} \right], \begin{bmatrix} \lambda_1 & 0 \\ 0 & \lambda_2 \end{bmatrix} = \text{eig}(\boldsymbol{A}); \\ \textit{and } \begin{bmatrix} a_1 \\ a_2 \end{bmatrix} = \begin{bmatrix} \begin{bmatrix} \hat{v}_{y1} \\ \hat{\omega}_{z1} \end{bmatrix} & \begin{bmatrix} \hat{v}_{y2} \\ \hat{\omega}_{z2} \end{bmatrix} \end{bmatrix}^{-1} \cdot \left(\begin{bmatrix} v_{y0} \\ \omega_{z0} \end{bmatrix} - \begin{bmatrix} v_{y\infty} \\ \omega_{z\infty} \end{bmatrix} \right); \end{cases} \quad [4.66]$$

Another way to express or compute this is the “exponential matrix exponential”, mentioned in 1.5.1.1.5.

Results from this model for step steer to +3 deg are shown in Figure 4-71. Left diagram shows step steer from straight line driving, while right diagram shows a step from steady state cornering with -3 deg steer angle. It can be noted that, if the steering step is sized so that same steady state path radius, i.e. same steady state yaw velocity, the understeered vehicle will require larger steering step, but it will respond quicker in yaw velocity and lateral acceleration.

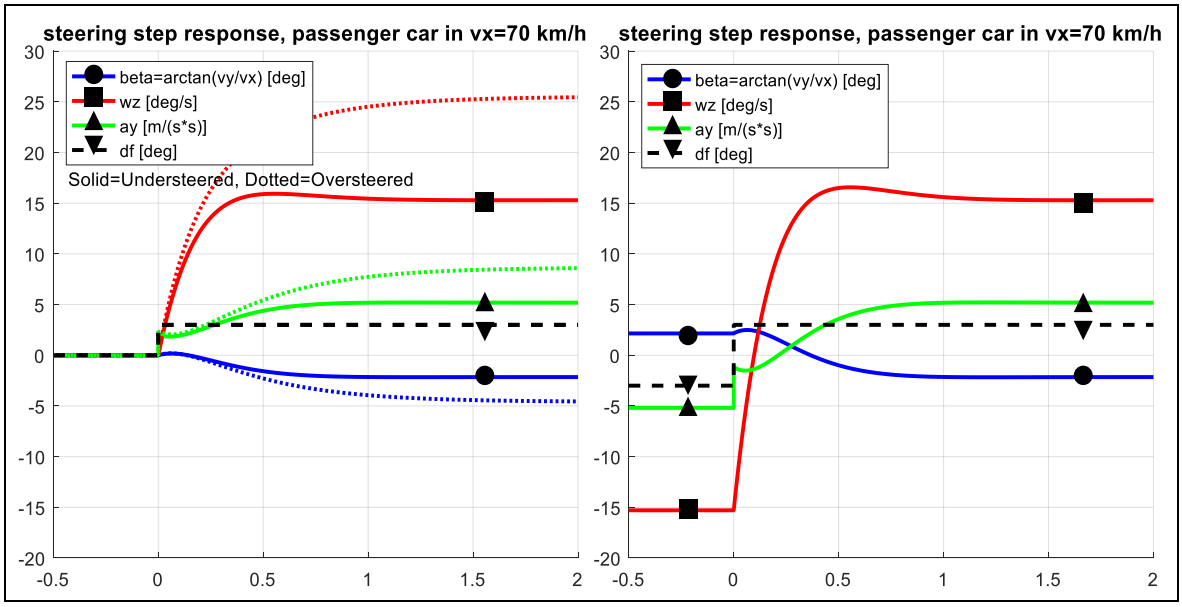

Figure 4-71: Steering step response. Simulation with model from Equation [4.66].

4.5.4.2 Violent Step Steering Response

This section is to be compared with 4.5.4.1 Mild Step Steering Response, which uses a model with linear tyre models without saturation. In present section, a more advanced model will be used, which might be needed when the step steering is more violent.

Most common interpretation is to make the steering step from an initial straight-line driving. In reality, the step will be a quick ramp. In simulations, an ideal step can be used.

The transients can easily be that violent that a model as Equations **Error! Reference source not found.**...**Error! Reference source not found.** is needed. If ESC is to be simulated, even more detailed models are needed (full two-track models, which are not presented in this compendium). Anyway, if we apply a step steer to the model in Equations **Error! Reference source not found.**...**Error! Reference source not found.**, we can simulate as in Figure 4-72.

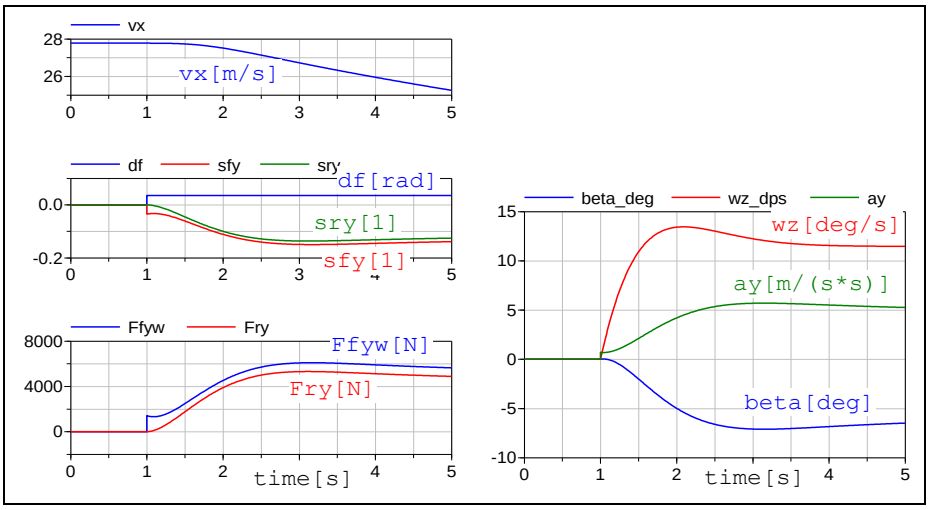

Figure 4-72: Step steer with 2 deg on road wheels at $v_x = 100$ km/h. Simulation using model from Eq ***Error! Reference source not found.****..Error! Reference source not found.*.

4.5.4.3 Steering Effort at High Speed *

Function definition: ***Steering effort at high speed*** *is the steering wheel torque (or subjectively assessed effort) needed to perform a certain avoidance manoeuvre at high road friction.*

At higher vehicle speeds, the steering effort is normally less of a problem since unless really high steering wheel rate. Hence, steering wheel torque in avoidance manoeuvres in e.g. 70 km/h can be a relevant requirement. In these situations, the subjective assessment of steering effort can also be the measure. Then, steering effort is probably assessed based on both steering wheel rate and steering wheel torque.

4.5.5 Phase Portrait

The transient from one steady state to another is seen after the steps in Figure 4-71 and Figure 4-72. Plotting several such transients as trajectories in a β, ω_z-diagram gives a phase portrait, which is a graphical representation of how a vehicle stabilize itself or gets unstable. For transients that stays within unsaturated tyre slip, the linear one-track model can be used, and the trajectories can then be explicit time expressions using Eq[4.66]. This is exemplified in left part of Figure 4-73. Some states can be confirmed stable already from this simple model. Simulations with higher fidelity model is exemplified in right part of Figure 4-73. With that one can confirm some more stable areas.

4.5.6 Long Heavy Combination Vehicles High Speed Functions

It is sometimes irrelevant to apply functions/measures from two axle vehicles on combinations of units. This can be the case for passenger cars with a trailer, but it is even more obvious for long combinations of heavy vehicles. Some typical measures for multi-unit combination vehicle are given in this section.

4.5.6.1 Rearward Amplification, RA *

Function definition: ***Rearward Amplification for long heavy combination vehicles*** *is the ratio of the maximum value of the motion variable of interest (e.g. yaw velocity or lateral acceleration of the centre of gravity) of the worst excited following vehicle unit to that of the first vehicle unit during a specified manoeuvre at a certain friction level and constant speed. From Reference [(Kati, 2013)].*

Figure 4-74 illustrates Rearward Amplification, RWA. RWA is defined for a special manoeuvre, e.g. a certain lane change or step steer. RWA is the ratio of the peak value of yaw velocity or lateral acceleration for the rearmost unit to that of the lead unit. This performance measure indicates the increased

risk for a swing out or rollover of the last unit compared to what the driver is experiencing in the lead unit.

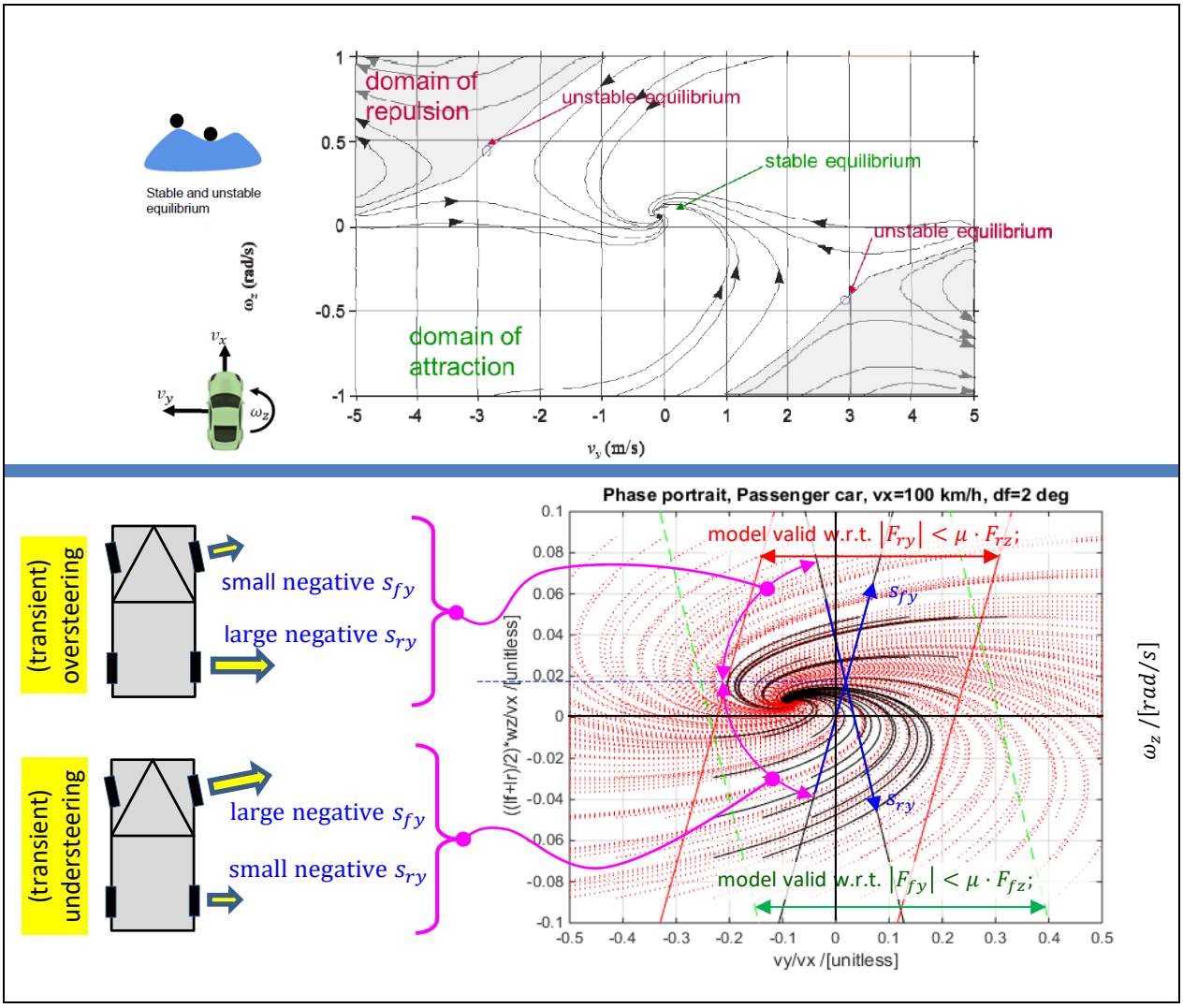

Figure 4-73: Phase portrait for constant v_x and constant steer angle δ_f. Bottom: Using simple model in Eq [4.50]. Only black solid trajectories credible, since they are completely within model validity. Upper: Using a model with larger validity. From Mats Jonasson, VCC.

4.5.6.2 High Speed Transient Off-tracking, HSTO *

Function definition: ***High speed transient off-tracking for long heavy combination vehicles*** *is the overshoot in the lateral distance between the paths of the centre of the front axle and the centre of the most severely off-tracking axle of any unit in a specified manoeuvre at a certain friction level and a certain constant longitudinal speed. From Reference [(Kati, 2013)].*

Figure 4-36 illustrates a manoeuvre where this Off-tracking can be defined. Off-tracking can be either determined in a steady state turn or in a transient manoeuvre such as lane change. The steady state version is described in 4.3.10.2.

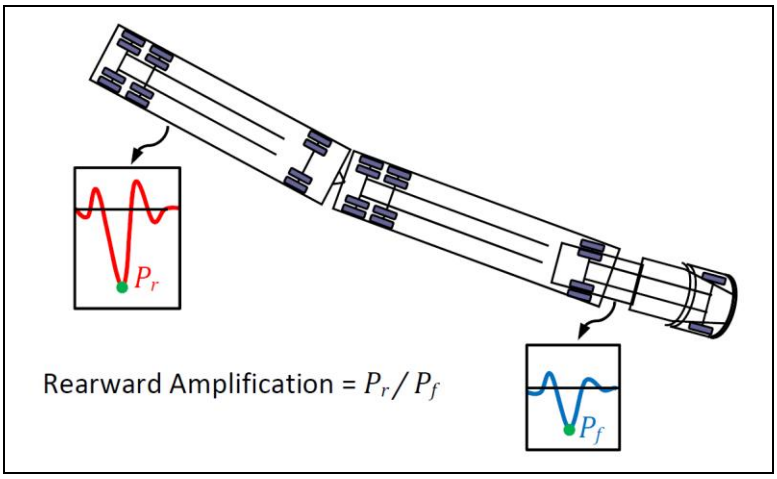

Figure 4-74: Rearward amplification, P is peak value of motion variable of interest. From (Kharrazi , 2012).

An alternative definition of RA is via the frequency response: $RA = |H_\delta \rightarrow \omega_1 / H_\delta \rightarrow \omega_{last}|$.

4.5.6.3 Yaw Damping, YD *

Function definition: Yaw Damping for long heavy combination vehicles is the ratio of decay of the least damped articulation joint's angle of the combination vehicle during free oscillations excited by actuating the steering wheel in a certain transient way, e.g. a step or single sine wave at a certain friction level. From Reference [(Kati, 2013)].

Figure 4-75 illustrates Yaw Damping. It is the ratio of two subsequent peaks, $YD = |\hat{\theta}_{i,j} / \hat{\theta}_{i,j+1}|$; where i=ordinal of coupling and j=ordinal of "half period" after steering disturbance has ended. Assuming linear model, it should not matter which two half periods one uses and, then it can give less sensitive definition to use several peaks, e.g. $YD = |\hat{\theta}_{i,j} / \hat{\theta}_{i,j+5}|/5$;. Sometimes other qualtities than articulation angle in coupling points, such as yaw velocity of units, can be used.

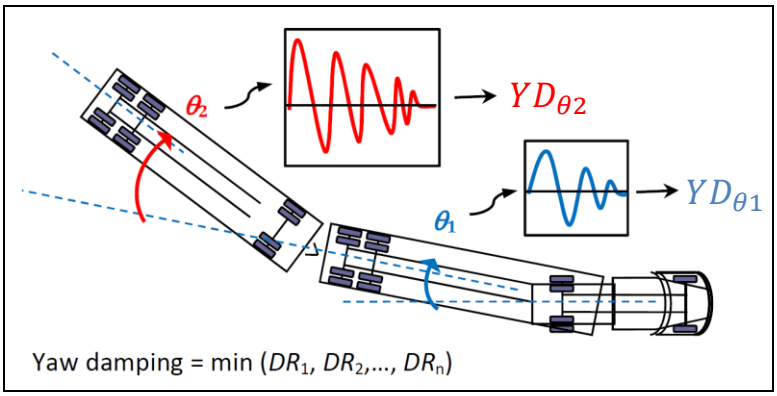

Figure 4-75: Yaw damping, YD_i denotes damping ratio of the articulation joint. From (Kharrazi , 2012).

4.5.6.4 Zero-Damping Speed *

Function definition: Zero-damping speed for long heavy combination vehicles is the longitudinal speed at which a yaw disturbance leads to undamped response.

The measure can be calculated from a linear model as the longitudinal speed when the damping coefficient, for any mode involving yaw velocity, equals zero. If the measure is applied on a two-axle vehicle it is same as critical speed.

4.6 Lateral Control Functions

Some control functions involving lateral vehicle dynamics will be presented briefly. There are more, but the following are among the most well-established ones. But initially, some general aspects of lateral control are given.

4.6.1 Lateral Control

Sensors available in production vehicles and used for lateral control are, generally those mentioned as available for Longitudinal Control, see 3.5 plus some more:

Steering wheel sensors gives at least steering wheel angle, if the vehicle is equipped with ESC (which is a legal requirement on many markets). Additionally, if the steering assistance is electrical, the steering wheel torque can be sensed.

High specification modern vehicles also have environment sensors (camera, radar, etc) that can give laterally interesting information, such as: Subject vehicle lateral position versus lane markers ahead and other vehicles to the side or rear of subject vehicle.

As general considerations for actuators, one can mention that interventions with friction brake normally have to have thresholds, because interventions are noticed by driver and also generate energy loss. Interventions with steering are less sensitive and can be designed without thresholds.

4.6.2 Lateral Control Functions

4.6.2.1 Electronic Stability Control, ESC *

*Function definition: **Electronic Stability Control** directs the vehicle to match a desired yaw behaviour, when the deviation from desired behaviour becomes above certain thresholds. ESC typically monitors vehicle speed, steer angle and yaw velocity to calculate a yaw velocity error and uses friction brakes as actuator to reduce it.*

There are 3 parts of ESC: Over-steer control, Under-steer control, Over-speed control. The actual control error that the vehicle reacts on is typically the yaw velocity error between a desired yaw velocity and the sensed yaw velocity. Desired yaw velocity is calculated from a so-called reference model. Some of today's advanced ESC also intervenes on difference between desired and estimated side slip.

Desired yaw velocity and side-slip is calculated using a reference model and a closed loop control on the reference, see Figure 4-76. The reference model requires at least steer angle and longitudinal velocity as input. The reference model can be either of steady state type (approximately as Eq [4.19] or the [4.15]) or transient (approximately as Eq [4.50]). The vehicle modelled by the reference model should rather be a desired vehicle than the controlled vehicle. Figure 4-76 does NOT show: Slide slip control, Reduction of C_f due to low friction detection, Coordination with Engine/Steering interventions, Arbitration with Pedal/ACC/ABS braking. (For single unit vehicles, $\dot{\omega}_{z,req}$ can be seen as a yaw moment.)

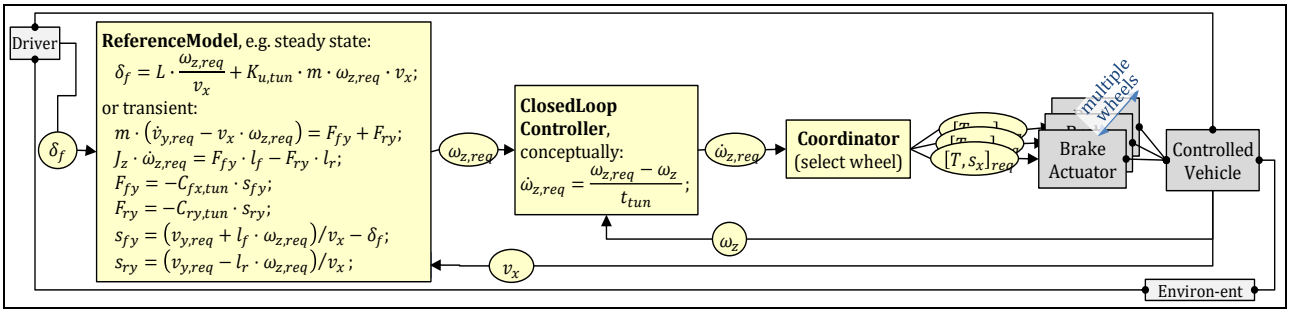

Figure 4-76: Concept for ESC.

The manoeuvre in Figure 4-20 shows an example of ESC interventions. But, in order to avoid too much friction brake interventions; the reference model cannot be too different. Also, in order to avoid that vehicle yaws more than its path curvature; the reference model cannot be much less understeered than the controlled vehicle, which typically can be arranged by saturating lateral tyre forces on the front axle in the reference model. This requires some kind of friction estimation, especially for low-mu driving.

When controlling yaw via wheel torques, one can identify some different concepts such as direct and in-direct yaw moment, see 4.3.6.6. For ESC there is also a "pre-cautious yaw control" which aims at reducing speed, see 4.6.2.1.3. The coordination of wheel torques handles these aspects, which are far

from trivial. Often, a dual-request concept for each wheel is used, see Figure 4-76 and 4.6.2.1.4. A simplest possible coordinator can be to request braking only on one wheel at the time:

4.6.2.1.1 Over-Steer Control

Over-steer control was the first and most efficient concept in ESC. When a vehicle over-steers, ESC will typically coordinate wheel torques so that outer front wheel is braked. It can brake to deep slip levels (typically -50%) since losing side grip on front axle is desired in an over-steer situation. More advanced ESC variants also brake outer rear, but less and not to same deep slip level, see Figure .

For combination vehicles with trailers that have controllable brakes, also the trailer is braked to avoid jack-knife effect, see upper part of Figure 4-77, or swing-out of the towed units.

4.6.2.1.2 Under-Steer Control

Under-steer control means that inner rear is braked when vehicle under-steers. This helps the vehicle turn-in. This intervention is most efficient on low mu, because on high mu the inner rear wheel normally has very little normal load. Also, the slip levels are not usually as deep as corresponding over-steer intervention, but rather -10%. This is because there is always a danger in braking too much on rear axle, since it can cause over-steering. More advanced ESC variants also brake inner front, see Figure . The more wheels that are braked, the more similar the understeer intervention becomes with the function in 4.6.2.1.3.

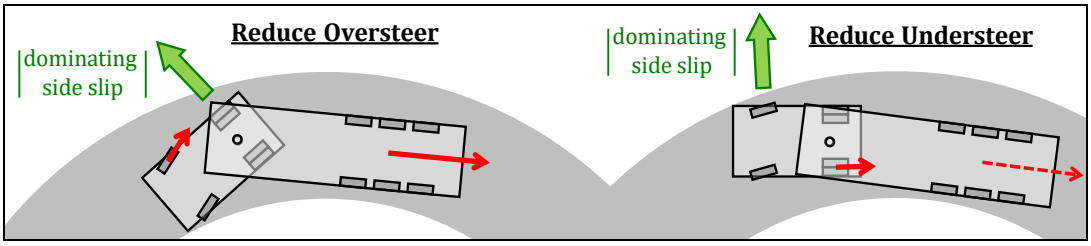

Figure 4-77: ESC brake interventions when oversteer and understeer, on a tractor with trailer.

4.6.2.1.3 Over-Speed Control

Over-speed control is not always recognised as a separate concept, but as a part of under-steer control. The actuation is that propulsion is reduced, or more than just inner rear wheels are braked. In this text, we identify this as done to decrease speed, which has a positive effect later in the curve.

4.6.2.1.4 Wheel-Level Control

A pre-requisite for all controls mentioned above in 4.6.2.1 is that the wheel torque actuator primarily responds to a torque request. However, one need to have another request channel to adjust the lateral force margin; normally one uses a longitudinal slip request, $s_{x,req}$ in Figure 4-76. The slip request is generally used as a "safety net" to avoid lock-up the wheel too much; so, it is a "max $|s_x|$ request". Typically, s_x is $-0.2..-0.1$, for braking, but at RSC interventions (see 4.6.2.2) the lateral grip should be braked away, so a deeper slip request is then used, typically 50-70%.

4.6.2.1.5 Other Intervention than Individual Wheel Brakes

4.6.2.1.5.1 Balancing with Propulsion per Axle

For vehicles with controllable distribution of propulsion torque between the axles, ESC can intervene also with a request for redistribution of the propulsion torque. If over-steering, the propulsion should be redistributed towards front and opposite for understeering.

4.6.2.1.5.2 Torque Vectoring

For vehicles with controllable distribution of propulsion torque between the left and right, ESC can intervene also with a request for redistribution of the propulsion torque. If over-steering, the propulsion should be redistributed towards inner side and opposite for understeering.

4.6.2.1.5.3 Steering Guidance

For vehicles with controllable steering wheel torque, ESC can intervene also with a request for additional steering wheel torque. The most obvious function is to guide driver to open up steering

(counter-steer) when the vehicle over-steers. Such functions are on market in passenger cars today. Less obvious is how to guide the driver when vehicle is under-steering.

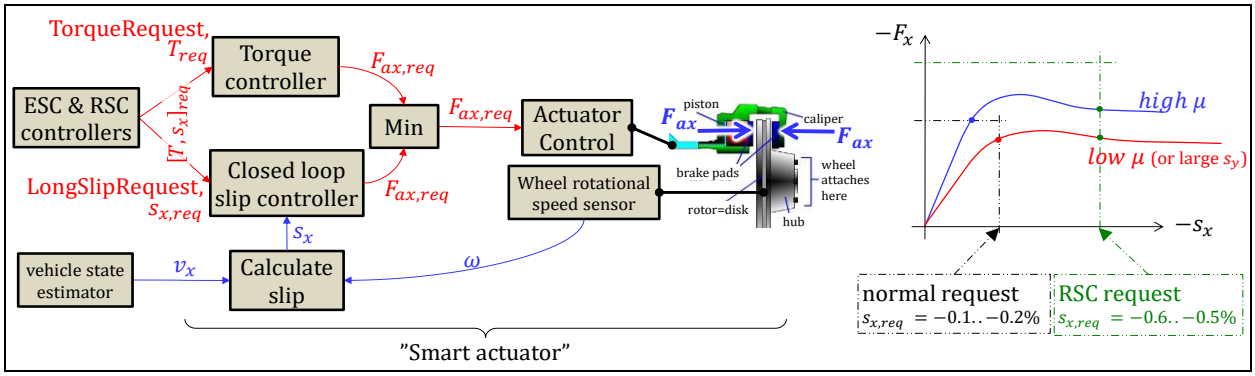

Figure 4-78: Individual wheel control by friction brakes for ESC-type functions. What is a "smart actuator" can depend on which function architecture that vehicle manufacturer and brake supplier has agreed.

4.6.2.1.6 ESC using Environment Information / ESC for the Virtual Driver

A prognosis of the future development of ESC like functions is that environment sensors can be used to better predict what driver tries to do; presently ESC can only look at steering wheel angle.

Related to this, but still somewhat different, would be to utilize the automated driving development by utilizing that a "virtual driver" can be much better predicted than a "manual driver". So, a predictive ESC control is more possible.

4.6.2.2 Roll Stability Control, RSC *

*Function definition: **Roll Stability Control, RSC**, prohibits vehicle to roll-over due to lateral wheel forces from road friction. RSC uses friction brake as actuator.*

The purpose of RSC is to avoid un-tripped roll-overs. The actuator used is the friction brake system. When roll-over risk is detected, via lateral acceleration sensor (or in some advanced RSC implementations, also roll velocity sensor), the outer front wheel is braked. RSC can brake to deep slip levels (typically -70%..-50%) since losing side grip on front axle is positive in this situation. To lock the wheels (slip= $-\infty$) is undesired since wheel rotational inertia makes it difficult to quickly regain lateral grip when needed after the intervention.

On heavy vehicles, RSC intervenes earlier and similar to function described in 4.6.2.1.3 Over-Speed Control. Future RSC might be developed towards also using steering, and potentially counteract also some tripped roll-overs.

4.6.2.3 Lane Keeping Aid, LKA *

*Function definition: **Lane Keeping Aid** steers the vehicle without driver having to steer, when probability for lane departure is predicted as high. It is normally actuated as an additional steering wheel torque. Conceptually, it can also be actuated as a steering wheel angle offset.*

Lane Keeping Aid (or *Lane Departure Prevention*) has the purpose to guide the driver to keep in the lane. Given the lane position from a camera, the function detects whether vehicle tends to leave the lane. If so, the function requests a mild steering wheel torque (typically 1..2 Nm) in appropriate direction. Driver can easily overcome the additional torque. Function does not intervene if too low speed or turning indicator (blinker) is used. There are different concepts whether the function continuously should aim at keeping the vehicle in centre of lane, or just intervene when close to leaving the lane, see Figure 4-79.

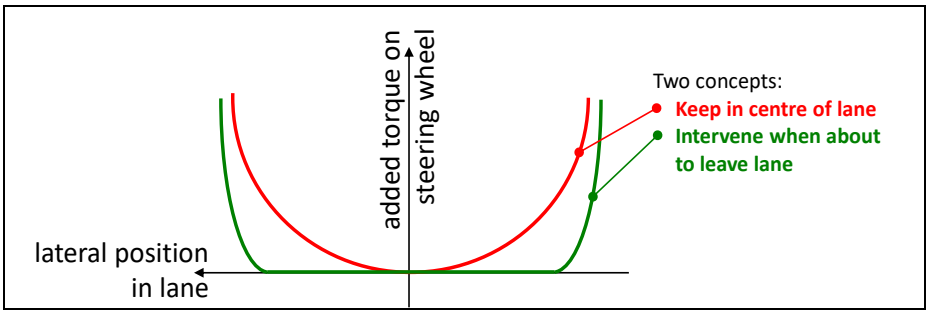

Figure 4-79: Two concepts for Lane Keeping Aid.

4.6.2.4 Lateral Collision Avoidance/Automatic Emergency Steering, LCA/AES *

Function definition: ***Lateral Collision Avoidance/Automatic Emergency Steering,*** *supports the driver when he has to do late lateral obstacle avoidance, when probability for forward collision is predicted as high.*

There are systems on the market for Automatic Emergency Brake, see 3.5. These do Longitudinal Collision Avoidance. Automotive industry also aims at AES/LCA functions, which would automatically steer away laterally from an obstacle ahead of subject vehicle. The market introduction is cautious, since many things can go wrong with such functions. However, the first systems on market triggers only if driver initiates steering. Another would be to trigger on a first collision impact, see Reference (Yang, 2013), when driver is less capable of steering by himself. A future similar situation could be AES/LCA functions active only during automated driving, when driver also is less likely to steer.

4.6.2.5 Automated Driving (AD)

Combining longitudinal control (such as ACC, in 3.5.2.2) with a lateral control (such as LKA, see 4.6.2.1) results in functionality which clearly approaches automated driving (AD). AD is a very general expression but are sometimes interpreted as more specific, but specific in different ways depending on context. In a way, AD is already reality since there are vehicles on the road which can have ACC and LKA active at the same time. On the other hand, AD can be seen as very futuristic, since completely driverless vehicle which can operate in all situations is far from mass-production.

It is not obvious if AD will mean higher or lower requirements on vehicle dynamics. Some (of many more!) examples of changes, relevant for vehicle dynamics are:

- The vehicle control can better **predict** the next few seconds of a virtual driver (AD algorithms) than of a (human) driver. This can facilitate loss-of-grip functions, such as ABS & ESC.
- There will be new requirements on vehicle response on **requests from the virtual driver**, in parallel with requirements on response on human drivers pedal and steering wheel operation.
- There will be new requirements on vehicle **relative** motion, relative to surrounding road and traffic, such as lane edges and other road users. These will be in synergy or conflict to corresponding requirement for absolute motion response.
- The motion actuation will have to be more **redundant**, since driver is less likely to take back control quickly. Emergency functions to reach safe stop will need to work with partly faulty sensors and actuators. Failures needs to be designed according to (ISO 26262, 2011-2012)
- The **maximum speed** for which the vehicle is designed can possibly be lower, since reduced transport efficiency could be accepted if driver can do something else or is not needed at all.
- Estimation of Road friction, Controlling to Safe stop, Self-Diagnose, etc.

5 VERTICAL DYNAMICS

5.1 Introduction

The vertical dynamics are needed since vehicles are operated on real roads, and real roads are not perfectly smooth. Also, vehicle can be operated off-road, where the ground unevenness is even larger.

The irregularities of the road can be categorized. A **transient** disturbance, such as a pothole or bump, can be represented as a step input or ramp. Undulating surfaces like grooves across the road may be a type of sinusoidal or other **stationary oscillating** (or periodic) input. More natural input like the random surface texture of the road may be a **random** noise distribution. In all cases, the same mechanical system must react when the vehicle travels over the road at varying speeds including doing manoeuvres in longitudinal and lateral directions.

The chapter is organised around the 3 complete vehicle functions: 5.5.1 Ride Comfort *, 5.5.2 Fatigue Life *, and 5.5.3 Road Grip *. It is, to a larger extent than Chapters 3 and 4, organised with mathematical theory first followed by the vehicle functions. In Figure 5-1 shows the 3 main functions. It explains the importance of the vehicle's dynamic structure. The vehicle's dynamic structure calls for a pretty extensive theory base, described mainly in 5.2.

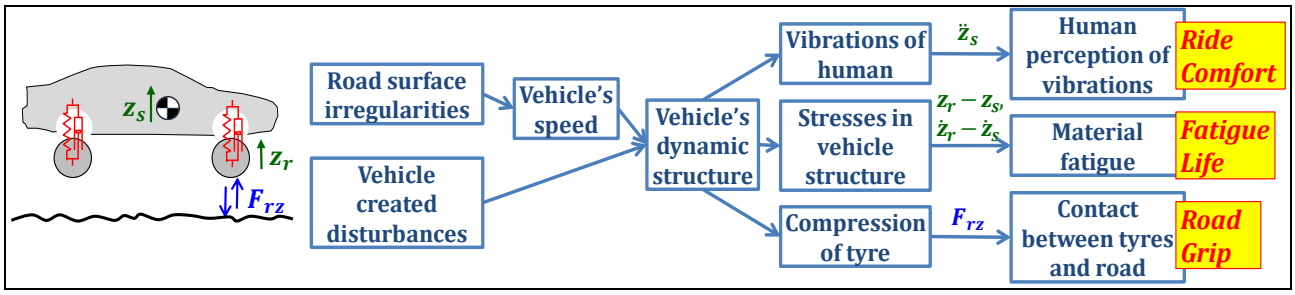

Figure 5-1: Different types of knowledge and functions in the area of vertical vehicle dynamics, organised around the vehicle's dynamic structure.

Models in this chapter focus the disturbance from vertical irregularities from the road, i.e. only the vertical forces on the tyre from the road and **not** the forces in road plane. This enables the use of simple models which are independent of exact wheel and axle suspension, such as pivot axes and roll centres. Only the wheel stiffness rate (effective stiffness) and wheel damping rate (effective damping), see Figure 2-54, influence. This has the benefit that the chapter becomes relatively independent of previous chapters, but it has the drawback that the presented models are **not** really suitable for studies of steep road irregularities (which have longitudinal components) and sudden changes in wheel torque or tyre side forces. Also, noise ($>\approx 25Hz$) is not covered in this compendium.

Furthermore, there is no section about Control functions for vertical dynamics in this compendium. Such do exist, e.g. levelling control and active damper control. However, they are less common and generally influence less than the stronger propulsion, brake and steering control functions.

5.1.1 References for this Chapter

- 2.3 Suspension System and *"Chapter 21 Suspension Systems"* in Ref (Ploechl, 2013)
- *"Chapter 29 Ride Comfort and Road Holding"* in Ref (Ploechl, 2013)

5.2 Stationary Oscillations Theory

Many vehicle functions in this chapter will be studied using stationary oscillations (cyclic repeating), as opposed to transiently varying. An example of transiently varying quantity is a single step function or single square pulse. A stationary oscillation can be as a sum of several harmonic terms, a multiple

frequency harmonic stationary oscillation. The special case with only one frequency is called a single frequency harmonic stationary oscillation. See Figure 5-2 and Equation [5.1].

Harmonic stationary oscillations:
Single frequency : $z(\xi) = \hat{z} \cdot \cos(\omega \cdot \xi + \varphi)$;
Multiple frequencies : $z(\xi) = \sum_{i=1}^{N} \hat{z}_i \cdot \cos(\omega_i \cdot \xi + \varphi_i)$;
where ξ *is the independent variable.* [5.1]

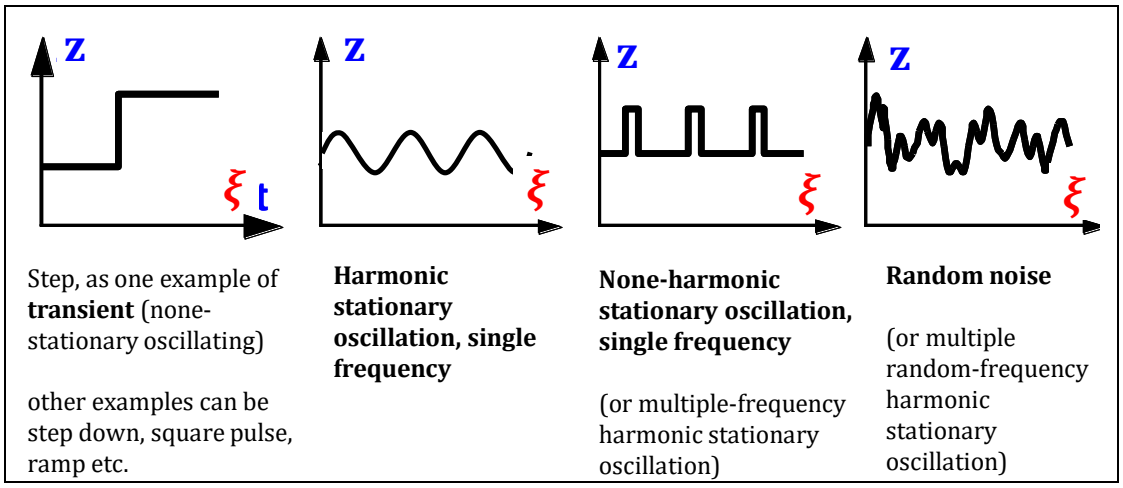

Step, as one example of **transient** (none-stationary oscillating)

other examples can be step down, square pulse, ramp etc.

Harmonic stationary oscillation, single frequency

None-harmonic stationary oscillation, single frequency

(or multiple-frequency harmonic stationary oscillation)

Random noise

(or multiple random-frequency harmonic stationary oscillation)

Figure 5-2: Different types of variables, both transient and stationary oscillating. The independent variable ξ can, typically, be either time or distance.

The most intuitive is probably to think of time as the independent variable, i.e. that the variation takes place as function of time and that $\xi = t$ in Equation [5.1]. However, for one specific road, the vertical displacement varies with longitudinal position, rather than with time. This is why we can either do analysis in **time domain** ($\xi = t$) and **space domain** ($\xi = x$).

Since the same oscillation can be described either as a function of ξ ($z = z(\xi)$) or as a function of frequency ω ($\hat{z} = \hat{z}(\omega)$), we can do analysis either in the **independent variable domain** (ξ) or in **frequency domain** (ω).

The four combinations of domains are shown in Figure 5-3.

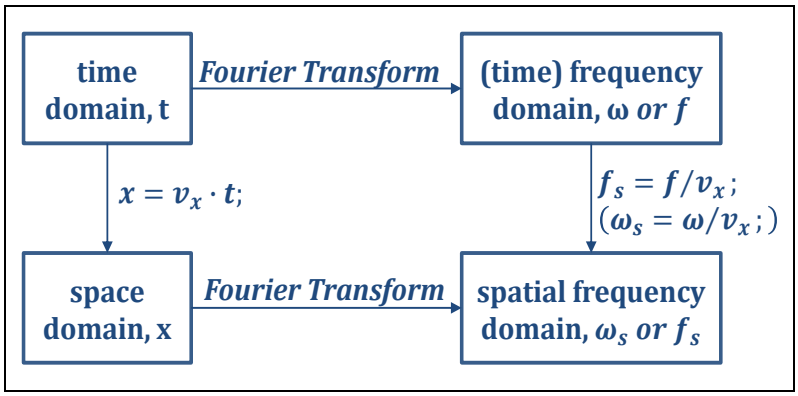

Figure 5-3: Four domains and transformations between them.

Time and space domains are treated in 5.2.1 and 5.2.2. In addition to the domains, we also need to differ between discrete and continuous representations in both domains.

5.2.1 Time as Independent Variable

With time as independent variable, the frequency has the meaning of "how often per time". Even so, there are two relevant ways to measure frequency: angular (time) frequency, and (time) frequency.

$$\omega = 2 \cdot \pi \cdot f;$$
$$where \quad \omega\,[rad/s] = angular\ (time)\ frequency;$$
$$and \quad f\,[1/s = oscillations/s] = (time)\ frequency;$$

[5.2]

The time for one oscillation is called the period time. It is denoted T:

$$T = 1/f = 2 \cdot \pi/\omega\,;$$

[5.3]

5.2.1.1 Mean Square (MS) and Root Mean Square (RMS)

For a variable, z, we can define MS and RMS values as follows:

$$Variable: \quad z = z(t);$$
$$MeanSquare: \quad MS(z) = \frac{\int_0^{t_{end}} z^2 \cdot dt}{t_{end}};$$
$$RootMeanSquare: \quad RMS(z) = \sqrt{\frac{\int_0^{t_{end}} z^2 \cdot dt}{t_{end}}};$$

[5.4]

If the variable is written as a single frequency harmonic stationary oscillation:

$$Variable: \quad z = \hat{z} \cdot \cos(\omega \cdot t + \varphi)\,;$$
$$MeanSquare: \quad MS(z) = \frac{\int_0^{t_{end}} z^2 \cdot dt}{t_{end}} = \frac{\int_0^{t_{end}} (\hat{z} \cdot \cos(\omega \cdot t + \varphi))^2 \cdot dt}{t_{end}} =$$
$$= \frac{\hat{z}^2 \cdot \left[\frac{t}{2} + \frac{\sin(2 \cdot \omega \cdot t)}{4 \cdot \omega}\right]_{t=0}^{t=t_{end}}}{t_{end}} = \frac{\hat{z}^2 \cdot \left(\frac{t_{end}}{2} + \frac{\sin(2 \cdot \omega \cdot t_{end})}{4 \cdot \omega}\right)}{t_{end}} \xrightarrow[t_{end} \to \infty]{} \frac{\hat{z}^2}{2};$$
$$RootMeanSquare: \quad RMS(z) = \sqrt{\frac{\int_0^{t_{end}} z^2 \cdot dt}{t_{end}}} = \sqrt{MS(z)} = \frac{|\hat{z}|}{\sqrt{2}};$$

[5.5]

If the variable is written as a multiple frequency harmonic stationary oscillation:

$$Variable: \quad z = \sum_{i=1}^{N} z_i = \sum_{i=1}^{N} \hat{z}_i \cdot \cos(\omega_i \cdot t + \varphi_i)\,;$$
$$MeanSquare: \quad MS(z) = \frac{\int_0^{t_{end}} z^2 \cdot dt}{t_{end}} = \frac{\int_0^{t_{end}} \left(\sum_{i=1}^{N} z_i\right)^2 \cdot dt}{t_{end}} =$$
$$= \frac{\int_0^{t_{end}} \left(\sum_{i=1}^{N} \hat{z}_i \cdot \cos(\omega_i \cdot t + \varphi_i)\right)^2 \cdot dt}{t_{end}} \xrightarrow[t_{end} \to \infty]{}$$
$$\xrightarrow[t_{end} \to \infty]{} \frac{\int_0^{t_{end}} \sum_{i=1}^{N} \hat{z}_i{}^2 \cdot (\cos(\omega_i \cdot t + \varphi_i))^2 \cdot dt}{t_{end}} = \sum_{i=1}^{N} MS(z_i) = \sum_{i=1}^{N} \frac{\hat{z}_i{}^2}{2};$$
$$RootMeanSquare: \quad RMS(z) = \sqrt{MS(z)} = \sqrt{\sum_{i=1}^{N} \frac{\hat{z}_i{}^2}{2}} = \sqrt{\sum_{i=1}^{N} MS(z_i)} = \sqrt{\sum_{i=1}^{N} \left(RMS(z_i)\right)^2};$$

[5.6]

5.2.1.2 Power Spectral Density and Frequency Bands

So far, the frequency has been a discrete number of frequencies, $\omega_1, \omega_2, \cdots, \omega_N$. There are reasons to treat the frequency as a continuous variable instead. The discrete amplitudes, $\hat{z}_1, \hat{z}_2, \cdots, \hat{z}_N$, should then be thought of as integrals of a "continuous amplitude curve", $\hat{z}_c$, where the integration is done over a small frequency interval, centred around a mid-frequency, ω_i:

$$\hat{z}_i = \int_{\omega=\frac{\omega_{i-1}+\omega_i}{2}}^{\frac{\omega_i+\omega_{i+1}}{2}} \hat{z}_c \cdot d\omega = \hat{z}_c(\omega_i) \cdot \frac{\omega_{i+1}-\omega_{i-1}}{2} = \hat{z}_c(\omega_i) \cdot \Delta\omega_i;\ \Rightarrow\ \hat{z}_c(\omega_i) = \frac{\hat{z}_i}{\Delta\omega_i}; \quad [5.7]$$

We realize that the unit of $\hat{z}_c$ has to be same as for z, but per [rad/s]. So, if z is a displacement in [m], $\hat{z}_c$ has the unit [m/(rad/s)]. Now, $\hat{z}_c$ is a way to understand the concept of a spectral density. A similar value, but more used, is the Power Spectral Density, PSD (also called Mean Square Spectral Density).

$PSD(\omega)$ is a continuous function, while $\hat{z}_i$ is a discrete function. That means that $PSD(\omega)$ is fully determined by a certain measured or calculated variable $z(t)$, while $\hat{z}_i$ depends on which discretization (which ω_i or which $\Delta\omega$) that is chosen.

$$PSD(z(t),\omega,\Delta\omega) = \frac{MS\big(filter(z(t),\omega,\Delta\omega)\big)}{\Delta\omega} = G(\omega);$$
$$where\ \text{filter} is\ a\ bandpass\ filter\ centered\ around\ \omega\ and\ with\ band\ width\ \Delta\omega; \quad [5.8]$$

PSD can also be defined with band width in time frequency instead of angular frequency. Eq [5.8] is the same but replacing $\Delta\omega$ with Δf.

When the variable to study (z) is known and the band width is known, one often writes simply $PSD(\omega)$ or $G(\omega)$. G has the same unit as z^2, but per [rad/s] or per [oscillations/s]. So, if z is a displacement in [m], G has the unit $[m^2/(rad/s)]$ or $[m^2/(1/s) = m^2 \cdot s]$.

RMS is square root of the area under the PSD curve:

$$RMS(z) = \sqrt{\sum_{i=1}^{N} MS(z_i)} = \sqrt{\sum_{i=1}^{N} G(\omega_i)\cdot\Delta\omega_i} = \sqrt{\int_{\omega=0}^{\infty} G(\omega)\cdot d\omega}\,; \quad [5.9]$$

5.2.1.2.1 Differentiation of PSD

Knowing the PSD of a variable, we can easily obtain the PSD for the derivative of the same variable:

$$G_{\dot{z}}(\omega) = \omega^2 \cdot G_z(\omega); \quad [5.10]$$

5.2.1.3 Transfer Function

In a minimum model for vertical dynamics there is at least one excitation, often road vertical displacement, z_r, and one response, e.g. vertical displacement of sprung mass (=vehicle body), z_s. A Transfer function, $H = H(j\cdot\omega)$, is the function which we can use to find the response, given the excitation:

$$Z_s(\omega) = H(\omega)\cdot Z_r(\omega); \quad \Leftrightarrow \quad \mathcal{F}\big(z_s(t)\big) = H(\omega)\cdot\mathcal{F}\big(z_r(t)\big);$$
$$where\ \mathcal{F}\ is\ the\ Fourier\ operator: Z(\omega) = \mathcal{F}\big(z(t)\big) = \int_0^{\infty} e^{-j\cdot\omega\cdot t}\cdot z(t)\cdot dt\,; \quad [5.11]$$

H is complex, with magnitude, $|H| = \sqrt{(\mathrm{Re}(H))^2 + (\mathrm{Im}(H))^2}$, and phase, $\arg\big(H(\omega)\big) = \arctan(\mathrm{Im}(H)/\mathrm{Re}(H))$.

$$Amplitude:\ \hat{z}_s(\omega) = |H(\omega)|\cdot\hat{z}_r(\omega);$$
$$Phase:\ \varphi_s(\omega) - \varphi_r(\omega) = \arg\big(H(\omega)\big);$$
$$where\ z = \sum_{i=1}^{N} \hat{z}(\omega_i)\cdot\cos(\omega_i\cdot t + \varphi_i)\,; \quad [5.12]$$

Since there can be different excitations and responses in a system, there are several transfer functions. To distinguish between those, a subscripting of H is often used: $H_{excitation\rightarrow response}$, which would be

$H_{z_r \to z_s} = H_{road\ displacement \to sprung\ mass\ displacement}$ in the example above. Other examples of relevant transfer functions in vertical vehicle dynamics are:

- $H_{road\ displacement \to sprung\ mass\ acceleration}$ $[(m/s^2)/m]$, see 5.5
- $H_{road\ displacement \to suspension\ deformation}$ $[m/m]$, see 5.5.2
- $H_{road\ displacement \to tyre\ force}$ $[N/m]$, see 5.5.2

When transfer function for one derivative is found, it is often easy to convert it to another:

$$\begin{aligned} &H_{z_1 \to \dot{z}_2} = j \cdot \omega \cdot H_{z_1 \to z_2}; \\ &H_{z_1 \to \ddot{z}_2} = j \cdot \omega \cdot j \cdot \omega \cdot H_{z_1 \to z_2} = -\omega^2 \cdot H_{z_1 \to z_2}; \\ &H_{z_1 \to z_2 - z_3} = H_{z_1 \to z_2} - H_{z_1 \to z_3}; \end{aligned} \qquad [5.13]$$

The usage of the transfer function is, primarily, to easily obtain the response from the excitation, as shown in Equation [5.12]. Also, the transfer function can operate on the Power Spectral Density, PSD=G, as shown in the following:

$$\begin{aligned} &G_{z_s}(\omega) = \frac{MS(z_s(t), \omega)}{\Delta\omega} = \frac{\left(\hat{z}_s(\omega)\right)^2/2}{\Delta\omega} = \frac{\left(|H(\omega)| \cdot \hat{z}_r(\omega)\right)^2/2}{\Delta\omega} = \\ &= \left|H_{z_r \to z_s}(\omega)\right|^2 \cdot \frac{\left(\hat{z}_r(\omega)\right)^2/2}{\Delta\omega} = \left|H_{z_r \to z_s}(\omega)\right|^2 \cdot G_{z_r}(\omega); \end{aligned} \qquad [5.14]$$

Using Equation [5.9], we can then express $RMS(z_s)$ (sprung mass), from knowing $G_{z_r}(\omega)$ (road):

$$RMS(z_s) = \sqrt{\int_{\omega=0}^{\infty} \left|H_{z_r \to z_s}(\omega)\right|^2 \cdot G_{z_r}(\omega) \cdot d\omega}\,; \qquad [5.15]$$

5.2.2 Space as Independent Variable

All transformations, in this compendium, between time domain and space domain requires a constant longitudinal speed, v_x, so that:

$$x = v_x \cdot t + x_0; \qquad [5.16]$$

The offset (x_0) is the phase (spatial) offset (x_0) is the correspondence to the phase angle (φ).

The corresponding formulas as given in Equations [5.2]..[5.13] can be formulated when changing to space domain, or spatial domain. It is generally a good idea to use a separate set of notations for the spatial domain. Hence the formulas are repeated with new notations, which is basically what will be done in present section.

In space domain, the frequency has the common understanding of "how often per **distance**". Even so, there are two relevant ways to measure frequency: spatial angular frequency and spatial frequency.

$$\begin{aligned} &\Omega = 2 \cdot \pi \cdot f_s; \\ &where \quad \Omega\ [rad/m] = angular\ spatial\ frequency; \\ &and \quad f_s\ [1/m = oscillations/m] = spatial\ frequency; \end{aligned} \qquad [5.17]$$

The correspondence to period time is wave length, denoted λ:

$$\lambda[m] = 1/f_s = 2 \cdot \pi/\Omega\,; \qquad [5.18]$$

Now, the basic assumption in Equation [5.16] and definitions of frequencies gives:

$$\omega = v_x \cdot \Omega; \quad and \quad f = v_x \cdot f_s; \qquad [5.19]$$

The relation between the phase (spatial) offset (x_0) and the phase angle (φ) is:

$$x_0 = \frac{\lambda \cdot \varphi}{2 \cdot \pi}; \qquad [5.20]$$

5.2.2.1 Spatial Mean Square and Spatial Root Mean Square

In space domain, a variable, z, varies with distance, x. We can define Mean Square and Root Mean Square values also in space domain. We subscript these with s for space.

$$\begin{aligned} &Variable: && z && = z(x); \\ &MeanSquare: && MS_s(z) && = \frac{\int_0^{x_{end}} z^2 \cdot dx}{x_{end}}; \\ &RootMeanSquare: && RMS_s(z) && = \sqrt{\frac{\int_0^{x_{end}} z^2 \cdot dx}{x_{end}}}; \end{aligned} \quad [5.21]$$

Because v_x is constant, the Mean Square and Root Mean Square will be the same in time and space domain. If the variable is written as a single frequency harmonic stationary oscillation, these values becomes as follows:

$$\begin{aligned} &Variable: && z && = \hat{z} \cdot \cos(\Omega \cdot x + x_0); \\ &MeanSquare: && MS_s(z) && = \cdots = \frac{\hat{z}^2}{2} = MS(z); \\ &RootMeanSquare: && RMS_s(z) && = \cdots = \frac{|\hat{z}|}{\sqrt{2}} = RMS(z); \end{aligned} \quad [5.22]$$

If the variable is written as a multiple frequency harmonic stationary oscillation:

$$\begin{aligned} &Variable: && z && = \sum_{i=1}^{N} z_i = \sum_{i=1}^{N} \hat{z}_i \cdot \cos(\Omega_i \cdot x + x_{0i}); \\ &MeanSquare: && MS_s(z) && = \sum_{i=1}^{N} \frac{\hat{z}_i^{\,2}}{2} = MS(z); \\ &RootMeanSquare: && RMS_s(z) && = \sqrt{MS_s(z)} = \sqrt{\sum_{i=1}^{N} \left(RMS(z_i)\right)^2} = RMS(z); \end{aligned} \quad [5.23]$$

5.2.2.2 Spatial Power Spectral Density and Frequency Bands

A correspondence to Power Spectral Density in space domain is denoted PSD_s in the following:

$$PSD_s(z(x), \Omega, \Delta\lambda) = \frac{MS(filter(z(x), \Omega, \Delta\lambda))}{\Delta\lambda} = \Phi(\Omega); \quad [5.24]$$

where "filter" is a band pass filter centred around ω and with band width Δf;

When the variable to study z is known and the band width is known, one often writes simply $PSD_s(\Omega)$ or $\Phi(\Omega)$. The Φ has the same unit as z^2, but per [rad/m] or per [oscillations/m]. So, if z is a displacement in [m], Φ has the unit $[\frac{m^2}{rad/m} = \frac{m^3}{rad}]$ or $[\frac{m^2}{1/m} = m^3]$.

5.3 Road Models

In general, a road model can include ground properties such as coefficient of friction, damping/elasticity of ground and vertical position. The independent variable is either one, along an assumed path, or generally two, x and y in ground plane. In vertical dynamics in this compendium, we only assume vertical displacement as function of a path. We use x as independent variable along the path, meaning that the road model is: $z_r = z_r(x)$. The function $z_r(x)$ can be either of the types in Figure 5-2. We will concentrate on stationary oscillations, which by Fourier series, always can be expressed as multiple (spatial) frequency harmonic stationary oscillation. This can be specialized to either single (spatial) frequency or random (spatial) frequency. Hence, the general form of the road model is multiple (spatial) frequencies:

$$z_r = z_r(x) = \sum_{i=1}^{N} \hat{z}_i \cdot \cos(\Omega_i \cdot x + x_{0i}) \; ; \qquad [5.25]$$

5.3.1 One Frequency Road Model

For certain roads, such as roads built with concrete blocks, a single (spatial) frequency can be a relevant approximation to study a certain single wave length. Also, the single (spatial) frequency road model is good for learning the different concepts. A single (spatial) frequency model is the same as a single wave length model ($\lambda = 2 \cdot \pi/\Omega$, from Equation [5.17]) and it can be described as:

$$z_r = z_r(x) = \hat{z} \cdot \cos(\Omega \cdot x + x_0) \; ; \qquad [5.26]$$

5.3.2 Multiple Frequency Road Models

Based on the general format in Equation [5.25], we will now specialise to models for different road qualities. In Figure 5-4, there are 4 types of road types defined. The 3 upper ones of those are also defined as PSD-plots in Figure 5-5. The mathematical formula is given in Equation [5.27] and numerical parameter values are given in Equation [5.28].

$$\Phi = \Phi(\Omega) = \Phi_0 \cdot \left(\frac{\Omega}{\Omega_0}\right)^{-w} = \frac{MS_s(z_r, \Omega)}{\Delta\Omega}; \qquad [5.27]$$

where Φ_0 = road severity $\left[\frac{\mathrm{m}^2}{\mathrm{rad/m}}\right]$;
w = road waviness [1];
Ω = spatial angular frequency [rad/m];
Ω_0 = 1 [rad/m];

Typical values are:

$$\text{Very good road:} \quad \Phi_0 = 1 \cdot 10^{-6} \left[\frac{\mathrm{m}^2}{\mathrm{rad/m}}\right];$$

$$\text{Bad road :} \quad \Phi_0 = 10 \cdot 10^{-6} \left[\frac{\mathrm{m}^2}{\mathrm{rad/m}}\right]; \qquad [5.28]$$

$$\text{Very bad road :} \quad \Phi_0 = 100 \cdot 10^{-6} \left[\frac{\mathrm{m}^2}{\mathrm{rad/m}}\right];$$

The waviness is normally in the range of $w = 2..3$ [1],
where smooth roads have larger waviness than bad roads.

The decreasing amplitude for higher (spatial) frequencies (i.e. for smaller wave length) can be explained by that height variation over a short distance requires large gradients. On micro-level, in the granular level in the asphalt, there can of course be steep slopes on each small stone in the asphalt. These are of less interest in vehicle vertical dynamics, since the wheel dimensions filter out wave length << tyre contact length, see Figure 2-51. Reference (ISO 8608) uses road waviness, w=2 for all roads. Figure 5-5 is based on measurements on real roads, which shows that waviness actually varies with road severity, Φ_0. A certain road can be described with:

- $\Omega_1, \cdots, \Omega_N$
- $\hat{z}_1, \cdots, \hat{z}_N$
- $x_{01}, \cdots, x_{0N}$

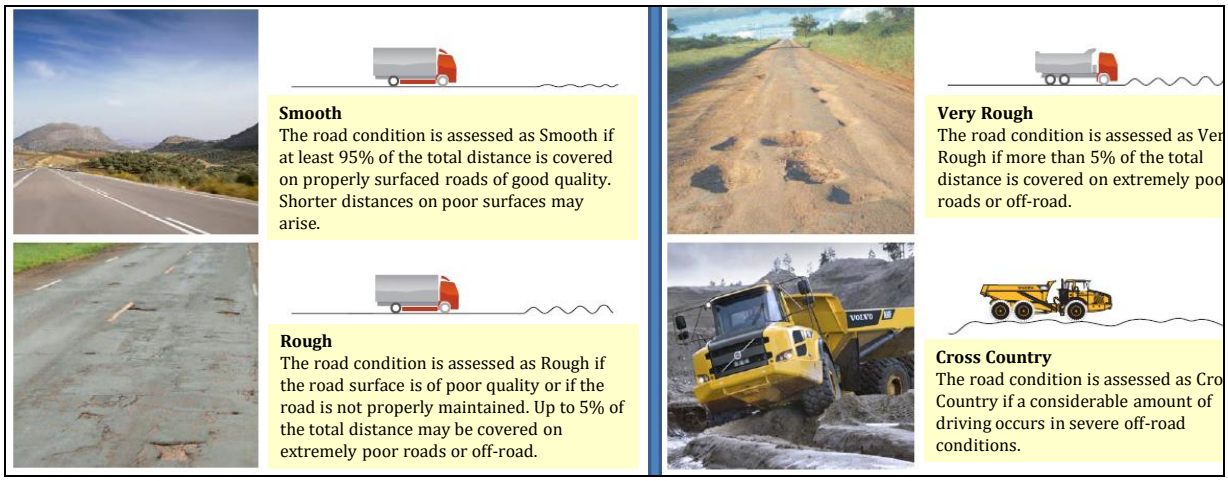

Figure 5-4: Four typical road types. From (AB Volvo, 2011).

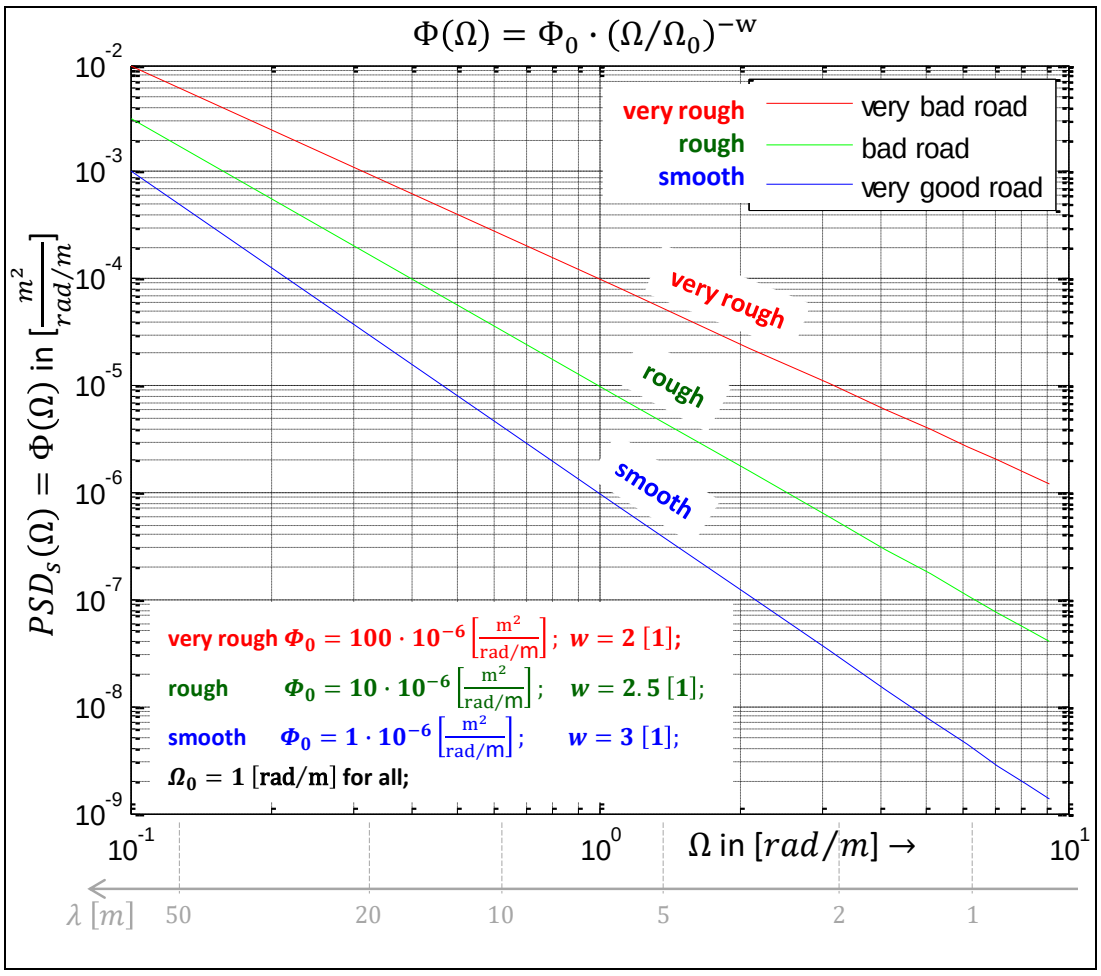

Figure 5-5: PSD spectra for the three typical roads in Figure 5-4.

Number of frequency components, N, to select is a matter of accuracy or experience. The offsets, $x_{01}, \cdots, x_{0N}$, can often be assumed to be zero. If phase is to be studied, as in Figure 5-5, a random generation of offsets is suitable. See also Reference (ISO 8608).

We can generate $z_r(x)$ curves for the 3 road types in Figure 5-5 as shown in Figure 5-6. To generate those plots, we have assumed different number of harmonic components (N in Equation [5.25]) and also randomly generate the phase for each component (each x_{0i}).

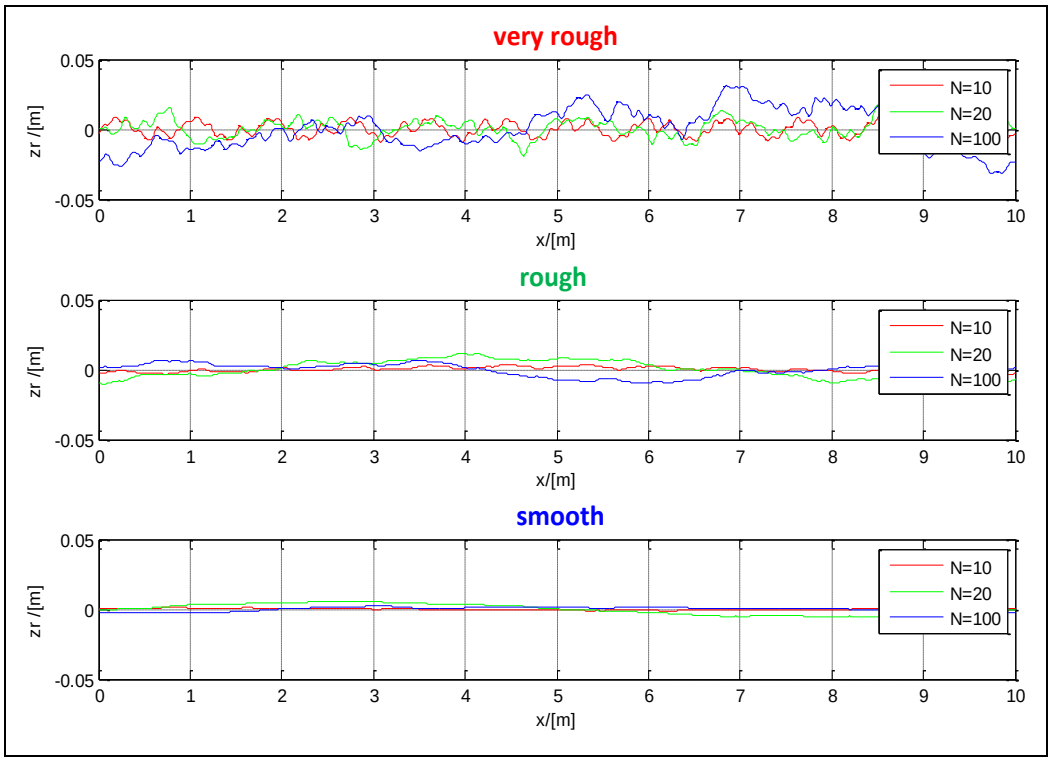

Figure 5-6: Road profiles, $z_r(x)$, for the three typical roads in Figure 5-4.

5.3.2.1 Transfer Function from Road Spectrum in Spatial Domain to System Response in Time Domain

Since we assume constant longitudinal velocity, v_x, the road spectrum can be transformed to the time-frequency domain:

$$G_{z_r}(\omega) = \frac{MS(z_r,\omega)}{\Delta\omega} = \{use: \omega = v_x \cdot \Omega\} = \frac{MS_s(z_r,\Omega)}{v_x \cdot \Delta\Omega} =$$
$$= \left\{use: \Phi_0 \cdot \left(\frac{\Omega}{\Omega_0}\right)^{-w} = \frac{MS_s(z_r,\Omega)}{\Delta\Omega}\right\} = \frac{\Phi_0 \cdot \left(\frac{\Omega}{\Omega_0}\right)^{-w}}{v_x} =$$
$$= \frac{\Phi_0 \cdot \Omega^{-w}}{{\Omega_0}^{-w} \cdot v_x} = \frac{\Phi_0}{{\Omega_0}^{-w}} \cdot \frac{\left(\frac{\omega}{v_x}\right)^{-w}}{v_x} = \frac{\Phi_0}{{\Omega_0}^{-w}} \cdot {v_x}^{w-1} \cdot \omega^{-w};$$

[5.29]

Then, we can use Equation [5.14] to obtain the responsez_s:

$$G_{z_s}(\omega) = \left|H_{z_r \to z_s}(\omega)\right|^2 \cdot G_{z_r}(\omega) = \left|H_{z_r \to z_s}(\omega)\right|^2 \cdot \frac{\Phi_0}{{\Omega_0}^{-w}} \cdot {v_x}^{w-1} \cdot \omega^{-w};$$

[5.30]

Then we can use Equation [5.9] to obtain the RMS of the response z_s:

$$RMS(z_s) = \sqrt{\sum_{i=1}^{N} G_{z_s}(\omega_i) \cdot \Delta\omega} = \sqrt{\frac{\Phi_0}{{\Omega_0}^{-w}} \cdot {v_x}^{w-1} \cdot \sum_{i=1}^{N} \left|H_{z_r \to z_s}(\omega_i)\right|^2 \cdot {\omega_i}^{-w} \cdot \Delta\omega};$$

or

$$RMS(z_s) = \sqrt{\int_{\omega=0}^{\infty} G_{z_s}(\omega) \cdot d\omega} = \sqrt{\frac{\Phi_0}{{\Omega_0}^{-w}} \cdot {v_x}^{w-1} \cdot \int_{\omega=0}^{\infty} \left|H_{z_r \to z_s}(\omega)\right|^2 \cdot \omega^{-w} \cdot d\omega};$$

[5.31]

5.4 1D Vehicle Models

"One-dimensional" refers to pure vertical motion, i.e. that the vehicle heaves without pitch and without roll. The tyre is stiff and massless.

This can be seen as that the whole vehicle mass, m, is modelled as suspended by the sum of all wheels' vertical forces, $F_z = F_{flz} + F_{frz} + F_{rlz} + F_{rrz}$. However, the model can sometimes be referred to as a "quarter-car-model". That is because one can see the model as a quarter of the vehicle mass, $m/4$, which is suspended by one of the wheel's vertical force, F_{ijz}. The exact physical interpolation of a quarter car is less obvious, since one can argue whether the fraction ¼ of the vehicle mass is the proper fraction or from which point of view it is proper. Using the fraction ¼ is as least debatable if the vehicle is completely symmetrical, both left/right and front/rear.

5.4.1 1D Model without Dynamic dofs

"Without dynamic degree of freedom" refers to that the (axle) suspension is modelled as ideally stiff. The model can be visualised as in Figure 5-7.

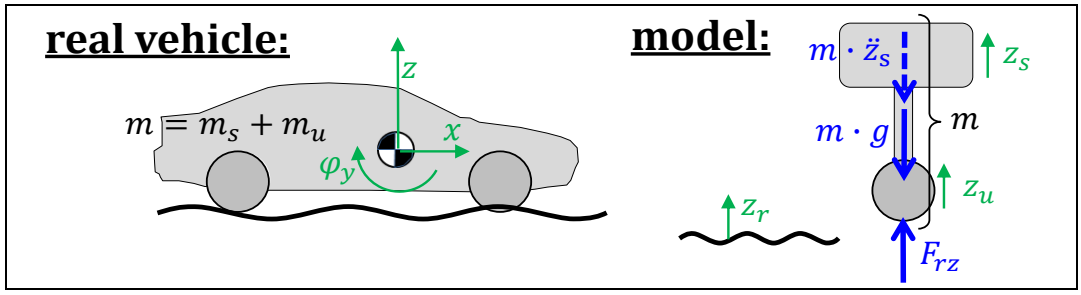

Figure 5-7: One-dimensional model without dynamic degree of freedom

The equations could be set up directly ($m \cdot \ddot{z}_s = F_{rz};\ \ and\ \ z_s = z_r(t);$), but the following equations gives a formalism which will be useful for the more complex models in 5.4.2 and 5.4.3.

$$\begin{aligned} &\textbf{\textit{Equilibrium}}: && m \cdot \ddot{z}_s + m \cdot g = F_{rz}; \\ &\textbf{\textit{Compatibility}}: && z_r = z_s;\ \ and\ \ z_r = z_u; \\ &\textbf{\textit{Excitation}}: && z_r = z_r(t); \end{aligned} \qquad [5.32]$$

5.4.1.1 Response to a Single Frequency Excitation

Assume that the road has only one (spatial) frequency, i.e. one wave length. Then the excitation is as follows:

$$\left.\begin{array}{c} z_r = z_r(x) = \hat{z}_r \cdot \cos(\Omega \cdot x + x_0) = \hat{z}_r \cdot \cos\left(\frac{2 \cdot \pi}{\lambda} \cdot x + x_0\right); \\ x = v_x \cdot t; \\ Assume\ x_0 = 0; \end{array}\right\} \Rightarrow$$

$$\Rightarrow z_r(t) = \hat{z}_r \cdot \cos\left(\frac{2 \cdot \pi \cdot v_x}{\lambda} \cdot t\right) = \hat{z}_r \cdot \cos(\omega \cdot t)\,; \Rightarrow$$

$$\Rightarrow \dot{z}_r(t) = -\frac{2 \cdot \pi \cdot v_x}{\lambda} \cdot \hat{z}_r \cdot \sin\left(\frac{2 \cdot \pi \cdot v_x}{\lambda} \cdot t\right) = -\omega \cdot \hat{z}_r \cdot \sin(\omega \cdot t)\,; \Rightarrow$$

$$\Rightarrow \ddot{z}_r(t) = -\left(\frac{2 \cdot \pi \cdot v_x}{\lambda}\right)^2 \cdot \hat{z}_r \cdot \cos\left(\frac{2 \cdot \pi \cdot v_x}{\lambda} \cdot t\right) = -\omega^2 \cdot \hat{z}_r \cdot \cos(\omega \cdot t)\,; \qquad [5.33]$$

Insertion in the model in Equation [5.32] (with eliminated z_u) gives directly the solution:

$$\begin{cases} F_{rz}(t) = m \cdot g + \Delta F(t) = m \cdot g + \widehat{\Delta F}_{rz} \cdot \cos(\omega \cdot t)\,; \\ z_r(t) = z_s(t) = \hat{z}_r \cdot \cos(\omega \cdot t);\ \ and\ \ \ddot{z}_r(t) = \ddot{z}_s(t) = \hat{a} \cdot \cos(\omega \cdot t)\,; \end{cases} \qquad [5.34]$$
$$where\ \ \hat{F}_{rz} = -m \cdot \omega^2 \cdot \hat{z}_r;\ \ and\ \ \hat{a} = -\omega^2 \cdot \hat{z}_r;$$

We can identify the magnitude of the transfer functions H. The negative sign in Equation [5.35] means 180 degrees phase shift:

$$
\begin{aligned}
H_{z_r \to z_s} &= \left\{ H_{z_r \to z_s} = \frac{\mathcal{F}(z_s)}{\mathcal{F}(z_r)} \right\} = \{ z_r(t) = z_s(t) \} = 1 + j \cdot 0; \\
H_{z_r \to z_r - z_s} &= \left\{ H_{z_r \to z_r - z_s} = H_{z_r \to z_s} - H_{z_s \to z_s} = H_{z_r \to z_s} - 1 \right\} = 0 + j \cdot 0; \\
H_{z_r \to \ddot{z}_s} &= \left\{ H_{z_r \to \ddot{z}_s} = (j \cdot \omega)^2 \cdot H_{z_r \to z_s} = -\omega^2 \cdot H_{z_r \to z_s} \right\} = -\omega^2 + j \cdot 0; \\
H_{z_r \to \Delta F_{rz}} &= \left\{ H_{z_r \to \Delta F_{rz}} = m \cdot H_{z_r \to \ddot{z}_s} \right\} = -m \cdot \omega^2 + j \cdot 0;
\end{aligned}
\qquad [5.35]
$$

The motivation to choose exactly those transfer functions is revealed later, in 5.5, 5.5.2 and 5.5.2. For now, we simply conclude that various transfer functions can be identified and plotted. The plots are found in Figure 5-8. Numerical values for m and λ are chosen.

5.4.1.1.1 Example Analysis

An example of how to use Figure 5-8 is: A certain road has amplitude of 1 cm ($\hat{z}_r = 0.01\ m$). The vehicle drives on it with a longitudinal velocity of 50 km/h ($v_x \approx 14\ m/s \mathrel{\widehat{=}} \approx 2.8 Hz$):

- $\left| H_{z_r \to \ddot{z}_s}(v_x) \right| \approx 305;\ \Rightarrow\ |\hat{a}| = 305 \cdot \hat{z}_r = 305 \cdot 0.01 = 3.05\ m/s^2;$. From this we can calculate $RMS(\ddot{z}_s) = |3.05|/\sqrt{2} \approx 2.16\ m/s^2$. The RMS value of acceleration will later be related to ride **comfort**, see 5.5.
- $\left| H_{z_r \to z_u - z_s}(v_x) \right| = 0$; is the transfer function to deformation of suspension, which later will be related to **fatigue life**, see 5.5.2. The model in 5.4.1 is not good for measuring fatigue, since the $\hat{z}_u - \hat{z}_s$ is intrinsically zero because of no compliance between unsprung and sprung mass.
- $\left| H_{z_r \to \Delta F_{rz}}(v_x) \right| \approx 487000;\ \Rightarrow\ \widehat{\Delta F}_{rz} = 487000 \cdot \hat{z}_r = 487000 \cdot 0.01 = 4870\ N;$. If $\widehat{\Delta F}_{rz} > m \cdot g \approx 16000\ N$, the model is outside its validity region, because it would require pulling forces between tyre and road. If changing to $\hat{z}_r = 0.1\ m$, this limit is defined by $\left| H_{z_r \to \Delta F_{rz}}(v_x) \right| >\approx \frac{16000}{0.1} = 1.6 \cdot 10^5\ [N/m]$, which is used to examplify the validity limit in Figure 5-8; model becomes invalid for $v_x >\approx 300\ m/s$. The variation in tyre road contact force will be related to **road grip**, see 5.5.2.

The phases for the studied variables can be found in Equation [5.35]. With this model, the phases become constant and $\pm 90\ deg$.

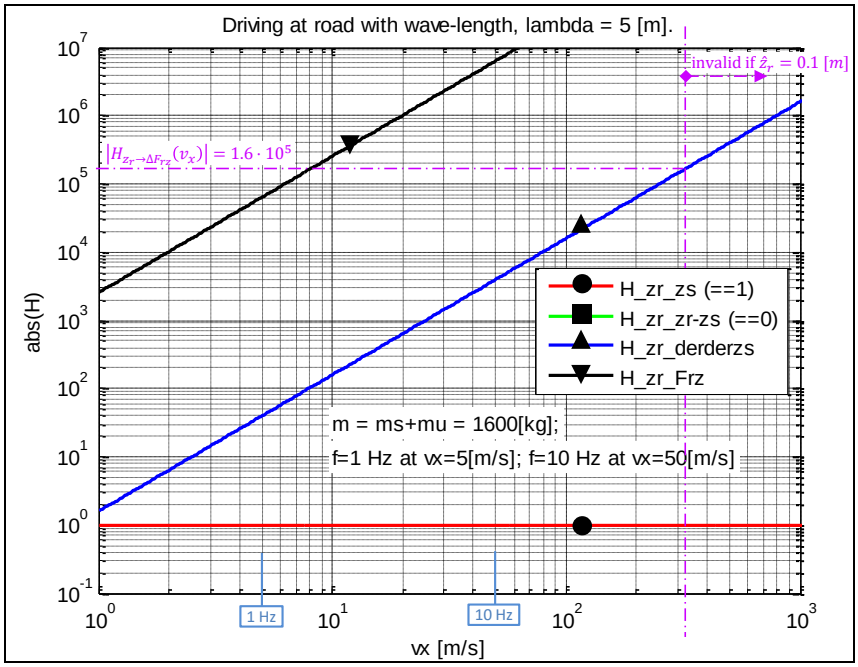

Figure 5-8: Transfer functions from model in Figure 5-7, excited with single frequencies.

5.4.1.2 Response to a Multiple Frequency Excitation

Using Eq [5.31], Eq [5.42] and values for road type "rough" in Figure 5-5, we can conclude:

$$RMS(z_s) = \sqrt{\frac{\Phi_0}{\Omega_0^{-w}} \cdot {v_x}^{w-1} \cdot \int_{\omega=0}^{\infty} \left|H_{z_r \to z_s}(\omega)\right|^2 \cdot \omega^{-w} \cdot d\omega} = \quad [5.36]$$

$$= \sqrt{\frac{10 \cdot 10^{-6}}{1} \cdot {v_x}^{2.5-1} \cdot \int_{\omega=0}^{\infty} \left|H_{z_r \to z_s}(\omega)\right|^2 \cdot \omega^{-2.5} \cdot d\omega};$$

For now, we simply note that it is possible to calculate this (scalar) RMS value for each vehicle speed over the assumed road. In corresponding way, an RMS value can be calculated for any of the oscillating variables, such as $\ddot{z}_s$, $z_r - z_s$ and F_{rz}. We will come back to Equation [5.36] in 5.5.1.2.

5.4.2 1D Model with 1 Dynamic dof

"With 1 dynamic dof" refers to that the axle suspension is modelled as a linear spring and linear (viscous) damper in parallel. Compared to the model in 5.4.1, the tyre is still stiff, but the unsprung parts are assigned a mass m_u. The model can be visualised as in Figure 5-9.

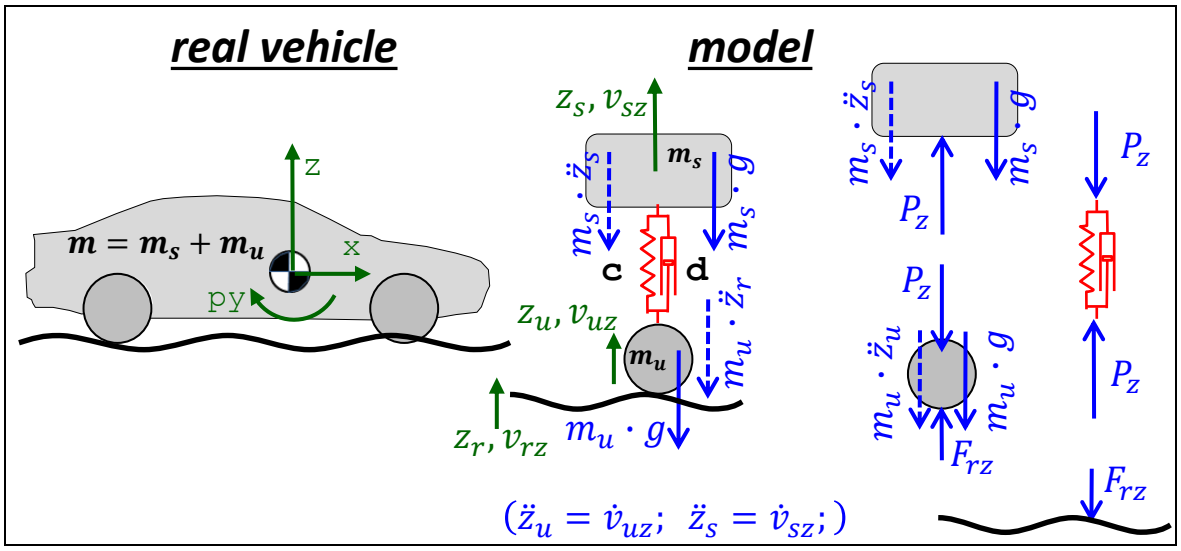

Figure 5-9: One-dimensional model with 1 dynamic degree of freedom

The mathematical model becomes as follows:

Equilibrium sprung mass: $P_z - m_s \cdot \ddot{z}_s - m_s \cdot g = 0;$
Equilibrium unsprung mass: $F_{rz} - P_z - m_u \cdot \ddot{z}_r - m_u \cdot g = 0;$
Constitution: $P_z = c \cdot (z_u - z_s) + d \cdot (\dot{z}_u - \dot{z}_s) + m_s \cdot g;$
Compatibility: $z_u = z_r;$
Excitation: $z_r = z_r(t);$ [5.37]

5.4.2.1 Response to a Single Frequency Excitation

Eliminating P_z, z_u and z_r gives:

$$m_s \cdot \ddot{z}_s = c \cdot (z_r(t) - z_s) + d \cdot (\dot{z}_r(t) - \dot{z}_s);$$
$$\underbrace{F_{rz} - (m_s + m_u) \cdot g}_{\Delta F_{rz}} = c \cdot (z_r(t) - z_s) + d \cdot (\dot{z}_r(t) - \dot{z}_s) + m_u \cdot \ddot{z}_r(t); \quad [5.38]$$

Note that since we measure z_u and z_s from the static equilibrium, the static load, $m_s \cdot g$, disappears when constitution is inserted in equilibrium. The ΔF_{rz} denotes the variation from static contact force between road and tyre.

Assume that the road has only one (spatial) frequency, i.e. one wave length. Then the excitation is as in Equation [5.26], in which we assume $x_0 = 0$. So, we can insert $z_r(t) = \hat{z}_r \cdot \cos(\omega \cdot t) \Rightarrow \dot{z}_r(t) = -\omega \cdot \hat{z}_r \cdot \sin(\omega \cdot t) \Rightarrow \ddot{z}_r(t) = -\omega^2 \cdot \hat{z}_r \cdot \cos(\omega \cdot t)$; in Equation [5.38] and solve it for $z_s(t)$ and $\Delta F_{rz}(t)$ with trigonometry or Fourier transform.

In 4.4.3.1.1, we applied Fourier transform on the linear state space form. To show a slightly other way, we do not rewrite to linear state space form, but apply Fourier transform on Eq [5.38] directly:

$$m_s \cdot \left(-\omega^2 \cdot \mathcal{F}(z_s)\right) = c \cdot \left(\mathcal{F}(z_r) - \mathcal{F}(z_s)\right) + d \cdot j \cdot \omega \cdot \left(\mathcal{F}(z_r) - \mathcal{F}(z_s)\right);$$
$$\mathcal{F}(\Delta F_{rz}) = c \cdot \left(\mathcal{F}(z_r) - \mathcal{F}(z_s)\right) + d \cdot j \cdot \omega \cdot \left(\mathcal{F}(z_r) - \mathcal{F}(z_s)\right) - m_u \cdot \omega^2 \cdot \mathcal{F}(z_r); \quad [5.39]$$

From this, we can then solve for the transfer functions:

$$H_{z_r \to z_s} = \frac{\mathcal{F}(z_s)}{\mathcal{F}(z_r)} = \frac{c + j \cdot d \cdot \omega}{c + j \cdot d \cdot \omega - m_s \cdot \omega^2};$$
$$H_{z_r \to \Delta F_{rz}} = \frac{\mathcal{F}(\Delta F_{rz})}{\mathcal{F}(z_r)} = (c + j \cdot \omega \cdot d - m_u \cdot \omega^2) - (c + j \cdot \omega \cdot d) \cdot \frac{\mathcal{F}(z_s)}{\mathcal{F}(z_r)} =$$
$$= (c + j \cdot \omega \cdot d - m_u \cdot \omega^2) - (c + j \cdot \omega \cdot d) \cdot H_{z_r \to z_s}; \quad [5.40]$$

We can elaborate further with Eq [5.40]:

Amplitude: $\left|H_{z_r \to z_s}\right| = \frac{\hat{z}_s}{\hat{z}_r} = \left|\frac{c + j \cdot d \cdot \omega}{(c - m \cdot \omega^2) + j \cdot d \cdot \omega}\right| =$

$$= \left\{ \begin{matrix} H_{z_r \to z_s} = \frac{c + j \cdot d \cdot \omega}{(c - m \cdot \omega^2) + j \cdot d \cdot \omega} = \\ = ReH + j \cdot ImH;\ Solve\ for\ ReH\ and\ ImH \end{matrix} \right\} = \cdots = \sqrt{\frac{c^2 + d^2 \cdot \omega^2}{(c - m \cdot \omega^2)^2 + d^2 \cdot \omega^2}};$$

Phase: $\varphi_s(\omega) - \varphi_r(\omega) = \arg\left(\frac{c + j \cdot d \cdot \omega}{-m \cdot \omega^2 + c + j \cdot d \cdot \omega}\right) =$

$$= \left\{ \begin{matrix} \tan\left(\arg\left(H_{z_r \to z_s}\right)\right) = ImH/ReH\ ; \\ Solve\ for\ ReH\ and\ ImH; \end{matrix} \right\} = \cdots = \arctan\left(\frac{m \cdot d \cdot \omega^3}{c^2 - m \cdot c \cdot \omega^2 + d^2 \cdot \omega^2}\right); \quad [5.41]$$

Equation [5.13] now allows us to get the magnitudes of the other transfer functions as well:

$$H_{z_r \to z_s} = \text{from Equation [5.40]};$$
$$H_{z_r \to z_r - z_s} = H_{z_r \to z_r} - H_{z_r \to z_s} = 1 - H_{z_r \to z_s};$$
$$H_{z_r \to \ddot{z}_s} = -\omega^2 \cdot H_{z_r \to z_s};$$
$$H_{z_r \to \Delta F_{rz}} = \left\{ \begin{matrix} \Delta F_{rz} = m_u \cdot \ddot{z}_u + P_z = m_u \cdot \ddot{z}_r + P_z = \\ = m_u \cdot \ddot{z}_r + c \cdot (z_r - z_s) + d \cdot (\dot{z}_r - \dot{z}_s) \end{matrix} \right\} =$$
$$= m_u \cdot H_{z_r \to \ddot{z}_r} + c \cdot \left(H_{z_r \to z_r} - H_{z_r \to z_s}\right) + d \cdot \left(H_{z_r \to \dot{z}_r} - H_{z_r \to \dot{z}_s}\right) =$$
$$= m_u \cdot (j \cdot \omega)^2 + (c + j \cdot d \cdot \omega) \cdot \left(H_{z_r \to z_r} - H_{z_r \to z_s}\right) =$$
$$= -m_u \cdot \omega^2 + (c + j \cdot d \cdot \omega) \cdot \left(1 - H_{z_r \to z_s}\right); \quad [5.42]$$

The motivation to choose exactly those transfer functions is revealed later, in 5.5. Some of those magnitudes are easily expressed in reel (non-complex) mathematics using Equation [5.41]:

$$\left|H_{z_r \to z_s}\right| = \sqrt{\frac{c^2 + d^2 \cdot \omega^2}{(c - m \cdot \omega^2)^2 + d^2 \cdot \omega^2}};$$
$$\left|H_{z_r \to \ddot{z}_s}\right| = \omega^2 \cdot \sqrt{\frac{c^2 + d^2 \cdot \omega^2}{(c - m \cdot \omega^2)^2 + d^2 \cdot \omega^2}}; \quad [5.43]$$

5.4.2.1.1 Example Analysis

The transfer functions in Equation [5.41] are plotted in Figure 5-10 and Figure 5-11. Numerical values for m and λ have been chosen.

If we use Figure 5-10 as the example in 0:

- Ride comfort related: $\left|H_{z_r \to \ddot{z}_s}(v_x)\right| \approx 120;\ \Rightarrow\ |\hat{a}| = 120 \cdot \hat{z}_r = 120 \cdot 0.01 = 1.20\, m/s^2$;. From this we can calculate $RMS(\ddot{z}_s) = |1.20|/\sqrt{2} \approx 0.8485\, m/s^2$.
- Fatigue life related: $\left|H_{z_r \to z_r - z_s}(v_x)\right| \approx 1.11;\ \Rightarrow\ |\hat{z}_r - \hat{z}_s| = 1.11 \cdot \hat{z}_r = 1.11 \cdot 0.01 = 0.0111\, m = 1.11\, cm$;.
- Road grip related: $\left|H_{z_r \to \Delta F_{rz}}(v_x)\right| \approx 59795;\ \Rightarrow\ |\Delta F_{rz}| = 59795 \cdot \hat{z}_r = 59795 \cdot 0.01 = 598\, N$;.

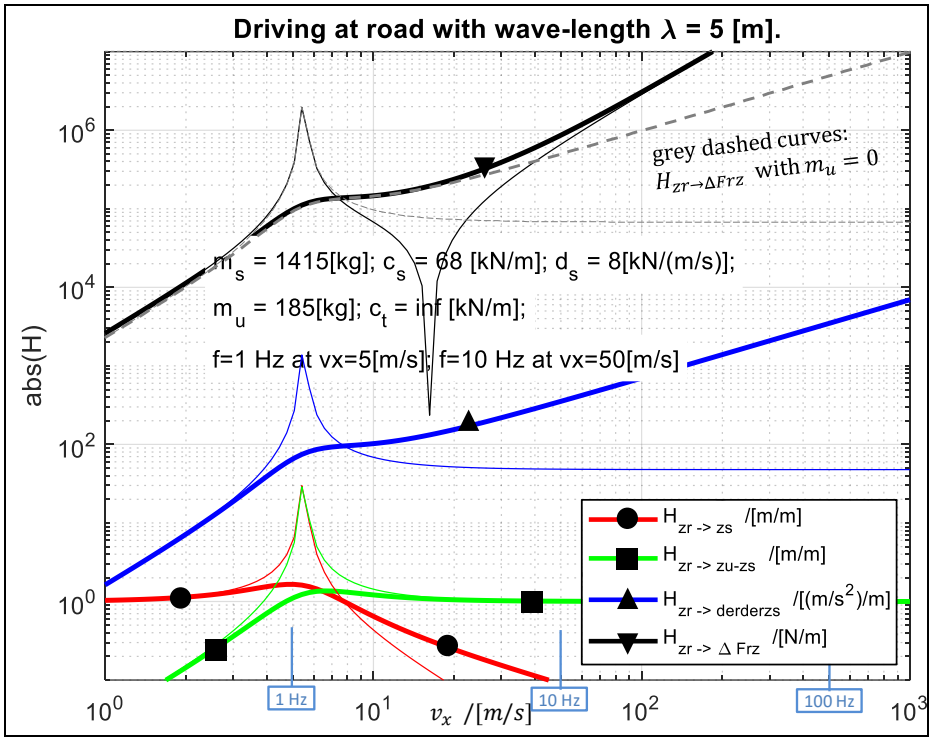

Figure 5-10: Transfer functions for amplitudes from model in Figure 5-9, excited with single frequencies. Thin lines are without damping. Notation: $H_{a \to b}$ is denoted `H_a_b`.

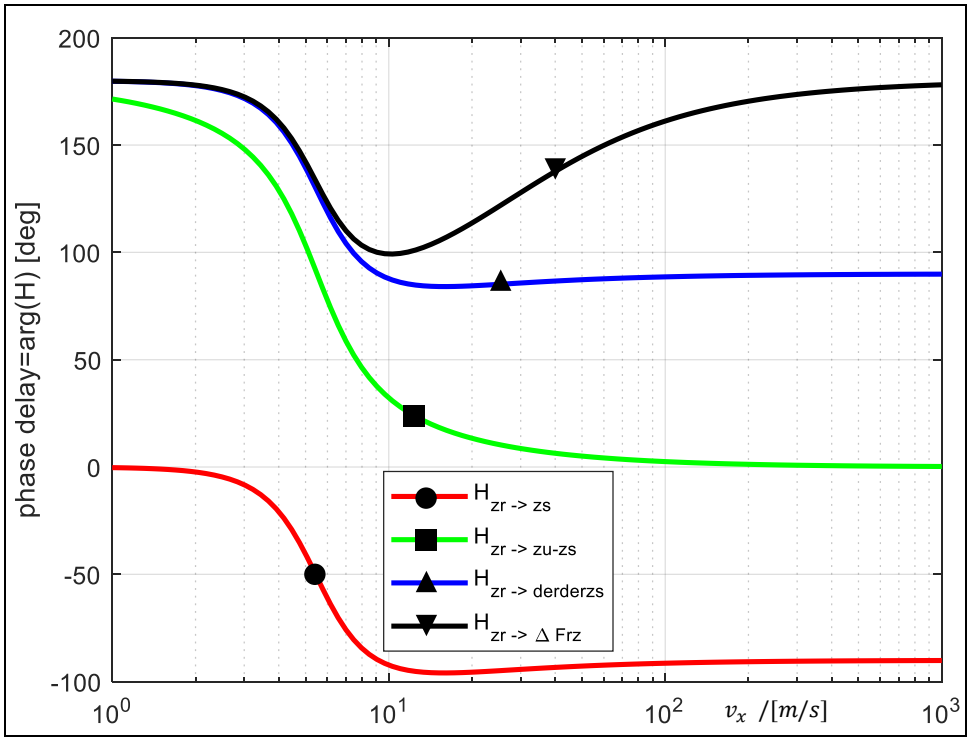

Figure 5-11: Transfer functions for phase delays from model in Figure 5-9, excited with single frequencies.

We compare these numbers with the corresponding numbers for the simpler model in 5.4.1. The comfort is better. The fatigue life and road grip have become more realistic.

Figure 5-10 also shows the curves for the undamped system (d=0). The highest peaks appear at approximately $v_x = 5..6$ m/s. This corresponds to the speed where the natural (=undamped) eigen frequency appears ($v_{x,crit} = \lambda \cdot f_{crit} = \lambda \cdot \omega_{crit}/(2 \cdot \pi) = \lambda \cdot \sqrt{c/m}/(2 \cdot \pi) \approx 5.5\ m/s$).

Figure 5-11 shows the phase angles for the different responses.

5.4.3 1D Model with 2 Dynamic dofs

The expression "2 dynamic dofs" refers to that both elasticity between road and wheel (unsprung mass) as well as between wheel (unsprung mass) and sprung mass is modelled. The model can be visualised as in Figure 5-12. No damping is modelled in tyre (in parallel with elasticity c_t) because it is generally relatively low.

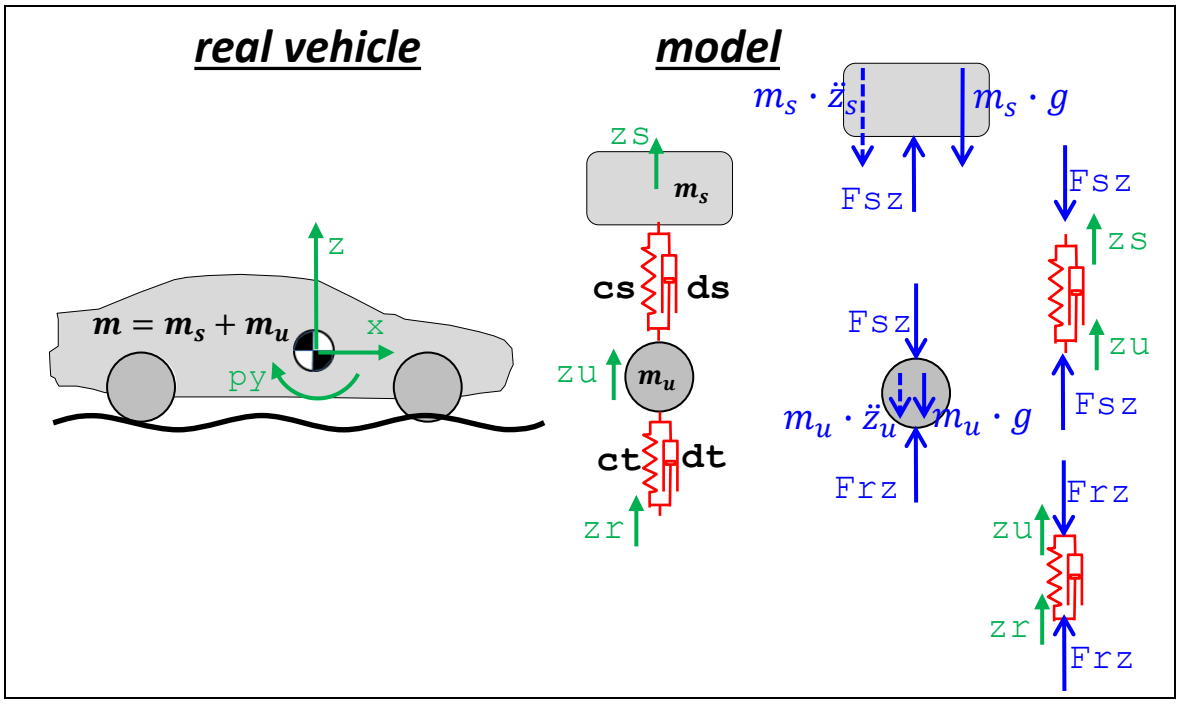

Figure 5-12: One-dimensional model with two dynamic degrees of freedom

The corresponding mathematical model becomes as follows:

Equilibrium:

$$m_s \cdot \ddot{z}_s = F_{sz} - m_s \cdot g;$$
$$m_u \cdot \ddot{z}_u = F_{rz} - F_{sz} - m_u \cdot g;$$

Constitution (displacements counted from static equilibrium):

$$F_{sz} = c_s \cdot (z_u - z_s) + d_s \cdot (\dot{z}_u - \dot{z}_s) + m_s \cdot g;$$
$$F_{rz} = c_t \cdot (z_r - z_u) + d_t \cdot (\dot{z}_r - \dot{z}_u) + (m_s + m_u) \cdot g;$$

Excitation: $z_r = z_r(t);$

[5.44]

The same can be formulated with matrices and Fourier transforms:

$$\begin{bmatrix} m_s & 0 \\ 0 & m_u \end{bmatrix} \cdot \begin{bmatrix} \ddot{z}_s \\ \ddot{z}_u \end{bmatrix} + \begin{bmatrix} d_s & -d_s \\ -d_s & d_s + d_t \end{bmatrix} \cdot \begin{bmatrix} \dot{z}_s \\ \dot{z}_u \end{bmatrix} + \begin{bmatrix} c_s & -c_s \\ -c_s & c_s + c_t \end{bmatrix} \cdot \begin{bmatrix} z_s \\ z_u \end{bmatrix} = \begin{bmatrix} 0 \\ d_t \end{bmatrix} \cdot \dot{z}_r + \begin{bmatrix} 0 \\ c_t \end{bmatrix} \cdot z_r; \Rightarrow$$

$$\Rightarrow \boldsymbol{M} \cdot \begin{bmatrix} \ddot{z}_s \\ \ddot{z}_u \end{bmatrix} + \boldsymbol{D} \cdot \begin{bmatrix} \dot{z}_s \\ \dot{z}_u \end{bmatrix} + \boldsymbol{C} \cdot \begin{bmatrix} z_s \\ z_u \end{bmatrix} = \boldsymbol{D_r} \cdot \dot{z}_r + \boldsymbol{C_r} \cdot z_r; \Rightarrow$$

$$\Rightarrow \boldsymbol{M} \cdot \left(-\omega^2 \cdot \begin{bmatrix} \mathcal{F}(z_s) \\ \mathcal{F}(z_u) \end{bmatrix} \right) + \boldsymbol{D} \cdot \left(j \cdot \omega \cdot \begin{bmatrix} \mathcal{F}(z_s) \\ \mathcal{F}(z_u) \end{bmatrix} \right) + \boldsymbol{C} \cdot \begin{bmatrix} \mathcal{F}(z_s) \\ \mathcal{F}(z_u) \end{bmatrix} =$$
$$= \boldsymbol{D_r} \cdot \left(j \cdot \omega \cdot \mathcal{F}(z_r) \right) + \boldsymbol{C_r} \cdot \mathcal{F}(z_r); \Rightarrow$$

$$\Rightarrow (-\omega^2 \cdot \boldsymbol{M} + j \cdot \omega \cdot \boldsymbol{D} + \boldsymbol{C}) \cdot \begin{bmatrix} \mathcal{F}(z_s) \\ \mathcal{F}(z_u) \end{bmatrix} = (j \cdot \omega \cdot \boldsymbol{D_r} + \boldsymbol{C_r}) \cdot \mathcal{F}(z_r);$$

[5.45]

5.4.3.1 Response to a Single Frequency Excitation

We can find the transfer functions via Fourier transform, starting from Eq [4.56]:

$$\begin{bmatrix} H_{z_r \to z_s} \\ H_{z_r \to z_u} \end{bmatrix} = \begin{bmatrix} \mathcal{F}(z_s) \\ \mathcal{F}(z_u) \end{bmatrix} \cdot \frac{1}{\mathcal{F}(z_r)} = (-\omega^2 \cdot \boldsymbol{M} + j \cdot \omega \cdot \boldsymbol{D} + \boldsymbol{C})^{-1} \cdot (j \cdot \omega \cdot \boldsymbol{D_r} + \boldsymbol{C_r}); \quad [5.46]$$

This format is very compact, since it includes both transfer functions for amplitude and phase. For numerical analyses, the expression in Eq [5.46] is explicit enough, since there are tools, e.g. Matlab, which do numerical matrix inversion and complex mathematics. Symbolic solution is rather lengthy, but one can use symbolic tools, e.g. Mathematica or Matlab Symbolic Toolbox.

Expression in real (without phase information) can be derived, see Eq [5.47].

$$\left| H_{z_r \to \ddot{z}_s} \right| = \omega^2 \cdot \frac{\sqrt{(c_s \cdot c_t - d_s \cdot d_t \cdot \omega^2)^2 + \left(\omega \cdot (d_s \cdot c_t + d_t \cdot c_s) \right)^2}}{\sqrt{A^2 + B^2}};$$

$$\left| H_{z_r \to z_u - z_s} \right| = \frac{m_s \cdot \sqrt{(c_t \cdot \omega^2)^2 + (d_t \cdot \omega^3)^2}}{\sqrt{A^2 + B^2}};$$

$$\left| H_{z_r \to z_r - z_u} \right| = \frac{\sqrt{(-m_s \cdot m_u \cdot \omega^4 + \omega^2 \cdot (m_s + m_u) \cdot c_s)^2 + (\omega^3 \cdot (m_s + m_u) \cdot d_s)^2}}{\sqrt{A^2 + B^2}};$$

$$A = \omega^4 \cdot m_s \cdot m_u - \omega^2 \cdot (m_s \cdot c_t + m_s \cdot c_s + d_s \cdot d_t + c_s \cdot m_u) + c_s \cdot c_t;$$

$$B = \omega^3 \cdot (m_s \cdot d_t + m_s \cdot d_s + m_u \cdot d_s) - \omega \cdot (d_s \cdot c_t + d_t \cdot c_s);$$

[5.47]

With $d_t = 0$, the solutions (with phase information, i.e. complex) becomes as follows:

$$H_{z_r \to z_s} = \frac{\mathcal{F}(z_s)}{\mathcal{F}(z_r)} = \frac{\dfrac{(-m_u \cdot \omega^2 + j \cdot d_s \cdot \omega + c_t + c_s) \cdot c_t}{-m_u \cdot \omega^2 + j \cdot d_s \cdot \omega + c_t + c_s - \dfrac{(c_s + j \cdot d_s \cdot \omega)^2}{-m_s \cdot \omega^2 + j \cdot d_s \cdot \omega + c_s}} - c_t}{c_s + j \cdot d_s \cdot \omega};$$

$$H_{z_r \to z_u} = \frac{\mathcal{F}(z_u)}{\mathcal{F}(z_r)} = \frac{c_t}{-m_u \cdot \omega^2 + j \cdot d_s \cdot \omega + c_t + c_s - \dfrac{(c_s + j \cdot d_s \cdot \omega)^2}{-m_s \cdot \omega^2 + j \cdot d_s \cdot \omega + c_s}};$$

where $\omega = \frac{2 \cdot \pi \cdot v_x}{\lambda}$;

[5.48]

Equation [5.13] now allows us to get the magnitudes of the other transfer functions as well:

$$
\begin{aligned}
&H_{z_r\to z_s} = \{\text{use Eq [5.48]}\};\\
&H_{z_r\to z_u} = \{\text{use Eq [5.48]}\};\\
&H_{z_r\to z_r-z_u} = H_{z_r\to z_r} - H_{z_r\to z_u} = 1 - H_{z_r\to z_u};\\
&H_{z_r\to z_u-z_s} = H_{z_r\to z_u} - H_{z_r\to z_s};\\
&H_{z_r\to \ddot{z}_s} = -\omega^2 \cdot H_{z_r\to z_s};\\
&H_{z_r\to \Delta F_{sz}} = \{\Delta F_{sz} = c_s\cdot(z_u - z_s) + d_s\cdot(\dot{z}_u - \dot{z}_s)\} =\\
&\qquad = c_s\cdot\left(H_{z_r\to z_u} - H_{z_r\to z_s}\right) + d_s\cdot j\cdot\omega\cdot\left(H_{z_r\to z_u} - H_{z_r\to z_s}\right) =\\
&\qquad = (c_s + j\cdot d_s\cdot\omega)\cdot\left(H_{z_r\to z_u} - H_{z_r\to z_s}\right);\\
&H_{z_r\to \Delta F_{rz}} = \{\Delta F_{rz} = c_t\cdot(z_r - z_u)\} = c_t\cdot\left(H_{z_r\to z_r} - H_{z_r\to z_u}\right) = c_t\cdot\left(1 - H_{z_r\to z_u}\right);
\end{aligned}
\qquad [5.49]
$$

The transfer functions in Equation [5.49] are plotted in Figure 5-13.

5.4.3.1.1 Example Analysis

If we use Figure 5-13 as the example in 0:

- Ride comfort related: $\left|H_{z_r\to \ddot{z}_s}(v_x)\right| \approx 123;\ \Rightarrow |\hat{a}| = 123\cdot\hat{z}_r = 123\cdot 0.01 = 1.23\ m/s^2;$. From this we can calculate $RMS(\ddot{z}_s) = |1.23|/\sqrt{2} \approx 0.8697\ m/s^2$.
- Fatigue life related: $\left|H_{z_r\to z_u-z_s}(v_x)\right| \approx 1.14;\ \Rightarrow\ |\hat{z}_u - \hat{z}_s| = 1.14\cdot\hat{z}_r = 1.14\cdot 0.01 = 0.0114\ m = 1.14\ cm;$.
- Road grip related: $\left|H_{z_r\to \Delta F_{rz}}(v_x)\right| \approx 177470;\ \Rightarrow\ |\Delta F_{rz}| = 177470\cdot\hat{z}_r = 177470\cdot 0.01 = 1775\ N;$.

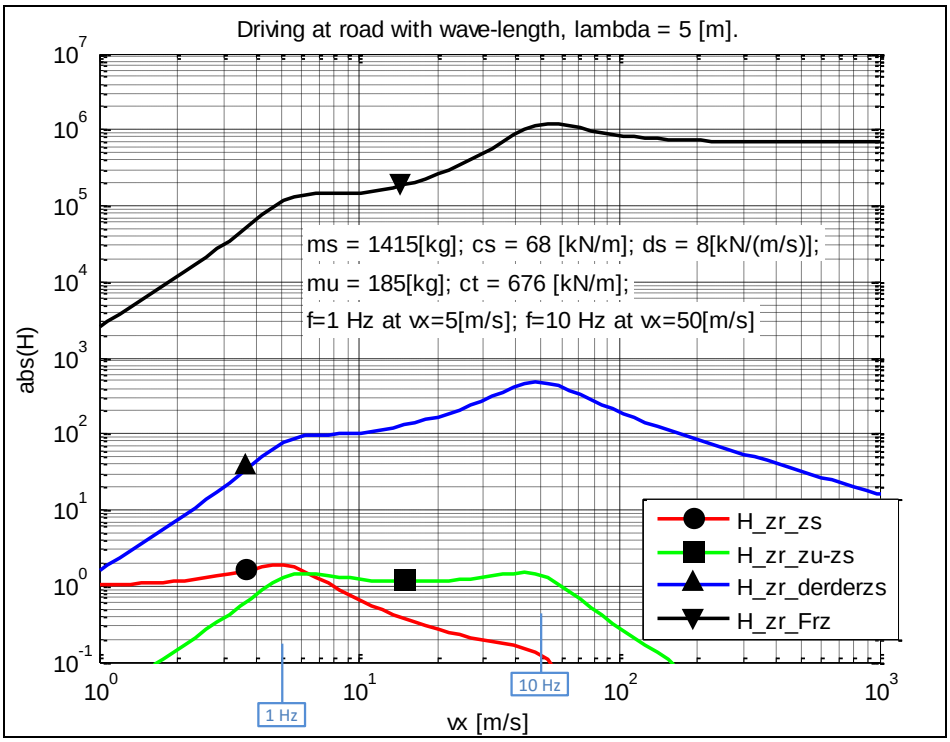

Figure 5-13: Transfer functions for amplitudes from model in Figure 5-12, excited with single frequencies.

This analysis can be compared with the analysis in 5.4.2.1.1. Ride comfort and fatigue does not change a lot, but road grip does. This indicates that the more advanced model is only needed for road grip evaluation.

Figure 5-14 shows the phase angles for the different responses.

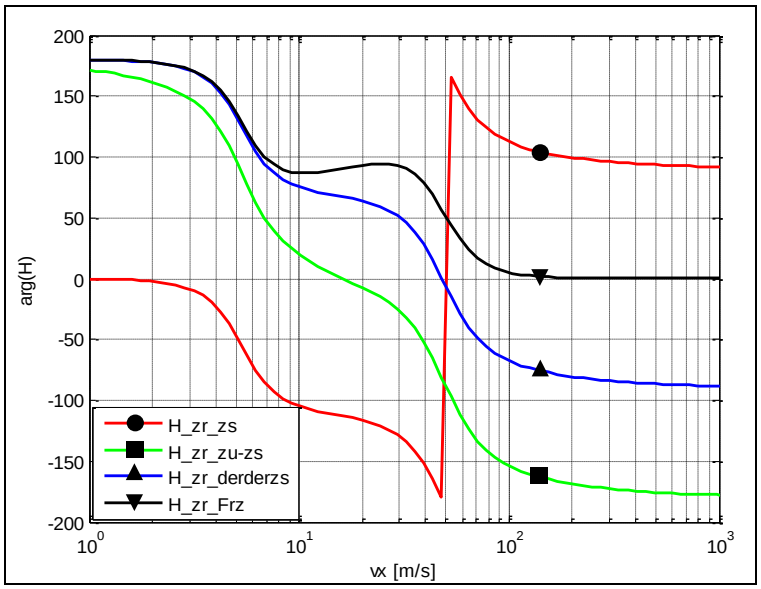

Figure 5-14: Transmission functions for phase delays. Same model and data as in Figure 5-13.

Figure 5-15, shows the amplitude gains for the corresponding un-damped system. Natural frequencies are around 5 m/s and 50 m/s. These two speeds correspond to frequencies $v_{x,crit}/\lambda$, i.e. approximately 1 Hz and 10 Hz. The 1Hz frequency is an oscillation mode where the both masses move in phase with each other, the so called "heave mode" or "bounce mode". The 10 Hz frequency comes from the mode where the masses are in counter-phase, the so called "wheel hop mode". In the wheel hop mode, the sprung mass is almost not moving at all. We will come back to these modes in 5.4.4.

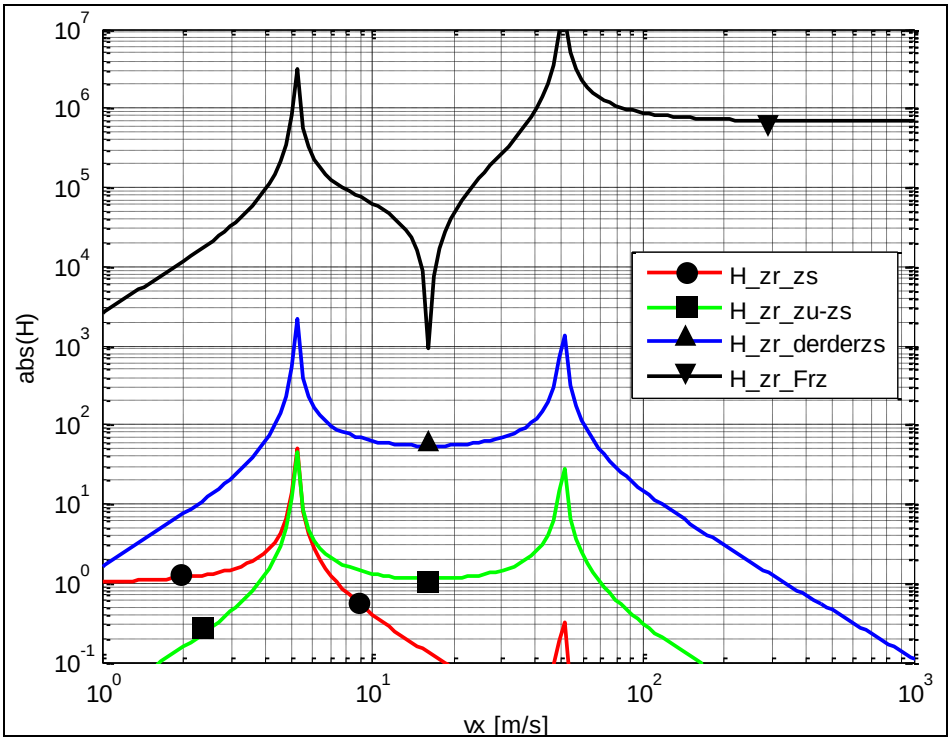

Figure 5-15: Un-damped transfer functions. Same model and data as in Figure 5-13, except $d_s = 0$.

5.4.4 One-Mode Models

The sprung mass is typically around 10 times larger than the unsprung mass and the suspension spring is usually around 10 times lower than the tyre stiffness. Hence, there are the 2 distinguished modes, identified in 0. If only interested in a certain frequency range around one of the eigenfrequencies, one can split the model in 2 models, which explains one mode each, see Figure 5-16.

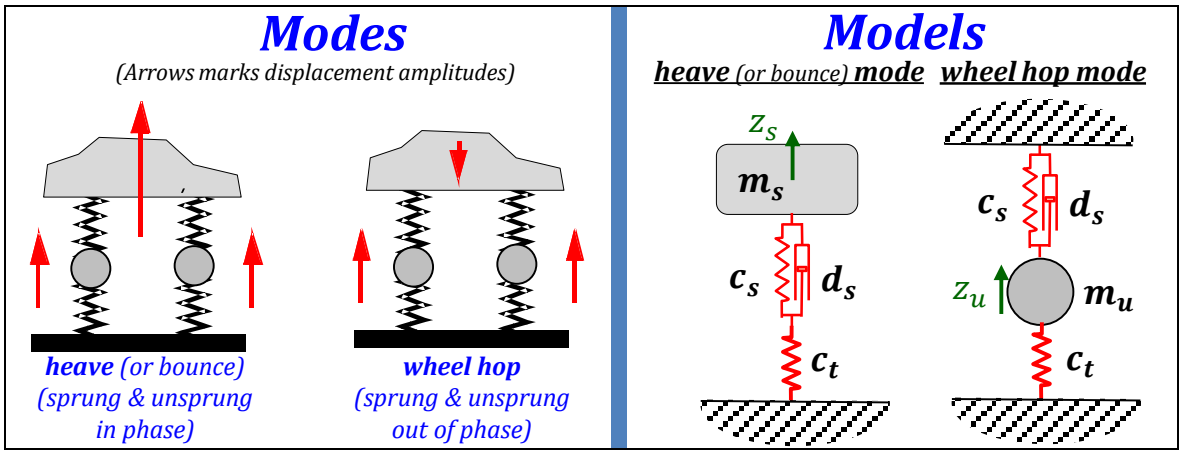

Figure 5-16: Modes and approximate models.

We will now derive the natural frequencies for the two models and compared with the natural frequencies ($d_s = 0$) found for the combined model, in Figure 5-15. Both models are one degree of freedom models with mass and spring, why the eigenfrequency is $\sqrt{\text{stiffness/mass}}$.

For the heave model, the mass is m_s. Stiffnesses c_s and c_t are series connected, which means that the total stiffness$= 1/\big((1/c_s) + (1/c_t)\big)$.

For the wheel hop model, the mass is m_u. Stiffnesses c_s and c_t are parallel connected, which means that the total stiffness$= c_s + c_t$.

$$\omega_{Bounce} = \sqrt{\frac{1/\left(\frac{1}{c_s}+\frac{1}{c_t}\right)}{m_s}} = 6.61\,\frac{\text{rad}}{\text{s}} = 1.05\text{ Hz};\ \omega_{WheelHop} = \sqrt{\frac{c_s+c_t}{m_u}} = 63.4\,\frac{\text{rad}}{\text{s}} = 10.1\text{ Hz};\quad [5.50]$$

Numerical values from 5.4.3 is used ($m_s = 1415\ kg; m_u = 185\ kg; c_s = 68\ kN/m; c_t = 676\ kN/m;$) and eigenfrequencies coincide well with Figure 5-15.

Heave (or Bounce) refers to the mode where the sprung mass has the greatest amplitude and wheel hop is related to the case when the unsprung mass exhibits the greatest amplitude. For a passenger car, the spring mass has the lowest frequency, typically around 1 Hz while tyre hop is more prevalent at frequencies around 10 Hz.

5.5 Functions for Stationary Oscillations

5.5.1 Ride Comfort *

Function definition: ***(Stationary) Ride comfort*** *is the comfort that vehicle occupants experience from stationary oscillations when the vehicle travels over a road with certain vertical irregularity in a certain speed. The measure is defined at least including driver (or driver seat) vertical acceleration amplitudes.*

Ride comfort is sometimes divided into:

- ***Primary Ride*** – the vehicle body on its suspension. Heave (Bounce), Pitch and Roll ≈0..4 Hz
- ***Secondary Ride*** – same but above body natural frequencies, i.e. ≈4..25 Hz

5.5.1.1 Single Frequency

It is generally accepted for stationary vibrations, that humans are sensitive to the RMS value of the acceleration. However, the sensitivity is frequency dependent, so that highest discomfort appears for a certain range of frequencies. Some human tolerance curves are shown in Figure 5-17 and Figure 5-18.

The curves can be considered a threshold for acceptance where everything above the line is unacceptable and points below the curve are acceptable. Discomfort is a subjective measure, and this is why the different diagrams cannot be directly compared to each other. The SAE has suggested that

frequencies from 4 to 8 Hz are the most sensitive and the accepted accelerations for these are no higher than 0.025 g (RMS).

The curves in Figure 5-17 mostly represent an extended exposure to the vibration. As one can expect, a human can endure exposure to more severe conditions for short periods of time. The SAE limits presented are indicative of 8 hours of continuous exposure. Curves for different exposure times can also be obtained from ISO, (ISO 2631). The ISO curves are from the first version of ISO 2631 and were later modified, see Figure 5-18.

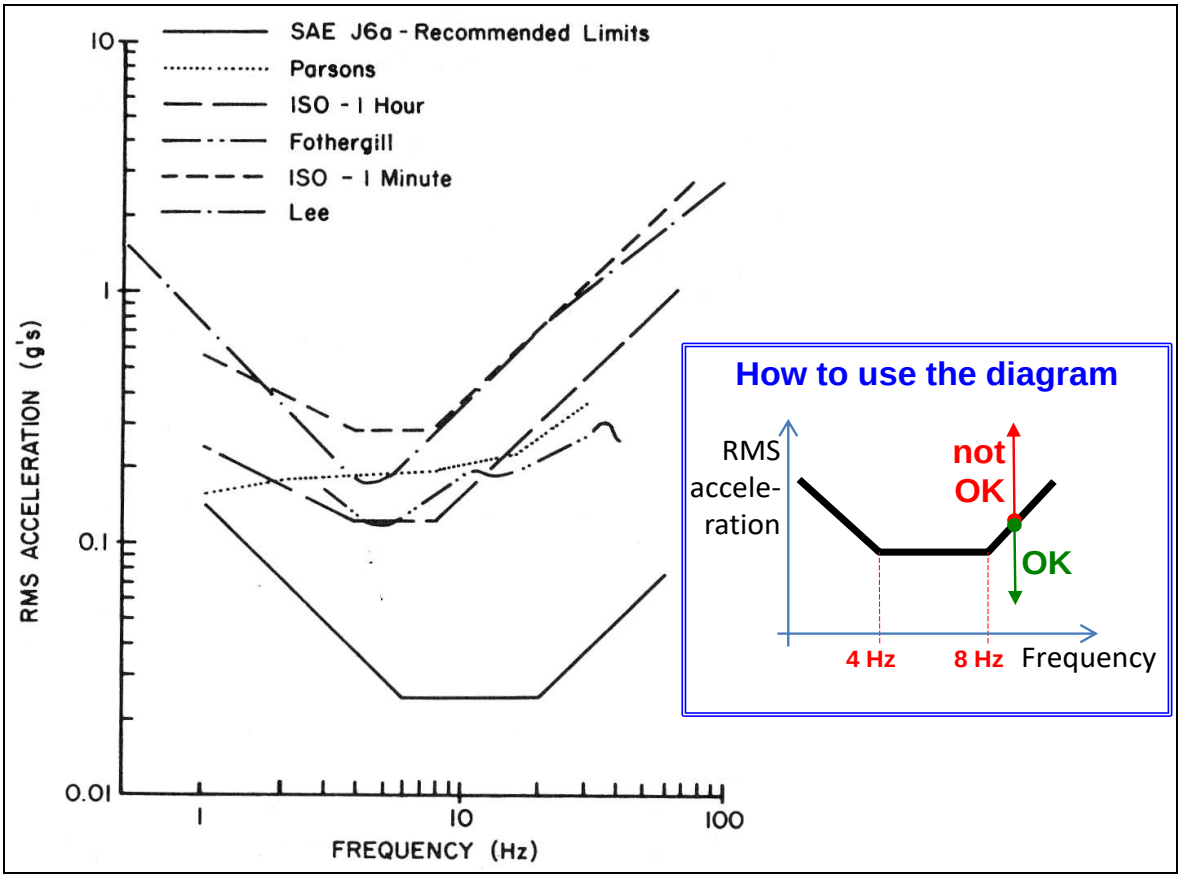

Figure 5-17: Various Human Tolerance Curves to Vertical Vibration, (Gillespie, 1992)

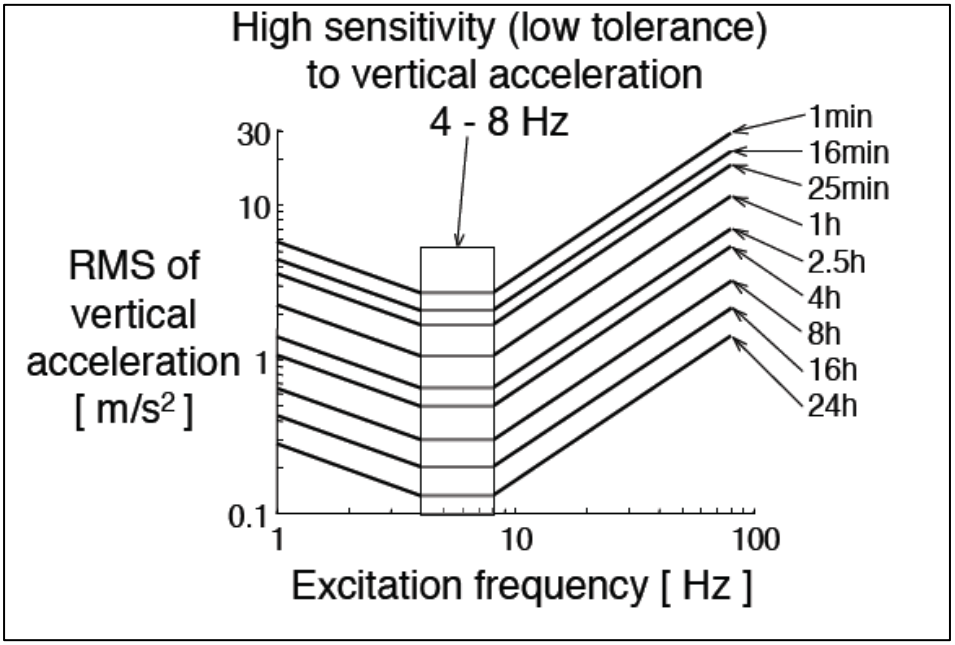

Figure 5-18: ISO 2631 Human Tolerance Curves

5.5.1.2 Multiple Frequencies

The curves in Figure 5-17 and Figure 5-18 can be interpreted as a filter, where the response of the human is influenced by the frequencies they are exposed to. This leads to the concept of a Human Filter Function $W_k(f)$. (W_k refers to vertical whole human body vibration sensitivity, while there are other for sensitivities for other directions and human parts.) This can be seen as a transfer function from driver seat to somewhere inside the driver's body or brain, where discomfort is perceived.

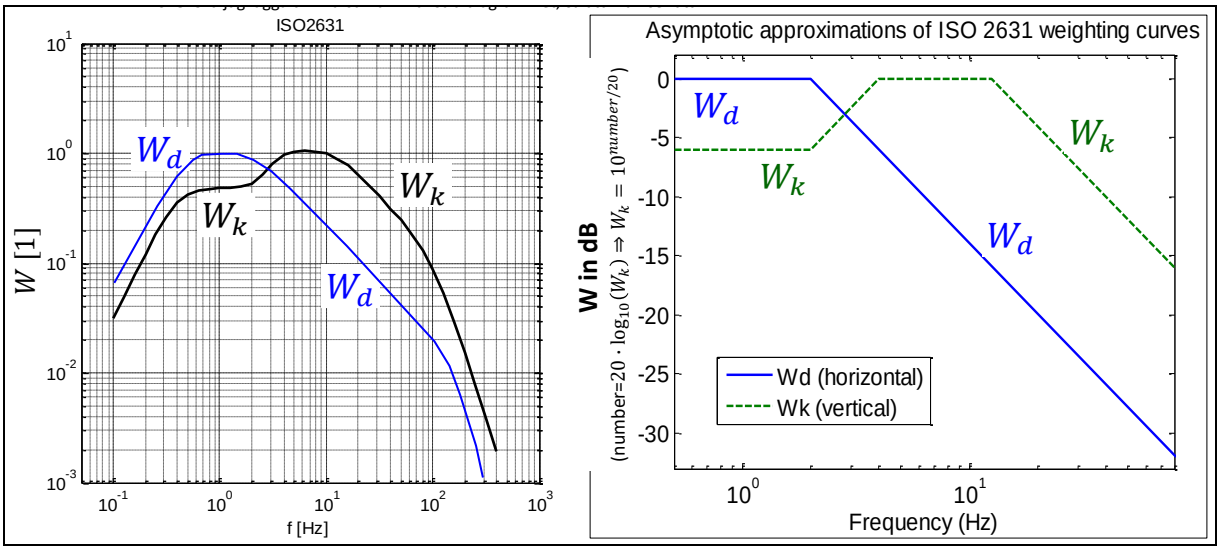

Figure 5-19: Human Sensitivity Filter Function. From (ISO 2631). Right: Asymptotic approximation

Frequency f Hz	W_k factor × 1 000	W_k dB
0,02		
0,025		
0,031 5		
0,04		
0,05		
0,063		
0,08		
0,1	31,2	– 30,11
0,125	48,6	– 26,26
0,16	79,0	– 22,05
0,2	121	– 18,33
0,25	182	– 14,81
0,315	263	– 11,60
0,4	352	– 9,07
0,5	418	– 7,57
0,63	459	– 6,77
0,8	477	– 6,43
1	482	– 6,33
1,25	484	– 6,29
1,6	494	– 6,12
1,6	494	– 6,12
2	531	– 5,49
2,5	631	– 4,01
3,15	804	– 1,90
4	967	– 0,29
5	1 039	0,33
6,3	1 054	0,46
8	1 036	0,31
10	988	– 0,10
12,5	902	– 0,89
16	768	– 2,28
20	636	– 3,93
25	513	– 5,80
31,5	405	– 7,86
40	314	– 10,05
50	246	– 12,19
63	186	– 14,61
80	132	– 17,56
100	88,7	– 21,04
125	54,0	– 25,35
160	28,5	– 30,91
200	15,2	– 36,38
250	7,90	– 42,04
315	3,98	– 48,00
400	1,95	– 54,20

Figure 5-20: Human Filter Function for vertical vibrations. Table from (ISO 2631).

With formulas from earlier in this chapter we can calculate an RMS value of a signal with multiple frequencies, see Equation [5.6]. Consequently, we can calculate RMS of multiple frequency acceleration. Since humans are sensitive to acceleration, it would give one measure of human discomfort. However, to get a measure which is useful for comparing accelerations with different frequency content, the measure has to take the human filter function into account. The Weighted RMS Acceleration, a_w, in the following formula is such measure:

$$a_w = a_w\big(\ddot{z}(t)\big) = \left\{ use: RMS\big(\ddot{z}(t)\big) = \sqrt{\sum_{i=1}^{N} \frac{\hat{\ddot{z}}_i^{\,2}}{2}} \right\} = \sqrt{\sum_{i=1}^{N} \frac{\big(W_k(\omega_i)\cdot \hat{\ddot{z}}_i\big)^2}{2}}; \quad \text{or}$$

$$a_w = a_w\big(\ddot{z}(t)\big) = \left\{ use: RMS\big(\ddot{z}(t)\big) = \sqrt{\int_{\omega=0}^{\infty} G_{\ddot{z}}(\omega)\cdot d\omega} \right\} = \sqrt{\int_{\omega=0}^{\infty} \big(W_k(\omega)\big)^2 \cdot G_{\ddot{z}}(\omega)\cdot d\omega}\,; \qquad [5.51]$$

Equation [5.51] is written for a case with only vertical vibrations, hence W_k and $G_{\ddot{z}}$. If vibrations in several directions, a total a_w can still be calculated, see (ISO 2631).

In (ISO 2631) one can also find the following equation, which weights together several time periods, with different vibrations spectra. Time averaged whole-body vibration exposure value is denoted $a_{w,av}$.

$$a_{w,av} = \sqrt{\frac{\sum_i {a_{wi}}^2 \cdot T_i}{\sum_i T_i}}; \qquad [5.52]$$

The a_w in Eq [5.52] is used both for vehicle customer requirement setting at OEMs and governmental legislation. One example of legislation is (DIRECTIVE 2002/44/EC, 2002). This directive stipulates that a_w in Eq [5.52] in any direction, normalized to 8 hours, may not exceed 1.15 m/s², and if the value exceeds 0.5 m/s² action must be taken.

5.5.1.2.1 Certain Combination of Road, Vehicle and Speed

Now we can use Equation [5.36] without assuming road type. However, we have to identify $\hat{\ddot{z}}_s$ and multiply it with $W_k(\omega)$, according to Equation [5.51]. Then we get [5.53].

Using Equation [5.53], we can calculate the weighted RMS value for the different models in 5.4.1, 5.4.2 and 5.4.3. For each model, it will vary with speed, v_x. A plot, assuming a certain road type ("Rough" from Figure 5-5) is shown in Figure 5-28. We can see that the simplest model "*stiff tyre, no unsprung mass*" gives much different comfort value than the two others, so the simplest is not goof to estimate comfort. However, the two other models give approximately same result, which indicates that the medium model, "*stiff tyre, no unsprung mass*", is enough for comfort evaluation. This is no general truth but an indication that the most advanced model, "*two masses, elastic tyre*", is not needed for comfort on normal roads. The advanced model is more needed for road grip.

We can also see that the comfort decreases, the faster the vehicle drives. If we read out at which speed we reach $a_w = 1\ m/s^2$ (which is a reasonable value for long time exposure) we get around $v_x \approx 70\ m/s \approx 250\ km/h$ on this road type ("Rough") with the medium (and advanced) model. With the simplest model, we get $v_x \approx 1\ m/s \approx 3..4\ km/h$.

$$RMS(\ddot{z}_s) = \left\{ \begin{matrix} \text{Eq} \\ [5.31] \end{matrix} \right\} = \sqrt{\frac{\Phi_0}{{\Omega_0}^{-w}} \cdot {v_x}^{w-1} \cdot \int_{\omega=0}^{\infty} \left|H_{z_r\to\ddot{z}_s}(\omega)\right|^2 \cdot \omega^{-w}\cdot d\omega} = \left\{ \begin{matrix} H_{z_r\to\ddot{z}_s} = \\ = -\omega^2 \cdot H_{z_r\to z_s} \end{matrix} \right\}$$

$$= \sqrt{\frac{\Phi_0}{{\Omega_0}^{-w}} \cdot {v_x}^{w-1} \cdot \int_{\omega=0}^{\infty} \left|\omega^2 \cdot H_{z_r\to z_s}(\omega)\right|^2 \cdot \omega^{-w}\cdot d\omega} =$$

$$= \sqrt{\frac{\Phi_0}{{\Omega_0}^{-w}} \cdot {v_x}^{w-1} \cdot \int_{\omega=0}^{\infty} \left|H_{z_r\to z_s}(\omega)\right|^2 \cdot \omega^{4-w}\cdot d\omega}\,; \Rightarrow \left\{ \begin{matrix} \text{Eq} \\ [5.51] \end{matrix} \right\} \Rightarrow$$

$$\Rightarrow a_w = \sqrt{\frac{\Phi_0}{{\Omega_0}^{-w}} \cdot {v_x}^{w-1} \cdot \int_{\omega=0}^{\infty} \big(W_k(\omega)\big)^2 \cdot \left|H_{z_r\to z_s}(\omega)\right|^2 \cdot \omega^{4-w}\cdot d\omega}\,; \qquad [5.53]$$

5.5.1.3 Other Excitation Sources

Present chapter focuses on the influence of excitation from vertical displacement of the road. Examples of other, but often co-operating, excitation sources are:

- Powertrain vibrations, non-uniform rotation in engine. Frequencies will be proportional to engine speed
- Wheel vibrations, e.g. due to non-round wheels or otherwise unbalanced wheels. Frequencies will be proportional to vehicle speed.
- Special machineries mounted on vehicles (e.g. climate systems or concrete mixers)

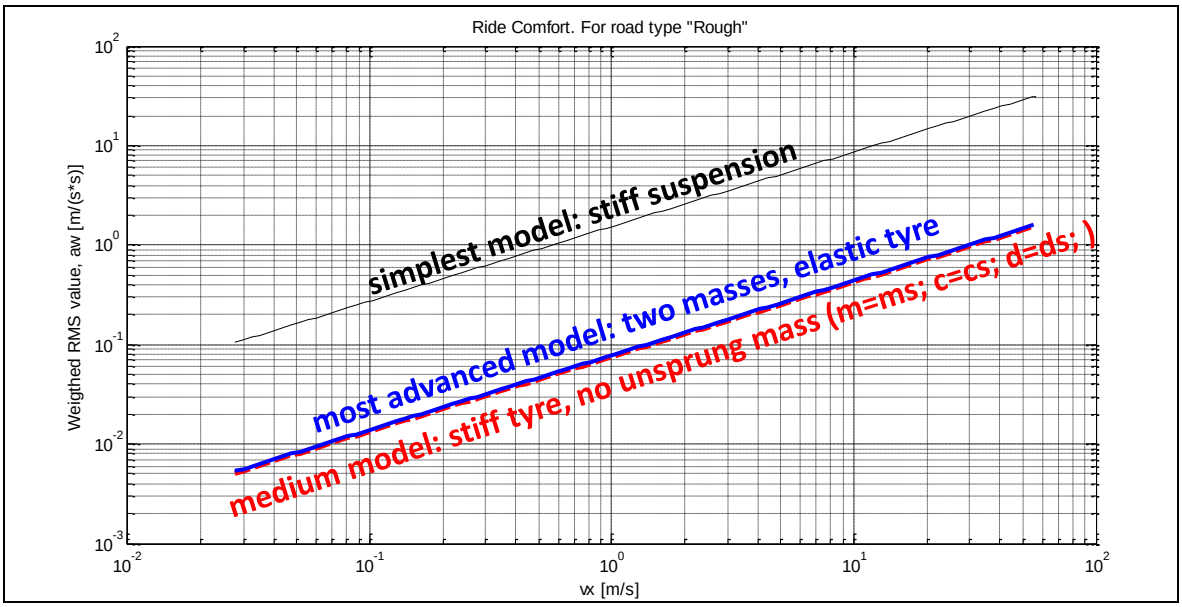

Figure 5-21: Weighted RMS values for road type "Smooth" from Figure 5-5. The 3 curves show 3 different models: Simplest (from 1.5.1), Medium (from 1.5.2) and Most advanced (from 1.5.3).

5.5.2 Fatigue Life *

> *Function definition:* ***(Vehicle) Fatigue life*** *is the life that the vehicle, mainly suspension, can reach due to stationary oscillations when vehicle travels over a road with certain vertical irregularity in a certain speed. One measure is the suspension vertical deformation amplitude.*

Beside human comfort, the fatigue of the vehicle structure itself is one issue to consider in vertical vehicle dynamics.

5.5.2.1 Single Frequency

5.5.2.1.1 Loads on Suspension Spring

In particular, the suspension spring may be subject to fatigue. The variation in spring material stress is dimensioning, which is why the force variation or amplitude in the springs should be under observation. Since spring force is proportional to deformation, the suspension deformation amplitude is proposed as a good measure (at least if spring design is not varied). This is the explanation to why the amplitude of $z_u - z_s$ is plotted in Figure 5-10.

Beside fatigue loads, $z_u - z_s$ is also relevant for judging whether suspension bump-stops become engaged or not. At normal driving, that limit should be far from reached, except possibly at high loads (many persons/much payload).

It can be noted that $z_u - z_s$ represents the variation in material stress only if spring is not changed. So, if different spring designs are compared, it is not sufficient to study only $z_u - z_s$.

5.5.2.1.2 Fatigue of Other Components

Fatigue of other parts may require other amplitudes.

One other example can be the damper fatigue. Damper fatigue would be more relevant to judge from amplitude of $\dot{z}_u - \dot{z}_s$, which determines the force level and hence the stress level.

Another example is to judge the force amplitude in parts that carry both spring and damper forces. For those it is motivated to consider $\Delta F_{sz} = c_s \cdot (z_u - z_s) + d_s \cdot (\dot{z}_u - \dot{z}_s)$; as in Eq [5.49].

Yet another example is the load of the road itself. For heavy trucks, it is relevant to consider how much they wear the road. At some roads with legislated maximum (static) axle load, one can be allowed to exceed that limit if the vehicle has especially road friendly suspensions. For these judgements, it is the contact force between tyre and road, $\hat{F}_{rz}$, which is important. These considerations are primarily for road authorities but becomes aspects for vehicle developers as legal requirements.

5.5.2.2 Multiple Frequencies

If the excitation is of one single frequency, the stress amplitude can be used when comparing two designs. However, for spectra of multiple frequencies, one cannot look at amplitudes solely, $[\hat{z}_1, \hat{z}_2, \cdots, \hat{z}_N]$, because the amplitudes will depend on how the discretization is done, i.e. the number N. Some kind of integral of a spectral density is more reasonable. In this compendium, it is proposed that a very approximate measure of fatigue load is calculated as follows, exemplified for the case of fatigue of the spring:

$$\begin{aligned} &Measure\ for\ spring\ fatigue\ life = RMS\big(z_u(t) - z_s(t)\big) = \\ &= \sqrt{\frac{\Phi_0}{\Omega_0{}^{-w}} \cdot v_x{}^{w-1} \cdot \int_{\omega=0}^{\infty} \left|H_{z_r \to z_u - z_s}(\omega)\right|^2 \cdot \omega^{-w} \cdot d\omega} = \begin{Bmatrix} use: H_{z_r \to z_u - z_s} = \\ = H_{z_r \to z_u} - H_{z_r \to z_s} \end{Bmatrix} = \\ &= \sqrt{\frac{\Phi_0}{\Omega_0{}^{-w}} \cdot v_x{}^{w-1} \cdot \int_{\omega=0}^{\infty} \left|H_{z_r \to z_u}(\omega) - H_{z_r \to z_s}(\omega)\right|^2 \cdot \omega^{-w} \cdot d\omega}\,; \end{aligned} \qquad [5.54]$$

Equation is written for application to a known road spectra (Φ_0, w) and vehicle dynamic structure ($H_{z_r \to z_u}, H_{z_r \to z_s}$), but the first expression ($RMS\big(z_u(t) - z_s(t)\big)$) is applicable on a measured or simulated time domain solution.

5.5.3 Road Grip *

Function definition: ***Road grip (on undulated roads)*** *is how well the longitudinal and lateral grip between tyres and road is retained due to stationary oscillations when the vehicle travels over a road with certain vertical irregularity in a certain speed.*

In **3.3** and **3.4**, the brush model explain how the tyre forces in the ground plane appears. It is a physical model where the contact length influences how stiff the tyre is for longitudinal and lateral slip. There is also a brief description of relaxation models for tyres. This together motivates that a tyre has more difficult to build up forces in ground plane if the vertical force varies. We can understand it as when contact length varies, the shear stress builds up has to start all over again. As an average effect, the tyre will lose more and more grip, the more the vertical force varies.

5.5.3.1 Multiple Frequencies

If the excitation is of one single frequency, the stress amplitude can be used when comparing two designs. However, for spectra of multiple frequencies, one cannot look at amplitudes solely, $[\hat{z}_1, \hat{z}_2, \cdots, \hat{z}_N]$, because the amplitudes will depend on how the discretization is done, i.e. the number N. Some kind of integral of a spectral density is more reasonable. In this compendium, it is proposed that a very approximate measure of road grip is calculated as follows:

$$Measure\ for\ (bad)road\ grip = RMS\left(\Delta F_{rz}(t)\right) =$$
$$= \sqrt{\frac{\Phi_0}{{\Omega_0}^{-w}} \cdot {v_x}^{w-1} \cdot \int_{\omega=0}^{\infty} \left|H_{z_r \to \Delta F_{rz}}(\omega)\right|^2 \cdot \omega^{-w} \cdot d\omega} =$$
$$= \left\{use\text{: } H_{z_r \to z_u - z_s} = c_t \cdot \left(1 - H_{z_r \to z_u}\right)\right\} =$$
$$= \sqrt{\frac{\Phi_0}{{\Omega_0}^{-w}} \cdot {v_x}^{w-1} \cdot \int_{\omega=0}^{\infty} \left|c_t \cdot \left(1 - H_{z_r \to z_u}\right)\right|^2 \cdot \omega^{-w} \cdot d\omega}\,; \qquad [5.55]$$

Equation is written for application to a known road spectrum (Φ_0, w) and vehicle dynamic structure ($H_{z_r \to z_u}$), but the first expression ($RMS\left(\Delta F_{rz}(t)\right)$) is applicable on a measured or simulated time domain solution.

5.5.4 Other Functions

Present chapter focuses on the functions, (vertical) ride comfort, fatigue and road grip. Examples of other functions are:

- An area of functions that encompasses the vertical dynamics is **Noise, Vibration, and Harshness – NVH**. It is similar to ride comfort, but the frequencies are higher, stretching up to sound which is heard by humans.
- **Ground clearance** (static and dynamic) between vehicle body and ground. Typically, important for off-road situations.
- **Longitudinal comfort**, due to drive line oscillations and/or vertical road displacements. Especially critical when driver cabin is separately suspended to the body. This is the case for heavy trucks.
- **Disturbances in steering wheel feel**, due to one-sided bumps. Especially critical for rigid steered axles. This is often the design of the front axle in heavy trucks.
- There are of course an infinite number of combined manoeuvres, in which functions with requirements can be found. Examples can be **bump during strong cornering** (possibly destabilizing vehicle) or **one-sided bump** (exciting both heave=bounce, pitch and roll modes). When studying such transients, the vertical dynamics is not enough to capture the comfort, but one often need to involve also **longitudinal** dynamics; the linkage with ant-dive/anti-squat geometry from Chapter **3** becomes important as well as tyre vertical (radial) deflection characteristics.
- Energy is dissipated in suspension dampers, which influence **energy consumption** for the vehicle. This energy loss is much related, but not same as, to (tyre) rolling resistance. Suspension characteristics do influence this energy loss, but it is normally negligible, unless driving very fast on very uneven road.

5.6 Variation of Suspension Design

The influence of design parameters on vehicle functions Ride comfort, Suspension fatigue and Road grip can now be made. E.g., it is important to not only use the transfer function, but also take the road and human sensitivity into account, which calls for different weighting for different frequencies.

Transfer function for the model in 5.4.3 is shown as dashed lines in

Figure 5-22. Same figure also shows the Road- and Human-weighted versions. Studying how these curves change with design parameters gives a quantitative understanding of how different suspension design parameters influence. Such variations will be done in 5.6.1 to 5.6.4.

There are two particular frequency intervals of the graphs to observe. These are the 2 peaks around the two the natural frequencies of the sprung and unsprung masses, the peak at lower frequency is mainly a resonance in heave mode, while the higher one is in wheel hop mode.

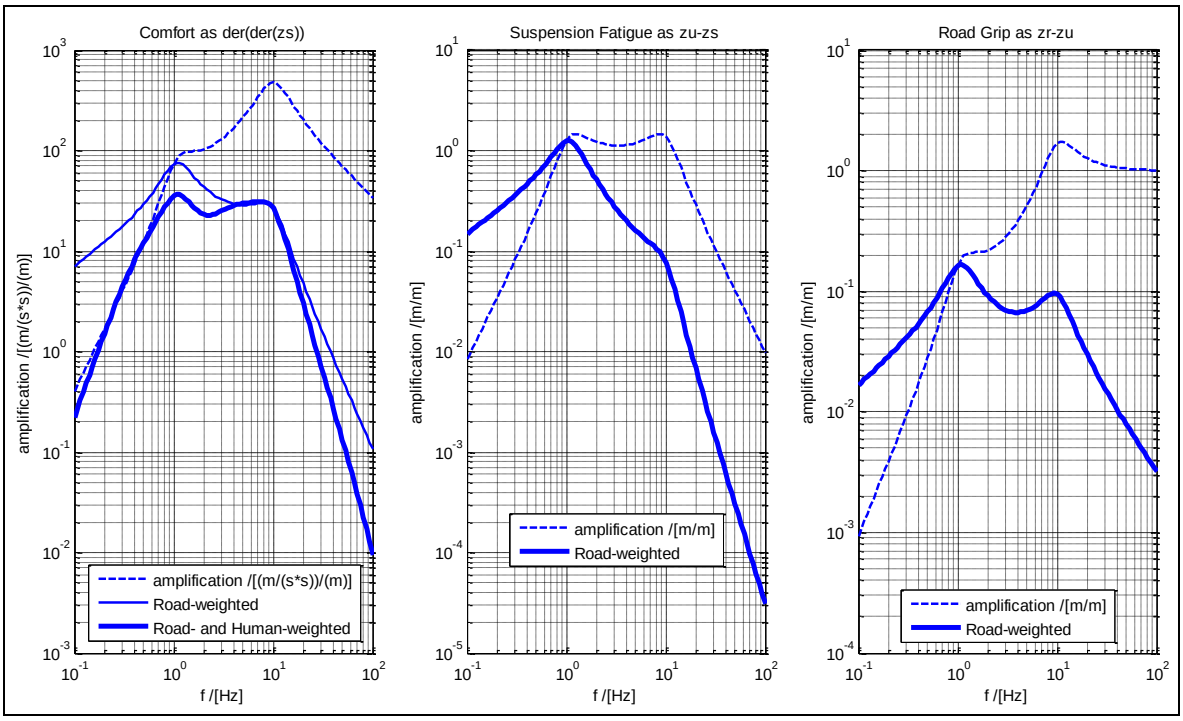

Figure 5-22: For a passenger car with $m_s = 1600\ [kg], m_u = 200\ [kg], c_s = 76\ [kN/m],\ d_s = 9\ [kN/(m/s)], c_t = 764\ [kN/m], d_t = 0$. Left is vertical acceleration (amplitude) of sprung mass for Ride Comfort. Middle is relative displacement (amplitude) between sprung and unsprung mass for Suspension Fatigue. Right is deformation (amplitude) of tyre spring for Road Grip. Weightings for typical road and for human sensitivity is shown.

5.6.1 Varying Suspension Stiffness

In Figure 5-23 the benefits of the low suspension stiffness (1 Hz) is seen for suspension travel and comfort without much change in the road grip performance.

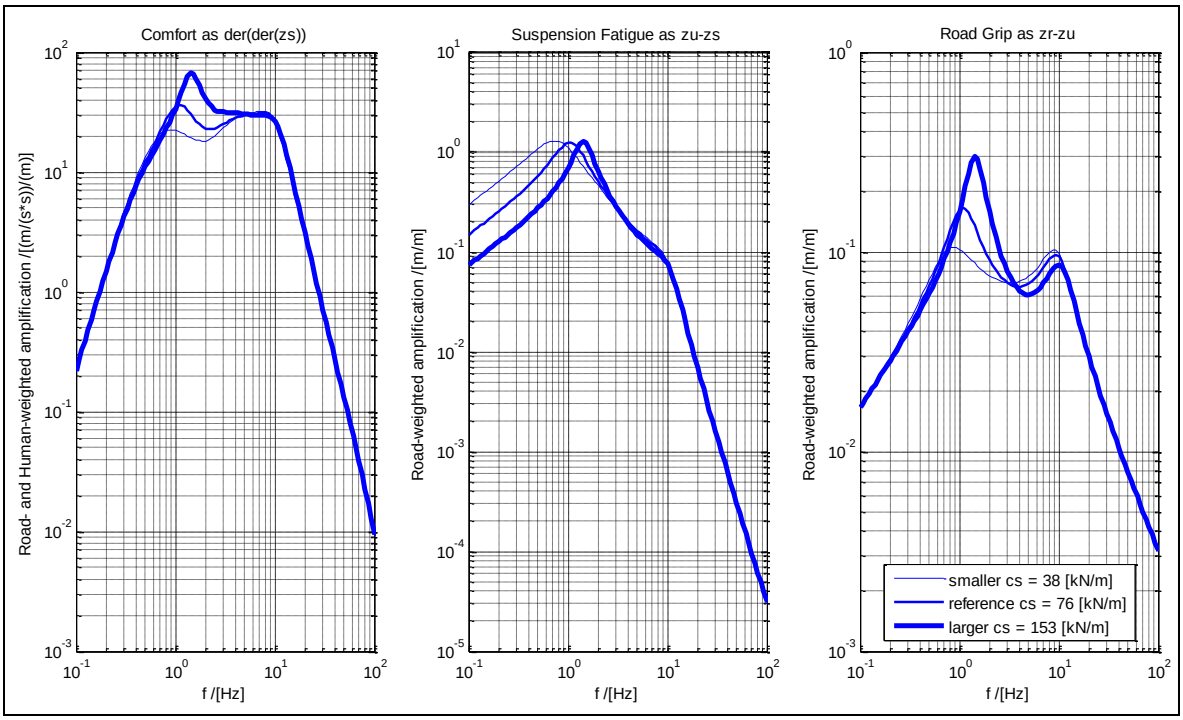

Figure 5-23: Result from varying suspension stiffness, c_s

Regarding Figure 5-23 and Figure 5-24 we see that there is a large influence of the acceleration gain at low frequencies with little change at the wheel hop and higher frequencies. The suspension stiffness and damping were seen to have little influence on the ride comfort / road grip response around 10 Hz.

5.6.2 Varying Suspension Damping

In Figure 5-24, we see that the changes in suspension damping have opposite effects for the heave and wheel hop frequency responses. High damping is good for reducing heave, but not so effective for wheel hop.

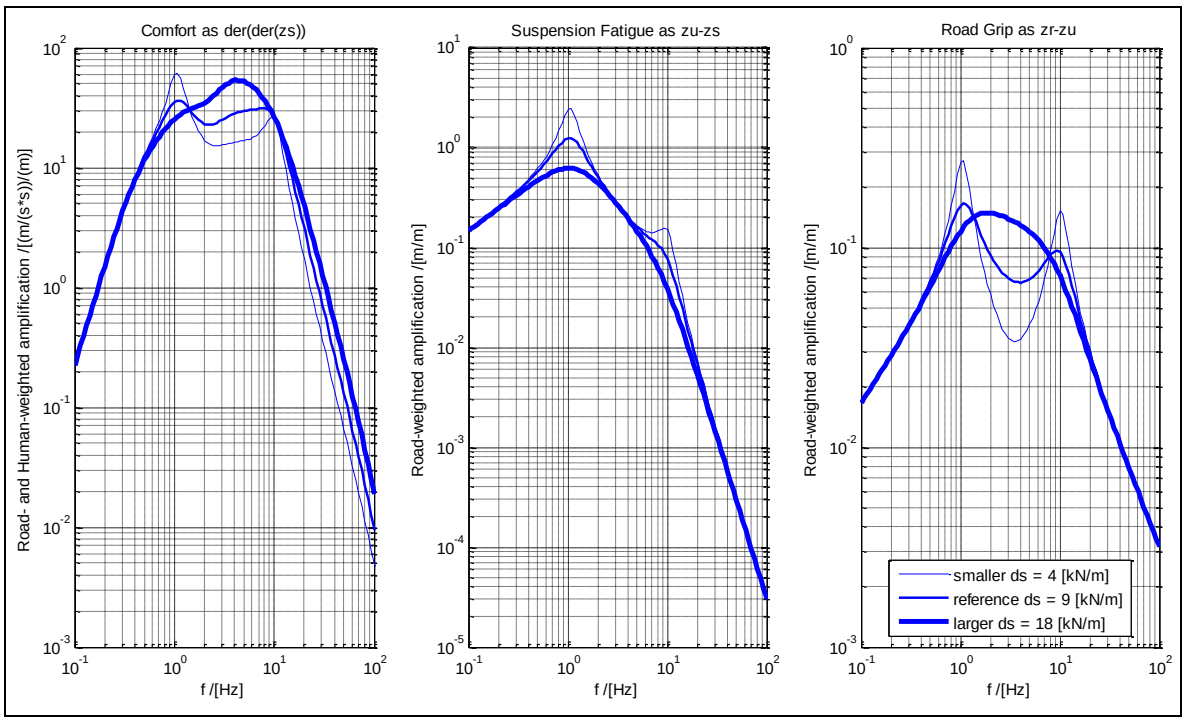

Figure 5-24: Result from varying suspension damping, d_s

5.6.3 Varying Unsprung Mass

In Figure 5-25, we see that if the response around the wheel hop frequency is to be changed, the unsprung mass is one of the most influential parameters. The unsprung mass is usually in the range of 10% of the sprung mass. Opposite to the suspension parameters, the unsprung mass influences frequencies around the wheel hop frequency with little influence around the heave frequency.

In Figure 5-25, the case with $m_u = 0$ is added. This is to demonstrate what a model with neglected mass gives and can be nearly compared with the model in 5.4.2.

5.6.4 Varying Tyre Stiffness

In Figure 5-26 a general observation is that low sprung mass natural frequencies are preferred for comfort considerations. Another parameter that has a strong affect near the wheel hop frequency is the tyre stiffness. The strongest response is noticed for the road grip function. (Note that, since c_t is now varying, we have to express road grip as $c_t \cdot (z_r - z_u)$; only $z_r - z_u$ does not give a fair comparison.)

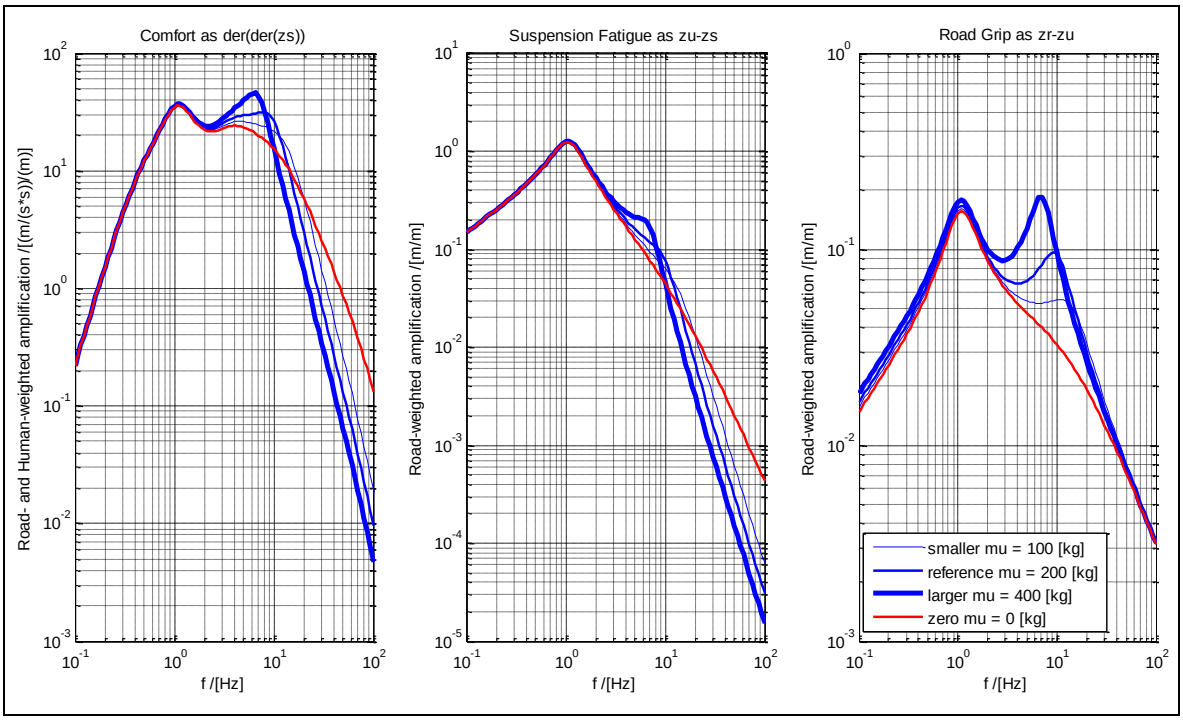

Figure 5-25: Result from varying unsprung mass, m_u

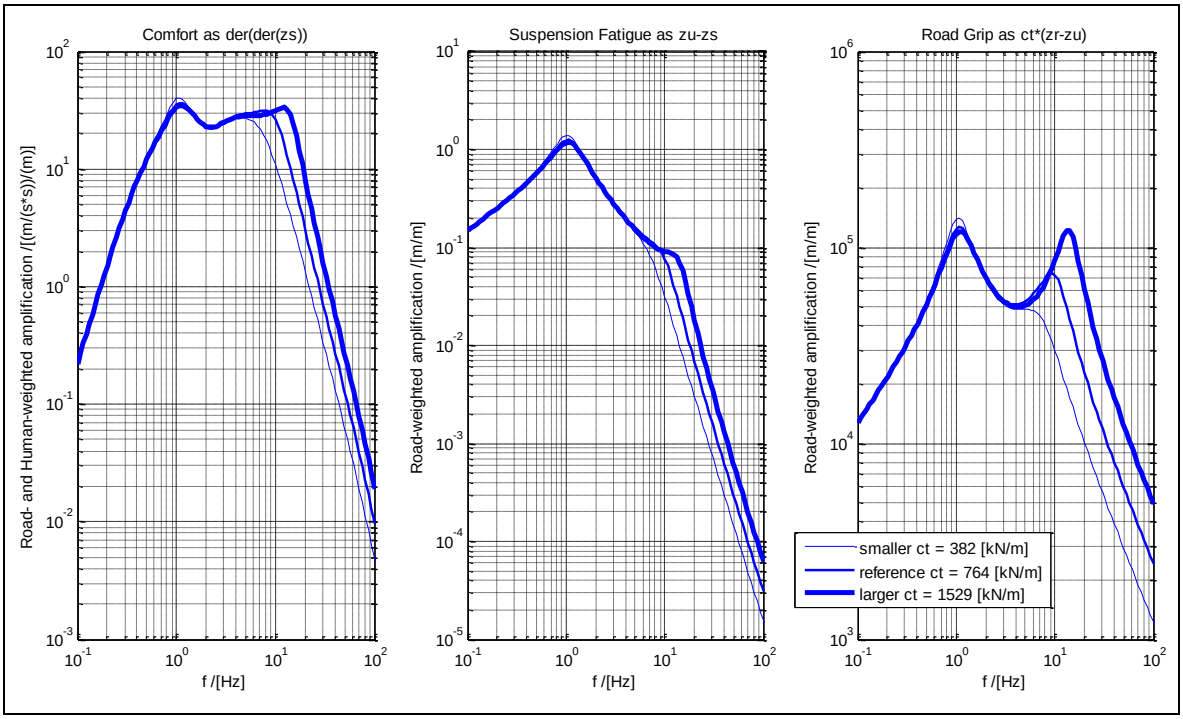

Figure 5-26: Result from varying Tyre Stiffness, c_t

5.7 Two Dimensional Oscillations

The one-dimensional model is useful for analysing the response of one wheel/suspension assembly. Some phenomena do connect other vehicle body motions than the vertical translation, especially pitch and roll. Here, other models are needed, such as Figure 5-28 and Figure 5-27.

5.7.1 Heave and Roll

A model like in Figure 5-27 is proposed. We have been studying Heave (bounce) and pitch before, in 4.3.9 and 4.5.2.3. Hence compare with corresponding model in Figur. In Chapter 4, the excitation was lateral tyre/axle forces, while the vertical displacement of the road was assumed to be zero. In vertical vehicle dynamics, it is the opposite. That means that the linkage geometry (roll centre or wheel pivot points) is not so relevant here. So, the model can be somewhat simpler.

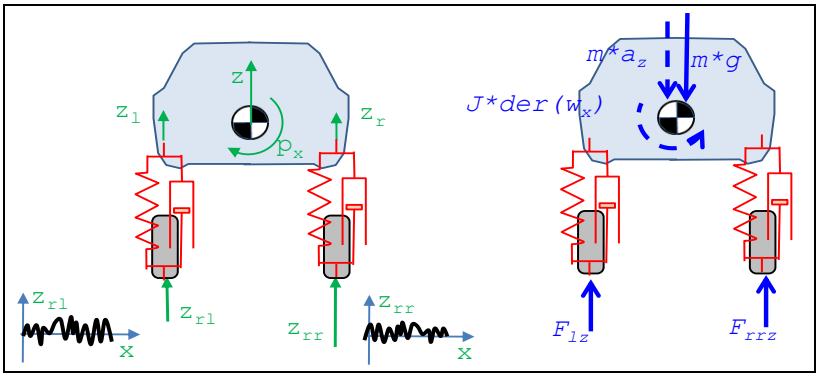

Figure 5-27: Heave and roll model. Anti-roll bar not drawn but can be included in equations in matrix ***C****.*

No equations are formulated for this model in this compendium, but a model will typically show two different modes, the heave and roll. Heave Eigen frequency is typically 1-1.5 Hz for a passenger car, as mentioned before. The roll frequency is similar or somewhat higher.

If modelling unsprung masses without inertia, we still get 2 state variables, heave z and roll φ_x. Using same mathematical form of equations as in Eq [5.45] we get this model (subscripts rl for "road left" and rr for "road right"):

$$\boldsymbol{M}\cdot\ddot{\boldsymbol{z}}+\boldsymbol{D}\cdot\dot{\boldsymbol{z}}+\boldsymbol{C}\cdot\boldsymbol{z}=\boldsymbol{D_r}\cdot\dot{\boldsymbol{z}}_{\boldsymbol{r}}+\boldsymbol{C_r}\cdot\boldsymbol{z_r};$$

$$where\ \boldsymbol{z}=\begin{bmatrix}z\\ \varphi_x\end{bmatrix}\ and\ \boldsymbol{z_r}=\begin{bmatrix}z_{rl}\\ z_{rr}\end{bmatrix};$$

The disturbances from the road are two independent ones, so the transfer functions will be a 2 × 2 matrix:

$$\begin{bmatrix}\mathcal{F}(z)\\ \mathcal{F}(\varphi_x)\end{bmatrix}=\boldsymbol{H}\cdot\begin{bmatrix}\mathcal{F}(z_{rl})\\ \mathcal{F}(z_{rr})\end{bmatrix}=\begin{bmatrix}H_{z_{rl}\to z} & H_{z_{rr}\to z}\\ H_{z_{rl}\to\varphi_x} & H_{z_{rr}\to\varphi_x}\end{bmatrix}\cdot\begin{bmatrix}\mathcal{F}(z_{rl})\\ \mathcal{F}(z_{rr})\end{bmatrix};$$

[5.56]

Note that the restoring matrix C might need to include both elastic restoring (wheel springs and anti-roll-bars) and pendulum effects, see 4.3.9.2 and Reference (Mägi, 1988). For high-loaded trucks, the pendulum effect is really relevant, while it often can be omitted for a low sportscar.

5.7.2 Heave and Pitch

A model like in Figure 5-28 is proposed. We have been studying heave (or bounce) and pitch before, in 3.4.5.2. Hence compare with corresponding model in Figure 3-28. In Chapter **3**, the excitation was longitudinal tyre forces, while the vertical displacement of the road was assumed to be zero. In vertical vehicle dynamics, it is the opposite. The importance of model with linkage geometry (pitch centre or axle pivot points above ground level) is that tyre forces are transferred correctly to the body. That means that the linkage geometry is not so relevant for vertical vehicle dynamics in Chapter 5. So, the model can be somewhat simpler.

A mathematical model would typically show two different modes, see Figure 5-29. The heave eigen-frequency is typically 1-1.5 Hz for a passenger car. The pitch frequency is somewhat higher.

We should reflect on that the models in 5.4 and 5.7.1 refer to the same bounce mode. But the models will most likely give different numbers of, e.g., Eigen frequency. A total model, with all degrees of freedom, would align those values, but the larger a model is the more data it produces which often leads to less easy design decisions.

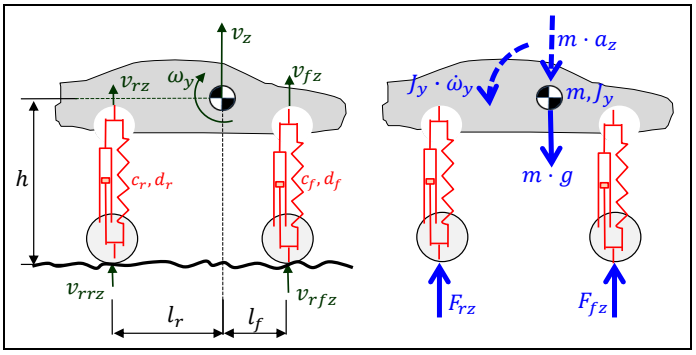

Figure 5-28: Heave and pitch physical model.

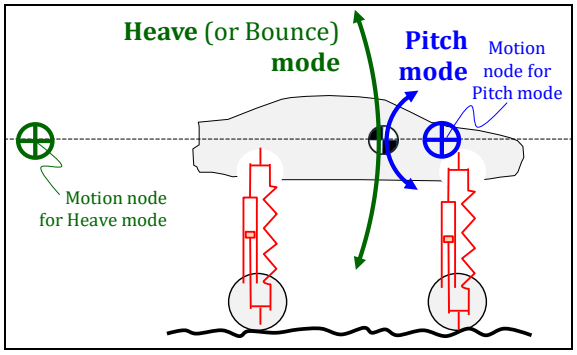

Figure 5-29: Oscillation modes of a Heave and Pitch model.

5.7.2.1 Wheel Base Filtering

See Figure 5-30. If the wheel base is an integer multiple of the wave length, only heave (bounce) will be excited. If wave length is in the middle between those, only pitch will be excited. This phenomenon is called "wheel base filtering".

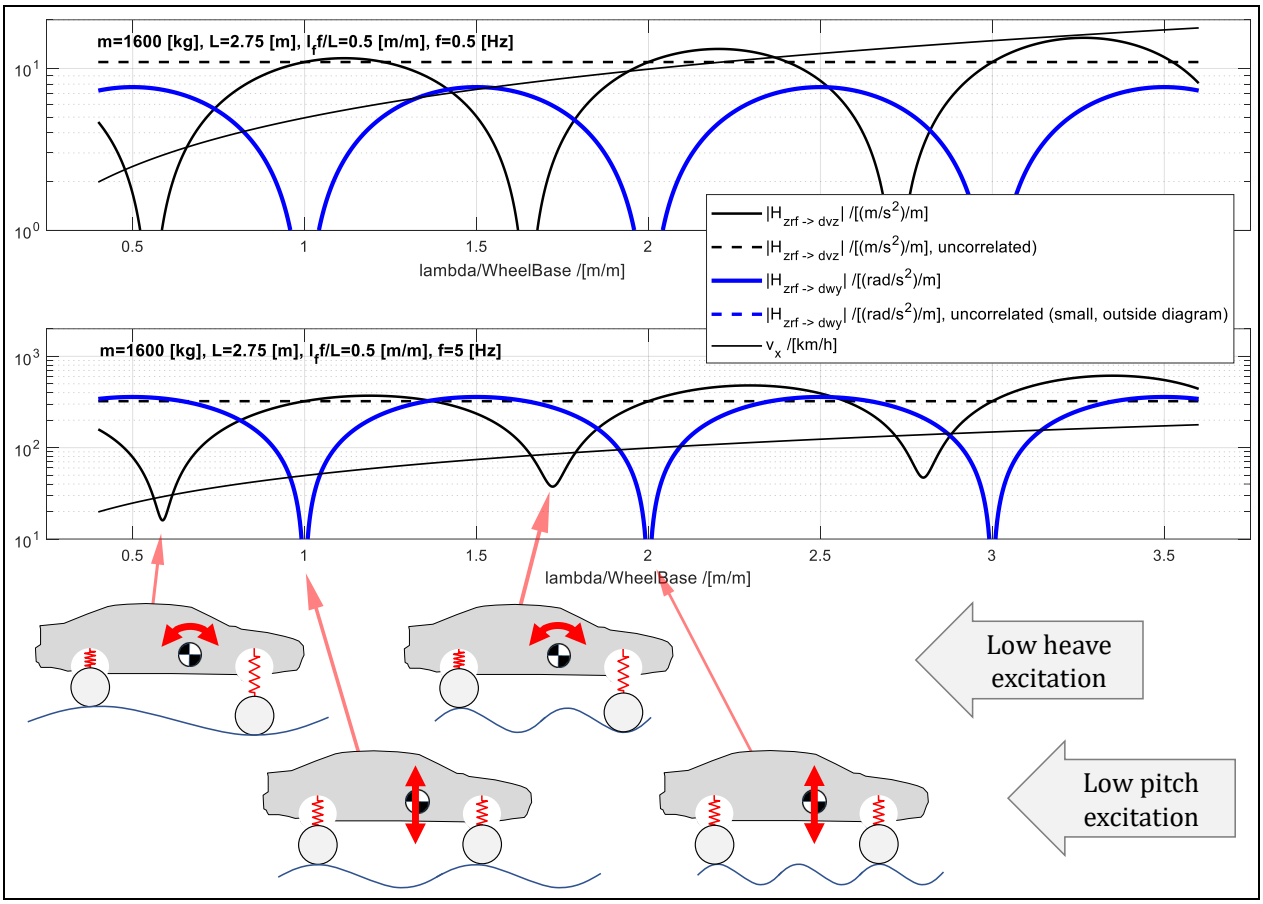

Figure 5-30: Wheel Base Filtering, as compared to "uncorrelated". Response $|H_{zrf \to vzg}|$ and $|H_{zrf \to \dot{\omega}y}|$. Two frequencies, 0.5 and 5 Hz. Varying Road Wavelengths, so also v_x has to vary.

5.7.2.2 Mathematical Model

From Figure 5-28 we can derive the following mathematical models:

Equilibrium: $F_{fz} + F_{rz} - m \cdot g - m \cdot a_z = 0; \quad and \quad -F_{fz} \cdot l_f + F_{rz} \cdot l_r - J_y \cdot \dot{\omega}_y = 0;$

Compatibility: $v_{fz} = v_z - l_f \cdot \omega_y; \quad and \quad v_{rz} = v_z + l_r \cdot \omega_y;$

Constitution: $F_{fz} = F_{fs} + d_f \cdot (v_{rfz} - v_{fz}); \quad and \quad \dot{F}_{fs} = c_f \cdot (v_{rfz} - v_{fz}); \quad and$

$F_{rz} = F_{rs} + d_r \cdot (v_{rrz} - v_{rz}); \quad and \quad \dot{F}_{rs} = c_r \cdot (v_{rrz} - v_{rz});$

Above model is formulated on first order form ($m \cdot \dot{v} \cdots$; and $\dot{F}_s = c \cdot (\cdots)$;) to show an alternative to second order differential equation form ($m \cdot \ddot{z} \cdots$;) used in 5.4.

We need to express a_z in differentiated variables. Then we can either assume $[v_x, v_z] = [v_{xg}, v_{zg}]$; (velocity components in ground fixed directions) or $[v_x, v_z] = [v_{xv}, v_{zv}]$; (vehicle fixed directions). Both are correct, in similar way as for the yaw rotation, see 4.4.2.3.3. If ground fix: $[a_{xg}, a_{zg}] = [\dot{v}_{xg}, \dot{v}_{zg}]$;. If ground fix: $[a_{xv}, a_{zv}] = [\dot{v}_{xv} + v_{zv} \cdot \omega_y \approx \dot{v}_{xv}, \dot{v}_{zv} - v_{xv} \cdot \omega_y]$;. The intention for 5.7.2 is to study constant speed over ground, so we know $\dot{v}_{xg} = 0$;. Therefore it is easiest to use ground fix directions. We can compare with the pitching model in 3.4.5, which is typically used for longitudinal acceleration and braking. Then it is most natural to use vehicle fix and solve v_{xv} and v_{zv} as state variables in an ode.

We formulate the matrix form of the model in ground fix direction:

$$\underbrace{\begin{bmatrix} m & 0 & 0 & 0 \\ 0 & J_y & 0 & 0 \\ 0 & 0 & 1/c_f & 0 \\ 0 & 0 & 0 & 1/c_r \end{bmatrix}}_{\boldsymbol{MC}} \cdot \begin{bmatrix} \dot{v}_{zg} \\ \dot{\omega}_y \\ \dot{F}_{fs} \\ \dot{F}_{rs} \end{bmatrix} =$$

$$= \underbrace{\begin{bmatrix} -d_f - d_r & d_f \cdot l_f - d_r \cdot l_r & 1 & 1 \\ d_f \cdot l_f - d_r \cdot l_r & -d_f \cdot l_f^2 - d_r \cdot l_r^2 & -l_f & +l_r \\ -1 & +l_f & 0 & 0 \\ -1 & -l_r & 0 & 0 \end{bmatrix}}_{\boldsymbol{D}} \cdot \underbrace{\begin{bmatrix} v_{zg} \\ \omega_y \\ F_{fs} \\ F_{rs} \end{bmatrix}}_{\boldsymbol{z_{vF}}} + \underbrace{\begin{bmatrix} -m \cdot g \\ 0 \\ 0 \end{bmatrix}}_{\boldsymbol{g}} + \underbrace{\begin{bmatrix} d_f & d_r \\ -d_f \cdot l_f & d_r \cdot l_r \\ 1 & 0 \\ 0 & 1 \end{bmatrix}}_{\boldsymbol{D_r}} \cdot \underbrace{\begin{bmatrix} v_{rfz} \\ v_{rrz} \end{bmatrix}}_{\boldsymbol{z_{vr}}};$$

Variable substitution $\boldsymbol{z_{vF}} = \boldsymbol{z_{vF0}} - \boldsymbol{D^{-1}} \cdot \boldsymbol{g}$; gives: $\boldsymbol{MC} \cdot \dot{\boldsymbol{z}}_{\boldsymbol{vF0}} = \boldsymbol{D} \cdot \boldsymbol{z_{vF0}} + \boldsymbol{D_r} \cdot \boldsymbol{z_{vrz}}$;.

Fourier transform gives: $j \cdot \omega \cdot \boldsymbol{MC} \cdot \boldsymbol{\mathcal{F}}(\boldsymbol{z_{vF0}}) = \boldsymbol{D} \cdot \boldsymbol{\mathcal{F}}(\boldsymbol{z_{vF0}}) + \boldsymbol{D_r} \cdot \boldsymbol{\mathcal{F}}(\boldsymbol{z_{vrz}})$;The Transfer functions in Figure 5-30 can now be plotted. Note that the driver comfort, earlier measured in vertical acceleration amplitude $\hat{a}_z = \text{amplitude}(\dot{v}_z)$;, now has two possibilities: $\hat{a}_{zg} = \text{amplitude}(\dot{v}_{zg}) = \hat{\dot{v}}_{zg}$; or $\hat{a}_{zv} = \text{amplitude}(\dot{v}_{zv} - v_{xv} \cdot \omega_y)$;. The latter one makes most sense, since seat and driver rotates with the vehicle. With this measure of driver comfort, the transfer function for a_z in Figure 5-30, $|H_{zrf \to \dot{v}z}| = |H_{zrf \to \dot{v}zg}|$, should be adjusted to $|H_{zrf \to \dot{v}zv}|$, for driver comfort measure.

If eliminating the forces, in the model in vehicle directions, we get the 2nd order differential equation:

$$\begin{bmatrix} m & 0 \\ 0 & J_y \end{bmatrix} \cdot \begin{bmatrix} \dot{v}_{zg} \\ \dot{\omega}_y \end{bmatrix} = \begin{bmatrix} -d_f - d_r & d_f \cdot l_f - d_r \cdot l_r \\ d_f \cdot l_f - d_r \cdot l_r & -d_f \cdot l_f^2 - d_r \cdot l_r^2 \end{bmatrix} \cdot \begin{bmatrix} \dot{v}_{zg} \\ \dot{\omega}_y \end{bmatrix} + \begin{bmatrix} 1 & 1 \\ -l_f & l_r \end{bmatrix} \cdot \begin{bmatrix} c_f & 0 \\ 0 & c_r \end{bmatrix}$$
$$\cdot \left(\begin{bmatrix} -1 & l_f \\ -1 & -l_r \end{bmatrix} \cdot \begin{bmatrix} v_{zg} \\ \omega_y \end{bmatrix} + \begin{bmatrix} v_{rfzg} \\ v_{rrzg} \end{bmatrix} \right) + \begin{bmatrix} d_f & d_r \\ -d_f \cdot l_f & d_r \cdot l_r \end{bmatrix} \cdot \begin{bmatrix} \dot{v}_{rfzg} \\ \dot{v}_{rrzg} \end{bmatrix};$$

5.7.2.2.1 Correlated or Wheel Base Filtered

Front and rear are excited with same frequencies, but delayed at the rear:

$$\boldsymbol{\mathcal{F}}(\boldsymbol{z_{vrz}}) = \begin{bmatrix} \mathcal{F}(v_{rfz}) \\ \mathcal{F}(v_{rrz}) \end{bmatrix} = \boldsymbol{\mathcal{F}}\left(\frac{d}{dt} \begin{bmatrix} z_{rf} \\ z_{rr} \end{bmatrix} \right) = \boldsymbol{\mathcal{F}}\left(\frac{d}{dt} \begin{bmatrix} \hat{z}_r \cdot \cos(\omega \cdot t) \\ \hat{z}_r \cdot \cos(\omega \cdot t - 2 \cdot \pi \cdot \lambda / L) \end{bmatrix} \right) =$$
$$= \begin{bmatrix} 1 \\ \cos(2 \cdot \pi \cdot \lambda / L) - j \cdot \sin(2 \cdot \pi \cdot \lambda / L) \end{bmatrix} \cdot \mathcal{F}(\hat{z}_r \cdot \cos(\omega \cdot t)) =$$
$$= \begin{bmatrix} 1 \\ \cos(2 \cdot \pi \cdot \lambda / L) - j \cdot \sin(2 \cdot \pi \cdot \lambda / L) \end{bmatrix} \cdot \mathcal{F}(v_{rfz}) =$$
$$= j \cdot \omega \cdot \begin{bmatrix} 1 \\ \cos(2 \cdot \pi \cdot \lambda / L) - j \cdot \sin(2 \cdot \pi \cdot \lambda / L) \end{bmatrix} \cdot \mathcal{F}(z_{rf}) = j \cdot \omega \cdot \boldsymbol{d_\lambda} \cdot \mathcal{F}(z_{rf});$$

Insertion gives: $j \cdot \omega \cdot \boldsymbol{MC} \cdot \boldsymbol{\mathcal{F}}(\boldsymbol{z_{vF0}}) = \boldsymbol{D} \cdot \boldsymbol{\mathcal{F}}(\boldsymbol{z_{vF0}}) + \boldsymbol{D_r} \cdot j \cdot \omega \cdot \boldsymbol{d_\lambda} \cdot \mathcal{F}(z_{rf}) \;\Rightarrow$

$$\Rightarrow \boldsymbol{\mathcal{F}}(\boldsymbol{z_{vF0}}) = (j \cdot \omega \cdot \boldsymbol{MC} - \boldsymbol{D})^{-1} \cdot \boldsymbol{D_r} \cdot j \cdot \omega \cdot \boldsymbol{d_\lambda} \cdot \mathcal{F}(z_{rf}) = \begin{bmatrix} H_{z_{rf} \to v_z} \\ H_{z_{rf} \to \omega_y} \\ H_{z_{rf} \to F_{fs}} \\ H_{z_{rf} \to F_{rs}} \end{bmatrix} \cdot \mathcal{F}(z_{rf}) = \boldsymbol{H_{z_{rf} \to v_z, corr}} \cdot \mathcal{F}(z_{rf});$$

All H depend on ω (or λ) and v_x.

5.7.2.2.2 Uncorrelated

We now assume that front and rear are excited "uncorrelated". This is wrong if driving on a road where rear axle follows front axle, but it is correct for a vehicle with independent excitation under each axle, which can be achieved e.g. in a shake rig.

$$\boldsymbol{\mathcal{F}}(\boldsymbol{z_{vr}}) = \begin{bmatrix}\mathcal{F}(v_{rfz})\\ \mathcal{F}(v_{rrz})\end{bmatrix} = \begin{bmatrix}\mathcal{F}(\dot{z}_{rf})\\ \mathcal{F}(\dot{z}_{rr})\end{bmatrix} = j\cdot\omega\cdot\begin{bmatrix}\mathcal{F}(z_{rf})\\ \mathcal{F}(z_{rr})\end{bmatrix};$$

$$\boldsymbol{\mathcal{F}}(\boldsymbol{z_{vF0}}) = (j\cdot\omega\cdot\boldsymbol{MC}-\boldsymbol{D})^{-1}\cdot\boldsymbol{D_r}\cdot j\cdot\omega\cdot\begin{bmatrix}\mathcal{F}(z_{rf})\\ \mathcal{F}(z_{rr})\end{bmatrix} = \begin{bmatrix}H_{z_{rf}\to v_z,uncorr} & H_{z_{rr}\to v_z,uncorr}\\ H_{z_{rf}\to\omega_y,uncorr} & H_{z_{rr}\to\omega_y,uncorr}\\ H_{z_{rf}\to F_{fs},uncorr} & H_{z_{rr}\to F_{fs},uncorr}\\ H_{z_{rf}\to F_{rs},uncorr} & H_{z_{rr}\to F_{rs},uncorr}\end{bmatrix}\cdot\begin{bmatrix}\mathcal{F}(z_{rf})\\ \mathcal{F}(z_{rr})\end{bmatrix};$$

If z_{rf} and z_{rf} have the same amplitude(frequency) content, and is called z_r, we can write:

$$\boldsymbol{\mathcal{F}}(\boldsymbol{z_{vF0}}) = \begin{bmatrix}H_{z_{rf}\to v_z,uncorr} & H_{z_{rr}\to v_z,uncorr}\\ H_{z_{rf}\to\omega_y,uncorr} & H_{z_{rr}\to\omega_y,uncorr}\\ H_{z_{rf}\to F_{fs},uncorr} & H_{z_{rr}\to F_{fs},uncorr}\\ H_{z_{rf}\to F_{rs},uncorr} & H_{z_{rr}\to F_{rs},uncorr}\end{bmatrix}\cdot\begin{bmatrix}1\\1\end{bmatrix}\cdot\mathcal{F}(z_r) = \boldsymbol{H_{z_r\to v_z,uncorr}}\cdot\mathcal{F}(z_r);$$

The elements in H depend on ω (or λ) and v_x.

5.8 Three Dimensional Oscillations

A real road generates motion in all out-of-road-plane dimensions: heave z, roll φ_x and pitch φ_y. One can, for instance, use [5.27] to generate a vertical profile for each side of the vehicle, but then randomly generate different phases for each side. Another way is to record a certain piece of a road where one does testing, typically at the vehicle manufacturer's test track. One then gets wheel base filtering one each side and a roll influence due to that left and right side are not in phase with each other.

If modelling unsprung masses without inertia, we still get 3 state variables: heave z, pitch φ_y and roll φ_y. Using same form of equations as in Eq [5.45] we get this model (subscripts rfl for "road front left" and so on):

$$\boldsymbol{M}\cdot\ddot{\boldsymbol{z}}+\boldsymbol{D}\cdot\dot{\boldsymbol{z}}+\boldsymbol{C}\cdot\boldsymbol{z} = \boldsymbol{D_r}\cdot\dot{\boldsymbol{z}}_{\boldsymbol{r}}+\boldsymbol{C_r}\cdot\boldsymbol{z_r};$$

$$where\ \boldsymbol{z} = \begin{bmatrix}z\\ \varphi_x\\ \varphi_y\end{bmatrix};$$

$$and\ \boldsymbol{z_r} = \begin{bmatrix}z_{rfl}\\ z_{rfr}\\ z_{rrl}\\ z_{rrr}\end{bmatrix} = \begin{bmatrix}1 & 0\\ 0 & 1\\ \cos(\varphi)+j\cdot\sin(\varphi) & 0\\ 0 & \cos(\varphi)+j\cdot\sin(\varphi)\end{bmatrix}\cdot\begin{bmatrix}z_{rfl}\\ z_{rfr}\end{bmatrix};$$

$$where\ \varphi = 2\cdot\pi\cdot L/v_x\ ;$$

The disturbances from the road are two independent ones, so the transfer functions will be a 3×2 matrix:

$$\begin{bmatrix}\mathcal{F}(z)\\ \mathcal{F}(\varphi_x)\\ \mathcal{F}(\varphi_y)\end{bmatrix} = \boldsymbol{H}\cdot\begin{bmatrix}\mathcal{F}(z_{rfl})\\ \mathcal{F}(z_{rfr})\end{bmatrix} = \begin{bmatrix}H_{z_{rfl}\to z} & H_{z_{rfr}\to z}\\ H_{z_{rfl}\to\varphi_x} & H_{z_{rfr}\to\varphi_x}\\ H_{z_{rfl}\to\varphi_y} & H_{z_{rfr}\to\varphi_y}\end{bmatrix}\cdot\begin{bmatrix}\mathcal{F}(z_{rl})\\ \mathcal{F}(z_{rr})\end{bmatrix};$$

[5.57]

5.9 Transient Vertical Dynamics

The majority of the chapter you read now, considers driving for during long time periods on roads with repetitive unevenness. This is one relevant use case and the functions are then suitably analysed using frequency analysis, since the quantities vary as stationary oscillations.

However, vertical vehicle dynamics also have transient disturbances to consider. Test cases can be one-sided or two sides road bumps or pot-holes. Two-sided bump is envisioned in Figure 5-31. It can represent driving over a speed bump or a low obstacle.

Models from earlier in this chapter are all relevant for two-sided bumps or holes, but one might need to consider non-linearities such as bump stops or wheel lift as well as different damping in compression and rebound. For one-sided bumps/holes, the models from earlier in this chapter are generally not enough. The computation is rather time simulation than frequency analysis. The function measures (and requirements) should be shifted somewhat:

- Human **comfort** for transients is often better described as time derivative of acceleration (called "jerk"). Peak-to-peak values of the variables can be used.
- The material **loads** are more of maximum load type than fatigue life dimensioning, i.e. higher material stress but fewer load cycles during vehicle life time.
- **Road grip** studies over road bumps and pot-holes are challenging. Qualitatively, the tyre models often must include relaxation, because that is the mechanism which reduces road grip when vertical load shifts. To get quantitatively correct tyre models is beyond the goal of the compendium you presently read.
- **Roll-over** can be tripped by large one-sided bumps. This kind of roll-overs is unusual and requires complex models.

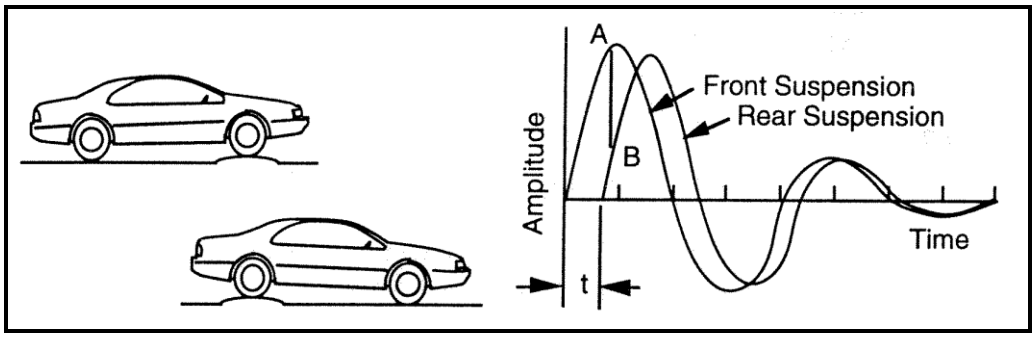

Figure 5-31: Response of Vehicle for Front and Rear Axle Impulses, (Gillespie, 1992)

Models for studying transient vertical dynamics can, in general be categorized as the stationary oscillation models, 1D, 2D and 3D. But they cannot generally be linear, so they require simulation, not frequency analysis. One typically need to add inertia of unsprung parts and vertical elasticities in each tyre. And "trivial linkage" suspension is generally not enough if sharp road unevenness, but instead one might identify the pivot axis in space for each wheel linkage.

A 3D model according to these concepts gets the states $\boldsymbol{z}$ containing $z,\ \varphi_x,\ \varphi_y,\ z_{fl},\ z_{fr},\ z_{rl},\ and\ z_{rr}$ if modelled with a second order differential equation ($\boldsymbol{f}(\ddot{\boldsymbol{z}}, \dot{\boldsymbol{z}}, \boldsymbol{z}, \boldsymbol{u}, t) = 0$;). If modelled with first order differential equations ($\boldsymbol{f}(\dot{\boldsymbol{z}}, \boldsymbol{z}, \boldsymbol{u}, t) = 0$;) and the concept of using forces in elasticities as states, see 1.5.2.2, the states z will instead contain $z,\ \varphi_x,\ \varphi_y,\ v_{flz},\ v_{frz},\ v_{rlz},\ v_{rrz},\ F_{sfl},\ F_{sfr},\ F_{srl},\ and\ F_{srr}$, where v_{ijz} is vertical velocity of unsprung mass in wheel ij and F_{sij} is elastic part of vertical force under wheel ij. The inputs (disturbance) $\boldsymbol{u} = \boldsymbol{z_r}$ will contain $z_{rfl},\ z_{rfr},\ z_{rrl},\ and\ z_{rrr}$.

Bibliography

AB Volvo. 2011. *Global Transport Application.* 2011.

Andreasson, Johan. 2007. *On Generic Road Vehicle Motion Modelling and Control.* Stockholm : KTH, 2007. Dissertation.

Bakker, E., Nyborg, L., Pacejka, H.B. 1987. *Tyre Modelling for use in Vehicle Dynamics Studies.* 1987. SAE Paper No.870495.

Barnard, R. H. *Road Vehicle Aerodynamic Design.* u.o. : Mechaero Publishing. ISBN 0954073479.

—. 2010. *Road Vehicle Aerodynamic Design.* u.o. : Mechaero Publishing, 2010.

Boerboom, Max. 2012. *Electric Vehicle Blended Braking maximizing energy recovery while maintaining vehicle stability and maneuverability.* Göteborg, Sweden : Chalmers University of Technology, 2012. Diploma work - Department of Applied Mechanics. ISSN 1652-8557; no 2012:01.

Clark, S, (ed). 1971. *Mechanics of Pneumatic Tires, Monograph 122.* u.o. : National Bureau of Standards, USA, 1971.

Cooper Tire & Rubber Co. 2007. Passenger radial tire cutaway. Online Art. [Online] Cooper Tire & Rubber Co., den 16 September 2007. http://deantires.com/us/en/information/info-construction.asp.

DIRECTIVE 2002/44/EC. 2002. *DIRECTIVE 2002/44/EC OF THE EUROPEAN PARLIAMENT AND OF THE COUNCIL.* 2002. http://europa.eu/legislation_summaries/employment_and_social_policy/health_hygiene_safety_at_work/c11145_en.htm.

Drenth, Edo F. 1993. *Brake Stability of Front Wheel Driven Cars at High Speed.* Delft, Netherlands : Delft University of Technology., 1993. Master thesis.

Encyclopædia Britannica Online. 2007. belted tire: tire designs." Online Art. Encyclopædia Britannica Online. [Online] 16 September 2007. http://www.britannica.com/eb/art-7786.

Gillespie, T. 1992. *Fundamentals of Vehicle Dynamics.* s.l. : Society of Automotive Engineers, 1992.

Grosch, K.A. and Schallamach, A. 1961. Tyre wear at controlled slip. *Wear.* September–October 1961, Vol. Volume 4, Issue 5, pp. Pages 356–371.

Happian-Smith, Julian. 2002. *An Introduction to Modern Vehicle Design.* u.o. : Butterwoth-Heinemann, ISBN 0-7506-5044-3, 2002.

Hirschberg, W., Rill, G. and Weinfurter, H. 2007. Tire model TMeasy. *Vehicle System Dynamics.* 2007, Vol. 45:1, pp. 101 — 119.

Hucho, Wolf-Heinric. 1998. *Aerodynamics of Road Vehicles.* u.o. : SAE International, 1998. R-177.

ISO 11026. *ISO 11026 Heavy commercial vehicles and buses - Test method for roll stability - Closing-curve test.* u.o. : International Organization for Standardization, Genève, Switzerland.

ISO 14791. *ISO 14791 Road vehicles - Heavy commercial vehicle combinations and articulated buses - Lateral stability test methods.* u.o. : International Organization for Standardization, Genève, Switzerland.

ISO 14792. *ISO 14792 Road vehicles - Heavy commercial vehicles and buses - Steady-state circular tests.* u.o. : International Organization for Standardization, Genève, Switzerland. ISO 14792.

ISO 14793. *ISO 14793 Road vehicles – Heavy commercial vehicles and buses – Lateral transient response test methods.* u.o. : International Organization for Standardization, Genève, Switzerland.

ISO 14794. 2011. *ISO 14794 Heavy commercial vehicles and buses - Braking in a turn - Open-loop test methods.* u.o. : International Organization for Standardization, Genève, Switzerland, 2011. ISO 14794.

ISO 26262. 2011-2012. *Road vehicles – Functional safety, 1-10.* u.o. : International Organization for Standardization, Genève, Switzerland, 2011-2012.

ISO 2631. *ISO 2631 – Evaluation of Human Exposure to Whole-Body Vibration.* s.l. : International Organization for Standardization, Genève, Switzerland.

ISO 3888. *ISO 3888 Passenenger Cars -- Test track for severe lane change manouvre -- Part 2: Obstacle Avoidance.* u.o. : International Organization for Standardization, Genève, Switzerland. ISO 3888.

ISO 4138. *ISO 4138 Passenger cars – Steady-state circular driving behaviour - Open-loop test methods.* u.o. : International Organization for Standardization, Genève, Switzerland. ISO 4138.

ISO 7401. *ISO 7401 Lateral transient response test methods - Open-loop test methods.* u.o. : International Organization for Standardization, Genève, Switzerland.

ISO 7975. 2006. *ISO 7975 Passenger cars – Braking in a turn – Open-loop test method.* u.o. : International Organization for Standardization, Genève, Switzerland, 2006. ISO 7975.

ISO 80000-3. 2013. *ISO 80000 – Quantities and units – Part 3: Space and time.* s.l. : International Organization for Standardization, Genève, Switzerland, 2013.

ISO 8608. *ISO 8608 Mechanical vibration - Road surface profiles - Reporting of measured data.* u.o. : International Organization for Standardization, Genève, Switzerland.

ISO 8855. *ISO 8855 – Road vehicle – Vehicle dynamics and road holding ability – Vocabulary.* s.l. : International Organization for Standardization, Genève, Switzerland.

ISO. 2011. *ISO 14794 Heavy commercial vehicles and buses - Braking in a turn - Open-loop test methods.* u.o. : ISO, 2011. ISO 14794.

—. 2006. *Passenger cars – Braking in a turn – Open-loop test method.* u.o. : ISO, 2006. ISO 7975.

ISO19377. 2017. *ISO 19377 Heavy commercial vehicles and buses - Emergency braking on a defined path - Test method for trajectory measurement.* u.o. : ISO, 2017. ISO 19377:2017, IDT.

ISO28580. 2018. *Passenger car, truck and bus tyre rolling resitance measurement method -- single point test and correlation of measurement results.* u.o. : ISO, 2018. ISO28580:2018.

Jacobson, Bengt, et al. 2014. *Vehicle Dynamics Compendium for Course MMF062.* Göteborg : Chalmers University of Technology, 2014. http://pingpong.chalmers.se/public/courseId/4042/lang-en/publicPage.do.

Jonsson, Axel och Olsson, Erik. 2016. *A Methodology for Identification of Magic Formula Tire Model Parameters from In-Vehicle Measurements.* u.o. : Chalmers University of Technology, 2016. MSc thesis.

Kati, Maliheh Sadeghi. 2013. *Definitions of Performance Based Characteristics for Long Heavy Vehicle Combinations.* Signals and Systems. u.o. : Chalmers University of Technology, 2013. ISSN 1403-266x.

Kharrazi , Sogol. 2012. *Steering Based Lateral Performance Control of Long Heavy Vehicle Combinations.* Göteborg, Sweden : Chalmers University of Technology, 2012. ISBN/ISSN: 978-91-7385-724-6.

Kiencke, U. and Nielsen, L. 2005 . *Automotive Control Systems.* 2005 .

Lex, Cornelia. 2015. *Estimation of the Maximum Coefficient of Friction between Tire and Road based on Vehicle State measurements.* Graz : Graz University of Technology, 2015. Doctoral thesis.

Ludwig, Christian och Kim, Chang Su. 2017. *Influence of testing surface on tire lateral force characteristics.* München : Springer Fachmedien, 2017. ss. 795-808.

Michelin. 2003. *The tyre Rolling resistance and fuel savings.* u.o. : Michelin, 2003.

Mägi, Mart. 1988. *The Significance of System Pre-Load at Modal Analysis of Low-Resonant Mechanical Systems.* Århus, Denmark : Modal Testing & FEM Seminar in Århus, 1988.

NHTSA. *Electronic Stability Control Systems.* u.o. : NHTSA. FMVSS 126.

Pacejka, H. 2005. *Tyre and Vehicle Dynamics, 2nd ed.* u.o. : Elsevier, 2005.

Pettersson, Pär. 2017. *On Numerical Descriptions of Road Transport Missions.* Gothenburg, Sweden : Chalmers University of Technology, 2017. Thesis for Licentate of Engineering.

—. 2019. *Operation cycles representations for road vehicles.* Göteborg : Chalmers University of Technology, 2019. PhD thesis.

Ploechl, Manfred, [red.]. 2013. *Road and Off-Road Vehicle System Dynamics Handbook.* u.o. : CRC Press, 2013. Print ISBN: 978-0-8493-3322-4; eBook ISBN: 978-1-4200-0490-8; http://www.crcnetbase.com/isbn/9781420004908.

Rajamani, Rajesh. 2012. *Vehicle Dynamics and Control.* u.o. : Springer, 2012. ISSN 0941-5122.

Rhyne, T. B. 2005. *Development of a Vertical Stiffness Relationship for Belted Radial Tires.* u.o. : Tire Science and Technology, TSTCA, Vol. 33, no. 3, July-September 2005, 2005. ss. pp. 136-155.

Rill, Georg. 2006. *FIRST ORDER TIRE DYNAMICS.* Lisbon, Portugal : III European Conference on Computational Mechanics Solids, Structures and Coupled Problems in Engineering, 5–8 June 2006, 2006.

Robert Bosch GmbH. 2004. *Bosch Automotive Handbook 6th Edition.* s.l. : Bentley Publishes, 2004.

Ross, I. Michael. 2015. *A Primer on Pontryagin's Principle in Optimal Control.* 2015.

Rösth, Markus. 2007. *Hydraulic Power Steering System Design in Road Vehicles: Analysis, Testing and Enhanced Functionality.* Linköping : Linköping Univeristy, Department of Management and Engineering, Fluid and Mechatronic Systems, 2007. Dissertation. Dissertations, ISSN 0345-7524; 1068.

SAE J1441. 2016.. *Standard J1441, Subjective Rating Scale for Vehicle Ride and Handling.* u.o. : SAE International, , 2016.

SAE_J3016. 2016. *SAE J3016 Taxonomy and Definitions for Terms Related toDriving Automation Systems for On-Road Motor Vehicles.* u.o. : SAE International, 2016. Tech. rep. 2016.

SAEJ670. *SAE J670e - Vehicle Dynamics Terminology.* u.o. : Society of Automotive Engineers, Warrendale, PA, USA.

Sander, Ulrich. 2018. *Predicting Safety Benefits of Automated Emergency Braking in Intersections -- Virtual simulations based on real-world accident data.* Göteborg : Chalmers University of Technology, PhD thesis, 2018.

Schuetz, Thomas. 2015. *Aerodynamics of Road Vehicles, Fifth Edition.* u.o. : SAE, 2015.

Sundström, Peter, Jacobson, Bengt och Laine, Leo. 2014. Vectorized single-track model in Modelica for articulated vehicles with arbitrary number of units and axles. Lund, Sweden : Modelica conference 2014, March 10-12, 2014, 2014.

Svendenius, Jacob. 2007. *Tire Modeling and Friction Estimation.* Lund, Sweden : Department of Automatic Control, Lund University, 2007. Dissertation.

Tagesson, Kristoffer. 2017. *Driver-centred Motion Control of Heavy Trucks.* Gothenburg, Sweden : Chalmers University of Technology, 2017. Dissertation.

Tagesson, Krsitoffer och Cole, David. 2017. Advanced emergency braking under split friction conditions and the influence of a destabilising steering wheel torque. *Vehicle System Dynamics.* 2017, Vol. 55.

Tiller, Michael. 2019. Modelica by example. [Online] 2019. [Citat: den 4 June 2019.] https://mbe.modelica.university/.

UN ECE 111. 2001. *UNIFORM PROVISIONS CONCERNING THE APPROVAL OF TANK VEHICLES OF CATEGORIES N AND O WITH REGARD TO ROLLOVER STABILITY.* u.o. : UNITED NATIONS, 2001. Regulation No. 111.

Weber, R. 1981. *Reifen Führungskräfte bei schnellen Änderungen von Schräglauf und Schlupf.* Karlsruhe : University of Karlsruhe, 1981. Dissertation.

Wedlin, Johan, Tillback, Lars-Runo och Bane, Olof. 1992. *Combining Properties for Driving Pleasure and Driving Safety: A Challenge for the Chassis Engineer.* u.o. : SAE, 1992. SAE Technical paper 921595.

Wipke, Keith B, Cuddy, Matthew R. och Burch, Steven D. 1999. ADVISOR 2.1: A User-Friendly Advanced Powertrain Simulation Using a Combined Backward/Forward Approach. *IEEE TRANSACTIONS ON VEHICULAR TECHNOLOGY.* 1999, Vol. 48, 6, ss. 1751-1761.

Wong, J.Y. 2001. *Theory of Ground Vehicles (3rd ed.).* s.l. : John Wiley and Sons, Inc., New York, 2001.

Yang, Derong. 2013. *Vehicle Dynamics Control after Impacts in Multiple-Event Accidents.* Göteborg : Chalmers University of Technology, 2013. PhD thesis. ISBN 978-91-7385-887-8.